MONASH University

Understanding the mechanisms involved in heat damage of testicular function in the rat testis

Rashid Abdulhameed R Aldahhan
MBBS, MClinEmb

A thesis submitted for the degree of *Doctor of Philosophy* at
Monash University in 2019
Department of Molecular and Translational Science (Hudson Institute of Medical Research)

Copyright notice

Abstract

In most mammals, the testes descend during prenatal or early neonatal life to reside in the scrotum, where the temperature is 2–7 °C lower than the core body temperature. Spermatogenesis is a temperature-sensitive process, and elevation above the normal scrotal temperature range can cause the death of heat-sensitive spermatogenic cells. Elevated scrotal temperature is considered to be a significant contributor to male factor infertility. Humans can be exposed to a wide range of sources of heat stress that adversely impact testis function. Although the physiological and cellular responses of the testes to heat stress have been well established, the molecular mechanisms that direct these responses remain mostly unknown. In this thesis, the effect of heat was investigated using two different heat exposure models: acute heat (43°C, 15 minutes) and experimental cryptorchidism in the adult rat testis.

In Chapter 2, the effects of acute heat on Sertoli cell functions, and inhibin/activin-related proteins were studied. The testicular response to heat stress displayed three phases: (I) onset (1–2 weeks), (II) peak damage (2–8 weeks) and (III) recovery (12–14 weeks). Expression of several key Sertoli and Leydig cell genes declined contemporaneously with the initial loss of meiotic germ cells. Activins were responsive to the subsequent loss of mature spermatids, leading to an increase in testicular activin B production relative to activin A. Critically, germ cell damage was not associated with a significant inflammatory response.

In Chapter 3, studies aimed to characterise the molecular mechanisms of this damage/recovery process via a detailed proteomic investigation of the testicular interstitial fluid (TIF) that surrounds seminiferous tubules in acute heat-treated rats. Overall, 1728 unique proteins were identified in TIF by LC-MS/MS, with 209 proteins altered ($p<0.05$) between 2–17-fold at 1, 8 and 14 weeks. Proteins essential for extracellular matrix regulation through their association with fibril formation showed the most acute response to heat at 1 and/or 8 weeks after exposure, corresponding with the peak loss of germ cells. Conversely, cytoskeletal proteins involved in Sertoli cell microtubule regulation were downregulated at 8-14 weeks. Additionally, a group of

germ-cell-specific proteins associated with spermatogenic regulation were also downregulated at 8-14 weeks.

In Chapter 4, the molecular effects of cryptorchidism on Sertoli cell and Leydig cell function were investigated by inducing cryptorchidism in adult rats for 7 and 14 weeks, which resulted in spermatogenic failure, fibrosis, accumulation of fluid in the testis and loss of feedback to the anterior pituitary gland via inhibin and testosterone. This damage coincided with a progressive decline of several critical Sertoli cell genes and the crucial Leydig cell steroidogenic enzymes. Activin A was largely unaffected at any time-point, but activin B and the activin-binding protein, follistatin, declined. Conversely, expression of genes involved in inflammation and fibrosis were strongly elevated throughout the experiment.

These data collectively indicate both direct and indirect detrimental effects of heat on multiple molecular functions in both the somatic and germ cell populations in the testis, involving disruption of intercellular and intercompartmental communication, and inflammatory and fibrotic response. This study also provides new insights into the proteome of TIF in response to testicular damage, indicating that further study of these proteins would be a promising diagnostic approach for identifying novel markers of male infertility.

Publications during enrolment

Aldahhan, R.A., Stanton, P.G., Ludlow, H., de Kretser, D.M., Hedger, M.P., 2019. Acute heat treatment disrupts inhibin-related protein production and gene expression in the adult rat testis. *Molecular and Cellular Endocrinology* 498, 110546.

Presentations arising from this thesis

Oral Presentations:

Rashid Aldahhan, David de Kretser, Peter Stanton, Mark Hedger (2016) *Understanding the role of activins in heat damage on testicular function in the rat*. 19th European Testis Workshop, Saint-Malo, France.

Poster Presentations:

Rashid Aldahhan, David de Kretser, Peter Stanton, Mark Hedger (2014) *Understanding the mechanisms involved in heat damage of testicular function in the rat.* Monash Health Translation Precinct Research Week, Melbourne, Australia

Rashid Aldahhan, Adnan Sali, Susan Hayward, Peter Stanton, Mark Hedger , David de Kretser (2017) *The effects of short-term heat treatment on spermatogenesis, inhibin-related protein production and gene expression in the adult rat. 50th Annual Meeting of the Society* of the Study of Reproduction (SSR), Washington D.C, USA **(also presented as a flash talk).**

Rashid Aldahhan, Julie Muir, Susan Hayward, Peter Stanton, Mark Hedger, David de Kretser (2017) *The effects of experimental cryptorchidism on spermatogenesis and inhibin-related protein production in the adult rat.* Annual Scientific Meeting of the Society for Reproductive Biology (SRB), Perth. Australia.

Aldahhan RA, Dagley LF, Infusini G, Webb AI, O'Donnell L, de Kretser DM, Hedger MP, Stanton PG (2018) *Changes in the proteomic profile of testicular interstitial fluid after short-term heat treatment in the adult rat*. Annual Scientific Meeting of the Society for Reproductive Biology (SRB), Adelaide. Australia.

Thesis including published works declaration

I hereby declare that this thesis contains no material which has been accepted for the award of any other degree or diploma at any university or equivalent institution and that, to the best of my knowledge and belief, this thesis contains no material previously published or written by another person, except where due reference is made in the text of the thesis.

This thesis includes **1** original paper published in a peer reviewed journal, and **2** unpublished manuscript. The core theme of the thesis is investigating the mechanisms involved in heat damage of testicular function in the rat testis**.** The ideas, development and writing up of all the papers in the thesis were the principal responsibility of myself, the student, working within the Department of Molecular and Translational Science under the supervision of Prof Mark Hedger, Assoc Prof Peter Stanton and Prof David de Kretser.

The inclusion of co-authors reflects the fact that the work came from active collaboration between researchers and acknowledges input into team-based research. In the case of chapter 2, my contribution to the work involved the following:

Thesis Chapter	**Publication Title**	**Status** *(published, in press, accepted or returned for revision, submitted)*	**Nature and % of student contribution**	**Co-author name(s) Nature and % of Co-author's contribution***	**Co-author(s), Monash student Y/N***
2	Acute heat treatment disrupts inhibin-related protein production and gene expression in the adult rat testis	Published	85% Experimental design, optimisation of protocols, experimental analyses and drafting of manuscript	1) Peter Stanton, Revisions of manuscript 2.5% 2) Helen Ludlow, Reagents/activin A and B assay techniques 2.5% 3) David de Kretser, Revisions of manuscript and intellectual input 5% 4) Mark Hedger, Revisions of manuscript and intellectual input 5%	No No No No

I have not renumbered sections of submitted or published papers in order to generate a consistent presentation within the thesis.

Student signature: **Date:** 10/5/2019

The undersigned hereby certify that the above declaration correctly reflects the nature and extent of the student's and co-authors' contributions to this work. In instances where I am not the responsible author I have consulted with the responsible author to agree on the respective contributions of the authors.

Main Supervisor signature: **Date:** 10/5/2019

Acknowledgements

First and foremost, all praise is due to God 'Allah' for giving me the ability and desire to undertake this study. I also express my sincere gratitude to Prof David de Kretser for accepting me as a PhD student at a time when he did not have enough funds for my project; he did not abandon me as I awaited funding. I am greatly indebted to my supervisors, Prof Mark Hedger and Assoc. Prof Peter Stanton, for familiarising me with my endeavours in this study, as well as for their tolerant and wholehearted administration, inestimable leadership and explanatory remarks, without which I would not have been able to conclude this thesis. Thank you for giving me the opportunity to run my ideas past you, for sharing with me your scientific skills and experience and for shaping me into a better scientist.

I also voice my heartfelt appreciation to all members in the Hedger and Stanton Labs, past and present. Adnan Sali, special thanks go to you for being patient, kind and supportive, and for teaching me many techniques and treating me as your son. Sue, many thanks for assisting me and teaching me different proteins assays. My special appreciation goes to Julie, who helped me in ordering, culling and collecting animals. Rukmali and Rajini, thank you for sharing your knowledge with me during my PhD journey. I sincerely thank my Aussie mom, Karen O`Keefe, for her continuous assistance and encouragement throughout my PhD candidature. I am grateful to my great professor in Saudi Arabia, Prof Mohammed Motabagani, for the motivation, enthusiasm and support he provided to allow me to complete my postgraduate studies.

I would especially like to thank my friends in Saudi Arabia, particularly Fiyad Alenazi, Abdullah Alfareed, Abdullah Alghamdi, Abdullah Alruqaib and Sultan Alzahrani, for their constant emotional support and prayers.

This work would not have been possible without the generous financial support of Imam Abdulrahman Bin Faisal University in Saudi Arabia. To Saudi Arabia Cultural Attaché in Canberra, thank you for your efforts during my PhD.

Nobody has been more important to me in the pursuit of this study than the members of my family. I thank my parents for their earlier support, without which I would not be in this position. My sincere thanks go to my aunt, Fatima Almana, for her love and reassurance. Most importantly, I thank my loving and supportive wife, Athari Alhomoud, and my three wonderful flowers, Omar, Bandar and Jana, who provide unending inspiration.

Abbreviations

Abbreviation	Description
17B-HSD	17 beta-hydroxysteroid dehydrogenase
3B-HSD	3 beta-hydroxysteroid dehydrogenase
ACTA2	Actin alpha 2, smooth muscle
ACVR2	Activin receptor type-2
ADAMTS	A disintegrin and metalloproteinase with thrombospondin motifs
ADP	Adenosine diphosphate
ALK	Activin receptor-like kinase
AMH	Anti-Müllerian hormone
APAF-1	Apoptotic protease activating factor 1
AR	Androgen receptor
BAG6	BCL2-associated athanogene 6
BAX	Apoptosis regulator BAX
BCL-2	B-cell lymphoma 2
BMP	Bone morphogenetic protein
BTB	Blood testis barrier
CDNA	Complementary deoxyribonucleic acid
CGRP	Calcitonin gene-related peptide
CLDN11	Claudin 11
CLDN3	Claudin 3
COL1A1	Collagen alpha-1(I) chain
CRYAB	Crystallin alpha B
CV	Coefficient of variation
CYP11A1	Cytochrome P450 family 11 subfamily a polypeptide 1
CYP17A1	Cytochrome P450 family 17 subfamily a polypeptide 1
DAB	Diaminobenzidine
DBD	DNA-binding domain
DCN	Decorin
DHT	Dihydrotestosterone
DMEM/HAM`S F12	Dulbecco's Modified Eagle's Medium (DMEM) and Ham's F-12 Nutrient Mixture
DNA	Deoxyribonucleic acid
DPP	Days post-partum
E2	Estradiol
ECM	Extracellular matrix
ELISA	Enzyme linked immunosorbant assay
ER	Endoplasmic reticulum
ERK	Extracellular signal–regulated kinase
FADD	Fas-associated death domain
FAS	FS-7-associated surface antigen
FGF	Fibroblast growth factors
FSH	Folicle stimulating hormone
FST	Follistatin

GAPDH	Glyceraldehyde-3-phosphate dehydrogenase
GCAP	Germ cell alkaline phosphatase
GJA1	Gap junction protein, alpha 1
GNRH	Gonadotropin-releasing hormone
HNRNPH1	Heterogeneous nuclear ribonucleoprotein H1
HPRT	Hypoxanthine phosphoribosyltransferase
HPT	Hypothalamic-Pituitary-Testicular
HSD17B3	Hydroxysteroid 17-beta dehydrogenase 3
HSD3B1	Hydroxy-delta-5-steroid dehydrogenase, 3 beta- and steroid delta-isomerase 1
HSF1	Heat shock factor 1
HSP	Heat shock protein
ICBS	Intercellular cytoplasmic bridges
IL6	Interleukin-6
INHA	Inhibin subunit alpha
INHBA	Inhibin subunit beta A
INHBB	Inhibin subunit beta B
INL3	Insulin-like 3
JNK	c-Jun N-terminal kinase
KRT18	Keratin 18
LC	Leydig cell
LH	Luteinising hormone
LPS	Lipopolysaccharide
MAGE-4	Melanoma antigen-A4
MAP	Mitogen-activated protein
MRNA	Messenger ribonucleic acid
MYD88	Myeloid differentiation primary response 88
PBS	Phosphate-buffered saline
PCPE	Procollagen C-proteinase enhancer
PDGF	Platelet-derived growth factor
PGC	Primordial germ cell
PO2	Partial pressure of oxygen
RIA	Radioimmunoassay
RN18S	18S ribosomal RNA
ROS	Reactive oxygen species
RT-QPCR	Real-time quantitative polymerase chain reaction
SACE	Somatic isoform of the angiotensin-converting enzyme
SC	Sertoli cell
SCPS	Synaptonemal complex proteins
SDHA	Succinate dehydrogenase complex flavoprotein subunit A
SOD1	Superoxide dismutase 1
SOX9	SRY box 9
SPATA2	Spermatogenesis-associated protein 20
SRY	Sex-determining region Y
SSCS	Spermatogonial stem cells
TDT	Terminal deoxynucleotidyl transferase
TGF-B	Transforming growth factor-β
TIF	Testicular interstitial fluid

TJP1	Tight junction protein 1
TLR	Toll-like-receptors
TNF	Tumour necrosis factor
TRAF	TNF receptor associated factor
TUNEL	Terminal deoxynucleotidyl transferase dUTP nick end labelling
VEGF	Vascular endothelial growth factor

Table of Contents

1. Chapter 1:

Literature Review

1.1. Introduction

In couples presenting with infertility, abnormal sperm production by the male partner is the cause in about 50 % of the cases (Kovac et al., 2013). While low sperm counts, poor sperm motility or morphology are defined as the reason, there is a very poor understanding of how these defects occur and very few therapeutic opportunities. A better understanding of spermatogenesis and its regulation is required in order to treat male factor infertility.

This literature review summarises the knowledge on the structure, function and regulation of the rat testis with inter-species comparisons. It reviews the recent developments in our knowledge concerning the endocrine regulation of the testis and their roles in process that damage testicular function. Moreover, the role of growth and endocrine factors including transforming growth factor β (TGF-β), pituitary gland hormones and others is discussed in relationship to heat-induced damage to spermatogenesis and the process of recovery.

1.2. Normal structure and function of the testis

1.2.1. Anatomy and histology of the testis

The testis is an ovoid, paired, reproductive and endocrine organ that produces spermatozoa by a well-ordered series of cytological events known as spermatogenesis. Sperm production and hormone secretion, are the most important functions of the testis and will be discussed in more detail in the next sections. The average adult rat testis dimensions are 2.4 cm in length, 1.3 cm in breadth and 0.9 cm in anterior-posterior diameter and weighs 1.7 g while the mouse testis measures 0.66 cm× 0.39 cm × 0.45 cm with an average weight of 0.06 g. In humans, the average testis weighs 21.6 g (right) or 20 g (left), with the right usually 10% heavier than the left. Each human testis measures 4.6 cm × 2.6 cm × 3 cm (Knoblaugh et al., 2018), with the average volume being 18mL/testis (normal range 15–30mL) (Behre et al., 2001).

The testis develops as an abdominal organ in most mammals and then descends, during foetal or neonatal life, into the scrotum, which is a cutaneous fibromuscular sac. In both rodents and humans, the paired testes are engulfed by multiple coverings within the scrotal sac (Figure 1). The outer layer is the tunica vaginalis, which is a pouch of peritoneum that is invaginated posteriorly by the testis and covers the anterior and lateral aspects of the testes, creating the visceral and parietal layers. The testis itself is encapsulated by the tunica albuginea, a thick, dense collagenous layer that projects posteriorly into the testis as thick, incomplete, fibrous septae to form the mediastinum testis, through which the blood supply enters.

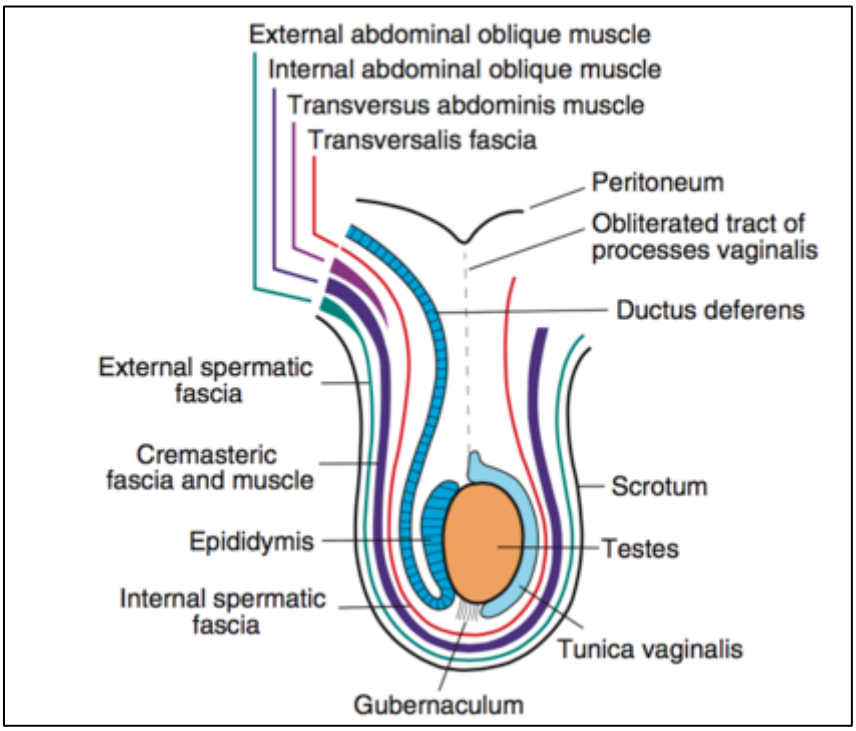

Figure 1. Illustration shows the coverings of the human testis that are derived from constituents of the abdominal wall. These coverings are formed as the testes migrate through the inguinal canal from their retroperitoneal location in the abdominal cavity into the scrotum [Adapted from (Sadler, 2011)].

The testicular parenchyma is incompletely divided by the septae, which extend internally from the mediastinum to form a series of about 200–300 conical lobules that contain convoluted seminiferous tubules (Kerr et al., 2006) (Figure 2). The seminiferous tubules are very fine coiled loops, with the two free ends connected by straight tubules to another network of tubules in the mediastinum called the rete testis. Each tubule is lined by the seminiferous epithelium that contains the germ cells, including spermatogonial stem cells and the radially arranged supporting Sertoli cells (Mescher, 2013). The Sertoli cells are highly specialised, tall, columnar cells that, together with the germ cells, form the lining of the seminiferous tubules. The base of the Sertoli cells is in contact with the basement membrane of the seminiferous tubules and the cytoplasm extends to the lumen of tubules. Where adjacent Sertoli cells are in contact with each other, various cell junctions (including tight junctions, basal ectoplasmic specialisations, desmosomes and gap junctions) are found and these junctions form the blood–testis barrier (BTB) (Cheng and Mruk, 2012).

The BTB divides the seminiferous tubules into a basal and an adluminal compartment, which maintains all germ cells, other than spermatogonia, in a specialised microenvironment. The adluminal compartment is an immunologically privileged site, which segregates the post-meiotic germ-cell antigens from the systemic circulation. The presence of the BTB results in the Sertoli cells controlling the entry of substances into the adluminal compartment of the seminiferous tubules. These cells also control the passage of large molecules and the passage of waste products into the intertubular compartment of the testis.

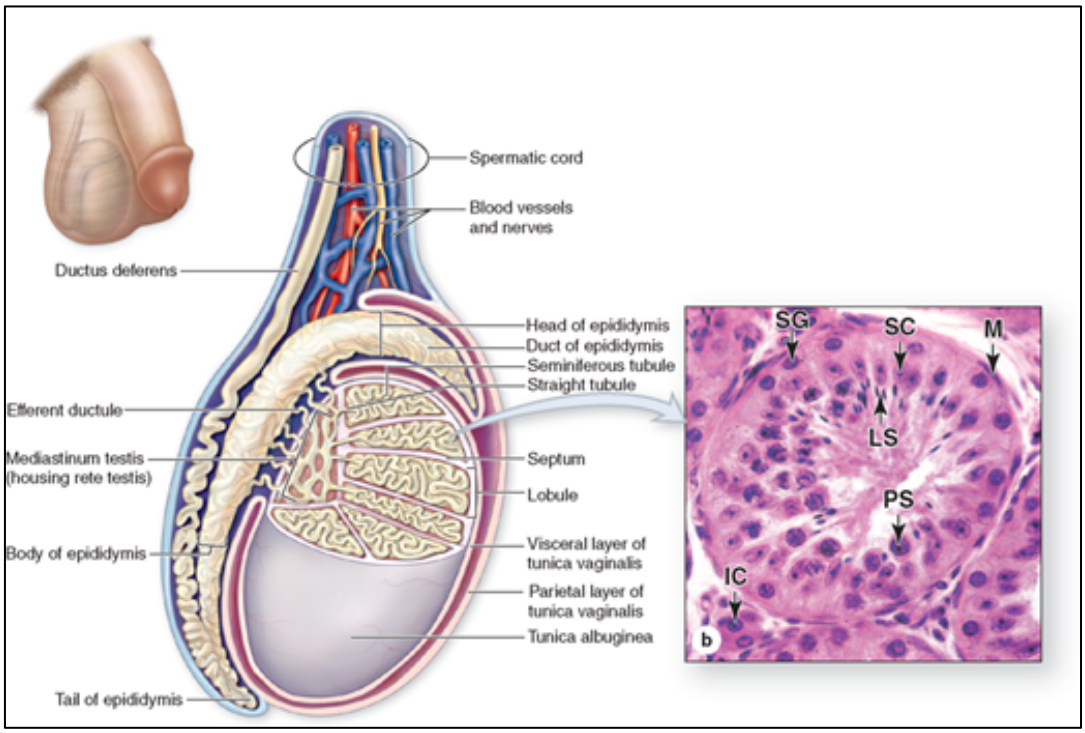

Figure 2. The anatomy and histology of the human testis. SG: spermatogonia, SC: Sertoli cell, LC: Leydig cell, M: myoid cells, PS: pachytene spermatocytes, LS: late spermatid [From (Mescher, 2013)].

The Sertoli cell has a basally placed nucleus and extends from the basal compartment to reach the lumen of the tubule. Its cytoplasm consists of a central core from which a complex of cytoplasmic processes extends between adjacent germ cells. It plays an essential role in the production of spermatozoa, as it supports a limited number of spermatogenic cells (O'Donnell et al., 2006; Orth et al., 1988). Thus, the number of Sertoli cells determines the total sperm output of the testis. Sertoli cells act as 'nurse' cells for the germ cells during their development, secreting

proteins required for spermatogenesis. They are also responsible for the production of fluid, secreted into the tubule lumen which facilitates sperm movement through the seminiferous tubules, via the rete testis, and into the epididymis. The Sertoli cells also phagocytise degenerated germ cells and residual bodies, mainly the residual spermatid cytoplasm that remains after sperm leave the epithelium. In addition, Sertoli cells participate in spermiation, a mechanism by which sperm are detached from the Sertoli cells to be released into the lumen (Jégou, 1992; Ravel and Jaillard, 2011; Russell et al., 1990).

Each seminiferous tubule is surrounded by peritubular myoid cells, which have a contractile function that gently 'squeezes' the tubules, thereby moving the sperm towards the rete testis. These cells are isolated from the basal lamina by a complex extracellular matrix. The interstitial compartment contains groups of specialised cells, including Leydig cells, blood vessels, lymphatics, monocytes, macrophages, dendritic cells, T cells, natural killer cells and, in some species, such as in rodent testes, the mast cells, found in close vicinity to blood vessels or the tunica albuginea (Anton et al., 1998; Kerr, 1991; Rival et al., 2006). The key role of the Leydig cell is production of various androgenic steroid hormones, particularly testosterone. Testosterone is pivotal for the development of reproductive organs in the male embryos, genesis of accessory organs, male fertility as it is essential for the maintenance of spermatogenesis, masculinisation of bone and muscle, and libido (McCarrey, 1993; Russell et al., 1990; Walker, 2011). It also exerts a variety of actions on many organs of the body (Table 1) (Weinbauer et al., 2010).

Males have a high sperm production rate, which requires high oxygen consumption. However, blood vessels are located in the interstitium, and oxygen reaches the lumen of the seminiferous tubules only by diffusion (Lysiak et al., 2000). The tubular compartment essentially operates on the verge of hypoxia because of the rather low PO_2 in the testis, due to the high oxygen extraction rate linked to the metabolic needs of spermatogenesis. The distance for oxygen diffusion is also comparatively long, and the testis has little capacity to elevate total blood flow (Setchell, 1978). Thus, the tubular compartment is dependent on the intertubular tissue for its blood supply and for androgen production.

Table 1. Targets of testosterone action in the male.

Target organ	Action
Brain	Cognitive function, socialisation, dominance and libido.
Larynx	Growth and resulting changes in voice
Muscles	Increase in volume, strength and lean body mass
Liver	Protein synthesis
Kidneys	Stimulation of erythropoietin
Male sexual organs	Testis size, Penile growth and potency; prostate, seminal vesicle and epididymis growth
Bone marrow	Stimulation of erythroid stem cell lineage leading to increased haemoglobin levels in men
Bone	Accelerated linear growth in bones and ultimately closure of epiphyses
Skin	Hair growth, balding and sebum production

The spermatozoa are transported from the seminiferous tubule into the rete testis by the peritubular myoid cell contractions. The rete testis is an anastomotic series of ducts that connect the seminiferous tubule to the efferent ducts of the epididymis. The spermatozoa then pass through the epididymis during which they mature and gain progressive motility and acquire the capacity for fertilisation during this transit. The testis is loosely connected to the epididymis along its posterior border.

The epididymis is structurally divided into three parts: the caput, corpus and cauda; it later becomes the vas deferens. The caput epididymis is flat in comparison with the globular cauda, with the corpus representing the narrow segment that connects the corpus and cauda (de Kretser et al., 1982). Histologically, connective tissue septa divide the epididymis into further segments (Turner et al., 2003), with the number differing between species. For instance, there are 19 segments in the rat, 10 segments in the mouse, and 7 in the human epididymis (Cornwall, 2009; Johnston et al., 2007).

The connective tissue septa provide structural support to the organ and may provide functional separation of different regions, as many genes and proteins are selectively expressed in different segments (Arrotéia et al., 2012; Turner et al., 2003). These connective tissue septa are capable of restricting the movement of agents with molecular weights of growth factors. Therefore, the epididymal segments can function as unique physiological compartments (Cornwall and von Horsten, 2007; Turner et al., 2003). These segments are viewed as important regulatory subunits which control the luminal fluid environment (Johnston et al., 2005). In addition, the epididymis has less prominent connective tissue strands that do not form complete septa and, hence, are called 'semi-septa'. These strands provide additional structural support to the organ (Turner et al., 2003).

In the seminiferous tubule of adult mammals, spermatogenesis takes place in a three phases: (1) mitosis in the basal compartment, (2) meiosis, and (3) spermiogenesis in the adhuminal compartment. The latter is a complex metamorphic process in which the round spermatid is transformed into an elongated spermatozoon, with the loss of its cytoplasm and without further cell division. The details of this process are described later in this review.

1.2.2. Embryology and development of the testis

The *primordial germ cell* (PGC) is the first cellular origin of the germ cell lineage in spermatogenesis as well as oogenesis. It is derived from the epiblast cells (Ginsburg et al., 1990), which originate from the embryonal ectoderm cells (Lawson and Pederson, 1992). The migration journey of the PGC starts from its origin through the primitive streak and then locates for a while in the wall of the yolk sac, adjacent to the base of the allantois. Afterwards, it passes along the dorsal mesentery of the hindgut to finally penetrate the genital ridges present at about embryonic day 13, 11 and 21 in rat, mouse and human embryo, respectively (Culty, 2009). Although the time points of the migration stages of the PGC differ between rodents and humans, they follow the same developmental pathway. The PGC becomes a gonocyte during migration and after migrating to the gonadal ridge. The gonocyte undergoes a series of mitotic divisions till 17.5 day post-coitum in the rat (Culty, 2009; Peters, 1970) and the division then is arrested in the G1 phase of the cell cycle

until after birth, when these cells give rise to spermatogonia. Various terms used to denote gonocytes, such as prospermatogonia (Byskov, 1986; Hilscher et al., 1974).

The genital ridge consists of the coelomic epithelium and underlying mesonephric mesenchyme, which is penetrated by epithelial cells prior to and during the approach of the PGC, to form irregular cords known as *primitive sex cords*. Under the influence of genetic products of the Y chromosome, more specifically SRY and SOX9, the primitive sex cords proceed with growth and penetration further into the mesenchyme to form the testis (Figure 3). At the hilum of the genital ridge, the cords form a network of minute cellular threads that subsequently produce the tubules of the rete testis. The tunica albuginea is formed with further development, forming a dense fibrous layer between the testis cords and the surface epithelium. As the testis cords develop, they become horseshoe-shaped and their ends join the tubules of the rete testis (Sadler, 2011). Gonocytes become enclosed within the testis cords with Sertoli precursor cells, which originate from the coelomic epithelial cells and are surrounded by the basal lamina and peritubular cells (Clermont and Perey, 1957; Sapsford, 1962). On the other hand, the mesonephric mesenchyme of the genital ridge gives rise to the interstitial cells of Leydig that are found between the testis cords. The testis cords persist until puberty, when they canalise to form the seminiferous tubules. Testicular macrophages were originally believed to originate mainly from blood monocytes derived from hematopoietic stem cells in the bone marrow (van Furth and Cohn, 1968), but this view has altered with the employment of recently-developed genomic techniques that demonstrated that macrophages of different tissues can also be derived from embryonic progenitors (Gomez Perdiguero et al., 2015; Hagemeyer et al., 2016; Mass et al., 2016; Yona et al., 2013). Recently, two macrophage populations have been identified in the adult testis, based on their specific localisation and morphology: interstitial and peritubular (DeFalco et al., 2015). Interstitial macrophages originate from yolk sac-derived progenitors, whereas bone marrow–derived progenitors give rise to peritubular macrophages, which appear postnatally in the prepubertal period (Mossadegh-Keller et al., 2017).

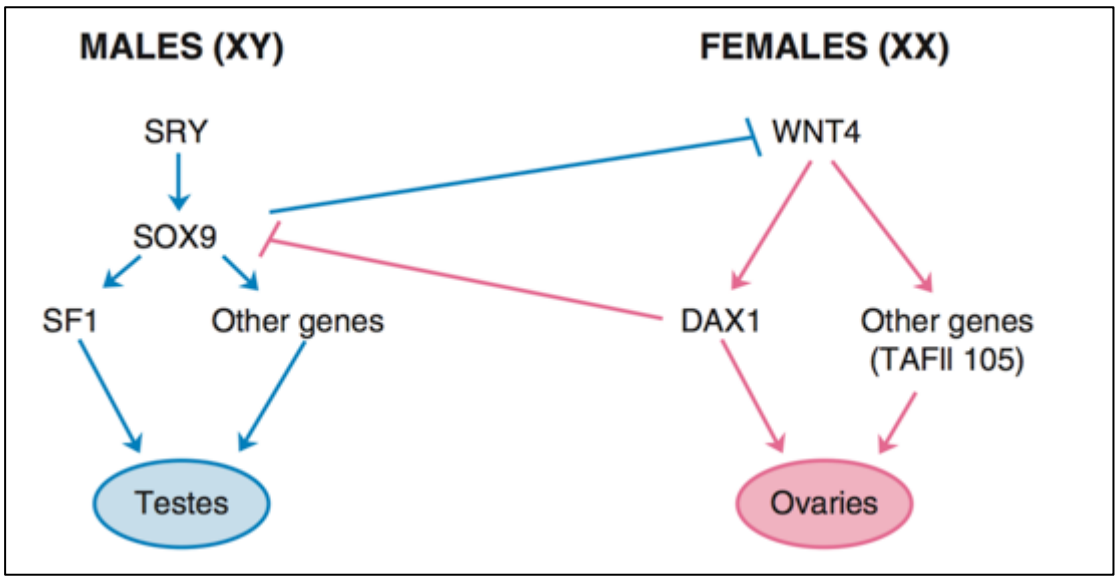

Figure 3. Schematic showing genes responsible for differentiation of the testes and ovaries. In both males and females. *SOX9* and *WNT4* are expressed in the gonadal ridges. In males, the expression of *SRY* upregulates *SOX9*, which in turn activates expression of *SF1* and other genes responsible for testes differentiation, while inhibiting expression of *WNT4*. In females, the uninhibited expression of *WNT4* upregulates *DAX1* that in turn inhibits *SOX9* expression. Then, under the continued influence of *WNT4*, other downstream target genes (perhaps *TAFII105*) induce ovarian differentiation [adapted from (Sadler, 2011)].

At the time of birth in rats, quiescent gonocytes appear uniformly round and are situated centrally in the seminiferous cords (Orth, 1993). At 2–5 days post-partum (dpp), the quiescent gonocytes show essential morphological alterations, which result in the presence of two subpopulations: round gonocytes and gonocytes that exhibit the development of pseudopodia, known as pseudopod gonocytes (Orwig et al., 2002). These gonocytes have different developmental roles. First, the pseudopod gonocytes develop cytoplasmic processes that result in their relocation to the basement membrane of the seminiferous cords (McGuinness and Orth, 1992a; McGuinness and Orth, 1992b; Roosen-Runge and Leik, 1968). Subsequently, they differentiate into spermatogonial germ cells; therefore, they can be considered the stem cells for the neonatal rat testis, as proposed by Orwig et al. (2002). The round cells, which lack this capability, consequently remain in the centre of the seminiferous cords and degenerate by apoptosis. The presence of two subpopulations is a feature of rodents (Manku and Culty, 2015; McLean et al., 2003).

In rats, the gonocytes resume their mitotic activity at 3 dpp (McGuinness and Orth, 1992b) after a 10-day period of quiescence (Clermont and Perey, 1957) and these cells relocate to the basement membrane of the seminiferous cords at 4 dpp. The proliferation and relocation of gonocytes are regulated by mechanisms that are independent of each other (McGuinness and Orth, 1992b; Nagano et al., 2000). The majority of gonocytes migrate to their location on the basement membrane by 5 dpp (Culty, 2009), which corresponds to the first appearance of spermatogonial stem cells (SSCs) (Figure 4).

The transition of foetal germ cells from PGCs to gonocytes and subsequently at a later time point to spermatogonia is clearly understood in rodents, given the good organisation in the seminiferous tubule. In humans, the foetal germ cell population is believed to be the same as that in rodents, where heterogeneous gonocyte populations are present during the second trimester (Bartkova et al., 2001; Castrillon et al., 2000; Manku and Culty, 2015; Ruggiu et al., 2000). The first cellular type is gonocyte, which comes into existence after successive stages of PGC proliferation and represents the dominant germ cell population in the first trimester (7–12 gestation weeks) in humans. The second type is prospermatogonium, which arises from the gonocytes in the second trimester (14–22 gestation weeks), and is divided into three types based on the morphology (Hilscher, 1991; Wartenberg, 1989): mitotically active (M) prospermatogonia, transitional (resting, T1) prospermatogonia (which are quiescent from gestation week 17 to 23), and (T2) prospermatogonia that resume mitotic activity from gestation week 25 (Franke et al., 2004). The prospermatogonia have also been classified on the basis of expression of markers, such as germ cell alkaline phosphatase (GCAP) as well as the somatic isoform of the angiotensin-converting enzyme (sACE) (Culty, 2009; Franke et al., 2004; Fukuda et al., 1975; Gaskell et al., 2004; Manku and Culty, 2015; Vergouwen et al., 1991; Wartenberg, 1976). Because of this gradual development, a mixture of gonocytes and prospermatogonia is seen at any given time during foetal growth in humans, unlike in rodents. This transition is recognised by a decrease in the expression of the pluripotent marker octamer-4 (Oct4) and c-kit and elevation in melanoma antigen-A4 (MAGE-4) (Franke et al., 2004; Gaskell et al., 2004). MAGE-4 is a member of the cancer-testis family of

antigens, which is observed in spermatogonia, primary spermatocyte and germ cell tumours (Aubry et al., 2001; De Plaen et al., 1999).

Data on the differentiation of prospermatogonia into type A spermatogonia are very scarce. These spermatogonial cells are termed type A-single (A_s) spermatogonia in rodents and type A-pale (A_p) and A-dark (A_d) spermatogonia in humans, with the latter based on haematoxylin staining of their nuclei (Clermont, 1966b; de Rooij and Russell, 2000; Desai et al., 2013; Dym et al., 2009). In humans, Paniagua and Nistal (1984) have found that the number of prospermatogonia at birth is similar to the number of type A_d and A_p spermatogonia, which may indicate their presence in the testis before birth. Prospermatogonia start declining continuously until they no longer exist by the age of six years. On the other hand, during the same period, the proportion of spermatogonia type A_d is increased 2-fold and of type A_p by 3-fold, approaching 4-fold more at puberty than at birth. Although the proportion of type A_d spermatogonia shows a slight diminution at age 4–5 years, type B spermatogonia start appearing and reach the peak quantity by puberty.

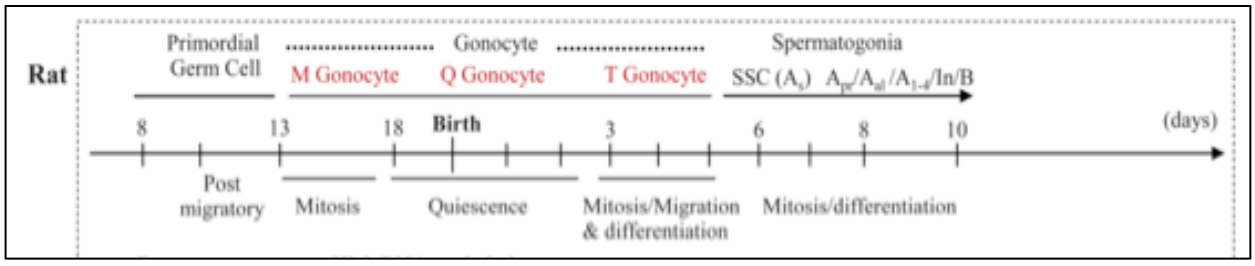

Figure 4. Schematic representation of the time-lines of gonocyte development in the rat, as summarised from the available literature (Culty, 2009).

1.2.2.1. Descent of the testis

In most mammals, the testes develop as abdominal organs, which, together with the mesonephros are connected to the posterior abdominal wall by the urogenital mesentery (Sadler, 2011). This attachment remains until the seventh month of gestation in humans, and then the testes descend through the inguinal canals into the scrotum. The testicular movement from the abdomen into the scrotum takes place in two phases. The first phase involves descent of the testes in the

abdomen to reach the entrance of the inguinal canal, a process is controlled by the anti-Müllerian hormone (AMH). In the second phase, the testes descend via the inguinal canal into the scrotum; this process occurs under androgen regulation. In rodents, data indicate that androgens stimulate the genitofemoral nerve to secrete calcitonin gene-related peptide (CGRP), which generates rhythmic contractions of the gubernaculum (Shenker et al., 2006). This is a ligament, which connects the testis to the scrotum and helps guide its descent into the scrotum, but a similar mechanism has not been demonstrated in humans because the tissue is unavailable for ethical reasons. Maldevelopment of the gubernaculum or deficiency or insensitivity to either AMH or testosterone therefore can prevent the testes from descending into the scrotum (Bartlett et al., 2002; Hutson et al., 1994). In many infants with inguinal testes, further descent of the testes into the scrotum occurs in the first six months of life. This is attributed to the postnatal surge of gonadotrophins and testosterone that normally occurs between the first and fourth months of life (Sadler, 2011).

1.2.3. Functions of the testis

1.2.3.1. Spermatogenesis

1.2.3.1.1. Overview

Spermatogenesis is a highly specialised process of germ cell development, involving proliferation of spermatogonia by mitosis, which gives rise to spermatocytes that progress through meiotic division to produce haploid round male germ cells, the spermatids. This process takes place under endocrine regulation through the secretion of gonadotrophins by the pituitary gland (Carreau and Hess, 2010; Kerr et al., 2006; O'Donnell et al., 2006).

The process starts with type A spermatogonia, which either undergo self-renewal or differentiation into type B spermatogonia. Type B spermatogonia lose all contact with the basement membrane and develop into primary spermatocytes, namely preleptotene spermatocytes, which cross the BTB and enter the adluminal compartment of the seminiferous epithelium. The primary spermatocytes give rise to the short-lived secondary spermatocytes in turn forming the round spermatids. The round spermatids undergo spermiogenesis, which involves several morphological steps, such as acrosome formation, nuclear changes, tail formation and maturation. Subsequently,

spermatozoa are developed and released from the Sertoli cells by a process called spermiation (Cooke and Saunders, 2002). Spermiogenesis comprises 16, 19 and 12 steps in the mouse, rat and human, respectively. The duration of spermatogenesis varies between species, taking 49 and 75 days in rats and humans, respectively, and continues throughout life, ensuring continuous sperm production in males (Clermont, 1963). The next sections discuss spermatogenesis in more detail.

1.2.3.1.2. Mitosis

SSCs are the early precursors of a male germ cell population that divides by mitosis to renew the stem cell population and differentiate into spermatogonia that are committed to entering the spermatogenesis transition to form sperm. These cells are also termed type A-single (A_s) spermatogonia in rodents and type A-pale (A_p) and A-dark (A_d) spermatogonia in humans, with the latter term based on haematoxylin staining of their nuclei (Clermont, 1966b; de Rooij and Russell, 2000; Desai et al., 2013; Dym et al., 2009). Rodents undergo about 9–11 spermatogonial divisions, starting from A_s through A-pair (A_{pr}), A-aligned (A_{al}), A_1, A_2, A_3, A_4, Intermediate (In), and B spermatogonia. The latter spermatogonia give rise to diploid primary spermatocytes, which undergo the first meiotic division (meiosis I) to produce the secondary spermatocyte. These cells then go through the second meiotic division (meiosis II) to give rise to haploid round spermatids. After that, no more cellular divisions occur, as the round spermatids progress through a complete series of changes called spermiogenesis resulting in the formation of spermatozoa.

SSCs (A_s) divide normally to renew the stem cell population and differentiate into spermatogonia (A_{pr}), which are connected by intercellular cytoplasmic bridges (ICBs) that share genetic material between cells to synchronise development (de Rooij and Grootegoed, 1998). These bridges result from incomplete cytokinesis, which characterise developing male germ cells and also play a crucial role in spermatogenesis and fertility. This has been demonstrated by several observations: in the absence of incomplete cytokinesis, spermatogenesis fails through the apoptotic response of multinucleated cells that form instead of ICBs, thereby reducing the transition from spermatogonia to spermatocytes (Di Cunto et al., 2002; Greenbaum et al., 2006). Although

spermatogenesis in rodents starts immediately after birth in a synchronous way, in humans there is a long prepubertal period since puberty occurs between 11.4 and 13.1 years (Crofton et al., 2002).

The proliferation and renewal mechanisms of SSCs in humans are still unclear. Earlier studies on human spermatogenesis showed that both types of A spermatogonia, A_{dark} and A_{pale}, are generally considered as stem cells (Clermont, 1966a, 1966b). The A_{dark} spermatogonia serve as reserve stem cells and divide less frequently, to renew their population as well as give rise to A_{pale} spermatogonia. The A_{dark} spermatogonia can be self-renewed in case of injury or disease, while the A_{pale} spermatogonia are the differentiating stem cells that divide frequently to form B spermatogonia, which further divide to give rise to cells that commence meiosis, primary spermatocytes (Clermont, 1963, 1966a, 1966b, 1972). Like non-human primates, humans have fewer mitotic steps prior to the beginning of meiosis to form spermatocytes. The efficiency of clonal expansion in humans is extremely low as compared with that in rodents. Nevertheless, recent observations in primates have revealed that A_{pale} spermatogonia are designed as progenitor cells to begin spermatogenesis. Thereafter, A_{pale} spermatogonia generate greater numbers of differentiated germ cells and reduce the risk for germline mutations and vulnerability to cytotoxic events due to the higher mitotic turnover required from spermatogonia (Ehmcke and Schlatt, 2006). Therefore, the function of A_{dark} spermatogonia is limited to stem cells, which replenish the progenitor compartment in situations where the more mature cells are damaged such as with cytotoxic depletion (Ehmcke and Schlatt, 2006; Waheeb and Hofmann, 2011). Since these studies were conducted on adult testes, further experiments are required to study the origin of B spermatogonia in the prepubertal testis and compare it with that in the adult testis.

1.2.3.1.3. Meiosis

Meiosis in male germ cells starts at puberty in both rodents and humans, even though rodent puberty begins shortly after birth, whereas human puberty does not start for several years. Meiosis begins after the last mitotic division of type B spermatogonia, which give rise to primary spermatocytes. It consists of two divisions: meiosis I and II which, in the ideal case, produce four haploid round spermatids from one diploid primary spermatocyte.

The DNA of primary spermatocytes is replicated in the pre-meiotic S phase of interphase, after which the primary spermatocytes become genetically 2N and 4C (N: chromosome number and C: DNA content). Primary spermatocytes go through a prolonged meiosis I prophase, which is subdivided into five stages: preleptotene, leptotene, zygotene, pachytene and diplotene, characterised by changes in chromosome configuration and structure (Handel and Schimenti, 2010). The leptotene stage is characterised by single unpaired chromosomes that subsequently pair with their homologous partner chromosome. A synaptonemal complex forms between homologous chromosomes and DNA recombination occurs between homologous chromosomes in the pachytene stage subsequent to which they then separate during the diplotene stage. The first meiosis is completed after rapid metaphase, anaphase and telophase by producing two secondary spermatocytes from each primary spermatocyte. The second meiotic division effectively results in the formation of four round spermatids within a shorter period, unlike the long first division (Rey, 2003).

The most unique meiotic-specific scaffold element linked to chromosomal pairing and synapsis is the synaptonemal complex. In rodents, seven synaptonemal complex proteins (SCPs) have been identified as well as expressed in meiosis. The SCP1, 2, and 3 proteins are pivotal for the initiation of synapsis, as central elements of the SC fail to form in their absence, causing arrest at zygotene I. In addition, the lack of SCP2 and 3 would result in serious synapse abnormalities and spermatocyte apoptosis through checkpoint-activation, which consequently influences testicular growth and fertility (Fraune et al., 2012; Yang and Wang, 2009; Yuan et al., 2000).

1.2.3.1.4. Spermiogenesis

Spermiogenesis is the final stage of spermatogenesis. During this stage, the round spermatids mature into elongated, mature, and highly-specialised motile spermatozoa**.** This process involves five fundamental metamorphic changes: chromatin remodelling, nuclear shaping, formation of the acrosome, development and specialisation of the tail, loss of cytoplasm and formation of the residual body; it ends with spermiation. Various species have different progressive structural steps of spermiogenesis, even though the major morphological changes are common to all

species. For instance, while rats and mice undergo 19 and 16 steps, respectively, 6 steps are defined in humans (Russell et al., 1990). The release of the first spermatozoa, known as spermarche, is seen at age 55 dpp in rats (Sengupta, 2015) and at 11.7–15.3 years in humans (Nielsen et al., 1986).

During spermiogenesis, chromatin remodelling occurs with alteration in the nuclear shape, conversion of negatively supercoiled nucleosomal DNA into a nonsupercoiled state (Ward et al., 1989), transient DNA breaks (McPherson and Longo, 1993) and chromatin condensation. These changes occur through the progressive 'exchange' of the sperm`s basic nuclear proteins termed as histones to transition proteins, and subsequently their replacement by protamine proteins (Dadoune, 1995; Kierszenbaum, 2001; Lee and Cho, 1999; Lewis et al., 2003a; Lewis et al., 2003b). Consequently, a broad cessation of RNA transcription occurs in the genome (Kierszenbaum and Tres, 1975). About 85% of the histones are replaced by protamines (Aoki and Carrell, 2003; Dadoune, 1995; Steger, 1999). Accordingly, this would facilitate molecular remodelling of the genome within the developing spermatid (Sassone-Corsi, 2002).

Two protamines, protamine 1 and 2, are expressed in rodents and humans in almost equal amounts. Normally, the average P1/P2 ratio is nearly 1.0 (Carrell et al., 2007; Carrell and Liu, 2001; Oliva, 2006). Cases of infertility show an imbalanced ratio and/or no detectable P2 in mature sperm, resulting in defects in the sperm count, morphology, DNA fragmentation, fertilisation ability and embryo implantation. While protamine abnormalities in the sperm of fertile men are very rare (Aoki et al., 2005; Jodar and Oliva, 2014), changes in the timing or ratio of protamine expression are common in infertile males. These alterations have been associated with aberrant spermatogenesis, which may be caused by inappropriate transcription or translational processing (Carrell et al., 2007; Carrell and Liu, 2001). Furthermore, protamines work as checkpoint regulators of spermatogenesis and defective protamine expression may result in stimulation of an apoptotic process and extremely low sperm quality (Carrell et al., 2007; Jodar and Oliva, 2014).

Spermatozoa acquire their motility from the flagellum that develops from the distal centriole from which the axoneme originates. The axoneme is made up of nine pairs of doublet microtubules

in a circular arrangement, with two single microtubules in the centre (9+2 arrangement) and it projects spermatid plasma membrane from the cell. The capacity for progressive sperm motility is conferred to sperm during their passage through the epididymis (Kerr et al., 2006; Russell et al., 1990; Sharma and Agarwal, 2011).

A characteristic feature of spermatogenesis is that the developing germ cells form associations of cells defined as stages of the seminiferous epithelial cycle. The cycle of spermatogenesis is divided into 14 stages (I to XIV) in rats (Figure 5), with spermiogenesis broken down further into 19 differentiation steps (from 1 to 19). The process of spermatogenesis provides a striking and unique example of cell differentiation, involving acrosome formation, nuclear condensation, and flagellar biogenesis. Another intriguing feature of spermatogenesis is the distinct ordering of cell associations along the length of the seminiferous tubules (segments), often referred to as the ‘wave of the seminiferous epithelium’ (Perey et al., 1961). A wave encompasses all 14 segments in the rat, 12 in the mouse, and 6 in the human, consisting of various cell associations (de Kretser and Kerr, 1988). A segment is defined as a longitudinal portion of the seminiferous tubule corresponding to a single cell association or stage (Hess and de Franca, 2009; Parvinen, 1982).

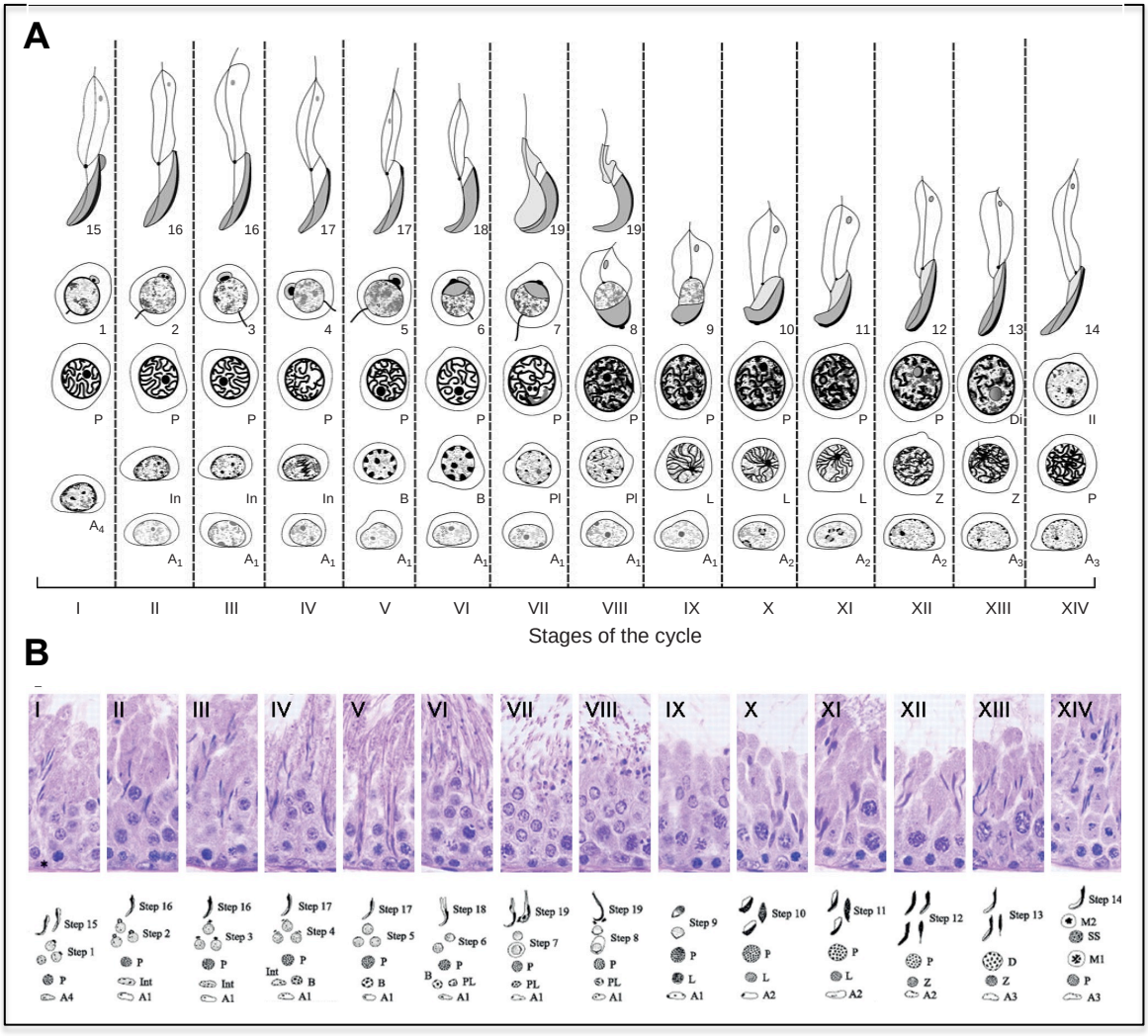

Figure 5. Diagram of the spermatogenic cycle of the rat spermatogenesis. A) The 14 stages of the rat spermatogenic cycle, denoted by I–XIV, are shown in the vertical columns and germ cell development is shown horizontally. B) Histological sections and schematic representations of the 14 stages (numbered from I to XIV) indicate all possible associations of germ cells that can be observed in tubules from a testis tissue section. This classification is essentially based on the morphogenesis of the acrosome of spermatids from the less differentiated step 1 to the highly differentiated step 19. The various types of spermatogonia (A1, A2, A3, A4, intermediate (*Int*), and B) and of spermatocytes (preleptotene (*PL*), leptotene (*L*), zygotene (*Z*), pachytene (*P*), diplotene (*D*), M1, and M2) are also represented [adapted from (O'Donnell et al., 2006; Lagarrigue et al., 2011].

1.2.3.2. Hormone secretion

The somatic Sertoli and Leydig cells of the testis are responsible for hormone secretion. While Leydig cells have the capacity for steroid biosynthesis, Sertoli cells can produce cholesterol but not androgens (Shi et al., 2018). The Sertoli cells produce growth factors and hormones, such as the activins and inhibins.

1.2.3.2.1. Steroidogenesis

Steroids are lipid-soluble hormones that simply can diffuse through the lipid bilayer cell membrane into the cytoplasm of target cells. Conversely, the actions of non-steroidal hormones, the hydrophilic peptide hormones, require membrane-bound receptors and intracellular second messenger systems to apply their effects. In the cytoplasm, steroids may undergo enzyme-mediated alteration, such as reduction, hydroxylation, or aromatisation, which changes the hormone to a more potent form. Steroids bind to specific intracellular receptors and upon binding, many kinds of steroid receptors dimerise, where two receptor subunits join together to form one functional DNA-binding unit that can enter the cell nucleus. In the nucleus, the steroid-receptor ligand complex binds to specific DNA sequences and induces transcription of its target genes (Frye, 2009).

In the testis, the production of androgens represents almost the entire synthesis of steroids in the interstitial compartment (Christensen and Mason, 1965; Eik-Nes and Hall, 1966) (For review see Landreh, 2014). In particular, interstitial Leydig cells make androgens, which are controlled by the pulsatile release of the pituitary gonadotrophin, luteinising hormone (LH). LH acts via the LH receptor (LHR) that is present on the surface of the Leydig cells (Ascoli et al., 2002; Dufau et al., 1983; Payne, 2007; Troppmann et al., 2013). Testosterone is the principal androgen synthesised in the testis. Testosterone may be converted to amplify or alter its biological actions, which is obtained by reduction to its 5α-reduced metabolite, dihydrotestosterone (DHT), or aromatisation to oestrogen. Testosterone plays a critical role in sex development, sexual function and reproduction. Early in foetal life, the neutral anlage is determined by 46,XY chromosomes to become a testis. From then on, testosterone production, together with Anti-Müllerian hormone and sex

differentiating factors, will lead to normal male sex differentiation (Jost et al., 1973). In this process, testosterone — and, more so, dihydrotestosterone (DHT) — are particularly crucial for the normal formation of male external genitalia.

While steroidogenesis virtually takes place in the interstitium of the testis, the intratubular Sertoli cells can synthesise cholesterol and a small quantity of pregnenolone; however, the physiological relevance of this production has not been identified (Ford et al., 1999; King and LaVoie, 2009). Testosterone is the major circulating androgen in the male and is synthesised by a sequence of enzymatic reactions (Figure 6) that convert the substrate for all steroid biosynthesis: cholesterol, the first steroid produced, pregnenolone, and then through a number of steroid intermediates to testosterone (Brady, 1951; Sharma et al., 1967; Steinberger and Ficher, 1968) (for more details see Stocco and McPhaul, 2006).

As mentioned above, testosterone produced by Leydig cells can be released into the circulatory system or it can be metabolised further to its 5α-reduced and highly active metabolite, DHT, or be aromatised to 17β-oestradiol (Payne, 2007). Sertoli cells also contain significant levels of aromatase and reductase activities that can convert testosterone into oestrogens or DHT, respectively (Canick et al., 1979; Dorrington and Armstrong, 1975; Nyman et al., 1959; Ritzen et al., 1981).

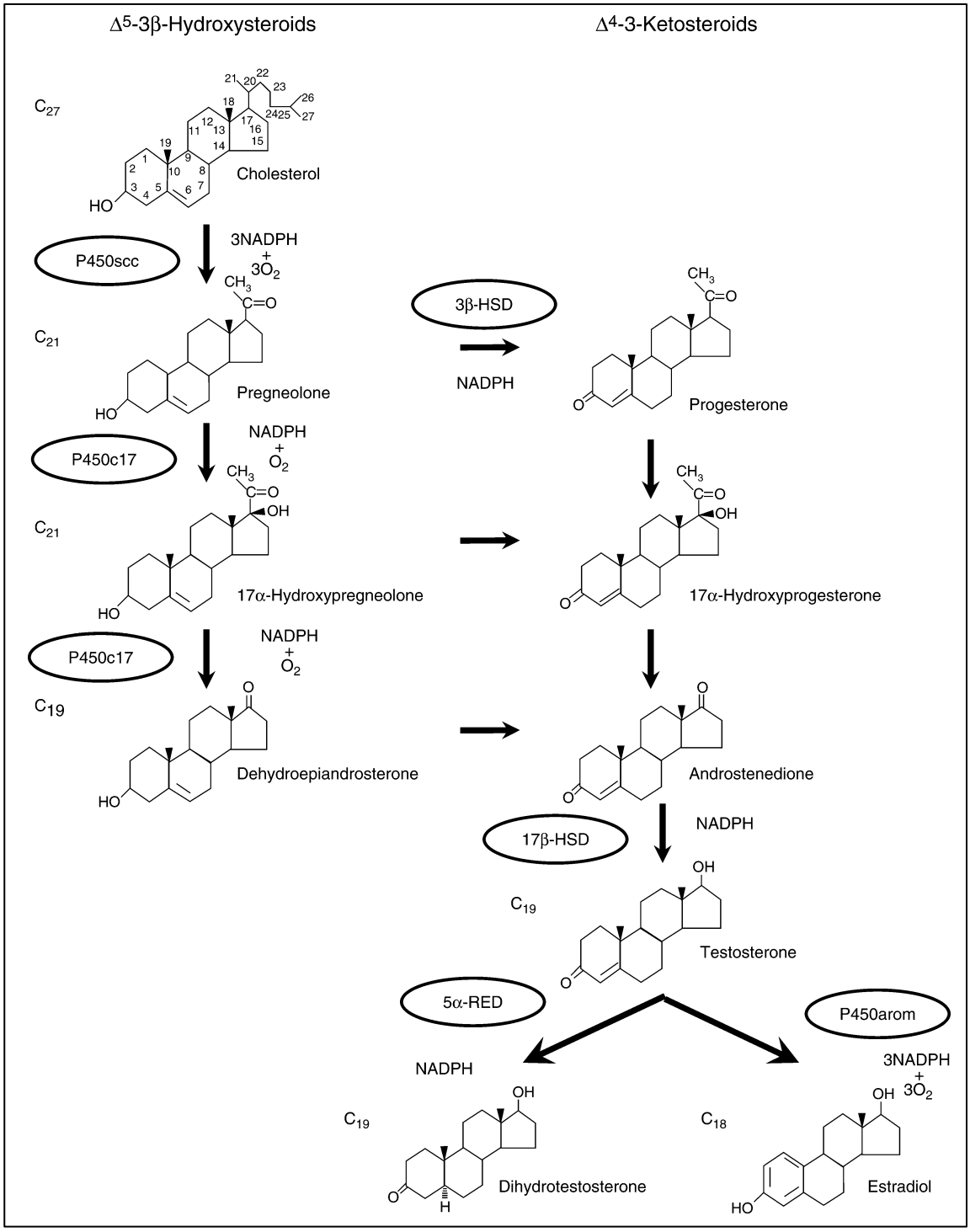

Figure 6. Steroid biosynthetic pathways in Leydig cells**.** The cytochrome P450 haeme-containing proteins CYP11A1 (P450scc), CYP17A1 (P450c17), P450arom, the hydroxysteroid dehydrogenases 3β-hydroxysteroid dehydrogenase (3β-HSD), 17β-hydroxysteroid dehydrogenase (17β-HSD), and 5α-reductase (5α-RED) [adapted from (Payne, 2007)].

Testosterone acts on the target cells via intracellular androgen receptors (ARs), which are present in Leydig cells, Sertoli cells and peritubular myoid cells. The AR is a prototypic member of the nuclear receptor family (Zoppi et al., 2002); in humans, it contains 48 different members (Evans and Mangelsdorf, 2014), including members that are regulated in response to ligands, such as the steroid receptors. *Orphan* receptors, with a similar structure, are other members of this family for which ligands have not yet been identified. The AR has a central DNA-binding domain (DBD), which is highly preserved in comparison with other nuclear receptor family members. This domain mediates the binding of target DNA sequences in the genome. Particular portions of the DBD play a role in the dimerisation of this domain and the identification of its recognition of specific DNA sequences. This mechanism, called the slow genomic effect, has focused on the direct control of responsive genes by nuclear receptor family members, which usually takes hours to become obvious. On the other hand, other responses have been identified that occur within seconds to minutes of hormone addition. These effects, which have been called 'nongenomic', are thought to be mediated by nuclear receptor family members by different mechanisms that include direct participation in cellular signalling cascades (Rousseau, 2013). Among the best characterised of these are regulation of genes such as nitric oxide synthase by oestrogen (Banerjee et al., 2014; Chen et al., 1999; Mendelsohn, 2002; Salerni et al., 2015) and regulation of MAP kinase by oestrogen and progesterone (Boonyaratanakornkit et al., 2001; Castoria et al., 1999; Coleman and Smith, 2001; Thomas, 2012).

Several studies have demonstrated the importance of AR by using AR knockout mouse models in various cellular locations. Total AR knockout mice have shown infertility with smaller testicular size, cryptorchidism, low Sertoli cell numbers, arrested spermatogenesis at the pachytene stage, large size Leydig cells, and the absence of the epididymis (Chang et al., 2013; Tan et al., 2005; Yeh et al., 2002). The AR in Sertoli cells is important for meiotic entry, which is an obvious cytological indication of the beginning of maturation of male gonad at puberty. This has been observed when the AR in Sertoli cells is targeted resulting in infertility due to pre-meiotic

spermatogenic arrest, smaller testes and normal well-developed Sertoli cells (Chang et al., 2013; Tsai et al., 2006; Wang et al., 2009). The absence of the AR in Leydig cells in mice arrests spermatogenesis at the round spermatid stage, leading to infertility, and comprises the steroidogenic pathway. However, these mice are still fertile when the ARs are lacking in the peritubular myoid cells. These cells require the ARs to keep the contractility of peritubular myoid cells and normal Sertoli cell function.

1.3. Control of testicular function

1.3.1. Endocrine regulation: the Hypothalamic-Pituitary-Testicular (HPT) Axis

The control of spermatogenesis and other reproductive functions in the male is determined by the neuroendocrine activity of the hypothalamic-pituitary-testicular (HPT) axis (Figure 7) and other auto/paracrine regulators, such as activin and follistatin (Cooke and Saunders, 2002). The HPT axis involves several hormones secreted by 1) the hypothalamus (gonadotrophin-releasing hormone, GnRH), 2) the anterior pituitary gland (follicle stimulating hormone, FSH and Luteinising hormone, LH), and 3) the testis (inhibins and testosterone)(Ramaswamy and Weinbauer, 2014).

GnRH is a decapeptide hormone produced in a characteristic pulsatile manner. It is an essential hypothalamic signal to the pituitary gonadotrophs, where it acts through the transmembrane GnRH receptor (Clayton et al., 1979; Marian and Conn, 1983) (for review see Gregory and Kaiser, 2004). In response to GnRH, the gonadotrophs in the anterior pituitary gland secrete two major heterodimeric glycoprotein hormones, called gonadotrophins: FSH and LH, which are vital regulators for the testis (Beitins et al., 1977). Although both gonadotrophins are released in a pulsatile fashion, LH secretion is a robust pulse like that of GnRH, while the pulse of FSH secretion is rather sluggish as it has longer half-life (Dierschke et al., 1970; Gay and Sheth, 1972; Chappel et al., 1984) (for details see Ramaswamy and Weinbauer, 2014).

The two gonadotrophins act via specific transmembrane receptors present in the somatic cells in the testis. Sertoli cells and spermatogonia express FSH receptors (FSHR) within the seminiferous tubules, whereas LH-R is expressed in the interstitial Leydig cells. These hormones act differently on spermatogenesis as FSH has a direct effect primarily via the control of the Sertoli cell, while LH works indirectly through the AR.

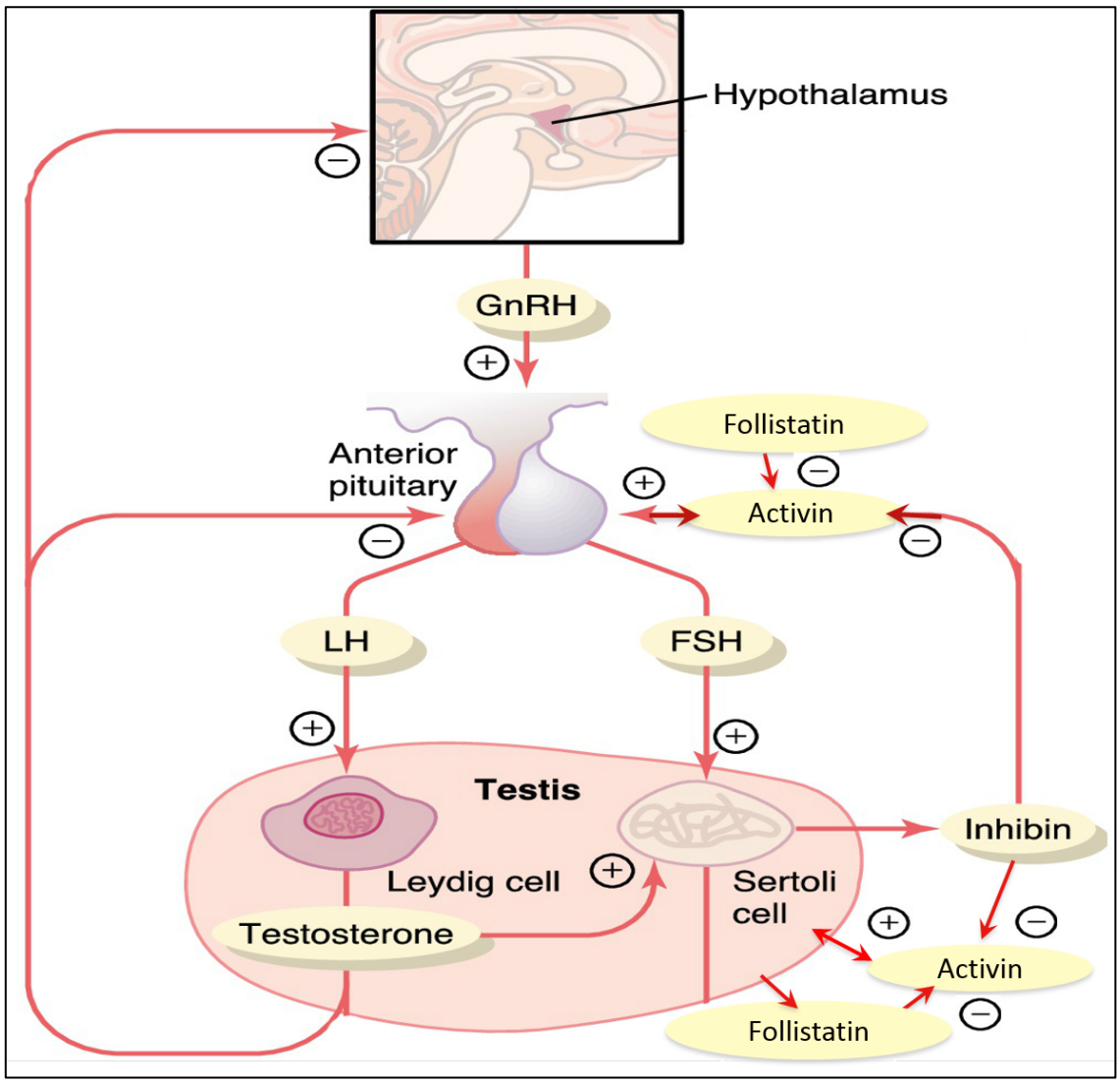

Figure 7. GnRH stimulates the release of FSH and LH from the gonadotrophs in the anterior pituitary gland. Activin and follistatin are produced by the gonad, pituitary gland, and hypothalamus. Activin synthesised in the pituitary gland mediates the paracrine control of FSH and GnRHR release and its actions are regulated by 1) follistatin which is locally synthesised by the folliculo-stellate cells and 2) inhibin produced in the testes. Inhibin acts in a classical endocrine manner to negatively control activin stimulation of FSH secretion. In the testis, activin works in synergy with FSH to trigger Sertoli cell proliferation and germ cell differentiation, where it is also modulated there by paracrine actions of follistatin and inhibin. LH targets Leydig cells in the testis to produce steroids, mainly testosterone (T), which can be aromatised in Sertoli cells to oestradiol (E2). T binds to the androgen-binding protein synthesised by Sertoli cells and works on androgen receptors in Sertoli, Leydig and peritubular cells. T stimulates spermatogenesis, Sertoli cell proliferation and Leydig cell development. T and E2 have a negative feedback effect at the level of the hypothalamus (via controlling GnRH secretion) and the pituitary gland, to limit LH and FSH secretion (the steroid negative feedback effect on FSH varies between species [Figure modified from (Hall and Guyton, 2011)].

Two separate signals are produced by the testis as a result of gonadotrophin stimulation: 1) the steroid hormone, testosterone, is secreted by the Leydig cells in a pulsatile manner due to LH signalling; 2) inhibin, which is a non-steroidal hormone, is produced in a non-pulsatile fashion by the Sertoli cells in response to FSH signalling (Schlatt and Ehmcke, 2014). Some studies have reported that testosterone may have an inhibitory role in inhibin B production (Ramaswamy et al., 2003). Together, these gonadal hormones are the major feedback signals that regulate the physiological operation of the HPT axis.

Activin is a pivotal regulatory factor in the HPT axis and exerts paracrine and/or autocrine action at the levels of hypothalamus, pituitary gland and testis. Activin is a key stimulator of GnRH from the hypothalamus and FSH from anterior pituitary gland, where it also elevates the number of GnRH receptors on the gonadotroph surface and increases the GnRH-mediated transcriptional activation of the receptors, which consequently activates the pituitary gland response to GnRH (Bliss et al., 2010). The bioactivity of activin is controlled by two different factors: the endocrine factor, inhibin, and the para/autocrine, follistatin, which ultimately control FSH secretion (Barakat et al., 2012). At the level of the testis, activin plays a crucial role in the development of germ cells and Sertoli cells, which will be discussed in more detail in the next sections.

In general, the function of gonadotrophins during puberty is mainly to form the adult populations of Sertoli, Leydig and stem germ cells and to support their roles that will result in normal spermatogenesis. Hence, the lack of these hormones during this critical phase will eventually affect the descent and development of the adult testis. Conversely, the effects of hormone deprivation in the adult are significant on the germ cells through impairment of the somatic cell function, namely the Sertoli cells (Ramaswamy and Weinbauer, 2014).

Gene knockout studies involving mice and mutations in humans have revealed the importance of the HPT axis, since any defect in this mechanism will result in infertility and loss of secondary sex features. The consequences can be severe if the damage occurs during embryonic life, which can lead to failure of male development [for more details see these references

(Huhtaniemi, 2003; Matsumoto, 1989; Seminara et al., 1998)]. HPT axis initiates and maintains normal spermatogenesis; therefore, any damage to this process, such as an increase in testicular temperature, would have an effect not just directly at the level of the testis but at many other indirect points along the HPT axis.

1.3.2. Testicular interstitial fluid (TIF)

The communication that occurs between the tubular and interstitial compartments in the testis is also pivotal for spermatogenesis and steroidogenesis (Hales, 2002; Rebourcet et al., 2014a, 2014b; Welsh et al., 2009). Not all cellular communications occur via direct physical contact; most are largely secretory, so the communication depends on the release of soluble factors into the testicular fluids, particularly the TIF. The TIF contains multiple proteins from various cellular origins (Stanton et al., 2016), including transferrin, androgen-binding protein, clusterin and inhibin from Sertoli cells (for review, see (Sharpe, 1992)) and testosterone and insulin-like 3 (Insl3) from Leydig cells (Anand-Ivell et al., 2009), as well as various germ-cell–derived proteins (phosphatidyl-binding protein, androgen-regulated protein 2, VASA homologue, fatty acid-binding protein 9 and lactate dehydrogenase-C4) (Elkin et al., 2010; Turner et al., 1996; Virji and Naz, 1995). Both the volume of the TIF and the individual concentrations of many of these proteins are highly responsive to changes in the endocrine hormones, which drive spermatogenesis (Hedger and Muir, 2000; Maddocks and Sharpe, 1989; Sharpe and Bartlett, 1987; Sharpe and Cooper, 1983), as well as to alterations in the local environment, including changes in germ cell types and number (Bartlett and Sharpe, 1987; Elkin et al., 2010; Sharpe et al., 1991). Collectively, the previous studies on TIF provide substantive preliminary evidence that this fluid contains factors representative of testicular function.

Substantial effort has been expended over the past decades to find biomarkers of spermatogenesis in easily accessible biological fluids, such as plasma and seminal plasma (Batruch et al., 2012; Drabovich et al., 2013; Elkin et al., 2010; Sharpe, 1992; Turner et al., 1996). Nevertheless, diagnosis of infertility still relies on (i) evaluation of sperm quantity and quality in the

ejaculate, (ii) testis volume, and (iii) serum hormone levels (Stahl et al., 2014; Wosnitzer et al., 2014). Unfortunately, these parameters provide only limited insights in azoospermic cases, when no sperm is present in the ejaculate, since they do not reliably relay information about cellular events occurring within the testis itself. For instance, these parameter measurements are incapable of differentiating between cases of primary spermatogenic failure (known as non-obstructive azoospermia, NOA) and those with complete spermatogenesis, but a physical post-testis blockage (obstructive azoospermia, OA). Similarly, current approaches provide little information about the potential for spermatogenic improvement with hormonal treatments (Toulis et al., 2010; Tunc et al., 2006; Zitzmann and Nieschlag, 2000) or about the presence of mature spermatids that can be recovered by testicular sperm extraction for use in assisted reproductive therapy (Ishikawa, 2012; Marconi et al., 2012; McLachlan et al., 2006; Ramasamy et al., 2013). For these applications, a testicular biopsy remains the key definitive test, but this requires specialist surgical skills and carries inherent risks (Ramasamy et al., 2013). The identification of proteins in testicular fluids and/or blood plasma that reflect spermatogenic function could therefore be very useful in exploring the mechanisms underlying infertility.

1.4. Activins, inhibins and follistatins

1.4.1. Biochemical structure

Activins and inhibins are members of the transforming growth factor (TGF)-β superfamily that have multiple effects. They act through membrane receptors and intracellular signalling molecules that are shared with many other TGF-β superfamily members, and their roles are regulated by several antagonists that have soluble and membrane bound signalling properties (Loveland and Hedger, 2015).

Inhibin is structurally one of the activin inhibitors and is composed of heterodimers of one β subunit and the inhibin α subunit, products of the Inhibin βA/B (*Inhba or Inhbb*) gene and α (*Inha*) gene, respectively (Hedger et al., 2011). While inhibins are synthesised mostly in the gonads, activins have numerous cellular sources (Winnall et al., 2013). The βA and βB genes are widely expressed throughout the body. Several studies have demonstrated that activins are secreted by the testis, epididymis (Winnall et al., 2013), neutrophils (Chen et al., 2011), macrophages, monocytes, mast cells, endothelial cells, bone marrow and several other tissues (Hedger et al., 2011).

Activins are dimeric proteins of inhibin β subunits encoded by one of four diverse *Inhb* A, B, C and E genes, and produced in various tissues (Loveland and Hedger, 2015). A number of activins have been identified on the basis of their type of β subunits. The best-studied activins are activin A, which is a homodimer of two βA subunits, activin B made of two βB subunits and, less frequently, activins C and E, with two βC and E subunits, respectively. While the βC subunit acts as a regulator of activin bioactivity by binding to a βA or βB subunit, a role for the βE has not been identified in the testis. Heterodimers of βA and βB have been determined to form activin AB that have different signalling features. The β subunits are synthesised as disulphide-linked dimers (Hedger et al., 2011). Acid proteolysis then cleaves the activin A precursor into a 25kDa protein, which is the main circulating form (Hedger et al., 2011).

Follistatin (FST), when originally isolated, was called FSH-suppressing protein because of its capacity to decrease FSH. It acts as an endogenous inhibitor of activin that binds to activins and

targets the complex to a lysosome degradation pathway and results in a decrease in activin bioactivity (Hashimoto et al., 1997; Hedger et al., 2011). Follistatin`s binding affinity to activin is considered extremely high (quite similar to the affinity of activin receptor), which is virtually an irreversible reaction to neutralise activin biological actions (Hashimoto et al., 1997; Phillips and de Kretser, 1998). The activin follistatin complex is formed from one activin dimer and two follistatin molecules, which means each activin subunit binds to one follistatin molecule. Thus, activins A, B and AB bind to follistatin with similar affinity (Nakamura et al., 1992; Phillips and de Kretser, 1998).

Like activin, follistatin is produced by various cell types in the body. In contrast to inhibin, follistatin exists as a monomeric polypeptide and is not a member of the TGF-β superfamily (Hedger and de Kretser, 2013). It is initially generated as 2 preproteins composed of 317 and 344 amino acids, following the alternative splicing of the follistatin gene (Patel, 1998) (Figure 8). Subsequent to cleavage of the signal peptide, two mature polypeptides are produced, known as FST315 and FST288, based on the length of their polypeptide chains (Patel, 1998; Phillips and de Kretser, 1998). Both forms of FST possess a heparin-binding site; however, the presence of a C-terminal extension in FST315 blocks this binding site. Consequently, FST315 circulates more freely, while FST288 is likely to be bound to cell surfaces through heparin sulphate proteoglycans (Hedger and de Kretser, 2013). Follistatin is expressed at very high levels in the vas deferens and skin (Winnall et al., 2013). The cell types that produce follistatin are often the ones that produce activin, or the cells adjacent to those producing activins (de Kretser et al., 2002).

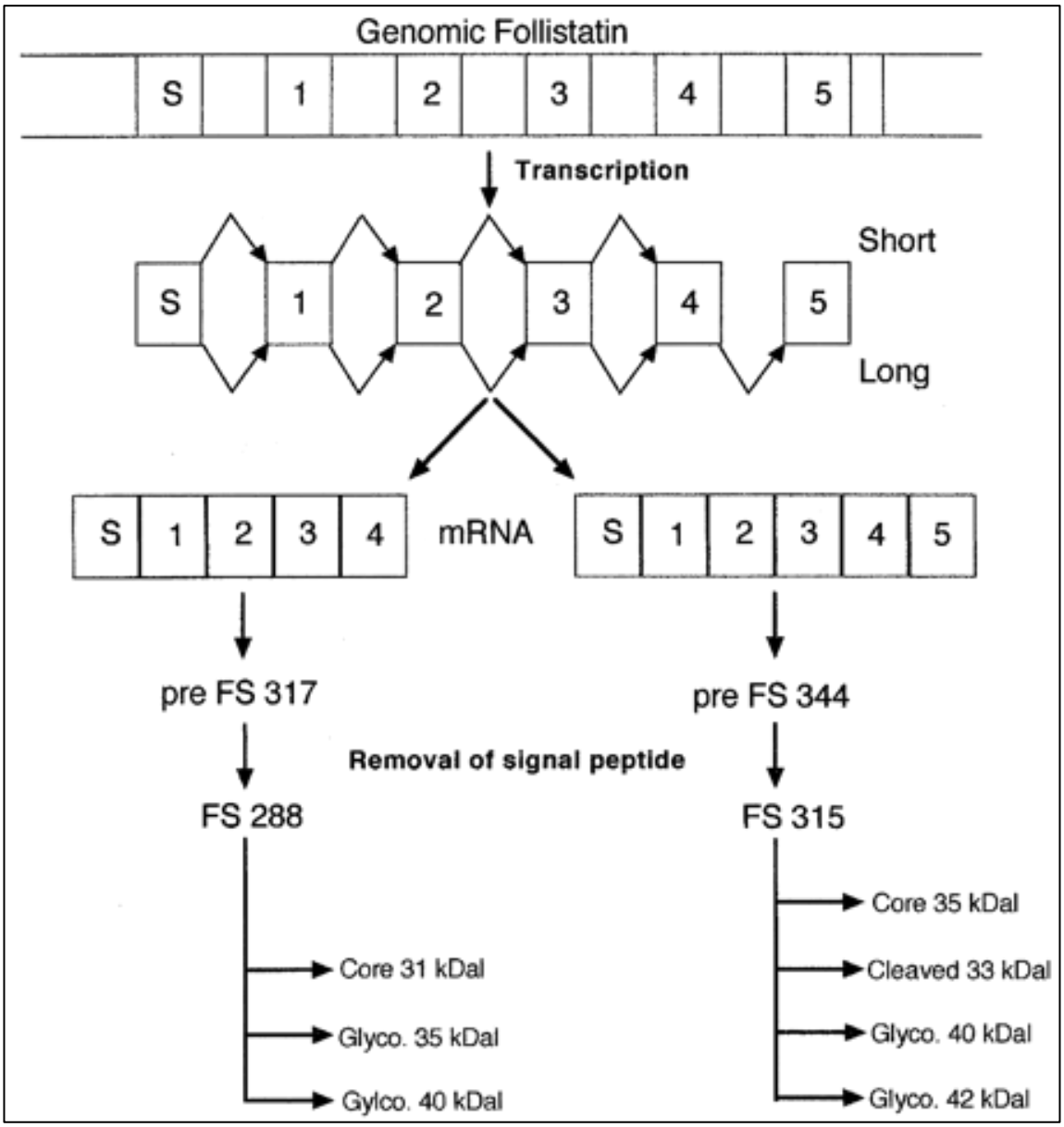

Figure 8. Nucleic and protein processing of follistatin. The follistatin gene encodes a signal peptide sequence (S) and 5 exon. The follistatin gene undergoes alternative splicing to produce short (missing exon 5) or long (exon 5 present) mRNAs. These are translated into pre-proteins that still have signal peptide at the 5^0 end (preFS) which is then removed (numbers refer to amino acid residue composition). The core protein can undergo cleavage or glycosylation (Glyco) [From (Patel, 1998)].

1.4.2. Activin signalling pathways

Activins act via TGF-β superfamily receptors with intracellular serine-threonine kinase activity (Figure 9) (Loveland and Hedger, 2015). Activin binds to specific type II activin receptors (ACVR2A or ACVR2B) that are present on the target cell surfaces (Hedger and de Kretser, 2013). The type II receptor then recruits and activates type I receptor with a serine-threonine kinase domain resulting in the formation of heterotetrameric receptor complexes. These complexes, in turn, phosphorylate intracellular signalling factors, termed receptor Smads (R-Smads), Smad2 or Smad3. These factors form a heteromeric complex transcription factor with a common factor, Smad4 (Loveland and Hedger, 2015). This complex enters the nucleus, where it selectively activates target genes in association with cell-specific factors, which results in various effects, in particular cellular proliferation, differentiation and apoptosis (Hedger et al., 2011). The activin type I receptor is also known as activin receptor-like kinase (ALK) (Hedger et al., 2011). Activin A acts through ALK 4, whereas activin B can act via both ALK 4 and ALK 7 (Tsuchida et al., 2004).

In addition to its role in the Smad signalling pathway, activin functions through the MAP kinase pathway, which is an inflammation-induced signalling pathway (Hedger and de Kretser, 2013). MAP kinases are essential gene regulators involved in inflammation and immunity and include ERK 1/2, JNK and p38. MAP Kinase signalling is triggered by inflammatory mediators, namely, interleukin-1 (IL-1) and Toll-like receptor (TLR) ligands, via the MyD88/TRAF pathway (Hedger et al., 2011).

Follistatin`s binding affinity to activin is considered extremely high (quite similar to the affinity of activin receptor) and it is a virtually irreversible reaction that neutralises activin`s biological actions (Hashimoto et al., 1997; Phillips and de Kretser, 1998). The activin follistatin complex is formed from one activin dimer and two follistatin molecules, which means each activin subunit binds to one follistatin molecule. Thus, activins A, B, and AB bind to follistatin with similar affinity (Nakamura et al., 1992; Phillips and de Kretser, 1998).

Both FST288 and FST215 bind to activin at the cellular level to form the complex, which is

removed via a lysosomal degradation pathway. In particular, activin binds to both FSTs, and finally this complex undergoes rapid endocytosis (Hashimoto et al. 1997). However, binding of activin to FST315 generates a conformational change in the protein, which in turn exposes its heparin binding site, resulting in endocytosis of the complex (Hashimoto et al., 1997; Hedger and de Kretser, 2013). Consequently, the binding of activin to follistatin is an irreversible process (Phillips and de Kretser, 1998).

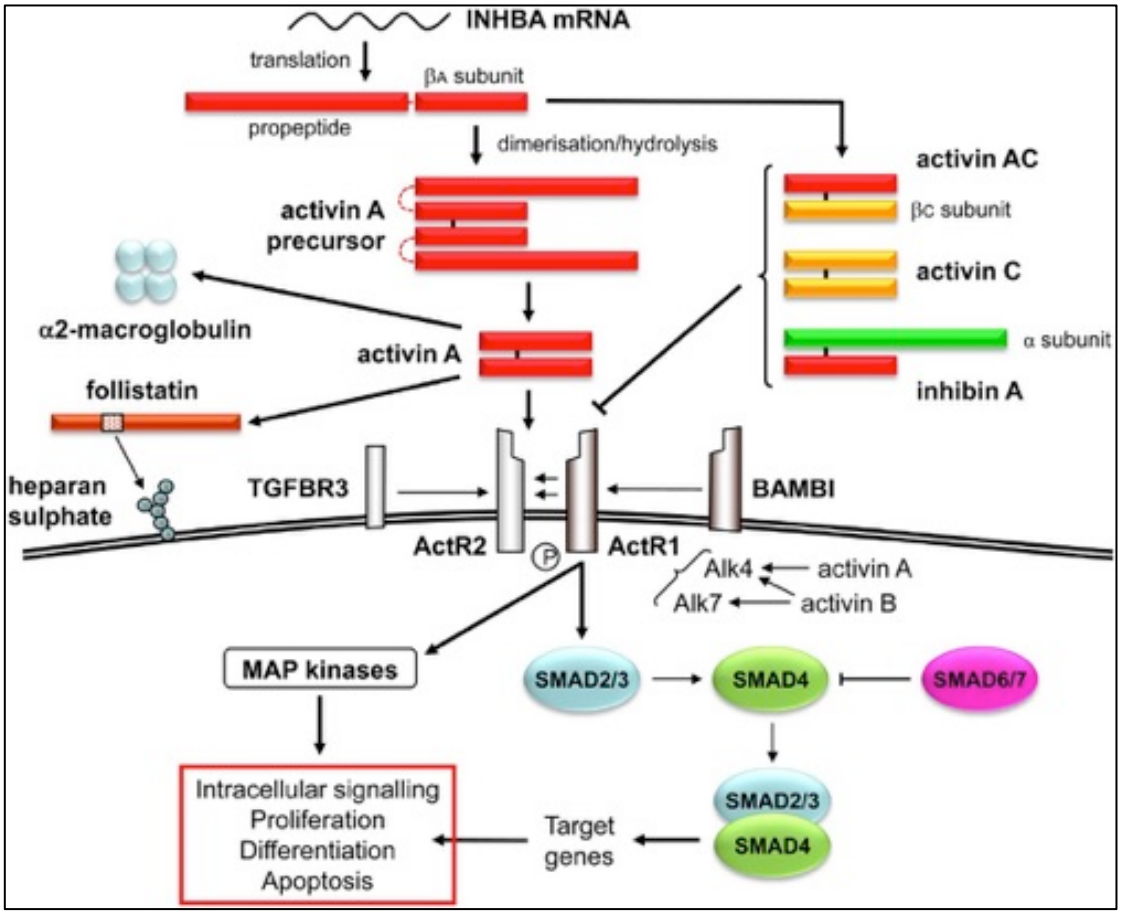

Figure 9. Activin structure, signalling pathway and its major biological effects [Adapted from (Hedger and de Kretser, 2013)].

1.4.3. Activin and follistatin in spermatogenesis

Activin and follistatin were first isolated from ovarian follicular fluid in 1987 (Phillips and de Kretser, 1998). These proteins play role in the well-known feedback regulation of the HPT axis in reproduction. Activin triggers the release of FSH from the anterior pituitary gland (Rombauts and Healy, 1995), while inhibin and follistatin inhibit FSH release from the pituitary gland and bind to

activin, respectively (de Kretser et al., 2002).

Activins function as both autocrine and paracrine regulators of testicular growth and function. Activins have been demonstrated to control germ cell development and steroidogenesis in the testis (de Kretser et al., 2002; Rombauts and Healy, 1995). During postnatal development, activin A regulates the proliferation of both Sertoli and germ cells in the testis (Archambeault and Yao, 2010; Mendis et al., 2011; Mithraprabhu et al., 2010). Meehan et al. (2000) have shown that high activin A levels regulate gonocyte development and Sertoli cell proliferation, whereas decreased activin A levels are needed for gonocyte differentiation into spermatogonia. On the other hand, exposure to higher follistatin levels and FSH may aid the migration of gonocytes to the basement membrane of the testicular cords (Buzzard et al., 2003; Meehan et al., 2000). In the adult rat testis, activin A may also have a critical role in the proliferation of spermatogonial stem cells and spermatocytes at immediate stages after spermiation (stages eight through eleven), which show peak activin A production and secretion (Figure 10) (Okuma et al., 2006). Hence, activin A might assist in the process of phagocytosis of residual bodies during these stages.

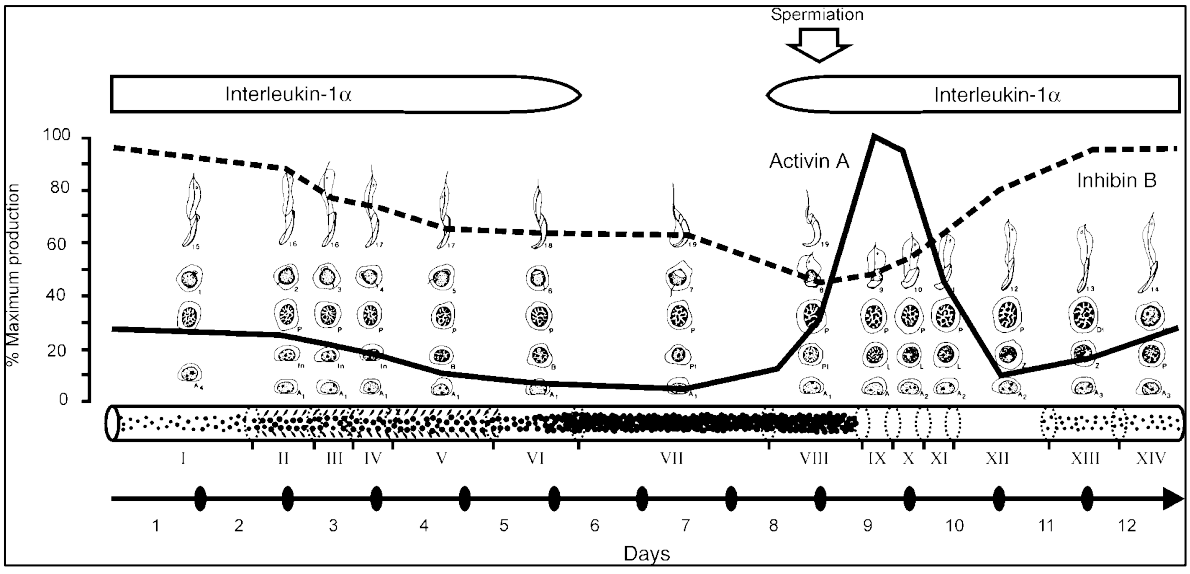

Figure 10. Summary diagram showing the pattern of activin A and inhibin B production, corresponding with events of the cycle of the seminiferous epithelium [From (Okuma et al., 2006)].

1.4.4. Activin and follistatin in inflammation and immunity

Activin is a key regulator of inflammation and immunity (Hedger et al., 2011; Jones et al., 2007). Activin A production is stimulated by IL-1 and TLR ligands, such as lipopolysaccharide (LPS) and tumour necrosis factor (TNF), during inflammation (Chen et al., 2011; Winnall et al., 2009), and activin A levels are increased in a range of inflammatory diseases (Jones et al., 2004). TLR and IL1 induce activation of MyD88 and the downstream TRAF/MAP Kinases are responsible for inflammation-induced activin synthesis (Hedger and de Kretser, 2013). On its own, activin can play two different roles, which is either pro-inflammatory or anti-inflammatory, depending on the stage of development of the immune response (Hedger and de Kretser, 2013; Jones et al., 2004).

Activin A is an effective stimulator of cachexia (Chen et al., 2014; Cipriano et al., 2000; Matzuk et al., 1992), and is also involved in controlling tumour angiogenesis (Hedger and de Kretser, 2013). Activin is a pivotal mediator of fibrosis, since it contributes to fibroblast development and differentiation into myofibroblasts (Hedger and de Kretser, 2013). While TGF-β stimulates activin secretion by fibroblasts during fibrosis, activin stimulates the production of TGF-β1, which is an important regulator of fibrosis (Hedger and de Kretser, 2013; Maeshima et al., 2014). The synthesis of activin is also stimulated by other fibrotic pathway mediators, such as angiotensin, endothelin, thrombin, and TNF (Hedger and de Kretser, 2013), indicating the significance of activin in fibrosis (Figure 11).

Follistatin, as a component of the acute phase reaction, ameliorates many inflammatory effects of activin (de Kretser et al., 2012). For example, follistatin inhibits dermal scarring and reduces inflammatory lung and liver damage (Hedger and de Kretser, 2013). While activin causes apoptosis of hepatocytes (Schwall et al., 1993) and induces hepatic fibrosis, follistatin aids liver regeneration following partial hepatectomy (Jones et al., 2004). Furthermore, follistatin reduces renal fibrosis (Maeshima et al., 2014). It is also capable of attenuating activin-induced cancer cachexia (Cipriano et al., 2000).

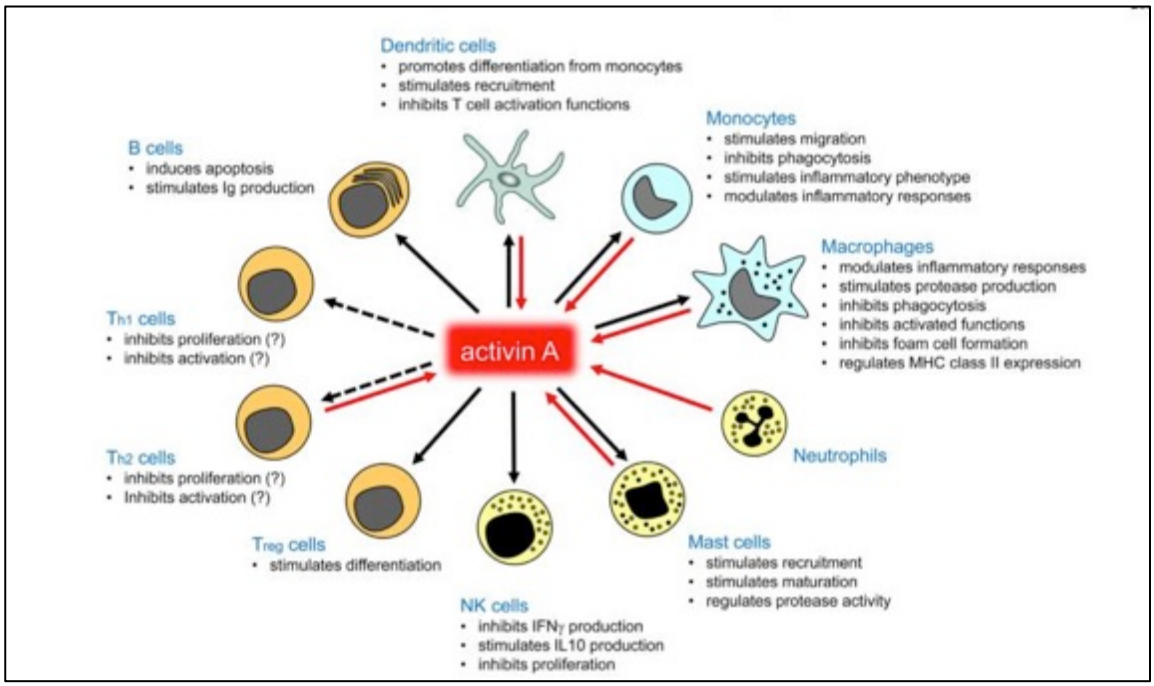

Figure 11. Roles of activins in immunophysiology [Adapted from (Hedger and de Kretser, 2013)].

1.5. Control of testicular temperature

Despite the abdominal origin of the testes, in many mammals they descend in the foetal or neonatal development to reside outside the abdominal cavity where the temperature is lower than the core body temperature by 2–7°C (Harrison and Weiner, 1949; Mieusset and Bujan, 1995). Spermatogenesis is a temperature-dependent process, and any elevation above the normal scrotal temperature range can disrupt its progression.

Numerous studies have demonstrated that low temperature is a pivotal requirement for spermatogenesis (Ivell, 2007; Werdelin and Nilsonne, 1999). Therefore, physiological mechanisms should offer and maintain the appropriate temperature environment for mammalian testis. These include the muscular response, which involves two main muscles. Firstly, the tunica dartos muscle, which forms the lining of the scrotum, relaxes when exposed to warm temperature and results in cooling of the testes by moving them further away from the core body temperature and regulating scrotal surface area. Second, the cremasteric muscle in the spermatic cord has the same action as the dartos; however, it exerts a greater forward action on the testicular distance from the body.

Another is the countercurrent heat exchange system, which acts via the pampiniform venous plexus to transfer heat from warm arterial blood to the cooler venous blood leaving the testes. This causes the arterial blood to be continuously cooler as it enters the testes (Dahl and Herrick, 1959; Harrison and Weiner, 1949). The pampiniform plexus has a further characteristic, which are arterio-venous (A-V) shunts that contribute to cooling of arterial blood. These shunts play an essential role in shunting about 40% of arterial blood into venous blood. Maddocks et al. (1993) have observed a reduction in the level of testosterone in the testicular venous blood that occurs due to the mixing with arterial blood in the rat, guinea pig, monkey and human.

Third, the scrotal sac structure is composed of a thin layer of skin with numerous apocrine glands and absence of subcutaneous fat (Fowler, 1969). These scrotal properties contribute to heat

loss either directly or indirectly through evaporative cooling (Waites and Voglmayr, 1963), although the significance of this mechanism still is queried in humans (Candas et al., 1993).

Heat stress affects the majority of reproductive functions in mammals. Male factor infertility has been reported to be a major cause in at least 50% of all infertile couples (Hou et al., 2015). High scrotal temperature is a significant cause of male factor infertility and is commonly due to 1) lifestyle and behavioural influences, e.g. hot baths and saunas, 2) occupational and environmental influences, like radiant and ambient heat and 3) pathophysiological causes, such as cryptorchidism and varicocele (Durairajanayagam et al., 2014a).

Various studies have discussed the effect of heat on the testes of the laboratory animals using a variety of techniques, such as: (1) general exposure to a heated environment; (2) duration-based insulation of the neck of the scrotum or the whole scrotum (i.e., continuous or intermittent); (3) surgically-induced cryptorchidism via returning one or both testes to the abdominal cavity; (4) immersing the scrotum in a warm water bath; (5) exposure to microwave radiation (Setchell, 2006).

Heat applied to the testis can have direct effects on specific germ cell types as well as indirect effects due to the influence of the germ cells on the Sertoli and Leydig cells. The severity of hyperthermic damage differs with the intensity, frequency and duration of heat exposure (Paul et al., 2008). Although heating the scrotum also might have systemic effects (Maloney et al., 2003), this review focuses on the local testicular effects. These effects can be analysed methodologically as changes in testicular weight, histology, hormone levels and molecular biology, as discussed in the next section.

1.6. Effects of heat on the testis

1.6.1. Effect on the testicular weight

Testicular weight is affected by short or long exposure to heat stress. The exposure of the testis to a single heat episode reduces testicular weight, which is observed 48 hours after heat treatment in the rat (Lue et al. 1999). Maximum effect is seen between 2 to 4 weeks after an acute episode of heat of 43°C for 15–30 minutes to about 60% of control weight (Au et al., 1987; Furland et al., 2011; Lue et al., 1999; Patil et al., 2014; Steinberg and Dixon, 1959). The testis weight starts gradually to recover after 4 weeks, a process that takes more than 4 months (Au et al., 1987). However, the testicular weight recovers to a value below normal, which suggests that the damage is not totally reversible. Some studies with extended time points of observation indicate that testicular weight had not recovered to normal even at 26 weeks post-heat (Setchell et al., 2001).

Repeated exposure of the rat testes to heat has greater effects than a single episode, with a decline in the testicular weight to around 50%, when exposed for 20 min to 43.5°C for 2–7 times in a 6 week interval. This 50% reduction persisted even after 24 weeks of recovery (Bowler, 1972). Kanter and his colleagues (2009, 2013) have also demonstrated a similar reduction in rat testis weight when they heated them for 30 minutes to 43°C, daily for 6 consecutive days.

Earlier studies on surgically-induced cryptorchidism in the rat have also shown that testicular weight drops when the testis is exposed to body temperature. A reduction has been seen within the first week in adult rats (Fujisawa et al., 1988), while in immature rats, it was observed by the second day (Shikone et al., 1994). The full testicular impact of cryptorchidism needs three weeks to be demonstrable (Wilson, 2014).

1.6.2. Histological effect

Exposure to heat stress causes several histological changes in the testis. It has been suggested that germ cells are more susceptible to testicular heating due to their high mitotic activity (Durairajanayagam et al., 2014a). Histological studies in rodents have shown that transient heating of the testis (43°C for 15/30 min) or surgical induction of cryptorchidism results in elevated germ

cell apoptosis (Chowdhury and Steinberger, 1970; Kandeel and Swerdloff, 1988; Setchell, 2006; Steinberg and Dixon, 1959), seminiferous epithelial atrophy and spermatogenic arrest (Munkelwitz and Gilbert, 1998; Wang et al., 2007), leading to decreased viability, disrupted morphology and reduced motility of spermatozoa, as well as diminished blood flow and changed vasomotion in the testis (Kim et al., 2013). Quantitative analysis has demonstrated that the cells most vulnerable to heat are pachytene spermatocytes at stages I–IV and IX–XII, diplotene and differentiating spermatocytes at stages XII–XIV, and early (steps 1– 4) round spermatids in humans (Carlsen et al., 2003; Wang et al., 2007), rats (Bowler, 1972; Chowdhury and Steinberger, 1970; Lue et al., 1999), and mice (Gasinska and Hill, 1989; Paul et al., 2008). This indicates that the development and maturation of these cells is temperature dependent. Since germ cell development is affected by testicular hyperthermia, the function and morphology of Sertoli and Leydig cells are also impacted (Cai et al., 2011; Kanter and Aktas, 2009). Testicular histopathology following exposure to heat stress shows formation of giant cells by pachytene spermatocytes, the presence of vacuoles in the germinal epithelium, degenerated mitochondria, dilated smooth endoplasmic reticulum, and widening of the intercellular spaces in both Sertoli cells and spermatids (Durairajanayagam et al., 2014b). The period in which testicular weight is diminished coincides with the germ cell death, while the return of weight to the control represents the recovery of germ cells (Durairajanayagam et al., 2014b; Setchell, 1998).

Spermatogonial stem cells are believed to be the least heat sensitive cells and are not affected by mild heating of the testis. However, some studies have revealed that the first fall in testicular weight following local heating of the testis is mainly attributed to the apoptosis of heat-sensitive germ cells, while the second decline in testis weight was observed at 182 days indicates the potential that heat also impacts the differentiation and growth of spermatogonia by unknown processes (Setchell et al., 2001, 2002).

1.6.3. Hormonal effect

Mild testicular heating would also result in a perturbation of the regulatory system that controls spermatogenesis, which includes endocrine as well as para/autocrine factors. Data from our lab investigating intratesticular inhibins have shown that the level of inhibin, which is a biomarker of spermatogenesis (Jensen et al., 1997), was decreased in the rat after mild scrotal hyperthermia (43°C for 15 min). This decrease corresponded with the significant damage seen in the seminiferous epithelium and the reduction in testis weight, as well as a large elevation in serum FSH within the first 4 weeks post heat treatment (Au et al., 1987). Hjollund et al. (2002) demonstrated a strong inverse correlation between increased daytime scrotal temperature and poor sperm concentrations and inhibin B in humans. Evidence supports the idea that increased serum FSH levels indicate an impairment of Sertoli cell function after mild testis heating, which is also reported a decreases in testicular content of androgen-binding protein (ABP). Serum LH is also elevated after 1 week of mild heating; however, this increase was preceded by a significant decline at 3 days after heat treatment (Au et al., 1987). Even though serum level of LH is increased, serum testosterone level remained within normal levels after mild heating, indicating a state of compensated Leydig cell damage, through activation of the HPT axis (Au et al., 1987; Jegou et al., 1984; Setchell, 1998). Similar changes have been observed in rat testes damaged by cryptorchidism (Au et al., 1983; Le Gac and de Kretser, 1982). Subfertile men with varicocele show a notable decrease in inhibin B in spermatic venous blood (Goulis et al., 2011). Thus, these data would indicate that Sertoli cell function is damaged by scrotal heating. Further efforts are required to investigate whether scrotal heating also distrupts the circulating inhibin levels by employing acute heat-treated models..

Testosterone has been proposed to play an essential role in protecting germ cells at specific stages from heat-induced programmed death. Lue and his colleagues (1999) have demonstrated that while germ cells at androgen-dependent stages (VII–VIII) are unaffected by heating in rats, administrating a GnRH antagonist increased heat-induced apoptosis in germ cells at these stages. The testosterone secretion in cryptorchidism has been a controversial subject. Some early reports suggested that androgen secretion in response to LH stimulation was elevated in cryptorchid rat

testes (Jegou et al., 1983). Conversely, no changes were reported for serum testosterone levels in cryptorchid mice (Mendis-Handagama et al., 1990), in models relevent to cryptorchidism or its treatement, such as INSL3/RXFP2 mutant mice (Agoulnik et al., 2012), or in response to a human chorionic gonadotrophin (Mendis-Handagama et al., 1990). Testosterone levels showed a progressive decline in long-term induced cryptorchidism in rats (more than 1 year) (Hedger et al., 1994).

1.6.4. Molecular effects

Various studies have reported the underlying molecular effects of hyperthermia on germ cells apoptosis, sperm DNA damage and alteration of gene expression by post-translational modification. In this section, a summary of the molecular mechanisms will be detailed.

1.6.4.1. Germ cell apoptosis

Germ cell apoptosis has long been identified as a characteristic of mammalian spermatogenesis. It occurs mainly during spermatogonial development and is less likely during division of spermatocytes and spermatid maturation in adult rats (Huckins, 1978). Evidence supports the stimulation of both spontaneous (during normal spermatogenesis) and elevated germ cell apoptosis by various regulatory factors, including local scrotal hyperthermia (Lue et al., 2000), lack of gonadotrophin support and reduced intratesticular testosterone (Hikim et al., 1995; Hikim et al., 1997) or by oestradiol therapy (Blanco-Rodriguez and Martinez-Garcia, 1998), Sertoli cell toxicants (Lee et al., 1999), and chemotherapy (Blanco-Rodriguez and Martinez-Garcia, 1998) in rats and humans. This indicates that apoptosis plays a pivotal role in male fertility (Hikim et al., 2003).

In testicular hyperthermia, germ cell apoptosis occurs in a stage and cell type-specific manner. Experimental cryptorchidism causes DNA fragmentation in germ cells (Ohta et al., 1996; Shikone et al., 1994; Yin et al., 1997b), which leads to apoptosis in rats (Henriksen et al., 1995). Transient immersion of the scrotum in a hot water bath at 43°C for 15–20 min also leads to germ

cell apoptosis (Lue et al., 1999; Rockett et al., 2001). Isolated male germ cells from immature rats undergo apoptosis within 1 h when kept at 43°C (Kim et al., 2013).

The use of apoptosis detection technology, namely the TdT terminal deoxynucleotidyl transferase mediated dUDP nick-end labelling (TUNEL) assay, has demonstrated that germ cells are lost via apoptotic processes in heat-treated rats and monkeys (Lue et al., 1999, 2002). Heat could also break cytoplasmic bridges, which are essential for cell survival in the normal testis (Durairajanayagam et al., 2014b; Légaré et al., 2004).

Apoptosis occurs through two major pathways, intrinsic and extrinsic, in mammalian cells (Kim et al., 2013; Morgentaler et al., 1999; Setchell, 1998). The intrinsic pathway is also called the mitochondria-dependent apoptotic pathway. BCL-2 protein family members play a role in controlling the mitochondria-dependent apoptotic pathway, with proteins such as BAX functioning as pro-apoptotic factors, and BCL-2 as an anti-apoptotic factor. The translocation of these proteins stimulates the intrinsic apoptotic pathway (Durairajanayagam et al., 2014a; Liu, 2010). While BAX is mainly found in the cytosol in normal cells, it increases greatly in the mitochondria and endoplasmic reticulum in response to heat stress and BCL-2 is limited to the mitochondrial membrane (Durairajanayagam et al., 2014a; Hikim et al., 2003). BAX repositioning is also accompanied by the concentration of ultra-condensed mitochondria in surrounding spermatocytes (Liu, 2010).

Cytochrome C is a small protein that plays a major role in the electron transport chain, and is commonly found on the inner mitochondrial membrane, where it takes part in redox reactions. In the cytosol, cytochrome C binds to apoptotic protease activating factor 1 (Apaf-1) to form a complex (Hikim et al., 2003). The activated form of Apaf-1 thereafter interacts with initiator (apical) caspase 9 leading to its activation and then proteolytically initiates the caspase cascade through executioner caspases 3, 6 and 7 (Vera et al., 2004). These active caspases are involved in the cleavage of several structural and repair proteins, like poly (ADP) ribose polymerase, lamin and actin, and lead to changes in morphology and, subsequently, apoptosis (Vera et al., 2005). Increased

reactive oxygen species (ROS) production possibly triggers this apoptotic pathway directly by causing the release of cytochrome c into the cytosol via altered functions of signalling molecules (Ishii et al., 2005).

Two pathways have been proposed to explain how germ cells undergo apoptosis extrinsically: the death receptor (Fas) and its ligand (FasL) system and the p53 system (Durairajanayagam et al., 2014a; Ishii et al., 2005). The Fas/FasL system requires the binding of FasL to Fas, which leads to Fas trimerisation and subsequent recruitment of the Fas-associated death domain (FADD) (Hikim et al., 2003). The Fas/FADD complex ligates to initiator caspases 8 or 10 with its N-terminal death effector domain (DED), and subsequently the activated DD stimulates the caspase cascade, including the activation of executioner/effector caspases 3, 6 and 7 (Hikim et al., 2003; Vera et al., 2005).

Some investigators have used genetically modified mouse models that show FasL-defective generalised lymphoproliferation disease (*gld*), or Fas-defective lymphoproliferation complementing *gld* (*lprcg*) mice, in order to determine the role of Fas system in germ cell apoptosis due to heat stress. These studies have demonstrated that heat stress-induced apoptosis still occurred and indicate that other pathways play a key role in inducing cell death (Durairajanayagam et al., 2014a; Vera et al., 2004).

The tumour suppressor *p53* is a transcription factor that expresses pro-apoptotic genes. It is a potential stimulator of germ cell apoptosis when exposed to heat stress as it elevates expression of pro-apoptotic genes and thus regulates the cell cycle (Absalan et al., 2010; Kim et al., 2013; Socher et al., 1997; Zhang et al., 2006). Following the exposure to testicular hyperthermia, p53 moves into the nucleus in order to bind to DNA, which leads to arrest or apoptosis of the cell cycle (Yin et al., 1997a). When cryptorchidism was induced in p53 knockout mice, male germ cell death was reduced and delayed, indicating that germ cell apoptosis involves both p53-dependent and p53-independent systems (Kim et al., 2013; Yin et al., 1998).

Cross-talk between these pathways occurs at multiple levels. A third subcellular compartment, the endoplasmic reticulum, is also involved in apoptotic execution. Both pathways converge on caspase 3 and other executioner caspases and nucleases that drive the terminal events of programmed cell death (Kim et al., 2013).

In conclusion, it appears that both apoptotic pathawys play an essential role in the response to heat stress. Using transgenic animal models, in conjunction with further studies to determine the function of each system in controlling specific phases of apoptosis in the heat stress response, will provide insight into how complex apoptotic pathways regulate the survival of male germ cells under heat stress conditions.

1.6.4.2. Sperm DNA damage

Heat may cause poor sperm quality in males, which is attributed to the ability of some germ cells to develop into mature sperms that contain damaged DNA (Durairajanayagam et al., 2014a). This could be explained by the protective role of heat shock proteins (HSP), which hinder protein denaturation and improper folding (Widlak et al., 2007b). DNA fragmentation has been observed in cryptorchid rodents, which show a loss of chromatin integrity and decreased mass (Sailer et al., 1997; Shiraishi, 2012). These defects are associated with oxidative stress, which results from the excessive production of ROS (Aitken and Baker, 2006; Durairajanayagam et al., 2014a; Shiraishi, 2012). Testicular hyperthermia results in chromosomal abnormalities, which can be regarded as defects in DNA synapsis and DNA strand breaks in pachytene spermatocytes (Paul et al., 2008) and X-Y bivalent dissociations during metaphase I primary spermatocytes (Garriott and Chrisman, 1980; Zupp et al., 1995). These damaged spermatocytes may avoid heat-induced apoptosis and develop to mature spermatozoa with defects in their chromatin integrity. The pairing failure in the X and Y chromosome is attributed to exposure to higher temperatures, which inhibits the normal functioning of the synaptonemal complex, leading to the formation of fewer and more distal chiasmas. Consequently, bivalents are loosely bound and unpaired Y chromosomes are present that will result in apoptosis of spermatocytes (Garriott and Chrisman, 1980). Furthermore, reduced DNA

synthesis and degraded mRNAs and proteins necessary for cell survival have been observed after exposure to heat stress (Durairajanayagam et al., 2014a; Izu et al., 2004).

1.6.4.3. Impaired DNA repair

Male germ cell development has unique DNA synthesis and chromosome-related features and the ability to repair DNA damage at each cellular stage (Favor, 1999). Heat stress causes an impairment in DNA repair mechanisms in germ cells due to decreased levels of gene expression of DNA polymerase β and DNA ligase III (Sottile and Nadin, 2018). This has also been observed in the testes of various acute heat treatment models, which showed a considerable decline in the DNA repair enzyme, poly (ADP) ribose polymerase (Eppink et al., 2012; Tramontano et al., 2000). Another hypothesis has been suggested that significant DNA damage occurs in the nuclei of meiotic germ cells during prophase following heat stress, but the majority of these cells are incapable of full repair of the DNA damage, although they are capable of appearing in the epididymis (Banks et al., 2005; Pérez-Crespo et al., 2008). Conversely, DNA repair mechanisms in premeiotic germ cells remain functional, while these mechanisms are unlikely to occur late in spermatogenesis (Pérez-Crespo et al., 2008). This would explain the presence of DNA damage in some spermatozoa, which may compromise assisted reproduction (Banks et al., 2005).

1.6.4.4. Heat shock proteins (HSPs)

Hyperthermia causes various changes in gene expression, post-translational modifications and proteins in male germ cells. These changes may be due to direct effects of hyperthermia or represent indirect effects due to other cellular modifications (Setchell, 1998). The changes in the protein composition of the spermatocytes result from altered gene expression levels, in concert with post-translational modification and changes in protein localisation (Kim et al., 2013). This would indicate that heat stress triggers the upregulation of genes that are potentially associated with apoptosis, whereas genes for DNA repair and cell cycle regulation are downregulated (Kim et al., 2013).

The HSPs have protective functions that prevent the nonspecific aggregation and denaturation of cellular proteins caused by heat stress. These protective mechanisms are preserved in all living cells (Richter et al., 2010). Specifically, the members of the 70-kDa heat shock protein (HSP70) family act as chaperones involved in folding, transport and assembly of proteins in the mitochondria, endoplasmic reticulum and cytoplasm (Radons, 2016). The HSP70 family consists of at least 7 different proteins in rodents and 13 in humans (Domanico et al., 1993; Giebel et al., 1988; Hunt et al., 1993; Radons, 2016). Two types of HSPs are found in male germ cells: constitutive HSPs and heat-inducible HSPs (Kim et al., 2013; Sarge and Cullen, 1997). The constitutively expressed HSPs, which include HSP70-2 (HSPA2), are molecular chaperones that ensure the correct formation and transfer of polypeptide. In the literature, there is an ambiguity in nomenclature of some HSPs gene products, e.g. the name HSP70-2 has been used for two different genes, *Hspa1b* and *Hspa2,* although *Hspa1b* showed a 83.5% protein homology to *Hspa2* (Kampinga et al., 2009; Scieglinska and Krawczyk 2015). The constitutive HSPs also play a role in the regulation of normal spermatogenesis (Dix et al., 1996; Rosario et al., 1992). Conversely, the inducible HSPs, which include HSP70-1 (HSPA1A) and HSP70-3 (HSPA8), are expressed in response to different hyperthermic conditions (Rockett et al., 2001; Widlak et al., 2007a). These proteins are capable of forming oligomers to mediate their functions (Sreedhar and Csermely, 2004), and protect cells from hyperthermia by interacting with other important proteins to hinder their denaturation and incorrect folding.

More specifically, HSPA2 is a testis-enriched member of the HSP70 chaperone family and has multifunctional roles in protein transport, DNA repair, assembly of the synaptonemal complex, sperm nuclear DNA protamination, and elimination of cytoplasmic residues following spermiogenesis (Beckmann et al., 1990; Chirico et al., 1988; Dix et al., 1997; Govin et al., 2006; Huszar et al., 2000). Deletion of *Hspa2* in mice results in arrest of the pachytene spermatocytes in prophase of meiosis I and extensive apoptosis of these cells (Dix et al., 1996). *Hspa2* in mature spermatozoa is also a crucial protein for sperm–oocyte binding (Redgrove et al., 2012). *Hspa2* underexpression has been observed in infertile men and can be considered a factor in failed sperm–

oocyte recognition (Cedenho et al., 2006; Redgrove et al., 2012, 2013). HSPA2 is modified by oxidative stress via the lipid aldehyde 4-hydroxynonenal, and the modified protein induces proteolytic degradation through the ubiquitin-proteasome system (Bromfield et al., 2017). A number of reports have demonstrated an essential role for BCL2-associated athanogene 6 (BAG6) in the stabilisation of HSPA2, as BCL2 protects these proteins against polyubiquitination and subsequent destruction, thereby allowing their normal function during spermatogenesis and maintaining fertility (Bromfield et al., 2015; Bromfield et al., 2017; Sasaki et al., 2008).

BAG6, which is mainly expressed in the testis, is involved in the regulation of spermatogenesis, apoptosis and heat shock proteins (Ozaki et al., 1999; Sasaki et al., 2008; Wang and Liew, 1994). BAG6 interacts with several apoptotic regulators, including p53, NCR3, AIFM1, and PBF (Desmots et al., 2008; Sasaki et al., 2007; Tsukahara et al., 2009; von Strandmann et al., 2007). Saski et al. (2008) have shown that *Bag6*-deficient mice exhibit degradation of HSPA2, apoptosis of meiotic germ cells and subsequent male infertility that mimics the infertility seen in *Hspa2* null males.

Heat shock factor 1 (HSF1) is an intracellular protein produced in sperm cells in response to activation of the HSF1 gene by hyperthermia (Izu et al., 2004). HSF1 has two opposing functions: 1) it causes a rapid increase in the production of HSPs and interferes with caspase activity, leading to cell survival (Radons, 2016; Widlak et al., 2007a), while 2) it also facilitates the direct removal of defective germ cells to assure a good quality of the mature cells (Izu et al., 2004). HSF1 activates HSP70, which is upregulated in the testis of heat-treated mice and rabbits (Pei et al., 2012; Rockett et al., 2001). HSF1 subsequently undergoes protein modification and is thereby activated in hyperthermic spermatocytes (Sarge and Cullen, 1997). HSF1 also has a reported role in Leydig cell steroidogenesis by maintaining cholesterol transport in cryptorchid mice lacking HSF1 (Oka et al., 2017).

1.6.4.5. Oxidative stress

Free radicals are individual atoms or molecules with a minimum of one unpaired electron in

the outer shell, giving them a high affinity for electron pairing (Agarwal et al., 2006). Reactive oxygen species are common free radicals in the body that arise from oxygen metabolism. The ROS are strongly oxidising and include chemical forms such as superoxide anions, hydrogen peroxide, and peroxyl and hydroxyl radicals (Bisht et al., 2017). The ROS are produced during normal body physiology, but their levels are kept under control by natural antioxidants, such as carotenoids and vitamins C and E. For instance, in the testis, ROS normally support several spermatozoal roles, like the acrosomal reaction, capacitation, hyperactivation and fusion of sperm & oocytes. However, failure to maintain the ROS/antioxidant balance results in oxidative stress, which interferes with vital metabolic processes (Durairajanayagam et al., 2014a; Paul et al., 2008; Shiraishi, 2012).

Oxidative stress impairs sperm function and structure, thereby leading to male infertility. Several studies have indicated that heat stress induces oxidative stress in the testis (Ahotupa and Huhtaniemi, 1992; Houston et al., 2018; Ikeda et al., 1999; Paul et al., 2008). In heat stress conditions, like experimentally-induced cryptorchidism, varicocele and acute heat, ROS are produced in the testis and may contribute to the heat stress response by direct and/or indirect pathways, both of which lead to apoptosis.

The direct pathway leads to apoptosis directly via oxidation of cellular elements such as DNA and lipids. Hydrogen peroxide levels increase following exposure to testicular hyperthermia, which results in lipid peroxidation and a reduction in the antioxidant activity of enzymes like superoxide dismutase and catalases (Durairajanayagam et al., 2014a). The result is increased ROS levels and further oxidative stress. These direct pathway responses have been confirmed in rats treated with catalase, as the rats showed a decline in the amount of peroxidation and cellular apoptosis. However, other data suggest that dramatic increases in ROS may be the main cause of elevated oxidative stress in rats, rather than a reduction in antioxidants (Peltola et al., 1995). This discrepancy may reflect an inconsistency in the decreased activity of manganese superoxide dismutase associated with the normally low levels of DNA (Durairajanayagam et al., 2014a). Therefore, elevated ROS levels may play an essential role in the DNA damage occurring during heat stress.

Alternatively, the indirect pathway activates apoptosis as a response to the generation of ROS, rather than as a direct effect of ROS (Shiraishi, 2012; Shiraishi et al., 2010). This has been confirmed in a SOD1-knockout mouse model subjected to mild transient scrotal hyperthermia. The duration of the exposure was too short to trigger ROS production sufficient to cause peroxidation and apoptosis (Ishii et al., 2005), suggesting that the generated ROS served as a signal to stimulate apoptosis.

1.6.4.6. Inflammation and fibrosis

The initial body response to cellular damage or infection is inflammation (Kumar et al., 2017). The hallmarks of inflammation are pyrexia or local hyperthermia, pain, redness and oedema of the affected tissue and, in severe cases, loss of function. Several inflammatory mediators are either released by cells or produced from plasma proteins in this process; these include vasoactive amines, lipid products, complement proteins and cytokines (e.g. TNF, IL-1, 6, 12 and 17, interferon-γ, and chemokines) (Kumar et al., 2017). Inflammation can be classified as acute or chronic, based on the extent of the damage.

Acute inflammation is a short-term reaction which normally occurs within minutes and lasts for days. It is an essential component of innate immunity and is characterised by the exudation of fluid and plasma proteins (oedema) and the migration of white blood cells (leukocytes), including neutrophils (Kumar et al., 2017). Acute inflammation subsides when the injurious agents are eliminated. By contrast, when these agents fail to clear, the result is a persistent reaction called chronic inflammation. Chronic inflammation is a long-term response that is associated with extensive cellular injury, the recruitment of lymphocytes, macrophages and monocytes, proliferation of the vasculature and the deposition of connective tissue. Chronic inflammation is an important factor in adaptive immunity. Overall, acute inflammation usually results in tissue repair by regeneration, whereas chronic inflammation usually ends with fibrotic damage (Kumar et al., 2017).

Fibrosis (also called scar formation) is a deposition of collagen in damaged tissue as a part

of healing process. Fibrosis takes place in three key steps: 1) angiogenesis, which is associated with various signalling pathways, cell-cell interactions, extracellular matrix proteins and tissue enzymes. 2) formation of granulation tissue via migration and proliferation of fibroblasts to deposit connective tissue, and 3) remodelling of the connective tissue (Kumar et al., 2017). Macrophages play an essential role in fibrosis by providing growth factors for the proliferation of different cells and by producing cytokines that trigger proliferation of fibroblasts and generation and deposition of connective tissue. The fibrotic process also involves the action of numerous growth factors, including vascular endothelial growth factors (VEGFs), Fibroblast growth factors (FGFs), angioproteins, TGF-β and Platelet-derived growth factor (PDGF). TGF-β1, which is an anti-inflammatory cytokine, is well recognised as a central contributor to fibrosis (Kumar et al., 2017). Activin, a member of the TGF-β superfamily, promotes the differentiation of fibroblasts into myofibroblasts and induces the expression of other fibrotic regulators (Hedger and de Kretser, 2013). Fibrosis is a basic mechanism of tissue repair, but it also can also be a pathological reaction caused by chronic injuries like persistent infections and immune reactions. In pathological cases, the abnormal fibrosis may end in permanent organ damage (Kumar et al., 2017).

The formation of fibrotic deposits occurs by the self-assembly of collagen molecules into fibrils, and this process requires the participation of several proteins. Collagens I, II and III are the most enriched proteins in the body and form the backbone of all collagen fibrils (Ricard-Blum, 2011). The fibril-forming collagens are produced and released as procollagens, which have a noncollagenous C-terminal propeptide and an N-terminal propeptide. The presence of the propeptide prevents the premature assembly of collagens into fibrils. Processing of the propeptides therefore regulates the initial assembly of collagen molecules into fibrils and requires numerous enzymes, including bone morphogenetic protein 1 (BMP-1)/tolloid proteinases, furin or ADAMTS 2, 3, and 14 (Birk and Brückner, 2011).

Procollagen C-proteinase enhancers (PCPE-1 and -2) are two closely related extracellular matrix glycoproteins that can stimulate the pace of C-terminal processing of fibrillar procollagens by tolloid metalloproteinases, such as BMP-1 and mammalian tolloid-like proteinase (Kessler et al.,

1996; Steiglitz et al., 2002). PCPE-1 acts as a regulator of collagen deposition and can be a potential therapeutic target in the treatment of hepatic and cardiac fibrosis (Kessler-Icekson et al., 2006; Ogata et al., 1997). It may also play a role in the proliferation of smooth muscle cells, in extracellular matrix (ECM) production during atheroma formation and in cell growth and differentiation. In the testis, Col1a1, Col1a2 and procollagen I are associated with the maintenance of spermatogonia and in germ cell detachment and migration during murine spermatogenesis (He et al., 2005). Silencing of Col1a1 results in inhibition of spermatogonial self-renewal and enhances spermatogonial differentiation (Chen et al., 2012).

Decorin and fibromodulin are members of the secreted small leucine-rich proteoglycans family and serve synergistic functions by regulating fibril formation and matrix assembly during the development of mature, functional tissues (Birk and Brückner, 2011). Decorin was named for its function of fibrillar collagen decoration in a periodic manner, which is an essential mechanism of ECM assembly and homeostasis (Schaefer and Iozzo, 2008). Decorin has other key biological functions, including cell migration, adhesion and proliferation (Ferdous et al., 2010; Nili et al., 2003). Decorin also binds to and regulates several soluble and insoluble ligands, such as TGF-β and platelet-derived growth factors (Macri et al., 2007; Nili et al., 2003), and it acts as a non-selective ligand for a variety of growth factor receptors (GFRs), such as epidermal GFR, insulin-like GFR 1, vascular endothelial GFR and hepatocyte GFR (Goldoni et al., 2009; Iacob et al., 2008; Schaefer and Iozzo, 2008). Adam et al. (2011) found an increase in decorin levels in the human testis due to the actions of mast-cell–derived tryptase and a consequent disruption of paracrine signalling pathways. These observations were also reported in mice and monkeys, indicating a potentially universal role for decorin in the functioning of the mammalian testis (Adam et al., 2012).

Despite an extensive body of literature regarding the effects of transient heat (ranging from 35–46°C) on the testis (Chowdhury and Steinberger, 1970; Houston et al., 2018; Jegou et al., 1984; Sailer et al., 1997; Yaeram et al., 2006), an inflammatory response was only reported within the tunica albuginea and adjacent peri-testicular tissues when the testis was exposed to 48°C for 15 minutes (Fridd et al., 1975). The inflammation also extended into the adjacent fibroadipose and

muscle tissue.

1.6.5. Proteomic effect

Proteomic technologies have emerged recently that can be used as effective tools for the comprehensive study of various biological system proteomes in mammals (Aebersold and Mann, 2016). Proteomics is the study of proteins, including their structure and function, with the aim of testing the total protein expression complement of the genome (Blackstock and Weir, 1999; Lamb, 2009). Proteomic analysis by mass-spectrometry (MS)-based methods can confirm the presence of a certain protein, measure its amount and detect its several forms, thereby leading to the production of thoroughly validated data. (Kovac et al., 2013). The use of proteomics is especially pivotal for spermatogenesis, since the quantitative relation between RNA and protein expression is lower in the testis than in other tissues (Lamb, 2009), suggesting that genomic studies are less explanatory in this context. Certain proteins that are differentially expressed in pathological conditions could be used as biomarkers and thereby serve as non-invasive diagnostic tools. Proteomic-based treatments may also demonstrate more effectiveness than currently used therapeutics (Agarwal et al., 2014). Hence, the use of novel proteomic techniques may hold the key to improving the accuracy of diagnoses treatment of male factor infertility.

Several studies have mapped the developmental changes in testicular proteomes from foetal germ cell development to adult spermatogenesis in pigs, rodents and humans (summarised in Table 2). Infertility biomarkers were explored in these studies by conducting proteomic analyses on different biological samples, including whole testis, isolated germ cells, sperm, seminal plasma, and seminiferous tubule fluid, but little attention has yet been paid to the TIF. Stanton et al. (2016) showed that the normal rat TIF contains 286 multicellular proteins. However, just one study has thus far investigated the effect of application of a transient mild local heat treatment to the testis on intratubular proteomics. Zhu and his colleagues (2010) used proteomics to demonstrate that mild scrotal hyperthermia in humans causes a reversible arrest of spermatogenesis by altering the expression of a sequence of proteins that have roles in proliferation, differentiation, apoptosis and cell survival. These differentially expressed proteins were the key molecular targets of heat

treatment related to spermatogenesis. For example, the expression of the HNRNPH1 protein altered the state of apoptosis following heat exposure. Further studies are needed to investigate the changes in intertubular proteomics that would reflect the cross-talk between the tubular and interstitial testicular compartments in response to testicular heating.

Table 2. Proteomic studies that investigated the different spermatogenesis proteomes in mammals.

Species	Age	Analysed sample	Reference
Mouse	Fetal	Whole testis	(Wilhelm et al., 2006)
		Multipotent Adult Germline Stem Cells and Embryonic Stem Cells	(Dihazi et al., 2009)
	Postnatal	Whole testis	(Paz et al., 2006)
			(Huang et al., 2008)
	Adult		(Zhu et al., 2006)
		Spermatids	(Govin et al., 2011)
Rat	Adult	Spermatogonia	(Com et al., 2003; Guillaume et al., 2000)
		Germ cells	(Lagarrigue et al., 2011; Rolland et al., 2007)
		TIF	(Stanton et al., 2016)
Pig	Postnatal	Whole testis	(Huang et al., 2011)
	Adult		(Huang et al., 2005)
Human	Adult	Whole testis	(Guo et al., 2008; Guo et al., 2010)
			(Li et al., 2011)
		Sperm	(de Mateo et al., 2011)
			(Intasqui et al., 2018)
			(Martínez□Heredia et al., 2006)
			(Chu et al., 2006)
			(Stein et al., 2006)
			(Zhao et al., 2007)
		Seminal plasma	(Cui et al., 2018)
			(Intasqui et al., 2015)
			(Agarwal et al., 2015)
			(Yamakawa et al., 2007)

1.7. Summary

Spermatogenesis is the process by which terminally differentiated sperm are produced from male germline stem cells. This complex developmental process requires the coordination of both somatic and germ cells through phases of differentiation to give rise to the cell that carries the paternal genome. The developmental processes of the male gamete may be influenced by various factors, including heat stress, which can lead to the production of poor quality sperm, thereby reducing fertility. The factors that can contribute to increased scrotal temperatures range from lifestyle, occupational, and environmental influences to pathophysiological changes. Many of these factors cannot be entirely avoided, so testicular thermoregulation is therefore of great importance to ensure the production of viable spermatozoa that will maintain fertility. Any failure in scrotal thermoregulation or exposure to high temperatures therefore runs the risk of causing testicular heat stress. Germs cells like pachytene spermatocytes and round spermatids have the greatest vulnerability to heat stress. The testicular response to hyperthermia varies according to the intensity and duration of the heat.

The impacts of hyperthermia on germ cells are not thoroughly understood. This area therefore needs further genomic and proteomic studies to elucidate the underlying pathways that regulate the heat stress responses of male germ cells and to identify new genes or proteomes that may be involved. A better understanding of the molecular mechanisms of testicular hyperthermia would aid in the development of targeted male infertility therapies, as well as contraception methods. Short-term heat and cryptorchidism studies have demonstrated that changes occur in gonadotrophin levels and testicular inhibin bioactivity, which would suggest that alterations also occur in the levels of inhibin-related proteins, activins and follistatin. These proteins have a crucial role in controlling gonadotrophin secretion. Furthermore, the results of these studies also suggest the existence of another potential role for intercompartmental communication, since the function of both the Sertoli cells and Leydig cells are changed by events such as cryptorchidism, mild transient hyperthermia or efferent duct ligation—all of which are known to impair spermatogenesis (de

Kretser et al., 1979; Jegou et al., 1983; Rich and de Kretser, 1977; Rich et al., 1979; Risbridger et al., 1981a, 1981b). The damage to spermatogenesis is therefore reflected in the Sertoli and Leydig cells functions. However, at the time these studies were performed, methods for measurement of inhibin-related proteins were not available, nor were modern proteomic or genomic techniques. These proteins, which are produced by the seminiferous tubules, could possibly be involved in the intercompartmental dialogue occurring within the testis; therefore, proteomics has enormous potential for identifying novel mechanisms by which the testicular compartments interact.

The studies in this thesis employed heat models that cause both reversible spermatogenic damage and reversible alterations in Sertoli cell and Leydig cell functions. Stanton et al. (2016) showed that testicular interstitial fluid (TIF) from normal adult rats contains proteins contributed by the main cell types in the seminiferous tubules, including Sertoli, Leydig, peritubular myoid and germ cells. These TIF proteins could therefore potentially reflect spermatogenic function. Thus, TIF was also investigated using recently developed proteomic techniques as a way to identify functional markers of spermatogenesis by comparing TIF from normal testes and testes subjected to a heat treatment that eliminates the spermatogenic cells. This strategy may also identify the factors that are responsible for the communication between the two compartments of the testis and reveal novel biomarkers of testis damage and recovery.

1.8. Hypothesis and aims

The work in this thesis addresses the hypothesis that heat disrupts activin-related pathways in the testis, and causes alterations in proteins secreted into the testicular interstitial fluid that collectively may provide novel insights into the mechanisms of heat damage and its recovery. In order to address this hypothesis, the following aims were undertaken:

1. To assess the time-course of the response to acute heat treatment and the impact of these changes on activin/inhibin-related protein production and gene expression in the adult rat testis.
2. To identify novel mechanisms involved in the response to acute heat by investigating changes in the proteome of testicular interstitial fluid during damage and following recovery.
3. To investigate activin/inhibin-related protein production and gene expression, and other inflammatory regulators in response to chronic heat treatment in the cryptorchid testis.

2. Chapter 2:

Acute heat treatment disrupts inhibin-related protein production and gene expression in the adult rat testis

Manuscript published in *Molecular and Cellular Endocrinology* (2019) 498, 110546.

DOI: 10.1016/j.mce.2019.110546

Acute heat treatment disrupts inhibin-related protein production and gene expression in the adult rat testis

Rashid A Aldahhan[a,b,c*], Peter G Stanton[a,b], Helen Ludlow[d], David M de Kretser[a,b] and Mark P Hedger[a,b]

[a]Centre for Reproductive Health, Hudson Institute of Medical Research, Clayton, Victoria, Australia

[b]Department of Molecular and Translational Sciences, Monash University, Clayton, Victoria, Australia

[c]Department of Anatomy, College of Medicine, Imam Abdulrahman Bin Faisal University, Dammam, Saudi Arabia

[d]Oxford Brookes University, Oxford, U.K

***Corresponding author and present Address:**

Rashid Aldahhan

Department of Anatomy, College of Medicine, Imam Abdulrahman Bin Faisal University, Dammam, Saudi Arabia.

P.O. Box 1982, Dammam 31441, Saudi Arabia

Email: raaldahhan@iau.edu.sa

Highlights

- The testicular response to heat stress displayed three phases: (I) onset (1–2 weeks), (II) peak damage (2–8 weeks) and (III) recovery (12–14 weeks)
- Expression of several key Sertoli and Leydig cell genes declined contemporaneously with the initial loss of meiotic germ cells.
- Activins were responsive to the subsequent loss of mature spermatids, leading to an increase in testicular activin B production relative to activin A.
- Critically, germ cell damage was not associated with a significant inflammatory response.

Abstract

Heat reversibly disrupts spermatogenesis, but the effects on Sertoli cell (SC) functions, and inhibin/activin-related proteins, are less well-defined. Adult rat testis weights decreased by 40% within 2 weeks after heat-treatment (43°C, 15 minutes), due to loss of pachytene spermatocytes and round spermatids. Coincident effects were reduced SC nuclear volume at one week and >50% reduction in several critical SC genes (*Inha*, *Cld11*, *Gja1*, *Tjp1, Cldn3*) by 2 weeks. Leydig cell steroidogenic enzymes, *Cyp11a1, Hsd3b1*, were also reduced. Activin gene expression was unaffected at this time, but expression of the activin-binding protein, follistatin (*Fst*), increased >2-fold. At 4-8 weeks, coincident with recovery of spermatocytes and early spermatids, but progressive loss of elongated spermatids, most SC genes had recovered; however, this corresponded with reduced testicular activin A and increased activin B. At 8 weeks, serum inhibin was decreased and, consequently, serum FSH increased. Crucially, germ cell damage was not associated with a significant inflammatory response. At 14 weeks, most testicular parameters had returned to normal, but testis weights remained slightly reduced. These data indicate that, following acute heat-treatment, expression of several key Sertoli and Leydig cell genes declined in parallel with the initial loss of meiotic germ cells, whereas activins were responsive to the subsequent loss of mature spermatids, leading to an increase in testicular activin B production relative to activin A.

Keywords:

Spermatogenesis – Heat stress – Sertoli cell - Activins – Steroidogenesis

1. Introduction

In most mammals, the testes descend during prenatal or early neonatal life to reside in the scrotum, where the temperature is 2–7 °C lower than the core body temperature. Spermatogenesis is a temperature-sensitive process, and elevation above the normal scrotal temperature range can cause the death of heat-sensitive spermatogenic cells (Durairajanayagam et al., 2014). Elevated scrotal temperature is considered to be a major contributor to male factor infertility (Durairajanayagam et al., 2014; Hou et al., 2015). The sources of heat stress that adversely impact testis function include: (1) lifestyle and behavioural factors, such as clothing, hot baths and saunas, (2) occupational and environmental exposure to radiant and ambient heat and (3) pathophysiological factors, such as cryptorchidism, fever and varicocele (Durairajanayagam et al., 2014).

Quantitative analysis in rats (Bowler, 1972; Chowdhury and Steinberger, 1970) and mice (Gasinska and Hill, 1989; Paul et al., 2008) has demonstrated that the germ cells most acutely susceptible to heat are pachytene spermatocytes and round spermatids at stages I–IV and IX-XII and the diplotene and differentiating primary or secondary spermatocytes at stages XII-XIV; similar stages are affected by heat in the human testis (Carlsen et al., 2003; Wang et al., 2007). Spermatogonia, in contrast to the meiotic and post-meiotic germ cells, appear to be relatively resistant to the detrimental effects of heat (McLean et al., 2002), which have been linked to oxidative stress and DNA damage (Houston et al., 2018). Sertoli and Leydig cell functions are also affected by heat (Au et al., 1987; Bergh and Söder, 2007; Jegou et al., 1984; Vallés et al., 2014). Changes documented in earlier studies include decreased production of seminiferous tubule fluid, androgen binding protein (ABP) and inhibin bioactivity by the Sertoli cells, as well as Leydig cell hypertrophy and hyper-responsiveness to stimulation (Jegou et al., 1984). These alterations in Sertoli and Leydig cell functions occur subsequent to the spermatogenic cell damage and appear to be, primarily, a response to the loss of the germ cells. However, the responses of the Sertoli and Leydig cells to a brief episode of heat have not been closely investigated at the gene expression level.

The disruption of the testis, in turn, causes increases in serum FSH due to decreases in feedback from inhibin from the testis (Au et al., 1987; Jegou et al., 1984). Activin A and B are homodimers of the inhibin β-subunits, which are able to stimulate FSH production by the pituitary gonadotrophs. The inhibitory action of inhibin on FSH is due to its ability to competitively block the binding of locally-produced activins to their receptors within the pituitary gland (de Kretser et al., 2002; Hedger et al., 2011). The activins are also implicated in the local regulation of testis function. Activin A plays a crucial role in the development and activity of male germ cells and Sertoli cells (Barakat et al., 2012; de Kretser et al., 2002; Meehan et al., 2000). In the adult rat testis, activin A is produced by Sertoli cells, but also by meiotic and post-meiotic germ cells, Leydig cells and interstitial macrophages (Hedger and Winnall, 2012). It appears to have a critical role in the regulation of spermatogonial stem cells, spermatocytes and Sertoli cell tight junctions during the restructuring of the seminiferous epithelium, particularly at stages VIII to XI of the rat spermatogenic cycle immediately after spermiation (Nicholls et al., 2012; Okuma et al., 2006). Activin A is also a key regulator of inflammation and immunity throughout the body (Hedger et al., 2011; Jones et al., 2007) and may be either pro-inflammatory or anti-inflammatory, depending on the setting within the immune response (Hedger et al., 2011; Wijayarathna and de Kretser, 2016). Activin A is also an essential mediator of fibrosis, since it regulates fibroblast development and differentiation into myofibroblasts (Hedger et al., 1989; Ohga et al., 1996; Yamashita et al., 2004).

In contrast to activin A, the role of activin B in the regulation of testis function is poorly defined. The inhibin/activin βB subunit is produced by the Sertoli cell, where it typically dimerises with the α-subunit to form inhibin B (de Kretser et al., 2002; Hedger and Winnall 2012), and studies on activin B in the testis have been limited in the past due to the absence of suitable immunoassays for the activin B homodimer. However, the βB subunit has been shown to be expressed by testicular cells other than the Sertoli cell, including the Leydig cells and meiotic- and post-meiotic germ cells (Marchetti et al., 2003; Roberts et al., 1989), indicating that these cell types are potential sources of activin B, as well. Bioactivity of the activins is regulated by inhibin and by the activin-binding

protein, follistatin, which is also widely expressed by testicular somatic and germ cells (Meinhardt et al., 1998; Phillips and de Kretser 1998).

While some previous studies have investigated inhibin production following heat-induced damage of the testis (Gao et al., 2012; Lue et al., 2002), the corresponding response of the activins and follistatin have not been investigated. At the time the earlier studies were performed, assays were not yet available for measurement of the activins or follistatin, nor had modern analytical techniques for mRNA expression been developed. Consequently, we set out to define the changes that occur in the inhibin-related proteins in the testis and serum in response to acute heat-treatment, their relationship with changes in gene expression by the Sertoli cells, Leydig cells and other testicular cells, and their relationship with markers of heat-stress and inflammation.

2. Materials and Methods

2.1. Animals and tissue collection

Adult male outbred Sprague-Dawley rats obtained from Monash Animal Services (Monash University, Clayton, Australia) were maintained at 20°C in a fixed 12-h light, 12-h dark cycle with free access to food and water. Rats (approximately 10 weeks old) were divided into two groups: control and heat-treated. Both groups were anaesthetised with intraperitoneal ketamine (40mg/kg) and xylazine (5mg/kg). The rats undergoing heat treatment had their scrota immersed in a water bath at 43°C for 15 minutes under anaesthesia, then were allowed to recover. Control rats were maintained at ambient room temperature for the same period of time. Groups of control and heat-treated rats were killed for evaluation at 1, 2, 4, 8, 12, and 14 weeks post-treatment (n = 7 rats/treatment group at each time-point).

For in vitro studies, control immature (day 20) Sprague-Dawley rats (n=12) were euthanised by CO_2 asphyxiation, and testes were removed for Sertoli cell culture. These studies were approved by the Monash Medical Centre Animal Ethics Committee.

2.2. Tissue handling and preparation

At each time point, control and heat-treated rats were anaesthetised (above), and blood was drawn by cardiac puncture until the rats were euthanised by exsanguination. The paired testes were dissected out and their weights recorded.

Immediately after dissection, tissues were collected for three analyses: histology, RNA and testicular interstitial fluid (see the details below) avoiding the presence of two testes from the same animal in each analysis. Testes collected for histology (n=4) were immersed intact in Bouin's fixative (Amber Scientific, Midvale, WA, Australia) for 24 hours, then stored in 70% ethanol. Tissues for RNA or protein extraction (n=6) were snap-frozen in dry ice and stored at -80°C until further processing. For mRNA and protein extraction, the tissues were homogenised using the Qiagen TissueLyser II and stainless steel beads (Qiagen GmBH, Hilden, Germany) prior to analysis. Blood was centrifuged at 4000 x g for 15 minutes and the separated serum was stored at -20°C, prior to use.

Testicular interstitial fluid (TIF) was collected (n=4 testes) as described elsewhere (Sharpe and Cooper, 1983). Briefly, a 2–4 mm incision was made in the tunica at the distal pole, and the testis was suspended on a thin needle placed through the tunica at the opposite pole in a 15 mL tube above 20 µL phosphate-buffered saline (0.01M PBS, pH 7.4) containing complete protease inhibitor cocktail (Roche, Castle Hill, Sydney). TIF was then collected by percolation overnight at 4°C, ultra-centrifuged (109,000g, 60 minutes, 4°C) and the supernatant was snap-frozen and stored at -80°C.

2.3. Tissue processing and histological staining

Bouin's fixed tissues were processed for routine histology and embedded in paraffin. Organs were sectioned at 5µm and attached to Superfrost Plus Glass slides (BioLabs Scientific, Melbourne, Australia). Sections were stained with periodic acid–Schiff reagent (PAS) for routine histological examination and staging of spermatogenesis.

2.4. Immunohistochemistry

Immunohistochemical localisation of Sox9 as a Sertoli cell-specific marker was performed as described previously (Wu et al., 2017). In brief, heat-mediated antigen retrieval was performed using 10mM citrate buffer (pH 6) and normal goat serum (5%) was used to block non-specific binding. Sections were incubated overnight incubated at 4°C with Sox9 rabbit polyclonal antibody (SC-20095, Santa Cruz Biotechnology, Inc., CA, USA), while negative controls were incubated with matched rabbit immunoglobulins (IgG). Signal detection was with Vectastain ABC kit reagents (Vector laboratories, Inc., Burlingame, CA, USA) (30 minutes, room temperature) followed by diaminobenzidine (DAB) (Dako North America, Inc., Carpinteria, CA, USA) and colour development was monitored under the microscope.

2.5. Terminal deoxynucleotidyl transferase dUTP nick end labelling (TUNEL) assay

The Apoptag peroxidase *in situ* apoptosis detection kit (Millipore Corporation, Billerica, MA, USA) was used to identify cells undergoing apoptosis. Testis sections were incubated with terminal deoxynucleotidyl transferase (TdT) enzyme, whereas phosphate-buffered saline (PBS) was added to negative control sections. CAS-block^{TM} solution (Life Technologies, Frederick, MD, USA) was added to the sections for 30 minutes, prior to colour development using DAB. For the quantification of apoptosis, areas of cross-sectioned testes were selected randomly, and all the tubules were included in the count by using x20 objective lens. The number of tubules containing apoptotic cells and the number of apoptotic cells per field were counted. A total of 100 tubules per testis were counted, moving across each section in a systematic manner. The percentage of tubules showing apoptosis and the number of TUNEL-positive cells was then calculated.

2.6. Stereological Techniques

Tubules containing Sox9-positive nuclear profiles were counted in a systematic manner by use of the 40x objective on an Olympus BX50 microscope (Olympus Corp., New York, NY, USA). Nuclear diameters were then calculated using the freehand polygon tool in the CELLSENS DIMENSIONS software 1.7.1 (Olympus Corp.). The numerical density of nuclei associated with an

immunopositive cell profile *(Nv)* was calculated as described (Abercrombie, 1946), in order to compensate for changes in nuclear size, as previously described (Wang et al 1994).

Nuclear profiles were counted for 20 tubules per animal at all timepoints. Subsequently, nuclear diameters for each immunopositive cell in the 1 week treatment group were calculated from 50 randomised nuclear profiles/animal. In order to eliminate under-estimation of nuclear diameters due to the presence of glancing sections of nuclear profiles, only the average of the upper 30% of diameter estimates/animal (i.e., the maximum observed diameter) was calculated. Section thickness was assumed to be as set (5 μm), and minor dimensional changes as a result of tissue processing or sectioning were ignored for the purposes of this study.

2.7. RNA Extraction, Reverse Transcription, and the Fluidigm Biomark™ HD Real-Time Polymerase Chain Reaction (PCR)

Fluidigm analysis was performed as described previously (Bienvenu et al., 2017). Briefly, total RNA was isolated from fragments of the snap-frozen testes and isolated Sertoli cells using an RNeasy kit (Qiagen, Venlo, Netherlands) followed by DNase treatment by the RNase-Free DNase set (Qiagen), according to the manufacturer's protocols. Synthesis of cDNA from RNA was performed using a Tetro cDNA synthesis kit (Bioline, Tauton, MA, USA), according to the manufacturer's instructions.

Quantitative digital PCR was carried out with Taqman® Gene Expression Assays (Life Technologies, CA, USA) using the Integrated Fluidic Circuits on the Biomark™ HD platform (Fluidigm, CA, USA). The TaqMan gene expression assays for testis and isolated Sertoli cells are listed in Table 1. All assays were available from the manufacturer except *Rn18s* TaqMan assays which were designed as the following: forward (5`-GGAGAGGGAGCCTGAGAAAC-3`), reverse (5`- CAATTACAGGGCCTCGAAAG-3`) and probe (CCACTCCCGACCC). Initially, three housekeepers per tissue source were evaluated; these were *Gapdh, Hprt* and *Sdha* for the testis and *Gapdh, Rn18s* and *Cryab* for the isolated Sertoli cells. From these, *Hprt* and *Rn18s* genes were stably expressed across all time-points and treatments for the testis and isolated Sertoli cells,

respectively. Data were analysed by Fluidigm Real-Time PCR Analysis software (version 4.12). The mean of duplicate Ct values from each reaction was converted into ΔΔCt values, from which the average fold change was expressed as the mean fold increase ± standard deviation (SD) of the gene relative to *Hprt* for the testis and *Rn18s* for the isolated Sertoli cells.

2.7.1. Real-Time quantitative PCR and standardisation of gene expression

An important concern of this study design was the fact that heat-treatment causes a major loss of the numerous meiotic and post-meiotic spermatogenic cells, but somatic cell numbers are largely unaltered, which would lead to significant distortions in the ratio of total germ cell mRNA to somatic cell mRNA following extraction. In order to compensate for this, genes that are specifically or preferentially expressed by the Sertoli cells are presented as a ratio with the constitutively-expressed Sertoli cell gene, *Sox9*, and the Leydig cell steroidogenic genes as a ratio with the Leydig cell-specific marker, *Insl3* (insulin-like 3). The fact that *Sox9* and *Insl3* are constitutively expressed by Sertoli and Leydig cells, respectively, has been demonstrated previously (Kent et al., 1996; Sadeghian et al., 2005). Genes that are expressed by both somatic cells and germ cells (excluding spermatogonia) are presented as the normalised data from the fluidigm analysis (Table 1).

For the purposes of the standardisation procedure, *Sox9, Insl3* and *Rn18s* were measured by qRT-PCR, using primers as published previously (Baburski et al., 2015; Wu et al., 2017; Zhang et al., 2016). The primers sequences were: *Sox9*: forward (5`-TGCTGAACGAGAGCGAGAAG-3`) and reverse (5`- ATGTGAGTCTGTTCGGTGGC-3`), *Insl3*: forward (5`-CGCAGTGTGGCCACCAA-3`) and reverse (5`-CCTGAGCCCTACAATCCTTCAG-3`), and *Rn18s*: forward (5`-GGAGAGGGAGCCTGAGAAAC-3`) and reverse (5`-CAATTACAGGGCCTCGAAAG-3`). Real-time PCR analyses to quantify gene expression were conducted using a QuantStudio™6 Flex Real-Time PCR System (Applied Biosystems, Carlsbad, CA, USA). Briefly, reactions included SYBR green PCR master mix (Life Technologies), primers (1 μM), and cDNA template in a final reaction volume of 10 μL. Following an initial denaturing step (95°C for 10 minutes), denaturation, annealing and extension steps (95°C for 15 sec, 60°C for 1 minute) were repeated 40 times, and a dissociation step (95, 60 and 95°C for 15 sec each) was.

Each sample was measured in triplicate, and the relative expression level of each target gene was normalised to that of the reference gene *Rn18s* and was quantified using the ΔΔCt method.

2.8. Immunoassays for protein measurements

2.8.1. Protein extraction and sample preparation

Fragments of the frozen testes pieces were weighed and homogenised (n=6) in cold PBS (0.01M, pH 7.4) containing protease inhibitor cocktail III (CalBiochem, La Jolla, CA), using a TissueLyser II (Qiagen) for 20 seconds, then centrifuged for 10 minutes (14,000 g) to collect the supernatants for protein measurement.

2.8.2. Activin A ELISA

A specific activin A enzyme immunoassay using antibodies supplied by Oxford Brookes University was used to determine serum, testis and culture media levels of activin A, as described previously (O'Connor et al., 1999). The limit of detection for serum and testis activin A levels was 14.3 pg/mL, or 6.8 pg/mL for culture media. The mean inter- and intra- assay CVs for serum and testis levels were 6.2% and 4.7%, respectively. The mean inter- and intra- assay CVs for the culture media were 6.6% and 5.6%, respectively.

2.8.3. Activin B ELISA

Serum and tissue concentrations of activin B were measured, as described previously (Ludlow et al., 2009), using antibodies kindly supplied from Oxford Brookes University, and validated for measurement of activin B in rat tissues. The limit of detection for serum and testis levels was 23.4 pg/mL, or 9.5 pg/mL for the culture media. The mean inter- and intra- assay CVs for serum and testis levels were 12% and 7.7%, respectively. The mean inter- and intra- assay CVs for the culture media were 5.2% and 6.8%, respectively.

2.8.4. FSH, LH, total inhibin and follistatin radioimmunoassay

A discontinuous radioimmunoassay (RIA) was used to measure serum FSH and LH levels, and total inhibin and follistatin levels in testis homogenates, serum and culture media samples, as described previously (Robertson et al., 1988; Sun et al., 1990; Winnall et al., 2013). The FSH and

LH assay detection limits were 1.33 and 0.01 ng/mL respectively, while the mean intra-assay CV values were 3.3 and 4.1%, respectively. The total inhibin and follistatin assays detection limits for serum and testis levels were 0.16 and 1.03 ng/mL, while the mean intra-assay CV values were 4.5 and 8.8%, respectively. For the culture media, the total inhibin and follistatin assay detection limits were 1.60 and 0.51 ng/mL, while the mean intra-assay CVs were 8.8 and 13.2%, respectively.

2.8.5. Testosterone radioimmunoassay

Serum and testicular homogenate supernatants were measured using the Immunotech IM1119 RIA Testosterone direct assay, supplied by Beckman Coulter (CA, USA), according to the manufacturer's instructions. Samples and testosterone standards were assayed in 25 uL duplicates. The sensitivity of the assay was 32.6 pg/mL, with an intra-assay CV of 7.0%.

2.9. In vitro studies

2.9.1. Sertoli cell isolation and culture

Sertoli cells were isolated from 19-21 day-old Sprague-Dawley rats (n=12), as previously described (Nicholls et al., 2013). Briefly, isolated cells were plated at a density of 2.5 x 10^6 cells per cm^2 into 24-well culture plates (Nunc; Nalge Nunc International, Roskilde, Denmark) precoated with Matrigel (BD Biosciences, Bedford, MA). Cell cultures proceeded in DMEM/Hams F12 (Gibco, Carlsbad, CA), supplemented with 2.5 mM L-glutamine, 29 mM sodium bicarbonate, 1 × non-essential amino acids, dialysed bovine serum albumin (1% w/v, Sigma, St. Louis, MO), HEPES (10mM, Gibco), insulin (5 µg/mL, Novo-Nordisk, Sydney, Australia), transferrin (5 µg/mL, Sigma), sodium selenite (50 ng/mL, Sigma), Amphotericin B/Penicillin/Streptomycin (Gibco), human FSH (150 mIU/mL, Puregon, N.V. Organon) testosterone (28 ng/mL, Sigma) and retinoic acid (100nM, Sigma). Cells were then incubated at 32°C in a humidified 5% CO2/95% air incubator with a medium change at 48 h. At 72 h, contaminating germ cells were removed by hypotonic shock treatment with 10% culture media in water for 45 sec (Sluka et al., 2006), after which Sertoli cells were allowed to recover for a further 24 hours at 32°C, 5% CO_2/95% air.

2.9.2. In vitro hyperthermia

To mimic the in vivo hyperthermia treatment, the experimental group was removed at 120 hours from the incubator, momentarily sealed with paraffin film, placed for 15 minutes in a 43°C water bath, and then returned to the incubator at 32°C. Cell dishes kept and incubated at 32°C were used as the corresponding controls. The conditioned culture medium was collected at three time-points 6, 24 and 48 hours after heating, and snap frozen for protein quantification, and plated cells were processed for mRNA quantification by real-time PCR.

2.10. Statistical analysis

All statistical analyses were performed using GRAPHPAD PRISM 6 (Graphpad Software, Inc., La Jolla, CA, USA). Data sets with two variables were analysed using two-way analysis of variance (ANOVA) following suitable transformation to normalise the data and equalise variance in conjunction with a Sidak's multiple comparisons test, as appropriate. Statistical significance was accepted when $p < 0.05$. Data are expressed as mean ± standard deviation (SD).

3. Results

3.1. The testicular response

The testicular response to heat stress displayed three phases: (I) onset (1–2 weeks), (II) peak damage (2–8 weeks) and (III) recovery (12–14 weeks) (Figure 1A). One week after heat treatment, testis weight was significantly decreased by about 20%, and continued to decline by a further 20% of control values by 2 weeks (Figure 1A). Testis weight was still 30% lower than control at 8 weeks after heat treatment. Testis weight returned toward control levels by 12 weeks after heat treatment, but was again 15% lower than normal at 14 weeks.

The volume of TIF doubled one week after heat treatment, when compared with controls and remained elevated at 4–8 weeks (Figure 1B). During the recovery phase, TIF volume had returned to control values by week 12 after the heat treatment.

There were no gross histological changes in spermatogonia at any stage of the spermatogenic cycle, or in Sertoli cells or other somatic cells across the experimental period (Figure 2). During the onset phase, a marked loss of pachytene spermatocyte (PSC) and round spermatid (rST) populations was observed in stages I–VI of the cycle of the seminiferous epithelium (Figure 2B). Moreover, these cells, when present, demonstrated signs of apoptosis, indicated by nuclear condensation and confirmed by TUNEL staining (Figure 2D). Multiple intraepithelial vacuoles were observed in regions of severe pachytene spermatocyte loss (Figure 2B). Elongated spermatids were not visibly affected during the onset phase (weeks 1-2), but this population of germ cells was clearly depleted during weeks 4-8 (the peak damage phase) (Figure 2F). The seminiferous epithelium appeared histologically normal during the recovery phase (Figure 2H).

TUNEL staining of DNA fragmentation was assessed at three time points, one from each phase of damage and recovery (1, 8 and 14 weeks). An increase in the percentage of tubules with TUNEL-positive spermatocytes and spermatids (Figure 2D) by 55% (data not shown), relative to control (Figure 2C), at one week coincided with the disruption of spermatogenesis and degeneration of seminiferous tubules. However, no significant difference was identified in the numbers of TUNEL-positive cells in the heat-treated testes at either 8 or 14 weeks (data not shown). There was no evidence of TUNEL staining among the Sertoli and Leydig cells or spermatogonia.

3.2. Response of the hypothalamic-pituitary-testis axis

Serum FSH in the heat-treated rats was increased by 8 weeks after heat treatment (150% of control), and then returned to control levels (Figure 3A). This increase in FSH coincided with a significant decrease in serum and total intratesticular inhibin levels, but not the intratesticular concentration of inhibin, at 8 weeks after heat treatment (Figure 3B – 3D). A reduction in serum inhibin was also observed at 14 weeks after heat treatment, although this did not correlate with alterations in serum FSH or intratesticular inhibin.

Serum LH and testosterone, and total intratesticular level testosterone concentrations were not different between the control and heat-treated rats at any time point (Supp Figure 1A, B and C), intratesticular testosterone concentration was only elevated relative to control at 4 weeks (Supp Figure 1D). However, there was a large variation in testosterone levels in both control and heat-treated rats between different time-points, and the level of intratesticular testosterone at 4 weeks was not different from the intratesticular testosterone concentration of control rats at other time-points. This suggests that intratesticular testosterone were minimally altered following heat-induced testicular damage.

3.3. Response of Sertoli cells

The number of Sertoli cell nuclei per tubule profile appeared to decrease by 20% at one week after heat treatment, and returned to control for the remainder of the experiment (Figure 4A). However, when the mean Sertoli cell nuclei diameters were also measured in the one week group, this apparent decrease was found to be due to a decline in the Sertoli cell nuclear diameters to 85% of the control value (Figure 4B), suggesting that Sertoli cell function was altered. When calculated as Sertoli cell nuclei per unit volume of testis (determined from the testis weight), Sertoli cell number was not different in control and heat-treated testes (data not shown).

In spite of the fact that Sertoli cell numbers were unchanged, a marked elevation in the normalised expression of *Sox9* mRNA was observed at 1-2 weeks (Figure 4C). This was attributed to the relative increase in the proportion of Sertoli cell-derived mRNAs due to a loss of contribution to total mRNA by the meiotic germ cells (spermatocytes and early spermatids) during the onset phase (weeks 1-2). Consequently, all Sertoli cell-specific gene expression was normalised to *Sox9* expression.

The mRNA expression ratios of key Sertoli cell-specific genes, inhibin α subunit (*Inha*), and the blood-testis barrier (BTB) protein claudin-11 (*Cldn11*), relative to Sox9 were decreased by approximately 80% at 2 weeks (Figure 5A and B), corresponding to the time of maximum

spermatogenic cell damage. Other BTB genes, which are preferentially expressed by the Sertoli cell but also by other cell types, including connexin 43 (*Gja1*), claudin-3 (*Cldn3*) and zonula occludens-1 (*Tjp1*), followed the same expression pattern as *Cldn11* (Figure 5C-E). An apparent decrease in the expression of interleukin-1α (*Il1a*), an inflammatory cytokine produced constitutively by the rat Sertoli cell under normal conditions, did not reach significance (Figure 5F).

3.4. Response of Leydig cells

Similar to *Sox9*, the relative expression of the Leydig cell biomarker insulin-like 3 (*Insl3*) appeared to be upregulated during the onset phase only (Figure 6A), again coinciding with the peak loss of germ cells. Although *Insl3* has been shown to be androgen-responsive (Paust et al., 2002; Laguë and Tremblay, 2008), serum and intratesticular testosterone levels were predominantely unchanged throughout this study. The ratio of the mRNA of several key Leydig cells-specific steroidogenic enzymes, cytochrome P450 family 11 subfamily a polypeptide 1 (*Cyp11a1*), 3β-hydroxysteroid dehydrogenase (*Hsd3b1*) and 17β-hydroxysteroid dehydrogenase (*Hsd17b3*), to *Insl3* diminished by 50% at 2 weeks after heat treatment (Figure 6B, C and D).

The androgen receptor (*Ar*) is expressed by most somatic cells in the testis, but is not expressed by germ cells. When normalised to the total testis housekeeping gene, *Hprt*, or calculated as a ratio with *Insl3* there was no significant change in *Ar* mRNA expression across the various heat treatment groups (Supp Figure 2A and B). However, *Ar* mRNA was significantly reduced at 1-2 weeks after heat-treatment when expressed as a ratio with the other somatic cell standardisation gene, *Sox9* (Supp Figure 2C), which may indicate that there was a significant reduction in *Ar* expression at this time.

3.5. Response of activins and activin-related proteins

Total testicular contents of activin A and follistatin, but not activin B, decreased in the heat-treated rats during the peak damage phase (weeks 2-8) (Figure 7A and G), although this was not reflected in the intratesticular concentrations (Figure 7B and H), attributable to the corresponding loss of meiotic germ cells. By contrast, both total testicular activin B (Figure 7D) and the

concentration of activin B (Figure 7E) were significantly elevated (approximately two-fold at 8 weeks) in the testis during the peak damage phase.

The decrease in total activin A protein during the peak damage phase (Figure 7A), was not accompanied by corresponding changes in the relative expression of mRNA for the inhibin βA subunit (*Inhba*) (Figure 7C). This may be attributable to reduced stability or increased clearance of the activin A protein, relative to its mRNA. By contrast, the mRNA expression of inhibin βB subunit (*Inhbb*) was elevated at 4 weeks after heat treatment (Figure 7F), consistent with the observed increase in activin B protein during the peak damage phase (Figure 7D and E). Overall, the data are consistent with a reduction in activin A protein and corresponding increase in activin B protein and gene expression during the peak damage period.

In contrast to the changes in follistatin protein, follistatin (*Fst*) mRNA expression, which is expressed by most testicular cells (Meinhardt et al., 1998; Phillips and de Kretser, 1998), was considerably increased throughout the onset and peak damage phases (Figure 7I), although this increase was not reflected by follistatin protein levels during this period (Figure 7G). As in the case of activin A, this may be attributable to differential stability or clearance of the mRNA and protein species.

Serum levels of activin A, activin B and follistatin did not differ significantly between control and heat-treated animals, with the exception of a small (25%) decrease in activin A at one week and a 22% increase at 4 weeks after heat treatment (data not shown).

In order to assess the direct effect of acute heat on the Sertoli cell activin-related protein production, we exposed isolated rat Sertoli cells cultured at 32°C to acute heat treatment (43°C). There was no significant difference in activin A and B, total inhibin, and follistatin production in conditioned media from these cells over 48h of culture (Supp Figure. 3A-D). Similarly, no significant changes Sertoli cell gene expression (*Sox9, Inha, Cldn11, Il1a, Gja1* and *Krt18*) were observed (data not shown).

3.6. Stress and inflammatory responses

No significant changes were observed in vivo for the mRNA expression of two key pro-inflammatory cytokines, tumour necrosis factor (*Tnf*) (Figure 8A), or interleukin-6 (*Il6*) (data not shown), which increase dramatically in tissues during inflammation due to the activation and recruitment of immune cells.

The expression of a fibrotic gene marker, collagen 1a1 (*Col1a1*), was increased approximately two-fold at 4 weeks after heat treatment, but returned to control levels during the recovery phase (Figure 8B). By contrast, expression of another fibrotic marker gene, α smooth muscle (*Acta2*), was not altered (data not shown).

During the onset and peak damage phases, the mRNA expression of the germ cell-specific heat shock proteins (HSPs), *Hspa1a* and *Hspa1b,* was not affected, (Figure 8C and D). In contrast, *Hspa1l* mRNA showed a dramatic decline to 30% of the control expression at 2 weeks after heat treatment (Figure 8E) consistent with the peak testicular damage; thereafter, it returned to control levels at 4 weeks. Interestingly, both *Hspa1a* and *Hspa1b* genes showed 4-6fold increases respectively at 14 weeks after heat treatment (Figure 8C and D) suggesting a second wave of damage. However, no changes were observed in the expression of the HSPs regulatory gene, heat shock transcription factor 1(*Hsf1)* (data not shown).

4. Discussion

The results of this study extend previous observations of the significant damage that acute mild heat causes to spermatogenesis in the adult rat testis. Overall, this damage reflects the loss of the most heat-sensitive germ cell types, specifically the pachytene spermatocytes and early round spermatids, as previously observed (Bowler, 1972; Chowdhury and Steinberger, 1970; Lue et al., 1999). The germ cells affected at later time points were the elongated spermatids, which would have been derived from the damaged or lost spermatocytes and round spermatids, consistent with

the observed decline in testicular weight at 1–8 weeks. These findings suggest that the heat damage extended through two spermatogenic cycles. The testis damage was also accompanied by a considerable elevation in serum FSH at 8 weeks, which differs slightly from earlier reports that showed this increase occurring within the first 4 weeks of heat treatment (Au et al., 1987; Bartlett and Sharpe, 1987; Jegou et al. 1984). This inconsistency may be attributed to differences in experimental conditions between the studies. There were no changes in the serum LH and negligible effects on serum or testicular testosterone concentrations, again consistent with earlier observations (Jegou et al., 1984).

In the present study, we were able to correct for the relative loss of spermatogenic cell genes versus somatic cell genes by normalising our gene expression data to the Sertoli cell-specific gene, *Sox9*, and the Leydig cell-specific gene, *Insl*3. Consequently, we found that the initial loss of spermatogenic cells was accompanied by a reduction in the expression of key Sertoli cell and Leydig cell genes, and this coincided with the peak loss of meiotic germ cells at 2 weeks after the heat treatment. Despite the transient decline in the size of the Sertoli cell nuclei, which could indicate an early effect on the Sertoli cells during the onset phase, germ cell loss has been reported elsewhere to occur as early as 3 days following heat exposure (Bartlett and Sharpe 1987; Sharpe et al. 1991). The fact that the effects on Sertoli and Leydig cell gene expression occur subsequent to the loss of the germ cells is consistent with the suggestion that functional changes in Sertoli and Leydig cell could be secondary to the germ cell loss rather than being a direct effect of the heat stress (Jegou et al., 1984).

However, Cai et al. (2011) have reported an elevation in the expression of the *Cldn11* gene at both the mRNA and protein levels following a long heat treatment (43°C for 30 minutes). This increased expression likely reflects a gene normalisation issue, as the housekeeping gene (60S ribosomal protein L32, *Rpl32*) used by the Cai group is largely expressed by germ cells. Alternatively, it could be due to the longer duration of heat exposure than was used in the present study. The duration of heat exposure would clearly determine the degree of induced testicular damage.

This is the first study to document changes in the inhibin-related proteins following acute heat treatment. The reduction in activin A and the increase in activin B were delayed until the elongated spermatids were lost, which may reflect a specific effect of the mature spermatids on epithelial activin levels. At least part of this loss may be due to germ cell depletion, as rat spermatocytes and spermatids express activin A but only low levels of activin B (Wijayarathna and de Kretser, 2016). By contrast, follistatin is produced by most testicular cell types (Meinhardt et al., 1998; Phillips and de Kretser, 1998). Activin A regulation has been well studied (Okuma et al., 2006; Winnall et al., 2013), but the regulation of activin B is poorly understood. These data suggest that activin B production by Sertoli cells is regulated by elongated spermatids.

The data of the present study also provide clear evidence for an increase in the protein level of activin B, occurring contemporaneously with the decreased inhibin levels at 8 weeks. This may indicate that the β_B subunits of inhibin are used to form activin B due to the decline in inhibin α subunits. Conversely, the observed reduction in activin A may reflect a lower production of inhibin βA subunits by the Sertoli cells, owing to the loss of germ cells. The apparent discordance between the mRNA expression and measurable levels of inhibin, follistatin and the activins, particularly during the peak damage phase, is consistent with a complex cellular distribution and regulation of these proteins. The data presented here suggest that these proteins are regulated both at the transcriptional level and at the level of protein subunit synthesis and homo-heterodimer formation (Hedger and Winnall, 2012). Therefore, changes may occur in the total protein content, but not in the relative expression or concentration.

Our *in vitro* study revealed no visible changes in the Sertoli-cell–specific genes and proteins within 48 hours of heat treatment. Nevertheless, other *in vitro* studies have shown that acute heat stress causes structural and metabolic changes and disrupts the junctions of adjacent Sertoli cells (Chen et al., 2008; Vallés et al., 2014). These changes were observed in the heat-treated Sertoli cell after 24 hours in the rhesus monkey and 5 days in the mouse. Although our study did not look at the structural and metabolic markers of the Sertoli cell, the alterations observed in the previous studies arose due to the longer duration of the heat stress (i.e. 30 minutes; Chen et al., 2008) or the repeated

exposures to heat over 5 days (Vallés et al., 2014), both of which would increase the severity of damage. Taken together, our *in vitro* and *in vivo* findings suggest that the alterations in Sertoli cell function may not represent a direct effect of heat but instead are secondary to the disruption of the germ cell complement as previously suggested by Jegou et al. (1984).

With respect to Leydig cell function, our data show that the steroidogenic activity was also disrupted following heat treatment with down-regulation of several key steroidogenic enzyme genes, *Cyp11a1*, *Hsd3b1* and *Hsd17b3* at 2 weeks. Nonetheless, no adverse effect was observed on serum and testicular testosterone levels. These data agree with the findings of Hwang et al. (2010), who showed a decline in the protein levels of the steroidogenic enzymes, StAR and P450c17, at 4 weeks after heat treatment in the adult rat. However, the heat treatment used by the Hwang group consisted of exposing the testis to a temperature ranges 41- 43°C for 10 minutes, twice daily for 3 days per week, over a 4 week period. In addition, this study only evaluated protein levels of the steroidogenic enzymes while no mRNA level was examined. Hence our data shows that these enzymes are acutely affected by heat, and that these changes continue within the epithelium in a model of chronic heat exposure, which would be expected to cause more damage.

The effects of acute heat treatments on Leydig cell functions were reported in earlier investigations that demonstrated changes in Leydig cell morphology and testosterone production. These morphological changes, which include accumulation of lipid droplets, the appearance of a dilated smooth endoplasmic reticulum, mitochondrial swelling, and the disappearance of mitochondrial cristae, have been observed by a number of investigators within the 35 days of heat exposure (Aktas and Kanter, 2009; Damber et al., 1980). The intracytoplasmic lipid droplets are documented to include substrates for steroidogenesis, and the lipid accumulation indicates impaired steroidogenesis (Christensen, 1975). However, the mechanisms by which heat induces functional alterations in Leydig cells are poorly characterised.

Our finding that testosterone secretion was mostly unaffected by heat is consistent with several previous observations (Au et al., 1987; Damber et al., 1980; Hwang et al., 2010). This was

in spite of the fact that the expression of several steroidogenic genes was decreased during the onset phase. However, other studies have reported a temporary alteration in serum testosterone in response to heat (Aktas and Kanter, 2009; Lue et al., 1999), which has been attributed to suppression of the steroidogenic enzymes (Murphy et al., 2001). Hwang et al. (2010) claimed that testosterone levels may be affected by a temporary elevation in the secretion of adrenal androgen. It would appear that the effects of heat on intratesticular and serum testosterone may be marginal, even though Leydig cell function is affected.

One critical point that arises from the findings of our study is that the data provide no evidence for any significant heat-stress, inflammatory or fibrotic response, either as a cause or consequence of the extensive germ cell damage. No consistent elevation was noted for heat-shock protein expression or for the production of the key inflammatory cytokine, TNF, and only minor effects were seen for key fibrotic gene expression. However, transient events may have been missed, particularly early in the process. An acute inflammatory response would be expected to occur within the first 24 hours of heat treatment, but this time point was not investigated in the current study.

The present results also emphasise that the effect of acute heat is not fully reversible, as evidenced by the failure of the testis weight to return to a normal level; this finding agrees with those of previous studies (Setchell et al., 2001, 2002). Notably, although Setchell's group used a 30-minute duration for heat exposure, whereas we used 15 minutes in the present study, we still observed damage for up to 14 weeks. Curiously, in the present study, *Hspa1a* and *Hspa1b* genes expression showed a maximum response at 14 weeks after heat exposure, which confirms the findings on testis weight, that indicated a second wave of damage. In contrast, the mRNA expression of *Hspa1l* was downregulated at 2 weeks only coinciding with peak germ cell loss. *Hspa1l* is a known inducible HSP, which is expressed in response to different hyperthermic conditions (Rockett et al., 2001; Widlak et al., 2007). The death of spermatogenic cells may be explained by the loss of anti-apoptotic properties of HSPs, and their ability to interfere with caspase activation (Radons, 2016). Germ cell apoptosis has been reported to occur as a result of disruption

of the testis-specific isoform of HSPs (Dix et al., 1996). Even though the *Hspa1l* response was exclusively seen in our study at 2 weeks, previous literature indicates that an acute response is observed within 3–5 hours following heat stress (Kiang and Tsokos, 1998).

In conclusion, the data presented here indicate that acute heat stress affects gene expression in Sertoli cells and Leydig cells and the production of inhibin-related proteins, particularly the activins, possibly mediated through changes in the germ cell complement, as previously suggested (Jegou et al., 1984). Changes in Leydig cell function are most likely the result of local factors produced by Sertoli cells or germ cells, suggesting intercompartmental communication (Bergh, 1982; de Kretser, 1982). The data from the present study also highlight the need to raise awareness, particularly for couples suffering from poor fertility, about the detrimental effects of prolonged heat exposure of the testes on fertility.

Acknowledgements

This research was supported by funding provided by Imam Abdulrahman Bin Faisal University in Saudi Arabia (8559246), the National Health and Medical Research Council of Australia and the Victorian State Government Operational Infrastructure Support Program. We thank Oxford Brookes University for kindly supplying the antibody reagents E4 and 46 A/F used in the activin A and B assays, Adnan Sali and Julie Muir for assistance in animal procedures, and Susan Hayward for her expert immunoassay skills and assistance. Furthermore, the authors thank the MHTP Medical Genomics Facility for assistance with the Fluidigm analysis.

Declaration of interest

The authors declare no conflict of interest with respect to this study.

Author's contributions

Conceived and designed the experiments: DDK, MPH, RA.

Performed the experiments: RA.

Reagents/activin A and B assay techniques: HL.

Analysed the data: RA, MPH.

Critical discussion of data: RA, MPH, DDK, PGS.

Wrote the manuscript: RA, MPH.

Critical review of manuscript: all authors.

Table 1. List of Taqman assays used

* indicates genes used in the in vivo study only, ** in vitro study only. Includes data from Chalmel et al. (2007), Gérard et al. (1991) and searchable GermOnline database (Lardenois et al., 2010).

Protein name	Gene symbol	Life Tech assay code	Main cell sites of expression in testis
Glyceraldehyde-3-phosphate dehydrogenase	*Gapdh*	Rn01775763_g1	All cell types
Succinate dehydrogenase complex flavoprotein subunit A	*Sdha**	Rn00590475_m1	
18S ribosomal RNA	*Rn18s***	Designed	
Inhibin βA subunit	*Inhba*	Rn01538592_m1	Somatic cells and germ cells
Inhibin βB subunit	*Inhbb*	Rn01753772_m1	
Follistatin	*Fst*	Rn00561225_m1	
Heat shock factor 1	*Hsf1*	Rn00801772_m1	
α smooth muscle actin	*Acta2*	Rn01759928_g1	
Collagen 1α type 1	*Col1a1*	Rn01463848_m1	
SRY box 9	*Sox9***	Rn01751070_m1	Sertoli cells
Inhibin α subunit	*Inha*	Rn00561423_m1	
Claudin 11	*Cldn11*	Rn00584941_m1	
Interleukin 1α	*Il1a*	Rn00566700_m1	
Claudin 3	*Cldn3**	Rn00581751_s1	
Hydroxy δ 5 steroid dehydrogenase 3 β and steroid δ isomerase 1	*Hsd3b1*	Rn01774741_m1	Leydig cells
Hydroxysteroid 17- β dehydrogenase 3	*Hsd17b3*	Rn00588942_m1	
Cytochrome P450 family 11 subfamily a polypeptide 1	*Cyp11a1*	Rn00568733_m1	
Heat shock protein 70-1	*Hspa1a*	Rn02532795_s1	Spermatogonia
Heat shock protein 70-2	*Hspa1b*	Rn04224718_u1	
Hypoxanthine phosphoribosyltransferase	*Hprt**	Rn01527840_m1	Sertoli cells and spermatogonia
Zonula occludens 1	*TJp1**	Rn02116071_s1	
Connexin 43	*Gja1*	Rn01433957_m1	
Keratin 18	*Krt18***	Rn01533360_g1	
Crystallin alpha B	*Cryab***	Rn01421541_m1	Sertoli and Leydig cells
Heat shock protein 70-3	*Hspa1l*	Rn01525984_m1	Spermatocytes and round spermatids
Interleukin 6	*Il6*	Rn01410330_m1	Activated immune cells, somatic cells and germ cells
TNFα	*Tnf*	Rn99999017_m1	
Androgen receptor	*Ar*	Rn00560747_m1	Somatic cells

Figures Legends

Figure 1. Changes in (A) testis weight and (B) the volume of recovered testicular interstitial fluid (TIF) of rats after heat-treatment. Data are mean ± SD (n = 7/group for testis weights and n=4/group for TIF volumes) and comparisons were made between the treatment and corresponding control values at each time-point using two-way ANOVA and Sidak`s multiple comparisons test: *p<0.05, **p<0.01, ***p<0.001 and **** p < 0.0001.

Figure 2. Histology and TUNEL staining of the testis in control and heat-treated rats. Periodic acid–Schiff stained tissue sections of the testis show the differences between the control and heat-treated rats at 1 week (A-D, representing the onset phase), 4 weeks (E and F, peak damage phase) and 12 weeks (G and H, recovery phase). Pachytene spermatocytes and round spermatids were lost from the seminiferous epithelium after 1 week of heat treatment (panel B: arrowhead), along with frequent degenerating cells (B: small arrow) and vacuoles (B: large arrow). TUNEL staining revealed differences in apoptosis in the heat-treated rats (panel D: arrows) compared with the control (C), especially during onset phase of heat damage at (1 week). Progression to loss of elongated spermatids during the peak damage phase was accompanied by recovery of the spermatocytes (panel F: arrows). All spermatogenic cells had largely reappeared by the recovery phase (12 weeks) (H) and the testes appeared similar to controls (G). All scale bars represent 25 μm. Roman numbers indicate the stages of seminiferous cycle.

Figure 3. Response of hypothalamic-pituitary-testis axis showing the changes in the serum FSH (A), serum inhibin (B), total testicular inhibin content (C) and inhibin concentration in the testis (D) after heat treatment. Data are mean ± SD (n = 7/group for serum FSH and inhibin, and n=6/group for testicular inhibin) and comparisons were made between the treatment and corresponding control values at each time-point using two-way ANOVA and Sidak`s multiple comparisons test: **p<0.01, ***p<0.001 and ****p < 0.0001.

Figure 4. Response of the Sertoli cells *in vivo* to heat treatment. Sertoli cell nuclear profiles per tubule were reduced by 20% at 1 week (A), but this corresponded with a significant decrease in nuclear diameter at this time (B). When corrected for the reduction in nuclear size, Sertoli cell numbers were found to be no different between control and heat-treated rats. The relative expression of the Sertoli cell marker gene *Sox9* was increased at 1 and 2 weeks after heat treatment, corresponding with the period of maximum depletion of spermatocytes. Data are mean ± SD (n = 4/ group for Sertoli cell counting, and n = 6 /group for mRNA expression) and comparisons were made between the treatment and corresponding control values at each time-point using two-way ANOVA and Sidak`s multiple comparisons test: ***p < 0.001, ****p <0.0001 and NS >0.05.

Figure 5. Response of Sertoli cell-specific genes *in vivo* to heat treatment. At the onset phase (1-2 weeks), there was a down-regulation of relative mRNA expression of several Sertoli cell-specific genes when normalised to the Sertoli cell constitutively expressed gene, *Sox9*: *Inha* (A), *Cldn11* (B), *Gja1* (C), *Tjp1* (D) *and Cldn3* (E). While *Il1a* expression also appeared to be reduced at this time, this difference was not significant (F). Data are mean ± SD (n = 6 /group) and comparisons were made between the treatment and corresponding control values at each time-point using two-way ANOVA and Sidak`s multiple comparisons test: *p < 0.05, **p <0.01, and ***p < 0.001, ****p <0.0001 and NS > 0.05.

Figure 6. Response of Leydig Cell specific genes**.** Comparison of mRNA expression of the Leydig cell-specific genes *Insl3* (A), *Cyp11a1* as a ratio with *Insl3* (B), *HSD3b1* as a ratio with *Insl3* (C) and *HSD17b3* as a ratio with *Insl3* (D) after heat treatment. Data are mean ± SD (n = 6 /group) and comparisons were made between the treatment and corresponding control values at each time-point using two-way ANOVA and Sidak`s multiple comparisons test: *p < 0.05, **p <0.01, and ***p < 0.001, and ****p <0.0001.

Figure 7. Response of activins and activin-related proteins and genes expression. Comparison of the total testicular content of activin A (A), activin B (D) and follistatin (G), and intratesticular concentrations of activin A (B), activin B (E) and follistatin (H), and mRNA expression of *Inhba* (C), *Inhbb* (F) and *Fst* (I) genes after heat treatment. Data are mean ± SD (n = 6/group) and comparisons were made between the treatment and corresponding control values at each time-point using two-way ANOVA and Sidak`s multiple comparisons test: *p<0.05, **p<0.01 and ****p<0.0001.

Figure 8. Stress and inflammatory responses. Comparison of mRNA expression of inflammatory marker gene, *Tnf* (A), fibrotic marker gene, *Col1a1* (B), and heat shock proteins (HSPs) genes, *Hspa1a* (C), *Hspa1*l (D) and *Hspa1b* (E) after heat treatment. Data are mean ± SD (n = 6 /group) and comparisons were made between the treatment and corresponding control values at each time-point using two-way ANOVA and Sidak`s multiple comparisons test: *p<0.05, ***p < 0.001 and ****p < 0.0001.

Supplementary data:

Supp Figure 1. Response of hypothalamic-pituitary-testis axis showing the changes in the serum LH (A), serum testosterone (B), total testicular testosterone content (C) and testosterone concentration in the testis (D) after heat treatment. Data are mean ± SD (n = 7/group for serum FSH and testosterone, and n=6/group for testicular testosterone) and comparisons were made between the treatment and corresponding control values at each time-point using two-way ANOVA and Sidak`s multiple comparisons test: **p<0.01.

Supp Figure 2. Response of androgen receptor (*Ar*) gene *in vivo* to heat treatment. At the onset phase (1-2 weeks), there was a down-regulation of the ratio of mRNA expression of *Ar* gene to the Sertoli cell constitutively expressed gene, *Sox9* (A). By contrast, the relative expression of *Ar* (B) and its ratio with *Insl3* (C*)* were not significantly different at any time point. Data are mean ± SD (n = 6 /group) and comparisons were made between the treatment and corresponding control values at each time-point using two-way ANOVA and Sidak`s multiple comparisons test: **p <0.01, ***p < 0.001, and NS > 0.05.

Supp Figure 3. Response of the Sertoli cells *in vitro* to heat treatment. Comparison of the immature Sertoli cells production of activin A (A), activin B (B), total inhibin (C), and follistatin (D) of rats at 6, 24 and 48 hours after heat exposure for 15 minutes at 43°C with control incubated at 32°C. Data are mean ± SD (n = 4/group) from a representative experiment and comparisons were made between the treatment and corresponding control values at each time-point using two-way ANOVA and Sidak`s multiple comparisons test: no significant differences were observed in two experiments. The broken line indicates the detection limit of the assay.

References

Abercrombie, M., 1946. Estimation of nuclear population from microtome sections. Anat. Rec. 94, 239–247.

Aktas, C., Kanter, M., 2009. A morphological study on Leydig cells of scrotal hyperthermia applied rats in short-term. J. Mol. Histol. 40, 31–39.

Au, C.L., Robertson, D.M., de Kretser, D.M., 1987. Changes in Testicular Inhibin after a Single Episode of Heating of Rat Testes. Endocrinology 120, 973–977.

Baburski, A.Z., Sokanovic, S.J., Janjic, M.M., Stojkov-Mimic, N.J., Bjelic, M.M., Andric, S.A., Kostic, T.S., 2015. Melatonin replacement restores the circadian behavior in adult rat Leydig cells after pinealectomy. Mol. Cell. Endocrinol. 413, 26–35.

Barakat, B., Itman, C., Mendis, S.H., Loveland, K.L., 2012. Activins and inhibins in mammalian testis development: New models, new insights. Mol. Cell. Endocrinol. 359, 66–77.

Bartlett, J.M.S., Sharpe, R.M., 1987. Effect of local heating of the rat testis on the levels in interstitial fluid of a putative paracrine regulator of the Leydig cells and its relationship to changes in Sertoli cell secretory function. J. Reprod. Fertil. 80, 279–287.

Bergh, A., 1982. Local differences in Leydig cell morphology in the adult rat testis: evidence for a local control of Leydig cells by adjacent seminiferous tubules. Int. J. Androl. 5, 325–330.

Bergh, A., Söder, O., 2007. Studies of cryptorchidism in experimental animal models. Acta Paediatr. 96, 617–621.

Bienvenu, L.A., Morgan, J., Reichelt, M.E., Delbridge, L.M., Young, M.J., 2017. Chronic in vivo nitric oxide deficiency impairs cardiac functional recovery after ischemia in female (but not male) mice. J. Mol. Cell. Cardiol. 112, 8–15.

Bowler, K., 1972. The effect of repeated applications of heat on spermatogenesis in the rat: a histological study. J. Reprod. Fertil. 28, 325–333.

Cai, H., Ren, Y., Li, X.X., Yang, J.L., Zhang, C.P., Chen, M., Fan, C.H., Hu, X.Q., Hu, Z.Y., Gao, F., 2011. Scrotal heat stress causes a transient alteration in tight junctions and induction of TGF- β expression. Int. J. Androl. 34, 352–362.

Carlsen, E., Andersson, A.M., Petersen, J.H., Skakkebæk, N.E., 2003. History of febrile illness and variation in semen quality. Hum. Reprod. 18, 2089–2092.

Chalmel, F., Rolland, A.D., Niederhauser-Wiederkehr, C., Chung, S.S., Demougin, P., Gattiker, A., Moore, J., Patard, J.-J., Wolgemuth, D.J., Jégou, B., 2007. The conserved transcriptome in human and rodent male gametogenesis. Proc. Natl. Acad. Sci. 104, 8346–8351.

Chen, M., Cai, H., Yang, J.L., Lu, C.L., Liu, T., Yang, W., Guo, J., Hu, X.Q., Fan, C.H., Hu, Z.Y. and Gao, F., , 2008. Effect of heat stress on expression of junction-associated molecules and upstream factors androgen receptor and Wilms' tumor 1 in monkey Sertoli cells. Endocrinology 149, 4871–4882.

Chowdhury, A., Steinberger, E., 1970. Early changes in the germinal epithelium of rat testes following exposure to heat. J. Reprod. Fertil. 22, 205–212.

Christensen, A.K. 1975. Leydig cells, in: Hamilton, D.W., Creep, R.O. (Eds.), Handbook of Physiology. American Physiological Society, Washington D.C., Section 7, Vol. 5, pp.57–94.

Damber, J.E., Bergh, A., Janson, P.O., 1980. Leydig cell function and morphology in the rat testis after exposure to heat. Andrologia 12, 12–19.

de Kretser, D.M., 1982. Sertoli cell—Leydig cell interaction in the regulation of testicular function. Int. J. Androl. 5, 11–17.

de Kretser, D.M., Hedger, M.P., Loveland, K.L., Phillips, D.J., 2002. Inhibins, activins and follistatin in reproduction. Hum. Reprod. Update 8, 529–541.

Dix, D.J., Allen, J.W., Collins, B.W., Mori, C., Nakamura, N., Poorman-Allen, P., Goulding, E.H., Eddy, E., 1996. Targeted gene disruption of Hsp70-2 results in failed meiosis, germ cell apoptosis, and male infertility. Proc. Natl. Acad. Sci. 93, 3264–3268.

Durairajanayagam, D., Agarwal, A., Ong, C., 2014. Causes, effects and molecular mechanisms of testicular heat stress. Reprod. Biomed. Online 30, 14–27.

Gao, J., Zuo, Y., So, K.-H., Yeung, W.S., Ng, E.H., Lee, K.-F., 2012. Electroacupuncture enhances spermatogenesis in rats after scrotal heat treatment. Spermatogenesis 2, 53–62.

Gasinska, A., Hill, S., 1989. The effect of hyperthermia on the mouse testis. Neoplasma 37, 357–366.

Gérard, N., Syed, V., Bardin, W., Genetet, N., Jégou, B., 1991. Sertoli cells are the site of interleukin-1 α synthesis in rat testis. Mol. Cell. Endocrinol. 82, R13–R16.

Hedger, M.P., Drummond, A.E., Robertson, D.M., Risbridger, G.P., de Kretse, D.M., 1989. Inhibin and activin regulate [^{3}H] thymidine uptake by rat thymocytes and 3T3 cells in vitro. Mol. Cell. Endocrinol. 61, 133–138.

Hedger, M.P., Winnall, W.R., 2012. Regulation of activin and inhibin in the adult testis and the evidence for functional roles in spermatogenesis and immunoregulation. Mol. Cell. Endocrinol. 359, 30–42.

Hedger, M.P., Winnall, W.R., Phillips, D.J., de Kretser, D.M., 2011. The regulation and functions of activin and follistatin in inflammation and immunity. Vitam. Horm. 85, 255–297.

Hou, Y., Wang, X., Lei, Z., Ping, J., Liu, J., Ma, Z., Zhang, Z., Jia, C., Jin, M., Li, X., 2015. Heat Stress Induced Metabolic Changes and Altered Male Reproductive Function. J. Proteome Res. 14, 1495–1503.

Houston, B.J., Nixon, B., Martin, J.H., De Iuliis, G.N., Trigg, N.A., Bromfield, E.G., McEwan, K.E., Aitken, R.J., 2018. Heat exposure induces oxidative stress and DNA damage in the male germ line. Biol. Reprod. 98, 593–606.

Hwang, E.C., Dai Min, K., Jung, S.I., Ryu, S.B., Ahn, K.Y., Lee, K., Park, K., 2010. Testicular steroidogenesis is decreased by hyperthermia in old rats. Urol. Int. 84, 347–352.

Jegou, B., Laws, A.O., de Kretser, D.M., 1984. Changes in testicular function induced by short‐term exposure of the rat testis to heat: further evidence for interaction of germ cells, Sertoli cells and Leydig cells. Int. J. Androl. 7, 244–257.

Jones, K.L., Mansell, A., Patella, S., Scott, B.J., Hedger, M.P., de Kretser, D.M., Phillips, D.J., 2007. Activin A is a critical component of the inflammatory response, and its binding protein, follistatin, reduces mortality in endotoxemia. Proc. Natl. Acad. Sci. 104, 16239–16244.

Kent, J., Wheatley, S.C., Andrews, J.E., Sinclair, A.H., Koopman, P., 1996. A male-specific role for SOX9 in vertebrate sex determination. Development 122, 2813–2822.

Kiang, J.G., Tsokos, G.C., 1998. Heat shock protein 70 kDa: molecular biology, biochemistry, and physiology. Pharmacol. Ther. 80, 183-201.

Laguë, E., Tremblay, J.J., 2008. Antagonistic effects of testosterone and the endocrine disruptor mono-(2-ethylhexyl) phthalate on INSL3 transcription in Leydig cells. Endocrinology 149, 4688–4694.

Lardenois, A., Gattiker, A., Collin, O., Chalmel, F., Primig, M., 2010. GermOnline 4.0 is a genomics gateway for germline development, meiosis and the mitotic cell cycle. Database 2010. (http://www.germonline.org/index.html).

Ludlow, H., Phillips, D.J., Myers, M., McLachlan, R.I., De Kretser, D.M., Allan, C.A., Anderson, R.A., Groome, N.P., Hyvönen, M., Colin Duncan, W., 2009. A new 'total'activin B enzyme‐linked immunosorbent assay (ELISA): development and validation for human samples. Clin. Endocrinol. 71, 867–873.

Lue, Y.H., Lasley, B.L., Laughlin, L.S., Swerdloff, R.S., Hikim, A.P.S., Leung, A., Overstreet, J.W., Wang, C., 2002. Mild testicular hyperthermia induces profound transitional spermatogenic suppression through increased germ cell apoptosis in adult cynomolgus monkeys (Macaca fascicularis). J. Androl. 23, 799–805.

Lue, Y.-H., Sinha Hikim, A.P., Swerdloff, R.S., Im, P., Taing, K.S., Bui, T., Leung, A., Wang, C., 1999. Single Exposure to Heat Induces Stage-Specific Germ Cell Apoptosis in Rats: Role of Intratesticular Testosterone on Stage Specificity. Endocrinology 140, 1709–1717.

Marchetti, C., Hamdane, M., Mitchell, V., Mayo, K., Devisme, L., Rigot, J.M., Beauvillain, J.C., Hermand, E., Defossez, A., 2003. Immunolocalization of inhibin and activin α and βB subunits and expression of corresponding messenger RNAs in the human adult testis. Biol. Reprod. 68, 230–235.

McLean, D.J., Russell, L.D., Griswold, M.D., 2002. Biological activity and enrichment of spermatogonial stem cells in vitamin A-deficient and hyperthermia-exposed testes from mice based on colonization following germ cell transplantation. Biol. Reprod. 66, 1374–1379.

Meehan, T., Schlatt, S., O'Bryan, M.K., de Kretser, D.M., Loveland, K.L., 2000. Regulation of germ cell and Sertoli cell development by activin, follistatin, and FSH. Dev. Biol. 220, 225–237.

Meinhardt, A., O'Bryan, M.K., McFarlane, J.R., Loveland, K.L., Mallidis, C., Foulds, L.M., Phillips, D.J., de Kretser, D.M., 1998. Localization of follistatin in the rat testis. J. Reprod. Fertil. 112, 233–241.

Murphy, B.D., Lalli, E., Walsh, L.P., Liu, Z., Soh, J., Stocco, D.M., Sassone-Corsi, P., 2001. Heat shock interferes with steroidogenesis by reducing transcription of the steroidogenic acute regulatory protein gene. Mol. Endocrinol. 15, 1255–1263.

Nicholls, P.K., Harrison, C.A., Rainczuk, K.E., Vogl, A.W., Stanton, P.G., 2013. Retinoic acid promotes Sertoli cell differentiation and antagonises activin-induced proliferation. Mol. Cell. Endocrinol. 377, 33–43.

Nicholls, P.K., Stanton, P.G., Chen, J.L., Olcorn, J.S., Haverfield, J.T., Qian, H., Walton, K.L., Gregorevic, P., Harrison, C.A., 2012. Activin signaling regulates Sertoli cell differentiation and function. Endocrinology 153, 6065–6077.

O'Connor, A.E., McFarlane, J.R., Hayward, S., Yohkaichiya, T., Groome, N.P., de Kretser, D.M., 1999. Serum activin A and follistatin concentrations during human pregnancy: a cross-sectional and longitudinal study. Hum. Reprod. 14, 827–832.

Ohga, E., Matsuse, T., Teramoto, S., Katayama, H., Nagase, T., Fukuchi, Y., Ouchi, Y., 1996. Effects of activin A on proliferation and differentiation of human lung fibroblasts. Biochem. Biophys. Res. Commun. 228, 391–396.

Okuma, Y., O'Connor, A.E., Hayashi, T., Loveland, K.L., de Kretser, D.M., Hedger, M.P., 2006. Regulated production of activin A and inhibin B throughout the cycle of the seminiferous epithelium in the rat. J. Endocrinol. 190, 331–340.

Paul, C., Murray, A.A., Spears, N., Saunders, P.T., 2008. A single, mild, transient scrotal heat stress causes DNA damage, subfertility and impairs formation of blastocysts in mice. Reproduction 136, 73–84.

Paust, H.J., Wessels, J., Ivell, R., Mukhopadhyay, A.K., 2002. The expression of the RLF/INSL3 gene is reduced in Leydig cells of the aging rat testis. Exp. Gerontol. 37, 1461–1467.

Phillips, D.J., de Kretser, D.M., 1998. Follistatin: a multifunctional regulatory protein. Front. Neuroendocrinol. 19, 287–322.

Radons, J., 2016. The human HSP70 family of chaperones: where do we stand? Cell Stress Chaperones 21, 379–404.

Roberts, V., Meunier, H., Sawchenko, P., Vale, W., 1989. Differential production and regulation of inhibin subunits in rat testicular cell types. Endocrinology 125, 2350–2358.

Robertson, D.M., Hayward, S., Irby, D., Jacobsen, J., Clarke, L., McLachlan, R.I., de Kretser, D.M., 1988. Radioimmunoassay of rat serum inhibin: changes after PMSG stimulation and gonadectomy. Mol. Cell. Endocrinol. 58, 1–8.

Rockett, J.C., Mapp, F.L., Garges, J.B., Luft, J.C., Mori, C., Dix, D.J., 2001. Effects of hyperthermia on spermatogenesis, apoptosis, gene expression, and fertility in adult male mice. Biol. Reprod. 65, 229–239.

Sadeghian, H., Anand-Ivell, R., Balvers, M., Relan, V., Ivell, R., 2005. Constitutive regulation of the Insl3 gene in rat Leydig cells. Mol. Cell. Endocrinol. 241, 10–20.

Setchell, B.P., Ploen, L., Ritzen, E.M., 2001. Reduction of long-term effects of local heating of the testis by treatment of rats with a GnRH agonist and an anti-androgen. Reproduction 122, 255–263.

Setchell, B.P., Ploen, L., Ritzen, E.M., 2002. Effect of local heating of rat testes after suppression of spermatogenesis by pretreatment with a GnRH agonist and an anti-androgen. Reproduction 124, 133–140.

Sharpe, R.M., Bartlett, J.M.S., Allenby, G., 1991. Evidence for the control of testicular interstitial fluid volume in the rat by specific germ cell types. J. Endocrinol. 128, 359–NP.

Sharpe, R.M., Cooper, I., 1983. Testicular interstitial fluid as a monitor for changes in the intratesticular environment in the rat. J. Reprod. Fertil. 69, 125–135.

Sluka, P., O'Donnell, L., Bartles, J.R., Stanton, P.G., 2006. FSH regulates the formation of adherens junctions and ectoplasmic specialisations between rat Sertoli cells in vitro and in vivo. J. Endocrinol. 189, 381–395.

Sun, Y.T., Wreford, N.G., Robertson, D.M., de Kretser, D.M., 1990. Quantitative cytological studies of spermatogenesis in intact and hypophysectomized rats: identification of androgen-dependent stages. Endocrinology 127, 1215–1223.

Vallés, A.S., Aveldaño, M.I., Furland, N.E., 2014. Altered lipid homeostasis in Sertoli cells stressed by mild hyperthermia. PLoS One 9, e91127.

Wang, C., Cui, Y.G., Wang, X.H., Jia, Y., Sinha Hikim, A., Lue, Y.H., Tong, J.-S., Qian, L.X., Sha, J.H., Zhou, Z.M., 2007. Transient scrotal hyperthermia and levonorgestrel enhance testosterone-induced spermatogenesis suppression in men through increased germ cell apoptosis. J. Clin. Endocrinol. Metab. 92, 3292–3304.

Wang, J., Wreford, N.G.M., Lan, H.Y., Atkins, R., Hedger, M.P., 1994. Leukocyte populations of the adult rat testis following removal of the Leydig cells by treatment with ethane dimethane sulfonate and subcutaneous testosterone implants. Biol. Reprod. 51, 551–561.

Widlak, W., Vydra, N., Malusecka, E., Dudaladava, V., Winiarski, B., Ścieglińska, D., Widlak, P., 2007. Heat shock transcription factor 1 down‐regulates spermatocyte‐specific 70 kDa heat shock protein expression prior to the induction of apoptosis in mouse testes. Genes to Cells 12, 487–499.

Wijayarathna, R., de Kretser, D.M., 2016. Activins in reproductive biology and beyond. Hum. Reprod. Update 22, 342–357.

Winnall, W.R., Wu, H., Sarraj, M.A., Rogers, P.A., de Kretser, D.M., Girling, J.E., Hedger, M.P., 2013. Expression patterns of activin, inhibin and follistatin variants in the adult male mouse reproductive tract suggest important roles in the epididymis and vas deferens. Reprod. Fertil. Dev. 25, 570–580.

Wu, X., Liu, J., Duan, Y., Gao, S., Lü, Y., Li, X., Zhu, Q., Chen, X., Lin, J., Ye, L., 2017. A Short-Term Exposure to Tributyltin Blocks Leydig Cell Regeneration in the Adult Rat Testis. Front. Pharmacol. 8, 704.

Yamashita, S., Maeshima, A., Kojima, I., Nojima, Y., 2004. Activin A is a potent activator of renal interstitial fibroblasts. J. Am. Soc. Nephrol. 15, 91–101.

Zhang, W.X., Fan, J., Ma, J., Rao, Y.S., Zhang, L., Yan, Y.E., 2016. Selection of suitable reference genes for quantitative real-time PCR normalization in three types of rat adipose tissue. Int. J. Mol. Sci. 17, 968.

Figure 1

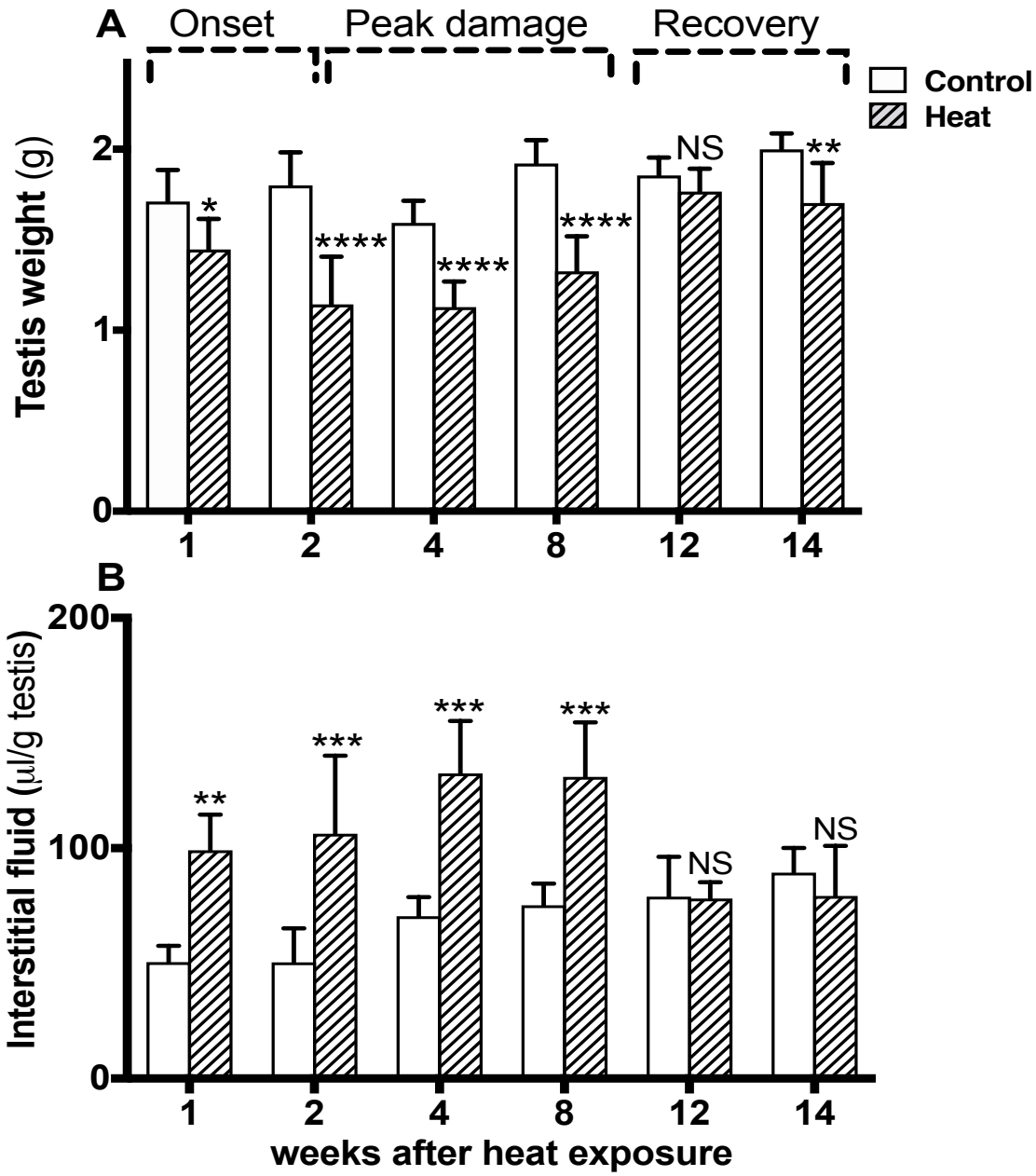
A
Onset
Peak damage
Recovery
Control
Heat
Testis weight (g)
2
1
0
*
****
****
****
NS
**
1
2
4
8
12
14
B
Interstitial fluid (µl/g testis)
200
100
0
**
***
***
***
NS
NS
1
2
4
8
12
14
weeks after heat exposure

Figure 2

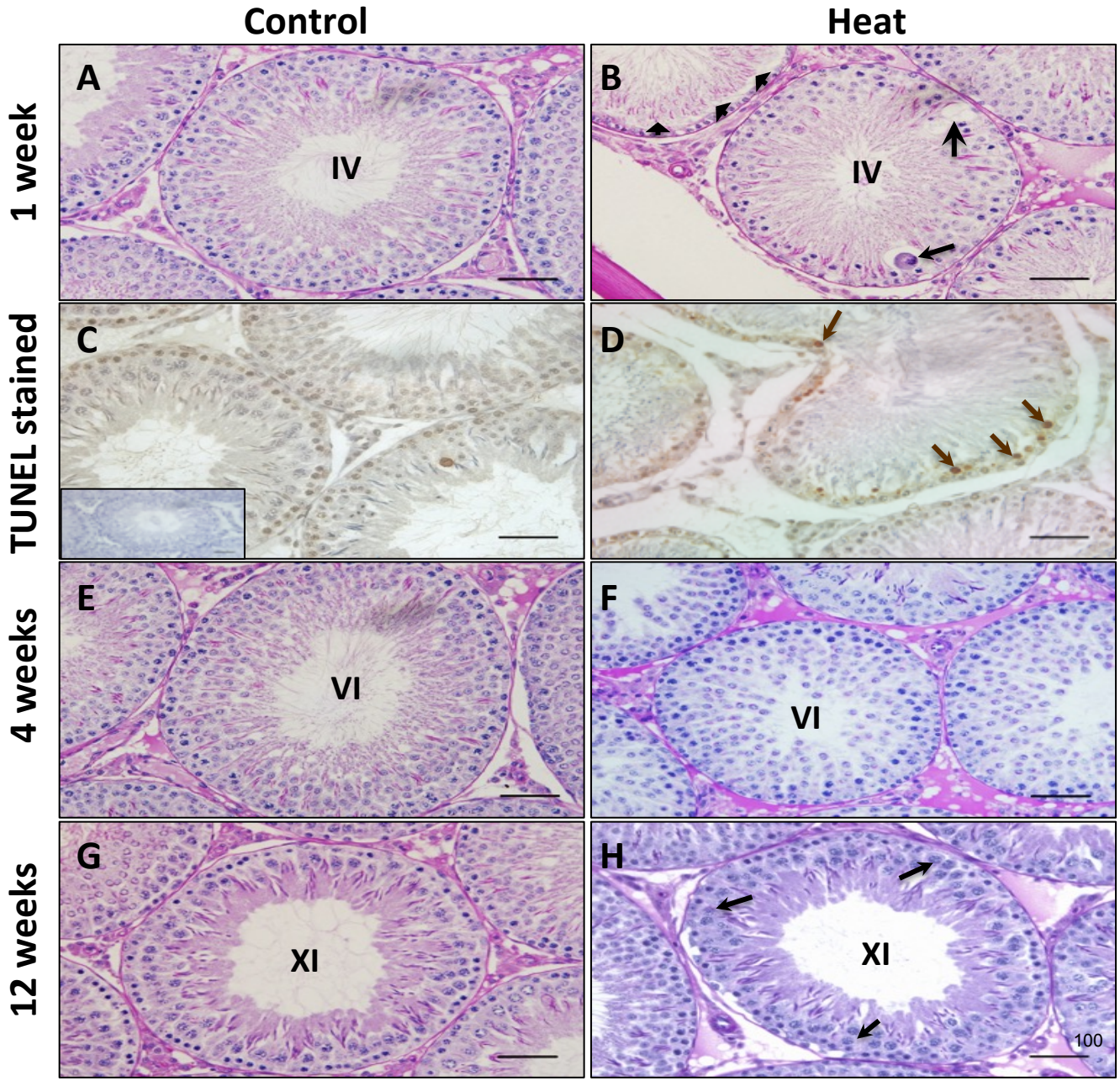
Control
Heat
1 week
TUNEL stained
4 weeks
12 weeks
A
B
C
D
E
F
G
H
IV
IV
VI
VI
XI
XI
100

Figure 3

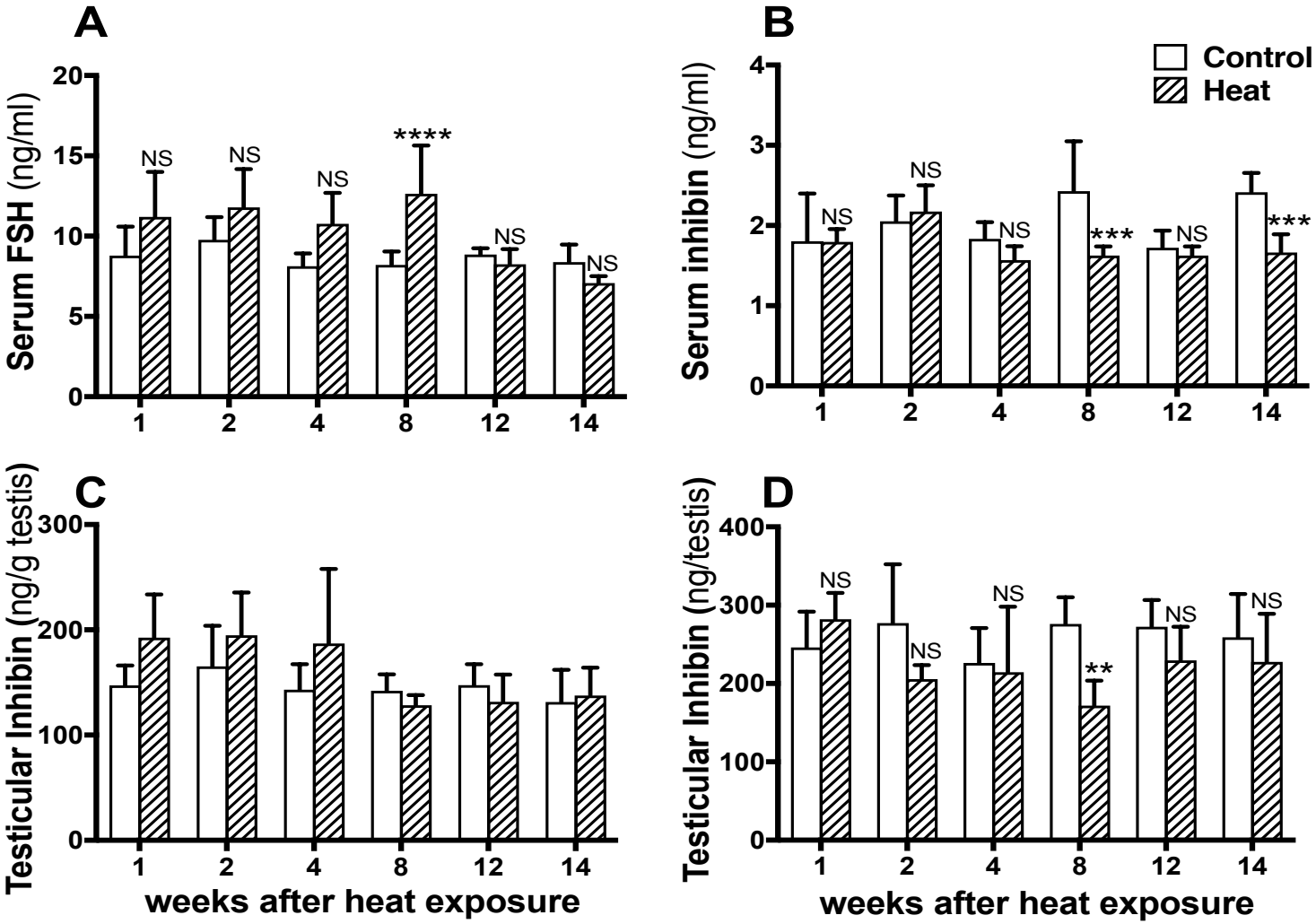
A
Serum FSH (ng/ml)
20
15
10
5
0
NS
NS
NS
****
NS
NS
1
2
4
8
12
14
B
Control
Heat
Serum inhibin (ng/ml)
4
3
2
1
0
NS
NS
NS
***
NS
***
1
2
4
8
12
14
C
Testicular Inhibin (ng/g testis)
300
200
100
0
1
2
4
8
12
14
weeks after heat exposure
D
Testicular Inhibin (ng/testis)
400
300
200
100
0
NS
NS
NS
**
NS
NS
1
2
4
8
12
14
weeks after heat exposure

Figure 4

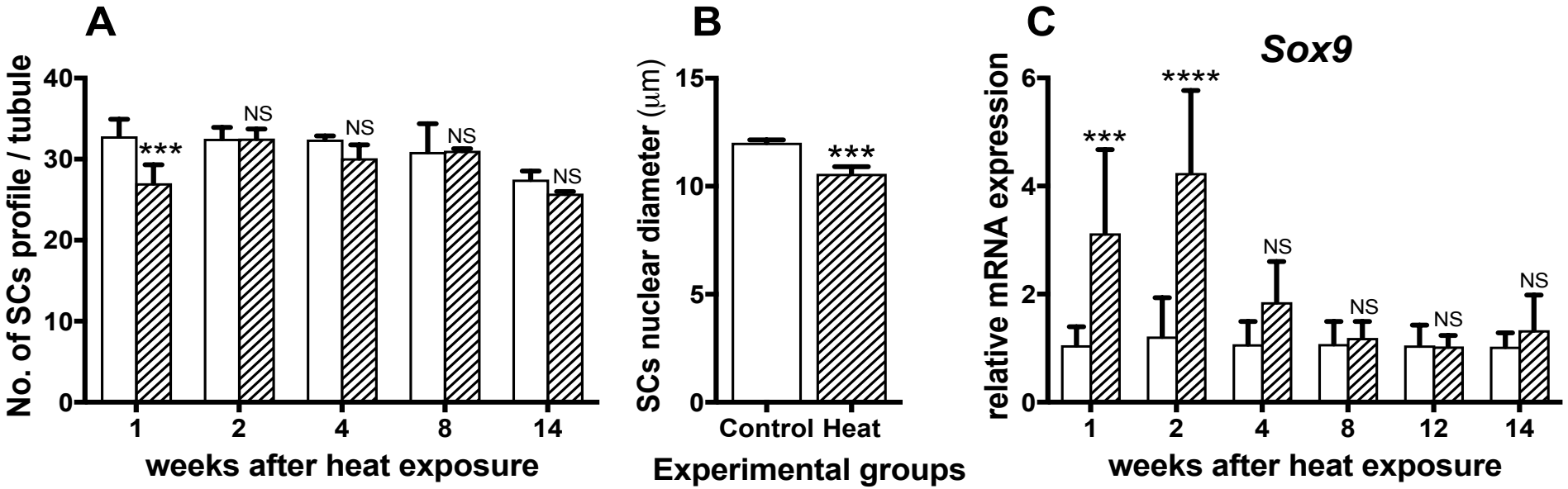
A
No. of SCs profile / tubule
40
30
20
10
0
***
NS
NS
NS
NS
1
2
4
8
14
weeks after heat exposure
B
SCs nuclear diameter (µm)
15
10
5
0
***
Control
Heat
Experimental groups
C
Sox9
relative mRNA expression
6
4
2
0
***
****
NS
NS
NS
NS
1
2
4
8
12
14
weeks after heat exposure

Figure 5

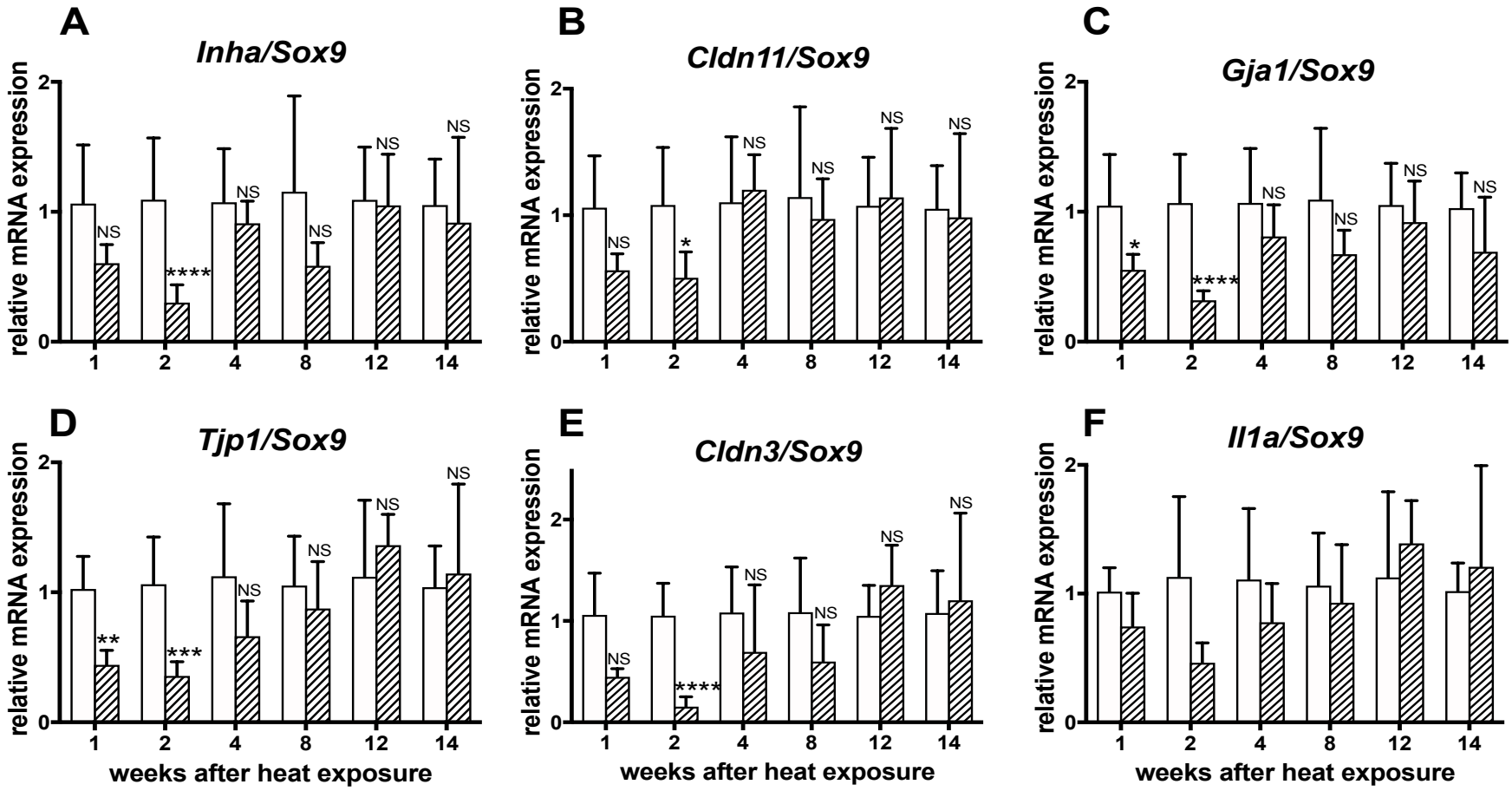
A
Inha/Sox9
B
Cldn11/Sox9
C
Gja1/Sox9
D
Tjp1/Sox9
E
Cldn3/Sox9
F
Il1a/Sox9
relative mRNA expression
weeks after heat exposure
1
2
4
8
12
14
NS
*
**
***
****

Figure 6

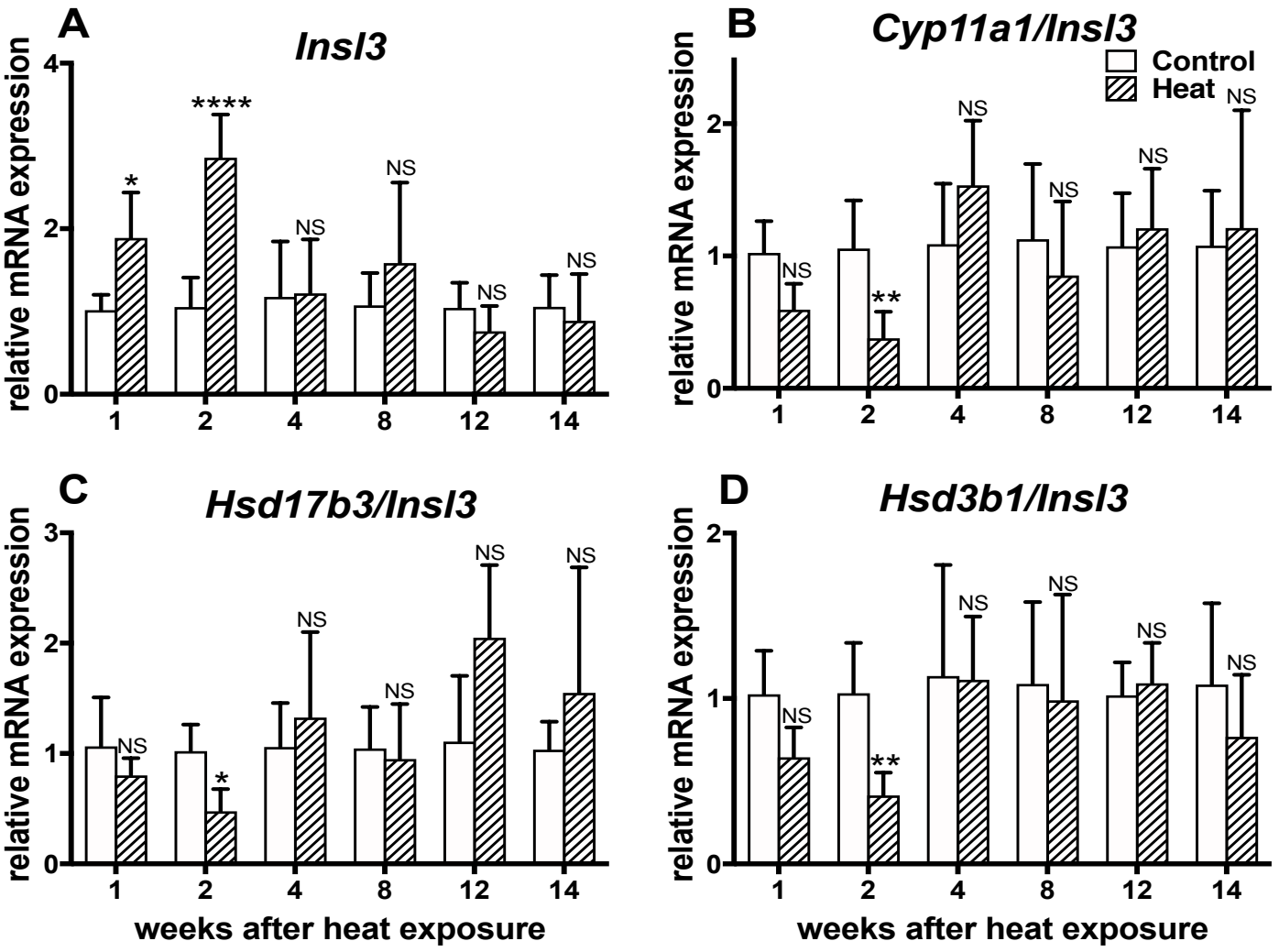
A
Insl3
relative mRNA expression
4
2
0
*
****
NS
NS
NS
NS
1
2
4
8
12
14
B
Cyp11a1/Insl3
Control
Heat
relative mRNA expression
2
1
0
NS
**
NS
NS
NS
NS
1
2
4
8
12
14
C
Hsd17b3/Insl3
relative mRNA expression
3
2
1
0
NS
*
NS
NS
NS
NS
1
2
4
8
12
14
weeks after heat exposure
D
Hsd3b1/Insl3
relative mRNA expression
2
1
0
NS
**
NS
NS
NS
NS
1
2
4
8
12
14
weeks after heat exposure

Figure 7

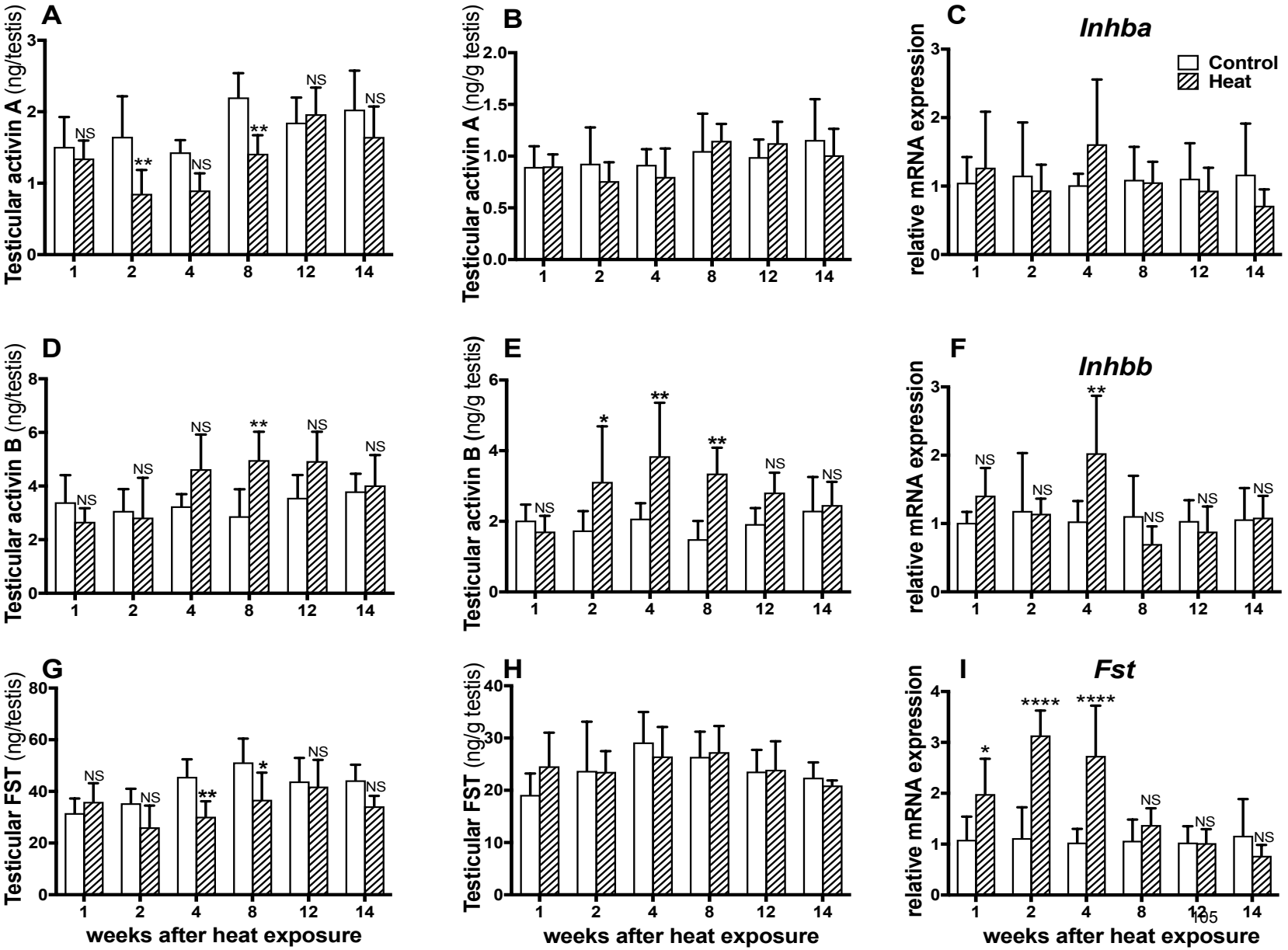
A
Testicular activin A (ng/testis)
B
Testicular activin A (ng/g testis)
C
Inhba
Control
Heat
relative mRNA expression
D
Testicular activin B (ng/testis)
E
Testicular activin B (ng/g testis)
F
Inhbb
relative mRNA expression
G
Testicular FST (ng/testis)
H
Testicular FST (ng/g testis)
I
Fst
relative mRNA expression
weeks after heat exposure
weeks after heat exposure
weeks after heat exposure

Figure 8

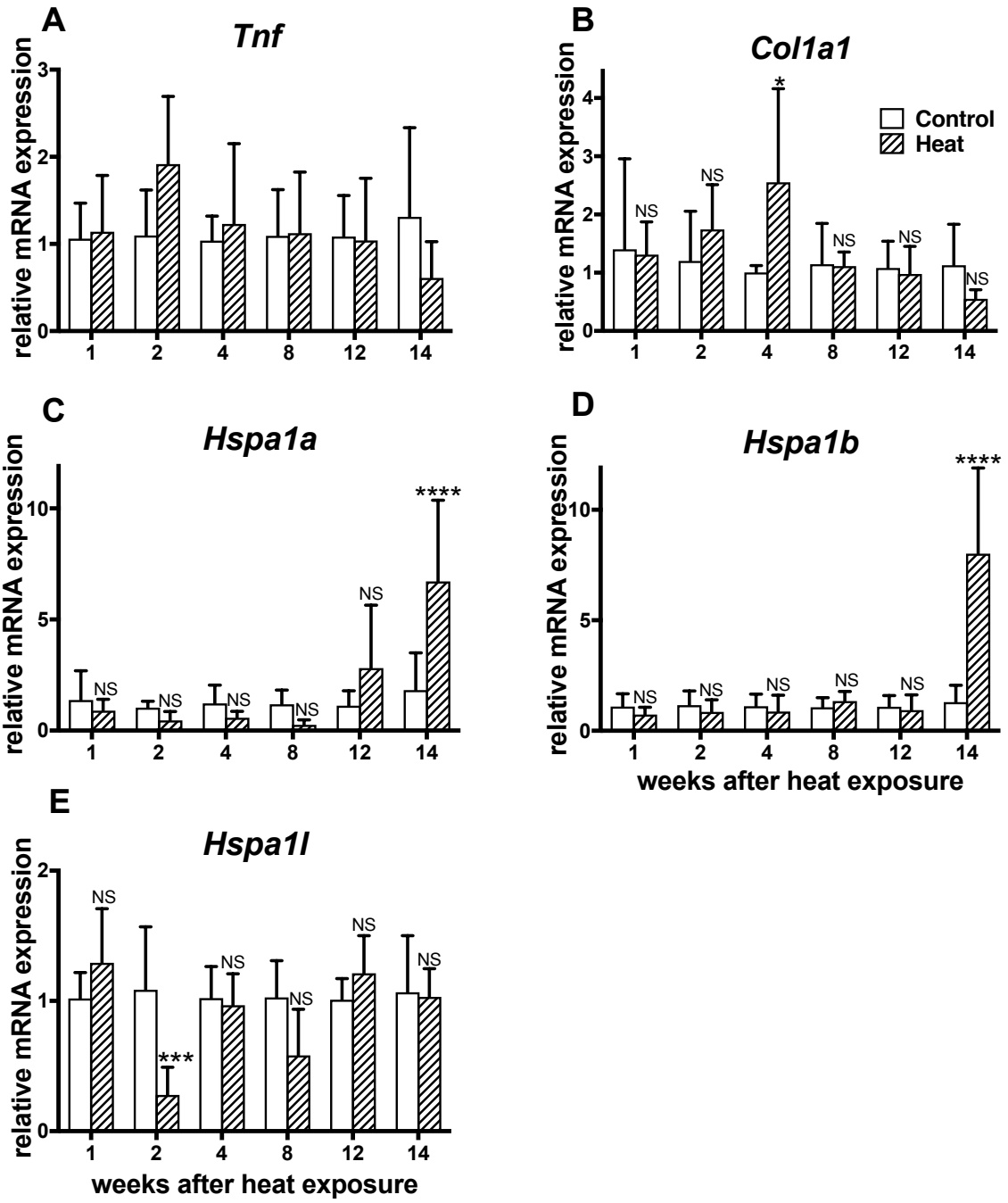
A
Tnf
relative mRNA expression
B
Col1a1
Control
Heat
C
Hspa1a
D
Hspa1b
E
Hspa1l
NS
*
***
****
1
2
4
8
12
14
weeks after heat exposure

Supp Figure 1

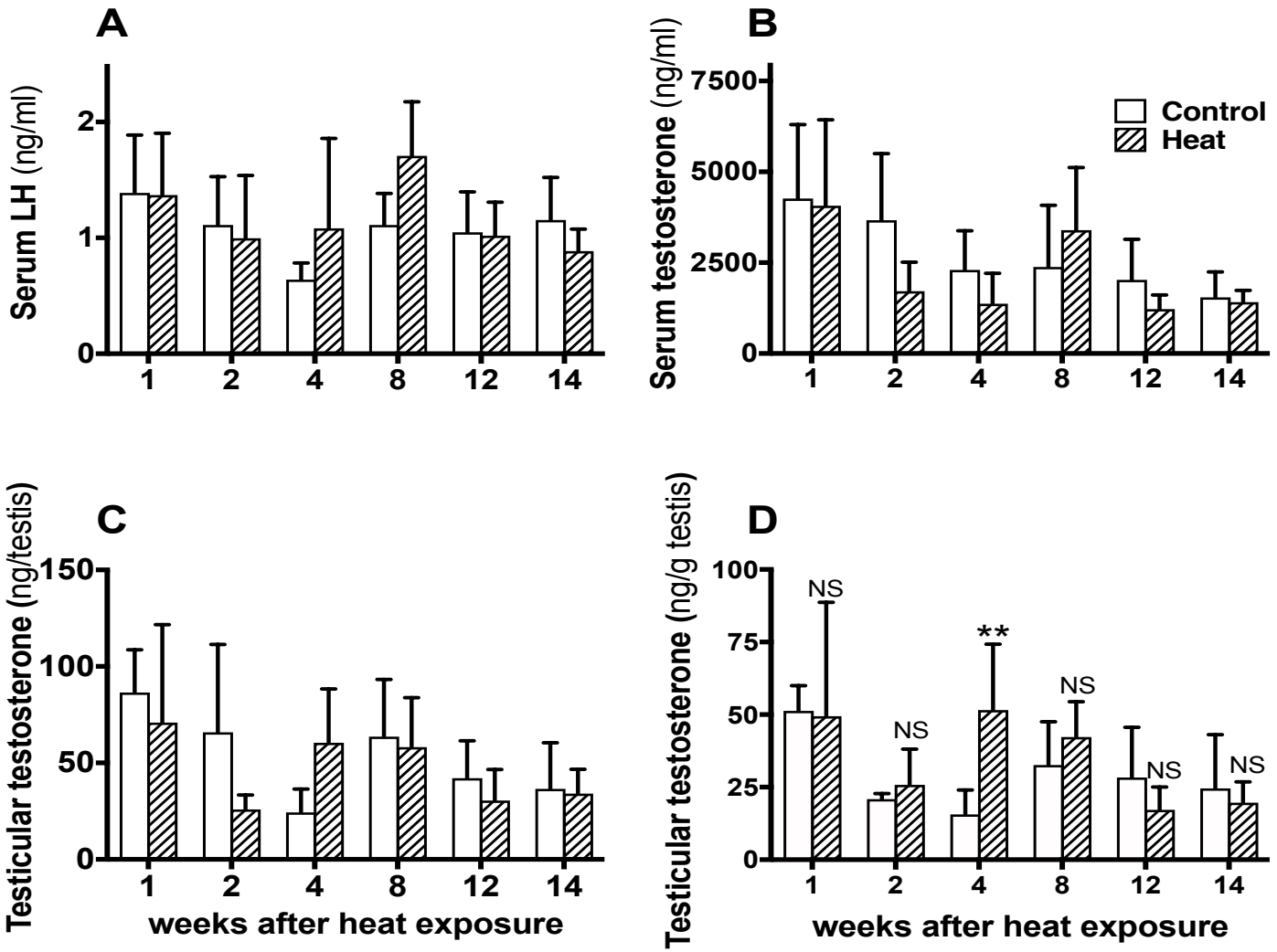

Supp Figure 2

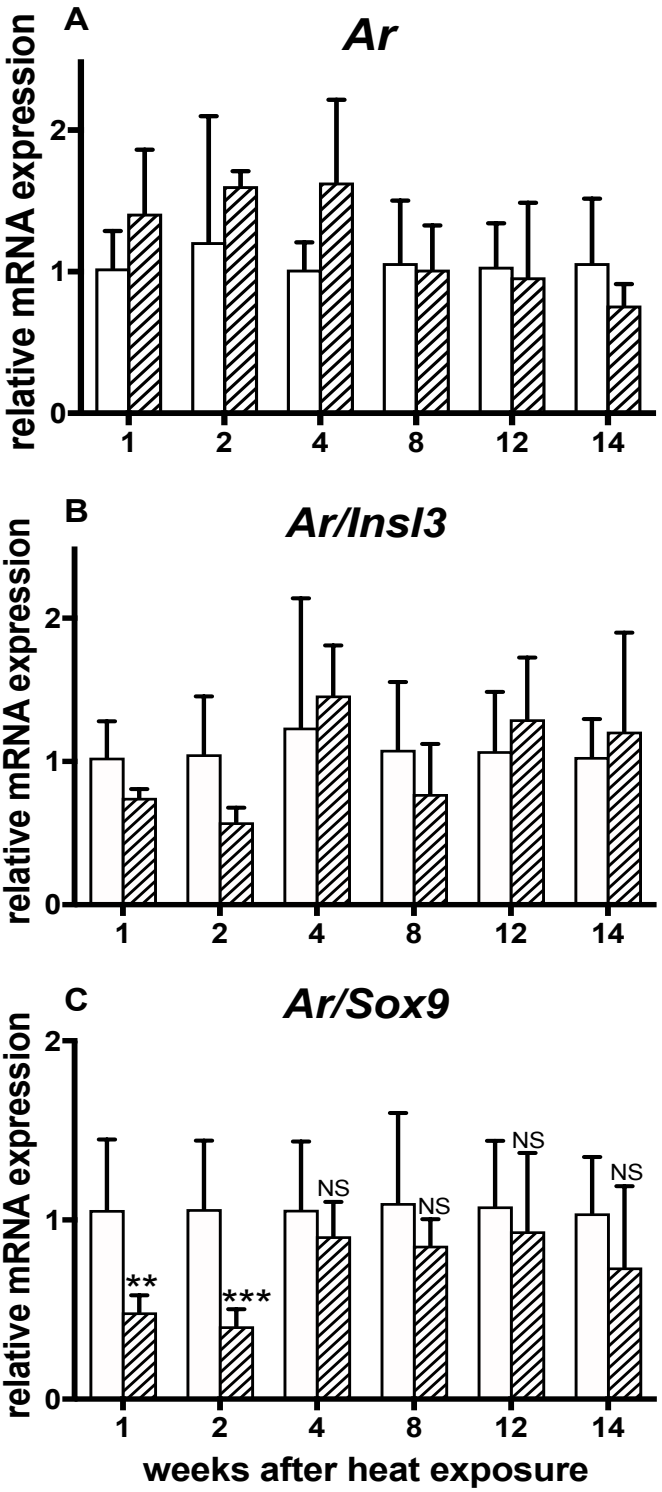

Supp Figure 3

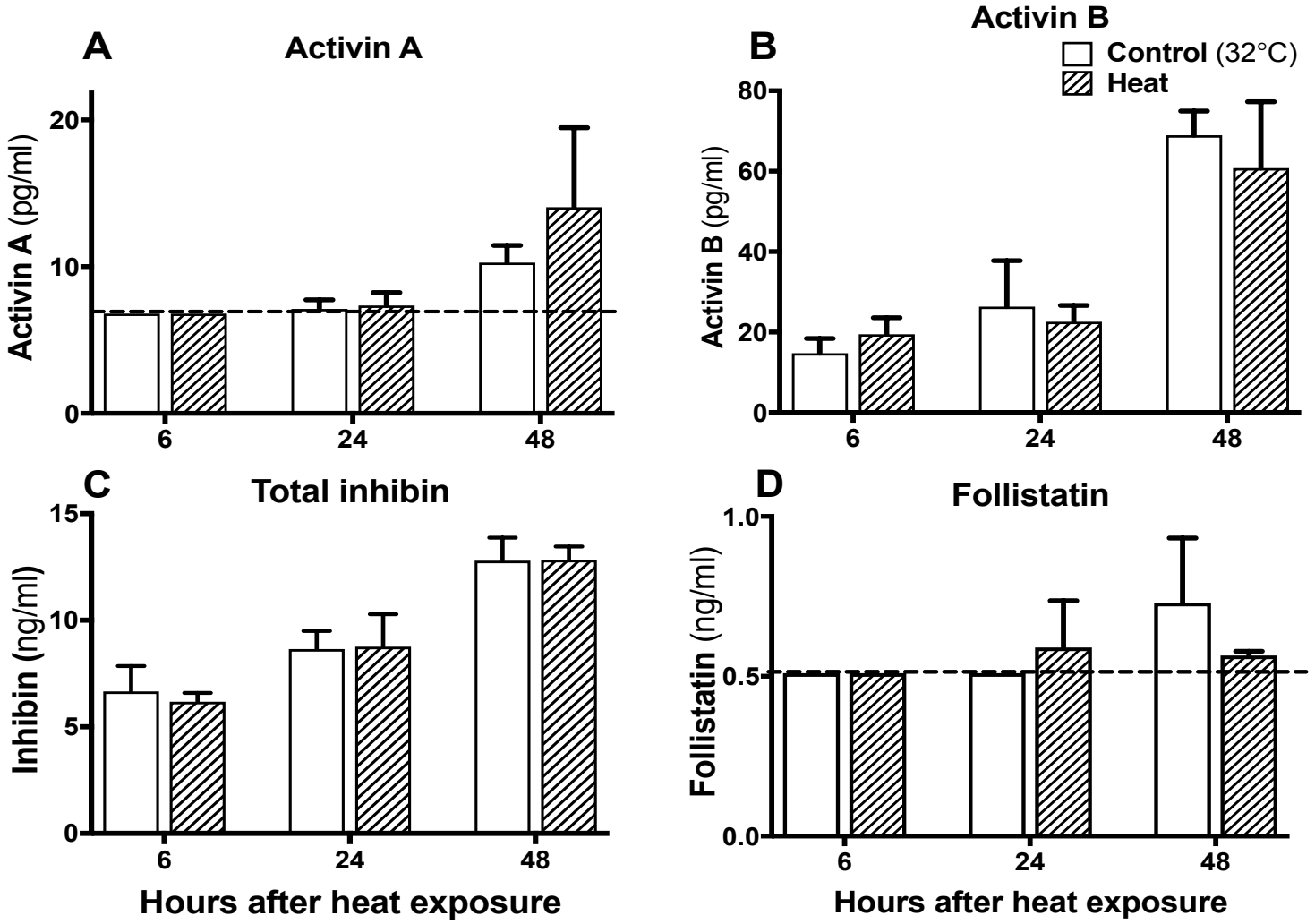

3. Chapter 3:

Acute heat treatment causes multifunctional damage in the adult rat testis

Manuscript prepared for submission to *Scientific Report*

DECLARATION FOR THESIS CHAPTER

Declaration by candidate

In the case of Chapter 3, the nature and extent of my contribution to the work was the following:

Nature of contribution	**Extent of contribution (%)**
Experimental design, optimisation of protocols, performing experiments, data analysis and drafting of manuscript	75%

The following co-authors contributed to the work. If co-authors are students at Monash University, the extent of their contribution in percentage terms must be stated:

Name	**Nature of contribution**	**Extent of contribution for student co-authors only (%)**
Laura Dagley	Proteomic specialists assisted with mass spectrometry data collection	NA
Giuseppe Infusini		NA
Andrew Webb		NA
Liza O'Donnell	Assisted with data analysis	NA
David de Kretser	Drafting of manuscript and intellectual input	NA
Mark Hedger	Drafting of manuscript and intellectual input	NA
Peter Stanton	Drafting of manuscript and intellectual input	NA

The undersigned hereby certify that the above declaration correctly reflects the nature and extent of the candidate's and co-authors' contributions to this work*.

Candidate`s Signature		Date: 10/5/2019

Main Supervisor`s Signature		Date: 10/5/2019

*Note: Where the responsible author is not the candidate's main supervisor, the main supervisor should consult with the responsible author to agree on the respective contributions of the authors.

Acute heat treatment causes multifunctional damage in the adult rat testis

Aldahhan RA[1,2,3*], Dagley LF[4], Infusini G[4], Webb AI[4], O'Donnell L[1,2], de Kretser DM[1,2,5], Hedger MP[1,2,5], Stanton PG[1,2*]

[1]Centre for Reproductive Health, Hudson Institute of Medical Research, Clayton, Victoria, Australia

[2]Department of Molecular and Translational Science, Monash University, Clayton, Victoria, Australia

[3]Department of Anatomy, College of Medicine, Imam Abdulrahman Bin Faisal University, Dammam, Saudi Arabia

[4]Systems Biology and Personalised Medicine Division, Walter and Eliza Hall Institute, Parkville, Victoria, Australia

[5]Department of Anatomy and Developmental Biology, Monash University, Clayton, Victoria, Australia

Abstract:

Spermatogenesis involves interactions between the seminiferous tubules, containing germ cells and somatic Sertoli cells, and the interstitial space, with steroidogenic Leydig cells, macrophages and blood vessels. Acute heat induces transient testicular damage, in particular to advanced germ cell types but possibly to somatic Sertoli and Leydig cells as well. We aimed to characterise the molecular mechanisms of this damage/recovery process via a detailed proteomic investigation of the testicular interstitial fluid (TIF) that surrounds the seminiferous tubules. Testes of adult Sprague-Dawley rats were subjected to acute heat treatment (43°C, 15 min) in vivo resulting in selective loss of pachytene spermatocytes and round spermatids, with maximum damage 2–8 weeks after treatment, but spermatogenesis was relatively restored by 12–14 weeks. Overall, 1728 unique proteins were identified in TIF by LC-MS/MS, with 209 proteins altered ($p<0.05$) 2–17-fold at various timepoints. Proteins essential for extracellular matrix regulation through their association with fibril formation (i.e. PCOLCE, COL1A1, TIMP1, SPARC, DCN, FMOD) showed the most acute response to heat at 1 and/or 8 weeks after exposure, corresponding with the peak loss of germ cells. Conversely, cytoskeletal proteins, EB1 and TUBA3A, involved in Sertoli cell microtubule regulation were downregulated at 8-14 weeks. Additionally, a group of germ-cell-specific proteins associated with spermatogenic regulation (including HSPA2, BAG6, NASP, SPATA20, CABS1) were also downregulated at 8-14 weeks. These data demonstrate that acute heat induces damage to multiple cellular functions in both the somatic and germ cell populations in the testis.

Key words:

Testicular interstitial fluid – Heat sress – Spermatogenesis – Sertoli cell – Leydig cell

Introduction

Spermatogenesis is a highly specialised process of male germ cell development that involves cell proliferation, maintenance and maturation. The end result of this process is the production of haploid germ cells, the spermatozoa, from diploid spermatogonial stem cells. Spermatogenesis involves interactions between the seminiferous tubules, which contain the developing germ cells and the somatic Sertoli cells, and the interstitial space, which contains steroidogenic Leydig cells, macrophages and blood vessels. The Sertoli cells are attached to each other through various junctions (i.e. tight junctions, basal ectoplasmic specialisations, desmosomes and gap junctions) to form the junctional component of the blood–testis barrier (BTB). The BTB divides the seminiferous tubules into a basal and an adluminal compartment and maintains all the germ cells, other than the spermatogonia and early spermatocytes, within a microenvironment that is both metabolically distinct and immunologically specialised (Stanton, 2016).

Spermatogenesis is a temperature-sensitive process and usually occurs at a temperature 2–7 °C lower than the core body temperature (Hou et al., 2015). Therefore, a temperature elevation above the normal scrotal temperature range can result in the temporary loss of the most heat-sensitive germ cells, these being pachytene spermatocytes and round spermatids (Kim et al., 2013). In fact, elevated scrotal temperature is considered a major contributor to male factor infertility (Durairajanayagam et al., 2014). The adverse effects of heat stress on testis function can be triggered by many factors, including (A) lifestyle and behavioural factors, such as clothing, hot baths and saunas; (B) occupational and environmental exposures to radiant and ambient heat; and (C) pathophysiological factors, such as cryptorchidism, fever and varicocele (Ilacqua et al., 2018). Previous studies in various species have demonstrated that the germ cells most acutely susceptible to mild transient heat stress are pachytene spermatocytes and round spermatids at stages I–IV and IX–XII and the diplotene and differentiating primary or secondary spermatocytes at stages XII–XIV (Bowler, 1972; Carlsen et al., 2003; Chowdhury and Steinberger, 1970; Gasinska and Hill, 1989; Paul et al., 2008; Wang et al., 2007). In contrast, spermatogonia seem to be somewhat resistant to the detrimental effects of heat (McLean et al., 2002). Hence, heat impact on spermatogenesis is not

permanent because the processes of germ cell meiosis and differentiation can resume from spermatogonial stem cells.

Sertoli and Leydig cell functions are also disrupted by heat (Aktas and Kanter, 2009; Au et al., 1987; Damber et al., 1980; Jegou et al., 1984). Alterations in Sertoli cell function include reductions in androgen binding protein (ABP) and inhibin secretion, and changed Sertoli cell fluid dynamics, with decreased production of apical seminiferous tubule fluid (STF) and increased basal testicular interstitial fluid (TIF) (Jegou et al., 1984; Sharpe et al., 1991). In contrast, Leydig cells undergo morphological changes, which include intracytoplasmic accumulation of lipid droplets, the appearance of a dilated smooth endoplasmic reticulum, mitochondrial swelling, and the disappearance of mitochondrial cristae, (Damber et al., 1980; Aktas and Kanter, 2009).. These changes in Sertoli and Leydig cell function occurred somewhat later (2−4 weeks) after heat treatment (Aktas and Kanter, 2009; Au et al., 1987; Jegou et al., 1984). Additionally, we recently found increased FSH due to a decline in feedback from inhibin 8 weeks after acute heat treatment in the rat (Aldahhan et al., Chapter 2). Collectively, these observations suggest that disruption of Sertoli cell function may occur subsequent to spermatogenic cell damage, and may therefore be primarily a response to germ cell loss. However, the molecular events that result in these cellular changes following exposure to acute heat remain poorly understood.

Intercellular communication in the testis is pivotal for spermatogenesis and steroidogenesis (Hales, 2002; Rebourcet et al., 2014a; Rebourcet et al., 2014b; Welsh et al., 2009). As most testicular cell types are not in direct physical contact, it is expected that intercellular communication likely happens via soluble factors released into the testicular fluids, particularly the TIF (Stanton et al., 2016). It is already known that TIF contains multiple proteins from various cellular origins (Stanton et al., 2016), including Sertoli (Sharpe, 1992), Leydig (Anand-Ivell et al., 2009), and germ cells (Turner et al., 1996). Because alterations in endocrine hormones and in the local environment, including changes in germ cells, can impact TIF volume and protein concentration (Hedger and Muir, 2000; Sharpe et al., 1991; Sharpe and Cooper, 1983), we therefore propose that TIF contains proteins and factors that can be representative of testicular function. However, the proteomic

changes in TIF in response to any dysfunctional state have yet to be investigated.

Our recent observations showed that acute heat treatment (43 °C for 15 min) of the rat testis *in vivo* resulted in a loss of vulnerable germ cell types (pachytene spermatocytes, round spermatids) from the epithelium after 1 week, and this loss persisted for up to 8 weeks (Aldahhan et al., Chapter 2). After 8 weeks, these cell types started to repopulate the testis, with a relatively full recovery observed after 14 weeks. In addition, TIF volumes were elevated when germ cell depletion was maximal at 8 weeks after heat treatment (Aldahhan et al., Chapter 2). The aim of this study was to characterise the molecular mechanism(s) contributing to cellular damage and recovery in the testis following acute heat treatment by investigating changes in the TIF proteome.

Materials and Methods

Animals

Scrotal heat stress (43°C for 15 minutes) was induced in the adult male Sprague-Dawley rats as described previously (Aldahhan et al., Chapter 2). Groups of control and heat-treated rats were euthanised for evaluation at 1, 2, 4, 8, 12, and 14 weeks post-treatment (n = 7 rats/treatment group at each time-point). These studies were approved by the Monash Medical Centre Animal Ethics Committee.

Tissue handling and preparation

In order to collect testicular interstitial fluid (TIF), a 2–4 mm incision was made in the tunica at the distal pole, and the testis was suspended on a thin needle placed through the tunica at the opposite pole in a 15 mL tube above 20 μL phosphate-buffered saline (PBS, pH 7.4) containing complete protease inhibitor cocktail (Roche, Penzberg, Germany). TIF was collected by percolation overnight at 4°C (Sharpe and Cooper, 1983), ultra-centrifuged (109,000g 60 min, 4°C) and the supernatant was snap-frozen and stored at -80°C.

Protein assay and enrichment

TIF samples collected 1, 8 and 14 weeks after heat treatment were chosen for proteomics analysis. These time-points were associated with the beginning of germ cell damage (1 week), peak damage (8 weeks) and recovery (14 weeks), according to our findings (Aldahhan et al., Chapter 2). TIF protein concentrations were determined by Bradford method (Bradford, 1976), prior to enrichment of low-abundance proteins using a ProteoMiner protein enrichment large capacity kit (Bio-Rad, Hercules, CA, USA) according to the manufacturer's instructions (Supplementary data Fig. 1).

Sample preparation for liquid chromatography and mass spectrometry (MS)

Rat TIF samples (40 µg protein) were prepared for mass spectrometry analysis using the SP3 protocol as described previously (Hughes et al., 2014; Hughes et al., 2019) but with some modifications (see Supp Data).

Peptides (2 µL) were separated by reverse-phase chromatography on a 1.9µm C18 fused silica column (I.D. 75 µm, O.D. 360 µm x 25 cm length) packed into an emitter tip (Ion Opticks, Australia), using a nano-flow HPLC (M-class, Waters). The HPLC was coupled to an Impact II UHR-QqTOF mass spectrometer (Bruker, Bremen, Germany) using a CaptiveSpray source and nanoBooster at 0.20 Bar using acetonitrile. Peptides were loaded directly onto the column at a constant flow rate of 400 nL/min with buffer A (99.9% Milli-Q water, 0.1% formic acid) and eluted with a 90 min linear gradient from 2 to 34% buffer B (99.9% acetonitrile, 0.1% formic acid). Mass spectra were acquired in a data-dependent manner including an automatic switch between MS and MS/MS scans using a 1.5 second duty cycle and 4 Hz MS1 spectra rate followed by MS/MS scans at 8-20 Hz dependent on precursor intensity for the remainder of the cycle. MS spectra were acquired between a mass range of 200–2000 m/z. Peptide fragmentation was performed using collision-induced dissociation (CID).

MS data analysis

Raw files consisting of high-resolution MS/MS spectra from the Bruker Impact II instrument were processed with MaxQuant (version 1.5.8.3) for feature detection and protein identification using the Andromeda search engine (Cox et al., 2011). Extracted peak lists were searched against the UniProtKB/Swiss-Prot *Rattus norvegicus* database (January 2018) and a separate reverse decoy database to empirically assess the false discovery rate (FDR) using strict trypsin specificity allowing up to 2 missed cleavages. The minimum required peptide length was set to 7 amino acids. In the main search, precursor mass tolerance was 0.006 Da and fragment mass tolerance was 40 ppm. The search included variable modifications of oxidation (methionine), amino-terminal acetylation, the addition of pyroglutamate (at N-termini of glutamate and glutamine) and a fixed modification of carbamidomethyl (cysteine). The "match between runs" option in MaxQuant was used to transfer identifications made between runs on the basis of matching precursors with high mass accuracy. Peptide spectrum match and protein identifications were filtered using a target-decoy approach at an FDR of 1%. Statistically-relevant protein expression changes were identified using a custom in-house designed label-free quantitative proteomics pipeline, as previously described (Delconte et al., 2016) where quantitation was performed at the peptide level. Missing values were imputed using a random normal distribution of values with the mean set at mean of the real distribution of values minus 1.8 standard deviation (SD), and an SD of 0.5 times the SD of the distribution of the measured intensities. The probability of differential expression between groups was calculated using the Mann–Whitney U test excluding any non-unique sequences and any features with modifications other than oxidation and carbamidomethylation. Probability values were corrected for multiple testing using Benjamini–Hochberg method. Cut-off lines with the function $y= -\log_{10}(0.05)+c/(x-x_0)$ (Keilhauer et al., 2015), were introduced to identify significantly enriched proteins. c was set to 0.2 while x_0 was set to 1, representing proteins with a twofold ($\log_2$ protein ratios of 1 or more) or fourfold ($\log_2$ protein ratio of 2) change in protein expression, respectively.

In silico analysis

The functional annotation-clustering tool within the Database for Annotation, Visualization and Integrated Discovery (DAVID; v6.8) was used to group proteins into related molecular functions, biological processes and cellular components (https://david.ncifcrf.gov/) (Huang et al., 2007). Cell specificity data were obtained from Chalmel et al. (2007) and searchable in the GermOnline database (Lardenois et al., 2010).

Western Blotting

All products for Western blots were purchased from Life Technologies (Carlsbad, CA, USA) unless otherwise specified and run according to manufacturer's protocols. Protein samples mixed with 4x Bolt LDS sample buffer and 10x Bolt sample reducing agent were heated to 70°C for 10 min and loaded into a Bolt 4–12% Bis–Tris Plus mini gel. Gels were immersed in Bolt MES SDS running buffer and run at 100 mV for ~60 min with Prestained Protein Ladder (Abcam, Cambridge, UK). Proteins were transferred onto polyvinylidene difluoride membranes using transfer buffer (38mM Tris Base, 280mM glycine and 20% methanol) at 30mV overnight at 4°C. Nonspecific binding was blocked with 1% bovine serum albumin (bSA, Sigma-Aldrich) in 25mM Tris Base, 140 mM NaCl, pH 7.9, 0.05% Tween-20 (TBST) for 1 h at room temperature. The blots were treated with the respective antibodies overnight at room temperature: rabbit anti-Dcn 1:1000 (14667-1-AP, Proteintech, Chicago, IL, USA), anti-Hspa2 1:1000 (ab108416, Abcam), and anti-Spata20 1:2000 (18373-1-AP, Proteintech). After washing three times (5 mins per wash) with TBST, membranes were probed the following day with horseradish peroxidase-conjugated goat anti-rabbit IgG (SAB3700878, SigmaAldrich) diluted in 5% non-fat milk in TBST (for Dcn and Hspa2) and in blocking buffer (for Spata20) at a dilution of 1:4000 for 1 h at room temperature. The membranes were then washed with TBST and the signals were revealed with Pierce ECL Western blotting substrate (Thermo Fisher) as per the manufacturer's instructions. The resultant image was developed, fixed, scanned, and quantified using ImageLab software (version 5.2.1, Bio-Rad).

Statistical analysis

Data are shown as mean ± SD. GRAPHPAD PRISM 7 (Graphpad Software, Inc., La Jolla, CA, USA) was used to perform the Student's t test to determine statistical significance among appropriate groups. A p value of < 0.05 was considered significant.

Results

The testicular response to heat treatment

The *in vivo* testicular response to acute heat treatment (15min, 43°C) has been reported in detail elsewhere (Aldahhan et al., Chapter 2), but a brief summary is provided here. Heat-treatment causes damage to cell populations that can be classified into three phases: (I) onset (1–2 weeks), (II) peak damage (2–8 weeks) and (III) recovery (12–14 weeks). In the onset phase, testis weights were significantly decreased to approximately 80% of control 1 week after heat treatment, with a further reduction to 60% of control at 2 weeks, due primarily to the loss of pachytene spermatocytes (SYT) and round spermatids (rST) from the seminiferous epithelium (Supp Fig. 2B) in comparison with control (Supp Fig. 2A). Although new SYT and rST started to repopulate the testis at 4 weeks, testis weight was still 30% lower than control at 8 weeks after heat treatment with partial re-appearance of SYT and rST (Supp Fig. 2D) compared with the control (Supp Fig. 2C). Testis weight returned toward control levels by 12 weeks after heat treatment, but remained 15% lower than normal at 14 weeks, although the testes exhibited a normal histological appearance (Supp Fig. 2F) (for more details refer to Aldahhan et al., Chapter 2).

Global proteomic analysis of interstitial fluid from heat-treated rats

Rat TIFs from three time-points representative of the three phases of damage were selected for proteomic analysis: onset (1 weeks), peak (8 weeks) and recovery (14 weeks). We identified a total of 1728 proteins in TIF from the control and heat-treated testes across all three time points (Supp Table 1). Provisional interrogation of the control TIF proteomes on the basis of shared

functional classification using DAVID Gene Ontology (GO) annotation tools returned dominant terms of 'nucleotide-binding' (GO: 166), 'ATP-binding' (GO: 5524) and 'calcium ion binding' (GO: 5509) among the top 10 GO molecular function categories when ranked on the basis of number of annotated proteins (Supp Fig. 3A). Similarly, the top 10 GO biological process categories were identified to be 'cell-cell adhesion' (GO: 98609), 'biosynthesis of antibiotic' (GO: 17000), 'immunity' (GO: 2376) and 'carbon metabolism' (GO: 6730), 'cell cycle' (GO: 7049), 'glutathoine metabolism' (GO: 6749), 'glycolysis/gluconeogenesis' (GO: 6096 and 6094), 'cell division' (GO: 6412), 'mRNA processing' (GO: 6397), and 'hemostasis' (GO: 7599) (Supp Fig. 3B). The dominant GO cellular component categories included 'extracellular space', 'cell-cell adherens junction' and 'proteasome' with 327, 101, and 39 proteins mapping to these respective categories (Supp Fig. 3C).

Analysis of the GO annotation of the heat-treated TIF proteome revealed that it was identical to the control proteome in terms of molecular process and cellular components (Supp Fig. 4A and C). Similarly, the GO annotation for biological process was comparable, although the number of annotated proteins per category were slightly different probably due to the heat effect (Supp Fig. 4B).

Among these 1728 proteins, a total of 209 proteins were differentially expressed ($p < 0.05$) following heat treatment (Fig. 1, Supp Tables 2 and 3). The majority of these proteins were down-regulated at the various time points (Fig 1), with a biphasic pattern showing limited change at 1 week (56 out of 58 $p<0.05$ proteins down-regulated), maximal change at 8 weeks (152 out of 167 $p<0.05$ proteins down-regulated) and ongoing change at 14 weeks (85 out of 85 $p<0.05$ proteins down-regulated) (Fig 1, Supp Tables 2 and 3).

In temporal terms, the MS results indicated that only 15 of the 209 proteins were downregulated at all three time points (Fig 2); these proteins were primarily of Sertoli cell and spermatogonial origin (see Supp Table 3A). At 1 week after heat treatment, expression of 58 proteins was disrupted; 23 proteins showed an acute response and were only altered at this time

(Supp Table 3B), whilst a further 35 proteins remained under-expressed till 8 weeks (Supp Table 3A and C). The majority (169/209) of the differentially regulated proteins were detected at 8 weeks, corresponding with the peak testicular damage (Fig 2). Of these, 81 proteins were predominantly enriched in Sertoli cells and spermatogonia (Supp Table 3D). The levels of these 81 proteins decreased at 8 weeks but had recovered by 14 weeks, whereas others (53) that were mainly of SYT and rST origin were still decreased at 14 weeks (Supp Table 3E). Furthermore, 17 proteins expressed by various epithelial cells revealed a late response at 14 weeks, suggesting persistent testicular damage (Supp Table 3F).

Provisional interrogation of this altered TIF proteome (209 proteins) on the basis of shared functional classification using DAVID GO annotation tools returned dominant terms of 'nucleotide-binding', 'ATP-binding' and 'ligase activity' (GO: 16874) among the top 10 GO molecular function categories when ranked on the basis of number of proteins with altered expression (Fig. 3A). Similarly, in terms of GO biological process categories, significant change was identified in the process of 'cell-cell adhesion' (GO: 98609), 'spermatogenesis' (GO: 7283) and 'protein biosynthesis' (GO: 6412) (Fig. 3B). A number of other GO biological process categories were equally affected and demonstrate a broad range of damage caused by heat treatment; these included 'wound healing' (GO: 42060), 'biosynthesis of antibiotic', 'amino acid biosynthesis' (GO: 8652), 'response to oxidative stress' (GO: 6979), 'Cellular response to amino acid' (GO: 71230), 'collagen fibril organisation' (GO: 30199), and 'glutathione metabolism'. The dominant GO cellular component categories were identified as 'extracellular space', 'cytoplasm' and 'nucleus' with 149, 134, and 42 proteins mapping to these respective categories (Fig. 3C).

Functional categories of altered TIF proteins

To study the response of the TIF proteome to acute heat, Table 1 and 2 categorise proteins into two groups based on the pattern of damage: (1) Proteins that were significantly up or down > 2-fold ($p<0.05$) at either 1 week or 8 weeks, or both, but return to normal at 14 weeks and thus reflect the pattern of spermatogenic damage (Table 1), (2) Proteins that were significantly down > 2-fold

($p<0.05$) at 14 weeks, regardless of whether they were up- or down- regulated at 1 and 8 weeks which may therefore be associated with persistent or ongoing damage (Table 2).

We next looked for associations between these disrupted proteins (209 in total, Tables 1 and 2) and their potential testicular functions. Table 3 summarises proteins that are associated with heat shock (6), oxidative stress (6), inflammation and/or fibrosis (8), spermatogenesis (11), proteasomes (3), Sertoli cell (2) and inhibin-related (1) regardless of whether they are up or down at any time point. These proteins provide information about the response, or lack of response, of the tissue to damage .

More specifically, the majority of inflammation/fibrosis-related proteins were downregulated at 1 week, corresponding to the loss of SYT and rST (Table 3). Conversely, an upregulation was observed in half of this protein category at 8 weeks (including PCOLCE, COL18A1, LYZ2 and TIMP1) as mature spermatids were lost. Among the inflammation/fibrosis-related proteins, only USP5 protein showed a long-term response for 14 weeks (Table 3). Most oxidative stress-related proteins were decreased at 1-8 weeks, but only three proteins, ALDH7A1, WARS and UCHL3, remaining downregulated at 14 weeks. Most of the heat shock-related proteins (HRSP12, HSPA2, HSPA4L, STIP1 and NASP) were unchanged at 1 week but were universally downregulated at 8 weeks, with some extended downregulation till 14 weeks; however, one protein (HSPD1) was exclusively altered at the 1 week time point (Table 3). In total, 20% of spermatogenesis-related proteins decreased at 1-8 weeks while 60% of these proteins including SPATA20, DAZAP1, CABS1, DBIL5, HSPA2, NCL and BAG6, showed persistent changes. This may indicate ongoing spermatogenic damage. Interestingly, although numerous proteins were downregulated in the recovery phase (14 weeks) when no histological damage was apparent in the germinal epithelium (Supp Fig 1E, F), most of these proteins (SPATA20, DAZAP1, CABS1, DBIL5, HSPA2 and BAG6) are highly expressed by the most heat vulnerable cells, SYT and rST. The remaining 20% of spermatogenesis-related proteins showed a limited reduction at 8 weeks only. Proteasomes and the Sertoli cell-related and inhibin-related proteins exhibited extended change to 14 weeks, but ATG3 protein showed alterations only during the peak phase (Table 3).

We then conducted a closer examination of several of the functional groupings that were altered in the heat-treated TIF by selecting 13 proteins that play roles in fibril formation, regulation of Sertoli cell microtubules or regulation of spermatogenesis (Table 4). Extracellular matrix proteins associated with fibril formation (including PCOLCE, COL1A1, SPARC, DCN and FMOD) were decreased at the onset and/or peak phases, coinciding with the loss of germ cells. Many of the fibril proteins are expressed in multiple cell types within the testis, so the changes in TIF protein expression could not be ascribed to specific cells. However, these data could equally suggest that heat has impacts on multiple cell types in both the interstitial and epithelial compartments of the testis.

Although the expression of the majority of these proteins was suppressed following heat treatment, TIMP1 expression showed a 3-fold upregulation at 8 weeks. TIMP1 is of particular interest because it has an essential role in spermatogenesis and steroidogenesis (see details in Table 4) (Mruk et al., 1997; Mruk et al., 2003; Nothnick et al., 1998). The observed elevation in TIMP1 could be explained by its contribution to the assembly of damaged epithelial adherens junctions (Mruk et al 2003) in response to heat exposure. The cytoskeletal proteins EB1 and TUBA3A, which both have pivotal roles in the regulation of Sertoli cell microtubules and germ cell translocation (Table 4) (Hess and Vogl, 2015), had an 8 week delay in response to acute heat and this lag extended to 14 weeks in the case of TUBA3A. This delayed response may suggest that the effect of heat treatment on the Sertoli cell function is indirect and may lead to functional damage that disrupts the translocation of the germ cells across the seminiferous epithelium. Most proteins that are involved in the regulation of the spermatogenesis and spermiogenesis revealed a persistent downregulation until 14 weeks.

Validation of differentially expressed proteins

Changes in TIF proteins detected by MS were confirmed by selecting three candidate proteins, based on their relative function, for orthogonal targeted validation via

immunoblotting. This analysis confirmed the differential alteration of the three targeted TIF proteins (Fig. 4), with each protein displaying a profile that closely paralleled the trends identified by the MS analyses. The first protein, decorin (DCN), is an extracellular matrix protein of the small leucine-rich proteoglycan family important in fibril formation and matrix assembly during the development of mature functional tissues (Birk and Brückner, 2011); it is enriched in spermatogonia, peritubular myoid cells and fibroblasts (Table 4) (Chalmel et al., 2007; Flenkenthaler et al., 2014). The expression of DCN was significantly reduced ($p<0.01$) 2.2-fold by western blot analysis at 1 week following heat treatment, comparable to the 4.0-fold decrease by mass spectrometry (Table 4). Because DCN is expressed by both spermatogonia and peritubular myoid cells (Table 4) this data suggests that one or both cell types is adversely affected by acute heat (Fig. 4A). We also confirmed by western blot that DCN expression was not significantly altered in the 8 week group (1.1-fold decrease, $p=0.353$ data not shown), consistent with the mass spectrometry data (Table 1).

The second protein, heat shock-related 70 kDa protein 2 (HSPA2), is a germ cell-specific member of the heat shock proteins 70 chaperone family that has multifunctional roles in protein transport, DNA repair, assembly of the synaptonemal complex, sperm nuclear DNA protamination, and elimination of cytoplasmic residues following spermiogenesis (Beckmann et al., 1990; Chirico et al., 1988; Dix et al., 1997; Govin et al., 2006; Huszar et al., 2000). HSPA2 is also an essential protein in mature spermatozoa for sperm–oocyte binding (Redgrove et al., 2012). HSPA2 was notably downregulated ($p < 0.05$) 2.4-fold at 8 weeks after the acute heat treatment (MS = 4.0 fold down, Table 4), due mainly to the loss of SYT and rST (Fig 4B). At 14 weeks, HSPA2 exhibited a further dramatic decrease of 5.3-fold (Fig 4C, MS = 7.0 fold down, Table 4), likely attributable to a parallel reduction in the level of the germ cell-specific protein, BAG6 (Table 4), which has a role in HSPA2 stability (Sasaki et al., 2008). The third protein, spermatogenesis-associated protein 20 (SPATA20), is constitutively expressed by heat-sensitive germ cells (Chalmel et al., 2007) and has an essential role in spermiogenesis (Liu et al., 2018); SPATA20 showed a marked 1.4-fold decrease in expression at 8 weeks following heat treatment (Fig 4D, MS 4.0 fold down, Table 4). Its

expression began to return to the control level by 14 weeks, but remained 1.25-fold lower than the unstressed control at 14 weeks (Fig 4E, MS 6.0 fold down, Table 4). Overall, although the fold changes observed by MS were higher than those detected by immunoblotting, the latter still confirmed significant declines in the expression of the selected proteins after exposure of the testis to acute heat.

Discussion

Although the physiological and cellular responses of the testes to heat stress have been well established, the molecular mechanisms that direct these responses remain mostly unknown. In the current study, our aims were to describe the testicular cell response to acute heat treatment and to explain the underlying molecular mechanism involved in the heat-induced disruption of spermatogenesis and intercellular communication in the testis. To gain an understanding of the relationship between damage and recovery of the functional changes in the epithelium, we looked at three time points: one corresponding to acute response (1 week), a second coinciding with the phase of maximal damage (8 weeks) and a third representative of long-term recovery phase (14 weeks). Extension of the duration of the investigation to 14 weeks after heat treatment was deliberately chosen to allow sufficient time for two full 49-day spermatogenic cycles (49 days in the rat, Russell et al., 1990) to occur. We found that 12% (209/1728) of the total quantified TIF proteins were altered following heat treatment, with the majority being downregulated. These data also reveal that most of the proteins affected by heat are extracellular space (secreted) proteins that have various key functional roles; this finding suggested multifunctional heat-induced damage. While few proteins showed an acute response at 1 week, most were altered at 8 weeks. These proteins are mostly enriched in Sertoli cells and spermatogonia although the maximum damage in the germinal epithelium had occurred in the meiotic and post-meiotic germ cells at this phase. Furthermore, long-term changes in protein expression 14 weeks after heat treatment indicated that damage persisted for two full cycles of spermatogenesis. This finding is consistent with our recent observation of a

reduction in testis weight at 14 weeks in the same heat model. Surprisingly, we found that the proteins showing decreases at 14 weeks are largely expressed by the heat-vulnerable germ cells, even though a qualitative assessment of their histology shows a relative recovery (Aldahhan et al., Chapter 2). These observations provide information about the functional damage of the new population of germ cells arising from the second cycle of spermatogenesis.

In total, 77 proteins showed acute and significant differential expression (> 2-fold) at 1 and/or 8 weeks after heat treatment, and the expression levels then recovered at 14 weeks. Interestingly, although more than 50% of these proteins are highly enriched in Sertoli cells and spermatogonia, the changes were predicted to occur in the proteins that highly expressed by heat-sensitive germ cells, SYT and rST, as these cells showed earlier losses at 1 week. Conversely, the proteins that showed persistent alterations throughout the experiment were largely expressed by the SYT and rST cells, even though these cells began to repopulate at 8 weeks following their initial decline in number in the first two weeks following heat treatment. These data suggest that Sertoli cells may alter their protein expression when the germ cells are damaged, consistent with our hypothesis.

In the present study, we were able to categorise the differentially expressed proteins in the TIF based on their functions and cellular origins, which in turn provided information about the response of the tissue to damage. The fibril formation-associated proteins (e.g. PCOLCE, COL1A1, TIMP1, SPARC, DCN and FMOD), which are preferentially expressed by Sertoli cell and spermatogonia, are essential regulators of the extracellular matrix (ECM) (Birk and Brückner, 2011). These proteins showed acute responses to heat at 1 and/or 8 weeks, corresponding to the peak loss of germ cells. The changes in the tissue inhibitor of metalloproteinase 1 (TIMP1) are particularly interesting, as this protein showed a 3-fold upregulation during the peak damage phase, when most of the other proteins were downregulated. TIMP1 plays an essential role in fibril formation by cleaving and inhibiting matrix metalloproteinases (MMPs) like collagenases or by cleaving and stimulating the pro-MMPs (Brew and Nagase, 2010). In the testis, TIMP1 is expressed mainly in spermatogonia, spermatocytes, and round spermatids, and is involved in the

assembly of the adherens junctions between the Sertoli and germ cells (Mruk et al., 1997; Mruk et al., 2003). Thus, the observed elevation of TIMP1 in our study is consistent with a role in adhesion. Moreover, TIMP1 has other reported functions (e.g. suppression of tumour growth, invasion and metastasis, modulation of cell morphology, control of growth factor availability and participation in gonadal steroidogenesis), suggesting that it plays multifunctional roles (Brew and Nagas, 2010). Therefore, our findings support the idea that heat treatment interrupts several regulatory proteins in the testis.

Acute heat also affected other likely TIF functional candidates, including the cytoskeletal proteins end-binding protein 1 (EB1) and tubulin alpha 3a (TUBA3A). These proteins are responsible for regulation of the Sertoli cell microtubules that serve as tracks for transporting the developing germ cells through the seminiferous epithelium (Hess and Vogl, 2015). EB1 has recently been of interest to a number of investigators because of its pivotal role as a regulator of microtubule dynamics and in the actin cytoskeletal network (Applewhite et al., 2013; Tamura and Draviam, 2012; Tian et al., 2014). EB1 knockdown disrupts the in vitro organisation of microtubules and actin microfilaments in rat Sertoli cells and causes functional damage that disrupts the translocation of the germ cells across the seminiferous epithelium (Tang et al., 2014). The downregulation of EB1 observed in our study suggests that acute heat perturbs the tubulin-based and actin-based cytoskeleton components of Sertoli cells. Functional disruption of Sertoli cells was also suggested by the concomitant reduction of inhibin expression at 8 weeks (Aldahhan et al., Chapter 2).

Our data for the spermatogenesis-related proteins (HSPA2, BAG6, NASP, SPATA20 and CABS1) show significant declines (≥3-fold) in these germ cell-specific proteins at 8 weeks after heat treatment, despite the earlier damage observed in the spermatogenic cells in the first 4 weeks. These findings, together with the assessments of spermatogonial proteins, suggest a possible disruption in the function of the spermatogonial stem cells by the generation of new, but functionally damaged, germ cell populations in the second spermatogenic cycle. Another intriguing candidate protein is BAG6 (BCL2-associated athanogene 6; formerly named Bat3, HLA-B-

associated transcript 3), which is predominantly expressed in the testis and is involved in the regulation of spermatogenesis, apoptosis and heat shock proteins (HSP) (Ozaki et al., 1999; Sasaki et al., 2008; Wang and Liew, 1994). BAG6 interacts with several apoptotic regulators, including p53, NCR3, AIFM1, and PBF (Desmots et al., 2008; Sasaki et al., 2007; Tsukahara et al., 2009; von Strandmann et al., 2007). Saski et al. (2008) have demonstrated that BAG6-deficient mice exhibited degradation of HSPA2 and apoptosis of meiotic germ cells, as well as subsequent male infertility that mimicked the infertility seen in HSPA2 null males.

The data presented here support the findings of the previous studies regarding the interaction between BAG6 and HSPA2. A number of studies have demonstrated a crucial role for BAG6 in the stabilisation of HSPA2. This stabilisation is achieved by protection of these heat shock proteins against polyubiquitination and subsequent destruction, thereby permitting their normal function during spermatogenesis to maintain fertility (Bromfield et al., 2015; Bromfield et al., 2017; Sasaki et al., 2008). HSPA2 underexpression has been observed in infertile men and can be considered a factor in failed sperm–oocyte recognition (Cedenho et al., 2006; Redgrove et al., 2013; Redgrove et al., 2012). BAG6 and HSPA2 were also underexpressed in the sperm proteomes of infertile men, suggesting an involvement of these proteins in male infertility (Intasqui et al., 2018). In the present study, we observed a significant decline in these proteins at 14 weeks following heat treatment. However, despite the earlier decrease in HSPA2 at 8 weeks, which may be attributed to a heat effect, this reduction became more significant at 14 weeks following the downregulation of BAG6.

This study is the first to identify 1728 proteins in the TIF from normal and heat-treated rats; this was accomplished using a form of MS that had greater sensitivity than the MS used in our previous investigation of 276 proteins in control rats (Stanton et al., 2016). In the current study, we speculate that the characterisation of TIF proteins could provide important clues for investigating intercellular communication in the testis. For example, TIMP1, which is exclusively expressed by Sertoli cells and spermatogonia, can act as a co-regulator of early basal Leydig cell steroidogenesis in the mouse in vivo (Nothnick et al., 1998). Serum testosterone levels were significantly lower in 21-day-old TIMP1 mutant male mice than in wild-type mice (Nothnick et al., 1998). We recently

observed a decline in the gene expression of key steroidogenic enzymes at 2 weeks following acute heat treatment (Aldahhan et al., Chapter 2). Hence, it is possible that TIMP1 secretion by the Sertoli cell may stimulate the steroidogenic activity of Leydig cells affected by the heat treatment.

In conclusion, this study demonstrates that acute heat induces damage to multiple molecular functions in both the somatic and germ cell populations in the testis. We were able to identify 1728 proteins in the TIF, of which 209 multifunctional proteins were altered, indicating that damage to numerous testicular functions (e.g. fibril formation, Sertoli cell cytoskeleton regulation, spermatogenesis and Hsp stabilisation) occurred subsequent to acute heat treatment. The findings described in this study provide evidence supporting the induction of persistent damage to the testis over two spermatogenic cycles by acute heat, as 40% (85/209) of the proteins normally expressed at 14 weeks were underexpressed following heat treatment. We propose, for the first time, that spermatogonia may be adversely impacted by heat. The proteomic approach taken here may assist in identifying novel markers for male infertility since TIF proteins show a high degree of similarity to blood plasma proteins (Stanton et al., 2016). Further mechanistic studies are needed to identify the pathways in which these proteins participate, as this information could be pivotal for understanding male reproduction.

Figures legends:

Figure 1. Heat map of control and heat-treated rat TIF proteomes. A total of 209 proteins showed various pattern of changes following heat treatment after the analysis with ANOVA $p < 0.05$.

Figure 2. Comparison of rat TIF proteomes that altered at 1, 8 and/or 14 weeks following heat treatment. Proteomes were compared based on common Uniprot accession number with total protein numbers in each group, and figures represent percentage of the total 209 TIF proteome that changed after acute heat.

Figure 3. GO annotation of heat-treated rat TIF proteins. A total of 209 TIF-associated proteins were altered after acute heat treatment in this study, from which 207 (99%) were able to be annotated according to GO information on the basis of (A) molecular function, (B) biological process, and (C) cellular component. The percentage of TIF proteins mapping to the 10 highest ranked (based on number of assigned proteins) (A) molecular function and (B) biological process categories are displayed. (C) Similarly, the percentage of TIF proteins mapping to the 3 highest ranked cellular component categories are also depicted.

Figure 4. Immunoblot validation of three candidate TIF proteins that downregulated following heat treatment: (A) Dcn at 1 week, (B and C) Hspa2 at 8 and 14 weeks, (E and F) Spata20 at 8 and 14 weeks. Data are mean ± SD and statistical comparisons were made against the corresponding controls using Student`s *t*-test: $*p<0.05$ and $**p<0.01$ ($n = 4$ /group). N/A indicates an outlier sample that was removed from the analysis after applying Grubb`s test.

Tables

Table 1. TIF proteins that were significantly altered (> 2-fold) following heat treatment at either 1 week or 8 weeks, or both, but return to normal at 14 weeks.

Table 2. TIF protein that were significantly declined (> 2-fold) following heat treatment at 14 weeks, regardless of whether they are up or down at 1 and 8 weeks – note that no proteins were elevated at 14 weeks.

Table 3. TIF proteins that are associated with heat shock (9), oxidative stress (13), inflammation and/or fibrosis (11), steroidogenesis (2), spermatogenesis (13), proteasomes (4) and Sertoli cell (3) regardless of whether they are up or down at any time point. These proteins provide information about the response, or lack of response, of the tissue to damage.

Table 4. Functional categorisation of selected TIF proteins that changed following acute heat treatment ($p<0.05$).

Supplementary data:

Supp Figure 1. SDS-PAGE on 4–12% SDS gradient gel of (1) adult rat non-enriched testicular interstitial fluid proteins, and (2) enriched TIF proteins. Approximately 500 ng total protein was loaded under reducing conditions, and the gel was stained with Oriole Fluorescent Gel Stain (Bio-rad, Hercules, California, USA). Molecular weight markers ranged from 250 to 15 kDa.

Supp Figure 2. Histology of testis in control and heat-treated rats. Periodic acid–Schiff stained tissue sections of the testis show clearly distinguishable histological differences between the control and heat-treated rats (A-F). Pachytene spermatocytes (SYT) (panel B: arrowhead) and round spermatids (rST) (panel B: large arrow) were lost after 1 week of heat treatment (onset phase). Although there is a re-population of new SYT and rST derived from the earlier germ cell types still present in the testis.at 8 weeks, the germinal epithelium still not recovered with presence of gaps in the damaged cells places (panel D: arrowhead and large arrow). The spermatogenic cells showed histological recovery at 14 weeks (F) and became similar to control (E). SG: Spermatogonia, SC: Sertoli cell and LC: Leydig cell. * indicates interstitial space from which TIF is harvested. All scale bars represent 25 μm. Roman numbers indicate the stages of seminiferous cycle.

Supp Figure 3. GO annotation of control rat TIF proteins. A total of 1538 proteins (89%) were able to be annotated according to GO information on the basis of (A) molecular function, (B) biological process, and (C) cellular component. The percentage of TIF proteins mapping to the 10 highest ranked (based on number of assigned proteins) (A) molecular function and (B) biological process categories are displayed. (C) Similarly, the percentage of TIF proteins mapping to the 3 highest ranked cellular component categories are also shown.

Supp Figure 4. GO annotation of heat-treated rat TIF proteins. A total of 1523 proteins (88%) were able to be annotated according to GO information on the basis of (A) molecular function, (B) biological process, and (C) cellular component. The percentage of TIF proteins mapping to the 10 highest ranked (based on number of assigned proteins) (A) molecular function and (B) biological process categories are displayed. (C) Similarly, the percentage of TIF proteins mapping to the 3

highest ranked cellular component categories are also shown.

Supp Table 1. Total of 1728 proteins identified in TIF from heat-treated and control rats (n=4/ experimental group/time-point). Note: the data presented here are for illustration purpose only and showed n=47 proteins. The whole dataset is shown in Appendix 4.

Supp Table 2. Total of 209 proteins that altered (up/down) following heat treatment at various time-points ($p<0.05$).

Supp Table 3. Proteins that displayed various patterns of changes at different timepoints following heat treatment. **(A)** Total of 15 proteins that changed (up/down) following heat treatment at all time-points ($p<0.05$). **(B)** Total of 23 proteins that altered (up/down) following heat treatment at 1 week only ($p<0.05$). **(C)** Total of 20 proteins that altered (up/down) following heat treatment at 1 and 8 weeks ($p<0.05$). **(D)** Total of 81 proteins that altered (up/down) following heat treatment at 8 weeks only ($p<0.05$). **(E)** Total of 53 proteins that disrupted (up/down) following heat treatment at 8 and 14 weeks ($p<0.05$). **(F)** Total of 17 proteins that downregulated subsequent to heat treatment at 14 weeks only ($p<0.05$).

References

Aktas, C., Kanter, M., 2009. A morphological study on Leydig cells of scrotal hyperthermia applied rats in short-term. J. Mol. Histol. 40, 31–39.

Anand-Ivell, R., Heng, K., Hafen, B., Setchell, B., Ivell, R., 2009. Dynamics of INSL3 peptide expression in the rodent testis. Biol. Reprod. 81, 480–487.

Applewhite, D.A., Grode, K.D., Duncan, M.C., Rogers, S.L., 2013. The actin-microtubule cross-linking activity of Drosophila Short stop is regulated by intramolecular inhibition. Mol. Biol. Cell 24, 2885–2893.

Au, C.L., Robertson, D.M., de Kretser, D.M., 1987. Changes in Testicular Inhibin after a Single Episode of Heating of Rat Testes. Endocrinology 120, 973–977.

Beckmann, R.P., Mizzen, L., Welch, W.J., 1990. Interaction of Hsp 70 with newly synthesized proteins: implications for protein folding and assembly. Science. 248, 850–854.

Birk, D.E., Brückner, P., 2011. Collagens, suprastructures, and collagen fibril assembly, in: Mecham R. (Ed.), The extracellular matrix: an overview. Springer, Berlin, Heidelberg, pp. 77–115

Bowler, K., 1972. The effect of repeated applications of heat on spermatogenesis in the rat: a histological study. J. Reprod. Fertil. 28, 325–333.

Bradford, M.M., 1976. A rapid and sensitive method for the quantitation of microgram quantities of protein utilizing the principle of protein-dye binding. Anal. Biochem. 72, 248–254.

Brew, K., Nagase, H., 2010. The tissue inhibitors of metalloproteinases (TIMPs): an ancient family with structural and functional diversity. Biochim. Biophys. Acta 1803, 55–71.

Bromfield, E.G., Aitken, R.J., Nixon, B., 2015. Novel characterization of the HSPA2-stabilizing protein BAG6 in human spermatozoa. Mol. Hum. Reprod. 21, 755–769.

Bromfield, E.G., Aitken, R.J., McLaughlin, E.A., Nixon, B., 2017. Proteolytic degradation of heat shock protein A2 occurs in response to oxidative stress in male germ cells of the mouse. Mol. Hum. Reprod. 23, 91–105.

Carlsen, E., Andersson, A.M., Petersen, J.H., Skakkebæk, N.E., 2003. History of febrile illness and variation in semen quality. Hum. Reprod. 18, 2089–2092.

Cedenho, A.P., Lima, S.B., Cenedeze, M.A., Spaine, D.M., Ortiz, V., Oehninger, S., 2006. Oligozoospermia and heat-shock protein expression in ejaculated spermatozoa. Hum. Reprod. 21, 1791–1794.

Chalmel, F., Rolland, A.D., Niederhauser-Wiederkehr, C., Chung, S.S., Demougin, P., Gattiker, A., Moore, J., Patard, J.-J., Wolgemuth, D.J., Jégou, B., 2007. The conserved transcriptome in human and rodent male gametogenesis. Proc. Natl. Acad. Sci. 104, 8346–8351.

Chirico, W.J., Waters, M.G., Blobel, G., 1988. 70K heat shock related proteins stimulate protein translocation into microsomes. Nature 332, 805–810.

Chowdhury, A., Steinberger, E., 1970. Early changes in the germinal epithelium of rat testes following exposure to heat. J. Reprod. Fertil. 22, 205–212.

Cox, J., Neuhauser, N., Michalski, A., Scheltema, R.A., Olsen, J.V., Mann, M., 2011. Andromeda: a peptide search engine integrated into the MaxQuant environment. J Proteom. Res. 10, 1794–1805.

Damber, J.E., Bergh, A., Janson, P.O., 1980. Leydig cell function and morphology in the rat testis after exposure to heat. Andrologia 12, 12–19.

Delconte, R.B., Kolesnik, T.B., Dagley, L.F., Rautela, J., Shi, W., Putz, E.M., Stannard, K., Zhang, J.G., Teh, C., Firth, M., Ushiki, T., Andoniou, C.E., Degli-Esposti, M.A., Sharp, P.P., Sanvitale, C.E., Infusini, G., Liau, N.P., Linossi, E.M., Burns, C.J., Carotta, S., Gray, D.H., Seillet, C., Hutchinson, D.S., Belz, G.T., Webb, A.I., Alexander, W.S., Li, S.S., Bullock, A.N., Babon, J.J.,

Smyth, M.J., Nicholson, S.E., Huntington, N.D., 2016. CIS is a potent checkpoint in NK cell-mediated tumor immunity. Nat. Immunol. 17, 816–824.

Desmots, F., Russell, H.R., Michel, D., McKinnon, P.J., 2008. Scythe regulates apoptosis-inducing factor stability during endoplasmic reticulum stress-induced apoptosis. J. Biol. Chem. 283, 3264–3271.

Dix, D.J., Allen, J.W., Collins, B.W., Poorman-Allen, P., Mori, C., Blizard, D.R., Brown, P.R., Goulding, E.H., Strong, B.D., Eddy, E., 1997. HSP70-2 is required for desynapsis of synaptonemal complexes during meiotic prophase in juvenile and adult mouse spermatocytes. Development 124, 4595–4603.

Durairajanayagam, D., Agarwal, A., Ong, C., 2014. Causes, effects and molecular mechanisms of testicular heat stress. Reprod. Biomed. Online 30, 14–27.

Flenkenthaler, F., Windschüttl, S., Fröhlich, T., Schwarzer, J.U., Mayerhofer, A., Arnold, G.J., 2014. Secretome analysis of testicular peritubular cells: a window into the human testicular microenvironment and the spermatogonial stem cell niche in man. J. Proteome Res. 13, 1259–1269.

Gasinska, A., Hill, S., 1989. The effect of hyperthermia on the mouse testis. Neoplasma 37, 357–366.

Govin, J., Caron, C., Escoffier, E., Ferro, M., Kuhn, L., Rousseaux, S., Eddy, E.M., Garin, J., Khochbin, S., 2006. Post-meiotic shifts in HSPA2/HSP70. 2 chaperone activity during mouse spermatogenesis. J. Biol. Chem. 281, 37888–37892.

Hales, D.B., 2002. Testicular macrophage modulation of Leydig cell steroidogenesis. J. Reprod. Immunol. 57, 3–18.

Hedger, M.P., Muir, J.A., 2000. Differential Actions of Gonadotropin‐Releasing Hormone and Human Chorionic Gonadotropin on Interstitial Fluid Volume and Immunoglobulin G Concentrations in Adult Rat Testis. J. Androl. 21, 747–752.

Hess, R.A., Vogl, A.W., 2015. Sertoli cell anatomy and cytoskeleton, in: Griswold, M.D. (Ed.), Sertoli Cell Biology. Academic Press, Oxford, pp. 1–55.

Hou, Y., Wang, X., Lei, Z., Ping, J., Liu, J., Ma, Z., Zhang, Z., Jia, C., Jin, M., Li, X., 2015. Heat Stress Induced Metabolic Changes and Altered Male Reproductive Function. J. Proteome Res. 14, 1495–1503.

Houston, B.J., Nixon, B., Martin, J.H., De Iuliis, G.N., Trigg, N.A., Bromfield, E.G., McEwan, K.E., Aitken, R.J., 2018. Heat exposure induces oxidative stress and DNA damage in the male germ line. Biol. Reprod. 98, 593–606.

Huang, D.W., Sherman, B.T., Tan, Q., Collins, J.R., Alvord, W.G., Roayaei, J., Stephens, R., Baseler, M.W., Lane, H.C., Lempicki, R.A., 2007. The DAVID Gene Functional Classification Tool: a novel biological module-centric algorithm to functionally analyze large gene lists. Genome Biol. 8, R183.

Hughes, C.S., Foehr, S., Garfield, D.A., Furlong, E.E., Steinmetz, L.M., Krijgsveld, J., 2014. Ultrasensitive proteome analysis using paramagnetic bead technology. Mol. Syst. Biol. 10, 757.

Hughes, C.S., Moggridge, S., Müller, T., Sorensen, P.H., Morin, G.B., Krijgsveld, J., 2019. Single-pot, solid-phase-enhanced sample preparation for proteomics experiments. Nat. Protoc. 14, 68–85.

Huszar, G., Stone, K., Dix, D., Vigue, L., 2000. Putative creatine kinase M-isoform in human sperm is identifiedas the 70-kilodalton heat shock protein HspA2. Biol. Reprod. 63, 925–932.

Ilacqua, A., Izzo, G., Emerenziani, G.P., Baldari, C., Aversa, A., 2018. Lifestyle and fertility: the influence of stress and quality of life on male fertility. Reprod. Biol. Endocrinol. 16, 115.

Intasqui, P., Agarwal, A., Sharma, R., Samanta, L., Bertolla, R., 2018. Towards the identification of reliable sperm biomarkers for male infertility: A sperm proteomic approach. Andrologia 50, e12919.

Jegou, B., Laws, A.O., de Kretser, D.M., 1984. Changes in testicular function induced by short‐term exposure of the rat testis to heat: further evidence for interaction of germ cells, Sertoli cells and Leydig cells. Int. J. Androl. 7, 244–257.

Keilhauer, E.C., Hein, M.Y., Mann, M., 2015. Accurate protein complex retrieval by affinity enrichment mass spectrometry (AE-MS) rather than affinity purification mass spectrometry (AP-MS). Mol. Cell. Proteom. 14, 120–135.

Kim, B., Park, K., Rhee, K., 2013. Heat stress response of male germ cells. Cell. Mol. Life Sci. 70, 2623–2636.

Lardenois, A., Gattiker, A., Collin, O., Chalmel, F., Primig, M., 2010. GermOnline 4.0 is a genomics gateway for germline development, meiosis and the mitotic cell cycle. Database 2010, p. baq030

Liu, M., Ru, Y., Gu, Y., Tang, J., Zhang, T., Wu, J., Yu, F., Yuan, Y., Xu, C., Wang, J., 2018. Disruption of Ssp411 causes impaired sperm head formation and male sterility in mice. Biochim. Biophys. Acta 1862, 660–668.

McLean, D.J., Russell, L.D., Griswold, M.D., 2002. Biological activity and enrichment of spermatogonial stem cells in vitamin A-deficient and hyperthermia-exposed testes from mice based on colonization following germ cell transplantation. Biol. Reprod. 66, 1374–1379.

Mruk, D.D., Zhu, L.J., Silvestrini, B., Lee, W.M., Cheng, C.Y., 1997. Interactions of proteases and protease inhibitors in Sertoli‐germ cell cocultures preceding the formation of specialized Sertoli‐germ cell junctions in vitro. J. Androl. 18, 612–622.

Mruk, D.D., Siu, M.K., Conway, A.M., Lee, N.P., Lau, A.S., Cheng, C.Y., 2003. Role of tissue inhibitor of metalloproteases‐1 in junction dynamics in the testis. J. Androl. 24, 510–523.

Nothnick, W.B., Soloway, P.D., Curry, J., Thomas E, 1998. Pattern of messenger ribonucleic acid expression of tissue inhibitors of metalloproteinases (TIMPs) during testicular maturation in male mice lacking a functional TIMP-1 gene. Biol. Reprod. 59, 364–370.

Ozaki, T., Hanaoka, E., Naka, M., Nakagawara, A., Sakiyama, S., 1999. Cloning and characterization of rat BAT3 cDNA. DNA Cell Biol. 18, 503–512.

Paul, C., Murray, A.A., Spears, N., Saunders, P.T., 2008. A single, mild, transient scrotal heat stress causes DNA damage, subfertility and impairs formation of blastocysts in mice. Reproduction 136, 73–84.

Rebourcet, D., O'Shaughnessy, P.J., Pitetti, J.L., Monteiro, A., O'Hara, L., Milne, L., Tsai, Y.T., Cruickshanks, L., Riethmacher, D., Guillou, F., 2014a. Sertoli cells control peritubular myoid cell fate and support adult Leydig cell development in the prepubertal testis. Development 141, 2139–2149.

Rebourcet, D., O'Shaughnessy, P.J., Monteiro, A., Milne, L., Cruickshanks, L., Jeffrey, N., Guillou, F., Freeman, T.C., Mitchell, R.T., Smith, L.B., 2014b. Sertoli cells maintain Leydig cell number and peritubular myoid cell activity in the adult mouse testis. PLoS One 9, e105687.

Redgrove, K.A., Anderson, A.L., McLaughlin, E.A., O'bryan, M.K., Aitken, R.J., Nixon, B., 2013. Investigation of the mechanisms by which the molecular chaperone HSPA2 regulates the expression of sperm surface receptors involved in human sperm–oocyte recognition. Mol. Hum. Reprod. 19, 120–135.

Redgrove, K.A., Nixon, B., Baker, M.A., Hetherington, L., Baker, G., Liu, D.-Y., Aitken, R.J., 2012. The molecular chaperone HSPA2 plays a key role in regulating the expression of sperm surface receptors that mediate sperm-egg recognition. PLoS One 7, e50851.

Russell L.D., Ettlin R.A., Hikim A.P., Clegg E.D., 1990. Histological and Histopathological Evaluation of the Testis, first ed. Cache River Press, Clearwater.

Sasaki, T., Gan, E.C., Wakeham, A., Kornbluth, S., Mak, T.W., Okada, H., 2007. HLA-B-associated transcript 3 (Bat3)/Scythe is essential for p300-mediated acetylation of p53. Genes Dev. 21, 848–861.

Sasaki, T., Marcon, E., McQuire, T., Arai, Y., Moens, P.B., Okada, H., 2008. Bat3 deficiency accelerates the degradation of Hsp70-2/HspA2 during spermatogenesis. J. Cell Biol. 182, 449–458.

Sharpe, R., 1992. Monitoring of spermatogenesis in man ‐ measurement of Sertoli cell ‐ or germ cell ‐ secreted proteins in semen or blood. Int. J. Androl. 15, 201–210.

Sharpe, R.M., Bartlett, J.M.S., Allenby, G., 1991. Evidence for the control of testicular interstitial fluid volume in the rat by specific germ cell types. J. Endocrinol. 128, 359–NP.

Sharpe, R.M., Cooper, I., 1983. Testicular interstitial fluid as a monitor for changes in the intratesticular environment in the rat. J. Reprod. Fertil. 69, 125–135.

Stanton, P.G., 2016. Regulation of the blood-testis barrier, Semin. Cell Dev. Biol. 59, 166–173.

Stanton, P.G., Foo, C.F., Rainczuk, A., Stephens, A.N., Condina, M., O'Donnell, L., Weidner, W., Ishikawa, T., Cruickshanks, L., Smith, L.B., 2016. Mapping the testicular interstitial fluid proteome from normal rats. Proteomics 16, 2391–2402.

Tamura, N., Draviam, V.M., 2012. Microtubule plus-ends within a mitotic cell are ‘moving platforms’ with anchoring, signalling and force-coupling roles. Open Biol. 2, 120–132.

Tang, E.I., Mok, K.-W., Lee, W.M., Cheng, C.Y., 2014. EB1 regulates tubulin and actin cytoskeletal networks at the sertoli cell blood-testis barrier in male rats: an in vitro study. Endocrinology 156, 680–693.

Tian, Y., Tian, X., Gawlak, G., O'Donnell, J.J., Sacks, D.B., Birukova, A.A., 2014. IQGAP1 regulates endothelial barrier function via EB1-cortactin crosstalk. Mol. Cell. Biol. 34, 3546–3558.

Tsukahara, T., Kimura, S., Ichimiya, S., Torigoe, T., Kawaguchi, S., Wada, T., Yamashita, T., Sato, N., 2009. Scythe/BAT3 regulates apoptotic cell death induced by papillomavirus binding factor in human osteosarcoma. Cancer Sci. 100, 47–53.

Turner, K.J., Mckinnell, C., Mclaren, T.T., Qureshi, S.J., Saunders, P.T., Foster, P.M., Sharpe, R.M., 1996. Detection of germ cell ‐ derived proteins in testicular interstitial fluid: potential for monitoring spermatogenesis in vivo. J. Androl. 17, 127–136.

von Strandmann, E.P., Simhadri, V.R., von Tresckow, B., Sasse, S., Reiners, K.S., Hansen, H.P., Rothe, A., Böll, B., Simhadri, V.L., Borchmann, P., 2007. Human leukocyte antigen-B-associated transcript 3 is released from tumor cells and engages the NKp30 receptor on natural killer cells. Immunity. 27, 965–974.

Wang, C., Cui, Y.G., Wang, X.H., Jia, Y., Sinha Hikim, A., Lue, Y.H., Tong, J.S., Qian, L.X., Sha, J.H., Zhou, Z.-M., 2007. Transient scrotal hyperthermia and levonorgestrel enhance testosterone-induced spermatogenesis suppression in men through increased germ cell apoptosis. J. Clin. Endocrinol. Metab. 92, 3292–3304.

Wang, R., Liew, C.C., 1994. The human BAT3 ortholog in rodents is predominantly and developmentally expressedin testis. Mol. Cell. Biochem. 136, 49–57.

Welsh, M., Saunders, P.T., Atanassova, N., Sharpe, R.M., Smith, L.B., 2009. Androgen action via testicular peritubular myoid cells is essential for male fertility. FASEB J. 23, 4218–4230.

Figure 1

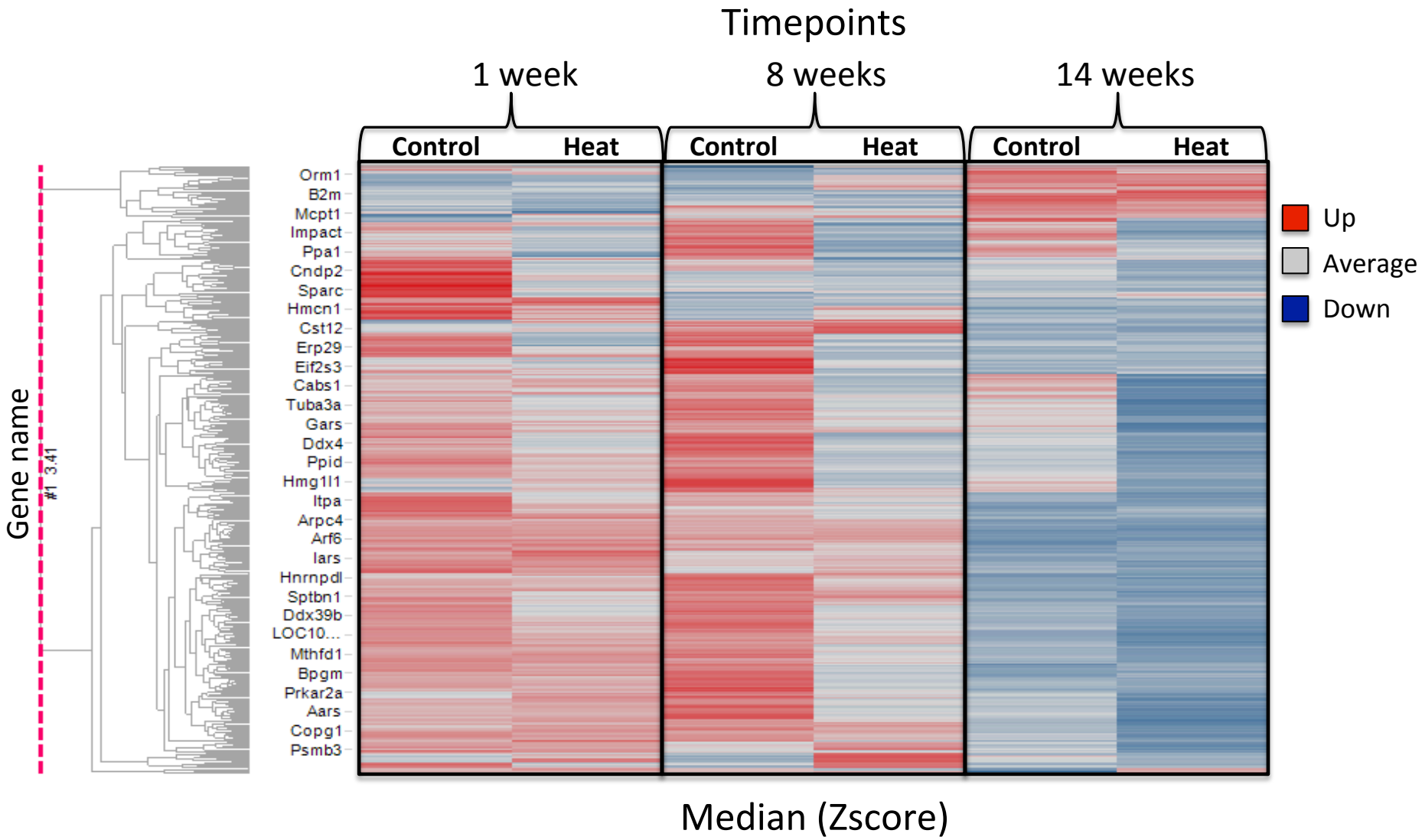
Timepoints
1 week
8 weeks
14 weeks
Control
Heat
Control
Heat
Control
Heat
Gene name
#1 3.41
Orm1
B2m
Mcpt1
Impact
Ppa1
Cndp2
Sparc
Hmcn1
Cst12
Erp29
Eif2s3
Cabs1
Tuba3a
Gars
Ddx4
Ppid
Hmg1l1
Itpa
Arpc4
Arf6
Iars
Hnrnpdl
Sptbn1
Ddx39b
LOC10...
Mthfd1
Bpgm
Prkar2a
Aars
Copg1
Psmb3
Up
Average
Down
Median (Zscore)

Figure 2

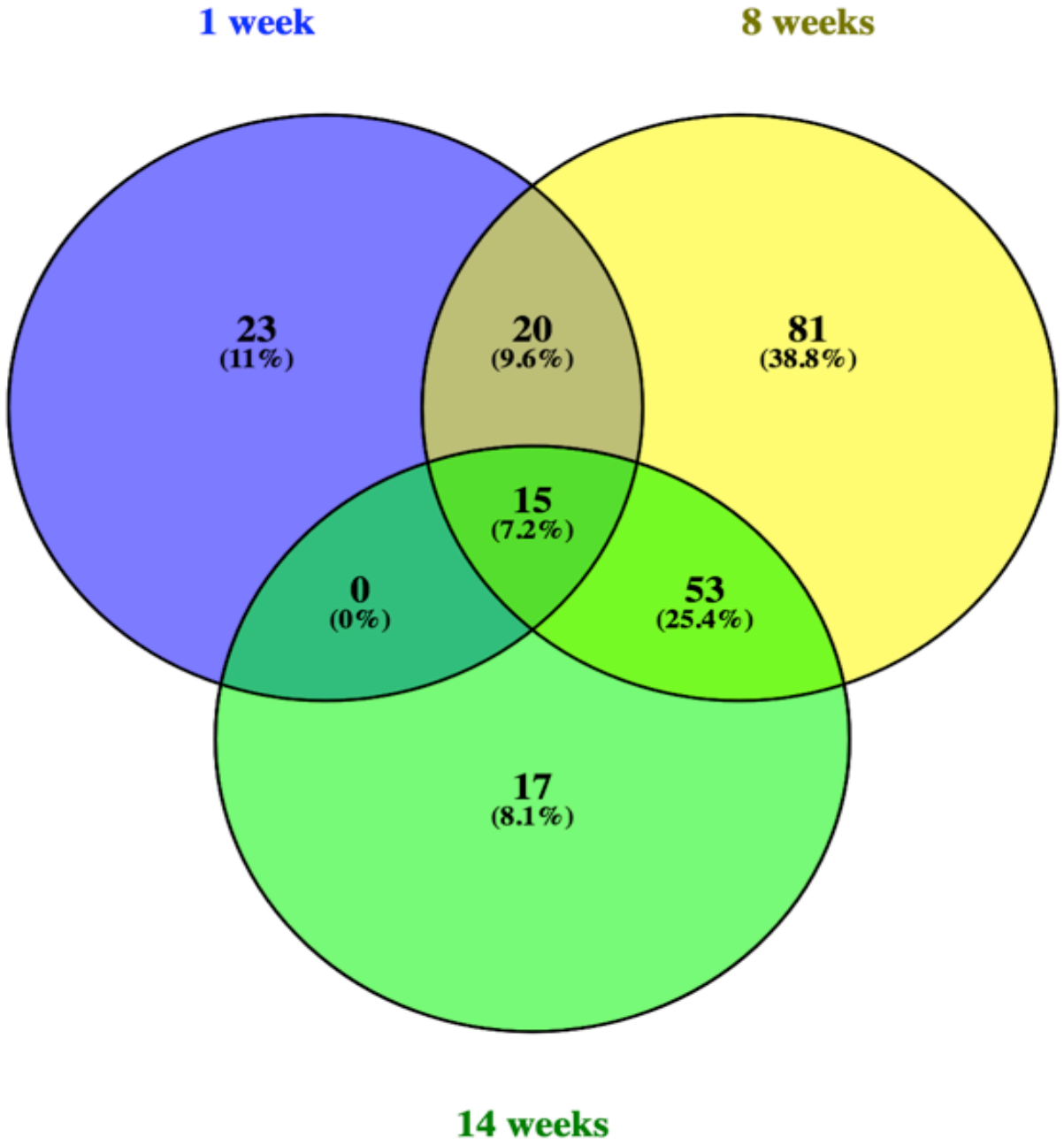

Figure 3

A Molecular function

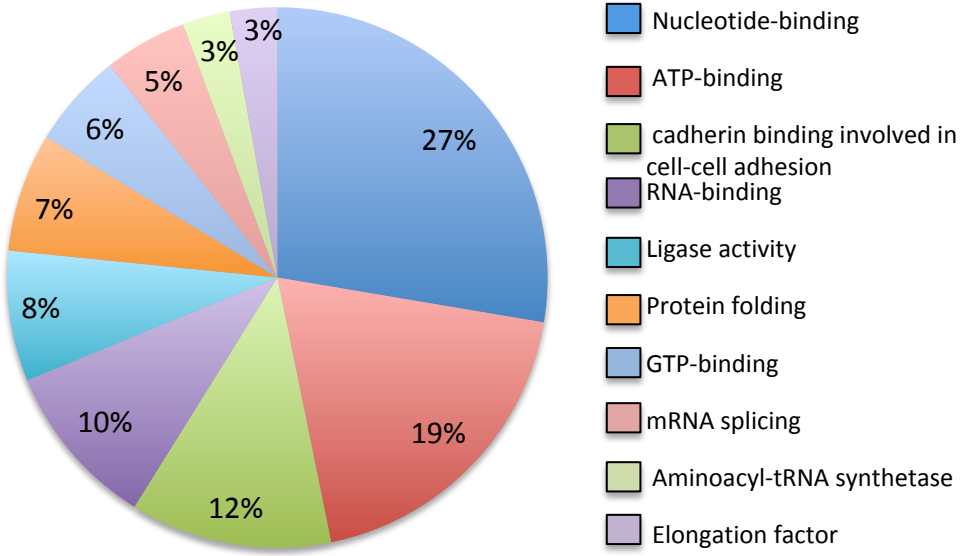

B Biological process

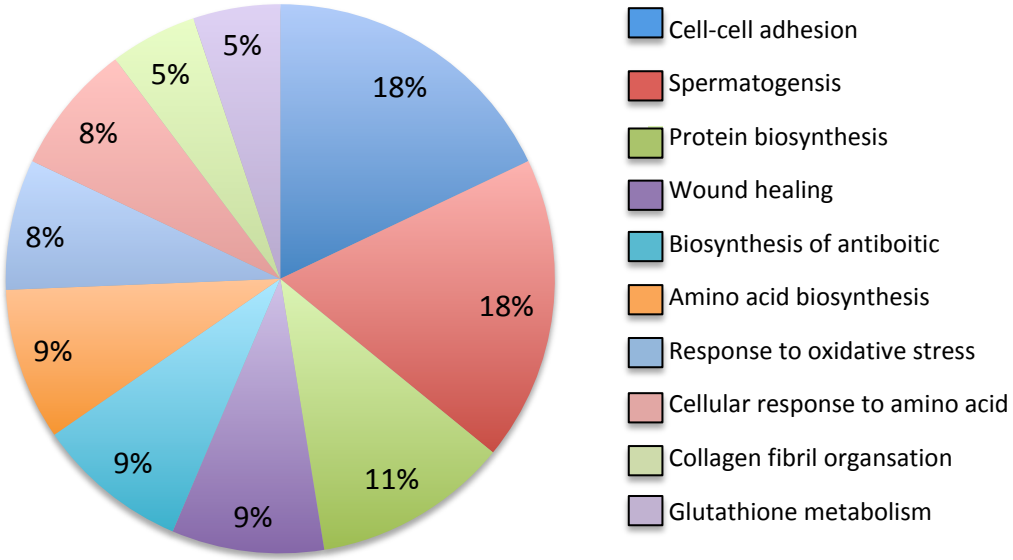

C Cellular component

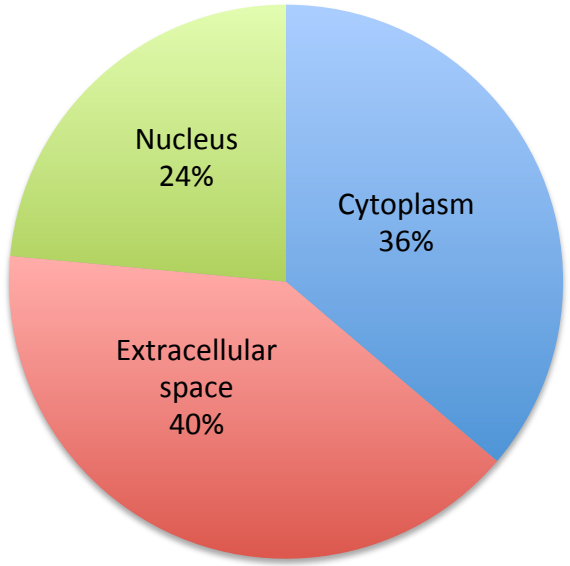

Figure 4

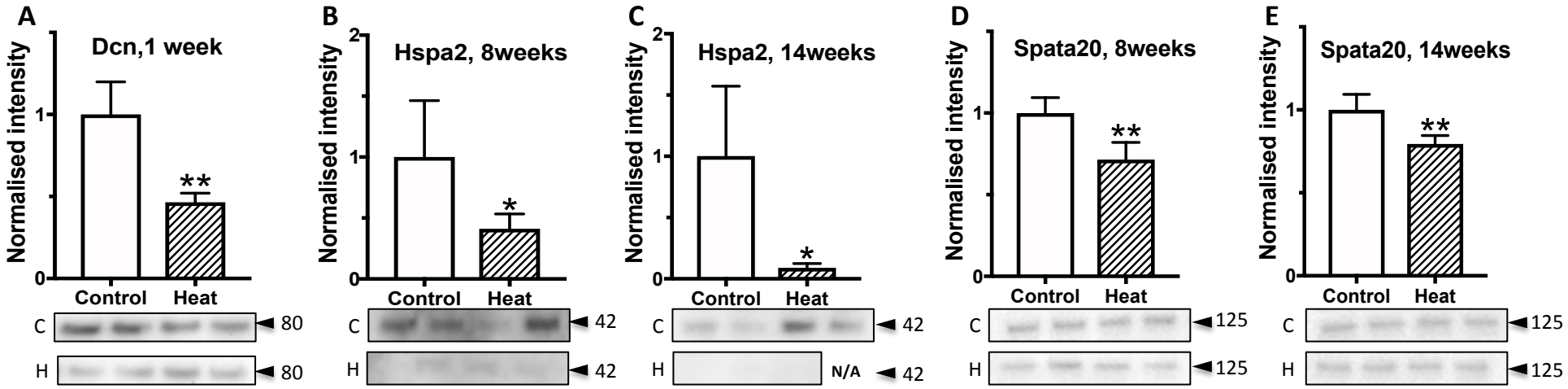
A
Dcn,1 week
Normalised intensity
1
0
**
Control
Heat
C
H
80
80
B
Hspa2, 8weeks
Normalised intensity
2
1
0
*
Control
Heat
C
H
42
42
C
Hspa2, 14weeks
Normalised intensity
2
1
0
*
Control
Heat
C
H
N/A
42
42
D
Spata20, 8weeks
Normalised intensity
1
0
**
Control
Heat
C
H
125
125
E
Spata20, 14weeks
Normalised intensity
1
0
**
Control
Heat
C
H
125
125

Table 1. TIF proteins that are significantly altered (> 2-fold, p<0.05) following heat treatment at either 1 week or 8 weeks, or both, but return to normal at 14 weeks.(See the explanatory notes at the end of the table)

			1 week				8 weeks				14 weeks				Tubular origin
Uniprot accession number	Gene symbol	Protein name	Fold change Heat / Control	P-Value Heat / Control	iBAQ Control	iBAQ Heat	Fold change Heat / Control	P-Value Heat / Control	iBAQ Control	iBAQ Heat	Fold change Heat / Control	P-Value Heat / Control	iBAQ Control	iBAQ Heat	
A0A096MJ40	Hmcn1	Hemicentin-1	0.32	7.45E-02	7.89E+04	3.38E+04	17.14	3.66E-02	4.78E+02	3.05E+04	–	–	7.56E+01	9.67E+03	below sensitivity
Q6P0K8	Jup	Junction plakoglobin	0.42	9.10E-02	4.56E+04	2.23E+04	10.00	3.00E-07	1.30E+04	3.59E+05	–	–	7.87E+02	2.98E+03	SC >> rST & SG
F1LR10	Lima1	LIM domain and actin-binding protein 1	0.67	4.22E-01	1.07E+04	1.37E+03	0.30	3.72E-03	2.04E+04	5.62E+03	0.84	7.08E-01	4.89E+03	2.79E+03	SC & SG
F1M9N7	Agfg1	Arf-GAP domain and FG repeat-containing protein 1	0.99	1.00E+00	1.83E+04	1.14E+04	0.37	1.18E-03	4.90E+04	1.51E+04	0.60	9.46E-01	1.51E+04	1.20E+04	rST & SYT > SC &
Q5RJK6	Inpp1	Inositol polyphosphate-1-phosphatase	0.52	1.24E-01	6.87E+04	2.10E+04	0.32	1.65E-04	8.90E+04	1.39E+04	0.87	8.46E-01	1.97E+04	1.84E+04	rST
B0BN85	Sugt1	Suppressor of G2 allele of SKP1 homolog	0.62	4.81E-01	1.61E+05	5.66E+04	0.26	5.62E-06	1.98E+05	1.21E+04	0.42	3.00E-01	1.74E+04	3.10E+03	Mixed
F1LQQ8	Gusb	Beta-glucuronidase	0.18	5.10E-03	2.40E+05	3.89E+04	1.35	7.41E-01	1.72E+04	2.51E+04	2.67	7.08E-01	8.71E+03	1.26E+04	SG & SC
G3V940	Coro1b	Coronin;Coronin-1B	0.72	4.97E-01	9.19E+04	4.65E+04	0.41	1.56E-02	1.18E+05	3.11E+04	0.99	1.00E+00	2.14E+04	1.03E+04	SYT > SC, rST &
A0A0G2JZ13	Cttn	Src substrate cortactin	0.75	5.63E-01	4.97E+04	3.00E+04	0.36	1.18E-03	1.21E+05	2.91E+04	0.70	5.26E-01	1.38E+04	1.24E+04	SG & SC
A0A0G2JSY5	Fam221a	Protein FAM221A	0.77	6.27E-01	5.18E+04	4.51E+04	0.36	2.63E-02	1.30E+05	1.95E+04	0.44	3.06E-01	3.54E+04	6.52E+03	**SYT >>** rST
F1LMA7	Mrc2	C-type mannose receptor 2	0.36	1.57E-07	1.69E+05	5.09E+04	0.65	1.58E-02	9.35E+04	4.48E+04	0.45	1.04E-01	3.14E+04	1.51E+04	SC & SG
D3ZZC1	Txndc5	Thioredoxin domain-containing protein 5	0.39	1.92E-02	2.92E+05	7.49E+04	0.48	1.65E-02	1.75E+05	6.79E+04	0.62	7.25E-01	4.65E+04	2.03E+04	SG & SC
Q64303	Pak2	Serine/threonine-protein kinase PAK 2	0.58	7.60E-02	1.21E+05	5.88E+04	0.36	1.39E-03	1.74E+05	5.18E+04	0.57	6.23E-02	2.86E+04	1.76E+04	SC & SG > SYT
F1LQD1	Ddx4	Probable ATP-dependent RNA helicase DDX4	0.59	1.79E-01	8.43E+04	5.90E+04	0.28	3.73E-04	2.26E+05	4.92E+04	0.37	1.33E-01	8.57E+04	1.80E+04	below sensitivity
Q4KMA2	Rad23b	UV excision repair protein RAD23 homolog B	0.63	1.79E-01	1.84E+05	6.26E+04	0.39	1.02E-02	2.62E+05	5.29E+04	0.54	8.81E-02	5.14E+04	1.02E+04	SC & SG >> rST &
A0A0G2K0X9	Sec31a	Protein transport protein Sec31A	0.83	4.97E-01	9.18E+04	5.43E+04	0.47	4.36E-04	1.21E+05	4.21E+04	0.64	9.73E-02	3.34E+04	7.88E+03	Mixed
D3ZHA7	RGD1560334	Similar to Myosin light chain 1 slow a	1.32	6.27E-01	8.72E+04	1.34E+05	0.39	1.62E-03	2.57E+05	9.12E+04	0.16	4.29E-01	2.27E+04	2.38E+03	SC & rST > SYT
P19468	Gclc	Glutamate--cysteine ligase catalytic subunit	0.85	7.73E-01	1.70E+05	1.27E+05	0.36	4.36E-03	3.29E+05	6.95E+04	0.65	7.31E-01	4.89E+04	2.06E+04	SG > SC
P50475	Aars	Alanine--tRNA ligase, cytoplasmic	0.91	8.48E-01	1.87E+05	1.41E+05	0.29	5.68E-06	3.28E+05	6.74E+04	0.50	7.79E-02	6.12E+04	2.20E+04	Mixed
Q6AYT3	Rtcb	tRNA-splicing ligase RtcB homolog	1.14	9.07E-01	8.10E+04	1.10E+05	0.37	2.21E-02	1.83E+05	6.81E+04	0.62	1.71E-01	7.08E+04	1.16E+04	SG & SC > SYT >
G3V6M1	Cst12	Cystatin-12	1.22	9.51E-01	1.80E+05	2.03E+05	3.51	1.46E-03	1.85E+05	5.02E+05	0.50	4.29E-01	4.25E+04	2.18E+04	SC
P30120	Timp1	Metalloproteinase inhibitor 1	1.04	9.63E-01	6.49E+04	1.16E+05	2.73	4.36E-03	4.97E+04	2.02E+05	0.98	9.46E-01	3.62E+04	2.09E+04	SG > SC
Q64298	Smcp	Sperm mitochondrial-associated cysteine-rich protein	1.24	7.71E-01	1.26E+06	2.06E+06	0.23	9.32E-04	2.25E+06	7.15E+05	0.26	9.24E-02	6.10E+05	9.30E+03	rST >> SYT
Q6AZ50	Atg3	Ubiquitin-like-conjugating enzyme ATG3	–	–	1.92E+04	2.52E+04	0.15	2.06E-03	1.50E+05	5.47E+03	–	–	0.00E+00	9.28E+03	Mixed
P52759	Hrsp12	Reactive intermediate imine deaminase A homolog	1.29	4.22E-01	1.58E+05	1.65E+05	0.35	2.63E-02	3.37E+05	8.59E+04	–	–	0.00E+00	1.48E+04	SG > SC
Q6AY84	Scrn1	Secernin-1	0.13	4.05E-02	1.61E+05	5.94E+04	0.60	4.83E-01	1.40E+05	4.93E+04	2.00	9.46E-01	1.16E+03	2.63E+04	SG > SC
F1LR02	Col18a1	Collagen type 18 alpha 1 chain	0.87	7.25E-01	5.82E+04	3.85E+04	2.39	1.88E-03	2.20E+04	5.83E+04	1.11	8.13E-01	2.44E+04	2.83E+04	SC & SG
F1LS40	Col1a2	Collagen alpha-2(I) chain	0.21	3.30E-11	4.32E+05	1.23E+05	0.87	6.32E-01	7.90E+04	6.36E+04	0.71	3.14E-01	1.04E+05	6.48E+04	SG > SC
P13941	Col3a1	Collagen alpha-1(III) chain	0.43	2.52E-05	1.45E+05	7.23E+04	1.29	3.25E-01	4.31E+04	4.51E+04	1.02	9.84E-01	3.47E+04	3.93E+04	**SG >>** SC
P46844	Blvra	Biliverdin reductase A	0.34	8.06E-05	4.61E+05	1.36E+05	0.56	5.70E-02	3.08E+05	1.39E+05	0.78	6.54E-01	9.60E+04	3.66E+04	SC
A0A1W2Q6E9	Msn	Moesin	0.30	1.02E-04	4.84E+05	1.82E+05	0.31	6.36E-04	3.45E+05	1.56E+05	1.10	8.91E-01	1.23E+05	9.62E+04	SG & SC
P63039	Hspd1	60 kDa heat shock protein, mitochondrial	0.27	2.69E-04	2.02E+05	3.99E+04	0.78	4.10E-01	3.95E+04	2.56E+04	0.40	1.12E-01	4.98E+04	2.99E+04	SG & SC
Q9ERA7	Msln	Mesothelin	0.39	5.00E-04	8.73E+04	3.50E+04	0.97	9.71E-01	2.62E+04	2.42E+04	0.99	1.00E+00	5.95E+04	5.46E+04	below sensitivity
A0A0G2JUA5	Ahnak	AHNAK nucleoprotein	0.66	2.30E-02	1.81E+05	1.74E+05	0.21	3.42E-12	2.44E+05	1.05E+05	0.64	1.04E-01	8.73E+04	6.00E+04	SC
A0A0G2JSL8	Adk	Adenosine kinase	0.58	6.22E-02	2.33E+05	1.42E+05	0.35	2.30E-03	2.38E+05	9.16E+04	0.66	3.36E-01	9.69E+04	4.31E+04	Mixed
Q02589	Adprh	[Protein ADP-ribosylarginine] hydrolase	0.51	1.47E-01	1.95E+05	4.31E+04	0.31	1.41E-02	2.98E+05	5.15E+04	0.62	2.73E-01	9.41E+04	2.69E+04	SG, SC & SYT
A0A0G2JSM3	Pdlim3	PDZ and LIM domain protein 3	0.37	1.48E-01	2.27E+05	6.53E+04	0.31	5.57E-03	3.66E+05	7.52E+04	0.91	9.46E-01	3.72E+04	2.43E+04	SG & SC
F1LP82	Rab2a	Ras-related protein Rab-2A	0.71	1.60E-01	3.24E+05	2.21E+05	0.41	5.79E-03	3.88E+05	1.28E+05	0.72	6.90E-01	7.78E+04	4.94E+04	Mixed
Q642F2	Ppm1b	protein phosphatase, Mg2+/Mn2+ dependent, 1B	0.66	1.79E-01	1.94E+05	1.09E+05	0.33	1.50E-04	3.48E+05	5.76E+04	0.40	6.12E-02	1.51E+05	6.82E+04	SC, SG & SYT
Q66HR2	Mapre1	Microtubule-associated protein RP/EB family member 1	0.70	4.04E-01	1.98E+05	1.48E+05	0.34	2.60E-04	3.60E+05	1.04E+05	0.44	6.86E-02	1.20E+05	3.46E+04	SC & SG >> SYT >
Q9WU49	Carhsp1	Calcium-regulated heat stable protein 1	0.77	5.68E-01	2.59E+05	1.56E+05	0.25	8.84E-03	3.19E+05	8.68E+04	0.58	3.36E-01	1.48E+05	7.63E+04	SC
B5DF46	Pmm2	Phosphomannomutase	0.69	6.27E-01	1.91E+05	1.02E+05	0.37	1.99E-04	3.27E+05	6.09E+04	0.43	8.81E-02	1.16E+05	3.29E+04	SYT > SG, rST &
Q6TXG7	Shmt1	Serine hydroxymethyltransferase	1.09	8.85E-01	2.08E+05	1.88E+05	0.17	4.53E-10	3.75E+05	8.98E+04	0.52	3.06E-01	6.63E+04	3.31E+04	SYT > SC & SG
Q6P688	Mat2a	S-adenosylmethionine synthase	1.00	1.00E+00	2.11E+05	1.95E+05	0.35	3.46E-02	2.91E+05	9.69E+04	0.42	6.84E-02	8.28E+04	4.16E+04	SG & SC > SYT
P02454	Col1a1	Collagen alpha-1(I) chain	0.25	5.22E-16	1.14E+06	3.02E+05	0.84	3.24E-01	1.98E+05	1.79E+05	0.62	6.50E-02	3.25E+05	2.19E+05	SG >> SC
A0A0G2JSZ5	Pdia6	Protein disulfide-isomerase A6	0.30	1.94E-08	6.82E+05	1.58E+05	0.50	4.36E-03	4.21E+05	1.49E+05	0.46	1.04E-01	2.18E+05	1.42E+05	Mixed
D3ZGK7	Ces1c	Carboxylic ester hydrolase	1.14	7.73E-01	5.84E+05	6.13E+05	14.69	2.36E-03	7.60E+04	4.67E+05	0.75	7.31E-01	5.14E+05	5.07E+05	below sensitivity

F1LQ48	Hnrnpl	Heterogeneous nuclear ribonucleoprotein L	0.60	2.02E-01	4.31E+05	2.79E+05	0.35	1.29E-03	7.07E+05	3.24E+05	0.44	6.29E-02	2.95E+05	1.01E+05	SC &SG > SYT >>
Q63228	Gmfb	Glia maturation factor beta	0.75	7.62E-01	4.26E+05	2.29E+05	0.28	5.05E-03	7.06E+05	1.53E+05	0.42	1.18E-01	2.74E+05	9.64E+04	rST & SYT > SC &
P62963	Pfn1	Profilin-1	0.20	4.10E-06	2.22E+06	4.55E+05	0.48	1.31E-01	5.89E+05	4.23E+05	0.82	8.13E-01	2.55E+05	2.67E+05	SC & SG > rST &
P18418	Calr	Calreticulin	0.31	2.13E-05	1.42E+06	4.48E+05	0.45	1.12E-03	1.00E+06	3.36E+05	0.47	9.88E-02	5.35E+05	3.32E+05	SC & SG > rST &
P36201	Crip2	Cysteine-rich protein 2	0.37	1.71E-03	5.92E+05	1.41E+05	0.23	1.37E-05	8.59E+05	2.14E+05	0.60	2.83E-01	2.90E+05	1.78E+05	SC > SG & rST
P17988	Sult1a1	Sulfotransferase 1A1	1.05	9.60E-01	5.53E+05	5.86E+05	0.32	3.49E-05	1.40E+06	3.11E+05	0.77	7.04E-01	1.89E+05	1.09E+05	Interstitial cell
Q8CFN2	Cdc42	Cell division control protein 42 homolog	0.71	3.54E-01	8.26E+05	6.76E+05	0.30	2.15E-03	1.30E+06	4.00E+05	0.77	6.90E-01	4.22E+05	2.99E+05	SC & SG >> SYT >
Q5M7T7	Pla2g7	Phospholipase A2 group VII	1.28	2.55E-01	2.88E+05	3.39E+05	2.91	4.11E-04	2.32E+05	6.03E+05	0.69	1.50E-01	2.91E+05	2.06E+05	Mixed
P02793	Ftl1	Ferritin light chain 1	0.36	1.64E-02	2.01E+06	4.79E+05	0.99	1.00E+00	2.35E+06	1.61E+06	0.98	1.00E+00	1.27E+05	8.67E+04	**SC & SG >>** rST &
Q6AY18	Sar1a	Secretion associated, Ras related GTPase 1A	0.51	2.55E-01	2.38E+05	9.18E+04	0.25	4.95E-02	3.73E+05	0.00E+00	0.66	5.53E-01	1.86E+05	1.25E+05	**SC & SG >>** rST &
B0BNE5	Esd	S-formylglutathione hydrolase	0.64	9.58E-02	1.20E+06	7.16E+05	0.14	2.66E-07	1.72E+06	3.18E+05	0.69	4.27E-01	5.68E+05	3.73E+05	SC & SG > rST
Q5RJN2	Pcolce	Procollagen C-endopeptidase enhancer 1	0.37	1.65E-10	2.49E+06	1.03E+06	1.73	4.96E-04	6.48E+05	9.05E+05	0.79	4.07E-01	6.14E+05	5.19E+05	SC >> SG
Q01129	Dcn	Decorin	0.23	9.32E-05	1.41E+06	3.37E+05	0.82	6.52E-01	3.74E+05	2.34E+05	1.50	5.09E-01	4.36E+05	6.24E+05	SG
P16975	Sparc	Secreted protein acidic and cysteine rich	0.39	1.85E-11	3.41E+06	1.26E+06	0.62	2.97E-02	1.18E+06	8.27E+05	0.91	8.32E-01	7.73E+05	6.63E+05	SC > SG
G3V6E7	Fmod	Fibromodulin	0.25	2.47E-11	1.21E+07	3.75E+06	0.88	6.35E-01	3.14E+06	2.27E+06	0.58	7.79E-02	2.92E+06	1.98E+06	SYT & rST
A0A0G2K135	Cfi	Complement factor I	0.57	1.44E-09	1.04E+07	5.99E+06	1.33	4.84E-02	5.66E+06	5.88E+06	1.11	4.70E-01	5.91E+06	6.66E+06	below sensitivity
Q6AXN2	Efemp1	EGF-containing fibulin-like extracellular matrix protein 1	0.65	2.35E-05	3.93E+06	2.49E+06	1.44	1.51E-03	2.63E+06	3.03E+06	0.84	3.39E-01	1.95E+06	1.65E+06	below sensitivity
P63029	Tpt1	Translationally-controlled tumor protein	0.18	1.54E-02	4.00E+06	2.32E+06	0.32	1.86E-02	3.44E+06	1.23E+06	0.74	6.01E-01	1.53E+06	9.86E+05	SG & SC >rST &
P62959	Hint1	Histidine triad nucleotide-binding protein 1	0.54	2.57E-02	2.31E+06	1.13E+06	0.26	4.02E-04	3.96E+06	8.02E+05	0.51	1.34E-01	2.44E+06	1.27E+06	Mixed
Q925N6	Igsf1	Immunoglobulin superfamily member 1	1.58	8.36E-02	7.20E+06	5.45E+06	2.93	6.69E-03	4.03E+06	5.03E+06	0.67	2.69E-01	5.51E+06	5.99E+06	SC
F1M8E9	Lyz2	Lysozyme	0.72	3.98E-01	2.48E+06	1.26E+06	2.55	2.15E-03	1.13E+06	2.21E+06	0.78	5.26E-01	1.53E+06	1.28E+06	rST
P11232	Txn	Thioredoxin	0.88	8.88E-01	5.08E+06	5.29E+06	0.32	2.36E-03	8.87E+06	3.62E+06	0.51	4.29E-01	3.42E+06	1.58E+06	SC & SG
A0A0G2K531	Gpx3	Glutathione peroxidase 3	1.69	3.82E-05	6.88E+06	1.03E+07	2.73	1.01E-07	6.48E+06	1.43E+07	0.89	7.38E-01	8.85E+06	7.67E+06	SG & SC
P14046	A1i3	Alpha-1-inhibitor 3	0.34	2.02E-03	9.14E+06	4.93E+06	1.09	7.22E-01	1.05E+07	8.01E+06	1.29	5.80E-01	1.36E+07	1.48E+07	below sensitivity
A0A0G2JTU6	Sbp	Prostatic spermine-binding protein	0.60	7.56E-01	6.72E+03	3.28E+03	0.08	2.63E-02	2.61E+05	4.33E+03	–	–	1.58E+03	0.00E+00	below sensitivity
E9PT65	Rdx	Radixin	0.85	7.51E-01	8.85E+04	5.89E+04	0.38	4.57E-02	1.31E+05	1.87E+04	0.49	4.29E-01	1.25E+04	0.00E+00	SYT & rST >> SG
M0R8P3	Cabyr	Calcium-binding tyrosine phosphorylation-regulated	0.24	6.27E-01	7.75E+04	3.13E+04	0.22	3.66E-02	1.47E+05	6.92E+03	0.25	1.18E-01	3.57E+04	0.00E+00	rST >> SYT
A0A0G2K824	Gmppa	Mannose-1-phosphate guanyltransferase alpha	0.31	1.37E-02	4.29E+04	5.09E+03	0.46	3.25E-01	1.71E+04	2.80E+03	–	–	0.00E+00	0.00E+00	Mixed
Q3B7D1	Ube2z	Ubiquitin-conjugating enzyme E2 Z	0.72	8.88E-01	2.06E+04	9.46E+03	0.27	3.66E-02	1.04E+05	1.21E+04	–	–	0.00E+00	0.00E+00	SG & SC >rST &
P43527	Casp1	Caspase-1	1.14	8.48E-01	5.70E+04	4.68E+04	0.40	3.46E-02	9.80E+04	1.04E+04	–	–	0.00E+00	0.00E+00	below sensitivity

Yellow cells:	Proteins that are changed (up/down) with $p < 0.05$.
Green cells:	Proteins that are unchanged or changed with $p > 0.05$.

Column explanations

Uniprot accession number: First, or leading, protein ID annotation in UniProtKB/Swiss-Prot Rattus norvegicus database (Nov 2018).

Gene symbol: Leading gene symbol in UniProtKB/Swiss-Prot Rattus norvegicus database (Nov 2018).

Protein name: Protein name from the UniProtKB/Swiss-Prot Rattus norvegicus database (Nov 2018).

iBAQ: The sum of all the peptides intensities divided by the number of observable peptides of a protein.

Relative abundance: Relative abundance score in 25 fold ranges, based on top most abundant protein iBAQ score.

Log2 Heat/Control: Log2 ratio of protein abundance in heat-treated rats/control rats.

Fold change Heat/Control: Linear ratio of protein abundance in heat-treated rats/control rats.

P-Value Heat/Control: p value of difference in protein abundance between heat-treated and control rats.

Tubular origin: Microarray dataset published by Chalmel et al 2007, PNAS, 104(20):8346. Data accessed via www.germonline.org

Note

Cell specificity: cell IDs are done by mRNA of purified cell types via Germonline.

'Mixed': indicates almost equal expression by all geminal epithelial cells.

'below sensitivity': indicates below detection limits.

‘>’: indicates expression greater than 2-fold, but less than 4-fold different to the next cell type.

‘>>’: indicates expression greater than 4-fold compared with next cell type.

Bold text and '>>': indicates 10-fold higher expression than next cell type.

‘&’: indicates expression differences between cell types is less than 2-fold.

'/': indicates another pattern of cell expression

Abbreviations	
SC	Sertoli cell
SG	Spermatogonia
SYT	Spermatocytes
rST	round spermatid

Table 2. TIF proteins that were significantly declined (> 2-fold, p<0.05) following heat treatment at 14 weeks, regardless of whether they are up or down at 1 and 8 weeks – note that no proteins were elevated at 14 weeks.

			1 week				8 weeks				14 weeks				Tubular origin
Uniprot accession number	Gene symbol	Protein name	Fold change Heat / Control	P-Value Heat / Control	iBAQ Control	iBAQ Heat	Fold change Heat / Control	P-Value Heat / Control	iBAQ Control	iBAQ Heat	Fold change Heat / Control	P-Value Heat / Control	iBAQ Control	iBAQ Heat	
B5DF80	Pabpc6	Polyadenylate-binding protein	0.74	8.16E-01	1.38E+04	5.47E+03	0.20	1.50E-02	6.68E+04	1.09E+04	0.15	2.29E-03	2.66E+04	1.45E+03	Not available
Q4QR76	Actl7b	Actin-like protein 7B	0.44	2.34E-02	8.43E+04	2.07E+04	0.46	1.41E-02	1.09E+05	1.71E+04	0.21	1.82E-03	7.31E+04	2.70E+03	rST > SYT
D3ZSC2	Pdcd2l	Programmed cell death 2-like	0.63	6.27E-01	3.30E+04	1.22E+04	0.12	7.84E-02	5.14E+04	1.08E+03	0.25	1.72E-02	5.78E+04	2.51E+03	SYT > rST >> SC &
P53042	Ppp5c	Serine/threonine-protein phosphatase 5	1.00	1.00E+00	3.16E+04	2.79E+04	0.47	1.53E-02	8.42E+04	6.48E+03	0.38	2.85E-02	4.44E+04	6.14E+03	SYT >> rST & SG &
F8WG67	Acot7	Cytosolic acyl coenzyme A thioester hydrolase	0.47	3.46E-01	6.09E+04	2.11E+04	0.82	9.87E-01	5.29E+04	4.00E+04	0.39	3.48E-02	5.76E+04	9.85E+03	**rST & SYT >>** SC &
G3V700	Nrd1	Nardilysin	1.67	1.98E-01	6.45E+04	9.46E+04	0.26	3.30E-05	2.53E+05	4.73E+04	0.17	1.48E-06	6.75E+04	6.02E+03	rST > **SYT >>** SC &
Q5XIM9	Cct2	T-complex protein 1 subunit beta	0.63	2.65E-01	1.82E+05	7.99E+04	0.70	2.90E-01	1.71E+05	8.20E+04	0.17	9.35E-03	6.80E+04	1.43E+04	Mixed
G3V7B2	Lrrc46	Leucine-rich repeat-containing protein 46	0.93	9.63E-01	1.54E+05	1.10E+05	0.39	1.56E-02	2.96E+05	5.97E+04	0.18	6.64E-04	1.93E+05	7.06E+03	SYT & rST
A0A0G2JZG7	Sars	Serine--tRNA ligase, cytoplasmic	1.01	1.00E+00	8.29E+04	8.30E+04	0.41	6.69E-03	1.44E+05	3.82E+04	0.26	3.67E-03	6.59E+04	1.04E+04	Mixed
G3V762	Tsta3	Tissue specific transplantation antigen P35B	1.18	8.17E-01	3.05E+05	3.09E+05	0.24	8.25E-04	5.50E+05	9.01E+04	0.30	3.41E-02	6.79E+04	1.92E+04	SYT & rST >> SC &
Q562C6	Lztfl1	Leucine zipper transcription factor-like protein 1	0.73	5.59E-01	1.01E+05	1.18E+05	0.32	1.39E-03	2.77E+05	6.49E+04	0.31	2.85E-02	9.63E+04	1.85E+04	SYT & rST >> SC &
Q5QD51	Akap12	A-kinase anchor protein 12	0.78	5.26E-01	5.47E+04	3.26E+04	0.27	3.44E-04	9.52E+04	2.67E+04	0.35	3.95E-03	3.35E+04	9.23E+03	rST & SYT >> SC &
G3V7G8	Gars	Glycine--tRNA ligase	0.62	1.47E-01	8.10E+04	4.58E+04	0.55	1.13E-01	9.25E+04	2.94E+04	0.36	2.03E-02	3.90E+04	7.26E+03	SG & SC > rST
P41499	Ptpn11	Tyrosine-protein phosphatase non-receptor type 11	1.26	6.21E-01	3.76E+04	6.01E+04	0.36	2.53E-06	1.46E+05	2.88E+04	0.37	2.12E-03	6.27E+04	1.29E+04	below sensitivity
G3V617	Mapk14	Mitogen-activated protein kinase	1.79	5.63E-01	1.34E+05	3.04E+05	1.45	6.69E-01	3.56E+05	6.51E+05	0.09	1.71E-02	4.68E+04	7.72E+03	SC & SG
Q5U328	Ncl	Nucleolin	–	–	0.00E+00	4.83E+03	0.28	4.80E-01	1.37E+04	0.00E+00	0.20	4.05E-03	3.48E+04	2.12E+03	SG > SC >> SYT >
O70177	Ces2c	Carboxylic ester hydrolase	2.29	5.15E-01	3.02E+04	5.12E+04	2.28	4.80E-01	1.05E+04	1.96E+04	0.38	1.41E-02	1.80E+05	8.84E+04	below sensitivity
F1LSR7	Spata20	Spermatogenesis-associated protein 20	1.12	7.73E-01	2.56E+05	2.51E+05	0.28	2.18E-07	4.62E+05	9.21E+04	0.18	1.38E-08	2.87E+05	3.75E+04	**rST>>** SYT
Q6MG49	Bag6	Large proline-rich protein BAG6	0.63	3.54E-01	2.16E+05	1.41E+05	0.62	2.79E-01	2.46E+05	1.38E+05	0.18	7.63E-03	1.10E+05	7.00E+04	rST & SYT > SC &
G3V6W6	Psmc6	Proteasome 26S subunit, ATPase 6	0.92	8.30E-01	2.85E+05	2.13E+05	0.77	3.08E-01	1.66E+05	1.93E+05	0.22	1.13E-02	1.95E+05	7.32E+04	SG > SC
D4A781	Ipo5	Importin 5	1.00	1.00E+00	3.47E+05	2.93E+05	0.54	2.86E-04	4.12E+05	1.61E+05	0.25	7.70E-11	2.79E+05	6.88E+04	rST >> SYT & SG >
Q66HD3	Nasp	Nuclear autoantigenic sperm protein	0.65	3.60E-01	8.96E+04	7.90E+04	0.33	2.94E-05	1.83E+05	3.24E+04	0.28	1.99E-03	1.67E+05	3.39E+04	SYT > rST >> SC &
C0JPT7	Flna	Filamin-A	0.82	1.80E-01	9.49E+04	7.16E+04	0.25	2.72E-18	2.46E+05	5.07E+04	0.29	5.84E-09	8.20E+04	3.19E+04	**SC & SG >>** rST
P47860	Pfkp	ATP-dependent 6-phosphofructokinase, platelet type	1.13	7.73E-01	2.32E+05	2.33E+05	0.52	3.14E-02	3.49E+05	1.05E+05	0.32	3.95E-04	1.27E+05	3.54E+04	SYT & SG > SC &
F2Z3Q8	Kpnb1	Importin subunit beta-1	0.71	4.22E-01	2.66E+05	3.28E+05	0.88	7.74E-01	1.39E+05	2.99E+05	0.32	4.28E-06	8.12E+04	2.84E+04	SYT >> SC, SG &
G3V8L9	Ptrf	Polymerase I and transcript release factor	0.37	2.63E-04	2.56E+05	9.23E+04	0.23	5.62E-06	3.21E+05	3.86E+04	0.33	8.80E-03	3.47E+05	9.54E+04	SG & SC
Q4KLZ3	Dazap1	Deleted in AZoospermia Associated Protein 1	0.95	9.63E-01	1.41E+05	1.26E+05	0.39	1.32E-02	2.77E+05	8.41E+04	0.34	1.72E-02	1.32E+05	2.96E+04	SYT > SG & rST >
P40112	Psmb3	Proteasome subunit beta type-3	0.78	5.80E-01	4.76E+05	3.59E+05	2.04	6.52E-03	2.44E+05	5.14E+05	0.36	4.61E-03	2.54E+05	6.35E+04	SC & SG >> rST &
A0A0G2JZY6	Sptbn1	Spectrin beta chain	1.01	9.93E-01	2.46E+05	1.84E+05	0.51	1.24E-04	4.15E+05	2.84E+05	0.36	1.39E-05	6.30E+04	3.33E+04	SG & SC > SYT &
Q9JLZ1	Glrx3	Glutaredoxin-3	0.98	1.00E+00	2.42E+05	2.04E+05	0.32	2.21E-03	3.46E+05	8.21E+04	0.37	1.99E-03	1.94E+05	4.04E+04	SYT & rST > SC &
A0A0G2K7X0	Anp32a	Acidic leucine-rich nuclear phosphoprotein 32 family	3.54	9.69E-02	1.15E+05	4.25E+05	0.11	7.00E-04	1.19E+06	1.31E+05	0.06	1.86E-03	2.90E+05	3.36E+04	SG & SC
F7F2F3	Hspa4l	Heat shock protein family A (Hsp70) member 4 like	1.22	5.22E-01	4.22E+05	4.17E+05	0.15	3.10E-13	7.65E+05	1.34E+05	0.06	4.06E-13	5.46E+05	7.95E+04	SYT >> SC & rST
Q68FR8	Tuba3a	Tubulin alpha-3 chain	0.82	9.58E-01	4.18E+05	3.72E+05	0.33	1.90E-02	7.60E+05	2.07E+05	0.10	2.50E-02	2.75E+05	5.07E+04	SC > SG > rST >>
D4A3P0	Ybx2	Y box-binding protein 2	0.63	3.22E-01	6.71E+05	4.17E+05	0.14	1.85E-06	1.54E+06	2.11E+05	0.14	3.16E-05	4.52E+05	6.10E+04	SYT & rST
A0A0G2JSU3	Set	Protein SET	0.51	3.64E-01	3.52E+05	2.92E+05	0.30	2.04E-02	6.61E+05	1.87E+05	0.22	2.67E-03	4.42E+05	5.32E+04	Mixed
O35814	Stip1	Stress-induced-phosphoprotein 1	0.78	4.22E-01	4.90E+05	3.84E+05	0.40	9.35E-04	7.79E+05	2.75E+05	0.24	2.13E-03	3.04E+05	1.28E+05	Mixed
P68511	Ywhah	14-3-3 protein eta	1.42	6.44E-01	5.33E+05	5.17E+05	0.32	2.91E-03	1.56E+06	3.56E+05	0.25	1.85E-02	4.01E+05	1.03E+05	SC & SG >> SYT
B5DEN5	Eef1b2	Eukaryotic translation elongation factor 1 beta 2	0.83	8.14E-01	5.65E+05	4.23E+05	0.35	1.88E-03	9.53E+05	2.73E+05	0.27	9.95E-03	4.09E+05	8.49E+04	Mixed
Q5D059	Hnrnpk	Heterogeneous nuclear ribonucleoprotein K	0.50	1.75E-03	7.80E+05	5.22E+05	0.57	7.79E-03	7.99E+05	4.40E+05	0.31	6.43E-05	3.83E+05	1.23E+05	SG & SC > SYT >>
O08651	Phgdh	D-3-phosphoglycerate dehydrogenase	0.40	4.35E-03	5.05E+05	1.99E+05	0.45	9.66E-04	6.07E+05	1.88E+05	0.34	5.36E-04	2.84E+05	1.09E+05	SC & SG >> rST >
G3V6H9	Nap1l1	Nucleosome assembly protein 1-like 1	0.69	3.02E-01	4.24E+05	3.05E+05	0.39	1.98E-03	8.42E+05	3.44E+05	0.38	6.73E-04	3.33E+05	1.31E+05	Two patterns:1-SG >
Q794E4	Hnrnpf	Heterogeneous nuclear ribonucleoprotein F	0.83	6.27E-01	7.57E+05	6.17E+05	0.41	5.12E-04	9.19E+05	4.47E+05	0.28	4.26E-02	3.00E+05	9.12E+04	Mixed
Q63413	Ddx39b	Spliceosome RNA helicase Ddx39b	0.60	7.45E-02	1.02E+06	6.30E+05	0.45	8.70E-03	1.11E+06	4.75E+05	0.32	9.78E-03	3.74E+05	1.42E+05	SG > SC > SYT >
D4ABI6	Uchl3	Ubiquitin carboxyl-terminal hydrolase	1.04	9.63E-01	6.65E+05	5.68E+05	0.40	2.46E-04	1.06E+06	3.23E+05	0.38	9.34E-04	4.51E+05	1.80E+05	Mixed
P17220	Psma2	Proteasome subunit alpha type-2	0.69	1.26E-01	1.34E+06	8.96E+05	1.63	7.16E-02	7.93E+05	1.12E+06	0.37	1.37E-02	4.34E+05	1.59E+05	SG & SC > SYT >
P05197	Eef2	Elongation factor 2	0.57	1.53E-03	1.39E+06	7.12E+05	0.52	1.03E-04	1.40E+06	7.28E+05	0.38	4.91E-06	5.03E+05	2.60E+05	Mixed
P56702	Dbil5	Diazepam-binding inhibitor-like 5	1.54	2.55E-01	3.29E+05	5.16E+05	0.22	3.59E-02	6.53E+05	2.25E+05	0.08	2.40E-03	5.92E+05	3.58E+04	rST >> SYT

D3ZDK7	Pgp	Glycerol-3-phosphate phosphatase	0.98	9.99E-01	7.17E+05	5.86E+05	0.33	7.14E-05	7.64E+05	2.04E+05	0.11	3.58E-10	9.97E+05	1.50E+05	**Two patterns:** 1-
Q68FX6	Cabs1	Calcium-binding and spermatid-specific protein 1	1.12	8.64E-01	5.19E+05	7.30E+05	0.13	5.54E-10	1.20E+06	1.38E+05	0.16	3.19E-05	5.91E+05	9.72E+04	**rST >>** SYT
Q6Q0N1	Cndp2	Cytosolic non-specific dipeptidase	0.51	2.68E-09	1.37E+06	6.40E+05	0.49	1.86E-08	1.19E+06	5.17E+05	0.35	4.28E-06	8.15E+05	3.86E+05	SC >> SG, rST &
A0A0G2JV31	Xpnpep1	X-prolyl aminopeptidase (Aminopeptidase P) 1, soluble,	0.75	1.35E-01	1.23E+06	8.69E+05	0.34	8.85E-10	1.71E+06	4.71E+05	0.36	2.89E-06	7.75E+05	2.89E+05	rST & SC > SYT &
P14659	Hspa2	Heat shock-related 70 kDa protein 2	0.73	3.80E-01	1.19E+06	9.60E+05	0.26	1.85E-06	2.30E+06	6.23E+05	0.14	7.39E-07	1.67E+06	3.14E+05	SYT & rST
P83868	Ptges3	Prostaglandin E synthase 3	1.27	7.66E-01	5.19E+05	7.53E+05	0.28	1.50E-04	2.30E+06	6.61E+05	0.20	5.00E-04	1.00E+06	2.82E+05	Mixed
Q08163	Cap1	Adenylyl cyclase-associated protein 1	0.57	1.17E-03	1.13E+06	6.74E+05	0.63	1.39E-02	1.42E+06	6.57E+05	0.30	6.32E-05	5.97E+05	2.80E+05	SC > SG & SYT >>
F1LNF1	Hnrnpa2b1	Heterogeneous nuclear ribonucleoproteins A2/B1	0.44	4.89E-03	1.42E+06	7.48E+05	0.50	1.80E-03	2.05E+06	7.82E+05	0.32	1.99E-03	7.95E+05	2.80E+05	Mixed
P55054	Fabp9	Fatty acid-binding protein 9	0.65	2.08E-01	3.14E+06	2.45E+06	0.23	3.14E-03	4.07E+06	1.06E+06	0.14	1.03E-04	3.49E+06	8.24E+05	SYT & rST
D3ZCR3	Hmgb1	High mobility group protein B1	1.60	3.22E-01	1.47E+06	2.14E+06	0.23	1.39E-04	5.92E+06	8.66E+05	0.28	1.10E-02	1.93E+06	7.96E+05	SG & SC
P09034	Ass1	Argininosuccinate synthase	1.32	2.92E-01	4.46E+06	4.53E+06	0.33	4.53E-10	1.07E+07	3.21E+06	0.28	3.16E-05	2.22E+06	9.05E+05	Interstitial cell
P62630	Eef1a1	Elongation factor 1-alpha 1	0.56	9.15E-07	7.06E+06	4.05E+06	0.43	4.37E-06	8.16E+06	3.20E+06	0.29	1.06E-08	3.52E+06	1.42E+06	Mixed

Yellow cells:	Proteins that are changed (up/down) with $p < 0.05$.
Green cells:	Proteins that are unchanged or changed with $p > 0.05$.

Column explanations

Uniprot accession number: First, or leading, protein ID annotation in UniProtKB/Swiss-Prot Rattus norvegicus database (Nov 2018).

Gene symbol: Leading gene symbol in UniProtKB/Swiss-Prot Rattus norvegicus database (Nov 2018).

Protein name: Protein name from the UniProtKB/Swiss-Prot Rattus norvegicus database (Nov 2018).

iBAQ: The sum of all the peptides intensities divided by the number of observable peptides of a protein.

Relative abundance: Relative abundance score in 25 fold ranges, based on top most abundant protein iBAQ score.

Log2 Heat/Control: Log2 ratio of protein abundance in heat-treated rats/control rats.

Fold change Heat/Control: Linear ratio of protein abundance in heat-treated rats/control rats.

P-Value Heat/Control: p value of difference in protein abundance between heat-treated and control rats.

Tubular origin: Microarray dataset published by Chalmel et al 2007, PNAS, 104(20):8346. Data accessed via www.germonline.org

Note

Cell specificity: cell IDs are done by mRNA of purified cell types via Germonline.

'Mixed': indicates almost equal expression by all geminal epithelial cells.

'below sensitivity': indicates below detection limits.

‘>’: indicates expression greater than 2-fold, but less than 4-fold different to the next cell type.

‘>>’: indicates expression greater than 4-fold compared with next cell type.

Bold text and '>>': indicates 10-fold higher expression than next cell type.

‘&’: indicates expression differences between cell types is less than 2-fold.

'/': indicates another pattern of cell expression

Abbreviations	
SC	Sertoli cell
SG	Spermatogonia
SYT	Spermatocytes
rST	round spermatid

Table 3. TIF proteins that are associated with heat shock (6), oxidative stress (6), inflammation and/or fibrosis (8), spermatogenesis (11), proteasomes (3), Sertoli cell (2) and inhibin-related (1) regardless of whether they are significantly up or down (> 2-fold, $p<0.05$) at any time point. These proteins provide information about the response, or lack of response, of the tissue to damage.

			1 week				8 weeks				14 weeks				
Uniprot accession number	Gene symbol	Protein name	Fold change Heat / Control	P-Value Heat / Control	iBAQ Control	iBAQ Heat	Fold change Heat / Control	P-Value Heat / Control	iBAQ Control	iBAQ Heat	Fold change Heat / Control	P-Value Heat / Control	iBAQ Control	iBAQ Heat	Tubular origin
Heat shock-related proteins															
P63039	Hspd1	60 kDa heat shock protein, mitochondrial	0.27	2.69E-04	2.02E+05	3.99E+04	0.78	4.10E-01	3.95E+04	2.56E+04	0.40	1.12E-01	4.98E+04	2.99E+04	SG & SC
P52759	Hrsp12	Reactive intermediate imine deaminase A homolog	1.29	4.22E-01	1.58E+05	1.65E+05	0.35	2.63E-02	3.37E+05	8.59E+04	–	–	0.00E+00	1.48E+04	SG > SC
P14659	Hspa2	Heat shock-related 70 kDa protein 2	0.73	3.80E-01	1.19E+06	9.60E+05	0.26	1.85E-06	2.30E+06	6.23E+05	0.14	7.39E-07	1.67E+06	3.14E+05	SYT & rST
F7F2F3	Hspa4l	Heat shock protein family A (Hsp70) member 4 like	1.22	5.22E-01	4.22E+05	4.17E+05	0.15	3.10E-13	7.65E+05	1.34E+05	0.06	4.06E-13	5.46E+05	7.95E+04	SYT >> SC & rST
O35814	Stip1	Stress-induced-phosphoprotein 1	0.78	4.22E-01	4.90E+05	3.84E+05	0.40	9.35E-04	7.79E+05	2.75E+05	0.24	2.13E-03	3.04E+05	1.28E+05	Mixed
Q66HD3	Nasp	Nuclear autoantigenic sperm protein	0.65	3.60E-01	8.96E+04	7.90E+04	0.33	2.94E-05	1.83E+05	3.24E+04	0.28	1.99E-03	1.67E+05	3.39E+04	SYT > rST >> SC &
Oxidative stress-related proteins															
Q3T1J1	Eif5a	Eukaryotic translation initiation factor 5A-1	0.47	1.54E-02	2.61E+06	1.33E+06	0.39	1.44E-04	3.07E+06	1.21E+06	0.54	6.12E-02	1.23E+06	7.61E+05	Mixed
A0A0G2K531	Gpx3	Glutathione peroxidase 3	1.69	3.82E-05	6.88E+06	1.03E+07	2.73	1.01E-07	6.48E+06	1.43E+07	0.89	7.38E-01	8.85E+06	7.67E+06	SG & SC
P19468	Gclc	Glutamate--cysteine ligase catalytic subunit	0.85	7.73E-01	1.70E+05	1.27E+05	0.36	4.36E-03	3.29E+05	6.95E+04	0.65	7.31E-01	4.89E+04	2.06E+04	SG > SC
Q64057	Aldh7a1	Alpha-aminoadipic semialdehyde dehydrogenase	0.79	4.56E-01	4.59E+05	3.25E+05	0.49	3.95E-03	5.84E+05	2.47E+05	0.49	4.18E-02	1.83E+05	8.72E+04	SC & SG
F8WFH8	Wars	Tryptophan--tRNA ligase, cytoplasmic;T1-TrpRS;T2-TrpRS	0.89	6.98E-01	1.57E+05	1.04E+05	0.36	2.13E-04	2.50E+05	6.94E+04	0.43	2.18E-03	1.10E+05	4.20E+04	Mixed
D4ABI6	Uchl3	Ubiquitin carboxyl-terminal hydrolase;Ubiquitin carboxyl-	1.04	9.63E-01	6.65E+05	5.68E+05	0.40	2.46E-04	1.06E+06	3.23E+05	0.38	9.34E-04	4.51E+05	1.80E+05	Mixed
Inflammation/fibrosis-related proteins															
A0A0G2JSZ5	Pdia6	Protein disulfide-isomerase A6	0.30	1.94E-08	6.82E+05	1.58E+05	0.50	4.36E-03	4.21E+05	1.49E+05	0.46	1.04E-01	2.18E+05	1.42E+05	Mixed
P02454	Col1a1	Collagen alpha-1(I) chain	0.25	5.22E-16	1.14E+06	3.02E+05	0.84	3.24E-01	1.98E+05	1.79E+05	0.62	6.50E-02	3.25E+05	2.19E+05	SG >> SC
F1LS40	Col1a2	Collagen alpha-2(I) chain	0.21	3.30E-11	4.32E+05	1.23E+05	0.87	6.32E-01	7.90E+04	6.36E+04	0.71	3.14E-01	1.04E+05	6.48E+04	SG > SC
Q5RJN2	Pcolce	Procollagen C-endopeptidase enhancer 1	0.37	1.65E-10	2.49E+06	1.03E+06	1.73	4.96E-04	6.48E+05	9.05E+05	0.79	4.07E-01	6.14E+05	5.19E+05	SC >> SG
D3ZVQ0	Usp5	Ubiquitin carboxyl-terminal hydrolase	0.70	1.92E-02	5.74E+05	3.96E+05	0.40	2.18E-08	7.78E+05	2.80E+05	0.43	1.96E-06	3.65E+05	1.57E+05	Mixed
F1LR02	Col18a1	Collagen type 18 alpha 1 chain	0.87	7.25E-01	5.82E+04	3.85E+04	2.39	1.88E-03	2.20E+04	5.83E+04	1.11	8.13E-01	2.44E+04	2.83E+04	SC & SG
F1M8E9	Lyz2	Lysozyme	0.72	3.98E-01	2.48E+06	1.26E+06	2.55	2.15E-03	1.13E+06	2.21E+06	0.78	5.26E-01	1.53E+06	1.28E+06	rST
P30120	Timp1	Metalloproteinase inhibitor 1	1.04	9.63E-01	6.49E+04	1.16E+05	2.73	4.36E-03	4.97E+04	2.02E+05	0.98	9.46E-01	3.62E+04	2.09E+04	SG > SC
Sertoli cell-related proteins															
Q68FR8	Tuba3a	Tubulin alpha-3 chain	0.82	9.58E-01	4.18E+05	3.72E+05	0.33	1.90E-02	7.60E+05	2.07E+05	0.10	2.50E-02	2.75E+05	5.07E+04	SC > SG > rST >>
Q6AZ50	Atg3	Ubiquitin-like-conjugating enzyme ATG3	–	–	1.92E+04	2.52E+04	0.15	2.06E-03	1.50E+05	5.47E+03	–	–	0.00E+00	9.28E+03	Mixed
Spermatogenesis-related proteins															
P18418	Calr	Calreticulin	0.31	2.13E-05	1.42E+06	4.48E+05	0.45	1.12E-03	1.00E+06	3.36E+05	0.47	9.88E-02	5.35E+05	3.32E+05	SC & SG > rST & SYT
P63029	Tpt1	Translationally-controlled tumor protein	0.18	1.54E-02	4.00E+06	2.32E+06	0.32	1.86E-02	3.44E+06	1.23E+06	0.74	6.01E-01	1.53E+06	9.86E+05	SG & SC >rST & SYT
F1M9N7	Agfg1	Arf-GAP domain and FG repeat-containing protein 1	0.99	1.00E+00	1.83E+04	1.14E+04	0.37	1.18E-03	4.90E+04	1.51E+04	0.60	9.46E-01	1.51E+04	1.20E+04	rST & SYT > SC & SG
Q4KMA2	Rad23b	UV excision repair protein RAD23 homolog B	0.63	1.79E-01	1.84E+05	6.26E+04	0.39	1.02E-02	2.62E+05	5.29E+04	0.54	8.81E-02	5.14E+04	1.02E+04	SC & SG >> rST &
F1LSR7	Spata20	Spermatogenesis-associated protein 20	1.12	7.73E-01	2.56E+05	2.51E+05	0.28	2.18E-07	4.62E+05	9.21E+04	0.18	1.38E-08	2.87E+05	3.75E+04	**rST>>** SYT
Q4KLZ3	Dazap1	Deleted in AZoospermia Associated Protein 1	0.95	9.63E-01	1.41E+05	1.26E+05	0.39	1.32E-02	2.77E+05	8.41E+04	0.34	1.72E-02	1.32E+05	2.96E+04	SYT > SG & rST > SC
Q68FX6	Cabs1	Calcium-binding and spermatid-specific protein 1	1.12	8.64E-01	5.19E+05	7.30E+05	0.13	5.54E-10	1.20E+06	1.38E+05	0.16	3.19E-05	5.91E+05	9.72E+04	**rST >>** SYT
P56702	Dbil5	Diazepam-binding inhibitor-like 5	1.54	2.55E-01	3.29E+05	5.16E+05	0.22	3.59E-02	6.53E+05	2.25E+05	0.08	2.40E-03	5.92E+05	3.58E+04	rST >> SYT
P14659	Hspa2	Heat shock-related 70 kDa protein 2	0.73	3.80E-01	1.19E+06	9.60E+05	0.26	1.85E-06	2.30E+06	6.23E+05	0.14	7.39E-07	1.67E+06	3.14E+05	SYT & rST
Q5U328	Ncl	Nucleolin	–	–	0.00E+00	4.83E+03	0.28	4.80E-01	1.37E+04	0.00E+00	0.20	4.05E-03	3.48E+04	2.12E+03	SG > SC >> SYT >>
Q6MG49	Bag6	Large proline-rich protein BAG6	0.63	3.54E-01	2.16E+05	1.41E+05	0.62	2.79E-01	2.46E+05	1.38E+05	0.18	7.63E-03	1.10E+05	7.00E+04	rST & SYT > SC & SG
Proteasomes															
P40112	Psmb3	Proteasome subunit beta type-3	0.78	5.80E-01	4.76E+05	3.59E+05	2.04	6.52E-03	2.44E+05	5.14E+05	0.36	4.61E-03	2.54E+05	6.35E+04	SC & SG >> rST &
G3V6W6	Psmc6	Proteasome 26S subunit, ATPase 6	0.92	8.30E-01	2.85E+05	2.13E+05	0.77	3.08E-01	1.66E+05	1.93E+05	0.22	1.13E-02	1.95E+05	7.32E+04	SG > SC
P17220	Psma2	Proteasome subunit alpha type-2	0.69	1.26E-01	1.34E+06	8.96E+05	1.63	7.16E-02	7.93E+05	1.12E+06	0.37	1.37E-02	4.34E+05	1.59E+05	SG & SC > SYT > rST
Inhibin-related proteins															
P63331	Ppp2ca	Serine/threonine-protein phosphatase 2A catalytic subunit	0.02	9.91E-01	5.42E+05	4.43E+05	0.54	2.04E-02	8.24E+05	3.58E+05	0.47	3.48E-02	2.45E+05	1.05E+05	SG & SC >rST & SYT

Yellow cells:	Proteins that are changed (up/down) with p < 0.05.
Green cells:	Proteins that are unchanged or changed with p > 0.05.

Column explanations

Uniprot accession number: First, or leading, protein ID annotation in UniProtKB/Swiss-Prot Rattus norvegicus database (Nov 2018).

Gene symbol: Leading gene symbol in UniProtKB/Swiss-Prot Rattus norvegicus database (Nov 2018).

Protein name: Protein name from the UniProtKB/Swiss-Prot Rattus norvegicus database (Nov 2018).

iBAQ: The sum of all the peptides intensities divided by the number of observable peptides of a protein.

Relative abundance: Relative abundance score in 25 fold ranges, based on top most abundant protein iBAQ score.

Log2 Heat/Control: Log2 ratio of protein abundance in heat-treated rats/control rats.

Fold change Heat/Control: Linear ratio of protein abundance in heat-treated rats/control rats.

P-Value Heat/Control: p value of difference in protein abundance between heat-treated and control rats.

Tubular origin: Microarray dataset published by Chalmel et al 2007, PNAS, 104(20):8346. Data accessed via www.germonline.org

Note

Cell specificity: cell IDs are done by mRNA of purified cell types via Germonline.

'Mixed': indicates almost equal expression by all geminal epithelial cells.

'below sensitivity': indicates below detection limits.

‘>’: indicates expression greater than 2-fold, but less than 4-fold different to the next cell type.

‘>>’: indicates expression greater than 4-fold compared with next cell type.

Bold text and '>>': indicates 10-fold higher expression than next cell type.

‘&’: indicates expression differences between cell types is less than 2-fold.

'/': indicates another pattern of cell expression

Abbreviations	
SC	Sertoli cell
SG	Spermatogonia
SYT	Spermatocytes
rST	round spermatid

Table 4. Functional categorisation of selected TIF proteins that changed following acute heat treatment.

Group	Function	Gene symbol	Protein name	Fold change	P-Value	Up/Down	Response time (weeks)	Tubular origin	Inter-tubular origin	Functional details	PMID
Extra-cellular matrix proteins	Fibril formation	Pcolce (PCPE-1)	procollagen C-proteinase enhancer-1	3.0 & 2.0	1.7E-10 & 4.96E-04	down & up	1 & 8	SC >> SG	PTMC*, LC***	N/A	Nothing about the testis
		Col1a1	Collagen alpha-1(I) chain	4.0	5.22E-16	down	1	SG >> SC	PTMC*, LC**	Col1a1 and Col1a2 are associated with the maintenance of spermatogonia and in germ cell detachment and migration during murine spermatogenesis. Silencing of Col1a1 results in inhibition of spermatogonial self-renewal and enhances spermatogonial differentiation.	16123240, 23064687, 24019537
		Timp1	Metalloproteinase inhibitor 1	3.0	4.36E-03	up	8	SG > SC	PTMC*, LC***, MG	In the testis, Timp-1 is involved in the assembly of the adherens junctions between the Sertoli and germ cells The secretion of Timp-1 from Sertoli cells is largely controlled by hormonal and local processes, suggesting that Timp-1 is of physiological importance during spermatogenesis. It also has a role in the regulation of junction dynamics. It is also a potent activator of steroidogenesis with procathepsin L protein, and may regulate steroid concentrations and, thus, germ cell development in both males and females.	12826691, 12488366, 10727275, 12815621, 29658577, 25966737
		Sparc	Secreted protein acidic and cysteine rich	3.0	1.85E-11	down	1 & 8	SC > SG	PTMC*, LC***, MG	Sparc is associated with changes in Leydig cell shape that accompany morphogenesis and tissue. Its remodeling has been shown to be required for insoluble collagen deposition.	2015346, 2775822, 29522370, 26582465
		Dcn	Decorin	4.0	9.32E-05	down	1	SG	PTMC*, FB	Dcn interferes with paracrine signalling growth factors in the testis. An elevated Dcn level is associated with impaired testicular function. It is also produced by stressed vascular endothelial cells, and smooth muscle cells. Dcn suppresses proliferation and protects macrophages from the induction of apoptosis.Dcn plays a role in macrophage activation via abolishing the binding of TGF-beta to macrophages.	29156766, 7626709, 21791437, 16177119,
		Fmod	Fibromodulin	4.0	2.47E-11	down	1	SYT & rST	PTMC*	Fmod regulates fibril formation. It binds to TGF-beta and may also regulate TGF-beta activities by sequestering TGF-beta into extracellular matrix.	Nothing about the testis
Cytoskeletal proteins	Regulation of Sertoli cell microtubules	Mapre1	Microtubule-associated protein RP (EB family member 1)	3.0	2.60E-04	down	8	SC & SG >> SYT > rST	None	Mapre1 has a pivotal role as a regulator of microtubule dynamics and in the actin cytoskeletal network in the seminiferous tubules .Its knockdown disrupts the in vitro organisation of microtubules and actin microfilaments in rat Sertoli cells and causes functional damage to the translocation of the germ cells across the seminiferous epithelium.	17964570, 29453575, 26894662, 25456071
		Tuba3a	Tubulin alpha-3 chain	3.0 & 10.0	1.90E-02	down	8 & 14	SC > SG > rST >> SYT	None	Tuba3a maintains Sertoli cell and sperm microtubules dynamic.	26894662, 25411052
Heat shock-and/or spermatogeneis related proteins	Regulation of spermatogenesis	Hspa2	Heat shock-related 70 kDa protein 2	4.0& 7.0	1.9E-06 &7.39E-07	down	8 & 14	SYT & rST	None	Hspa2 is required for normal spermatogenesis. It can also be an infertility biomarker. BAG6 is likely a key regulator of HSPA2 stability/function in human germ cells.	29205438, 28389751, 26676989, 26153132,
		Bag6	Large proline-rich protein BAG6	6.0	7.63E-03	down	14	rST & SYT > SC & SG	None	Bag6 plays a key role in regulating the stability of HSPA2 in the testis, by preventing its ubiquitination and subsequent proteolytic degradation. It could also be a sperm biomarker for infertility.	29205438, 27932549, 26153132,
		Nasp	Nuclear autoantigenic sperm protein	3.0 & 4.0	3E-05 & 2E-03	down	8 & 14	SYT > rST >> SC & SG	None	Testicular Nasp's acts as a functional link between linker histones and cell cycle progression during meiosis. Nasp also forms a cytoplasmic complex with HSP90 and H1 linker histones and stimulates HSP90 ATPase activity. The antibody against Nasp can result in reproductive failure while its knockdown effectively inhibits the proliferation and causes G1 phase arrest through ERK/MAPK signal pathway.	15533935, 19553603, 19219058, 25669170
	Regulation of spermiogenesis	Spata20 (Ssp411)	Spermatogenesis-associated protein 20	4.0 & 6.0	2.2E-07 & 1.4E-08	down	8 & 14	**rST>>** SYT	None	Spata20 is required for spermiogenesis particularly in sperm head shaping since the lack of Spata20 causes sperm deformation and results in male infertility.	29247744, 15223837
		Cabs1	Calcium-binding and spermatid-specific protein 1	8.0 & 6.0	5.5E-10 & 3.2E-05	down	8 & 14	**rST >>** SYT	None	Cabs1 is involved in the extremely complex structural rearrangements occurring in haploid germ cells during spermiogenesis. It was identified in mitochondria of step 17 to 18 spermatids.	19271754, 19208547, 19374365

Blue cells:	indicates germ cell-specific proteins

Column explanations

Gene symbol: Leading gene symbol in UniProtKB/Swiss-Prot Rattus norvegicus database (Nov 2018).

Protein name: Protein name from the UniProtKB/Swiss-Prot Rattus norvegicus database (Nov 2018).

Fold change: Linear ratio of protein abundance in heat-treated rats/control rats.

P-Value: p value of difference in protein abundance between heat-treated and control rats.

Tubular origin: Microarray dataset published by Chalmel et al 2007, PNAS, 104(20):8346. Data accessed via www.germonline.org

* Data from secreted proteins in Supporting Information Table 5 (Flenkenthaler et al., Proteome Res. 2014)

** Data from Supporting Information Table S3 (Stanley et al., Biol. Reprod. 2011).

*** Data from Dataset S2 Leydig cell enriched genes (Sanz et al., PLoS One 2013).

PMID: is the unique identifier number used in PubMed for articles from which functional details were prepared

Underlined: indicates macrophage and its reference

Note

Cell specificity: cell IDs are done by mRNA of purified cell types via Germonline.

'Mixed': indicates almost equal expression by all geminal epithelial cells.

'below sensitivity': indicates below detection limits.

‘>’: indicates expression greater than 2-fold, but less than 4-fold different to the next cell type.

‘>>’: indicates expression greater than 4-fold compared with next cell type.

Bold text and '>>': indicates 10-fold higher expression than next cell type.

‘&’: indicates expression differences between cell types is less than 2-fold.

'/': indicates another pattern of cell expression

Abbreviations	
SC	Sertoli cell
SG	Spermatogonia
SYT	Spermatocytes
rST	round spermatid
SC	Sertoli cell
LC	Leydig cell
MG	Macrophage
FB	Fibroblast

Supp Figure 1

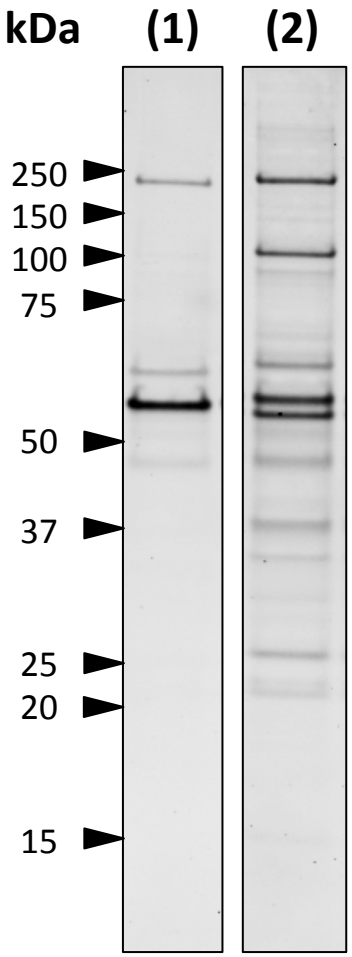

Supp Figure 2

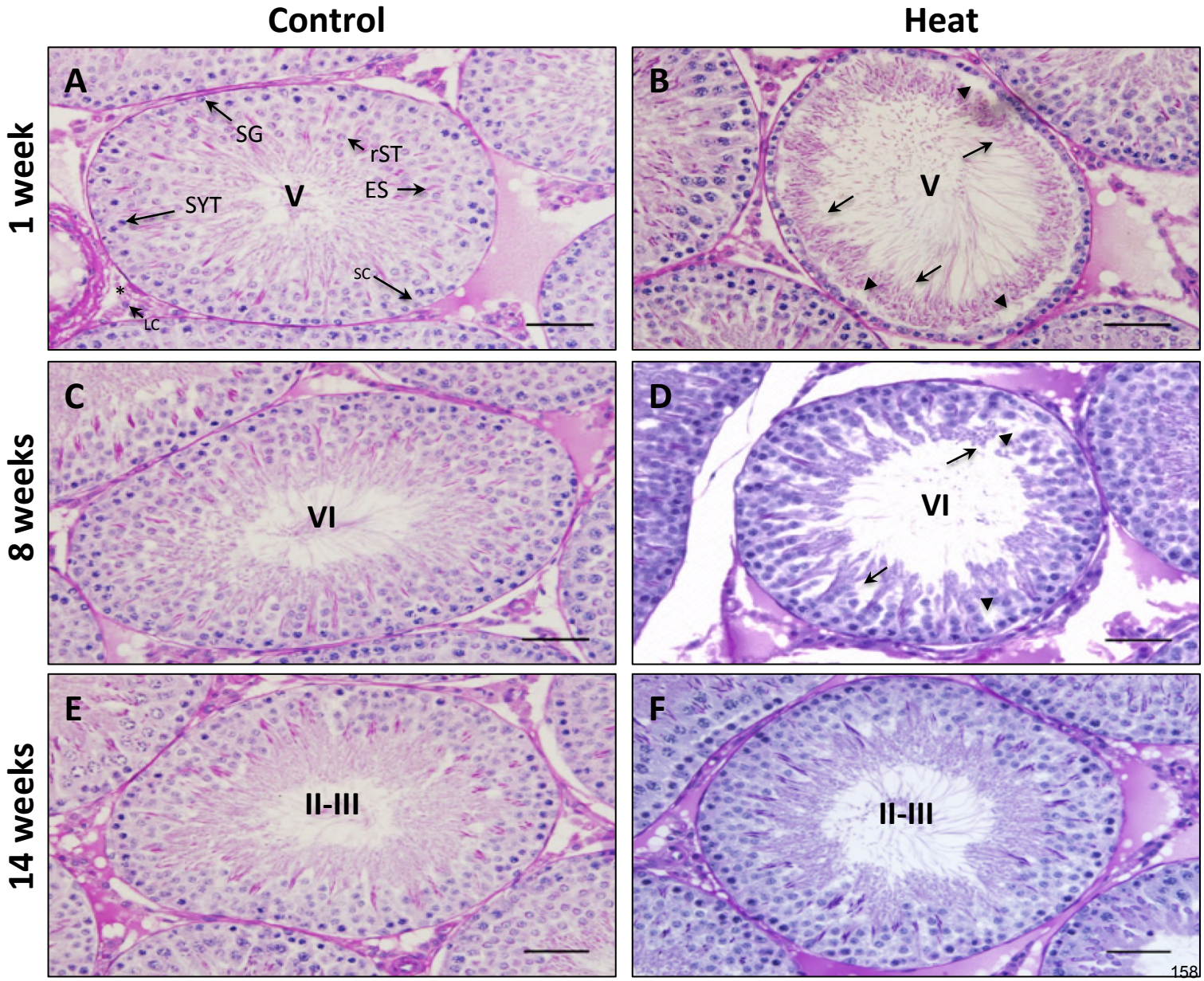

Supp Figure 3

A Molecular function

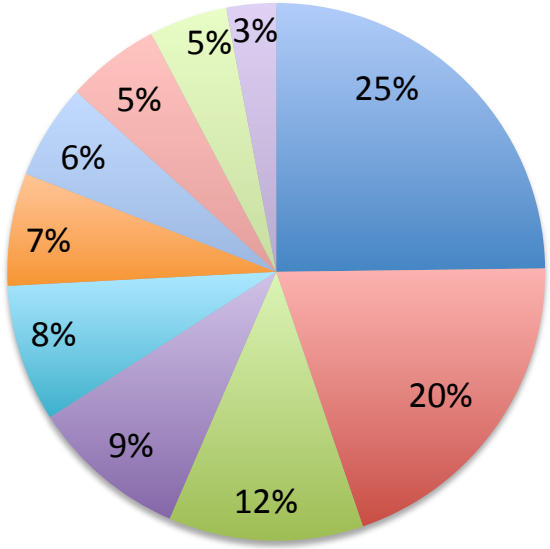

- Nucleotide-binding
- ATP-binding
- Calcium ion binding
- Protease
- GTP-binding
- RNA-binding
- GTPase activity
- Chaperone
- Ligase activity
- Structural constituent of cytoskeleton

B Biological process

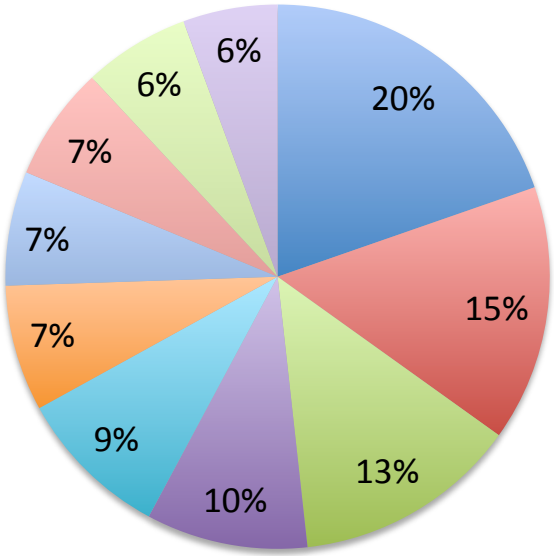

- Cell-cell adhesion
- Biosynthesis of antibotic
- negative regulation of endopeptidase activity
- Immunity
- Carbon metabolism
- Protein biosynthesis
- Amino-acid biosynthesis
- Glutathione metabolic process
- Glycolysis / Gluconeogenesis
- Cell division

C Cellular component

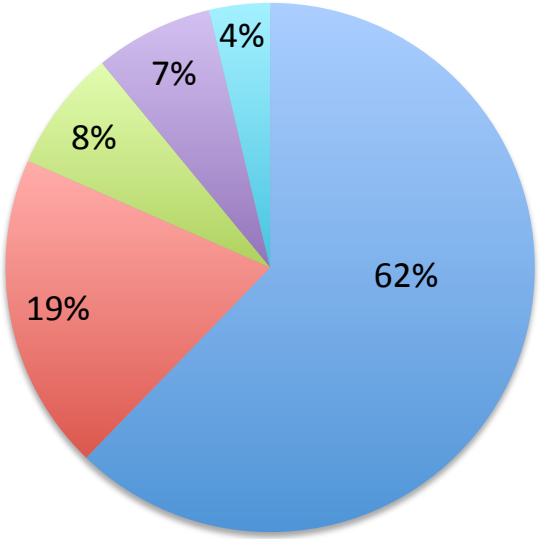

- Extracellular space
- cell-cell adherens junction
- Lysosome
- Proteasome
- Endoplasmic reticulum

Supp Figure 4

A Molecular function

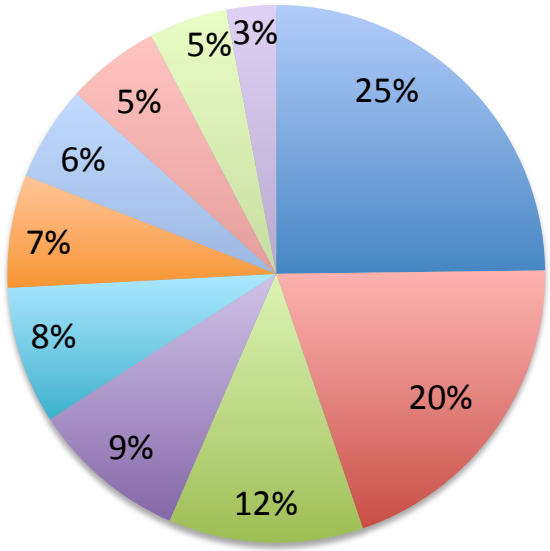

- Nucleotide-binding
- ATP-binding
- Calcium ion binding
- Protease
- GTP-binding
- RNA-binding
- GTPase activity
- Chaperone
- Ligase activity
- Structural constituent of cytoskeleton

B Biological process

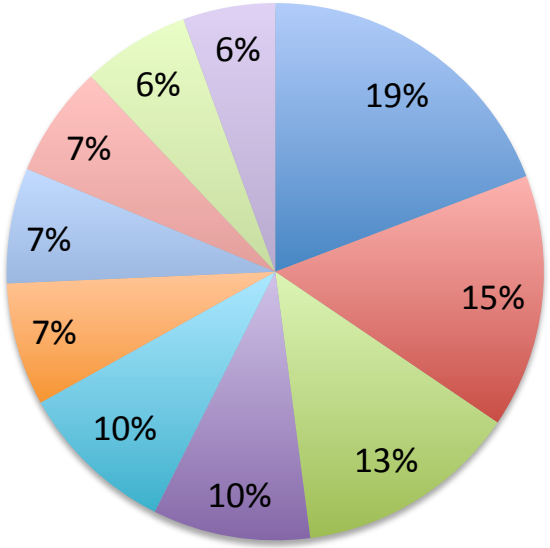

- Cell-cell adhesion
- Biosynthesis of antibotic
- negative regulation of endopeptidase activity
- Immunity
- Carbon metabolism
- Protein biosynthesis
- Glutathione metabolic process
- Amino-acid biosynthesis
- Glycolysis / Gluconeogenesis
- Cell division

C Cellular component

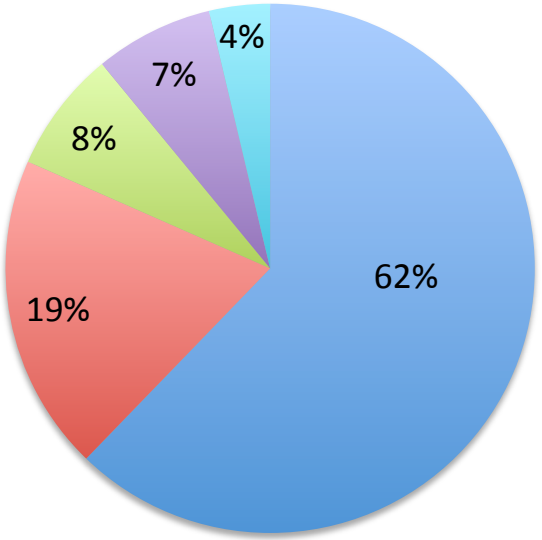

- Extracellular space
- cell-cell adherens junction
- Lysosome
- Proteasome
- Endoplasmic reticulum

Supp Table 1. Total of 1728 proteins identified in TIF from heat-treated and control rats (n=4/ experimental group/time-point). Note: The data presented here are for illustration purpose only and showed n= 47 proteins. The whole dataset is shown in Appendix 4.

Uniprot accession number	Gene symbol	Protein name	Mol. weight [kDa]	No. Peptides Control wk1	No. Peptides Control wk8	No. Peptides Control wk14	No. Peptides Heat wk1	No. Peptides Heat wk8	No. Peptides Heat wk14	No. Unique peptides Control wk1	No. Unique peptides Control wk8	No. Unique peptides Control wk14	No. Unique peptides Heat wk1	No. Unique peptides Heat wk8	No. Unique peptides Heat wk14	iBAQ Control wk1	iBAQ Control wk8	iBAQ Control wk14	iBAQ Heat wk1	iBAQ Heat wk8	iBAQ Heat wk14	Sequence coverage Control wk1 [%]	Sequence coverage Control wk8 [%]	Sequence coverage Control wk14 [%]	Sequence coverage Heat wk1 [%]	Sequence coverage Heat wk8 [%]	Sequence coverage Heat wk14 [%]
P14046	A1i3	Alpha-1-inhibitor 3	163.77	128	133	131	131	129	131	4	5	4	5	6	5	9.14E+06	1.05E+07	1.36E+07	4.93E+06	8.01E+06	1.48E+07	74.3	74.9	74.9	76.1	76	76
Q63041	A1m	Alpha-1-macroglobulin	167.12	99	106	102	103	105	102	99	106	102	103	105	102	5.23E+07	3.61E+07	5.12E+07	4.67E+07	4.81E+07	4.72E+07	77.2	78	77.3	77.3	77.6	76.7
P06238	A2m	Alpha-2-macroglobulin	163.78	22	13	20	17	18	19	19	11	18	15	16	17	2.43E+05	3.42E+04	1.43E+05	5.75E+04	7.22E+04	9.80E+04	22.5	13.9	20.4	16.8	18.1	19.2
D3ZS19	A2ml1	Alpha-2-macroglobulin-like 1	162.77	6	6	7	5	5	5	6	6	7	5	5	5	1.12E+04	1.80E+04	4.82E+04	2.08E+04	1.24E+04	2.93E+04	6.3	6.9	7.8	6	6.2	6.2
G3V7V2	Aamp	Angio-associated migratory protein	46.94	2	2	2	3	2	2	2	2	2	3	2	2	4.85E+04	9.06E+04	3.45E+04	5.62E+04	4.34E+04	3.07E+04	6.9	6.9	5.5	9.9	6.9	6.9
P50475	Aars	Alanine--tRNA ligase, cytoplasmic	106.79	15	16	10	16	13	8	15	16	10	16	13	8	1.87E+05	3.28E+05	6.12E+04	1.41E+05	6.74E+04	2.20E+04	23.5	25.3	16.4	25.3	20	13.1
Q9QYJ4	Abcb9	ATP-binding cassette sub-family B member 9	82.83	1	1	1	1	1	1	1	1	1	1	1	1	1.66E+04	2.57E+03	9.81E+03	6.42E+03	6.15E+03	6.41E+03	0.9	0.9	0.9	0.9	0.9	0.9
D3ZD23	Abce1	ATP-binding cassette subfamily E member 1	67.30	2	2	1	2	2	1	2	2	1	2	2	1	3.89E+04	3.65E+04	1.17E+04	1.47E+04	1.48E+04	3.97E+03	5.3	5.3	1.7	5.3	5.3	1.7
Q6DGG1	Abhd14b	PAlpha/beta hydrolase domain-containing protein 14B	22.62	4	5	3	3	3	4	4	5	3	3	3	4	3.13E+05	7.29E+05	1.76E+05	2.44E+05	1.38E+05	1.09E+05	37.1	42.4	21.4	22.4	22.4	27.6
D3ZAW4	Abhd4	Abhydrolase domain containing 4	40.37	9	9	5	9	7	5	9	9	5	9	7	5	3.63E+05	9.67E+05	1.62E+05	4.18E+05	2.58E+05	7.98E+04	44.2	44.2	23.9	44.2	32.1	26.5
F1M305	Abi3bp	ABI family member 3-binding protein	94.55	2	2	1	2	3	2	2	2	1	2	3	2	3.84E+04	1.35E+04	8.27E+03	1.80E+04	1.79E+04	9.92E+03	2.8	2.8	1.5	2.8	4	2.8
D3ZSL2	Abracl	ABRA C-terminal-like	9.03	3	4	3	3	3	2	3	4	3	3	3	2	8.72E+05	1.19E+06	7.34E+05	8.05E+05	5.37E+05	3.56E+05	46.9	51.9	46.9	46.9	46.9	30.9
P13437	Acaa2	3-ketoacyl-CoA thiolase, mitochondrial	41.75	1	1	1	1	1	1	1	1	1	1	1	1	3.65E+04	2.09E+04	4.08E+04	7.03E+03	1.39E+04	2.45E+04	5.1	5.1	5.1	5.1	5.1	5.1
P15650	Acadl	Long-chain specific acyl-CoA dehydrogenase, mitochondrial	47.87	2	2	2	2	2	2	2	2	2	2	2	2	5.17E+04	4.59E+04	3.00E+04	2.46E+04	1.88E+04	2.05E+04	6.5	6.5	6.5	6.5	6.5	6.5
Q5FVC7	Acap2	Arf-GAP with coiled-coil, ANK repeat and PH domain-containing protein 2	91.57	1	1	1	1	1	2	1	1	1	1	1	2	3.54E+03	7.27E+03	2.88E+04	2.83E+03	1.80E+03	3.83E+04	1.4	1.4	1.9	1.4	1.4	3.2
Q5XI22	Acat2	Acetyl-CoA acetyltransferase, cytosolic	41.11	5	6	4	6	5	4	5	6	4	6	5	4	3.93E+05	4.80E+05	2.23E+05	2.85E+05	1.32E+05	7.75E+04	29.5	37	23.4	37	33.2	23.4
P16638	Acly	ATP-citrate synthase	120.54	20	21	12	20	19	13	20	21	12	20	19	13	3.38E+05	4.28E+05	1.23E+05	2.81E+05	2.68E+05	5.65E+04	27.9	28.4	17.5	27.8	26.5	18.3
Q63270	Aco1	Cytoplasmic aconitate hydratase	98.19	5	3	4	3	5	5	5	3	4	3	5	5	4.57E+04	2.71E+04	1.87E+04	1.51E+04	1.75E+04	2.13E+04	7.3	4.4	7	4.4	7.3	8.2
Q9ER34	Aco2	Aconitate hydratase, mitochondrial	85.43	2	1	2	1	1	2	2	1	2	1	1	2	6.72E+03	3.66E+03	4.63E+03	1.28E+03	2.82E+03	5.78E+03	3.6	1.7	3.6	1.9	1.7	3.6
Q64559	Acot7	Cytosolic acyl coenzyme A thioester hydrolase	40.97	2	2	2	2	2	2	2	2	2	2	2	2	6.09E+04	5.29E+04	5.76E+04	2.11E+04	4.00E+04	9.85E+03	5.9	5.9	5.9	5.9	5.9	5.9
P41498	Acp1	Low molecular weight phosphotyrosine protein phosphatase	18.22	4	4	2	4	4	2	4	4	2	4	4	2	2.08E+05	2.04E+05	1.41E+04	1.43E+05	5.73E+04	3.10E+04	27	27	18.9	27	27	15.7
Q6AY33	Acrbp	Acrosin-binding protein	35.92	2	1	1	2	0	0	2	1	1	2	0	0	1.24E+04	1.51E+04	2.14E+05	1.38E+04	0.00E+00	0.00E+00	8.2	3.2	3.2	8.2	0	0
Q9WUY6	Acrv1	Acrosomal vesicle protein 1	28.59	2	2	1	1	1	0	2	2	1	1	1	0	3.51E+04	6.18E+04	9.85E+03	3.85E+03	1.60E+04	0.00E+00	9.7	9.7	2.6	7.1	2.6	0
Q924N5	Acsbg1	Long-chain-fatty-acid--CoA ligase ACSBG1	80.52	38	39	33	37	37	32	38	39	33	37	37	32	4.11E+06	8.88E+06	1.96E+06	5.32E+06	3.62E+06	1.27E+06	55.6	58.5	54	55.6	55.6	50.2
P18163	Acsl1	Long-chain-fatty-acid--CoA ligase 1	78.18	4	3	2	3	2	3	4	3	2	3	2	3	2.74E+04	8.88E+03	8.18E+03	2.67E+03	8.54E+02	2.87E+03	7	5.3	3.7	4.4	3.7	5.3
P60711	Actb	Actin, cytoplasmic 1	41.74	29	33	29	31	30	23	1	1	1	1	1	1	4.48E+07	5.34E+07	3.95E+07	3.07E+07	2.23E+07	2.33E+07	90.4	92.5	91.5	91.7	91.7	85.6
P63259	Actg1	Actin, cytoplasmic 2	41.79	29	33	29	31	30	23	1	1	1	1	1	1	2.47E+05	2.92E+05	1.95E+05	1.13E+05	1.40E+05	8.90E+04	90.4	92.5	91.5	91.7	91.7	85.6
P63269	Actg2	Actin, gamma-enteric smooth muscle	42.01	23	28	26	27	22	21	1	2	2	2	1	1	8.37E+06	1.41E+07	9.83E+06	6.61E+06	5.60E+06	6.73E+06	71.9	81.4	80.6	79.6	77.7	74.3
Q4KM87	Actl6a	Actin-like 6A	47.42	1	2	1	0	1	1	1	2	1	0	1	1	6.01E+03	2.00E+04	1.65E+04	0.00E+00	1.61E+03	1.63E+03	3.3	7.5	4.2	0	4.2	4.2
Q4QR76	Actl7b	Actin-like protein 7B	45.49	6	5	5	3	3	2	6	5	5	3	3	2	8.43E+04	1.09E+05	7.31E+04	2.07E+04	1.71E+04	2.70E+03	27.8	22.3	27.6	14.9	15.1	10.6
Q6GMN8	Actn1	Alpha-actinin-1	102.61	27	25	25	24	21	23	16	14	15	14	11	13	1.82E+05	1.67E+05	1.38E+05	7.78E+04	5.16E+04	8.09E+04	42.2	37.3	38.9	34.7	32.1	35.2
Q9QXQ0	Actn4	Alpha-actinin-4	102.97	28	31	26	23	27	24	17	20	16	13	17	14	1.05E+06	9.11E+05	6.63E+05	4.00E+05	4.11E+05	4.12E+05	45.2	47	42	38	43.5	38.2
P85515;B2RYJ7	Actr1a	Alpha-centractin	42.61	5	7	3	4	3	3	5	7	3	4	3	3	1.23E+05	1.69E+05	3.40E+04	8.32E+04	5.39E+04	4.00E+04	20.5	22.6	12.5	15.7	13.3	13
Q5M7U6	Actr2	Actin-related protein 2	44.73	5	6	2	6	4	2	5	6	2	6	4	2	2.71E+05	9.63E+04	2.72E+04	1.12E+05	6.19E+04	2.57E+04	21.6	27.4	6.1	27.4	12.7	6.1
A0A0G2K1C0	Actr3	Actin-related protein 3	47.58	6	8	4	6	6	2	6	8	4	6	6	2	1.73E+05	1.67E+05	4.13E+04	5.90E+04	1.32E+05	5.99E+03	23.9	28.9	14.3	23.9	23.9	5.3
Q5M876	Acy3	N-acyl-aromatic-L-amino acid amidohydrolase (carboxylate-forming)	35.42	7	7	6	7	4	4	7	7	6	7	4	4	3.49E+05	3.01E+05	1.51E+05	3.15E+05	2.13E+05	8.17E+04	26	26	25.7	26	15.4	23.2
Q920P6	Ada	Adenosine deaminase	39.90	1	1	0	1	1	0	1	1	0	1	1	0	1.02E+04	3.67E+04	0.00E+00	3.64E+03	4.97E+03	0.00E+00	5.4	5.4	0	5.4	5.4	0
D4A4X6	Adamsl2	ADAMTS-like 2	105.57	1	1	1	1	1	1	1	1	1	1	1	1	1.42E+04	9.15E+03	8.81E+03	9.38E+03	5.44E+03	6.60E+03	2	2	2	2	2	2
Q63028	Add1	Alpha-adducin	80.34	14	15	13	14	15	10	14	15	13	14	15	10	1.61E+05	4.28E+05	7.22E+04	1.89E+05	1.48E+05	4.82E+04	33.6	36.1	30.1	32.8	36.1	20.3
D3ZCH7	Add3	Adducin 3 (Gamma), isoform CRA_a	74.96	5	6	2	6	6	1	5	6	2	6	6	1	2.47E+04	1.71E+05	1.42E+04	3.77E+04	4.84E+04	7.40E+03	12.8	14.5	5.2	14.9	15.5	2.7
A0A0G2JSI4	Adgre5	Adhesion G protein-coupled receptor E5	99.39	4	4	3	4	3	3	4	4	3	4	3	3	6.14E+04	3.71E+04	3.46E+04	6.01E+04	3.57E+04	3.02E+04	7.1	7.1	3.7	7.1	3.7	3.7
P06757	Adh1	Alcohol dehydrogenase 1	39.65	16	18	11	16	17	11	16	18	11	16	17	11	4.55E+06	1.37E+07	3.00E+06	5.78E+06	3.19E+06	1.79E+06	58	64.4	46.8	58	58	46.8
Q7TQ80	Adh4	Alcohol dehydrogenase 4 class-2	93.85	3	3	3	3	3	3	3	3	3	3	3	3	4.19E+04	8.71E+04	2.46E+04	3.52E+04	2.78E+04	1.24E+04	6.8	6.8	6.8	6.8	6.8	6.8
Q562C9	Adi1	1,2-dihydroxy-3-keto-5-methylthiopentene dioxygenase	21.46	6	6	4	5	3	5	6	6	4	5	3	5	2.05E+05	5.88E+05	7.13E+05	2.83E+05	5.21E+05	5.32E+05	44.7	44.7	28.5	33	26.3	33
A0A0G2K845	Adipoq	Adiponectin, C1Q and collagen domain-containing	23.47	2	2	2	2	2	2	2	2	2	2	2	2	4.24E+05	9.11E+05	8.02E+05	1.79E+05	1.40E+06	8.02E+05	12.4	12.4	12.4	12.4	12.4	12.4
Q64640	Adk	Adenosine kinase	40.13	7	6	5	6	4	6	7	6	5	6	4	6	2.33E+05	2.38E+05	9.69E+04	1.42E+05	9.16E+04	4.31E+04	24.1	21.9	17.2	21.9	14.1	20.5
Q02589	Adprh	[Protein ADP-ribosylarginine] hydrolase	39.96	5	6	3	4	5	4	5	6	3	4	5	4	1.95E+05	2.98E+05	9.41E+04	4.31E+04	5.15E+04	2.69E+04	21	23.8	11.9	16.3	21	18

Column explanations

Uniprot accession number: First, or leading, protein ID annotation in UniProtKB/Swiss-Prot Rattus norvegicus database (Nov 2018).

Gene symbol: Leading gene symbol in UniProtKB/Swiss-Prot Rattus norvegicus database (Nov 2018).

Protein name: Protein name from the UniProtKB/Swiss-Prot Rattus norvegicus database (Nov 2018).

iBAQ: The sum of all the peptides intensities divided by the number of observable peptides of a protein.

N/A: Data not available/ applicable.

Supp Table 2. Total of 209 proteins with altered expression (up/down, p<0.05) following heat treatment at various time-points

			1 week			8 weeks			14 weeks		
Uniprot accession number	Gene name	Protein name	Log2 Heat / Control	Fold change Heat / Control	P-Value Heat / Control	Log2 Heat / Control	Fold change Heat / Control	P-Value Heat / Control	Log2 Heat / Control	Fold change Heat / Control	P-Value Heat / Control
A0A0G2K7X0	Anp32a	Acidic leucine-rich nuclear phosphoprotein 32 family member A	1.82	3.54	9.69E-02	-3.22	0.11	7.00E-04	-4.02	0.06	1.86E-03
F7F2F3	Hspa4l	Heat shock 70 kDa protein 4L	0.28	1.22	5.22E-01	-2.75	0.15	3.10E-13	-4.02	0.06	4.06E-13
P56702	Dbil5	Diazepam-binding inhibitor-like 5	0.63	1.54	2.55E-01	-2.16	0.22	3.59E-02	-3.66	0.08	2.40E-03
G3V617	Mapk14	Mitogen-activated protein kinase 14	0.84	1.79	5.63E-01	0.53	1.45	6.69E-01	-3.54	0.09	1.71E-02
Q68FR8	Tuba3a	Tubulin alpha-3 chain	-0.29	0.82	9.58E-01	-1.61	0.33	1.90E-02	-3.31	0.10	2.50E-02
D3ZDK7	Pgp	Glycerol-3-phosphate phosphatase	-0.03	0.98	9.99E-01	-1.60	0.33	7.14E-05	-3.22	0.11	3.58E-10
D4A3P0	Ybx2	Y box-binding protein 2	-0.67	0.63	3.22E-01	-2.83	0.14	1.85E-06	-2.87	0.14	3.16E-05
P55054	Fabp9	Fatty acid-binding protein 9	-0.62	0.65	2.08E-01	-2.13	0.23	3.14E-03	-2.81	0.14	1.03E-04
P14659	Hspa2	Heat shock-related 70 kDa protein 2	-0.45	0.73	3.80E-01	-1.93	0.26	1.85E-06	-2.79	0.14	7.39E-07
B5DF80	Pabpc6	Polyadenylate-binding protein	-0.43	0.74	8.16E-01	-2.35	0.20	1.50E-02	-2.75	0.15	2.29E-03
D3ZHA7	RGD1560334	Similar to Myosin light chain 1 slow a	0.40	1.32	6.27E-01	-1.35	0.39	1.62E-03	-2.63	0.16	4.29E-01
Q68FX6	Cabs1	Calcium-binding and spermatid-specific protein 1	0.17	1.12	8.64E-01	-3.00	0.13	5.54E-10	-2.62	0.16	3.19E-05
G3V700	Nrd1	Nardilysin	0.74	1.67	1.98E-01	-1.95	0.26	3.30E-05	-2.57	0.17	1.48E-06
Q5XIM9	Cct2	T-complex protein 1 subunit beta	-0.66	0.63	2.65E-01	-0.51	0.70	2.90E-01	-2.56	0.17	9.35E-03
G3V7B2	Lrrc46	Leucine-rich repeat-containing protein 46	-0.11	0.93	9.63E-01	-1.38	0.39	1.56E-02	-2.51	0.18	6.64E-04
F1LSR7	Spata20	Spermatogenesis-associated protein 20	0.17	1.12	7.73E-01	-1.83	0.28	2.18E-07	-2.51	0.18	1.38E-08
Q6MG49	Bag6	Large proline-rich protein BAG6	-0.68	0.63	3.54E-01	-0.69	0.62	2.79E-01	-2.44	0.18	7.63E-03
Q5U328	Ncl	Nucleolin	–	–	–	-1.85	0.28	4.80E-01	-2.36	0.20	4.05E-03
P83868	Ptges3	Prostaglandin E synthase 3	0.35	1.27	7.66E-01	-1.85	0.28	1.50E-04	-2.35	0.20	5.00E-04
Q4QR76	Actl7b	Actin-like protein 7B	-1.17	0.44	2.34E-02	-1.12	0.46	1.41E-02	-2.23	0.21	1.82E-03
A0A0G2JSU3	Set	Protein SET	-0.96	0.51	3.64E-01	-1.74	0.30	2.04E-02	-2.21	0.22	2.67E-03
G3V6W6	Psmc6	26S protease regulatory subunit 10B	-0.12	0.92	8.30E-01	-0.39	0.77	3.08E-01	-2.16	0.22	1.13E-02
O35814	Stip1	Stress-induced-phosphoprotein 1	-0.35	0.78	4.22E-01	-1.33	0.40	9.35E-04	-2.03	0.24	2.13E-03
P68511	Ywhah	14-3-3 protein eta	0.51	1.42	6.44E-01	-1.63	0.32	2.91E-03	-2.02	0.25	1.85E-02
D4A781	Ipo5	Importin 5	-0.01	1.00	1.00E+00	-0.88	0.54	2.86E-04	-2.02	0.25	7.70E-11
M0R8P3	Cabyr	Calcium-binding tyrosine phosphorylation-regulated	-2.08	0.24	6.27E-01	-2.20	0.22	3.66E-02	-2.02	0.25	1.18E-01
D3ZSC2	Pdcd2l	Programmed cell death 2-like	-0.67	0.63	6.27E-01	-3.06	0.12	7.84E-02	-2.01	0.25	1.72E-02
P49088	Asns	Asparagine synthetase [glutamine-hydrolyzing]	0.11	1.08	8.88E-01	-1.01	0.50	2.05E-03	-1.98	0.25	3.52E-03
Q64298	Smcp	Sperm mitochondrial-associated cysteine-rich protein	0.31	1.24	7.71E-01	-2.11	0.23	9.32E-04	-1.97	0.26	9.24E-02
A0A0G2JZG7	Sars	Serine--tRNA ligase, cytoplasmic	0.01	1.01	1.00E+00	-1.29	0.41	6.69E-03	-1.92	0.26	3.67E-03
B5DEN5	Eef1b2	Elongation factor 1-beta 2	-0.27	0.83	8.14E-01	-1.53	0.35	1.88E-03	-1.90	0.27	9.95E-03
D3ZCR3	Hmgb1	High mobility group protein B1 pseudogene	0.68	1.60	3.22E-01	-2.13	0.23	1.39E-04	-1.86	0.28	1.10E-02
Q794E4	Hnrnpf	Heterogeneous nuclear ribonucleoprotein F	-0.28	0.83	6.27E-01	-1.28	0.41	5.12E-04	-1.84	0.28	4.26E-02
Q66HD3	Nasp	Nuclear autoantigenic sperm protein	-0.61	0.65	3.60E-01	-1.59	0.33	2.94E-05	-1.84	0.28	1.99E-03
Q9Z1B2	Gstm5	Glutathione S-transferase Mu 5	0.14	1.10	8.88E-01	-1.31	0.40	8.94E-04	-1.84	0.28	1.87E-04
P09034	Ass1	Argininosuccinate synthase	0.40	1.32	2.92E-01	-1.60	0.33	4.53E-10	-1.82	0.28	3.16E-05
C0JPT7	Flna	Filamin A	-0.29	0.82	1.80E-01	-2.01	0.25	2.72E-18	-1.78	0.29	5.84E-09
P62630	Eef1a1	Elongation factor 1-alpha 1	-0.84	0.56	9.15E-07	-1.20	0.43	4.37E-06	-1.78	0.29	1.06E-08
Q08163	Cap1	Adenylyl cyclase-associated protein 1	-0.82	0.57	1.17E-03	-0.66	0.63	1.39E-02	-1.75	0.30	6.32E-05
G3V762	Tsta3	Tissue specific transplantation antigen P35B	0.24	1.18	8.17E-01	-2.08	0.24	8.25E-04	-1.74	0.30	3.41E-02
P48508	Gclm	Glutamate--cysteine ligase regulatory subunit	-0.16	0.90	9.31E-01	-1.16	0.45	2.28E-02	-1.70	0.31	5.80E-01
Q5D059	Hnrnpk	Heterogeneous nuclear ribonucleoprotein K	-0.99	0.50	1.75E-03	-0.82	0.57	7.79E-03	-1.68	0.31	6.43E-05
Q562C6	Lztfl1	Leucine zipper transcription factor-like protein 1	-0.46	0.73	5.59E-01	-1.65	0.32	1.39E-03	-1.68	0.31	2.85E-02
F1LNF1	Hnrnpa2b1	Heterogeneous nuclear ribonucleoproteins A2/B1	-1.18	0.44	4.89E-03	-1.00	0.50	1.80E-03	-1.64	0.32	1.99E-03
P47860	Pfkp	ATP-dependent 6-phosphofructokinase, platelet type	0.18	1.13	7.73E-01	-0.94	0.52	3.14E-02	-1.64	0.32	3.95E-04
Q63413	Ddx39b	Spliceosome RNA helicase Ddx39b	-0.73	0.60	7.45E-02	-1.15	0.45	8.70E-03	-1.64	0.32	9.78E-03
F2Z3Q8	Kpnb1	Importin subunit beta-1	-0.50	0.71	4.22E-01	-0.19	0.88	7.74E-01	-1.64	0.32	4.28E-06
Q5U216	Ddx39a	ATP-dependent RNA helicase DDX39A	0.19	1.14	8.16E-01	-1.00	0.50	2.59E-02	-1.62	0.33	1.18E-01
G3V8L9	Ptrf	Polymerase I and transcript release factor	-1.42	0.37	2.63E-04	-2.13	0.23	5.62E-06	-1.60	0.33	8.80E-03
O08651	Phgdh	D-3-phosphoglycerate dehydrogenase	-1.31	0.40	4.35E-03	-1.17	0.45	9.66E-04	-1.55	0.34	5.36E-04
Q4KLZ3	Dazap1	DAZ associated protein 1	-0.08	0.95	9.63E-01	-1.38	0.39	1.32E-02	-1.55	0.34	1.72E-02
Q6Q0N1	Cndp2	Cytosolic non-specific dipeptidase	-0.98	0.51	2.68E-09	-1.04	0.49	1.86E-08	-1.51	0.35	4.28E-06
Q5QD51	Akap12	A-kinase anchor protein 12	-0.36	0.78	5.26E-01	-1.90	0.27	3.44E-04	-1.50	0.35	3.95E-03
A0A0G2JV31	Xpnpep1	Xaa-Pro aminopeptidase 1	-0.41	0.75	1.35E-01	-1.54	0.34	8.85E-10	-1.48	0.36	2.89E-06
P40112	Psmb3	Proteasome subunit beta type-3	-0.35	0.78	5.80E-01	1.03	2.04	6.52E-03	-1.48	0.36	4.61E-03
G3V7G8	Gars	Glycine--tRNA ligase	-0.69	0.62	1.47E-01	-0.85	0.55	1.13E-01	-1.47	0.36	2.03E-02
A0A0G2JZY6	Sptbn1	Spectrin beta chain, non-erythrocytic 1	0.02	1.01	9.93E-01	-0.96	0.51	1.24E-04	-1.46	0.36	1.39E-05
P41499	Ptpn11	Tyrosine-protein phosphatase non-receptor type 11	0.33	1.26	6.21E-01	-1.49	0.36	2.53E-06	-1.44	0.37	2.12E-03
F1LQD1	Ddx4	Probable ATP-dependent RNA helicase DDX4	-0.76	0.59	1.79E-01	-1.81	0.28	3.73E-04	-1.43	0.37	1.33E-01
Q9JLZ1	Glrx3	Glutaredoxin-3	-0.02	0.98	1.00E+00	-1.63	0.32	2.21E-03	-1.42	0.37	1.99E-03
P17220	Psma2	Proteasome subunit alpha type-2	-0.53	0.69	1.26E-01	0.71	1.63	7.16E-02	-1.42	0.37	1.37E-02
O70177	LOC100365112	Carboxylic ester hydrolase	1.20	2.29	5.15E-01	1.19	2.28	4.80E-01	-1.41	0.38	1.41E-02
Q6PCT3	Tpd52l2	Tumor protein D54	-0.08	0.95	9.63E-01	-1.11	0.46	4.95E-02	-1.41	0.38	5.80E-01
P05197	Eef2	Elongation factor 2	-0.81	0.57	1.53E-03	-0.94	0.52	1.03E-04	-1.41	0.38	4.91E-06
G3V6H9	Nap1l1	Nucleosome assembly protein 1-like 1	-0.53	0.69	3.02E-01	-1.36	0.39	1.98E-03	-1.40	0.38	6.73E-04
D4ABI6	Uchl3	Ubiquitin carboxyl-terminal hydrolase isozyme L3	0.05	1.04	9.63E-01	-1.33	0.40	2.46E-04	-1.39	0.38	9.34E-04
P53042	Ppp5c	Serine/threonine-protein phosphatase 5	0.01	1.00	1.00E+00	-1.08	0.47	1.53E-02	-1.39	0.38	2.85E-02
F8WG67	Acot7	Cytosolic acyl coenzyme A thioester hydrolase	-1.10	0.47	3.46E-01	-0.29	0.82	9.87E-01	-1.36	0.39	3.48E-02
P63039	Hspd1	60 kDa heat shock protein, mitochondrial	-1.90	0.27	2.69E-04	-0.36	0.78	4.10E-01	-1.33	0.40	1.12E-01
Q642F2	Ppm1b	Protein phosphatase 1B	-0.60	0.66	1.79E-01	-1.62	0.33	1.50E-04	-1.32	0.40	6.12E-02
Q62785	Pdap1	28 kDa heat- and acid-stable phosphoprotein	-0.02	0.99	1.00E+00	-1.24	0.42	2.06E-03	-1.31	0.40	6.84E-02
A0A0G2K911	Nsfl1c	NSFL1 cofactor p47	-0.28	0.82	6.01E-01	-0.56	0.68	9.03E-02	-1.30	0.41	6.43E-05
E2RUH2	Rnh1	Ribonuclease inhibitor	-0.36	0.78	4.22E-01	-1.28	0.41	5.37E-05	-1.26	0.42	3.19E-03
B0BN85	Sugt1	Suppressor of G2 allele of SKP1 homolog	-0.70	0.62	4.81E-01	-1.93	0.26	5.62E-06	-1.26	0.42	3.00E-01
Q63228	Gmfb	Glia maturation factor beta	-0.41	0.75	7.62E-01	-1.86	0.28	5.05E-03	-1.25	0.42	1.18E-01
Q6P688	Mat2a	S-adenosylmethionine synthase	-0.01	1.00	1.00E+00	-1.50	0.35	3.46E-02	-1.25	0.42	6.84E-02
F1M779	Cltc	Clathrin heavy chain;Clathrin heavy chain 1	-0.28	0.83	5.57E-01	-0.02	0.99	9.87E-01	-1.24	0.42	2.67E-02
B5DF46	Pmm2	Phosphomannomutase	-0.54	0.69	6.27E-01	-1.45	0.37	1.99E-04	-1.23	0.43	8.81E-02
Q68FS2	Cops4	COP9 signalosome complex subunit 4	-0.02	0.99	1.00E+00	-1.02	0.49	1.69E-03	-1.23	0.43	4.16E-03
Q6AYK3	Isyna1	Inositol-3-phosphate synthase 1	-0.15	0.90	7.49E-01	-0.85	0.55	7.27E-03	-1.21	0.43	1.60E-03
D3ZVQ0	Usp5	Ubiquitin carboxyl-terminal hydrolase	-0.52	0.70	1.92E-02	-1.32	0.40	2.18E-08	-1.21	0.43	1.96E-06
F1M3H8	LOC681410	Hypothetical protein	-0.56	0.68	1.80E-01	-1.03	0.49	5.54E-02	-1.21	0.43	2.40E-03
D4A1Q9	Ttll12	Tubulin tyrosine ligase-like 12	-0.34	0.79	5.28E-01	-1.12	0.46	3.89E-03	-1.20	0.43	2.48E-02
F8WFH8	Wars	Tryptophan--tRNA ligase, cytoplasmic	-0.17	0.89	6.98E-01	-1.46	0.36	2.13E-04	-1.20	0.43	2.18E-03
A0A0G2JSY5	Fam221a	Protein FAM221A	-0.37	0.77	6.27E-01	-1.46	0.36	2.63E-02	-1.19	0.44	3.06E-01
A0A140TAJ3	Fubp1	Far upstream element-binding protein 1	0.18	1.13	7.73E-01	-0.89	0.54	4.15E-02	-1.17	0.44	2.75E-02
Q7TPB1	Cct4	T-complex protein 1 subunit delta	-0.54	0.69	3.80E-01	-0.60	0.66	2.69E-01	-1.17	0.44	4.23E-04
Q66HR2	Mapre1	Microtubule-associated protein RP/EB family member 1	-0.52	0.70	4.04E-01	-1.55	0.34	2.60E-04	-1.17	0.44	6.86E-02
F1LQ48	Hnrnpl	Heterogeneous nuclear ribonucleoprotein L	-0.75	0.60	2.02E-01	-1.50	0.35	1.29E-03	-1.17	0.44	6.29E-02
F1LMA7	Mrc2	C-type mannose receptor 2	-1.46	0.36	1.57E-07	-0.63	0.65	1.58E-02	-1.17	0.45	1.04E-01
P97532	Mpst	3-mercaptopyruvate sulfurtransferase	-0.38	0.77	6.64E-01	-1.06	0.48	1.18E-03	-1.15	0.45	7.90E-02
A0A0G2JSZ5	Pdia6	Protein disulfide-isomerase A6	-1.73	0.30	1.94E-08	-1.01	0.50	4.36E-03	-1.13	0.46	1.04E-01
G3V6S5	Mthfd1	C-1-tetrahydrofolate synthase	-0.01	0.99	1.00E+00	-0.96	0.51	4.41E-02	-1.12	0.46	4.24E-01
A0A140TAA4	Pdcd6ip	Programmed cell death 6-interacting protein	-0.35	0.79	4.22E-01	-1.64	0.32	1.36E-05	-1.10	0.47	5.64E-04
G3V8U9	Psmb4	Proteasome subunit beta type-4	-0.33	0.80	4.33E-01	0.30	1.23	4.72E-01	-1.10	0.47	9.43E-03
F7EPH4	Ppa1	Pyrophosphatase (inorganic) 1	-0.50	0.71	2.18E-01	-1.85	0.28	1.71E-06	-1.09	0.47	3.95E-03
P63331	Ppp2ca	Serine/threonine-protein phosphatase 2A catalytic subunit alpha isoform	0.02	1.01	9.91E-01	-0.88	0.54	2.04E-02	-1.08	0.47	3.48E-02
P18418	Calr	Calreticulin	-1.68	0.31	2.13E-05	-1.14	0.45	1.12E-03	-1.08	0.47	9.88E-02
Q5M9H7	Dnaja2	DnaJ homolog subfamily A member 2	-0.35	0.79	7.28E-01	-1.17	0.44	2.97E-02	-1.07	0.48	1.09E-01
Q64057	Aldh7a1	Alpha-aminoadipic semialdehyde dehydrogenase	-0.35	0.79	4.56E-01	-1.02	0.49	3.95E-03	-1.04	0.49	4.18E-02
E9PT65	Rdx	Radixin	-0.24	0.85	7.51E-01	-1.39	0.38	4.57E-02	-1.02	0.49	4.29E-01
B0BNM1	Apoa1bp	NAD(P)H-hydrate epimerase	-1.09	0.47	5.05E-02	-1.11	0.46	7.26E-03	-1.01	0.50	4.29E-01

G3V6M1	Cst12	Cystatin-12	0.29	1.22	9.51E-01	1.81	3.51	1.46E-03	-1.01	0.50	4.29E-01
A0A0G2K405	Prkar2a	cAMP-dependent protein kinase type II-alpha regulatory subunit	0.06	1.04	9.63E-01	-1.16	0.45	1.02E-02	-1.00	0.50	4.29E-01
P50475	Aars	Alanine--tRNA ligase, cytoplasmic	-0.13	0.91	8.48E-01	-1.78	0.29	5.68E-06	-0.99	0.50	7.79E-02
P11232	Txn	Thioredoxin	-0.19	0.88	8.88E-01	-1.66	0.32	2.36E-03	-0.98	0.51	4.29E-01
M0R961	Khsrp	Far upstream element-binding protein 2	0.02	1.02	9.63E-01	-1.20	0.44	7.22E-06	-0.98	0.51	1.37E-03
G3V852	Tln1	Talin-1	-0.62	0.65	1.02E-05	-1.49	0.36	2.66E-14	-0.97	0.51	5.95E-06
P62959	Hint1	Histidine triad nucleotide-binding protein 1	-0.90	0.54	2.57E-02	-1.95	0.26	4.02E-04	-0.97	0.51	1.34E-01
B5DF91	Elavl1	ELAV-like protein	0.09	1.06	9.31E-01	-1.27	0.42	1.08E-02	-0.97	0.51	3.06E-01
P11762	Lgals1	Galectin-1	-1.92	0.26	3.99E-11	-1.82	0.28	9.73E-09	-0.94	0.52	3.11E-02
Q6TXG7	Shmt1	Serine hydroxymethyltransferase	0.12	1.09	8.85E-01	-2.52	0.17	4.53E-10	-0.94	0.52	3.06E-01
D3ZB30	Ptbp1	Polypyrimidine tract-binding protein 1	-0.98	0.51	1.64E-02	-1.16	0.45	1.30E-02	-0.91	0.53	1.12E-01
Q4KMA2	Rad23b	UV excision repair protein RAD23 homolog B	-0.67	0.63	1.79E-01	-1.34	0.39	1.02E-02	-0.89	0.54	8.81E-02
Q3T1J1	Eif5a	Eukaryotic translation initiation factor 5A-1	-1.10	0.47	1.54E-02	-1.36	0.39	1.44E-04	-0.89	0.54	6.12E-02
F1LRL9	Map1b	Microtubule-associated protein 1B	0.23	1.17	6.98E-01	-1.71	0.31	1.27E-07	-0.89	0.54	2.88E-02
A0A0G2K1C0	Actr3	Actin-related protein 3	-1.12	0.46	1.61E-02	0.15	1.11	7.90E-01	-0.81	0.57	4.63E-01
P06761	Hspa5	78 kDa glucose-regulated protein	-0.69	0.62	1.84E-03	-0.53	0.69	1.57E-02	-0.81	0.57	1.58E-03
Q64303	Pak2	Serine/threonine-protein kinase PAK 2	-0.79	0.58	7.60E-02	-1.46	0.36	1.39E-03	-0.80	0.57	6.23E-02
Q9WU49	Carhsp1	Calcium-regulated heat stable protein 1	-0.38	0.77	5.68E-01	-2.00	0.25	8.84E-03	-0.80	0.58	3.36E-01
G3V6E7	Fmod	Fibromodulin	-2.01	0.25	2.47E-11	-0.18	0.88	6.35E-01	-0.78	0.58	7.79E-02
P62944	Ap2b1	AP-2 complex subunit beta	0.07	1.05	9.51E-01	-1.27	0.41	3.59E-02	-0.77	0.59	6.90E-01
P06214	Alad	Delta-aminolevulinic acid dehydratase	-0.07	0.95	9.63E-01	-0.72	0.61	1.24E-01	-0.76	0.59	2.57E-02
F1M9N7	Agfg1	Arf-GAP domain and FG repeat-containing protein 1	-0.01	0.99	1.00E+00	-1.42	0.37	1.18E-03	-0.74	0.60	9.46E-01
P36201	Crip2	Cysteine-rich protein 2	-1.43	0.37	1.71E-03	-2.13	0.23	1.37E-05	-0.74	0.60	2.83E-01
P05065	Aldoa	Fructose-bisphosphate aldolase A	-0.78	0.58	2.69E-02	-0.58	0.67	5.69E-02	-0.72	0.61	1.18E-01
Q9QZR6	Sept9	Septin-9	0.28	1.21	6.56E-01	-0.89	0.54	3.73E-02	-0.72	0.61	1.07E-01
A0A0G2K2R5	Efemp2	EGF-containing fibulin extracellular matrix protein 2	-0.34	0.79	5.03E-01	0.61	1.52	2.54E-02	-0.71	0.61	9.98E-02
A0A0H2UH90	Vwa5a	von Willebrand factor A domain-containing protein 5A	0.20	1.15	8.16E-01	-1.23	0.43	1.41E-03	-0.71	0.61	1.20E-01
Q6AYT3	Rtcb	tRNA-splicing ligase RtcB homolog	0.19	1.14	9.07E-01	-1.42	0.37	2.21E-02	-0.70	0.62	1.71E-01
P02454	Col1a1	Collagen alpha-1(I) chain	-1.98	0.25	5.22E-16	-0.25	0.84	3.24E-01	-0.70	0.62	6.50E-02
Q02589	Adprh	[Protein ADP-ribosylarginine] hydrolase	-0.96	0.51	1.47E-01	-1.68	0.31	1.41E-02	-0.69	0.62	2.73E-01
D3ZZC1	Txndc5	Thioredoxin domain-containing protein 5	-1.35	0.39	1.92E-02	-1.05	0.48	1.65E-02	-0.68	0.62	7.25E-01
P52631	Stat3	Signal transducer and activator of transcription 3	-0.11	0.93	8.76E-01	-1.06	0.48	1.86E-02	-0.67	0.63	5.39E-01
O35567	Atic	Bifunctional purine biosynthesis protein PURH	-0.79	0.58	4.30E-02	-1.07	0.48	8.41E-04	-0.66	0.63	3.45E-01
A0A0G2K0X9	Sec31a	Protein transport protein Sec31A	-0.28	0.83	4.97E-01	-1.09	0.47	4.36E-04	-0.65	0.64	9.73E-02
A0A0G2JUA5	Ahnak	AHNAK nucleoprotein	-0.61	0.66	2.30E-02	-2.24	0.21	3.42E-12	-0.65	0.64	1.04E-01
Q4KM73	Cmpk1	UMP-CMP kinase	-0.07	0.95	8.93E-01	-1.13	0.46	1.18E-03	-0.64	0.64	3.62E-01
P19468	Gclc	Glutamate--cysteine ligase catalytic subunit	-0.23	0.85	7.73E-01	-1.48	0.36	4.36E-03	-0.62	0.65	7.31E-01
Q6AY18	Sar1a	GTP-binding protein SAR1a	-0.97	0.51	2.55E-01	-1.98	0.25	4.95E-02	-0.61	0.66	5.53E-01
A0A0G2JSL8	Adk	Adenosine kinase	-0.79	0.58	6.22E-02	-1.53	0.35	2.30E-03	-0.61	0.66	3.36E-01
Q925N6	Igsf1	Immunoglobulin superfamily member 1	0.66	1.58	8.36E-02	1.55	2.93	6.69E-03	-0.58	0.67	2.69E-01
G3V8R1	Nucb2	Nucleobindin-2;Nesfatin-1	-0.25	0.84	7.78E-01	-1.22	0.43	1.65E-02	-0.57	0.67	4.29E-01
Q5M7T7	Pla2g7	Platelet-activating factor acetylhydrolase	0.36	1.28	2.55E-01	1.54	2.91	4.11E-04	-0.54	0.69	1.50E-01
B0BNE5	Esd	S-formylglutathione hydrolase	-0.65	0.64	9.58E-02	-2.79	0.14	2.66E-07	-0.53	0.69	4.27E-01
A0A0G2JZ13	Cttn	Src substrate cortactin	-0.41	0.75	5.63E-01	-1.47	0.36	1.18E-03	-0.51	0.70	5.26E-01
F1LS40	Col1a2	Collagen alpha-2(I) chain	-2.25	0.21	3.30E-11	-0.20	0.87	6.32E-01	-0.49	0.71	3.14E-01
F1LP82	Rab2a	Ras-related protein Rab-2A	-0.49	0.71	1.60E-01	-1.28	0.41	5.79E-03	-0.47	0.72	6.90E-01
P63029	Tpt1	Translationally-controlled tumor protein	-2.50	0.18	1.54E-02	-1.66	0.32	1.86E-02	-0.43	0.74	6.01E-01
A0A0H2UHJ0	Shbg	Sex hormone-binding globulin	0.44	1.36	3.14E-03	0.83	1.77	5.53E-05	-0.42	0.75	1.65E-02
D3ZGK7	Ces1c	Carboxylic ester hydrolase	0.19	1.14	7.73E-01	3.88	14.69	2.36E-03	-0.41	0.75	7.31E-01
F1M9V7	Npepps	Aminopeptidase	-0.58	0.67	4.31E-03	-0.69	0.62	2.68E-02	-0.38	0.77	3.81E-01
P17988	Sult1a1	Sulfotransferase 1A1	0.07	1.05	9.60E-01	-1.65	0.32	3.49E-05	-0.38	0.77	7.04E-01
Q8CFN2	Cdc42	Cell division control protein 42 homolog	-0.50	0.71	3.54E-01	-1.73	0.30	2.15E-03	-0.38	0.77	6.90E-01
A0A0G2K737	Txnl1	Thioredoxin-like protein 1	-0.28	0.82	6.46E-01	-1.12	0.46	4.23E-03	-0.37	0.77	6.10E-01
P46844	Blvra	Biliverdin reductase A	-1.54	0.34	8.06E-05	-0.84	0.56	5.70E-02	-0.35	0.78	6.54E-01
F1M8E9	Lyz2	Lysozyme	-0.48	0.72	3.98E-01	1.35	2.55	2.15E-03	-0.35	0.78	5.26E-01
Q5RJN2	Pcolce	Procollagen C-endopeptidase enhancer 1	-1.43	0.37	1.65E-10	0.79	1.73	4.96E-04	-0.35	0.79	4.07E-01
D4A7U1	Zyx	Zyxin	-0.25	0.84	6.47E-01	-1.01	0.50	3.71E-02	-0.34	0.79	4.81E-01
Q68FY4	Gc	Vitamin D-binding protein	-0.81	0.57	1.96E-21	-1.17	0.44	1.74E-30	-0.34	0.79	1.06E-02
G3V826	Tkt	Transketolase	-1.19	0.44	1.10E-03	-1.06	0.48	5.75E-02	-0.33	0.79	5.42E-01
P62963	Pfn1	Profilin-1	-2.29	0.20	4.10E-06	-1.04	0.48	1.31E-01	-0.29	0.82	8.13E-01
Q6P6Q5	App	Amyloid beta A4 protein	-0.19	0.88	6.99E-01	-0.31	0.81	8.84E-03	-0.29	0.82	6.20E-01
P20767	N/A	Ig lambda-2 chain C region	0.51	1.43	7.45E-02	0.74	1.67	6.36E-04	-0.27	0.83	5.91E-01
Q6DGG0	Ppid	Peptidyl-prolyl cis-trans isomerase D	-0.50	0.71	3.54E-01	-0.66	0.63	3.59E-02	-0.25	0.84	7.98E-01
F1LR10	Lima1	LIM domain and actin-binding protein 1	-0.58	0.67	4.22E-01	-1.73	0.30	3.72E-03	-0.25	0.84	7.08E-01
Q6AXN2	Efemp1	EGF-containing fibulin-like extracellular matrix protein 1	-0.61	0.65	2.35E-05	0.53	1.44	1.51E-03	-0.24	0.84	3.39E-01
O88794	Pnpo	Pyridoxine-5-phosphate oxidase	-0.22	0.86	8.48E-01	-1.11	0.46	1.86E-02	-0.23	0.85	9.23E-01
D3ZUB0	Rcn1	Reticulocalbin 1	-0.82	0.57	4.67E-03	-0.82	0.57	9.77E-02	-0.23	0.86	8.42E-01
Q5RJK6	Inpp1	Inositol polyphosphate-1-phosphatase	-0.95	0.52	1.24E-01	-1.65	0.32	1.65E-04	-0.21	0.87	8.46E-01
A0A0G2K531	Gpx3	Glutathione peroxidase 3	0.76	1.69	3.82E-05	1.45	2.73	1.01E-07	-0.17	0.89	7.38E-01
D3ZQN7	Lamb1	Laminin subunit beta-1	-0.46	0.73	3.12E-03	0.35	1.27	3.65E-01	-0.15	0.90	7.85E-01
P16975	Sparc	Secreted protein acidic and cysteine rich	-1.36	0.39	1.85E-11	-0.70	0.62	2.97E-02	-0.14	0.91	8.32E-01
A0A0G2JSM3	Pdlim3	PDZ and LIM domain protein 3	-1.43	0.37	1.48E-01	-1.67	0.31	5.57E-03	-0.13	0.91	9.46E-01
Q5RJR2	Twf1	Twinfilin-1	-0.39	0.76	5.33E-01	-1.05	0.48	3.05E-02	-0.12	0.92	9.23E-01
Q9EPB1	Dpp7	Dipeptidyl peptidase 2	-1.06	0.48	9.85E-03	-0.60	0.66	1.60E-01	-0.09	0.94	9.95E-01
Q6AYP7	Nt5c3b	7-methylguanosine phosphate-specific 5-nucleotidase	-0.33	0.79	5.59E-01	-0.86	0.55	4.14E-02	-0.09	0.94	9.21E-01
P02793	Ftl1	Ferritin light chain 1	-1.46	0.36	1.64E-02	-0.01	0.99	1.00E+00	-0.03	0.98	1.00E+00
P30120	Timp1	Metalloproteinase inhibitor 1	0.06	1.04	9.63E-01	1.45	2.73	4.36E-03	-0.03	0.98	9.46E-01
D3ZHC4	Hebp2	Heme binding protein 2	0.15	1.11	9.51E-01	-1.15	0.45	8.84E-03	-0.03	0.98	9.46E-01
G3V940	Coro1b	Coronin-1B	-0.47	0.72	4.97E-01	-1.28	0.41	1.56E-02	-0.02	0.99	1.00E+00
Q9ERA7	Msln	Mesothelin	-1.37	0.39	5.00E-04	-0.04	0.97	9.71E-01	-0.01	0.99	1.00E+00
A0A0G2JV28	Mea1	Male-enhanced antigen 1	0.68	1.60	6.27E-01	-1.22	0.43	5.87E-03	–	–	–
P13941	Col3a1	Collagen alpha-1(III) chain	-1.21	0.43	2.52E-05	0.36	1.29	3.25E-01	0.02	1.02	9.84E-01
B1WC26	Nans	N-acetylneuraminate synthase	-0.92	0.53	5.81E-03	-1.20	0.44	1.77E-03	0.06	1.04	9.83E-01
Q5XI38	Lcp1	Lymphocyte cytosolic protein 1	-0.66	0.63	1.43E-02	-0.58	0.67	4.17E-02	0.10	1.07	8.69E-01
E9PSQ1	Amy1a	Alpha-amylase	-0.53	0.69	4.63E-02	0.75	1.68	8.68E-02	0.11	1.08	4.99E-01
A0A1W2Q6E9	Msn	Moesin	-1.76	0.30	1.02E-04	-1.67	0.31	6.36E-04	0.14	1.10	8.91E-01
A0A0G2K135	Cfi	Complement factor I	-0.82	0.57	1.44E-09	0.41	1.33	4.84E-02	0.16	1.11	4.70E-01
F1LR02	Col18a1	Collagen type 18 alpha 1 chain	-0.21	0.87	7.25E-01	1.26	2.39	1.88E-03	0.16	1.11	8.13E-01
P81795	Eif2s3	Eukaryotic translation initiation factor 2 subunit 3	-0.17	0.89	8.16E-01	-1.21	0.43	3.06E-02	0.18	1.13	8.46E-01
D4A8H3	Uba6	Ubiquitin-like modifier-activating enzyme 6	0.06	1.04	9.63E-01	-1.26	0.42	3.73E-05	0.19	1.14	8.37E-01
P14046	A1i3	Alpha-1-inhibitor 3	-1.54	0.34	2.02E-03	0.13	1.09	7.22E-01	0.36	1.29	5.80E-01
G3V734	Decr1	2,4-dienoyl-CoA reductase, mitochondrial	-0.84	0.56	1.37E-02	-0.36	0.78	6.85E-01	0.47	1.39	7.08E-01
Q01129	Dcn	Decorin	-2.14	0.23	9.32E-05	-0.28	0.82	6.52E-01	0.58	1.50	5.09E-01
Q6AY84	Scrn1	Secernin-1	-2.97	0.13	4.05E-02	-0.73	0.60	4.83E-01	1.00	2.00	9.46E-01
F1LQQ8	Gusb	Beta-glucuronidase	-2.47	0.18	5.10E-03	0.43	1.35	7.41E-01	1.41	2.67	7.08E-01
A0A0G2JTU6	Sbp	Prostatic spermine-binding protein	-0.73	0.60	7.56E-01	-3.69	0.08	2.63E-02	–	–	–
Q6AZ50	Atg3	Ubiquitin-like-conjugating enzyme ATG3	–	–	–	-2.69	0.15	2.06E-03	–	–	–
P52759	Hrsp12	Ribonuclease UK114	0.37	1.29	4.22E-01	-1.52	0.35	2.63E-02	–	–	–
P43527	Casp1	Caspase-1	0.19	1.14	8.48E-01	-1.32	0.40	3.46E-02	–	–	–
A0A0G2K824	Gmppa	Mannose-1-phosphate guanyltransferase alpha	-1.68	0.31	1.37E-02	-1.12	0.46	3.25E-01	–	–	–
Q6AY48	Pcbp3	Poly(rC)-binding protein 3	-0.34	0.79	5.15E-01	-1.11	0.46	4.84E-02	–	–	–
Q2LAP6	Tes	Testin	-0.43	0.74	7.56E-01	-1.08	0.47	4.84E-02	–	–	–
A0A0G2K905	Arpc2	Actin-related protein 2/3 complex subunit 2	-1.26	0.42	2.74E-03	-0.41	0.75	7.74E-01	–	–	–
Q6P0K8	Jup	Junction plakoglobin	-1.25	0.42	9.10E-02	3.32	10.00	3.00E-07	–	–	–
A0A096MJ40	Hmcn1	Hemicentin 1	-1.63	0.32	7.45E-02	4.10	17.14	3.66E-02	–	–	–
Q3B7D1	Ube2z	Ubiquitin-conjugating enzyme E2 Z	-0.47	0.72	8.88E-01	-1.90	0.27	3.66E-02	–	–	–
Q6P6G4	Bpgm	Phosphoglycerate mutase	-0.33	0.79	7.25E-01	-1.10	0.47	1.18E-03	–	–	–

Yellow cells:	Proteins that are changed (up/down) with $p < 0.05$.
Green cells:	Proteins that are unchanged or changed with $p > 0.05$.

Column explanations

Uniprot accession number: First, or leading, protein ID annotation in UniProtKB/Swiss-Prot Rattus norvegicus database (Nov 2018).

Gene symbol: Leading gene symbol in UniProtKB/Swiss-Prot Rattus norvegicus database (Nov 2018).

Protein name: Protein name from the UniProtKB/Swiss-Prot Rattus norvegicus database (Nov 2018).

Log2 Heat/Control: Log2 ratio of protein abundance in heat-treated rats/control rats.

Fold change Heat/Control: Linear ratio of protein abundance in heat-treated rats/control rats.

P-Value Heat/Control: p value of difference in protein abundance between heat-treated and control rats.

Supp Table 3A. Total of 15 proteins with altered expression (up/down, p<0.05) at all time-points following heat treatment.

			1 week			8 weeks			14 weeks			
Uniprot accession number	**Gene name**	**Protein name**	**Log2 Heat / Control**	**Fold change Heat / Control**	**P-Value Heat / Control**	**Log2 Heat / Control**	**Fold change Heat / Control**	**P-Value Heat / Control**	**Log2 Heat / Control**	**Fold change Heat / Control**	**P-Value Heat / Control**	**Tubular origin**
Q4QR76	Actl7b	Actin-like protein 7B	-1.17	0.44	2.34E-02	-1.12	0.46	1.41E-02	-2.23	0.21	1.82E-03	rST > SYT
Q08163	Cap1	Adenylyl cyclase-associated protein 1	-0.82	0.57	1.17E-03	-0.66	0.63	1.39E-02	-1.75	0.30	6.32E-05	SC > SG & SYT >> rST
Q6Q0N1	Cndp2	Cytosolic non-specific dipeptidase	-0.98	0.51	2.68E-09	-1.04	0.49	1.86E-08	-1.51	0.35	4.28E-06	SC >> SG, rST & SYT
P62630	Eef1a1	Elongation factor 1-alpha 1	-0.84	0.56	9.15E-07	-1.20	0.43	4.37E-06	-1.78	0.29	1.06E-08	Mixed
P05197	Eef2	Elongation factor 2	-0.81	0.57	1.53E-03	-0.94	0.52	1.03E-04	-1.41	0.38	4.91E-06	Mixed
Q68FY4	Gc	Vitamin D-binding protein	-0.81	0.57	1.96E-21	-1.17	0.44	1.74E-30	-0.34	0.79	1.06E-02	below sensitivity
F1LNF1	Hnrnpa2b1	Heterogeneous nuclear ribonucleoproteins A2/B1	-1.18	0.44	4.89E-03	-1.00	0.50	1.80E-03	-1.64	0.32	1.99E-03	Mixed
Q5D059	Hnrnpk	Heterogeneous nuclear ribonucleoprotein K	-0.99	0.50	1.75E-03	-0.82	0.57	7.79E-03	-1.68	0.31	6.43E-05	SG & SC > SYT >> rST
P06761	Hspa5	78 kDa glucose-regulated protein	-0.69	0.62	1.84E-03	-0.53	0.69	1.57E-02	-0.81	0.57	1.58E-03	Mixed
P11762	Lgals1	Galectin-1	-1.92	0.26	3.99E-11	-1.82	0.28	9.73E-09	-0.94	0.52	3.11E-02	**SC >>** SG
O08651	Phgdh	D-3-phosphoglycerate dehydrogenase	-1.31	0.40	4.35E-03	-1.17	0.45	9.66E-04	-1.55	0.34	5.36E-04	SC & SG >> rST > SYT
G3V8L9	Ptrf	Polymerase I and transcript release factor	-1.42	0.37	2.63E-04	-2.13	0.23	5.62E-06	-1.60	0.33	8.80E-03	SG & SC
A0A0H2UHJ0	Shbg	Sex hormone-binding globulin	0.44	1.36	3.14E-03	0.83	1.77	5.53E-05	-0.42	0.75	1.65E-02	**SC >>** SG & SYT
G3V852	Tln1	Talin-1	-0.62	0.65	1.02E-05	-1.49	0.36	2.66E-14	-0.97	0.51	5.95E-06	SC & SG >> rST & SYT
D3ZVQ0	Usp5	Ubiquitin carboxyl-terminal hydrolase	-0.52	0.70	1.92E-02	-1.32	0.40	2.18E-08	-1.21	0.43	1.96E-06	Mixed

Supp Table 3B. Total of 23 proteins with altered expression (up/down, p<0.05) at 1 week only following heat treatment.

			1 week			8 weeks			14 weeks			
Uniprot accession number	**Gene name**	**Protein name**	**Log2 Heat / Control**	**Fold change Heat / Control**	**P-Value Heat / Control**	**Log2 Heat / Control**	**Fold change Heat / Control**	**P-Value Heat / Control**	**Log2 Heat / Control**	**Fold change Heat / Control**	**P-Value Heat / Control**	**Tubular origin**
P02454	Col1a1	Collagen alpha-1(I) chain	-1.98	0.25	5.22E-16	-0.25	0.84	3.24E-01	-0.70	0.62	6.50E-02	SG >> SC
G3V6E7	Fmod	Fibromodulin	-2.01	0.25	2.47E-11	-0.18	0.88	6.35E-01	-0.78	0.58	7.79E-02	SYT & rST
F1LS40	Col1a2	Collagen alpha-2(I) chain	-2.25	0.21	3.30E-11	-0.20	0.87	6.32E-01	-0.49	0.71	3.14E-01	SG > SC
P62963	Pfn1	Profilin-1	-2.29	0.20	4.10E-06	-1.04	0.48	1.31E-01	-0.29	0.82	8.13E-01	SC & SG > rST & SYT
P13941	Col3a1	Collagen alpha-1(III) chain	-1.21	0.43	2.52E-05	0.36	1.29	3.25E-01	0.02	1.02	9.84E-01	**SG >>** SC
P46844	Blvra	Biliverdin reductase A	-1.54	0.34	8.06E-05	-0.84	0.56	5.70E-02	-0.35	0.78	6.54E-01	SC
Q01129	Dcn	Decorin	-2.14	0.23	9.32E-05	-0.28	0.82	6.52E-01	0.58	1.50	5.09E-01	SG
P63039	Hspd1	60 kDa heat shock protein, mitochondrial	-1.90	0.27	2.69E-04	-0.36	0.78	4.10E-01	-1.33	0.40	1.12E-01	SG & SC
Q9ERA7	Msln	Mesothelin	-1.37	0.39	5.00E-04	-0.04	0.97	9.71E-01	-0.01	0.99	1.00E+00	below sensitivity
G3V826	Tkt	Transketolase	-1.19	0.44	1.10E-03	-1.06	0.48	5.75E-02	-0.33	0.79	5.42E-01	SC & SG
P14046	A1i3	Alpha-1-inhibitor 3	-1.54	0.34	2.02E-03	0.13	1.09	7.22E-01	0.36	1.29	5.80E-01	below sensitivity
A0A0G2K905	Arpc2	Actin-related protein 2/3 complex subunit 2	-1.26	0.42	2.74E-03	-0.41	0.75	7.74E-01	–	–	–	Mixed
D3ZQN7	Lamb1	Laminin subunit beta-1	-0.46	0.73	3.12E-03	0.35	1.27	3.65E-01	-0.15	0.90	7.85E-01	SG & SC
D3ZUB0	Rcn1	Reticulocalbin 1	-0.82	0.57	4.67E-03	-0.82	0.57	9.77E-02	-0.23	0.86	8.42E-01	SG & SC
F1LQQ8	Gusb	Beta-glucuronidase	-2.47	0.18	5.10E-03	0.43	1.35	7.41E-01	1.41	2.67	7.08E-01	SG & SC
Q9EPB1	Dpp7	Dipeptidyl peptidase 2	-1.06	0.48	9.85E-03	-0.60	0.66	1.60E-01	-0.09	0.94	9.95E-01	Mixed
G3V734	Decr1	2,4-dienoyl-CoA reductase, mitochondrial	-0.84	0.56	1.37E-02	-0.36	0.78	6.85E-01	0.47	1.39	7.08E-01	SC & SG
A0A0G2K824	Gmppa	Mannose-1-phosphate guanyltransferase alpha	-1.68	0.31	1.37E-02	-1.12	0.46	3.25E-01	_	_	_	Mixed
A0A0G2K1C0	Actr3	Actin-related protein 3	-1.12	0.46	1.61E-02	0.15	1.11	7.90E-01	-0.81	0.57	4.63E-01	SC & SG
P02793	Ftl1	Ferritin light chain 1	-1.46	0.36	1.64E-02	-0.01	0.99	1.00E+00	-0.03	0.98	1.00E+00	**SC & SG >>** rST & SYT
P05065	Aldoa	Fructose-bisphosphate aldolase A	-0.78	0.58	2.69E-02	-0.58	0.67	5.69E-02	-0.72	0.61	1.18E-01	SC, SG & rST >> SYT
Q6AY84	Scrn1	Secernin-1	-2.97	0.13	4.05E-02	-0.73	0.60	4.83E-01	1.00	2.00	9.46E-01	SG > SC
E9PSQ1	Amy1a	Alpha-amylase	-0.53	0.69	4.63E-02	0.75	1.68	8.68E-02	0.11	1.08	4.99E-01	below sensitivity

Supp Table 3C. Total of 20 proteins with altered expression (up/down, p<0.05) at 1 and 8 weeks following heat treatment.

			1 week			8 weeks			14 weeks			
Uniprot accession number	**Gene name**	**Protein name**	**Log2 Heat / Control**	**Fold change Heat / Control**	**P-Value Heat / Control**	**Log2 Heat / Control**	**Fold change Heat / Control**	**P-Value Heat / Control**	**Log2 Heat / Control**	**Fold change Heat / Control**	**P-Value Heat / Control**	**Tubular origin**
A0A0G2JU	Ahnak	AHNAK nucleoprotein	-0.61	0.66	2.30E-02	-2.24	0.21	3.42E-12	-0.65	0.64	1.04E-01	SC
O35567	Atic	Bifunctional purine biosynthesis protein PURH	-0.79	0.58	4.30E-02	-1.07	0.48	8.41E-04	-0.66	0.63	3.45E-01	SC & SG >> SYT
P18418	Calr	Calreticulin	-1.68	0.31	2.13E-05	-1.14	0.45	1.12E-03	-1.08	0.47	9.88E-02	SC & SG > rST & SYT
A0A0G2K13	Cfi	Complement factor I	-0.82	0.57	1.44E-09	0.41	1.33	4.84E-02	0.16	1.11	4.70E-01	below sensitivity
P36201	Crip2	Cysteine-rich protein 2	-1.43	0.37	1.71E-03	-2.13	0.23	1.37E-05	-0.74	0.60	2.83E-01	SC > SG & rST
Q6AXN2	Efemp1	EGF-containing fibulin-like extracellular matrix protein 1	-0.61	0.65	2.35E-05	0.53	1.44	1.51E-03	-0.24	0.84	3.39E-01	below sensitivity
Q3T1J1	Eif5a	Eukaryotic translation initiation factor 5A-1	-1.10	0.47	1.54E-02	-1.36	0.39	1.44E-04	-0.89	0.54	6.12E-02	Mixed
A0A0G2K5	Gpx3	Glutathione peroxidase 3	0.76	1.69	3.82E-05	1.45	2.73	1.01E-07	-0.17	0.89	7.38E-01	SG & SC
P62959	Hint1	Histidine triad nucleotide-binding protein 1	-0.90	0.54	2.57E-02	-1.95	0.26	4.02E-04	-0.97	0.51	1.34E-01	Mixed
Q5XI38	Lcp1	Lymphocyte cytosolic protein 1	-0.66	0.63	1.43E-02	-0.58	0.67	4.17E-02	0.10	1.07	8.69E-01	SC >> SG
F1LMA7	Mrc2	C-type mannose receptor 2	-1.46	0.36	1.57E-07	-0.63	0.65	1.58E-02	-1.17	0.45	1.04E-01	SC & SG
A0A1W2Q6E	Msn	Moesin	-1.76	0.30	1.02E-04	-1.67	0.31	6.36E-04	0.14	1.10	8.91E-01	SG & SC
B1WC26	Nans	N-acetylneuraminate synthase	-0.92	0.53	5.81E-03	-1.20	0.44	1.77E-03	0.06	1.04	9.83E-01	SYT > SC, rST & SG
F1M9V7	Npepps	Aminopeptidase	-0.58	0.67	4.31E-03	-0.69	0.62	2.68E-02	-0.38	0.77	3.81E-01	SYT & rST > SC & SG
Q5RJN2	Pcolce	Procollagen C-endopeptidase enhancer 1	-1.43	0.37	1.65E-10	0.79	1.73	4.96E-04	-0.35	0.79	4.07E-01	SC >> SG
A0A0G2JSZ5	Pdia6	Protein disulfide-isomerase A6	-1.73	0.30	1.94E-08	-1.01	0.50	4.36E-03	-1.13	0.46	1.04E-01	Mixed
D3ZB30	Ptbp1	Polypyrimidine tract-binding protein 1	-0.98	0.51	1.64E-02	-1.16	0.45	1.30E-02	-0.91	0.53	1.12E-01	SG & SC > rST & SYT
P16975	Sparc	Secreted protein acidic and cysteine rich	-1.36	0.39	1.85E-11	-0.70	0.62	2.97E-02	-0.14	0.91	8.32E-01	SC > SG
P63029	Tpt1	Translationally-controlled tumor protein	-2.50	0.18	1.54E-02	-1.66	0.32	1.86E-02	-0.43	0.74	6.01E-01	SG & SC >rST & SYT
D3ZZC1	Txndc5	Thioredoxin domain-containing protein 5	-1.35	0.39	1.92E-02	-1.05	0.48	1.65E-02	-0.68	0.62	7.25E-01	SG & SC

Supp Table 3D. Total of 81 proteins with altered expression (up/down, p<0.05) at 8 weeks only following heat treatment.

			1 week			8 weeks			14 weeks			
Uniprot accession number	Gene name	Protein name	Log2 Heat / Control	Fold change Heat / Control	P-Value Heat / Control	Log2 Heat / Control	Fold change Heat / Control	P-Value Heat / Control	Log2 Heat / Control	Fold change Heat / Control	P-Value Heat / Control	Tubular origin
P50475	Aars	Alanine--tRNA ligase, cytoplasmic	-0.13	0.91	8.48E-01	-1.78	0.29	5.68E-06	-0.99	0.50	7.79E-02	Mixed
A0A0G2JSL8	Adk	Adenosine kinase	-0.79	0.58	6.22E-02	-1.53	0.35	2.30E-03	-0.61	0.66	3.36E-01	Mixed
Q02589	Adprh	[Protein ADP-ribosylarginine] hydrolase	-0.96	0.51	1.47E-01	-1.68	0.31	1.41E-02	-0.69	0.62	2.73E-01	SG, SC & SYT
F1M9N7	Agfg1	Arf-GAP domain and FG repeat-containing protein 1	-0.01	0.99	1.00E+00	-1.42	0.37	1.18E-03	-0.74	0.60	9.46E-01	Mixed
P62944	Ap2b1	AP-2 complex subunit beta	0.07	1.05	9.51E-01	-1.27	0.41	3.59E-02	-0.77	0.59	6.90E-01	SYT > rST > SC & SG
B0BNM1	Apoa1bp	NAD(P)H-hydrate epimerase	-1.09	0.47	5.05E-02	-1.11	0.46	7.26E-03	-1.01	0.50	4.29E-01	Mixed
Q6P6Q5	App	Amyloid beta A4 protein	-0.19	0.88	6.99E-01	-0.31	0.81	8.84E-03	-0.29	0.82	6.20E-01	SC > SG
Q6AZ50	Atg3	Ubiquitin-like-conjugating enzyme ATG3	–	–	–	-2.69	0.15	2.06E-03	–	–	–	Mixed
Q6P6G4	Bpgm	Phosphoglycerate mutase	-0.33	0.79	7.25E-01	-1.10	0.47	1.18E-03	–	–	–	Mixed
M0R8P3	Cabyr	Calcium-binding tyrosine phosphorylation-regulated	-2.08	0.24	6.27E-01	-2.20	0.22	3.66E-02	-2.02	0.25	1.18E-01	rST >> SYT
Q9WU49	Carhsp1	Calcium-regulated heat stable protein 1	-0.38	0.77	5.68E-01	-2.00	0.25	8.84E-03	-0.80	0.58	3.36E-01	SC
P43527	Casp1	Caspase-1	0.19	1.14	8.48E-01	-1.32	0.40	3.46E-02	_	_	_	below sensitivity
Q8CFN2	Cdc42	Cell division control protein 42 homolog	-0.50	0.71	3.54E-01	-1.73	0.30	2.15E-03	-0.38	0.77	6.90E-01	SC & SG >> SYT > rST
D3ZGK7	Ces1c	Carboxylic ester hydrolase	0.19	1.14	7.73E-01	3.88	14.69	2.36E-03	-0.41	0.75	7.31E-01	below sensitivity
Q4KM73	Cmpk1	UMP-CMP kinase	-0.07	0.95	8.93E-01	-1.13	0.46	1.18E-03	-0.64	0.64	3.62E-01	SG & SC
F1LR02	Col18a1	Collagen type 18 alpha 1 chain	-0.21	0.87	7.25E-01	1.26	2.39	1.88E-03	0.16	1.11	8.13E-01	SC & SG
G3V940	Coro1b	Coronin-1B	-0.47	0.72	4.97E-01	-1.28	0.41	1.56E-02	-0.02	0.99	1.00E+00	SYT > SC, rST & SG
G3V6M1	Cst12	Cystatin-12	0.29	1.22	9.51E-01	1.81	3.51	1.46E-03	-1.01	0.50	4.29E-01	SC
A0A0G2JZ13	Cttn	Src substrate cortactin	-0.41	0.75	5.63E-01	-1.47	0.36	1.18E-03	-0.51	0.70	5.26E-01	SG & SC
Q5U216	Ddx39a	ATP-dependent RNA helicase DDX39A	0.19	1.14	8.16E-01	-1.00	0.50	2.59E-02	-1.62	0.33	1.18E-01	SYT >> SC, rST & SG
F1LQD1	Ddx4	Probable ATP-dependent RNA helicase DDX4	-0.76	0.59	1.79E-01	-1.81	0.28	3.73E-04	-1.43	0.37	1.33E-01	below sensitivity
Q5M9H7	Dnaja2	DnaJ homolog subfamily A member 2	-0.35	0.79	7.28E-01	-1.17	0.44	2.97E-02	-1.07	0.48	1.09E-01	Mixed
A0A0G2K2	Efemp2	EGF-containing fibulin extracellular matrix protein 2	-0.34	0.79	5.03E-01	0.61	1.52	2.54E-02	-0.71	0.61	9.98E-02	SG > SC
P81795	Eif2s3	Eukaryotic translation initiation factor 2 subunit 3	-0.17	0.89	8.16E-01	-1.21	0.43	3.06E-02	0.18	1.13	8.46E-01	SG & SC
B5DF91	Elavl1	ELAV-like protein	0.09	1.06	9.31E-01	-1.27	0.42	1.08E-02	-0.97	0.51	3.06E-01	SG > SC > SYT
B0BNE5	Esd	S-formylglutathione hydrolase	-0.65	0.64	9.58E-02	-2.79	0.14	2.66E-07	-0.53	0.69	4.27E-01	SC & SG > rST
A0A0G2JSY3	Fam221a	Protein FAM221A	-0.37	0.77	6.27E-01	-1.46	0.36	2.63E-02	-1.19	0.44	3.06E-01	SYT >> rST
P19468	Gclc	Glutamate--cysteine ligase catalytic subunit	-0.23	0.85	7.73E-01	-1.48	0.36	4.36E-03	-0.62	0.65	7.31E-01	SG > SC
P48508	Gclm	Glutamate--cysteine ligase regulatory subunit	-0.16	0.90	9.31E-01	-1.16	0.45	2.28E-02	-1.70	0.31	5.80E-01	SYT > SC, rST & SG
Q63228	Gmfb	Glia maturation factor beta	-0.41	0.75	7.62E-01	-1.86	0.28	5.05E-03	-1.25	0.42	1.18E-01	rST & SYT > SC & SG
D3ZHC4	Hebp2	Heme binding protein 2	0.15	1.11	9.51E-01	-1.15	0.45	8.84E-03	-0.03	0.98	9.46E-01	SC
A0A096MJ	Hmcn1	Hemicentin 1	-1.63	0.32	7.45E-02	4.10	17.14	3.66E-02	–	–	–	below sensitivity
F1LQ48	Hnrnpl	Heterogeneous nuclear ribonucleoprotein L	-0.75	0.60	2.02E-01	-1.50	0.35	1.29E-03	-1.17	0.44	6.29E-02	SC &SG > SYT >> rST
P52759	Hrsp12	Ribonuclease UK114	0.37	1.29	4.22E-01	-1.52	0.35	2.63E-02	–	–	–	SG > SC
Q925N6	Igsf1	Immunoglobulin superfamily member 1	0.66	1.58	8.36E-02	1.55	2.93	6.69E-03	-0.58	0.67	2.69E-01	SC
Q5RJK6	Inpp1	Inositol polyphosphate-1-phosphatase	-0.95	0.52	1.24E-01	-1.65	0.32	1.65E-04	-0.21	0.87	8.46E-01	rST
Q6P0K8	Jup	Junction plakoglobin	-1.25	0.42	9.10E-02	3.32	10.00	3.00E-07	–	–	–	SC >> rST & SG
F1LR10	Lima1	LIM domain and actin-binding protein 1	-0.58	0.67	4.22E-01	-1.73	0.30	3.72E-03	-0.25	0.84	7.08E-01	SC & SG

F1M8E9	Lyz2	Lysozyme	-0.48	0.72	3.98E-01	1.35	2.55	2.15E-03	-0.35	0.78	5.26E-01	rST
Q66HR2	Mapre1	Microtubule-associated protein RP/EB family member 1	-0.52	0.70	4.04E-01	-1.55	0.34	2.60E-04	-1.17	0.44	6.86E-02	SC & SG >> SYT > rST
Q6P688	Mat2a	S-adenosylmethionine synthase	-0.01	1.00	1.00E+00	-1.50	0.35	3.46E-02	-1.25	0.42	6.84E-02	SG & SC > SYT
A0A0G2JV28	Mea1	Male-enhanced antigen 1	0.68	1.60	6.27E-01	-1.22	0.43	5.87E-03	–	–	–	**rST & SYT >>** SG & SC
P97532	Mpst	3-mercaptopyruvate sulfurtransferase	-0.38	0.77	6.64E-01	-1.06	0.48	1.18E-03	-1.15	0.45	7.90E-02	SG & SC
G3V6S5	Mthfd1	C-1-tetrahydrofolate synthase	-0.01	0.99	1.00E+00	-0.96	0.51	4.41E-02	-1.12	0.46	4.24E-01	SG > SC
P20767	N/A	Ig lambda-2 chain C region	0.51	1.43	7.45E-02	0.74	1.67	6.36E-04	-0.27	0.83	5.91E-01	rST
Q6AYP7	Nt5c3b	7-methylguanosine phosphate-specific 5-nucleotidase	-0.33	0.79	5.59E-01	-0.86	0.55	4.14E-02	-0.09	0.94	9.21E-01	rST & SC > SG > SYT
G3V8R1	Nucb2	Nucleobindin-2;Nesfatin-1	-0.25	0.84	7.78E-01	-1.22	0.43	1.65E-02	-0.57	0.67	4.29E-01	SC > SYT & SG
Q64303	Pak2	Serine/threonine-protein kinase PAK 2	-0.79	0.58	7.60E-02	-1.46	0.36	1.39E-03	-0.80	0.57	6.23E-02	SC & SG > SYT
Q6AY48	Pcbp3	Poly(rC)-binding protein 3	-0.34	0.79	5.15E-01	-1.11	0.46	4.84E-02	–	–	–	SYT > rST
Q62785	Pdap1	28 kDa heat- and acid-stable phosphoprotein	-0.02	0.99	1.00E+00	-1.24	0.42	2.06E-03	-1.31	0.40	6.84E-02	Mixed
A0A0G2JSM1	Pdlim3	PDZ and LIM domain protein 3	-1.43	0.37	1.48E-01	-1.67	0.31	5.57E-03	-0.13	0.91	9.46E-01	SG & SC
Q5M7T7	Pla2g7	Platelet-activating factor acetylhydrolase	0.36	1.28	2.55E-01	1.54	2.91	4.11E-04	-0.54	0.69	1.50E-01	Mixed
B5DF46	Pmm2	Phosphomannomutase	-0.54	0.69	6.27E-01	-1.45	0.37	1.99E-04	-1.23	0.43	8.81E-02	SYT > SG, rST & SC
O88794	Pnpo	Pyridoxine-5-phosphate oxidase	-0.22	0.86	8.48E-01	-1.11	0.46	1.86E-02	-0.23	0.85	9.23E-01	SC & SG
Q6DGG0	Ppid	Peptidyl-prolyl cis-trans isomerase D	-0.50	0.71	3.54E-01	-0.66	0.63	3.59E-02	-0.25	0.84	7.98E-01	SG >> SYT & SC > rST
Q642F2	Ppm1b	Protein phosphatase 1B	-0.60	0.66	1.79E-01	-1.62	0.33	1.50E-04	-1.32	0.40	6.12E-02	SC, SG & SYT
A0A0G2K405	Prkar2a	cAMP-dependent protein kinase type II-alpha regulatory	0.06	1.04	9.63E-01	-1.16	0.45	1.02E-02	-1.00	0.50	4.29E-01	rST
F1LP82	Rab2a	Ras-related protein Rab-2A	-0.49	0.71	1.60E-01	-1.28	0.41	5.79E-03	-0.47	0.72	6.90E-01	Mixed
Q4KMA2	Rad23b	UV excision repair protein RAD23 homolog B	-0.67	0.63	1.79E-01	-1.34	0.39	1.02E-02	-0.89	0.54	8.81E-02	SC & SG >> rST & SYT
E9PT65	Rdx	Radixin	-0.24	0.85	7.51E-01	-1.39	0.38	4.57E-02	-1.02	0.49	4.29E-01	SYT & rST >> SC & SG
D3ZHA7	RGD156033	Similar to Myosin light chain 1 slow a	0.40	1.32	6.27E-01	-1.35	0.39	1.62E-03	-2.63	0.16	4.29E-01	Unavailable data
Q6AYT3	Rtcb	tRNA-splicing ligase RtcB homolog	0.19	1.14	9.07E-01	-1.42	0.37	2.21E-02	-0.70	0.62	1.71E-01	SG & SC > SYT > rST
Q6AY18	Sar1a	GTP-binding protein SAR1a	-0.97	0.51	2.55E-01	-1.98	0.25	4.95E-02	-0.61	0.66	5.53E-01	**SC & SG >>** rST & SYT
A0A0G2JTU6	Sbp	Prostatic spermine-binding protein	-0.73	0.60	7.56E-01	-3.69	0.08	2.63E-02	–	–	–	below sensitivity
A0A0G2K0X5	Sec31a	Protein transport protein Sec31A	-0.28	0.83	4.97E-01	-1.09		4.36E-04	-0.65	0.64	9.73E-02	Mixed
Q9QZR6	Sept9	Septin-9	0.28	1.21	6.56E-01	-0.89	0.54	3.73E-02	-0.72	0.61	1.07E-01	SC & SG
Q6TXG7	Shmt1	Serine hydroxymethyltransferase	0.12	1.09	8.85E-01	-2.52	0.17	4.53E-10	-0.94	0.52	3.06E-01	SYT > SC & SG
Q64298	Smcp	Sperm mitochondrial-associated cysteine-rich protein	0.31	1.24	7.71E-01	-2.11	0.23	9.32E-04	-1.97	0.26	9.24E-02	rST >> SYT
P52631	Stat3	Signal transducer and activator of transcription 3	-0.11	0.93	8.76E-01	-1.06	0.48	1.86E-02	-0.67	0.63	5.39E-01	SG > SC
B0BN85	Sugt1	Suppressor of G2 allele of SKP1 homolog	-0.70	0.62	4.81E-01	-1.93	0.26	5.62E-06	-1.26	0.42	3.00E-01	Mixed
P17988	Sult1a1	Sulfotransferase 1A1	0.07	1.05	9.60E-01	-1.65	0.32	3.49E-05	-0.38	0.77	7.04E-01	Interstitial cell
Q2LAP6	Tes	Testin	-0.43	0.74	7.56E-01	-1.08	0.47	4.84E-02	–	–	–	SC / rST & SC >> SG & SYT
P30120	Timp1	Metalloproteinase inhibitor 1	0.06	1.04	9.63E-01	1.45	2.73	4.36E-03	-0.03	0.98	9.46E-01	SG > SC
Q6PCT3	Tpd52l2	Tumor protein D54	-0.08	0.95	9.63E-01	-1.11	0.46	4.95E-02	-1.41	0.38	5.80E-01	rST & SG > SC
Q5RJR2	Twf1	Twinfilin-1	-0.39	0.76	5.33E-01	-1.05	0.48	3.05E-02	-0.12	0.92	9.23E-01	SC > SG >rST & SYT
P11232	Txn	Thioredoxin	-0.19	0.88	8.88E-01	-1.66	0.32	2.36E-03	-0.98	0.51	4.29E-01	SC & SG
A0A0G2K737	Txnl1	Thioredoxin-like protein 1	-0.28	0.82	6.46E-01	-1.12	0.46	4.23E-03	-0.37	0.77	6.10E-01	SG > SC > SYT & rST
D4A8H3	Uba6	Ubiquitin-like modifier-activating enzyme 6	0.06	1.04	9.63E-01	-1.26	0.42	3.73E-05	0.19	1.14	8.37E-01	SC > SG
Q3B7D1	Ube2z	Ubiquitin-conjugating enzyme E2 Z	-0.47	0.72	8.88E-01	-1.90	0.27	3.66E-02	–	–	–	SG & SC >> rST & SYT
A0A0H2UH96	Vwa5a	von Willebrand factor A domain-containing protein 5A	0.20	1.15	8.16E-01	-1.23	0.43	1.41E-03	-0.71	0.61	1.20E-01	SC & SG
D4A7U1	Zyx	Zyxin	-0.25	0.84	6.47E-01	-1.01	0.50	3.71E-02	-0.34	0.79	4.81E-01	SC & SG

Supp Table 3E. Total of 53 proteins with altered expression (up/down, p<0.05) at 8 and 14 weeks following heat treatment.

			1 week			8 weeks			14 weeks			
Uniprot accession number	**Gene name**	**Protein name**	**Log2 Heat / Control**	**Fold change Heat / Control**	**P-Value Heat / Control**	**Log2 Heat / Control**	**Fold change Heat / Control**	**P-Value Heat / Control**	**Log2 Heat / Control**	**Fold change Heat / Control**	**P-Value Heat / Control**	**Tubular origin**
Q5QD51	Akap12	A-kinase anchor protein 12	-0.36	0.78	5.26E-01	-1.90	0.27	3.44E-04	-1.50	0.35	3.95E-03	rST > SYT >> SG > SC
Q64057	Aldh7a1	Alpha-aminoadipic semialdehyde dehydrogenase	-0.35	0.79	4.56E-01	-1.02	0.49	3.95E-03	-1.04	0.49	4.18E-02	SC & SG
A0A0G2K7X0	Anp32a	Acidic leucine-rich nuclear phosphoprotein 32 family member A	1.82	3.54	9.69E-02	-3.22	0.11	7.00E-04	-4.02	0.06	1.86E-03	SG & SC
P49088	Asns	Asparagine synthetase [glutamine-hydrolyzing]	0.11	1.08	8.88E-01	-1.01	0.50	2.05E-03	-1.98	0.25	3.52E-03	rST & SG & SC
P09034	Ass1	Argininosuccinate synthase	0.40	1.32	2.92E-01	-1.60	0.33	4.53E-10	-1.82	0.28	3.16E-05	Interstitial cell
Q68FX6	Cabs1	Calcium-binding and spermatid-specific protein 1	0.17	1.12	8.64E-01	-3.00	0.13	5.54E-10	-2.62	0.16	3.19E-05	**rST >>** SYT
Q68FS2	Cops4	COP9 signalosome complex subunit 4	-0.02	0.99	1.00E+00	-1.02	0.49	1.69E-03	-1.23	0.43	4.16E-03	SYT & rST >> SC & SG
Q4KLZ3	Dazap1	DAZ associated protein 1	-0.08	0.95	9.63E-01	-1.38	0.39	1.32E-02	-1.55	0.34	1.72E-02	SYT > SG & rST > SC
P56702	Dbil5	Diazepam-binding inhibitor-like 5	0.63	1.54	2.55E-01	-2.16	0.22	3.59E-02	-3.66	0.08	2.40E-03	rST >> SYT
Q63413	Ddx39b	Spliceosome RNA helicase Ddx39b	-0.73	0.60	7.45E-02	-1.15	0.45	8.70E-03	-1.64	0.32	9.78E-03	SG > SC > SYT > rST
B5DEN5	Eef1b2	Elongation factor 1-beta 2	-0.27	0.83	8.14E-01	-1.53	0.35	1.88E-03	-1.90	0.27	9.95E-03	Mixed
P55054	Fabp9	Fatty acid-binding protein 9	-0.62	0.65	2.08E-01	-2.13	0.23	3.14E-03	-2.81	0.14	1.03E-04	SYT & rST
C0JPT7	Flna	Filamin A	-0.29	0.82	1.80E-01	-2.01	0.25	2.72E-18	-1.78	0.29	5.84E-09	**SC & SG >>** rST
A0A140TAJ3	Fubp1	Far upstream element-binding protein 1	0.18	1.13	7.73E-01	-0.89	0.54	4.15E-02	-1.17	0.44	2.75E-02	Mixed
Q9JLZ1	Glrx3	Glutaredoxin-3	-0.02	0.98	1.00E+00	-1.63	0.32	2.21E-03	-1.42	0.37	1.99E-03	SYT & rST > SC & SG
Q9Z1B2	Gstm5	Glutathione S-transferase Mu 5	0.14	1.10	8.88E-01	-1.31	0.40	8.94E-04	-1.84	0.28	1.87E-04	rST & SYT >> SG & SC
D3ZCR3	Hmgb1	High mobility group protein B1 pseudogene	0.68	1.60	3.22E-01	-2.13	0.23	1.39E-04	-1.86	0.28	1.10E-02	SG & SC
Q794E4	Hnrnpf	Heterogeneous nuclear ribonucleoprotein F	-0.28	0.83	6.27E-01	-1.28	0.41	5.12E-04	-1.84	0.28	4.26E-02	Mixed
P14659	Hspa2	Heat shock-related 70 kDa protein 2	-0.45	0.73	3.80E-01	-1.93	0.26	1.85E-06	-2.79	0.14	7.39E-07	SYT & rST
F7F2F3	Hspa4l	Heat shock 70 kDa protein 4L	0.28	1.22	5.22E-01	-2.75	0.15	3.10E-13	-4.02	0.06	4.06E-13	SYT >> SC & rST
D4A781	Ipo5	Importin 5	-0.01	1.00	1.00E+00	-0.88	0.54	2.86E-04	-2.02	0.25	7.70E-11	rST >> SYT & SG > SC
Q6AYK3	Isyna1	Inositol-3-phosphate synthase 1	-0.15	0.90	7.49E-01	-0.85	0.55	7.27E-03	-1.21	0.43	1.60E-03	**SYT & rST >>** SC & SG
M0R961	Khsrp	Far upstream element-binding protein 2	0.02	1.02	9.63E-01	-1.20	0.44	7.22E-06	-0.98	0.51	1.37E-03	Mixed
G3V7B2	Lrrc46	Leucine-rich repeat-containing protein 46	-0.11	0.93	9.63E-01	-1.38	0.39	1.56E-02	-2.51	0.18	6.64E-04	SYT & rST
Q562C6	Lztfl1	Leucine zipper transcription factor-like protein 1	-0.46	0.73	5.59E-01	-1.65	0.32	1.39E-03	-1.68	0.31	2.85E-02	SYT & rST >> SC & SG
F1LRL9	Map1b	Microtubule-associated protein 1B	0.23	1.17	6.98E-01	-1.71	0.31	1.27E-07	-0.89	0.54	2.88E-02	SC & SG
G3V6H9	Nap1l1	Nucleosome assembly protein 1-like 1	-0.53	0.69	3.02E-01	-1.36	0.39	1.98E-03	-1.40	0.38	6.73E-04	SG > SC & SYT >> rST/
Q66HD3	Nasp	Nuclear autoantigenic sperm protein	-0.61	0.65	3.60E-01	-1.59	0.33	2.94E-05	-1.84	0.28	1.99E-03	SYT > rST >> SC & SG
G3V700	Nrd1	Nardilysin	0.74	1.67	1.98E-01	-1.95	0.26	3.30E-05	-2.57	0.17	1.48E-06	rST > **SYT >>** SC & SG
B5DF80	Pabpc6	Polyadenylate-binding protein	-0.43	0.74	8.16E-01	-2.35	0.20	1.50E-02	-2.75	0.15	2.29E-03	Unavailable data
A0A140TAA4	Pdcd6ip	Programmed cell death 6-interacting protein	-0.35	0.79	4.22E-01	-1.64	0.32	1.36E-05	-1.10	0.47	5.64E-04	SC > SG > rST & SYT
P47860	Pfkp	ATP-dependent 6-phosphofructokinase, platelet type	0.18	1.13	7.73E-01	-0.94	0.52	3.14E-02	-1.64	0.32	3.95E-04	SYT & SG > SC & rST
D3ZDK7	Pgp	Glycerol-3-phosphate phosphatase	-0.03	0.98	9.99E-01	-1.60	0.33	7.14E-05	-3.22	0.11	3.58E-10	**SYT & rST >>** SC &
F7EPH4	Ppa1	Pyrophosphatase (inorganic) 1	-0.50	0.71	2.18E-01	-1.85	0.28	1.71E-06	-1.09	0.47	3.95E-03	**SC & SG >>** rST & SYT
P63331	Ppp2ca	Serine/threonine-protein phosphatase 2A catalytic subunit alpha	0.02	1.01	9.91E-01	-0.88	0.54	2.04E-02	-1.08	0.47	3.48E-02	SG > SC
P53042	Ppp5c	Serine/threonine-protein phosphatase 5	0.01	1.00	1.00E+00	-1.08	0.47	1.53E-02	-1.39	0.38	2.85E-02	SYT > SG & rST & SC
P40112	Psmb3	Proteasome subunit beta type-3	-0.35	0.78	5.80E-01	1.03	2.04	6.52E-03	-1.48	0.36	4.61E-03	SC & SG >> rST & SYT
P83868	Ptges3	Prostaglandin E synthase 3	0.35	1.27	7.66E-01	-1.85	0.28	1.50E-04	-2.35	0.20	5.00E-04	Mixed
P41499	Ptpn11	Tyrosine-protein phosphatase non-receptor type 11	0.33	1.26	6.21E-01	-1.49	0.36	2.53E-06	-1.44	0.37	2.12E-03	below sensitivity
E2RUH2	Rnh1	Ribonuclease inhibitor	-0.36	0.78	4.22E-01	-1.28	0.41	5.37E-05	-1.26	0.42	3.19E-03	SG & SC >> SYT
A0A0G2JZG7	Sars	Serine--tRNA ligase, cytoplasmic	0.01	1.01	1.00E+00	-1.29	0.41	6.69E-03	-1.92	0.26	3.67E-03	Mixed
A0A0G2JS	Set	Protein SET	-0.96	0.51	3.64E-01	-1.74	0.30	2.04E-02	-2.21	0.22	2.67E-03	Mixed

F1LSR7	Spata20	Spermatogenesis-associated protein 20	0.17	1.12	7.73E-01	-1.83	0.28	2.18E-07	-2.51	0.18	1.38E-08	**rST>>** SYT
A0A0G2JZ	Sptbn1	Spectrin beta chain, non-erythrocytic 1	0.02	1.01	9.93E-01	-0.96	0.51	1.24E-04	-1.46	0.36	1.39E-05	SG & SC > SYT & rST
O35814	Stip1	Stress-induced-phosphoprotein 1	-0.35	0.78	4.22E-01	-1.33	0.40	9.35E-04	-2.03	0.24	2.13E-03	Mixed
G3V762	Tsta3	Tissue specific transplantation antigen P35B	0.24	1.18	8.17E-01	-2.08	0.24	8.25E-04	-1.74	0.30	3.41E-02	SYT & rST >> SC & SG
D4A1Q9	Ttll12	Tubulin tyrosine ligase-like 12	-0.34	0.79	5.28E-01	-1.12	0.46	3.89E-03	-1.20	0.43	2.48E-02	SC >> SYT, rST & SG
Q68FR8	Tuba3a	Tubulin alpha-3 chain	-0.29	0.82	9.58E-01	-1.61	0.33	1.90E-02	-3.31	0.10	2.50E-02	SC > SG > rST >> SYT
D4ABI6	Uchl3	Ubiquitin carboxyl-terminal hydrolase isozyme L3	0.05	1.04	9.63E-01	-1.33	0.40	2.46E-04	-1.39	0.38	9.34E-04	Mixed
F8WFH8	Wars	Tryptophan--tRNA ligase, cytoplasmic	-0.17	0.89	6.98E-01	-1.46	0.36	2.13E-04	-1.20	0.43	2.18E-03	Mixed
A0A0G2JV	Xpnpep1	Xaa-Pro aminopeptidase 1	-0.41	0.75	1.35E-01	-1.54	0.34	8.85E-10	-1.48	0.36	2.89E-06	rST & SC > SYT & SG
D4A3P0	Ybx2	Y box-binding protein 2	-0.67	0.63	3.22E-01	-2.83	0.14	1.85E-06	-2.87	0.14	3.16E-05	SYT & rST
P68511	Ywhah	14-3-3 protein eta	0.51	1.42	6.44E-01	-1.63	0.32	2.91E-03	-2.02	0.25	1.85E-02	SC & SG >> SYT

Supp Table 3F. Total of 17 proteins with altered expression (up/down, p<0.05) at 14 weeks only following heat treatment.

			1 week			8 weeks			14 weeks			
Uniprot accession number	**Gene name**	**Protein name**	**Log2 Heat / Control**	**Fold change Heat / Control**	**P-Value Heat / Control**	**Log2 Heat / Control**	**Fold change Heat / Control**	**P-Value Heat / Control**	**Log2 Heat / Control**	**Fold change Heat / Control**	**P-Value Heat / Control**	**Tubular origin**
F8WG67	Acot7	Cytosolic acyl coenzyme A thioester hydrolase	-1.10	0.47	3.46E-01	-0.29	0.82	9.87E-01	-1.36	0.39	3.48E-02	rST & SYT
P06214	Alad	Delta-aminolevulinic acid dehydratase	-0.07	0.95	9.63E-01	-0.72	0.61	1.24E-01	-0.76	0.59	2.57E-02	SC > SG
Q6MG49	Bag6	Large proline-rich protein BAG6	-0.68	0.63	3.54E-01	-0.69	0.62	2.79E-01	-2.44	0.18	7.63E-03	rST & SYT > SC & SG
Q5XIM9	Cct2	T-complex protein 1 subunit beta	-0.66	0.63	2.65E-01	-0.51	0.70	2.90E-01	-2.56	0.17	9.35E-03	Mixed
Q7TPB1	Cct4	T-complex protein 1 subunit delta	-0.54	0.69	3.80E-01	-0.60	0.66	2.69E-01	-1.17	0.44	4.23E-04	SYT >> SC, SG & rST
F1M779	Cltc	Clathrin heavy chain;Clathrin heavy chain 1	-0.28	0.83	5.57E-01	-0.02	0.99	9.87E-01	-1.24	0.42	2.67E-02	below sensitivity
G3V7G8	Gars	Glycine--tRNA ligase	-0.69	0.62	1.47E-01	-0.85	0.55	1.13E-01	-1.47	0.36	2.03E-02	SC & SG > rST > SYT
F2Z3Q8	Kpnb1	Importin subunit beta-1	-0.50	0.71	4.22E-01	-0.19	0.88	7.74E-01	-1.64	0.32	4.28E-06	SG & SC
O70177	LOC100365112	Carboxylic ester hydrolase	1.20	2.29	5.15E-01	1.19	2.28	4.80E-01	-1.41	0.38	1.41E-02	SYT >> SC, SG & rST
F1M3H8	LOC681410	Hypothetical protein	-0.56	0.68	1.80E-01	-1.03	0.49	5.54E-02	-1.21	0.43	2.40E-03	Unavailable data
G3V617	Mapk14	Mitogen-activated protein kinase 14	0.84	1.79	5.63E-01	0.53	1.45	6.69E-01	-3.54	0.09	1.71E-02	SC & SG
Q5U328	Ncl	Nucleolin	–	–	–	-1.85	0.28	4.80E-01	-2.36	0.20	4.05E-03	SG > SC >> SYT > rST
A0A0G2K911	Nsfl1c	NSFL1 cofactor p47	-0.28	0.82	6.01E-01	-0.56	0.68	9.03E-02	-1.30	0.41	6.43E-05	Mixed
D3ZSC2	Pdcd2l	Programmed cell death 2-like	-0.67	0.63	6.27E-01	-3.06	0.12	7.84E-02	-2.01	0.25	1.72E-02	SYT > rST
P17220	Psma2	Proteasome subunit alpha type-2	-0.53	0.69	1.26E-01	0.71	1.63	7.16E-02	-1.42	0.37	1.37E-02	SG & SC > SYT > rST
G3V8U9	Psmb4	Proteasome subunit beta type-4	-0.33	0.80	4.33E-01	0.30	1.23	4.72E-01	-1.10	0.47	9.43E-03	Mixed
G3V6W6	Psmc6	26S protease regulatory subunit 10B	-0.12	0.92	8.30E-01	-0.39	0.77	3.08E-01	-2.16	0.22	1.13E-02	SG > SC

Yellow cells:	Proteins that are changed (up/down) with p < 0.05.
Green cells:	Proteins that are unchanged or changed with p > 0.05.

Column explanations

Uniprot accession number: First, or leading, protein ID annotation in UniProtKB/Swiss-Prot Rattus norvegicus database (Nov 2018).

Gene symbol: Leading gene symbol in UniProtKB/Swiss-Prot Rattus norvegicus database (Nov 2018).

Protein name: Protein name from the UniProtKB/Swiss-Prot Rattus norvegicus database (Nov 2018).

Log2 Heat/Control: Log2 ratio of protein abundance in heat-treated rats/control rats.

Fold change Heat/Control: Linear ratio of protein abundance in heat-treated rats/control rats.

P-Value Heat/Control: p value of difference in protein abundance between heat-treated and control rats.

Tubular origin: Microarray dataset published by Chalmel et al 2007, PNAS, 104(20):8346. Data accessed via www.germonline.org

Note

Cell specificity: cell IDs are done by mRNA of purified cell types via Germonline.

'Mixed': indicates almost equal expression by all geminal epithelial cells.

'below sensitivity': indicates below detection limits.

‘>’: indicates expression greater than 2-fold, but less than 4-fold different to the next cell type.

‘>>’: indicates expression greater than 4-fold compared with next cell type.

Bold text and '>>': indicates 10-fold higher expression than next cell type.

‘&’: indicates expression differences between cell types is less than 2-fold.

'/': indicates another pattern of cell expression

Abbreviations	
SC	Sertoli cell
SG	Spermatogonia
SYT	Spermatocytes
rST	round spermatid

4. Chapter 4:

Experimental cryptorchidism causes chronic inflammation and a progressive decline in Sertoli cell and Leydig cell function in the adult rat testis

Manuscript prepared for submission to *Andrology*

DECLARATION FOR THESIS CHAPTER

Declaration by candidate

In the case of Chapter 4, the nature and extent of my contribution to the work was the following:

Nature of contribution	**Extent of contribution (%)**
Experimental design, performing experiments, data analysis, drafting of manuscript.	85%

The following co-authors contributed to the work. If co-authors are students at Monash University, the extent of their contribution in percentage terms must be stated:

Name	**Nature of contribution**	**Extent of contribution for student co-authors only (%)**
Peter Stanton	Drafting the manuscript	NA
Helen Ludlow	Assisted with experiments	NA
David de Kretser	Drafting of manuscript and intellectual input	NA
Mark Hedger	Drafting of manuscript and intellectual input	NA

The undersigned hereby certify that the above declaration correctly reflects the nature and extent of the candidate's and co-authors' contributions to this work*.

Candidate`s Signature		Date: 10/5/2019

Main Supervisor`s Signature		Date: 10/5/2019

*Note: Where the responsible author is not the candidate's main supervisor, the main supervisor should consult with the responsible author to agree on the respective contributions of the authors.

Experimental cryptorchidism causes chronic inflammation and a progressive decline in Sertoli cell and Leydig cell function in the adult rat testis

Rashid A Aldahhan[a,b,c*], Peter G Stanton[a,b], Helen Ludlow[d], David M de Kretser[a,b] and Mark P Hedger[a,b]

[a]Centre for Reproductive Health, Hudson Institute of Medical Research, Clayton, Victoria, Australia

[b]Department of Molecular and Translational Sciences, Monash University, Clayton, Victoria, Australia

[c]Department of Anatomy, College of Medicine, Imam Abdulrahman Bin Faisal University, Dammam, Saudi Arabia

[d]Oxford Brookes University, Oxford, U.K

Abstract

Cryptorchidism disrupts testicular function, leading to spermatogenic failure, fibrosis and accumulation of fluid in the testis, and reduced serum androgens. However, the molecular effects of cryptorchidism on Sertoli cell and Leydig cell function are less well defined. Cryptorchidism was surgically induced in adult rats for 7 and 14 weeks. Testis weights decreased to 40% of normal within 7 weeks, due to loss of all developing spermatogenic cells, except spermatogonia, but did not decrease further at 14 weeks. This decrease was accompanied by progressive fluid accumulation and peritubular fibrosis. Serum FSH and LH increased, consistent with the loss of feedback by inhibin and testosterone. This damage coincided with a progressive decline of several critical Sertoli cell genes [*Sox9*, *Inha* (inhbin α-subunit)*, Cldn11* (claudin 11), *Gja1* (connexin 43) and *Il1a* (interleukin-1α)] and the crucial Leydig cell steroidogenic enzymes, *Cyp11a1*, *Hsd3b1* and *Hs17b3*. Activin A was largely unaffected at any time-point, but activin B and the activin-binding protein, follistatin, also declined. In contrast, expression of genes involved in inflammation (*Tnf, Il10, Il1b, Mcp1*) and fibrosis (*Acta2*, *Col1a1*) were strongly elevated. These data indicate that depletion of the germinal epithelium by induction of experimental cryptorchidism in the adult rat causes chronic inflammation, oedema and fibrosis, and is followed by a progressive decline of Sertoli and Leydig cell gene expression and function.

Key words:

Spermatogenesis – Cryptorchidism – Sertoli cell - Activins – Steroidogenesis

Introduction

The testes originate in the abdomen, but descend during foetal or neonatal life into the scrotum. This allows the intratesticular temperature to be maintained at 2–7°C below the core body temperature to ensure the production of normal sperm (Harrison and Weiner, 1949; Mieusset and Bujan, 1995). Failure of the testis to descend, a pathological condition known as cryptorchidism, is one of the most common congenital anomalies reported in 2–4% of male births (Fantasia et al., 2015). This condition is a known risk factor for infertility and testis cancer (Fantasia et al., 2015), hence surgical intervention to translocate the testis into the scrotum is recommended within the first year after birth (Schneuer et al., 2016).

Cryptorchidism, whether pathological or induced experimentally, causes extensive damage to the seminiferous epithelium by arresting spermatogonial differentiation and inducing the death of post-and meiotic germ cells, followed by increased peritubular fibrosis (Agoulnik et al., 2012). The effects also extend to the supporting Sertoli cells, which show several physiological changes such as the accumulation of lipid droplets, secretion of excessive seminiferous tubule fluid, and reduced androgen-binding protein and inhibin production (Hagenas and Ritzen, 1976; Kerr et al., 1979b; Ren et al., 2006). Other changes include Leydig cell hypertrophy and elevated levels of serum LH, but low to normal serum testosterone levels, indicating a state of compensatory pituitary gland stimulation, that accompany tubular damage, as well as alterations in blood flow and vascular permeability (Bergh et al., 1984b; Risbridger et al., 1981b). The effects of experimental cryptorchidism studies on inhibin suggests that the activins, which are structurally and functionally related to inhibin, may also be affected. The response of the activins to cryptorchidism can now be investigated due to the development of specific assays for these proteins (Knight, 1996; Ludlow et al., 2009; O'Connor et al., 1999).

Activins A and B are homodimers of the inhibin β-subunits (β_A and β_B) that stimulate FSH secretion by paracrine and/or autocrine interactions with inhibin in the pituitary gland (Hedger et al., 2011; Wijayarathna and de Kretser, 2016). However, the activins are also implicated in the local regulation of testis function; for example, activin A plays a crucial role in the development of male

germ cells and Sertoli cells (Barakat et al., 2012; Meehan et al., 2000). In the adult testis, activin A is implicated in regulating the production of spermatogonial stem cells and spermatocytes and the development of Sertoli cell tight junctions required for restructuring of the seminiferous epithelium, particularly at stages VIII to XI of the rat spermatogenic cycle immediately after spermiation (Nicholls et al., 2012; Okuma et al., 2006). Crucially, activin A is a key regulator of inflammation and immunity and has both pro- and anti- inflammatory actions, depending on the maturity of the immune response (Gasinska and Hill, 1989; Hedger et al., 2011; Jones et al., 2007). Activin A is also an essential mediator of fibrosis, by regulating fibroblast development and differentiation into myofibroblasts (Hedger et al., 1989; Ohga et al., 1996; Ota et al., 2003; Yamashita et al., 2004). The bioactivity of the activins is controlled by two different proteins: inhibin and the activin-binding protein, follistatin (Barakat et al., 2012). In contrast to activin A, the roles of activin B in the regulation of testis function or immunity are poorly described.

Studies on the exact pathogenesis of cryptorchidism in boys plus experimental cryptorchid animal models have indicated the involvement of inflammatory and oxidative stress responses, which are known to have temporary or even permanent effects on male fertility due to spermatogenic damage (Ahotupa and Huhtaniemi, 1992; Hedger and Meinhardt, 2003; Houston et al., 2018; Imamoğlu et al., 2012). Imamoğlu et al (2012) found higher serum interleukin-6 (IL-6) levels in cryptorchid boys than in a control group, and markedly higher serum IL-6 in bilaterally cryptorchid- versus unilaterally cryptorchid- subjects, indicating that an inflammatory response may be another risk factor present in cryptorchid patients. Nevertheless, serum IL-6 is not a definitive marker of intratesticular inflammation, and the response of other key proinflammatory cytokines that would confirm the presence of inflammation in cryptorchidism is required.

In the present study, we hypothesised that experimental cryptorchidism causes chronic inflammation and a progressive decline in Sertoli cell and Leydig cell function in the adult rat testis. Therefore, the aim of this study was to investigate the effects of extended experimental cryptorchidism on the expression of key functional genes in Sertoli and Leydig cells, and the response of the activins and other inflammatory regulators.

Materials and Methods

Animals

Adult male outbred Sprague-Dawley rats obtained from Monash Animal Services (Monash University, Clayton, Australia) were maintained at 20°C in a fixed 12-h light, 12-h dark cycle with free access to food and water. Rats (approximately 10 weeks old) were divided into two groups: control and cryptorchid. Bilateral cryptorchidism was induced surgically by translocating the testes into the abdomen, as previously described (Kerr et al., 1979b). Briefly, rats were anaesthetised with isoflurane and the testes exposed via an incision in the inguinal canal. The distal gubernaculum was cut and the testes were transferred through the inguinal canal into the abdomen which was then closed with a suture to prevent the re-descent of the testis into the scrotum. Control rats underwent the same procedure without translocation of the testis or closure of the inguinal canal (sham-operated)**.** Control and cryptorchid rats were killed for evaluation at 7 weeks and 14 weeks after the surgery (n = 10/treatment group at each time-point). These time-points were chosen to span the duration of spermatogenesis in the rat, which is approximately 49 days. These studies were approved by the Monash Medical Centre Animal Ethics Committee.

Tissue handling and preparation

At each time point, control and cryptorchid rats were anaesthetised and blood was drawn by cardiac puncture. The paired testes were dissected out and their weights were recorded.

Immediately after dissection, tissues were collected for three analyses: histology, RNA, and testicular interstitial fluid (as detailed below), to avoid the presence of two testes from the same animal in each analysis. Testes collected for histology (one testis from 9 animals) were immersed intact in Bouin's (5 testes) or 10% formalin (4 testes) fixative solutions (Amber Scientific, Midvale, WA, Australia) immediately after dissection for 24 or 48 hours, respectively. The tissues were transferred into 70% ethanol and stored until processing. Tissues for RNA or protein extraction (one testis from 7 animals) were snap-frozen in dry ice and stored at -80°C until further processing. For mRNA and protein extraction, 6 testes were homogenised using the Qiagen TissueLyser II and

stainless-steel beads (Qiagen GmBH, Hilden, Germany) prior to analysis. Blood was centrifuged at 4000 x g for 15 minutes and the separated serum was stored at -20°C, prior to use.

In order to collect testicular interstitial fluid (TIF) (one testis from 4 animals), a 2–4 mm incision was made in the tunica at the distal pole, and the testis was suspended on a thin needle placed through the tunica at the opposite pole in a 15 mL tube above 20 μL phosphate-buffered saline (PBS, pH 7.4) containing complete protease inhibitor cocktail (Roche, Castle Hill, Sydney). TIF was collected by percolation overnight at 4°C, as previously described (Sharpe and Cooper, 1983), then weighed the next day and ultra-centrifuged at 109,000 x g for 60 minutes. The supernatant was snap-frozen and stored at -80°C.

Tissue processing and histological staining

The Bouin's-fixed tissues were processed for routine histology and embedded in paraffin. Organs were sectioned at 5 μm and attached to Superfrost Plus Glass slides (BioLabs Scientific, Melbourne, Australia). The tissues were stained with periodic acid–Schiff reagent (PAS) for routine histological examination and staging of spermatogenesis. Sections were stained with Masson's trichrome to identify fibrosis.

Protein extraction and sample preparation

Testes were weighed and homogenised in cold PBS (0.01M, pH 7.4) containing 1:200 protease inhibitor (PI) cocktail III (CalBiochem, La Jolla, CA), using a TissueLyser II (Qiagen) for 20 seconds. A mixture (PBS & PI) volume was equal to 10 times of the net weight of the tissue. The homogenates then were centrifuged (14,000 x g) for 10 minutes to collect the supernatants for protein measurement.

Activin A ELISA

A specific activin A enzyme immunoassay using antibodies supplied by Oxford Brookes University was used to determine serum and tissue levels of activin A, as described previously

(Knight, 1996; O'Connor et al., 1999). The limit of detection was 22 pg/mL. The mean inter-assay coefficient of variation (CV) was 4%, and the mean intra-assay CV was 5.1%.

Activin B ELISA

Serum and tissue concentrations of activin B were measured, as described previously (Ludlow et al., 2009), using antibodies kindly supplied from Oxford Brookes University, and validated for measurement of mouse tissues. The limit of detection was 22.95 pg/mL. The mean inter-assay CV was 10% and the mean intra-assay CV was 7%.

FSH, LH, total inhibin and follistatin radioimmunoassay

Discontinuous radioimmunoassays (RIA) were used to measure serum FSH and LH levels, and total inhibin and follistatin levels in tissue homogenates and serum samples, as described previously (Robertson et al., 1988; Sun et al., 1990; Winnall et al., 2013). The FSH and LH assays detection limits were 2.48 and 0.10 ng/mL respectively, and the mean intra-assay CV was 4.8 % for both assays. The total inhibin and follistatin assays detection limits were 0.31 and 0.89 ng/mL respectively, with mean intra-assay CVs of 9.0% and 7.6%, respectively.

Testosterone radioimmunoassay

Serum and testicular homogenates were assayed using the Immunotech IM1119 RIA Testosterone direct (Beckman Coulter) using testosterone as the standard, according to the manufacturer's instructions. The sensitivity of the assay was 19.3 pg/mL with an intra-assay CV of 12%. The cross-reactivity of the assay for other steroids was DHT; 26.8%, antrodstenediol; 2.0%, 11 β –hydroxytestosterone; 5.8%, androstenedione; 1.8% and 5α-androstane-3β.17 β–diol; 1.5%.

RNA Extraction, Reverse Transcription, and Fluidigm Biomark™ HD Real-Time PCR

Fluidigm analysis was performed, as described previously (Aldahhan et al., Chapter 2). Briefly, Total RNA was isolated from snap-frozen testes (n=6, to fit Fluidigm array spaces) with β-

mercaptoethanol (14.3M, Sigma-Aldrich, MO, USA) and Rneasy kit (Qiagen, Venlo, Netherlands) followed by DNase treatment by the RNase-Free DNase set (Qiagen), according to the manufacturer's protocols. Synthesis of cDNA from RNA was performed using a Tetro cDNA synthesis kit (Bioline, Tauton, MA, USA), according to the manufacturer's instructions. Quantitative digital PCR was carried out with Taqman® Gene Expression Assays (Life Technologies, CA, USA) using the Integrated Fluidic Circuits on the Biomark™ HD platform (Fluidigm, CA, USA). The TaqMan gene expression assays are listed in Table 1. All assays were available from the manufacturer except *Rn18s* TaqMan assays which were designed as detailed previously (Adahhan et al., Chapter 2). Initially, 3 housekeeper genes were evaluated: *Gapdh, Rn18s* and *Cryab*. From these, the *Rn18s* gene was found to be most stably expressed across all time-points and experimental procedures. Data were analysed by Fluidigm Real-Time PCR Analysis software (version 4.12). The mean of each duplicate Ct value from each reaction was converted into ΔΔCt values using the housekeeping Rn18s gene, and then into 2(-ΔΔCt). A single 2(-ΔΔCt) value from the control group for each time-point was selected as a reference against which the other samples were compared. This provided the fold increase for the gene in question relative to the housekeeping gene. The average fold change is expressed as the mean fold increase of the gene relative to Rn18s and standard deviation (SD).

Real-Time quantitative PCR

Initially, Fluidigm was performed to investigate multiple testicular genes after which RT-qPCR was performed as a follow-up to determine the expression of the Leydig cell-specific gene, *Insl3,* and inflammatory markers genes*, Il10, Ilb* and *Mcp1*. RT-qPCR data were validated by examining two genes, *Rn18s* and *Sox9*, that were also tested by Fluidigm. Primers in Table 2 were designed as published previously (Baburski et al., 2015; Bhushan et al., 2015; Xie et al., 2015; Zhang et al., 2016). mRNA expression was analysed using SYBR green PCR master mix (Life Technologies) with primers (1 μM), and cDNA template in a final reaction volume of 10 μL. Following an initial denaturing step (95 °C for 10 minutes), denaturation, annealing and extension

steps (95 °C for 15 sec, 60 °C for 1 minute) were repeated 40 times, and a dissociation step (95, 60 and 95 °C for 15 seconds each) was performed using QuantStudio™ 6 Flex Real-Time PCR System (Applied Biosystems, Carlsbad, CA, USA). Each sample was measured in triplicate, and the relative expression level of each target gene was normalized to that of the reference gene Rn18s and was quantified using the ΔΔCt method.

As cryptorchidism causes a selective loss of the spermatogenic cell component of the testis, genes that are normally constitutively-expressed by the Sertoli cell and Leydig cell respectively, *Sox9* and *Insl3*, were included in the Fluidigm and RT-qPCR analyses (Kent et al., 1996; Sadeghian et al., 2005). This was done to provide an indication of the relative increase in the proportion of mRNA from the somatic cells in the samples from testes containing few spermatogenic cells, as previously described (Aldahhan et al, Chapter 2).

Statistical analysis

All statistical analyses were performed using Graphpad Prism 6 software (Graphpad Software, Inc., La Jolla, CA, USA). Data sets with two variables (treatment and time-point) were analysed using two-way analysis of variance (ANOVA) following suitable transformation to normalise the data and equalise variance in conjunction with a Sidak's multiple comparisons test, as appropriate. Statistical significance was accepted when $p < 0.05$. All data are presented as mean and standard deviation (SD).

Results

Testicular and hormonal responses to cryptorchidism

Testis weights declined to 40% of control values after 7 weeks of experimentally-induced cryptorchidism (Figure 1A), but did not decrease further at 14 weeks. At the same time, TIF volume showed displayed a progressive increase of 8-fold compared with control by 14 weeks (Figure 1B).

Seven weeks after inducing cryptorchidism, there was a complete loss of all spermatogenic cells, except spermatogonia, leading to reduced seminiferous tubule volume, increased interstitial volume and peritubular fibrosis (Figure 2B and D) compared with controls (Figure 2A and C). At 14 weeks post-cryptorchidism, the damage was similar to that observed at 7 weeks (Figure 2F and 3H).

Seven weeks after inducing cryptorchidism, serum FSH increased more than 2-fold (Figure 3A), while inhibin levels were reduced in both the serum (Figure 3B) and testis (Figure 3C and D) Serum LH was also elevated 2.5-fold (Figure 4E), and the concentration of testosterone in the testis was elevated by a similar amount (Figure 3F), but total testicular testosterone content and serum testosterone were not different from normal (data not shown).

These results showed that spermatogenesis was completely arrested at the spermatogonial stage within 7 weeks of induced cryptorchidism in the adult rat, accompanied by a compensatory increase in gonadotrophin secretion due to reduced feedback by inhibin and testosterone from the testis, consistent with previous studies using this model in the rat (Au et al., 1987; Jegou et al., 1984). Moreover, there were minimal further changes in the histological and hormonal variables between 7 and 14 weeks.

Response of the Sertoli cells

The relative expression of the critical Sertoli cell transcription factor, *Sox9*, was elevated at 7 weeks (Figure 4A), which would be consistent with loss of the contribution of mRNA from the developing spermatogenic cells. However, the relative expression of *Sox9* displayed an ongoing decline between 7 and 14 weeks. A similar pattern of decline was observed for the inhibin α-subunit gene (*Inha*), *Cldn11*, *Gja1* and *Il1a* (Figure 4B-E), all of which are genes that are primarily expressed by the Sertoli cell in the testis (Chalmel et al., 2007; Gérard et al., 1991; Lardenois et al., 2010) and in the androgen receptor gene (*Ar*) (Figure 4F), which is expressed on most somatic cells in the testis. These data indicate that there was a progressive decline in Sertoli cell function caused by cryptorchidism, which continued even after the spermatogenic cells had been depleted from the epithelium.

Response of the Leydig cells

The relative expression of the Leydig cell constitutive gene insulin like-3 (*Insl3*) was upregulated 5- to 8-fold at 7 weeks and 14 weeks after cryptorchidism (Figure 5A). As with the initial increase in *Sox9* expression, this relative increase would be consistent with the loss of the developing spermatogenic cells. In contrast to the Sertoli cell genes; however, the relative expression of *Insl3* was maintained between 7 and 14 weeks albeit *Insl3* has been shown to be androgen-regulated (Laguë and Tremblay, 2008; Paust et al., 2002) and that intratesticular androgens were maintained throughout the experiment. Significantly, expression of the crucial Leydig cell steroidogenic enzymes, cytochrome P450 family 11 subfamily a polypeptide 1 (*Cyp11a1*), 3β-hydroxysteroid dehydrogenase (*Hsd3b1*) and 17β-hydroxysteroid dehydrogenase (*Hsd17b3*), when normalised to the constitutive expression of *Insl3*, were all maintained at 7 weeks, but declined by 60% or more at 14 weeks (Figure 5B-D). These data indicate that Leydig cell function, like Sertoli cell function, declines after the loss of spermatogenic cells in cryptorchidism, although the loss in activity may be relatively delayed.

Response of activins and follistatin

The concentration of activin A in the testis was not affected by cryptorchidism (Figure 6A), but total activin A was reduced (Figure 6B), consistent with the loss of testis volume. In contrast, the testicular concentration and total amount of both activin B (Figure 6D and E) and follistatin (Figure 6G and H) were reduced in the cryptorchid testis. These differences may reflect the fact that the Sertoli cells, which were declining in their function, are the principal source of activin B and follistatin, but not of activin A, in cryptorchidism. Although the relative expression of the βA-subunit of activin A (*Inhba*) was not different between control and cryptorchid testes (Figure 6C), the βB-subunit of activin B (*Inhbb*) (Figure 6F) and follistatin (*Fst*) (Figure 6I) both showed a similar pattern of progressive decline in their expression during cryptorchidism, broadly similar to the response of the other Sertoli cell genes.

Serum activin A, activin B and follistatin levels were not different between control and cryptorchid animals at both 7 and 14 weeks (data not shown).

Stress and inflammatory responses

The expression of the key inflammatory cytokines, tumour necrosis factor (*Tnf*), interleukin-10 (*Il10*), interleukin-1β (Il1b), and monocyte chemoattractant protein 1 (*Mcp1*) was increased between 10- and 20-fold at 7 weeks after induction of cryptorchidism (Figure 7A-D). The large increase in these genes is evidence of an ongoing inflammatory response due to the cryptorchid state. In contrast, no alteration was observed in the expression of interleukin-6 (*Il6*) (data not shown). Likewise, expression of the fibrotic gene markers, α smooth muscle (*Acta2*) and collagen 1a1 (*Col1a1*), was increased two- and four-fold, respectively, at 7 weeks (Figure 7E and F). The inflammatory genes remained significantly elevated at 14 weeks, but there was a clear trend towards resolution of the inflammatory and profibrotic response between 7 and 14 weeks.

The expression of the heat-inducible heat shock protein (HSP) HSP70-1 (*Hspa1a*) and constitutive HSP70-2 (*Hspa1b*) was not altered at any time-point (data not shown). However, HSP70-3 (*Hspa1l*), which is a heat-inducible HSP, showed a dramatic decline by 95% at 7 weeks and minimal expression at 14 weeks (Figure 7G). The heat-shock transcription factor (*Hsf1*) was also reduced in expression by 75% at 14 weeks (Figure 7H).

Discussion

In the present study, the induction of cryptorchidism in the adult rat caused loss of all developing spermatogenic cells, as well as oedema, peritubular fibrosis and increased gonadotrophin secretion. The germ cell death in the cryptorchid testes has been reported to result primarily from exposure of the testes to the core body temperature (Setchell, 2006) and is also associated with oxidative stress involved in heat-mediated damage (Ahotupa and Huhtaniemi, 1992; Houston et al., 2018). Selective signalling pathway regulation in various testicular cell types could possibly be responsible for the observed selective cellular damage (Li et al., 2006).

The significant increase in serum FSH, LH and intratesticular testosterone levels, and the decrease in serum and intratesticular inhibin concentrations at 7 and 14 weeks are consistent with earlier studies that showed elevated FSH and LH levels within 2–10 weeks after induction of cryptorchidism in the adult rat (Jegou et al., 1983; Jones et al., 1977; Kerr et al., 1979a; Risbridger et al., 1981a; Seethalakshmi and Steinberger, 1983). However, other reports have shown no change or even a decrease in the LH level following experimental cryptorchidism in the rat and mouse (Jones et al., 1977; Mendis-Handagama et al., 1990; Ren et al., 2006). The inhibin response occurred earlier, as indicated by reports of initiation of the decline in inhibin during the first 3 days after the surgery and persistence of this effect for 2 weeks (Gonzales et al., 1989; Ren et al., 2006). We also found no changes in the serum or total testicular testosterone levels, even though the intratesticular concentration was markedly elevated at both time points. This finding could be explained by changes in the testicular vasculature caused by cryptorchidism; these changes could elevate intratesticular testosterone while reducing passage of testosterone into the circulation (Bergh et al., 1984a; Damber et al., 1978). Nevertheless, the data on testosterone secretion in the cryptorchid testis is somewhat contradictory.

In mice, the serum testosterone level was similar to the control level following experimentally induced cryptorchidism (Mendis-Handagama et al., 1990). Conversely, other experiments have shown a considerable decrease in the serum or intratesticular testosterone levels (Kerr et al., 1979a; Murphy and O'Shaughnessy, 1991; Ren et al., 2006). This inconsistency in the hormone levels may be explained by differences in the experimental conditions such as species specificity, evaluation timepoints or type of cryptorchid surgery (uni/bilateral). Overall, the hormonal observations in the present study are consistent with a reduced feedback to the anterior pituitary gland via inhibin and testosterone, even though intratesticular testosterone levels are maintained or even elevated, indicating a state of compensated Leydig cell function through hyperstimulation.

The findings in the present study indicate that Sertoli cell and Leydig cell functions continue

to decline, even after all the spermatogenic cells have been depleted from the testis. In our previous study on the effects of heat on the testis (Aldahhan et al, Chapter 3), the expression of the Sertoli cell-specific gene, *Sox9*, and of the Leydig cell-specific gene, *Insl3*, were used to control for the relative loss of spermatogenic cell genes versus somatic cell genes due to depletion of the germinal epithelium. However, the expression of *Sox9* and of several other key Sertoli cell genes, including inhibin α-subunit (*Inha*), interleukin-1α (*Il1a*), claudin-11 (*Cldn11*), and connexin 43 (*Gja1*) was observed to fall during cryptorchidism, even though the Sertoli cell numbers are known to be maintained in the cryptorchid testis (Bergh, 1981; Zhang et al., 2002); this finding indicated that the function of the Sertoli cell was progressively declining in the absence of the spermatogenic cells. The decline in expression of the Sertoli cell tight junction proteins, claudin-11 and connexin 43, was consistent with earlier studies indicating morphological and functional disruption of the integrity of the inter-Sertoli cell tight junctions at 7–12 days after cryptorchidism induction (Hagenäs et al., 1977; Kerr et al., 1979b).

Expression of the constitutive Leydig cell gene, *Insl3*, appeared to be maintained during cryptorchidism, suggesting the possiblility of using this as an indicator of absolute Leydig cell mRNA levels. When expressed as a ratio with *Insl3*, the expression of the key steroidogenic genes, *Cyp11a1*, *Hsd3b1* and *Hsd17b3*, was apparently maintained at 7 weeks, but declined at 14 weeks after induction of cryptorchidism. In spite of the reduced expression of these genes, the intratesticular levels of testosterone were maintained in the cryptorchid testis, suggesting that the increase in LH coming from the pituitary gland and the vascular changes associated with cryptorchidism favoured the retention of testosterone within the testis. These data indicate that the progressive decline in Sertoli and Leydig cell function is not directly due to the raised testicular temperature, the depletion of the spermatogenic cells or a loss of androgens in the cryptorchid testis.

The findings in the present study indicate that the concentration of intratesticular activin A was maintained in cryptorchidism, but the levels of activin B and of the activin-binding protein, follistatin, decreased. The decreased mRNA expression of the inhibin B subunits, *Inha* and *Inhbb*, was reflected in a reduction in the protein levels of total inhibin and activin B, which are primarily,

although not exclusively, products of the Sertoli cells within the testis. Earlier observations in rats indicated a regulation of inhibin B levels by spermatogenic cells, suggesting an association between the loss of post-meiotic germ cells and a reduction in inhibin B levels (Allenby et al., 1991; Guitton et al., 2000). However, *in vitro* studies have shown an inhibition of Sertoli cell *Inhbb* mRNA by meiotic germ cells in culture (Clifton et al., 2002). Therefore, the changes in inhibin seen in the present study may be associated with a disruption of the normal stage-dependent regulation of Sertoli cell activity (Okuma et al., 2006). The fact that activin A was not altered following experimental cryptorchidism may indicate that activin A is more widely expressed within the testis when compared with inhibin, activin B or follistatin, at least in the cryptorchid condition. Overall, the data suggest that activin A plays a significant role in the cryptorchid testis, and that its effects are enhanced by the reduction in the corresponding level of its binding protein, follistatin.

The observation that several key inflammatory and fibrotic genes are strongly increased in the cryptorchid testis, along with the persistence of activin A, indicate that cryptorchidism causes a strong inflammatory response in the testis, and this response persists even after all the spermatogenic cells have been lost. Although the inflammatory response has not been investigated previously in other animal models, Imamoğlu et al. (2012) have shown an increase in the serum interleukin-6 in cryptorchid boys aged 1–14 years. We did not evaluate proinflammatory cytokine protein production; however, the mRNA expression of interleukin-6 did not differ significantly at either time points. We speculate the inflammation occurring in cryptorchidism may play a role in the pathophysiology of the sub-/infertility, as seen in patients with varicocoele (Nallella et al., 2004).

The occurrence of peritubular fibrosis was also consistent with the observed alterations in marker transcript levels, which included upregulation of the fibrotic genes *Acta2* and *Col1a1*. Since chronic inflammation is known to have detrimental effects on cell function, a valid hypothesis is that chronic inflammation may be the main cause of the progressive decline in Sertoli and Leydig cell function in this model, even after the loss of the spermatogenic cells. The principal drivers of the inflammatory response remain to be determined, but the ongoing production of activin A, along

with the reduced follistatin levels, and the elevated temperature, are likely to be factors.

The HSPs protect cells from thermal stress, reduce the consequences of damage and facilitate cellular recovery. In the testis, 70-kDa HSPs are essential for spermatogenesis and are expressed by various germ cells (Table 1). In the present study, expression of HSP70-3 mRNA decreased significantly, along with the loss of the spermatogenic cells in the cryptorchid testis while the mRNA of *Hsf1* showed late downregulation at 14 weeks. Nevertheless, HSP70-1 and -2 was not significantly changed at any timepoint. HSF1 has a cytoprotective role against several forms of stress by regulation of HSP molecular chaperone genes (He et al. 2003; Shiraishi, 2012). HSPs and *Hsf1* would be predicted to show acute activation following the increase in the testis temperature (Kiang and Tsokos, 1998). Since HSP70-3 is highly enriched in pachytene spermatocytes and round spermatids, the initial downregulation of HSP70-3 mRNA at 7 weeks could possibly due to the loss of these germ cells while the reduction became more prominent at 14 weeks after the downregulation of *Hsf1*. These data indicate potential regulation of HSP70-3 by HSF.

HSPs also play an anti-apoptotic role by interfering with caspase activation (Radons, 2016); however, the anti-apoptotic properties of HSPs70 have shown conflicting results in other cryptorchid models. Overexpression of HSP70 does not add further protection to the germinal epithelium following experimental cryptorchidism in mice (Widlak et al., 2007), but Zhou et al (2001) suggested that HSP70 may suppress the germ cell apoptosis induced by experimental cryptorchidism at a later stage.

In conclusion, the current study indicate that depletion of the germinal epithelium in experimental cryptorchidism in the adult rat results in chronic inflammation, oedema and fibrosis, and is followed by a progressive decline of Sertoli and Leydig cell gene expression and function. Evaluating inflammatory markers may therefore assist in the diagnosis of male sub-/infertility. Treatment of this infertility condition with anti-inflammatory agents may also reduce the severity of the cryptorchidism consequences. Furthermore, these findings, taken together with those of earlier studies, suggest that changes in Leydig cell function are most likely the result of local factors

produced by Sertoli cells, indicating the importance of intercellular communication between Leydig and Sertoli cells. Future studies that focus on the specific local mechanisms may advance our understanding of the molecular cues driving spermatogenesis and identify the potential targets for fertility regulation.

Acknowledgements

This research was supported by funding provided by Imam Abdulrahman Bin Faisal University in Saudi Arabia (8559246), the National Health and Medical Research Council of Australia and the Victorian State Government Operational Infrastructure Support Program. We thank Oxford Brookes University for kindly supplying the antibody reagents E4 and 46 A/F used in the activin A and B assays, Adnan Sali and Julie Muir for assistance in animal procedures, and Susan Hayward for her expert immunoassay skills and assistance. Furthermore, the authors thank the MHTP Medical Genomics Facility for assistance with the Fluidigm analysis.

Declaration of interest

The authors declare no conflict of interest with respect to this study.

Author's contributions

Conceived and designed the experiments: DDK, MPH, RA.

Performed the experiments: RA.

Reagents/activin A and B assay techniques: HL.

Analysed the data: RA, MPH.

Critical discussion of data: RA, MPH, DDK, PGS.

Wrote the manuscript: RA, MPH.

Critical review of manuscript: all authors.

Tables

Table 1. List of Taqman assays used. Includes data from Chalmel et al. (2007), Gérard et al. (1991) and searchable GermOnline database (Lardenois et al., 2010).

Protein name	Gene symbol	Life Tech assay code	Main cell sites of expression in testis
Glyceraldehyde-3-phosphate dehydrogenase	*Gapdh*	Rn01775763_g1	All cell types
18S ribosomal RNA	*Rn18s*	Designed	
Inhibin βA subunit	*Inhba*	Rn01538592_m1	Somatic cells and germ cells
Inhibin βB subunit	*Inhbb*	Rn01753772_m1	
Follistatin	*Fst*	Rn00561225_m1	
Heat shock factor 1	*Hsf1*	Rn00801772_m1	
α smooth muscle actin	*Acta2*	Rn01759928_g1	
Collagen 1α type 1	*Col1a1*	Rn01463848_m1	
SRY box 9	*Sox9*	Rn01751070_m1	Sertoli cells
Inhibin α subunit	*Inha*	Rn00561423_m1	
Claudin 11	*Cldn11*	Rn00584941_m1	
Interleukin 1α	*Il1a*	Rn00566700_m1	
Hydroxy δ 5 steroid dehydrogenase 3 β and steroid δ isomerase 1	*Hsd3b1*	Rn01774741_m1	Leydig cells
Hydroxysteroid 17- β dehydrogenase 3	*Hsd17b3*	Rn00588942_m1	
Cytochrome P450 family 11 subfamily a polypeptide 1	*Cyp11a1*	Rn00568733_m1	
Heat shock protein 70-1	*Hspa1a*	Rn02532795_s1	Spermatogonia
Heat shock protein 70-2	*Hspa1b*	Rn04224718_u1	
Connexin 43	*Gja1*	Rn01433957_m1	Sertoli cells and spermatogonia
Keratin 18	*Krt18*	Rn01533360_g1	
Crystallin alpha B	*Cryab*	Rn01421541_m1	Sertoli and Leydig cells
Heat shock protein 70-3	*Hspa1l*	Rn01525984_m1	Spermatocytes and round spermatids
Interleukin 6	*Il6*	Rn01410330_m1	Activated immune cells, somatic cells and germ cells
TNFα	*Tnf*	Rn99999017_m1	
Androgen receptor	*Ar*	Rn00560747_m1	Somatic cells

Table 2. List of forward and reverse primer sequences for quantitative RT-PCR.

Gene name	**Forward primer (5`-3`)**	**Reverse primer (5`-3`)**	**Product size**	**Accession number**
Insl3	CGCAGTGTGGCCACCAA	CCTGAGCCCTACAATCCTTCAG	102	NM_053680.1
Il10	TAAAAGCAAGGCAGTGGAGC	GATGCCGGGTGGTTCAATTT	149	NM_012854.2
Il1b	TGCCTCGTGCTGTCTGACCCA	AGGCCCAAGGCCACAGGGAT	137	NM_031512.2
Mcp1	TGTTCACAGTTGCTGCCTGT	CCGACTCATTGGGATCATCT	110	NM_031530.1
Rn18s	GGAGAGGGAGCCTGAGAAAC	CAATTACAGGGCCTCGAAAG	128	NR 046237.1

Figures

Figure 1. Testis weight (A) and the volume of recovered testicular interstitial fluid (TIF) (B) of sham-operated control and cryptorchid rats at 7 and 14 weeks after surgery. Data are mean ± SD (n = 10 animals for testis weights, and n = 4 animals for TIF volumes): NS $p > 0.05$, **** $p < 0.0001$.

Figure 2. Testicular histology in sham-operated control and cryptorchid rats. Sections stained with Periodic acid–Schiff (A, B, E and F) and Masson's trichrome (C, D, G and H). After 7 weeks of experimental cryptorchidism most cells were lost from the seminiferous epithelium, with the exception of spermatogonia and Sertoli cells (B and D). Seminiferous tubule diameters were considerably reduced, with increased evidence of peritubular fibrosis (D: arrows) and increased acellular interstitial spaces. After 14 weeks, there was little further change in the seminiferous tubules, although the peritubular fibrosis became more conspicuous (H: arrows). Sham-operated control rats showed no pathological changes. All scale bars represent 50 μm.

Figure 3. Response of the hypothalamic-pituitary-testis axis in sham-operated control and cryptorchid rats. Serum levels of FSH (A), inhibin (B) and LH (E), intratesticular concentrations of inhibin (C) and testosterone (F) expressed as ng/g testis, and total testicular inhibin content (D) at 7 and 14 weeks after induction of cryptorchidism. Data are mean ± SD (n = 10 animals for serum FSH, inhibin and LH values, and n = 6 for intratesticular inhibin and testosterone): *$p < 0.05$, **$p < 0.01$, ***$p < 0.001$ and ****$p < 0.0001$.

Figure 4. Response of Sertoli cell genes in sham-operated control and cryptorchid rats. Comparison of relative expression of Sertoli cell-specific mRNA: *Sox9* (A), *Inha* (B) and *Il1a* (C), the blood testis-barrier proteins, *Cldn11* (D) and *Gja1* (E), and the androgen receptor (*Ar*) (F) at 7 and 14 weeks after induction of cryptorchidism. Data are mean ± SD (n = 6 animals): NS $p > 0.05$, *$p <$

0.05, **p <0.01, ***p < 0.001 and ****p < 0.0001.

Figure 5. Response of Leydig cell genes in sham-operated control and cryptorchid rats**.** Comparison of relative expression of Leydig cell-specific mRNA: *Insl3* (A) and steroidogenic enzymes*, Cyp11a1* (B), *Hsd17b3* (C) and *Hsd3b1* (D) at 7 and 14 weeks after induction of cryptorchidism. Data are mean ± SD (n = 6 animals): NS p > 0.05, *p < 0.05, ***p < 0.001 and ****p <0.0001. (n = 6 /group). *Insl3* mRNA expression was normalised to *Rn18s* in respective controls, and all other genes are expressed as a ratio with *Insl3*.

Figure 6. Response of activins and activin-related proteins in sham-operated control and cryptorchid rats. Comparison of the intratesticular concentrations (ng/g testis) of activin A (A), activin B (D) and follistatin (G), total testicular content of activin A (B), activin B (E) and follistatin (H), and mRNA expression of *Inhba* (C), *Inhbb* (F) and *Fst* (I) at 7 and 14 weeks after induction of cryptorchidism. Data are mean ± SD (n = 6 animals): NS p > 0.05, **p<0.01 and ****p<0.0001.

Figure 7. Inflammatory, fibrotic and stress responses in sham-operated control and cryptorchid rats. Comparison of expression of inflammatory markers genes: *Tnf* (A)*, Il10* (B*), Il1b (C)* and *Mcp1* (D); fibrotic marker genes: Acta2 (E) and *Col1a1* (F); and heat shock proteins: *Hspa1*l (G) and *Hsf1* (H)**,** at 7 and 14 weeks after induction of cryptorchidism. Data are mean ± SD (n = 6 animals): NS p>0.05, **p<0.01, ***p < 0.001 and ****p < 0.0001.

References

Agoulnik A.I., Huang Z., Ferguson L., 2012. Spermatogenesis in Cryptorchidism, in: Chan W.Y., Blomberg L. (Eds.) Germline Development: Methods and Protocols. Springer, New York, pp.127–147.

Ahotupa, M., Huhtaniemi, I., 1992. Impaired detoxification of reactive oxygen and consequent oxidative stress in experimentally cryptorchid rat testis. Biol. Reprod. 46, 1114–1118.

Allenby, G., Foster, P.M., Sharpe, R.M., 1991. Evidence that secretion of immunoactive inhibin by seminiferous tubules from the adult rat testis is regulated by specific germ cell types: correlation between in vivo and in vitro studies. Endocrinology 128, 467–476.

Au, C.L., Robertson, D.M., de Kretser, D.M., 1987. Changes in Testicular Inhibin after a Single Episode of Heating of Rat Testes. Endocrinology 120, 973–977.

Baburski, A.Z., Sokanovic, S.J., Janjic, M.M., Stojkov-Mimic, N.J., Bjelic, M.M., Andric, S.A., Kostic, T.S., 2015. Melatonin replacement restores the circadian behavior in adult rat Leydig cells after pinealectomy. Mol. Cell. Endocrinol. 413, 26–35.

Barakat, B., Itman, C., Mendis, S.H., Loveland, K.L., 2012. Activins and inhibins in mammalian testis development: New models, new insights. Mol. Cell. Endocrinol. 359, 66–77.

Bergh, A., 1981. Morphological signs of a direct effect of experimental cryptorchidism on the Sertoli cells in rats irradiated as fetuses. Biol. Reprod. 24, 145–152.

Bergh, A., Berg, A.Å., Damber, J.E., Hammar, M., Selstam, G., 1984a. Steroid biosynthesis and Leydig cell morphology in adult unilaterally cryptorchid rats. Eur. J. Endocrinol. 107, 556–562.

Bergh, A., Berg, A.Å., Damber, J.E., Hammar, M., Selstam, G., 1984b. Steroid biosynthesis and Leydig cell morphology in adult unilaterally cryptorchid rats. Acta Endocrinol. 107, 556–562.

Bhushan, S., Tchatalbachev, S., Lu, Y., Fröhlich, S., Fijak, M., Vijayan, V., Chakraborty, T., Meinhardt, A., 2015. Differential activation of inflammatory pathways in testicular macrophages provides a rationale for their subdued inflammatory capacity. J. Immunol. 194, 5455–5464.

Bienvenu, L.A., Morgan, J., Reichelt, M.E., Delbridge, L.M., Young, M.J., 2017. Chronic in vivo nitric oxide deficiency impairs cardiac functional recovery after ischemia in female (but not male) mice. J. Mol. Cell. Cardiol. 112, 8–15.

Chalmel, F., Rolland, A.D., Niederhauser-Wiederkehr, C., Chung, S.S., Demougin, P., Gattiker, A., Moore, J., Patard, J.J., Wolgemuth, D.J., Jégou, B., 2007. The conserved transcriptome in human and rodent male gametogenesis. Proc. Natl. Acad. Sci. 104, 8346–8351.

Clifton, R.J., O'Donnell, L., Robertson, D.M., 2002. Pachytene spermatocytes in co-culture inhibit rat Sertoli cell synthesis of inhibin beta B-subunit and inhibin B but not the inhibin alpha-subunit. J. Endocrinol. 172, 565–574.

Damber, J.E., Bergh, A., Janson, P.O., 1978. Testicular blood flow and testosterone concentrations in the spermatic venous blood in rats with experimental cryptorchidism. Eur. J. Endocrinol. 88, 611–618.

Eddy, E., 1998. HSP70‐2 heat‐shock protein of mouse spermatogenic cells. J. Exp. Zool. 282, 261–271.

Fantasia, J., Aidlen, J., Lathrop, W., Ellsworth, P., 2015. Undescended testes: a clinical and surgical review. Urol. Nurs. 35, 117–127.

Gasinska, A., Hill, S., 1989. The effect of hyperthermia on the mouse testis. Neoplasma 37, 357–366.

Gérard, N., Syed, V., Bardin, W., Genetet, N., Jégou, B., 1991. Sertoli cells are the site of interleukin-1α synthesis in rat testis. Mol. Cell. Endocrinol. 82, R13–R16.

Gonzales, G.F., Risbridger, G.P., de Kretser, D.M., 1989. In vivo and in vitro production of inhibin by cryptorchid testes from adult rats. Endocrinology 124, 1661–1668.

Guitton, N., Touzalin, A.M., Sharpe, R.M., Cheng, C.Y., Pinon‐Lataillade, G., Meritte, H., Chenal, C., Jegou, B., 2000. Regulatory influence of germ cells on Sertoli cell function in the pre‐pubertal rat after acute irradiation of the testis. Int. J. Androl. 23, 332–339.

Hagenäs, L., Plöen, L., Ritzen, E.M., Ekwall, H., 1977. Blood‐testis barrier: Maintained function of inter‐Sertoli cell junctions in experimental cryptorchidism in the rat, as judged by a simple lanthanum‐immersion technique. Andrologia 9, 250–254.

Hagenas, L., Ritzen, E.M., 1976. Impaired Sertoli cell function in experimental cryptorchidism in the rat. Mol. Cell. Endocrinol. 4, 25–34.

Harrison, R.G., Weiner, J.S., 1949. Vascular patterns of the mammalian testis and their functional significance. J. Exp. Biol. 26, 304–316.

He, H., Soncin, F., Grammatikakis, N., Li, Y., Siganou, A., Gong, J., Brown, S.A., Kingston, R.E. and Calderwood, S.K., 2003. Elevated expression of heat shock factor (HSF) 2A stimulates HSF1-induced transcription during stress. J. Biol. Chem. 278, 35465–35475.

Hedger, M.P., Drummond, A.E., Robertson, D.M., Risbridger, G.P., de Kretse, D.M., 1989. Inhibin and activin regulate [3 H] thymidine uptake by rat thymocytes and 3T3 cells in vitro. Mol. Cell. Endocrinol. 61, 133–138.

Hedger, M.P., Meinhardt, A., 2003. Cytokines and the immune-testicular axis. J. Reprod. Immunol. 58, 1–26.

Hedger, M.P., Winnall, W.R., Phillips, D.J., de Kretser, D.M., 2011. The regulation and functions of activin and follistatin in inflammation and immunity. Vitam. Horm. 85, 255–297.

Houston, B.J., Nixon, B., Martin, J.H., De Iuliis, G.N., Trigg, N.A., Bromfield, E.G., McEwan, K.E., Aitken, R.J., 2018. Heat exposure induces oxidative stress and DNA damage in the male germ line. Biol. Reprod. 98, 593–606.

Imamoğlu, M., Bülbül, S.S., kaklikkaya, N., Sarihan, H., 2012. Oxidative, inflammatory and immunologic status in children with undescended testes. Pediatr. Int. 54, 816–819.

Jegou, B., Laws, A.O., de Kretser, D.M., 1984. Changes in testicular function induced by short‐term exposure of the rat testis to heat: further evidence for interaction of germ cells, Sertoli cells and Leydig cells. Int. J. Androl. 7, 244–257.

Jegou, B., Risbridger, G.P., de Kretser, D.M., 1983. Effects of experimental cryptorchidism on testicular function in adult rats. J. Androl. 4, 88–94.

Jones, K.L., Mansell, A., Patella, S., Scott, B.J., Hedger, M.P., de Kretser, D.M., Phillips, D.J., 2007. Activin A is a critical component of the inflammatory response, and its binding protein, follistatin, reduces mortality in endotoxemia. Proc. Natl. Acad. Sci. 104, 16239–16244.

Jones, T.M., Anderson, W., Fang, V.S., Landau, R.L., Rosenfield, R.L., 1977. Experimental cryptorchidism in adult male rats: histological and hormonal sequelae. Anat. Rec. 189, 1–27.

Kent, J., Wheatley, S.C., Andrews, J.E., Sinclair, A.H., Koopman, P., 1996. A male-specific role for SOX9 in vertebrate sex determination. Development 122, 2813–2822.

Kerr, J.B., Rich, K.A., de Kretser, D.M., 1979a. Alterations of the fine structure and androgen secretion of the interstitial cells in the experimentally cryptorchid rat testis. Biol. Reprod. 20, 409–422.

Kerr, J.B., Rich, K.A., de Kretser, D.M., 1979b. Effects of experimental cryptorchidism on the ultrastructure and function of the Sertoli cell and peritubular tissue of the rat testis. Biol. Reprod. 21, 823–838.

Knight, P., 1996. Roles of inhibins, activins, and follistatin in the female reproductive system. Front. Neuroendocrinol. 17, 476–509.

Laguë, E., Tremblay, J.J., 2008. Antagonistic effects of testosterone and the endocrine disruptor mono-(2-ethylhexyl) phthalate on INSL3 transcription in Leydig cells. Endocrinology 149, 4688–4694.

Lardenois, A., Gattiker, A., Collin, O., Chalmel, F., Primig, M., 2010. GermOnline 4.0 is a genomics gateway for germline development, meiosis and the mitotic cell cycle. Database 2010. (http://www.germonline.org/index.html).

Li, Y.C., Hu, X.-Q., Xiao, L.J., Hu, Z.Y., Guo, J., Zhang, K.Y., Song, X.X., Liu, Y.X., 2006. An oligonucleotide microarray study on gene expression profile in mouse testis of experimental cryptorchidism. Front. Biosci. 11, 2465–2482.

Liu, F., Xu, Z.L., Qian, X.J., Qiu, W.Y. and Huang, H., 2011. Expression of Hsf1, Hsf2, and Phlda1 in cells undergoing cryptorchid-induced apoptosis in rat testes. Mol. Reprod. Dev. 78, 283-291.

Ludlow, H., Phillips, D.J., Myers, M., McLachlan, R.I., de Kretser, D.M., Allan, C.A., Anderson, R.A., Groome, N.P., Hyvönen, M., Colin Duncan, W., 2009. A new ‘total’ activin B enzyme‐linked immunosorbent assay (ELISA): development and validation for human samples. Clin. Endocrinol. 71, 867–873.

Meehan, T., Schlatt, S., O'Bryan, M.K., de Kretser, D.M., Loveland, K.L., 2000. Regulation of germ cell and Sertoli cell development by activin, follistatin, and FSH. Dev. Biol. 220, 225–237.

Mendis-Handagama, S.C., Kerr, J.B., de Kretser, D.M., 1990. Experimental cryptorchidism in the adult mouse: II. A hormonal study. J. Androl. 11, 548–554.

Mieusset, R., Bujan, L., 1995. Testicular heating and its possible contributions to male infertility: a review. Int. J. Androl. 18, 169–184.

Murphy, L., O'Shaughnessy, P., 1991. Effect of cryptorchidism on testicular and Leydig cell androgen production in the mouse. Int. J. Androl. 14, 66–74.

Nallella, K.P., Allamaneni, S.S., Pasqualotto, F.F., Sharma, R.K., Thomas Jr, A.J., Agarwal, A., 2004. Relationship of interleukin-6 with semen characteristics and oxidative stress in patients with varicocele. Urology 64, 1010–1013.

Nicholls, P.K., Stanton, P.G., Chen, J.L., Olcorn, J.S., Haverfield, J.T., Qian, H., Walton, K.L., Gregorevic, P., Harrison, C.A., 2012. Activin signaling regulates Sertoli cell differentiation and function. Endocrinology 153, 6065–6077.

O'Connor, A.E., McFarlane, J.R., Hayward, S., Yohkaichiya, T., Groome, N.P., de Kretser, D.M., 1999. Serum activin A and follistatin concentrations during human pregnancy: a cross-sectional and longitudinal study. Hum. Reprod. 14, 827–832.

Ohga, E., Matsuse, T., Teramoto, S., Katayama, H., Nagase, T., Fukuchi, Y., Ouchi, Y., 1996. Effects of activin A on proliferation and differentiation of human lung fibroblasts. Biochem. Biophys. Res. Commun. 228, 391–396.

Okuma, Y., O'Connor, A.E., Hayashi, T., Loveland, K., de Kretser, D.M., Hedger, M.P., 2006. Regulated production of activin A and inhibin B throughout the cycle of the seminiferous epithelium in the rat. J. Endocrinol. 190, 331–340.

Ota, F., Maeshima, A., Yamashita, S., Ikeuchi, H., Kaneko, Y., Kuroiwa, T., Hiromura, K., Ueki, K., Kojima, I., Nojima, Y., 2003. Activin A induces cell proliferation of fibroblast‐like synoviocytes in rheumatoid arthritis. Arthritis Rheum. 48, 2442–2449.

Paust, H.J., Wessels, J., Ivell, R., Mukhopadhyay, A.K., 2002. The expression of the RLF/INSL3 gene is reduced in Leydig cells of the aging rat testis. Exp. Gerontol. 37, 1461–1467.

Radons, J., 2016. The human HSP70 family of chaperones: where do we stand? Cell Stress Chaperones 21, 379–404.

Ren, L., Medan, M.S., Ozu, M., LI, C., Watanabe, G., Taya, K., 2006. Effects of experimental cryptorchidism on sperm motility and testicular endocrinology in adult male rats. J. Reprod. Dev. 52, 219–228.

Risbridger, G.P., Kerr, J., de Kretser, D.M., 1981a. Evaluation of Leydig cell function and gonadotropin binding in unilateral and bilateral cryptorchidism: evidence for local control of Leydig cell function by the seminiferous tubule. Biol. Reprod. 24, 534–540.

Risbridger, G.P., Kerr, J.B., Peake, R.A., Rich, K.A., de Kretser, D.M., 1981b. Temporal changes in rat Leydig cell function after the induction of bilateral cryptorchidism. J. Reprod. Fertil. 63, 415–423.

Robertson, D.M, Hayward, S., Irby, D., Jacobsen, J., Clarke, L., McLachlan, R.I., de Kretser, D.M., 1988. Radioimmunoassay of rat serum inhibin: changes after PMSG stimulation and gonadectomy. Mol. Cell. Endocrinol. 58, 1–8.

Sadeghian, H., Anand-Ivell, R., Balvers, M., Relan, V., Ivell, R., 2005. Constitutive regulation of the Insl3 gene in rat Leydig cells. Mol. Cell. Endocrinol. 241, 10–20.

Schneuer, F.J., Holland, A.J., Pereira, G., Jamieson, S.E., Bower, C., Nassar, N., 2016. Age at surgery and outcomes of an undescended testis. Pediatrics, 137, 2015–2768.

Seethalakshmi, L., Steinberger, A., 1983. Effect of cryptorchidism and orchidopexy on inhibin secretion by rat Sertoli cells. J. Androl. 4, 131–135.

Setchell, B.P., 2006. The effects of heat on the testes of mammals. Anim. Reprod. 3, 81–91.

Sharpe, R.M, Cooper, I., 1983. Testicular interstitial fluid as a monitor for changes in the intratesticular environment in the rat. J. Reprod. Fertil. 69, 125–135.

Shiraishi K., 2016. HSF is required for gametogenesis, in: Nakai A. (Ed.), Heat Shock Factor. Springer, Tokyo, pp. 147-164.

Sun, Y.T., Wreford, N.G., Robertson, D.M., de Kretser, D.M., 1990. Quantitative cytological studies of spermatogenesis in intact and hypophysectomized rats: identification of androgen-dependent stages. Endocrinology 127, 1215–1223.

Widlak, W., Winiarski, B., Krawczyk, A., Vydra, N., Malusecka, E., Krawczyk, Z., 2007. Inducible 70 kDa heat shock protein does not protect spermatogenic cells from damage induced by cryptorchidism. Int. J. Androl. 30, 80–87.

Wijayarathna, R., de Kretser, D.M, 2016. Activins in reproductive biology and beyond. Hum. Reprod. Update 22, 342–357.

Winnall, W.R., Wu, H., Sarraj, M.A., Rogers, P.A., de Kretser, D.M., Girling, J.E., Hedger, M.P., 2013. Expression patterns of activin, inhibin and follistatin variants in the adult male mouse reproductive tract suggest important roles in the epididymis and vas deferens. Reprod. Fertil. Dev. 25, 570–580.

Xie, L., Choudhury, G.R., Winters, A., Yang, S.H., Jin, K., 2015. Cerebral regulatory T cells restrain microglia/macrophage‐mediated inflammatory responses via IL‐10. Eur. J. Immunol. 45, 180–191.

Yamashita, S., Maeshima, A., Kojima, I., Nojima, Y., 2004. Activin A is a potent activator of renal interstitial fibroblasts. J. Am. Soc. Nephrol. 15, 91–101.

Zhang, R., Wen, X., Kong, L., Deng, X., Peng, B., Huang, A., Wan, Y., Yang, Z., 2002. A quantitative (stereological) study of the effects of experimental unilateral cryptorchidism and subsequent orchiopexy on spermatogenesis in adult rabbit testis. Reproduction 124, 95–105.

Zhang, W.X., Fan, J., Ma, J., Rao, Y.S., Zhang, L., Yan, Y.-E., 2016. Selection of suitable reference genes for quantitative real-time PCR normalization in three types of rat adipose tissue. Int. J. Mol. Sci. 17, 968.

Zhou, X.C., Han, X.B., Hu, Z.Y., Zhou, R.J., Liu, Y.X., 2001. Expression of Hsp70-2 in unilateral cryptorchid testis of rhesus monkey during germ cell apoptosis. Endocrine 16, 89–95.

Figure 1

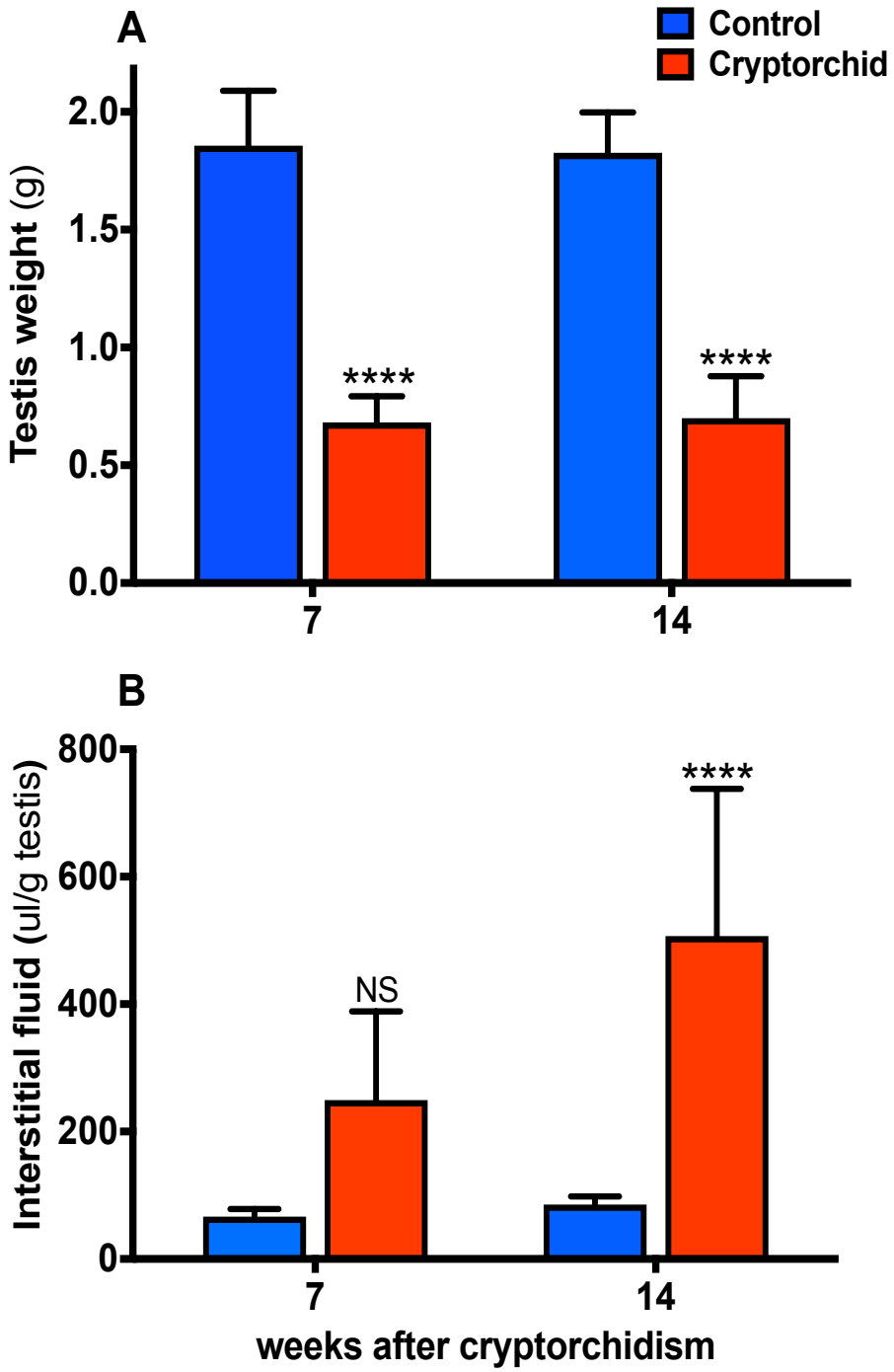
A
Control
Cryptorchid
Testis weight (g)
2.0
1.5
1.0
0.5
0.0
****
****
7
14
B
Interstitial fluid (ul/g testis)
800
600
400
200
0
NS
****
7
14
weeks after cryptorchidism

Figure 2

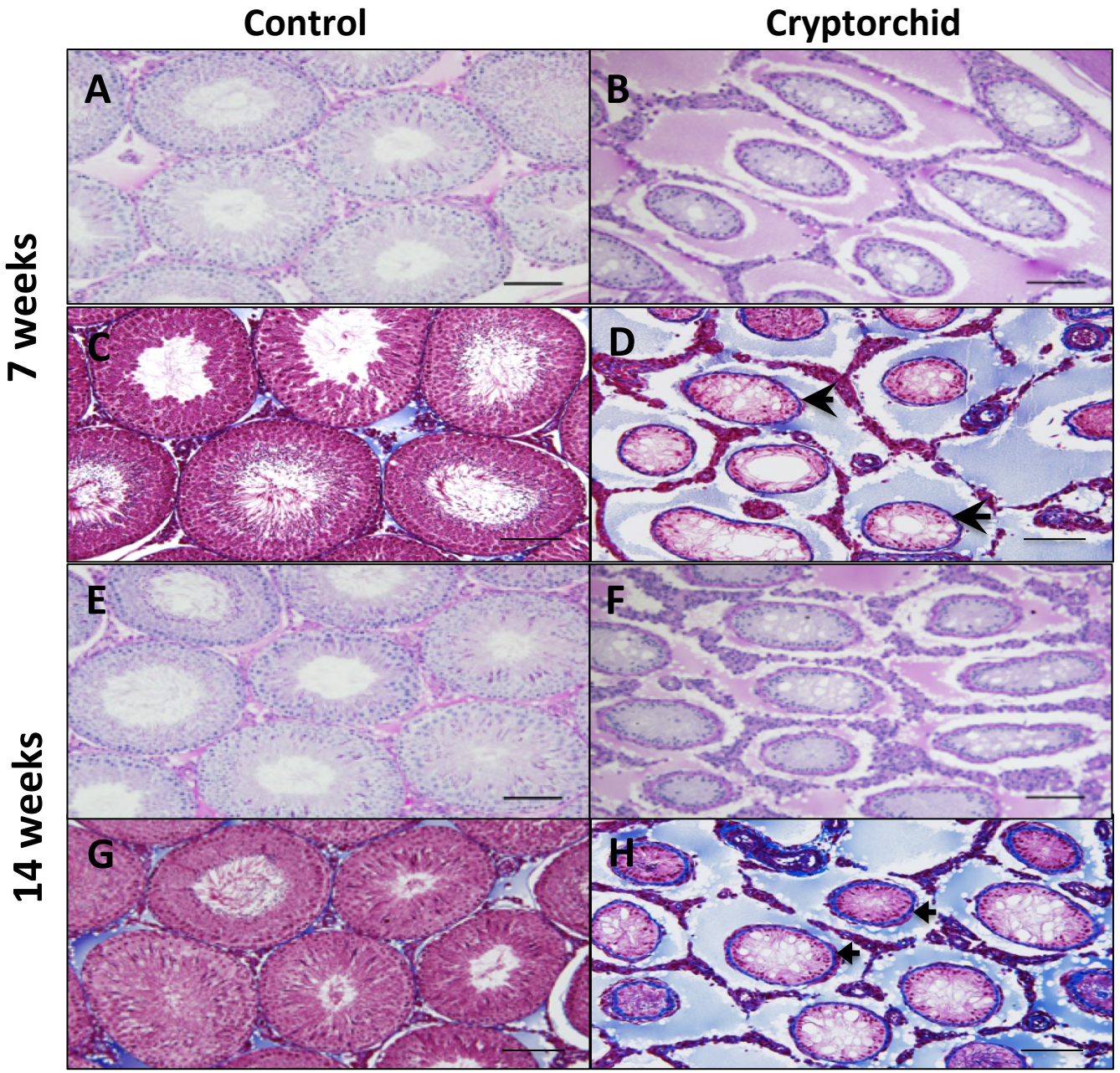

Figure 3

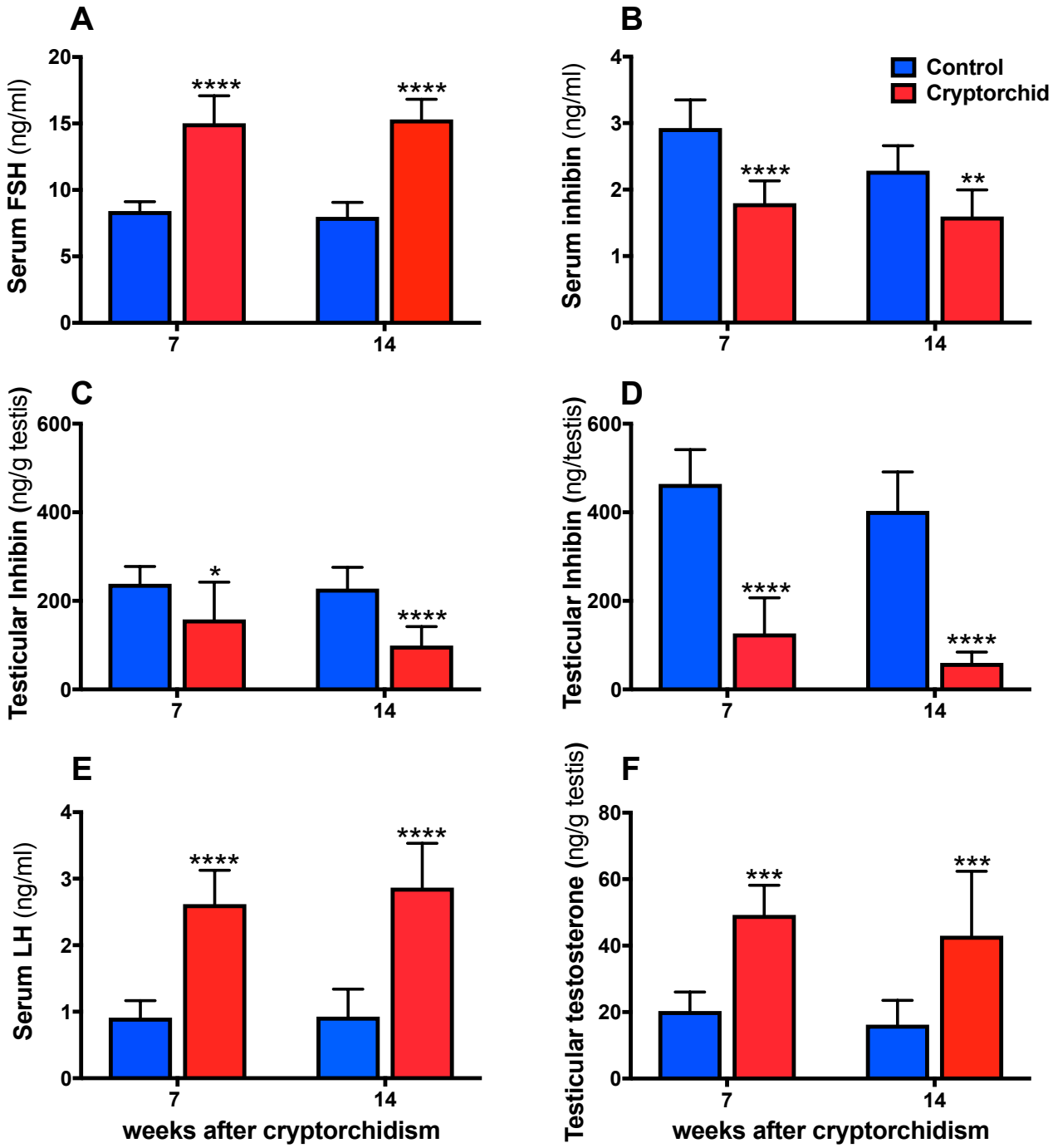
A
Serum FSH (ng/ml)
20
15
10
5
0
****
****
7
14
B
Serum inhibin (ng/ml)
4
3
2
1
0
****
**
7
14
Control
Cryptorchid
C
Testicular Inhibin (ng/g testis)
600
400
200
0
*
****
7
14
D
Testicular Inhibin (ng/testis)
600
400
200
0
****
****
7
14
E
Serum LH (ng/ml)
4
3
2
1
0
****
****
7
14
weeks after cryptorchidism
F
Testicular testosterone (ng/g testis)
80
60
40
20
0
***
***
7
14
weeks after cryptorchidism

Figure 4

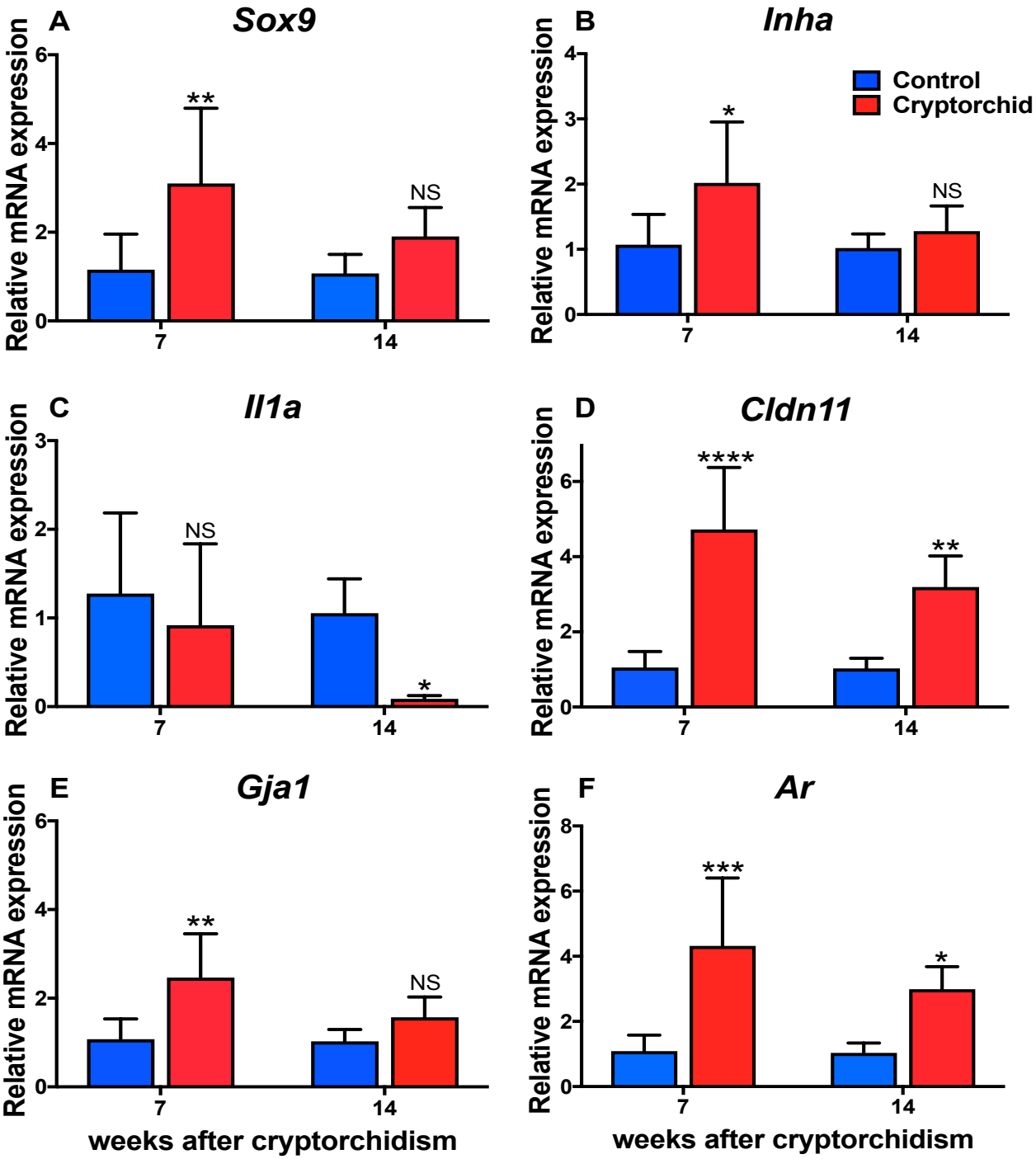
A
Sox9
Relative mRNA expression
**
NS
7
14
B
Inha
Control
Cryptorchid
*
NS
C
Il1a
NS
*
D
Cldn11
****
**
E
Gja1
**
NS
F
Ar
***
*
weeks after cryptorchidism

Figure 5

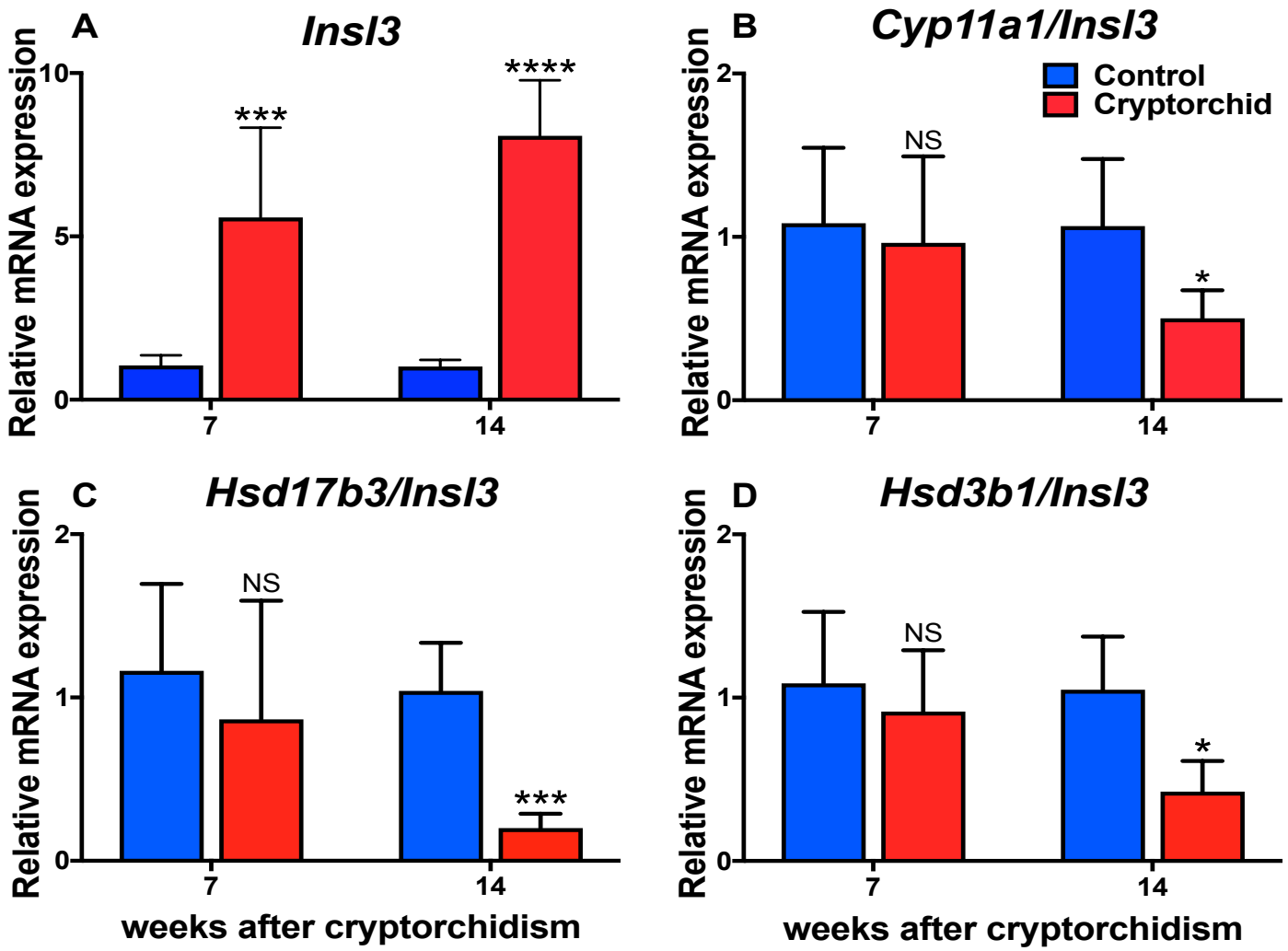
A
Insl3
Relative mRNA expression
10
5
0
***
****
7
14
B
Cyp11a1/Insl3
Control
Cryptorchid
Relative mRNA expression
2
1
0
NS
*
7
14
C
Hsd17b3/Insl3
Relative mRNA expression
2
1
0
NS
***
7
14
weeks after cryptorchidism
D
Hsd3b1/Insl3
Relative mRNA expression
2
1
0
NS
*
7
14
weeks after cryptorchidism

Figure 6

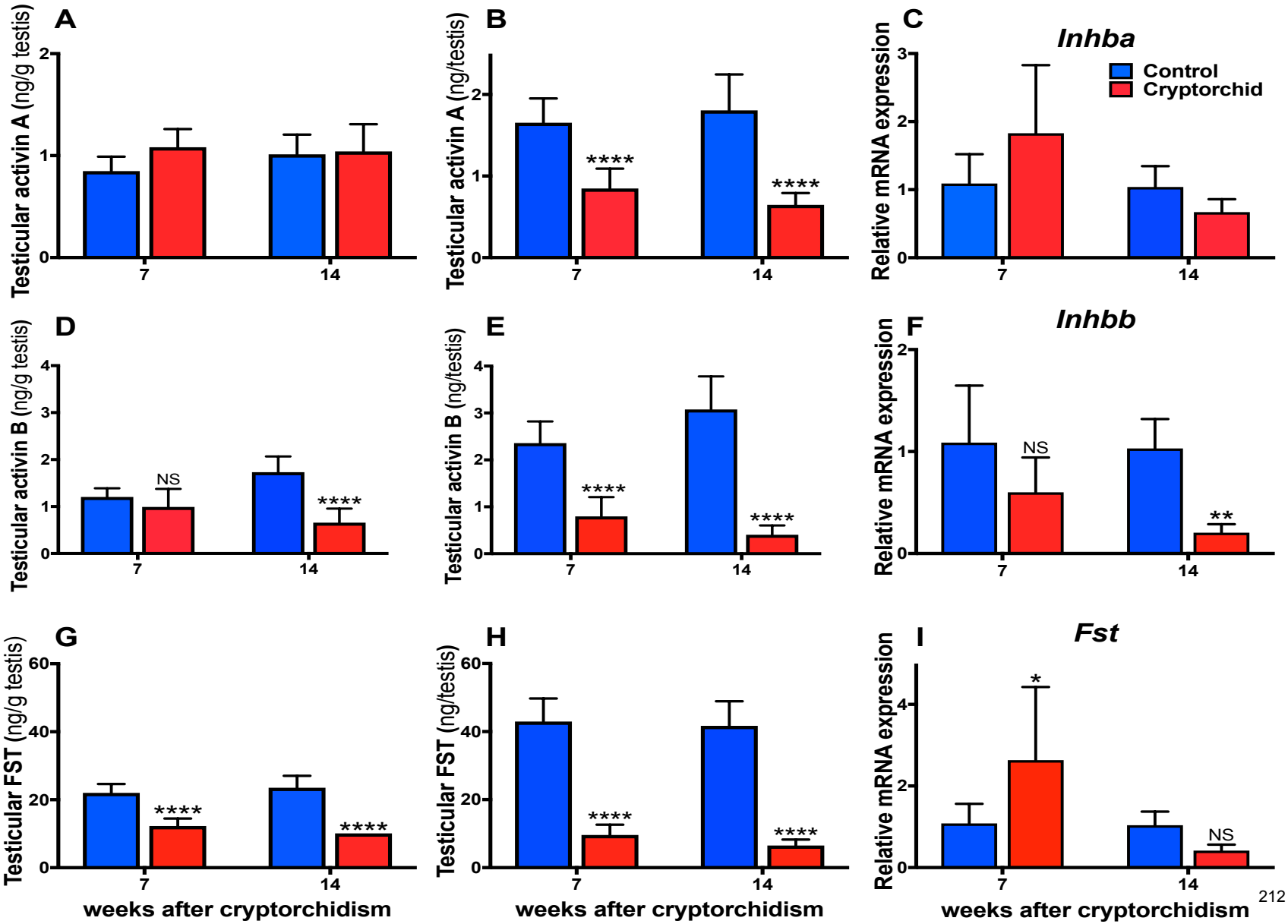
A
Testicular activin A (ng/g testis)
B
Testicular activin A (ng/testis)
C
Inhba
Relative mRNA expression
Control
Cryptorchid
D
Testicular activin B (ng/g testis)
NS
E
Testicular activin B (ng/testis)
F
Inhbb
Relative mRNA expression
G
Testicular FST (ng/g testis)
H
Testicular FST (ng/testis)
I
Fst
Relative mRNA expression
****
*
**
7
14
weeks after cryptorchidism

Figure 7

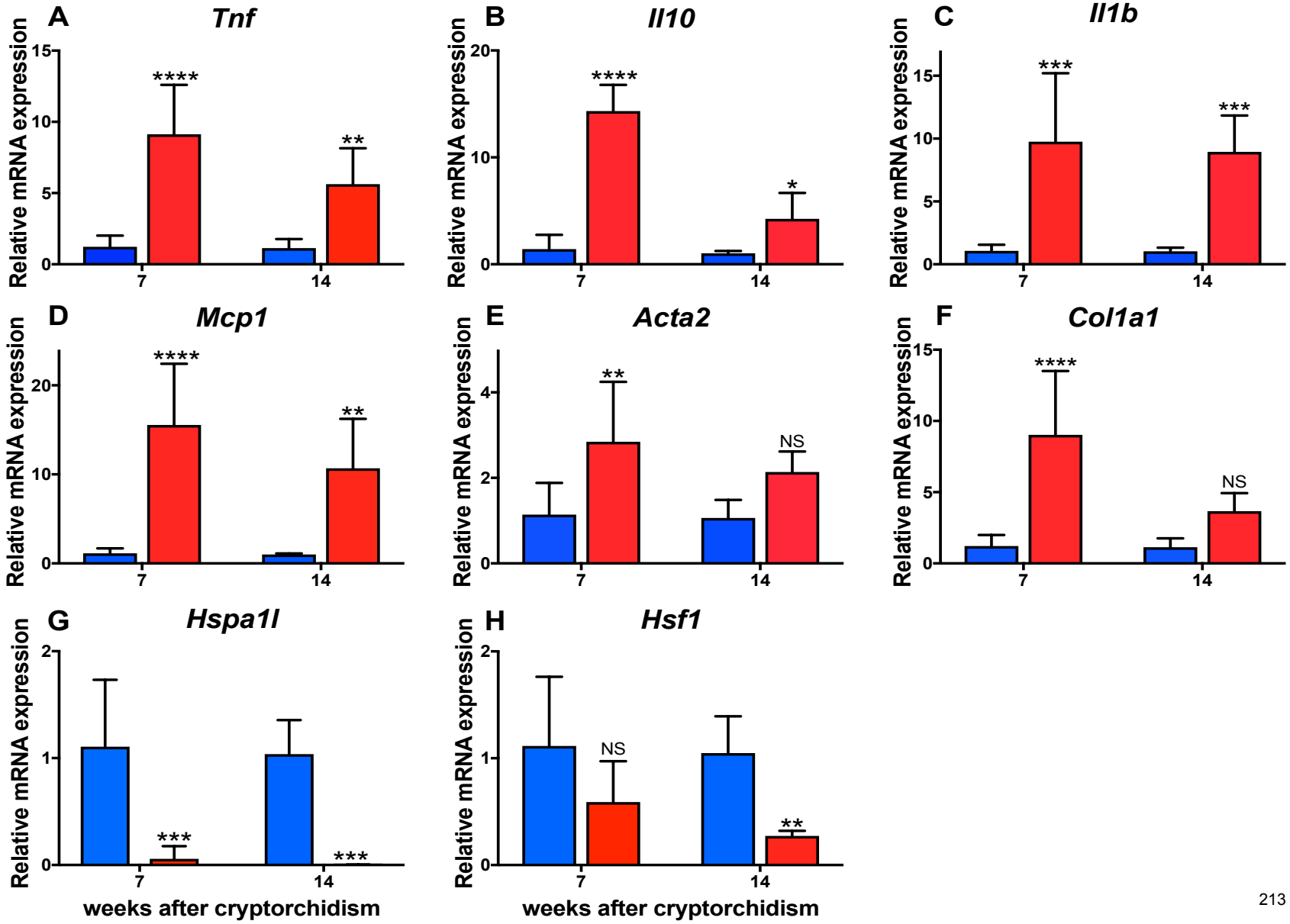
A
Tnf
B
Il10
C
Il1b
D
Mcp1
E
Acta2
F
Col1a1
G
Hspa1l
H
Hsf1
Relative mRNA expression
****
**
*
***
NS
7
14
weeks after cryptorchidism

5. Chapter 5:

General Discussion

These studies contribute to the field of andrology by extending our knowledge regarding the impact of short-term and long-term heat on the testis function, with particular emphasis on the response of activin/inhibin-related proteins and the functions of Sertoli and Leydig cells. They also involved investigation of heat-induced changes at the molecular level (for the first time) using TIF proteomic to provide new insights into the regulation of male reproduction.

The novel data presented in this thesis support the following conclusions and new hypotheses: 1) acute heat can cause persistent testicular damage that extends for at least two spermatogenic cycles in the rat; 2) mature spermatids may play a role in the regulation of activin B, since their loss following acute heat coincides with an elevation of testicular activin B production relative to activin A; 3) activin A is relatively maintained despite the complete loss of developing spermatogenic cells in cryptorchidism, but all other activin/inhibin-related proteins, including activin B, progressively decline; 4) acute heat induces multifunctional damage, as indicated by the changes in the TIF proteome that include fibril formation, cytoskeletal and spermatogenic regulation proteins; 5) acute and chronic heat treatment causes a loss of key gene expression in Sertoli and Leydig cells, which may be associated with germ cell loss; 6) the changes in Leydig cell function arising from exposure to acute or chronic heat may be triggered by local factors, such as TIMP1, produced by Sertoli cells and spermatogonia, thereby suggesting a potential role for this protein in intercellular communication; 7) reduction in spermatogonial-specific proteins in TIF following heat treatment indicates that these cells are potentially heat-sensitive, leading to longer term effects on spermatogenic recovery; 8) experimental cryptorchidism induces chronic inflammation in the testis, which may contribute to the progressive failure of the Sertoli and Leydig cells; 9) TIF is composed of numerous multifunctional and multicellular proteins (1728, in total, identified here), indicating that further study of these proteins would be a promising approach for identifying novel markers of male reproductive function.

These studies have confirmed and extended previously reported observations that heat stress causes spermatogenic damage in mammalian species with scrotal testis and that the severity of damage depends on the duration and intensity of the heat. The research using an experimentally

induced cryptorchid model (Chapter 4) showed that exposure of the testis to body temperature [37°C] caused a depletion of all germ cells except the spermatogonia and this depletion persisted for the duration of the cryptorchidism. In contrast, a single exposure to 43°C for 15 minutes (Chapter 2) induced the death of the heat-vulnerable germ cells, pachytene spermatocytes and round spermatids, within the first 2 weeks following heat treatment. Although spermatogenesis recovered in this model, as indicated by the increase in the testis weight at 12 weeks, testis weight was not completely restored at 14 weeks suggesting ongoing damage. This finding was further supported by the observation that germ cell-specific proteins in TIF were still suppressed at this timepoint (Chapter 3), even though the germ cells appeared histologically normal. However, testis weights did return to normal in earlier studies that investigated longer recovery times (17 and 21 weeks) in the same heat model (Au et al., 1987; Jegou et al., 1984). Overall, the present findings confirm that acute heat-treatment is detrimental to spermatogenesis and that the damage persists for two 49-day spermatogenic cycles in the rat.

The studies presented here are the first to document alterations in the activin/inhibin-related proteins after short-term and long-term heat exposures. Following acute heat-treatment (Chapter 2), activin A levels declined, but activin B increased after the loss of elongated spermatids. This increase may reflect a specific role of the mature spermatids in the control of activin B levels. Data in Appendix 1 indicate that activin B production is associated with spermatogenic stages XII-I suggesting that the elongating spermatids at these stages are involved. At least part of the reduction in activin A levels following acute heat treatemnt may be a consequence of germ cell depletion, since rat spermatocytes and spermatids express activin A but only low levels of activin B (Wijayarathna and de Kretser, 2016). The data from the cryptorchid model (Chapter 4) also confirm these findings, as they verify a reduction in levels of both activins when all germ cells, with the exception of spermatogonia, are depleted. The regulation of activin A in the testis is well characterised (Okuma et al., 2006; Winnall et al., 2013), but the regulation of activin B is poorly understood. These findings suggest for first time that elongated spermatids have a role in the regulation of activin B production.

A number of earlier reports using various experimental models have proposed the concept of intercompartmental communication in the testis (Bergh, 1982; Jegou et al., 1984; Rich and de Kretser, 1977; Rich et al., 1979; Risbridger et al., 1981a, 1981b). In these studies, the induction of unilateral spematogenic damage resulted in alterations in Leydig cell functions, suggesting the possibility that the seminiferous tubules influence Leydig cell function (Jegou et al.,1984; Risbridger et al., 1981a; Risbridger et al., 1981b). This possibility was supported by the observed restoration of normal Leydig cell function upon recovery of seminiferous tubule function (Bergh, 1982). Interestingly, Aoki and Fawcett (1978) observed that alterations in Leydig cell size were related to the stage of the seminiferous epithelium in the tubules adjacent to those cells, indicating that Leydig cell size was modulated by a tubular factor.

The nature of the factors responsible for this interaction between the two testicular compartments is unknown. However, the data from the acute heat-treatment model (Chapter 3) show an upregulation of TIMP1 in TIF at 8 weeks following testis exposure to acute heat, when the initial damage to Leydig cell function has been reversed. TIMP1, which is predominantly expressed by Sertoli cells and spermatogonia in the testis, has been reported to exert a modulating influence on the Leydig cell by stimulating steroidogenesis. Therefore, a working hypothesis would be that the secretion of TIMP1 triggers the steroidogenic activity of the Leydig cell, which had been disrupted by exposure to acute heat. Although the precise time point at which steroidogenic gene expression was most reduced (2 weeks) was not investigated with regard to TIF proteins, the TIMP1 levels would be expected to increase afterwards. The proteomic approach used in the present study supports the concept that the two compartments of the testis are functionally interdependent.

The proteomic analyis of TIF (Chapter 3) demonstrated the existence of a great number of multifunctional and multicellular proteins (1728 proteins) in TIF, thereby supporting the idea that TIF analysis may be a useful method for studying spermatogenesis and male reproduction. In particular, this proteomic approach provides a practical means to identify signalling pathways between compartments in the normal testis and to assess the effect of alterations in a single cell type

on the functions of other cell types. Generally, this strategy could assist in the evaluation of the cellular and molecular processes pertinent to testicular disease and infertility. A recent study showed a homology of >80% between the TIF proteins and the human plasma proteome, indicating the occurrence of a ready exchange of proteins between these biological fluids (Stanton et al., 2016).

Acute heat treatment leading to selective germ cell damage caused a disruption of 209 of the total identified proteins in TIF. The data show that acute heat causes extensive functional damage through the modulation of 12% of the total TIF proteins. In the heat-stressed rat testis, 40% of disrupted proteins were downregulated and remained downregulated even after 14 weeks, suggesting that acute heat exposure is detrimental to the testis for a long period. These changes in multifunctional proteins also provide information about the response of the tissue to damage, as the majority of the proteins with reduced expression at 14 weeks were germ cell-specific and play essential roles in spermatogenesis (e.g. BAG6, HSPA2, NASP, SPATA20 and CABS1). Underexpression of BAG6 and HSPA2 has also been reported in the sperm proteomes of infertile men, indicating that these proteins may contribute to male infertility (Intasqui et al., 2018). Testicular NASPs serve as a functional bridge between linker histones and cell cycle progression during meiosis in the mouse testis (Alekseev et al., 2009). The knockdown of human testicular NASP suppresses cell proliferation and leads to cell cycle arrest (in the G1 phase) via the ERK/MAPK signalling pathway (Fang et al., 2015). A lack of SPATA20 results in sperm deformation, and therefore male infertility, in mice (Liu et al., 2018). CABS1 is involved in the intricate structural rearrangements in postmeiotic germ cells during spermiogenesis (Calvel et al., 2009). Other important functions that are affected by acute heat treatment as revealed by proteome analysis were fibril formation, Sertoli cell cytoskeleton regulation, heat shock protein stabilisation and oxidative stress.

The studies presented in this thesis provide evidence that the duration of heat exposure determines the nature of the tissue response. The data from the acute heat-treatment model (Chapter 2) do not indicate an inflammatory reaction in the testis after a short-term heat treatment, whereas

cryptochidism was characterised by chronic inflammation as indicated by a large upregulation in inflammatory cytokines. This study is the first to document chronic inflammation in a cryptorchid animal model. Increased immune cell infiltration was not evident, but the persistence of the elevated expression of the genes coding for pro-inflammatory mediators (e.g. *Tnf*, *Il10*, *Il1b* and *Mcp1)* and fibrosis for 14 weeks suggest that the intratesticular immune cells are activated. Activin A is also a marker of inflammation in most tissues (Hedger et al., 2011). Although activin A was not increased, it did not decline, in spite of the loss of testicular somatic cells function and absence of germ cells. This maintenance may have been due to the ongoing inflammatory environment. It would be interesting to investigate the composition and function of the intratesticular leukocyte population in this condition.

This inflammatory response has not been reported previously in other animal models of cryptorchidism, although an elevation in the serum level of IL-6 was observed in cryptorchid boys aged 1–14 years (Imamoğlu et al., 2012). However, no changes were observed in the expression of interleukin-6 at any time point in the present study. This finding indicates that IL-6 may not be a reliable marker of inflammation in the testis, at least in the cryptorchid condition. Furthermore, the data indicate that the causes of suppression of Sertoli and Leydig cell function are different in the acute and chronic models. The acute heat model reflects the role of spermatogenic cells in regulating somatic cell function, whereas the chronic model illustrates the effect of persistent inflammation on the function of these cells.

Future directions, speculations and conclusions

The production of activin A by Sertoli cells, meiotic and post-meiotic germ cells and other interstitial cells is well documented (Hedger and Winnall, 2012); however, little is known about the production of activin B. The data in this thesis have highlighted the role of post-meiotic germ cells in activin B regulation, but further studies should be performed to investigate activin B biology in the testis.

The proteomic analysis of TIF is powerful technique that provides new insights into the regulation of spermatogenesis and intercellular communication.. This analysis showed evidence for the persistence of testicular damage for 14 weeks following acute heat exposure. A more complete understanding of the effects of the duration of heat damage in the testis could be gained by assessing further timepoints using this proteomic method. The data from this thesis also point to a need to raise awareness, especially among males suffering from poor fertility, regarding the deleterious impacts of prolonged heat exposure of the testes on fertility.

This proteomic study identified 1728 multifunctional and multicellular proteins in the TIF, which may assist in identifying novel markers for male infertility since the TIF proteins are 80% similar to blood plasma proteins. Further mechanistic studies could provide information about the pathways in which these proteins are involved, thereby advancing our understanding of male reproduction.

Finally, the presence of chronic inflammation subsequent to experimental cryptorchidism documented in this thesis has not been reported previously. Hence, in-depth investigations into the inflammatory responses in cryptorchidism may aid in the diagnosis of male infertility. Treatment of this infertility condition with anti-inflammatory agents may also minimise the impact of cryptorchidism damage.

6. Appendices

6.1. Appendix (App.) 1: Activin B regulation throughout the seminiferous tubule stages

Materials and Methods

Animals

Adult male Sprague–Dawley rats (approximately 10 weeks old, n=8) were obtained from the Central Animal House (Monash University, Victoria, Australia), and maintained at 20 C in a fixed 12-h light, 12-h dark cycle with free access to food and water. Rats were euthanised by CO2 asphyxiation, and testes were removed for seminiferous tubules. All studies were approved by the Monash University Animal Ethics Committee and conformed to the Australian Code of Practice for the Care and Use of Animals for Experimental Purposes.

Seminiferous tubule (ST) dissection and staging

Seminiferous tubules were isolated form the testes as described previously (Okuma et al., 2006). Briefly, testes were decapsulated immediately post-mortem and individual tubules were isolated using fine forceps under sterile conditions in a Petri dish containing Dulbecco's modified Eagle's medium (DMEM), under an Olympus SZX12 transillumination inverted stereomicroscope (Olympus, Tokyo, Japan). Tubules were staged according to the 14-stage classification (I–XIV) for rat spermatogenesis (Leblond & Clermont 1952), using the transillumination identification criteria of Parvinen and colleagues (Parvinen & Ruokonen 1982) and cut into 2 mm long fragments. Immediately after dissection, tissues were collected for two analyses: activin B measurement by ELISA, RNA (as detailed below).

Protein extraction and sample preparation

ST tubule fragements were weighed and homogenised in cold PBS (0.01M, pH 7.4) containing 1:200 protease inhibitor (PI) cocktail III (CalBiochem, La Jolla, CA), using a TissueLyser II (Qiagen) for 20 seconds. A mixture (PBS & PI) volume was equal to 10 times of the

net weight of the tissue. The homogenates then were centrifuged (14,000 x g) for 10 minutes to collect the supernatants for protein measurement.

Activin B ELISA

ST tubules concentrations of activin B were measured, as described previously (Ludlow et al., 2009), using antibodies kindly supplied from Oxford Brookes University, and validated for measurement of mouse tissues. The limit of detection was 22.95 pg/mL. The mean inter-assay CV was 10% and the mean intra-assay CV was 7%.

RNA Extraction, Reverse Transcription, and Fluidigm Biomark™ HD Real-Time PCR

Fluidigm analysis was performed, as described previously (Aldahhan et al., Chapter 2). Briefly, Total RNA was isolated from snap-frozen ST fragments/stage with β-mercaptoethanol (14.3M, Sigma-Aldrich, MO, USA) and Rneasy kit (Qiagen, Venlo, Netherlands) followed by DNase treatment by the RNase-Free DNase set (Qiagen), according to the manufacturer's protocols. Synthesis of cDNA from RNA was performed using a Tetro cDNA synthesis kit (Bioline, Tauton, MA, USA), according to the manufacturer's instructions. Quantitative digital PCR was carried out with Taqman® Gene Expression Assays (Life Technologies, CA, USA) using the Integrated Fluidic Circuits on the Biomark™ HD platform (Fluidigm, CA, USA). The TaqMan gene expression assays are listed in Table 1 (Aldahhan et al., Chapter 4). Data were analysed by Fluidigm Real-Time PCR Analysis software (version 4.12). The mean of each duplicate Ct value from each reaction was converted into ΔΔCt values using the housekeeping *Rn18s* gene, and then into 2(-ΔΔCt). A single 2(-ΔΔCt) value from the control group for each time-point was selected as a reference against which the other samples were compared. This provided the fold increase for the gene in question relative to the housekeeping gene. The average fold change is expressed as the mean fold increase of the gene relative to *Rn18s* and standard deviation (SD).

Results

App. Figure 1. Activin B content measured in homogenates of isolated staged tubules. Values are for homogenates of pooled 30 fragments from each stage in a final extract volume of 0.15 ml. The broken line indicates the detection limit of the assay. Data are mean (n = 8 animals).

App. Figure 2. The relative expression of activins and activin-related mRNA: *Inha* (A), *Inhba* (B) *Inhbb* (C) and *Fst* (D) throughout the stages of ST cycle. Data are mean (n = 8 animals).

App. Figure 3. The relative expression of Sertoli cell-specific mRNA: *Sox9* (A), *Il1a* (B), the blood testis barrier proteins, *Cldn11* (C) and *Gja1* (D), and the androgen receptor (*Ar*) (E) and keratin 18 (*Krt18*) (F) throughout the stages of ST cycle. Data are mean (n = 8 animals).

App. 1 Figure 1

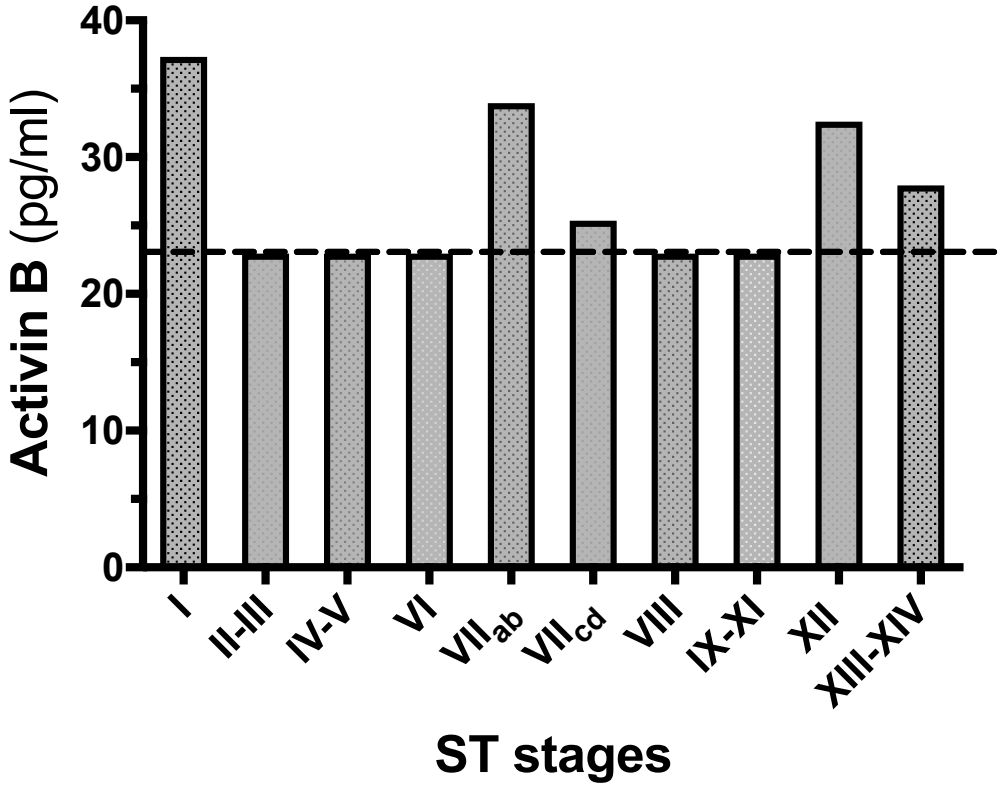

App. 1 Figure 2

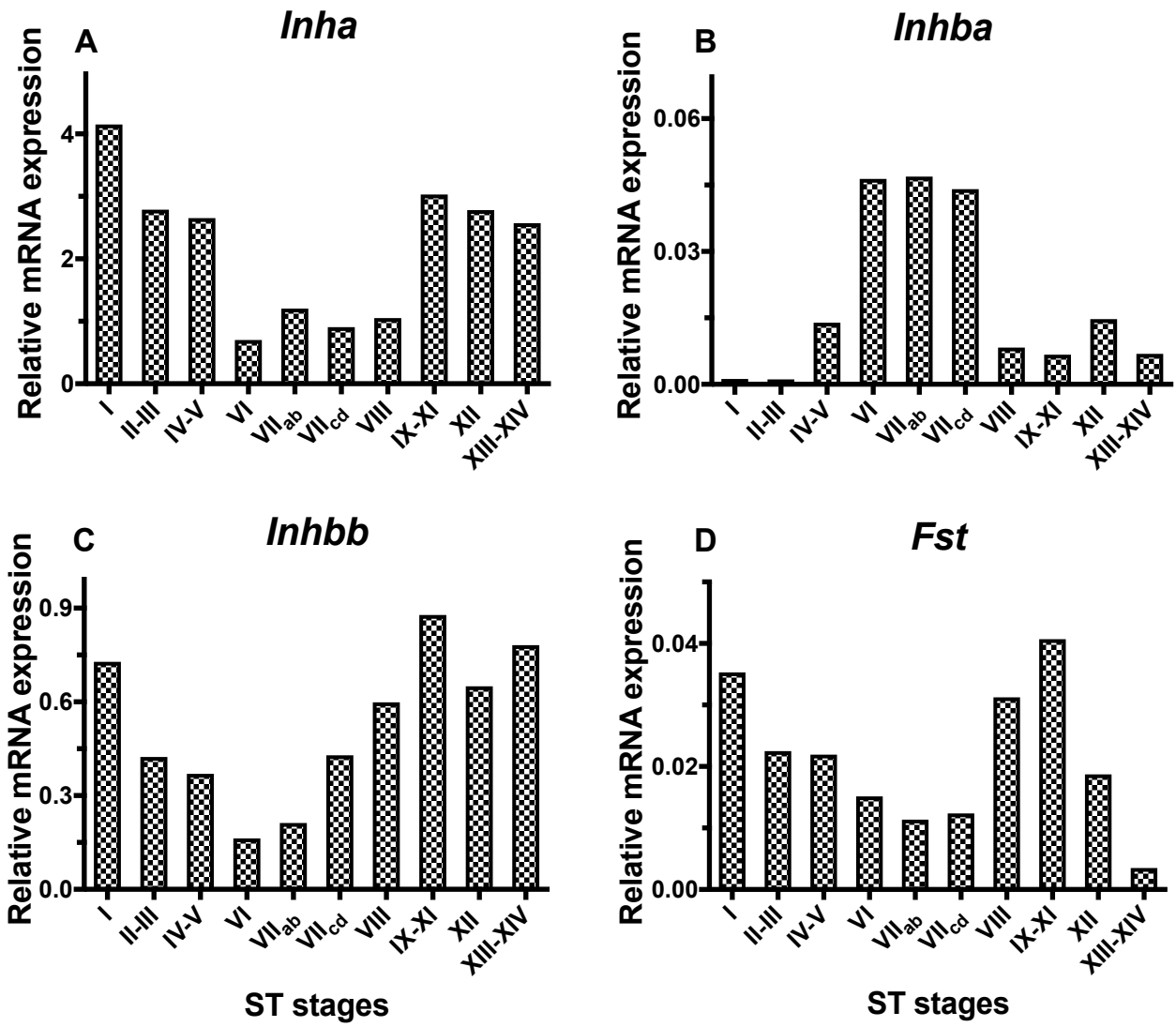

App. 1 Figure 3

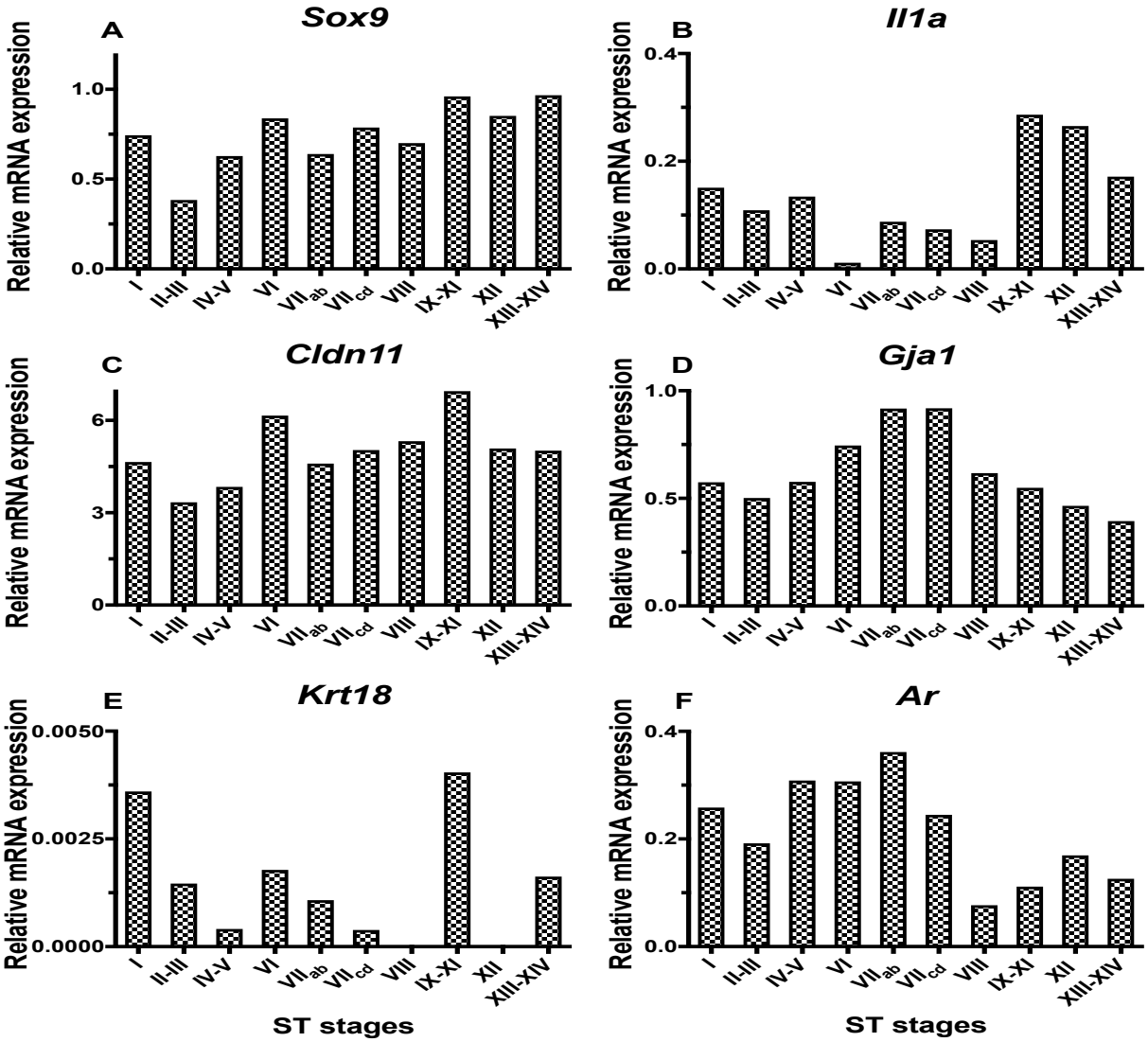

6.2. Appendix 2:

Published version of Chapter 2

Molecular and Cellular Endocrinology 498 (2019) 110546

Contents lists available at ScienceDirect

Molecular and Cellular Endocrinology

journal homepage: www.elsevier.com/locate/mce

Acute heat-treatment disrupts inhibin-related protein production and gene expression in the adult rat testis

Rashid A. Aldahhan[a,b,c,*], Peter G. Stanton[a,b], Helen Ludlow[d], David M. de Kretser[a,b], Mark P. Hedger[a,b]

[a] Centre for Reproductive Health, Hudson Institute of Medical Research, Clayton, Victoria, Australia
[b] Department of Molecular and Translational Sciences, Monash University, Clayton, Victoria, Australia
[c] Department of Anatomy, College of Medicine, Imam Abdulrahman Bin Faisal University, Dammam, Saudi Arabia
[d] Oxford Brookes University, Oxford, UK

ARTICLE INFO

Keywords:
Spermatogenesis
Heat stress
Sertoli cell
Activins
Steroidogenesis

ABSTRACT

Heat reversibly disrupts spermatogenesis, but the effects on Sertoli cell (SC) function and inhibin/activin-related proteins are less well-defined. Adult rat testis weights decreased by 40% within 2 weeks after heat-treatment (43 °C, 15 min), due to loss of pachytene spermatocytes and round spermatids. Coincident effects were reduced SC nuclear volume at one week and > 50% reduction in expression of several critical SC genes (*Inha*, *Cld11*, *Gja1*, *Tjp1*, *Cldn3*) by 2 weeks. Leydig cell steroidogenic enzymes, *Cyp11a1*, *Hsd3b1*, were also reduced. Activin gene expression was unaffected at this time, but expression of the activin-binding protein, follistatin (*Fst*), increased > 2-fold. At 4–8 weeks, coincident with the recovery of spermatocytes and early spermatids, but progressive loss of elongated spermatids, most SC genes had recovered; however, testicular activin A was reduced and activin B increased. At 8 weeks, serum inhibin was decreased and, consequently, serum FSH increased. Crucially, germ cell damage was not associated with a significant inflammatory response. At 14 weeks, most testicular parameters had returned to normal, but testis weights remained slightly reduced. These data indicate that, following acute heat-treatment, expression of several key Sertoli and Leydig cell genes declined in parallel with the initial loss of meiotic germ cells, whereas activins were responsive to the subsequent loss of mature spermatids, leading to an increase in testicular activin B production relative to activin A.

1. Introduction

In most mammals, the testes descend during prenatal or early neonatal life to reside in the scrotum, where the temperature is 2–7 °C lower than the core body temperature. Spermatogenesis is a temperature-sensitive process, and elevation above the normal scrotal temperature range can cause the death of heat-sensitive spermatogenic cells (Durairajanayagam et al., 2014). Elevated scrotal temperature is considered to be a major contributor to male factor infertility (Durairajanayagam et al., 2014; Hou et al., 2015). The sources of heat stress that adversely impact testis function include: (1) lifestyle and behavioural factors, such as clothing, hot baths and saunas, (2) occupational and environmental exposure to radiant and ambient heat, and (3) pathophysiological factors, such as cryptorchidism, fever and varicocele (Durairajanayagam et al., 2014).

Quantitative analysis in rats (Chowdhury and Steinberger, 1970; Bowler, 1972) and mice (Gasinska and Hill, 1989; Paul et al., 2008) has demonstrated that the germ cells most acutely susceptible to heat are pachytene spermatocytes and round spermatids at stages I–IV and IX-XII and the diplotene and differentiating primary or secondary spermatocytes at stages XII-XIV; similar stages are affected by heat in the human testis (Carlsen et al., 2003; Wang et al., 2007). In contrast to the meiotic and post-meiotic germ cells, spermatogonia appear to be relatively resistant to the detrimental effects of heat (McLean et al., 2002), which have been linked to oxidative stress and DNA damage (Houston et al., 2018). Sertoli and Leydig cell functions are also affected by heat (Jegou et al., 1984; Au et al., 1987; Bergh and Söder, 2007; Vallés et al., 2014). Changes documented in earlier studies include decreased production of seminiferous tubule fluid, androgen binding protein (ABP) and inhibin bioactivity by the Sertoli cells, as well as Leydig cell hypertrophy and hyper-responsiveness to stimulation (Jegou et al., 1984). These alterations in Sertoli and Leydig cell function occur subsequent to

* Corresponding author and present address: Department of Anatomy, College of Medicine, Imam Abdulrahman Bin Faisal University, Dammam, Saudi Arabia P.O. Box 1982, Dammam, 31441, Saudi Arabia.
E-mail address: raaldahhan@iau.edu.sa (R.A. Aldahhan).

https://doi.org/10.1016/j.mce.2019.110546
Received 11 January 2019; Received in revised form 9 August 2019; Accepted 15 August 2019
Available online 15 August 2019
0303-7207/

the spermatogenic cell damage and appear to be a response to the loss of the germ cells. However, the responses of the Sertoli and Leydig cells to a brief episode of heat have not been closely investigated at the gene expression level.

The disruption of the testis, in turn, causes increased serum FSH due to decreased feedback from testicular inhibin (Jegou et al., 1984; Au et al., 1987). Inhibin, which is a heterodimer of homologous α- and β-subunits, blocks FSH secretion by antagonising the action of activins within the anterior pituitary. Activin A and B are homodimers of the inhibin β-subunits that stimulate FSH production and secretion by pituitary gonadotrophs (de Kretser et al., 2002; Hedger et al., 2011). The activins are also implicated in the local regulation of testis function. Activin A plays a crucial role in the development and activity of male germ cells and Sertoli cells (Meehan et al., 2000; de Kretser et al., 2002; Barakat et al., 2012). In the adult rat testis, activin A is produced primarily by Sertoli cells, but also by meiotic and post-meiotic germ cells, Leydig cells and interstitial macrophages (Hedger and Winnall, 2012). It appears to have a critical role in the regulation of spermatogonial stem cells, spermatocytes and Sertoli cell tight junctions during the restructuring of the seminiferous epithelium, particularly at stages VIII to XI of the rat spermatogenic cycle immediately after spermiation (Okuma et al., 2006; Nicholls et al., 2012). Activin A is also a key regulator of inflammation and immunity throughout the body (Jones et al., 2007; Hedger et al., 2011) and may be either pro-inflammatory or anti-inflammatory, depending on the setting within the immune response (Wijayarathna and de Kretser, 2016; Hedger et al., 2011). Activin A is also an essential mediator of fibrosis, since it regulates fibroblast development and differentiation into myofibroblasts (Hedger et al., 1989; Ohga et al., 1996; Yamashita et al., 2004).

In contrast to activin A, the role of activin B in the regulation of testis function is poorly defined. The inhibin/activin βB-subunit is produced by the Sertoli cell, where it typically dimerises with the α-subunit to form inhibin B (de Kretser et al., 2002; Hedger and Winnall, 2012). Until recently, studies on activin B actions in the testis have been limited due to the absence of suitable immunoassays for the activin B homodimer. Bioactivity of the activins is regulated by inhibin and by the activin-binding protein, follistatin, which is widely expressed by testicular somatic and germ cells (Meinhardt et al., 1998; Phillips and de Kretser, 1998).

While some previous studies have investigated inhibin production following heat-induced damage of the testis (Lue et al., 2002; Gao et al., 2012), the corresponding response of the activins and follistatin have not been investigated. At the time the earlier studies were performed, assays were not yet available for measurement of the activins or follistatin, nor had modern analytical techniques for mRNA expression been developed. Consequently, we set out to define the changes that occur in the inhibin-related proteins in the testis and serum in response to acute heat-treatment, their relationship with changes in gene expression by the Sertoli cells, Leydig cells and other testicular cells, and their relationship with markers of heat-stress and inflammation.

2. Materials and methods

2.1. Animals and tissue collection

Adult male outbred Sprague-Dawley rats (10 weeks old, weight range 250–350 g) were obtained from Monash Animal Services (Monash University, Clayton, Australia), and randomly assigned to one of two experimental groups: control and heat-treatment. Both groups were anaesthetised with intraperitoneal ketamine (40 mg/kg) and xylazine (5 mg/kg). The rats undergoing heat-treatment had their lower abdomen and scrotum immersed in a water-bath at 43 °C for 15 min under anaesthesia. Controls were maintained at ambient room temperature for the same period of time. All rats were allowed to recover, and were maintained at 20 °C in a fixed 12-h light, 12-h dark cycle with free access to food and water for up to 14 weeks. Groups of control and heat-treated rats were killed for evaluation at 1, 2, 4, 8, 12, and 14 weeks post-treatment (n = 7 rats/treatment group at each time-point). All procedures were approved by the Monash Medical Centre Animal Ethics Committee.

2.2. Tissue handling and preparation

At each time point, control and heat-treated rats were anaesthetised as described above, and blood was collected by cardiac puncture. Following exsanguination, the testes were dissected out, weighed, and processed for histology, RNA and protein measurement, or collection of testicular interstitial fluid (see details below). Testes collected for histology (from 4 separate rats) were immersed intact in Bouin's fixative (Amber Scientific, Midvale, WA, Australia) for 24 h, then stored in 70% ethanol. Tissues for RNA or protein extraction (from 6 separate animals) were snap-frozen in dry ice and stored at −80 °C. Blood was allowed to clot and was centrifuged at 4000 × *g* for 15 min and the separated serum was stored at −20 °C.

Testicular interstitial fluid (TIF) was collected (from 4 separate rats), as described previously (Sharpe and Cooper, 1983; Stanton et al., 2016). Briefly, a 2–4 mm incision was made in the tunica at the distal pole, and the testis was suspended on a thin needle placed through the tunica at the opposite pole in a 15 mL tube above 20 µL phosphate-buffered saline (0.01M PBS, pH 7.4) containing complete protease inhibitor cocktail (Roche, Castle Hill, Sydney). The TIF was then collected by percolation overnight at 4 °C, ultra-centrifuged (109,000 × *g*, 60 min, 4 °C) and the supernatant was snap-frozen and stored at −80 °C.

2.3. Tissue processing and histological staining

Bouin's-fixed tissues were processed for routine histology and embedded in paraffin. Organs were sectioned at 5 µm and attached to Superfrost Plus Glass slides (BioLabs Scientific, Melbourne, Australia). Sections were stained with periodic acid–Schiff reagent (PAS) for histological examination and staging of spermatogenesis.

2.4. Immunohistochemistry

Immunohistochemical localisation the Sertoli cell-specific marker, Sox9, was performed as described previously (Wu et al., 2017). In brief, heat-mediated antigen retrieval was performed in 10 mM citrate buffer (pH 6), and normal goat serum (5%) was used to block non-specific binding. Sections were incubated overnight at 4 °C with rabbit antiSox9 polyclonal antibody (SC-20095, Santa Cruz Biotechnology, Inc., CA, USA), while negative controls were incubated with matched rabbit immunoglobulins (IgG). Signal detection was with Vectastain ABC kit reagents (Vector laboratories, Inc., Burlingame, CA, USA) (30 min, room temperature) followed by diaminobenzidine (DAB) (Dako North America, Inc., Carpinteria, CA, USA) and colour development was monitored under the microscope.

2.5. Terminal deoxynucleotidyl transferase dUTP nick end labelling (TUNEL) assay

The Apoptag peroxidase *in situ* apoptosis detection kit (Millipore Corporation, Billerica, MA, USA) was used to identify cells undergoing apoptosis. Testis sections were incubated with terminal deoxynucleotidyl transferase (TdT) enzyme, whereas PBS was added to negative control sections. The casein-blocking solution CAS-block™ (Life Technologies, Frederick, MD, USA) was added to the sections for 30 min, prior to colour development using DAB. For the quantification of apoptosis, areas of cross-sectioned testes were selected at random, and examined using a 20x objective lens on an Olympus B × 50 microscope (Olympus Corp., New York, NY, USA). The number of tubules containing TUNEL-positive apoptotic cells and the number of apoptotic cells per field were counted. A total of 100 tubules per testis were

Table 1
List of Taqman assays used.

Protein name	Gene symbol	Life Tech assay code	Main cell sites of expression in testis
Glyceraldehyde-3-phosphate dehydrogenase	*Gapdh*	Rn01775763_g1	All cells
Succinate dehydrogenase complex flavoprotein subunit A	*Sdha*[a]	Rn00590475_m1	
18S ribosomal RNA	*Rn18s*[b]	Designed	
Inhibin βA-subunit	*Inhba*	Rn01538592_m1	Somatic cells and germ cells
Inhibin βB-subunit	*Inhbb*	Rn01753772_m1	
Follistatin	*Fst*	Rn00561225_m1	
Heat shock factor 1	*Hsf1*	Rn00801772_m1	
α smooth muscle actin	*Acta2*	Rn01759928_g1	
Collagen 1α type 1	*Col1a1*	Rn01463848_m1	
SRY box 9	*Sox9*[b]	Rn01751070_m1	Sertoli cells
Inhibin α subunit	*Inha*	Rn00561423_m1	
Claudin 11	*Cldn11*	Rn00584941_m1	
Interleukin 1α	*Il1a*	Rn00566700_m1	
Claudin 3	*Cldn3*[a]	Rn00581751_s1	
Hydroxy Δ5 steroid dehydrogenase 3β and steroid δ isomerase 1	*Hsd3b1*	Rn01774741_m1	Leydig cells
Hydroxysteroid 17- β dehydrogenase 3	*Hsd17b3*	Rn00588942_m1	
Cytochrome P450 family 11 subfamily a polypeptide 1	*Cyp11a1*	Rn00568733_m1	
Heat shock protein 70-1	*Hspa1a*	Rn02532795_s1	Spermatogonia
Heat shock protein 70-2	*Hspa1b*	Rn04224718_u1	
Hypoxanthine phosphoribosyltransferase	*Hprt*[a]	Rn01527840_m1	Somatic cells and germ cells
Zonula occludens 1	*Tjp1*[a]	Rn02116071_s1	
Connexin 43	*Gja1*	Rn01433957_m1	
Keratin 18	*Krt18*[b]	Rn01533360_g1	
Crystallin alpha B	*Cryab*[b]	Rn01421541_m1	Sertoli and Leydig cells
Heat shock protein 70-3	*Hspa1l*	Rn01525984_m1	Spermatocytes and round spermatids
Interleukin 6	*Il6*	Rn01410330_m1	Activated immune cells (somatic cells and germ cells)
tumour necrosis factor	*Tnf*	Rn99999017_m1	
Androgen receptor	*Ar*	Rn00560747_m1	Somatic cells only

[a] Indicates genes used in the in vivo study only.
[b] In vitro study only. Includes data from Chalmel et al. (2007), Gérard et al. (1991) and a searchable GermOnline database (Lardenois et al., 2010).

counted, moving across each section in a systematic manner.

2.6. Stereological techniques

Tubules containing Sox9-positive nuclear profiles were counted in a systematic manner by use of a 40x objective. Nuclear diameters were calculated using the freehand polygon tool of the cellSens Dimension software 1.7.1 (Olympus Corp.). The numerical density of nuclei associated with an immunopositive cell profile *(Nv)* was calculated as described (Abercrombie, 1946), in order to compensate for changes in nuclear size, as previously described (Wang et al., 1994).

Nuclear profiles were counted in 20 tubules per animal at all timepoints. Nuclear diameters for each immunopositive cell in the one week treatment group were calculated from 50 randomised nuclear profiles/animal. In order to eliminate under-estimation of nuclear diameters due to the presence of glancing sections of nuclear profiles, only the average of the upper 30% of diameter estimates/animal (i.e., the maximum observed diameter) was calculated. Section thickness was assumed to be as set (5 μm), and minor dimensional changes as a result of tissue processing or sectioning were ignored for the purposes of this study.

2.7. In vitro studies

2.7.1. Sertoli cell isolation and culture

Sertoli cells were isolated from 19 to 21 day-old Sprague-Dawley rats, as previously described (Nicholls et al., 2013). Briefly, isolated cells were plated at a density of 2.5×10^6 cells per cm^2 into 24-well culture plates (Nunc; Nalge Nunc International, Roskilde, Denmark) precoated with Matrigel (BD Biosciences, Bedford, MA). Cells were cultured in DMEM/Hams F12 (Gibco, Carlsbad, CA), supplemented with 2.5 mM L-glutamine, 29 mM sodium bicarbonate, non-essential amino acids, dialysed bovine serum albumin (1% w/v, Sigma, St. Louis, MO), HEPES (10 mM, Gibco), insulin (5 μg/mL, Novo-Nordisk, Sydney, Australia), transferrin (5 μg/mL, Sigma), sodium selenite (50 ng/mL, Sigma), Amphotericin B/Penicillin/Streptomycin (Gibco), human FSH (150 mIU/mL, Puregon, N.V. Organon), testosterone (28 ng/mL, Sigma) and retinoic acid (100 nM, Sigma). Cells were then incubated at 32 °C in a humidified 5% CO2/95% air incubator with a medium change at 48 h. At 72 h, contaminating germ cells were removed by hypotonic shock treatment with 10% culture media in water for 45 s (Sluka et al., 2006), after which Sertoli cells were allowed to recover for a further 24 h at 32 °C, 5% CO_2/95% air.

2.7.2. In vitro hyperthermia

Culture dishes containing the isolated Sertoli cells were sealed with paraffin film, placed for 15 min in a 43 °C water bath for 15 min, to replicate the in vivo heat-treatment protocol, and then returned to the incubator at 32 °C. Culture dishes maintained at 32 °C were used as the corresponding controls. The conditioned culture medium was collected at three time-points, 6, 24 and 48 h after heating, and snap frozen for protein quantification, and the attached cells were processed for mRNA and protein measurements.

2.8. RNA measurements

Fluidigm analysis was performed as described previously (Bienvenu et al., 2017). Briefly, fragments of snap-frozen testes and isolated Sertoli cells were homogenised using the Qiagen TissueLyser II and stainless steel beads (Qiagen GmBH, Hilden, Germany). Total RNA was isolated using an RNeasy kit (Qiagen, Venlo, Netherlands) followed by DNase treatment by the RNase-Free DNase kit (Qiagen), according to the manufacturer's protocols. Synthesis of cDNA from RNA was performed using a Tetro cDNA synthesis kit (Bioline, Tauton, MA, USA), according to the manufacturer's instructions.

Quantitative digital PCR was carried out with Taqman® Gene Expression Assays (Life Technologies, CA, USA) using the Integrated Fluidic Circuits on the Biomark™ HD platform (Fluidigm, CA, USA). The TaqMan gene expression assays used for the testes and isolated Sertoli cells are listed in Table 1. All assays were available from the

manufacturer except *Rn18s* TaqMan assays, which were designed as the following: forward (5′-GGAGAGGGAGCCTGAGAAAC-3′), reverse (5′-CAATTACAGGGCCTCGAAAG-3′) and probe (CCACTCCCGACCC). Initially, three housekeeping genes per tissue source were evaluated: *Gapdh, Hprt* and *Sdha* for the testis and *Gapdh, Rn18s* and *Cryab* for the isolated Sertoli cells. From these, the *Hprt* (whole testis extracts) and *Rn18s* (isolated Sertoli cells) genes were the most stably expressed across all time-points and treatments and were used as controls. Data were analysed by Fluidigm Real-Time PCR Analysis software (version 4.12). The mean of duplicate Ct values from each reaction was converted into ΔΔCt values, from which the average fold change was expressed as the mean fold increase ± standard deviation (SD) of the gene relative to *Hprt* for the testis and *Rn18s* for the isolated Sertoli cells.

2.8.1. Real-time quantitative PCR and standardisation of gene expression

An important concern of this study design was the fact that heat-treatment causes a major loss of the numerous meiotic and post-meiotic spermatogenic cells, but somatic cell numbers are largely unaltered, which would lead to significant distortions in the ratio of total germ cell mRNA to somatic cell mRNA following extraction. In order to compensate for this, genes that are specifically or preferentially expressed by the Sertoli cells were standardised as a ratio with the Sertoli cell-specific gene, *Sox9* (Kent et al., 1996; Fröjdman et al., 2000), and the Leydig cell steroidogenic genes as a ratio with the Leydig cell-specific gene, *Insl3* (insulin-like 3)(Sadeghian et al., 2005). Genes that are expressed by both somatic cells and spermatogenic cells are presented as the normalised data from the fluidigm analysis (Table 1).

For the purposes of this Sertoli cell and Leydig cell standardisation procedure, *Sox9, Insl3* and *Rn18s* were measured by qRT-PCR, using primers as published previously (Baburski et al., 2015; Zhang et al., 2016; Wu et al., 2017). The primers sequences used were: Sox9 forward (5′-TGCTGAACGAGAGCGAGAAG-3′) and reverse (5′- ATGTGAGTCTG TTCGGTGGC-3′), Insl3 forward (5′-CGCAGTGTGGCCACCAA-3′) and reverse (5′-CCTGAGCCCTACAATCCTTCAG-3′), and Rn18s forward (5′-GGAGAGGGAGCCTGAGAAAC-3′) and reverse (5′-CAATTACAGGGC CTCGAAAG-3′). Gene expression analyses were conducted using a QuantStudio™ 6 Flex Real-Time PCR System (Applied Biosystems, Carlsbad, CA, USA). Briefly, reactions included SYBR green PCR master mix (Life Technologies), primers (1 μM), and cDNA template in a final reaction volume of 10 μL. Following an initial denaturing step (95 °C for 10 min), denaturation, annealing and extension steps (95 °C for 15 s, 60 °C for 1 min) were repeated 40 times, and a dissociation step (95, 60 and 95 °C for 15 s each) was. Each sample was measured in triplicate, and the relative expression level of *Sox9* and *Insl3* was normalised to that of the reference gene *Rn18s* and was quantified using the ΔΔCt method.

2.9. Immunoassays

2.9.1. Protein extraction and sample preparation

Fragments of the frozen testes were weighed and homogenised in cold PBS (0.01M, pH 7.4) containing protease inhibitor cocktail III (CalBiochem, La Jolla, CA), using a TissueLyser II (Qiagen) for 20 s, then centrifuged for 10 min (14,000 × *g*) to collect the supernatants for protein measurement.

2.9.2. Activin A ELISA

A specific activin A enzyme immunoassay using antibodies supplied by Oxford Brookes University was used to determine serum, testis and culture media levels of activin A, as described previously (O'Connor et al., 1999). The limit of detection for activin A in serum and testis extracts was 14.3 pg/mL, and 6.8 pg/mL for culture media. The mean inter- and intra-assay CVs for serum and testis assays were 6.2% and 4.7%, respectively. The mean inter- and intra-assay CVs for the culture media assays were 6.6% and 5.6%, respectively.

2.9.3. Activin B ELISA

Serum and tissue concentrations of activin B were measured, as described previously (Ludlow et al., 2009), using antibodies kindly supplied from Oxford Brookes University, and validated for measurement of activin B in rat tissues. The limit of detection for serum and testis extracts was 23.4 pg/mL, and 9.5 pg/mL for culture media. The mean inter- and intra-assay CVs for serum and testis assays were 12% and 7.7%, respectively. The mean inter- and intra-assay CVs for the culture media assays were 5.2% and 6.8%, respectively.

2.9.4. FSH, LH, total inhibin and follistatin radioimmunoassay

A discontinuous radioimmunoassay (RIA) was used to measure serum FSH and LH levels, and total inhibin and follistatin levels in testis homogenates, serum and culture media samples, as described previously (Robertson et al., 1988; Sun et al., 1990; Winnall et al., 2013). The FSH and LH assay detection limits were 1.33 and 0.01 ng/mL respectively, while the mean intra-assay CV values were 3.3 and 4.1%, respectively. The total inhibin and follistatin assays detection limits for serum and testis extracts were 0.16 and 1.03 ng/mL, while the mean intra-assay CV values were 4.5 and 8.8%, respectively. For culture media, the total inhibin and follistatin assay detection limits were 1.60 and 0.51 ng/mL, while the mean intra-assay CVs were 8.8 and 13.2%, respectively.

2.9.5. Testosterone radioimmunoassay

Serum and testicular homogenate supernatants were assayed for testosterone using the Immunotech IM1119 RIA Testosterone direct assay, supplied by Beckman Coulter (CA, USA), according to the manufacturer's instructions. Samples and testosterone standards were assayed in 25 μL duplicates. The sensitivity of the assay was 32.6 pg/mL, with an intra-assay CV of 7.0%.

2.10. Statistical analysis

All statistical analyses were performed using GRAPHPAD PRISM 6 (Graphpad Software, Inc., La Jolla, CA, USA). Data sets with two variables were analysed using two-way analysis of variance (ANOVA) following suitable transformation to normalise the data and equalise variance in conjunction with a Sidak's multiple comparisons test, as appropriate. Statistical significance was accepted when $p < 0.05$. All data are expressed as mean ± standard deviation (SD).

3. Results

3.1. Testicular responses to heat-treatment

The testicular response to heat displayed three phases: (I) onset (1–2 weeks), (II) peak damage (2–8 weeks) and (III) recovery (12–14 weeks) (Fig. 1A). One week after heat-treatment, testis weight was decreased by about 20%, and continued to decline by a further 20% of control values by 2 weeks (Fig. 1A). Testis weight was still 30% lower than control at 8 weeks after heat-treatment. Testis weight returned toward control levels by 12 weeks after heat-treatment, but was again 15% lower than control at 14 weeks.

The volume of TIF doubled one week after heat-treatment, when compared with controls, and remained elevated at 4–8 weeks (Fig. 1B). During the recovery phase, TIF volume returned to control values by week 12 after the heat-treatment.

There were no gross histological changes in spermatogonia at any stage of the spermatogenic cycle, or in Sertoli cells or other somatic cells across the experimental period (Fig. 2). During the onset phase, a marked loss of pachytene spermatocyte and round spermatid populations was observed in stages I–VI of the cycle of the seminiferous epithelium (Fig. 2B). Moreover, these cells, when present, demonstrated signs of apoptosis, indicated by nuclear condensation and confirmed by TUNEL staining (Fig. 2D). Multiple intraepithelial vacuoles were

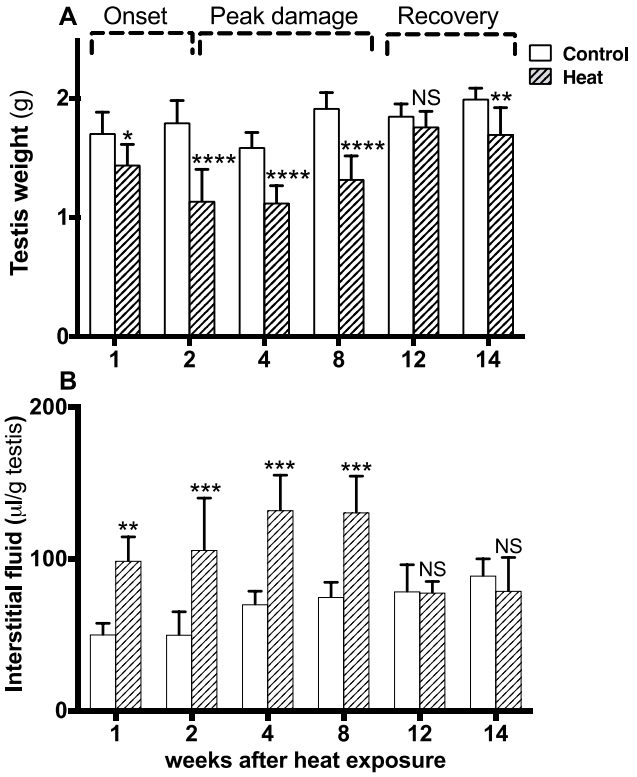

Fig. 1. Changes in (A) testis weight and (B) the volume of recovered testicular interstitial fluid (TIF) of rats after heat-treatment. Data are mean ± SD (n = 7/group for testis weights and n = 4/group for TIF volumes) and comparisons were made between the treatment and corresponding control values at each time-point using two-way ANOVA and Sidak's multiple comparisons test: *p < 0.05, **p < 0.01, ***p < 0.001 and ****p < 0.0001.

observed in regions of severe pachytene spermatocyte loss (Fig. 2B). Elongated spermatids were not visibly affected during the onset phase (weeks 1–2), but this population of germ cells was clearly depleted during weeks 4–8 (the peak damage phase) (Fig. 2F). The seminiferous epithelium appeared histologically normal during the recovery phase (Fig. 2H).

TUNEL staining of DNA fragmentation was assessed at three time points, one from each phase of damage and recovery (1, 8 and 14 weeks). An increase in the percentage of tubules with TUNEL-positive spermatocytes and spermatids (Fig. 2D) by 55% ($p < 0.05$; data not shown), relative to control (Fig. 2C), at one week coincided with the disruption of spermatogenesis and degeneration of seminiferous tubules. However, no significant difference was identified in the numbers of TUNEL-positive cells in the heat-treated testes at either 8 or 14 weeks (data not shown). There was no evidence of TUNEL staining among the Sertoli and Leydig cells or spermatogonia.

3.2. Response of the hypothalamic-pituitary-testis axis to heat-treatment

Serum FSH in the heat-treated rats increased 150% by 8 weeks after heat-treatment, and then returned to control levels (Fig. 3A). This increase in FSH coincided with a significant decrease in serum and total intratesticular inhibin levels, but not the intratesticular concentration of inhibin, at 8 weeks after heat-treatment (Fig. 3B–D). A reduction in serum inhibin was also observed at 14 weeks after heat-treatment, although this was not accompanied by alterations in serum FSH or intratesticular inhibin.

Serum LH and testosterone, and total testosterone per testis were not different between control and heat-treated rats at any time point

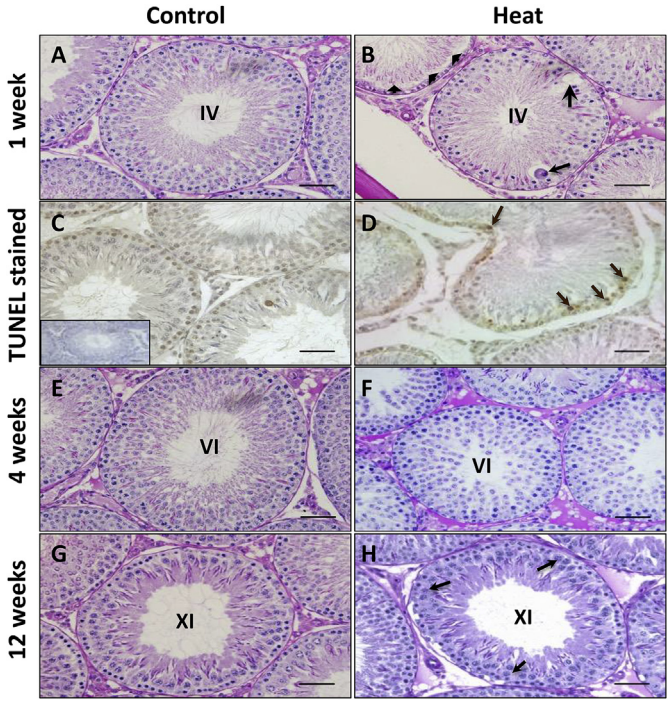

Fig. 2. Histology and TUNEL staining of the testis in control and heat-treated rats. Periodic acid–Schiff stained tissue sections of the testis show the differences between the control and heat-treated rats at 1 week (A and B, representing the onset phase), 4 weeks (E and F, peak damage phase) and 12 weeks (G and H, recovery phase). Pachytene spermatocytes and round spermatids were lost from the seminiferous epithelium after 1 week of heat-treatment (panel B: arrowhead), along with frequent degenerating cells (B: small arrow) and vacuoles (B: large arrow). TUNEL staining revealed differences in apoptosis in the heat-treated rats (panel D: arrows) compared with the control (C), especially during onset phase of heat damage at (1 week). Progression to loss of elongated spermatids during the peak damage phase was accompanied by recovery of the spermatocytes (panel F: arrows). All spermatogenic cells had largely reappeared by the recovery phase (12 weeks) (H) and the testes appeared similar to controls (G). All scale bars represent 25 µm. Roman numbers indicate the stages of the cycle of the seminiferous epithelium.

(Supp Fig. 1A–C). Similarly, the intratesticular concentration of testosterone was unaffected following heat-treatment with the exception of a single timepoint at 4 weeks (Supp Figure 1D), thought likely to be due to the large number of multiple comparisons and within-group variations in testosterone rather than a significant outcome. Altogether, the data suggest that intratesticular testosterone was minimally affected following heat-induced testicular damage.

3.3. Response of Sertoli cells to heat-treatment

The number of Sertoli cell nuclei per tubule profile appeared to decrease by 20% at one week after heat-treatment, and returned to control for the remainder of the experiment (Fig. 4A). However, when the mean Sertoli cell nuclei diameters were also measured in the one week group, this apparent decrease was found to be due to a decline in the Sertoli cell nuclear diameters to 85% of the control value (Fig. 4B), suggesting that Sertoli cell function was altered at this time point. When calculated as Sertoli cell nuclei per unit volume of testis (determined from the testis weight), Sertoli cell number was not different in control and heat-treated testes (data not shown).

In spite of the fact that Sertoli cell numbers were unchanged, a marked elevation in the normalised expression of *Sox9* mRNA measured by Fluidigm analysis (Fig. 4C) or by qRT-PCR (data not shown) was observed at 1–2 weeks. This can be attributed to a relative increase in the proportion of Sertoli cell-derived mRNAs due to a loss of

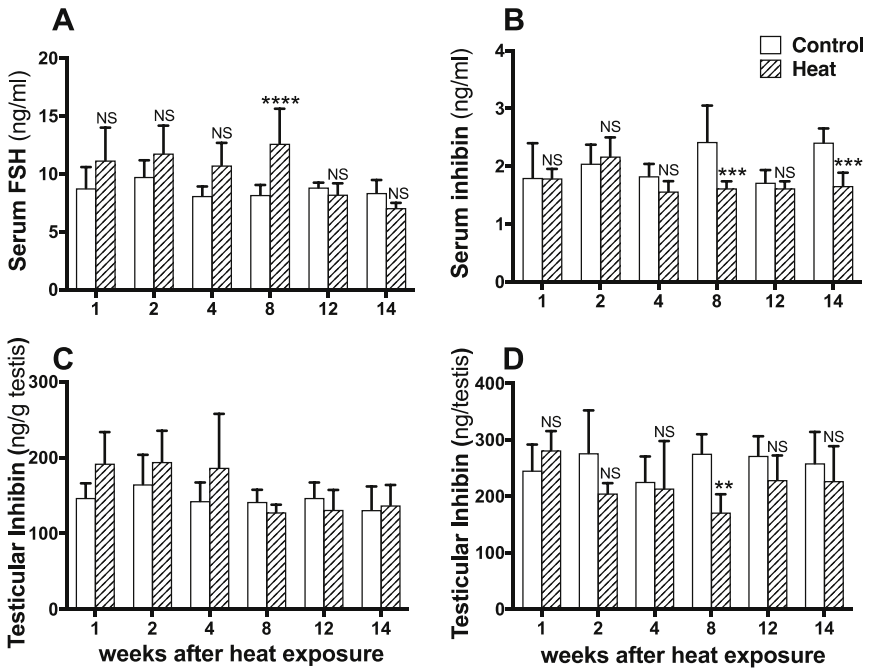

Fig. 3. Response of hypothalamic-pituitary-testis axis showing the changes in the serum FSH (A), serum inhibin (B), intratesticular inhibin concentration (C) and total intratestiuclar inhibin level (D) after heat-treatment. Data are mean ± SD (n = 7/group for serum FSH and inhibin, and n = 6/group for testicular inhibin) and comparisons were made between the treatment and corresponding control values at each time-point using two-way ANOVA and Sidak's multiple comparisons test: **p < 0.01, ***p < 0.001 and ****p < 0.0001.

contribution to total mRNA by the meiotic germ cells (spermatocytes and early spermatids) during the onset phase (weeks 1–2). Consequently, all Sertoli cell-specific gene expression was normalised to *Sox9* expression, measured by qRT-PCR.

The mRNA expression ratios of key Sertoli cell-specific genes, inhibin α-subunit (*Inha*), and the blood-testis barrier protein claudin-11 (*Cldn11*), relative to Sox9 were decreased by 50% or more at 2 weeks (Fig. 5A and B), corresponding to the time of maximum spermatogenic cell damage. Other blood-testis barrier genes, which are preferentially expressed by the Sertoli cell but also by other cell types, including connexin 43 (*Gja1*), claudin-3 (*Cldn3*) and zonula occludens-1 (*Tjp1*), followed the same expression pattern as *Cldn11* (Fig. 5C–E). An apparent decrease in the expression of interleukin-1α (*Il1a*), an inflammatory cytokine produced constitutively by the rat Sertoli cell under normal conditions, did not reach significance (Fig. 5F).

3.4. Response of Leydig cells to heat-treatment

Similar to the observation for *Sox9*, the relative expression of the Leydig cell biomarker insulin-like 3 (*Insl3*), measured by qRT-PCR, appeared to be increased during the onset phase only (Fig. 6A), again coinciding with the peak loss of germ cells. Although *Insl3* has been shown to be androgen-responsive (Paust et al., 2002; Laguë and Tremblay, 2008), as already noted (Supp Figure 1), serum and intratesticular testosterone levels were effectively unchanged throughout this study. In spite of this lack of change in testosterone levels, the mRNA of several key Leydig cells-specific steroidogenic enzymes, cytochrome P450 family 11 subfamily a polypeptide 1 (*Cyp11a1*), 3β-hydroxysteroid dehydrogenase (*Hsd3b1*) and 17β-hydroxysteroid dehydrogenase (*Hsd17b3*), diminished by 50% at 2 weeks after heat-treatment when calculated as a ratio with *Insl3* (Fig. 6B, C and D).

The androgen receptor (*Ar*) is expressed by most somatic cells in the testis, but is not expressed by germ cells. When normalised to the total testis housekeeping gene, *Hprt*, or calculated as a ratio with *Insl3* there

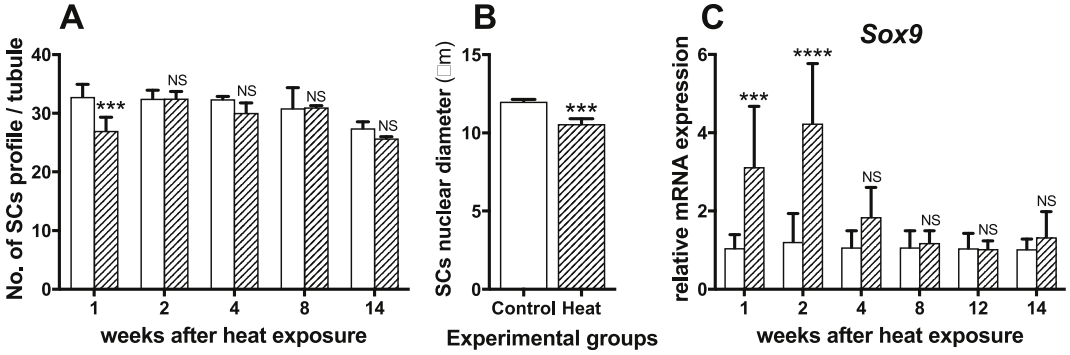

Fig. 4. Response of the Sertoli cells to heat-treatment in vivo. Sertoli cell nuclear profiles per tubule were reduced by 20% at 1 week (A), but this corresponded with a significant decrease in nuclear diameter at this time (B). When corrected for the reduction in nuclear size, Sertoli cell numbers were found to be no different between control and heat-treated rats. The relative expression of the Sertoli cell marker gene *Sox9* was increased at 1 and 2 weeks after heat-treatment, corresponding with the period of maximum depletion of spermatocytes. Data are mean ± SD (n = 4/group for Sertoli cell counting, and n = 6/group for mRNA expression) and comparisons were made between the treatment and corresponding control values at each time-point using two-way ANOVA and Sidak's multiple comparisons test: ***p < 0.001, ****p < 0.0001 and NS > 0.05.

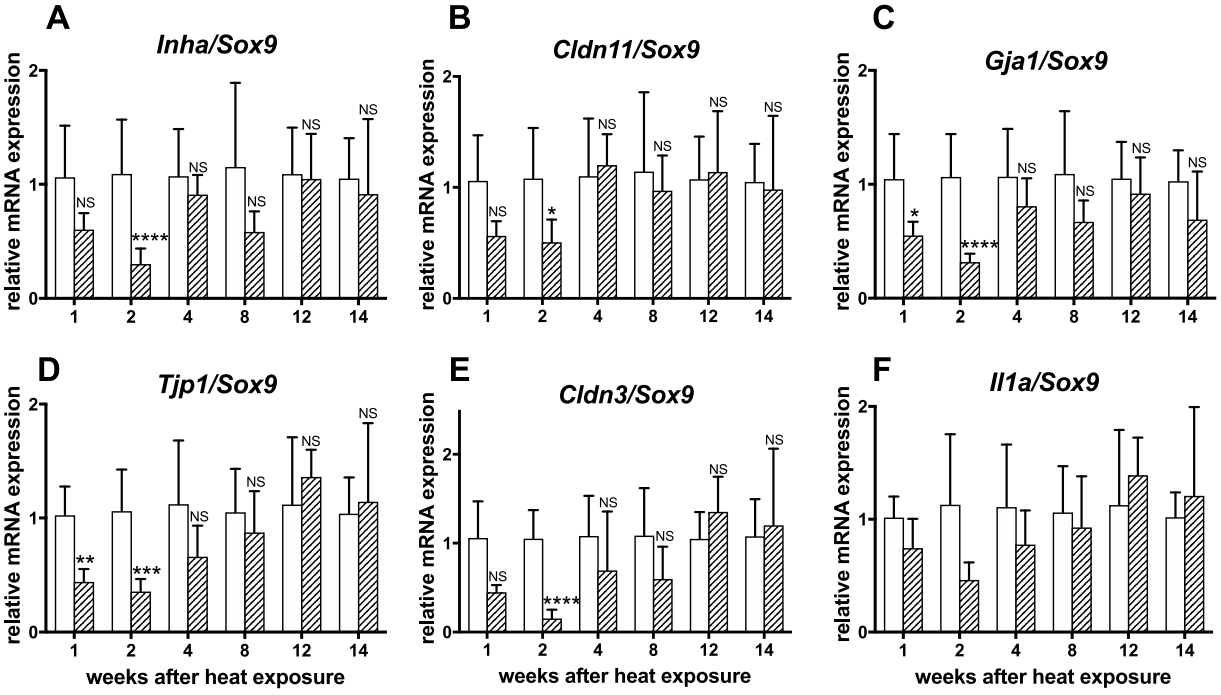

Fig. 5. Response of Sertoli cell-specific genes to heat-treatment in vivo. At the onset phase (1–2 weeks), there was a down-regulation of relative mRNA expression of several Sertoli cell-specific genes when normalised to the Sertoli cell-specific gene, *Sox9*: *Inha* (A), *Cldn11* (B), *Gja1* (C), *Tjp1* (D) *and Cldn3* (E). While *Il1a* expression also appeared to be reduced at this time, this difference was not significant (F). Data are mean ± SD (n = 6/group) and comparisons were made between the treatment and corresponding control values at each time-point using two-way ANOVA and Sidak's multiple comparisons test: *p < 0.05, **p < 0.01, and ***p < 0.001, ****p < 0.0001 and NS > 0.05.

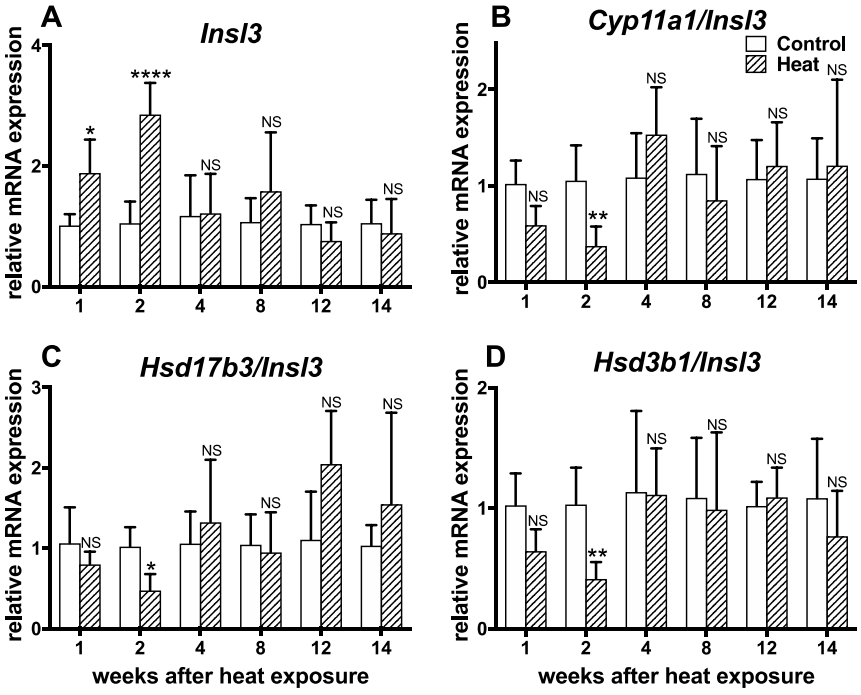

Fig. 6. Response of Leydig Cell specific genes to heat-treatment in vivo. Comparison of mRNA expression of the Leydig cell-specific genes *Insl3* (A), *Cyp11a1* as a ratio with *Insl3* (B), *HSD3b1* as a ratio with *Insl3* (C) and *HSD17b3* as a ratio with *Insl3* (D) after heat-treatment. Data are mean ± SD (n = 6/group) and comparisons were made between the treatment and corresponding control values at each time-point using two-way ANOVA and Sidak's multiple comparisons test: *p < 0.05, **p < 0.01, and ***p < 0.001, and ****p < 0.0001.

was no significant change in *Ar* mRNA expression across the various heat-treatment groups (Supp Fig. 2A and B). However, *Ar* mRNA was significantly reduced at 1–2 weeks after heat-treatment when expressed as a ratio with the other somatic cell standardisation gene, *Sox9* (Supp Figure 2C), which may indicate that there was a small, but significant, reduction in *Ar* expression by the somatic cells at this time.

3.5. Response of activins and activin-related proteins to heat-treatment

Total testicular contents of activin A and follistatin, but not activin B, decreased in the heat-treated rats during the peak damage phase (weeks 2–8) (Fig. 7A and G), although this was not reflected by changes in the intratesticular concentrations (Fig. 7B and H), attributable to the

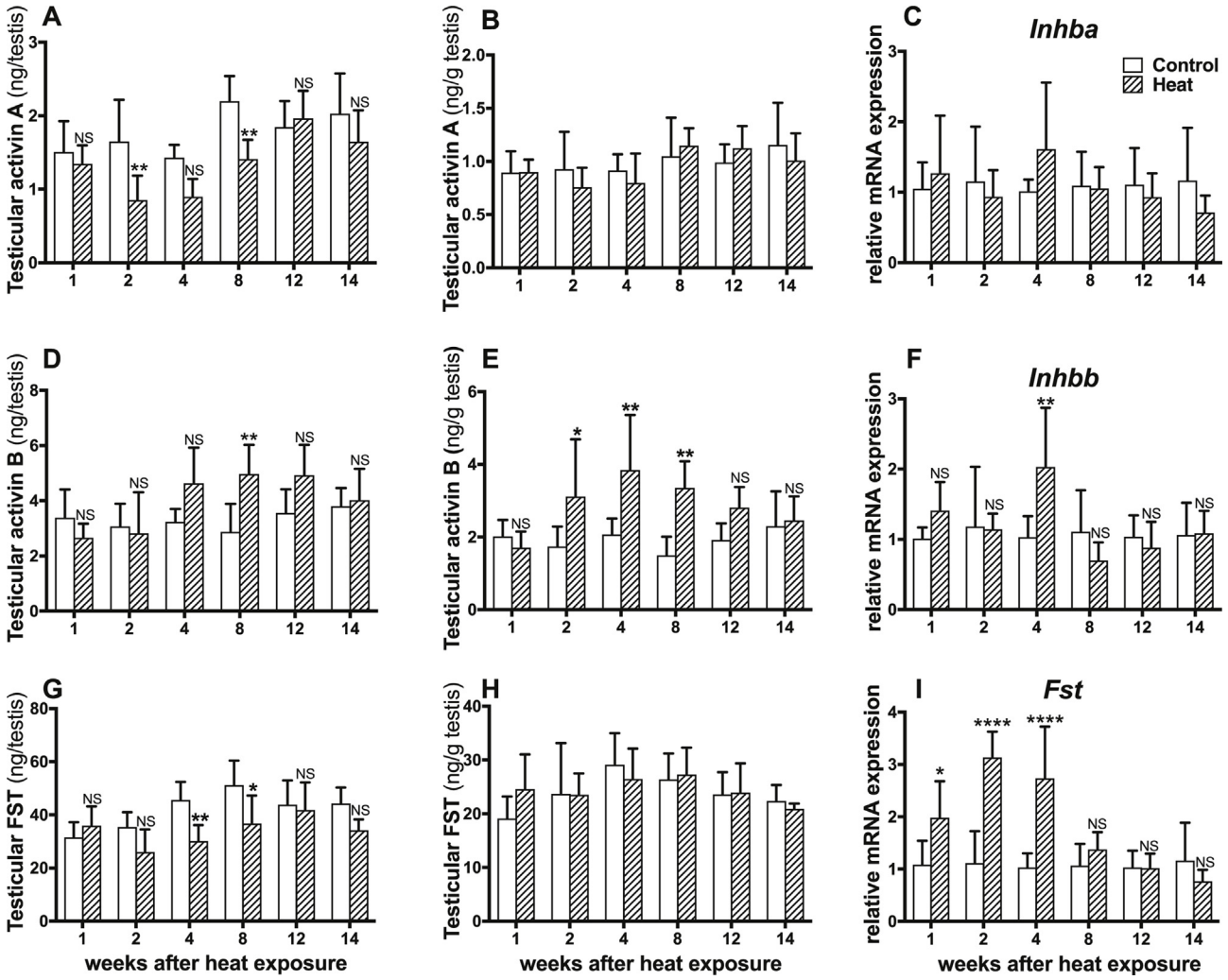

Fig. 7. Response of activins and activin-related proteins and genes expression to heat-treatment in vivo. Comparison of the total testicular content of activin A (A), activin B (D) and follistatin (G), and intratesticular concentrations of activin A (B), activin B (E) and follistatin (H), and mRNA expression of *Inhba* (C), *Inhbb* (F) and *Fst* (I) genes after heat-treatment. Data are mean ± SD (n = 6/group) and comparisons were made between the treatment and corresponding control values at each time-point using two-way ANOVA and Sidak's multiple comparisons test: *p < 0.05, **p < 0.01 and ****p < 0.0001.

corresponding loss of meiotic germ cells. By contrast, both total testicular activin B (Fig. 7D) and the concentration of activin B (Fig. 7E) were significantly elevated (approximately two-fold at 8 weeks) in the testis during the peak damage phase.

The decrease in total activin A protein during the peak damage phase (Fig. 7A), was not accompanied by corresponding changes in the relative expression of mRNA for the inhibin βA subunit (*Inhba*) (Fig. 7C). This may be attributable to reduced stability or increased clearance of the activin A protein, relative to its mRNA. In contrast with the inhibin βA subunit, the mRNA expression of inhibin βB subunit (*Inhbb*) was elevated at 4 weeks after heat-treatment (Fig. 7F), coinciding with the observed increase in activin B protein during the peak damage phase (Fig. 7D and E). Overall, the data are consistent with a reduction in activin A protein and corresponding increase in activin B protein and gene expression during the peak damage period.

Follistatin is expressed by most testicular cells (Meinhardt et al., 1998; Phillips and de Kretser, 1998). Follistatin (*Fst*) mRNA expression was considerably increased throughout the onset and peak damage phases (Fig. 7I), although this increase was not reflected by changes in follistatin protein levels during this period, and follistatin content actually decreased in parallel with the loss of spermatogenic cells at 4 and 8 weeks (Fig. 7G). As appeared to be the case of activin A, this may be attributable to differential stability or clearance of the mRNA and protein species in different cell types.

Serum levels of activin A, activin B and follistatin did not differ significantly between control and heat-treated animals, with the exception of a small (25%) decrease in activin A at one week and a 22% increase at 4 weeks after heat-treatment (data not shown).

In order to assess the direct effect of acute heat on activin-related protein production by the Sertoli cell, isolated rat Sertoli cells cultured at 32 °C were exposed to an episode of acute heat-treatment (43 °C) for 15 min. There was no significant difference in activin A and B, total inhibin, and follistatin production in conditioned media from these cells up to 48 h later (Supp Fig. 3A–D). Moreover, no significant changes in expression of any Sertoli cell gene (*Sox9, Inha, Cldn11, Il1a, Gja1* and *Krt18*) was observed (data not shown).

3.6. Stress and inflammatory responses to heat-treatment

No significant changes were observed in vivo for the mRNA expression of two key pro-inflammatory cytokines, tumour necrosis factor (*Tnf*) (Fig. 8A), or interleukin-6 (*Il6*) (data not shown), which typically increase dramatically in tissues during inflammation due to the activation and recruitment of immune cells.

The expression of a fibrotic gene marker, collagen 1a1 (*Col1a1*), was increased approximately two-fold at 4 weeks after heat-treatment, but

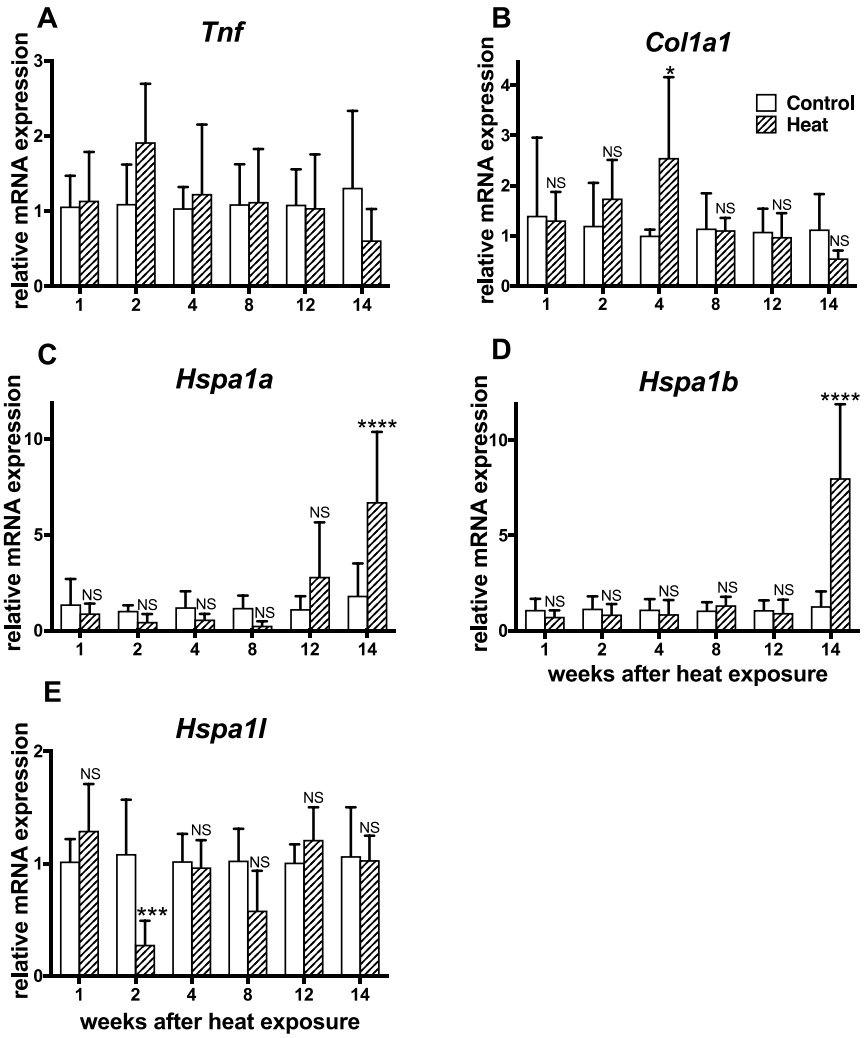

Fig. 8. Stress and inflammatory responses. Comparison of mRNA expression of inflammatory marker gene, *Tnf* (A), fibrotic marker gene, *Col1a1* (B), and heat shock proteins (HSPs) genes, *Hspa1a* (C), *Hspa1*l (D) and *Hspa1b* (E) after heat-treatment. Data are mean ± SD (n = 6/group) and comparisons were made between the treatment and corresponding control values at each time-point using two-way ANOVA and Sidak's multiple comparisons test: *p < 0.05, ***p < 0.001 and ****p < 0.0001.

returned to control levels during the recovery phase (Fig. 8B). By contrast, expression of another fibrotic marker gene, α smooth muscle (*Acta2*), was not altered (data not shown).

During the onset and peak damage phases, mRNA expression of the germ cell-specific heat shock proteins (HSPs), *Hspa1a* and *Hspa1b,* was not affected, (Fig. 8C and D). In contrast, *Hspa1l* mRNA showed a dramatic decline to 30% of control expression at 2 weeks after heat-treatment (Fig. 8E) consistent with peak testicular damage; thereafter, it returned to control levels at 4 weeks. Interestingly, both *Hspa1a* and *Hspa1b* showed 4–6fold increases, respectively, at 14 weeks after heat-treatment (Fig. 8C and D), suggesting the onset of a second wave of damage. However, no changes were observed in the expression of the HSP regulatory gene, heat shock transcription factor 1(*Hsf1)* at any time-point (data not shown).

4. Discussion

The results of this study extend previous observations of the significant damage that acute mild heat causes to spermatogenesis in the adult rat testis. Overall, this damage reflects the loss of the most heat-sensitive germ cell types, specifically the pachytene spermatocytes and early round spermatids, as previously observed (Bowler, 1972; Chowdhury and Steinberger, 1970; Lue et al., 1999). The germ cells affected at later time points were the elongated spermatids, which would have been derived from the damaged or lost spermatocytes and round spermatids, consistent with the observed decline in testicular weight at 1–8 weeks. These findings suggest that heat damage extended through two spermatogenic cycles. The testis damage was also accompanied by an elevation in serum FSH, and corresponding reduction in serum inhibin, at 8 weeks, which differs slightly from earlier reports that this occurred within the first 4 weeks of heat-treatment (Jegou et al., 1984; Au et al., 1987; Bartlett and Sharpe, 1987). The explanation for the differences in the timing of the alteration in the inhibin-FSH axis between these studies and in the present study is not clear, but may be attributable to differences in the sensitivity and specificity of the assays methods employed. There were no changes in serum LH and negligible effects on serum or testicular testosterone concentrations, consistent with earlier observations in this model (Jegou et al., 1984).

Transient heat-treatment causes a substantial loss of meiotic and post-meiotic spermatogenic cells, but not somatic cells, causing significant distortions in the ratio of total germ cell mRNA to somatic cell mRNA following extraction. In the present study, it was observed that expression of the Sertoli cell specific gene, *Sox9*, and the Leydig cell specific gene, *Insl3*, was significantly elevated at the time of maximum

loss of transcriptionally active spermatogenic cells (pachytene spermatocytes and early round spermatids), following heat treatment. It was established by stereological analysis that the actual number of Sertoli cells did not increase during this period, and previous studies indicate that Leydig cells can undergo hypertrophic changes, but do not actually increase in number, in response to mild or severe heat damage (Kerr et al., 1979; Jegou et al., 1984), suggesting that these coincident increases in relative *Sox9* and *Insl3* expression are indicators of the relative loss of spermatogenic cell mRNA. Consequently, the relative loss of spermatogenic cell mRNA was compensated for by standardising gene expression against *Sox9*, for Sertoli cell-specific genes, and *Insl*3, for Leydig cell-specific genes. On the other hand, genes that are known to be expressed by both somatic cells and spermatogenic cells were expressed relative to the housekeeping gene, *Hprt*, which was consistently expressed across all time-points.

Although the first time-point in this study was one week, germ cell loss has been reported to occur as early as 3 days following heat exposure (Bartlett and Sharpe, 1987; Sharpe et al., 1991). The fact that the reduction in expression of genes involved in Sertoli and Leydig cell function, observed in the present study, occur subsequent to the loss of the germ cells is consistent with the probability, previously suggested by Jegou and colleagues (Jegou et al., 1984), that alterations in Sertoli and Leydig cell function could be secondary to the germ cell loss rather than due to a direct effect of heat stress in this model. However, the transient decline in the size of the Sertoli cell nuclei measured at one week also indicates an early effect of heat on the Sertoli cells during the onset phase. Investigation of the response of the Sertoli cells to transient heat *in vitro* revealed no visible changes in Sertoli-cell–specific genes and proteins within 48 h. However, other *in vitro* studies have reported that acute heat stress causes structural and metabolic changes and disrupts the formation of junctions by Sertoli cells (Chen et al., 2008; Vallés et al., 2014). These changes were observed in Sertoli cell within 24 h after 30 min of heat in the rhesus monkey and after repeated exposures to heat over 5 days in the mouse, so the absence of effects in the present study may be attributable to the differences in experimental protocols. Taken together, these data indicate that heat has immediate direct effects on Sertoli cell function, as well as longer-term indirect effects subsequent to the loss of adjacent spermatogenic cells.

This is the first study to document changes in the inhibin-related proteins following acute heat-treatment. In contrast to the majority of the Sertoli and Leydig cell-specific genes measured, the reduction in activin A and the increase in activin B were delayed until the elongated spermatids were lost, which may reflect a specific effect of the mature spermatids on epithelial activin levels. At least part of this loss may be due to germ cell depletion, as rat spermatocytes and spermatids express activin A, but only low levels of activin B (Wijayarathna and de Kretser, 2016). Activin A regulation in the testis has been well studied (Okuma et al., 2006; Winnall et al., 2013), but the regulation of activin B is poorly understood. These data provide the first evidence to suggest that activin B production by Sertoli cells is regulated by the presence of the elongated spermatids. The data of the present study provide clear evidence for an increase in the protein level of activin B, occurring contemporaneously with the decreased inhibin levels at 8 weeks. This may indicate that the β_B-subunits of inhibin are being freed up to form activin B due to the decline in production of inhibin α-subunit.

In contrast, the observed reduction in activin A may reflect a lower production of inhibin βA-subunits by the Sertoli cells. The apparent discordance between the mRNA expression and measurable levels of inhibin, follistatin and the activins, particularly during the peak damage phase, is consistent with the emerging picture of the complex cellular distribution and regulation of these proteins. The data presented here suggest that these proteins are regulated both at the transcriptional level and at the level of protein subunit synthesis and homo-heterodimer formation (Hedger and Winnall, 2012).

With respect to Leydig cell function, the expression of several key steroidogenic enzyme genes, *Cyp11a1*, *Hsd3b1* and *Hsd17b3*, was also reduced at 2 weeks following heat-treatment. Nonetheless, no significant effect was observed on serum and testicular testosterone levels, consistent with several previous observations (Damber et al., 1980; Jegou et al., 1984; Au et al., 1987). However, other studies have reported a temporary alteration in serum testosterone in response to heat (Lue et al., 1999; Aktas and Kanter, 2009), which has been attributed to suppression of steroidogenesis (Murphy et al., 2001). A decline in the steroidogenic proteins, StAR and P450c17, after heat-treatment in the adult rat has been reported by Hwang et al. (2010), although this involved exposing the testis to a temperature ranges 41–43 °C for 10 min, twice daily for 3 days per week, over a 4 week period. Significant morphological changes in the steroidogenic machinery of the Leydig cells, which include accumulation of lipid droplets, the appearance of a dilated smooth endoplasmic reticulum, mitochondrial swelling, and the disappearance of mitochondrial cristae, have been reported by a number of investigators within 35 days of heat exposure (Damber et al., 1980; Aktas and Kanter, 2009). Overall, the data suggest that the Leydig cell can undergo significant functional changes following heat-treatment, including reduction in steroidogenic gene expression, but that other compensatory changes in the steroidogenic machinery of the cell result in the maintenance of normal testosterone production.

Another critical observation is the lack of evidence for a significant stress, inflammatory or fibrotic response, either as a cause or a consequence of the germ cell damage. No elevation in expression of several heat-shock-related genes or key inflammatory cytokine genes was observed and there was only a small, transient increase in the expression of the fibrotic gene, *Col1a1*, during the onset and period of maximum testicular damage. However, it is likely that transient heat-stress and inflammatory events have been missed early in the process (less than one week). Significantly, expression of the heat shock protein genes, *Hspa1a* and *Hspa1b*, was dramatically increased at 14 weeks after heat exposure, coinciding with a small, but significant, secondary decline in testis weight, and potentially indicating a second wave of spermatogenic damage at this time-point. This could indicate a long-term effect of heat on the spermatogonial precursor cells that merits further investigation.

Curiously, the expression of *Hspa1l*, but not that of any other HSP-related gene, was considerably downregulated at 2 weeks, at the time of peak spermatogenic cell damage. *Hspa1l* is an inducible HSP, which is expressed within 3–5 h following heat stress (Rockett et al., 2001; Widlak et al., 2007; Kiang and Tsokos, 1998). Germ cell apoptosis has been reported to occur as a result of disruption of the testis-specific isoform of HSPs (Dix et al., 1996), and the loss of this anti-apoptotic protein and its ability to interfere with caspase activation (Radons, 2016), may contribute to the severity of the damage observed at this time.

In conclusion, the data presented here indicate that acute heat stress affects gene expression in Sertoli cells and Leydig cells and the production of inhibin-related proteins, particularly the activins, which may be primarily mediated through changes in the germ cell complement. The changes in Leydig cell function, most likely the result of local factors produced by Sertoli cells or germ cells, supports the concept of intercompartmental communication (Bergh, 1982; de Kretser, 1982; Jegou et al., 1984). The data from the present study also highlight the need to raise awareness, particularly for couples suffering from poor fertility, about the detrimental effects of prolonged heat exposure of the testes on fertility.

Declaration of interest

The authors declare no conflict of interest with respect to this study.

Author's contributions

Conceived and designed the experiments: DDK, MPH, RA.
Performed the experiments: RA.

Reagents/activin A and B assay techniques: HL.
Analysed the data: RA, MPH.
Critical discussion of data: RA, MPH, DDK, PGS.
Wrote the manuscript: RA, MPH.
Critical review of manuscript: all authors.

Acknowledgements

This research was supported by funding provided by Imam Abdulrahman Bin Faisal University in Saudi Arabia (8559246), the National Health and Medical Research Council of Australia and the Victorian State Government Operational Infrastructure Support Program. We thank Oxford Brookes University for kindly supplying the antibody reagents E4 and 46 A/F used in the activin A and B assays, Adnan Sali and Julie Muir for assistance in animal procedures, and Susan Hayward for her expert immunoassay skills and assistance. Furthermore, the authors thank the MHTP Medical Genomics Facility for assistance with the Fluidigm analysis.

Appendix A. Supplementary data

Supplementary data to this article can be found online at https://doi.org/10.1016/j.mce.2019.110546.

References

Abercrombie, M., 1946. Estimation of nuclear population from microtome sections. Anat. Rec. 94, 239–247.
Aktas, C., Kanter, M., 2009. A morphological study on Leydig cells of scrotal hyperthermia applied rats in short-term. J. Mol. Histol. 40, 31–39.
Au, C.L., Robertson, D.M., de Kretser, D.M., 1987. Changes in testicular inhibin after a single episode of heating of rat testes. Endocrinology 120, 973–977.
Baburski, A.Z., Sokanovic, S.J., Janjic, M.M., Stojkov-Mimic, N.J., Bjelic, M.M., Andric, S.A., Kostic, T.S., 2015. Melatonin replacement restores the circadian behavior in adult rat Leydig cells after pinealectomy. Mol. Cell. Endocrinol. 413, 26–35.
Barakat, B., Itman, C., Mendis, S., Loveland, K., 2012. Activins and inhibins in mammalian testis development: new models, new insights. Mol. Cell. Endocrinol. 359, 66–77.
Bartlett, J., Sharpe, R., 1987. Effect of local heating of the rat testis on the levels in interstitial fluid of a putative paracrine regulator of the Leydig cells and its relationship to changes in Sertoli cell secretory function. J. Reprod. Fertil. 80, 279–287.
Bergh, A., 1982. Local differences in Leydig cell morphology in the adult rat testis: evidence for a local control of Leydig cells by adjacent seminiferous tubules. Int. J. Androl. 5, 325–330.
Bergh, A., Söder, O., 2007. Studies of cryptorchidism in experimental animal models. Acta Paediatr. 96, 617–621.
Bienvenu, L.A., Morgan, J., Reichelt, M.E., Delbridge, L.M., Young, M.J., 2017. Chronic in vivo nitric oxide deficiency impairs cardiac functional recovery after ischemia in female (but not male) mice. J. Mol. Cell. Cardiol. 112, 8–15.
Bowler, K., 1972. The effect of repeated applications of heat on spermatogenesis in the rat: a histological study. J. Reprod. Fertil. 28, 325–333.
Carlsen, E., Andersson, A.M., Petersen, J.H., Skakkebæk, N.E., 2003. History of febrile illness and variation in semen quality. Hum. Reprod. 18, 2089–2092.
Chalmel, F., Rolland, A.D., Niederhauser-Wiederkehr, C., Chung, S.S., Demougin, P., Gattiker, A., Moore, J., Patard, J.-J., Wolgemuth, D.J., Jégou, B., 2007. The conserved transcriptome in human and rodent male gametogenesis. Proc. Natl. Acad. Sci. U.S.A. 104, 8346–8351.
Chen, M., Cai, H., Yang, J.L., Lu, C.L., Liu, T., Yang, W., Guo, J., Hu, X.Q., Fan, C.H., Hu, Z.Y., Gao, F., 2008. Effect of heat stress on expression of junction-associated molecules and upstream factors androgen receptor and Wilms' tumor 1 in monkey Sertoli cells. Endocrinology 149, 4871–4882.
Chowdhury, A., Steinberger, E., 1970. Early changes in the germinal epithelium of rat testes following exposure to heat. J. Reprod. Fertil. 22, 205–212.
Damber, J., Bergh, A., Janson, P., 1980. Leydig cell function and morphology in the rat testis after exposure to heat. Andrologia 12, 12–19.
de Kretser, D., 1982. Sertoli cell—Leydig cell interaction in the regulation of testicular function. Int. J. Androl. 5, 11–17.
de Kretser, D., Hedger, M., Loveland, K., Phillips, D., 2002. Inhibins, activins and follistatin in reproduction. Hum. Reprod. Update 8, 529–541.
Dix, D.J., Allen, J.W., Collins, B.W., Mori, C., Nakamura, N., Poorman-Allen, P., Goulding, E.H., Eddy, E., 1996. Targeted gene disruption of Hsp70-2 results in failed meiosis, germ cell apoptosis, and male infertility. Proc. Natl. Acad. Sci. U.S.A. 93, 3264–3268.
Durairajanayagam, D., Agarwal, A., Ong, C., 2014. Causes, effects and molecular mechanisms of testicular heat stress. Reprod. Biomed. Online 30, 14–27.
Fröjdman, K., Harley, V.R., Pelliniemi, L.J., 2000. Sox9 protein in rat Sertoli cells is age and stage dependent. Histochem. Cell Biol. 113, 31–36.
Gao, J., Zuo, Y., So, K.-H., Yeung, W.S., Ng, E.H., Lee, K.-F., 2012. Electroacupuncture enhances spermatogenesis in rats after scrotal heat treatment. Spermatogenesis 2, 53–62.
Gasinska, A., Hill, S., 1989. The effect of hyperthermia on the mouse testis. Neoplasma 37, 357–366.
Gérard, N., Syed, V., Bardin, W., Genetet, N., Jégou, B., 1991. Sertoli cells are the site of interleukin-1α synthesis in rat testis. Mol. Cell. Endocrinol. 82, R13–R16.
Hedger, M., Drummond, A., Robertson, D., Risbridger, G., de Kretse, D., 1989. Inhibin and activin regulate [^{3}H] thymidine uptake by rat thymocytes and 3T3 cells in vitro. Mol. Cell. Endocrinol. 61, 133–138.
Hedger, M.P., Winnall, W.R., 2012. Regulation of activin and inhibin in the adult testis and the evidence for functional roles in spermatogenesis and immunoregulation. Mol. Cell. Endocrinol. 359, 30–42.
Hedger, M.P., Winnall, W.R., Phillips, D.J., de Kretser, D.M., 2011. The regulation and functions of activin and follistatin in inflammation and immunity. Vitam. Horm. 85, 255–297.
Hou, Y., Wang, X., Lei, Z., Ping, J., Liu, J., Ma, Z., Zhang, Z., Jia, C., Jin, M., Li, X., 2015. Heat stress induced metabolic changes and altered male reproductive function. J. Proteome Res. 14, 1495–1503.
Houston, B.J., Nixon, B., Martin, J.H., De Iuliis, G.N., Trigg, N.A., Bromfield, E.G., McEwan, K.E., Aitken, R.J., 2018. Heat exposure induces oxidative stress and DNA damage in the male germ line. Biol. Reprod. 98, 593–606.
Hwang, E.C., Dai Min, K., Jung, S.I., Ryu, S.B., Ahn, K.Y., Lee, K., Park, K., 2010. Testicular steroidogenesis is decreased by hyperthermia in old rats. Urol. Int. 84, 347–352.
Jegou, B., Laws, A., de Kretser, D., 1984. Changes in testicular function induced by short-term exposure of the rat testis to heat: further evidence for interaction of germ cells, Sertoli cells and Leydig cells. Int. J. Androl. 7, 244–257.
Jones, K.L., Mansell, A., Patella, S., Scott, B.J., Hedger, M.P., de Kretser, D.M., Phillips, D.J., 2007. Activin A is a critical component of the inflammatory response, and its binding protein, follistatin, reduces mortality in endotoxemia. Proc. Natl. Acad. Sci. U.S.A. 104, 16239–16244.
Kent, J., Wheatley, S.C., Andrews, J.E., Sinclair, A.H., Koopman, P., 1996. A male-specific role for SOX9 in vertebrate sex determination. Development 122, 2813–2822.
Kerr, J.B., Rich, K.A., de Kretser, D.M., 1979. Alterations of the fine structure and androgen secretion of the interstitial cells in the experimentally cryptorchid rat testis. Biol. Reprod. 20, 409–422.
Kiang, J.G., Tsokos, G.C., 1998. Heat shock protein 70 kDa: molecular biology, biochemistry, and physiology. Pharmacol. Ther. 80, 183–201.
Laguë, E., Tremblay, J.J., 2008. Antagonistic effects of testosterone and the endocrine disruptor mono-(2-ethylhexyl) phthalate on INSL3 transcription in Leydig cells. Endocrinology 149, 4688–4694.
Lardenois, A., Gattiker, A., Collin, O., Chalmel, F., Primig, M., 2010. GermOnline 4.0 Is a Genomics Gateway for Germline Development, Meiosis and the Mitotic Cell Cycle. Database 2010. http://www.germonline.org/index.html.
Ludlow, H., Phillips, D.J., Myers, M., McLachlan, R.I., De Kretser, D.M., Allan, C.A., Anderson, R.A., Groome, N.P., Hyvönen, M., Colin Duncan, W., 2009. A new 'total'activin B enzyme-linked immunosorbent assay (ELISA): development and validation for human samples. Clin. Endocrinol. 71, 867–873.
Lue, Y.-H., Lasley, B.L., Laughlin, L.S., Swerdloff, R.S., Hikim, A.P.S., Leung, A., Overstreet, J.W., Wang, C., 2002. Mild testicular hyperthermia induces profound transitional spermatogenic suppression through increased germ cell apoptosis in adult cynomolgus monkeys (Macaca fascicularis). J. Androl. 23, 799–805.
Lue, Y.-H., Sinha Hikim, A.P., Swerdloff, R.S., Im, P., Taing, K.S., Bui, T., Leung, A., Wang, C., 1999. Single exposure to heat induces stage-specific germ cell apoptosis in rats: role of intratesticular testosterone on stage specificity. Endocrinology 140, 1709–1717.
McLean, D.J., Russell, L.D., Griswold, M.D., 2002. Biological activity and enrichment of spermatogonial stem cells in vitamin A-deficient and hyperthermia-exposed testes from mice based on colonization following germ cell transplantation. Biol. Reprod. 66, 1374–1379.
Meehan, T., Schlatt, S., O'Bryan, M.K., de Kretser, D.M., Loveland, K.L., 2000. Regulation of germ cell and Sertoli cell development by activin, follistatin, and FSH. Dev. Biol. 220, 225–237.
Meinhardt, A., O'Bryan, M., McFarlane, J., Loveland, K., Mallidis, C., Foulds, L., Phillips, D., de Kretser, D., 1998. Localization of follistatin in the rat testis. J. Reprod. Fertil. 112, 233–241.
Murphy, B.D., Lalli, E., Walsh, L.P., Liu, Z., Soh, J., Stocco, D.M., Sassone-Corsi, P., 2001. Heat shock interferes with steroidogenesis by reducing transcription of the steroidogenic acute regulatory protein gene. Mol. Endocrinol. 15, 1255–1263.
Nicholls, P.K., Harrison, C.A., Rainczuk, K.E., Vogl, A.W., Stanton, P.G., 2013. Retinoic acid promotes Sertoli cell differentiation and antagonises activin-induced proliferation. Mol. Cell. Endocrinol. 377, 33–43.
Nicholls, P.K., Stanton, P.G., Chen, J.L., Olcorn, J.S., Haverfield, J.T., Qian, H., Walton, K.L., Gregorevic, P., Harrison, C.A., 2012. Activin signaling regulates Sertoli cell differentiation and function. Endocrinology 153, 6065–6077.
O'Connor, A., McFarlane, J., Hayward, S., Yohkaichiya, T., Groome, N., De Kretser, D., 1999. Serum activin A and follistatin concentrations during human pregnancy: a cross-sectional and longitudinal study. Hum. Reprod. 14, 827–832.
Ohga, E., Matsuse, T., Teramoto, S., Katayama, H., Nagase, T., Fukuchi, Y., Ouchi, Y., 1996. Effects of activin A on proliferation and differentiation of human lung fibroblasts. Biochem. Biophys. Res. Commun. 228, 391–396.
Okuma, Y., O'Connor, A., Hayashi, T., Loveland, K., De Kretser, D., Hedger, M., 2006. Regulated production of activin A and inhibin B throughout the cycle of the seminiferous epithelium in the rat. J. Endocrinol. 190, 331–340.
Paul, C., Murray, A.A., Spears, N., Saunders, P.T., 2008. A single, mild, transient scrotal heat stress causes DNA damage, subfertility and impairs formation of blastocysts in mice. Reproduction 136, 73–84.

Paust, H., Wessels, J., Ivell, R., Mukhopadhyay, A., 2002. The expression of the RLF/INSL3 gene is reduced in Leydig cells of the aging rat testis. Exp. Gerontol. 37, 1461–1467.
Phillips, D.J., de Kretser, D.M., 1998. Follistatin: a multifunctional regulatory protein. Front. Neuroendocrinol. 19, 287–322.
Radons, J., 2016. The human HSP70 family of chaperones: where do we stand? Cell Stress Chaperones 21, 379–404.
Robertson, D., Hayward, S., Irby, D., Jacobsen, J., Clarke, L., McLachlan, R., De Kretser, D., 1988. Radioimmunoassay of rat serum inhibin: changes after PMSG stimulation and gonadectomy. Mol. Cell. Endocrinol. 58, 1–8.
Rockett, J.C., Mapp, F.L., Garges, J.B., Luft, J.C., Mori, C., Dix, D.J., 2001. Effects of hyperthermia on spermatogenesis, apoptosis, gene expression, and fertility in adult male mice. Biol. Reprod. 65, 229–239.
Sadeghian, H., Anand-Ivell, R., Balvers, M., Relan, V., Ivell, R., 2005. Constitutive regulation of the Insl3 gene in rat Leydig cells. Mol. Cell. Endocrinol. 241, 10–20.
Sharpe, R., Bartlett, J., Allenby, G., 1991. Evidence for the control of testicular interstitial fluid volume in the rat by specific germ cell types. J. Endocrinol. 128, 359–367.
Sharpe, R., Cooper, I., 1983. Testicular interstitial fluid as a monitor for changes in the intratesticular environment in the rat. J. Reprod. Fertil. 69, 125–135.
Sluka, P., O'Donnell, L., Bartles, J., Stanton, P.G., 2006. FSH regulates the formation of adherens junctions and ectoplasmic specialisations between rat Sertoli cells in vitro and in vivo. J. Endocrinol. 189, 381–395.
Stanton, P.G., Foo, C.F.H., Rainczuk, A., Stephens, A.N., Condina, M., O'Donnell, L., Weidner, W., Ishikawa, T., Cruickshanks, L., Smith, L.B., McLachlan, R.I., 2016. Mapping the testicular interstitial fluid proteome from normal rats. Proteomics 16, 2391–2402.
Sun, Y.-T., Wreford, N.G., Robertson, D.M., de Kretser, D.M., 1990. Quantitative cytological studies of spermatogenesis in intact and hypophysectomized rats: identification of androgen-dependent stages. Endocrinology 127, 1215–1223.
Vallés, A.S., Aveldaño, M.I., Furland, N.E., 2014. Altered lipid homeostasis in Sertoli cells stressed by mild hyperthermia. PLoS One 9, e91127.
Wang, C., Cui, Y.-G., Wang, X.-H., Jia, Y., Sinha Hikim, A., Lue, Y.-H., Tong, J.-S., Qian, L.-X., Sha, J.-H., Zhou, Z.-M., 2007. Transient scrotal hyperthermia and levonorgestrel enhance testosterone-induced spermatogenesis suppression in men through increased germ cell apoptosis. J. Clin. Endocrinol. Metab. 92, 3292–3304.
Wang, J., Wreford, N., Lan, H., Atkins, R., Hedger, M., 1994. Leukocyte populations of the adult rat testis following removal of the Leydig cells by treatment with ethane dimethane sulfonate and subcutaneous testosterone implants. Biol. Reprod. 51, 551–561.
Widlak, W., Vydra, N., Malusecka, E., Dudaladava, V., Winiarski, B., Ścieglińska, D., Widlak, P., 2007. Heat shock transcription factor 1 down-regulates spermatocyte--specific 70 kDa heat shock protein expression prior to the induction of apoptosis in mouse testes. Genes Cells 12, 487–499.
Wijayarathna, R., de Kretser, D., 2016. Activins in reproductive biology and beyond. Hum. Reprod. Update 22, 342–357.
Winnall, W.R., Wu, H., Sarraj, M.A., Rogers, P.A., de Kretser, D.M., Girling, J.E., Hedger, M.P., 2013. Expression patterns of activin, inhibin and follistatin variants in the adult male mouse reproductive tract suggest important roles in the epididymis and vas deferens. Reprod. Fertil. Dev. 25, 570–580.
Wu, X., Liu, J., Duan, Y., Gao, S., Lü, Y., Li, X., Zhu, Q., Chen, X., Lin, J., Ye, L., 2017. A short-term exposure to tributyltin blocks Leydig cell regeneration in the adult rat testis. Front. Pharmacol. 8, 704.
Yamashita, S., Maeshima, A., Kojima, I., Nojima, Y., 2004. Activin A is a potent activator of renal interstitial fibroblasts. J. Am. Soc. Nephrol. 15, 91–101.
Zhang, W.-X., Fan, J., Ma, J., Rao, Y.-S., Zhang, L., Yan, Y.-E., 2016. Selection of suitable reference genes for quantitative real-time PCR normalization in three types of rat adipose tissue. Int. J. Mol. Sci. 17, 968.

6.3. Appendix 3: Western Blotting Optimisation for TIF

In order to confirm changes in TIF proteins detected by MS, eight candidate proteins were selected, based on their relative function, for orthogonal targeted validation by immunoblotting. Because western blotting (WB) has not been tested on TIF previously, this experiment took a while to optimise, since TIF contains abundant immunoglobulins which interfere with the analysis. Although WB was optimised as detailed below, only three candidate proteins were identified by WB at the end of this experiment.

All products for WB were purchased from Life Technologies (Carlsbad, CA, USA), unless otherwise specified, and were used according to the manufacturer's protocols. The following steps were conducted unchanged throughout the optimisation process, unless specified: Protein samples were mixed with 4× Bolt LDS sample buffer and 10× Bolt sample reducing agent and then heated to 70°C for 10 min for loading onto a Bolt 4–12% Bis–Tris Plus minigel. The loaded gels were immersed in Bolt MES SDS running buffer and run at 100 mV for ~60 min with a Prestained Protein Ladder (Abcam, Cambridge, UK). The separated proteins were transferred onto polyvinylidene difluoride membranes using a transfer buffer (38 mM Tris Base, 280 mM glycine and 20% methanol) at 30 mV overnight at 4°C.

Most of the optimisation work was focused on determining different conditions and/or times for blocking and for treatment with primary and secondary antibodies, as outlined in Table 1. The rationale for adjusting these steps was to maximise the specific bindings and minimise non-specific bands. Before testing the antibodies on TIF samples, they were trialled on Sertoli cell extracts to ensure each antibody's efficiency. Once the antibody was confirmed to work, it was then checked on pooled TIF samples from various animals which also served as a quality control sample for the real experiments.

The blocking buffer, which was also used as an antibody diluent unless otherwise specified, consisted of 1% bovine serum albumin (BSA, Sigma-Aldrich) in 25mM Tris Base, 140 mM NaCl, and 0.05% Tween-20, adjusted to pH 7.9 (TBST). In general, the membranes were washed three

times (5 mins per wash) with TBST after incubation with the primary and secondary antibodies. The signals were revealed with Pierce ECL western blotting substrate (Thermo Fisher), following the manufacturer's instructions. The resulting images were developed, fixed, scanned and quantified using ImageLab software (version 5.2.1, Bio-Rad).

App. 3 Table 1. Different WB conditions

Primary antibodies	Blocking time	Incubation time with 1ry antibody	2ry antibody	2ry antibody diluent	Incubation time with 2ry antibody	Comments
1-Polyclonal rabbit **Spata20** antibody (Proteintech, 18373-1-AP, 1:2000) 2- Polyclonal rabbit **Decorin** antibody (Proteintech, 14667-1-AP, 1:1000) 3-Monoclonal rabbit **Hspa2** (Abcam, Ab108416, 1:1000)	1 hour	1 hour	Goat anti-Rabbit IgG H&L (HRP) preadsorbed, Abcam (ab7090)	1%BSA/0.05%TBST	1 hour	No specific bands with many nonspecific bands
	*Overnight	1 hour			1 hour	No specific bands with many nonspecific bands
	Overnight	Overnight			1 hour	Faint specific bands with many nonspecific bands
	1 hour	1 hour	Goat anti-Rabbit IgG (H+L), highly cross adsorbed, Sigma (SAB3700878)	1%BSA/0.05%TBST	1 hour	Faint specific bands with some nonspecific bands
	Overnight	1 hour			1 hour	Faint specific bands with some nonspecific bands
	Overnight	Overnight			1 hour	Clear specific bands with some nonspecific bands
	1 hour	Overnight			1 hour	**Clear specific bands with some nonspecific bands
	1 hour	Overnight		***5% Skim milk/0.05%TBST	1 hour	Very good quality bands with a very few non-specific bands

* All overnight incubations were at room temperature.

** This condition showed a good quality Spata20 bands with a very few nonspecific bands.

*** This diluent was used for Decorin and Hspa2 antibodies only.

Appendix 4: Whole dataset for Supp Table 1 in Chapter 3

Table 1. Total of 1728 proteins identified in TIF from heat-treated and control rats (n=4/ experimental group/time-point)

Uniprot accession number	Gene symbol	Protein name	Mol. weight [kDa]	No. Peptides Control wk1	No. Peptides Control wk8	No. Peptides Control wk14	No. Peptides Heat wk1	No. Peptides Heat wk8	No. Peptides Heat wk14	No. Unique peptides Control wk1	No. Unique peptides Control wk8	No. Unique peptides Control wk14	No. Unique peptides Heat wk1	No. Unique peptides Heat wk8	No. Unique peptides Heat wk14	iBAQ Control wk1	iBAQ Control wk8	iBAQ Control wk14	iBAQ Heat wk1	iBAQ Heat wk8	iBAQ Heat wk14	Sequence coverage Control wk1 [%]	Sequence coverage Control wk8 [%]	Sequence coverage Control wk14 [%]	Sequence coverage Heat wk1 [%]	Sequence coverage Heat wk8 [%]	Sequence coverage Heat wk14 [%]
P14046	A1i3	Alpha-1-inhibitor 3	163.77	128	133	131	131	129	131	4	5	4	5	6	5	9.14E+06	1.05E+07	1.36E+07	4.93E+06	8.01E+06	1.48E+07	74.3	74.9	74.9	76.1	76	76
Q63041	A1m	Alpha-1-macroglobulin;Alpha-1-macroglobulin 45 kDa subunit	167.12	99	106	102	103	105	102	99	106	102	103	105	102	5.23E+07	3.61E+07	5.12E+07	4.67E+07	4.81E+07	4.72E+07	77.2	78	77.3	77.3	77.6	76.7
P06238	A2m	Alpha-2-macroglobulin	163.78	22	13	20	17	18	19	19	11	18	15	16	17	2.43E+05	3.42E+04	1.43E+05	5.75E+04	7.22E+04	9.80E+04	22.5	13.9	20.4	16.8	18.1	19.2
D3ZS19	A2ml1	Alpha-2-macroglobulin-like 1	162.77	6	6	7	5	5	5	6	6	7	5	5	5	1.12E+04	1.80E+04	4.82E+04	2.08E+04	1.24E+04	2.93E+04	6.3	6.9	7.8	6	6.2	6.2
G3V7V2	Aamp	Angio-associated migratory protein	46.94	2	2	2	3	2	2	2	2	2	3	2	2	4.85E+04	9.06E+04	3.45E+04	5.62E+04	4.34E+04	3.07E+04	6.9	6.9	5.5	9.9	6.9	6.9
P50475	Aars	Alanine--tRNA ligase, cytoplasmic	106.79	15	16	10	16	13	8	15	16	10	16	13	8	1.87E+05	3.28E+05	6.12E+04	1.41E+05	6.74E+04	2.20E+04	23.5	25.3	16.4	25.3	20	13.1
Q9QYJ4	Abcb9	ATP-binding cassette sub-family B member 9	82.83	1	1	1	1	1	1	1	1	1	1	1	1	1.66E+04	2.57E+03	9.81E+03	6.42E+03	6.15E+03	6.41E+03	0.9	0.9	0.9	0.9	0.9	0.9
D3ZD23	Abce1	ATP-binding cassette subfamily E member 1	67.30	2	2	1	2	2	1	2	2	1	2	2	1	3.89E+04	3.65E+04	1.17E+04	1.47E+04	1.48E+04	3.97E+03	5.3	5.3	1.7	5.3	5.3	1.7
Q6DGG1	Abhd14b	PAlpha/beta hydrolase domain-containing protein 14B	22.62	4	5	3	3	3	4	4	5	3	3	3	4	3.13E+05	7.29E+05	1.76E+05	2.44E+05	1.38E+05	1.09E+05	37.1	42.4	21.4	22.4	22.4	27.6
D3ZAW4	Abhd4	Abhydrolase domain containing 4	40.37	9	9	5	9	7	5	9	9	5	9	7	5	3.63E+05	9.67E+05	1.62E+05	4.18E+05	2.58E+05	7.98E+04	44.2	44.2	23.9	44.2	32.1	26.5
F1M305	Abi3bp	ABI family member 3-binding protein	94.55	2	2	1	2	3	2	2	2	1	2	3	2	3.84E+04	1.35E+04	8.27E+03	1.80E+04	1.79E+04	9.92E+03	2.8	2.8	1.5	2.8	4	2.8
D3ZSL2	Abracl	ABRA C-terminal-like	9.03	3	4	3	3	3	2	3	4	3	3	3	2	8.72E+05	1.19E+06	7.34E+05	8.05E+05	5.37E+05	3.56E+05	46.9	51.9	46.9	46.9	46.9	30.9
P13437	Acaa2	3-ketoacyl-CoA thiolase, mitochondrial	41.75	1	1	1	1	1	1	1	1	1	1	1	1	3.65E+04	2.09E+04	4.08E+04	7.03E+03	1.39E+04	2.45E+04	5.1	5.1	5.1	5.1	5.1	5.1
P15650	Acadl	Long-chain specific acyl-CoA dehydrogenase, mitochondrial	47.87	2	2	2	2	2	2	2	2	2	2	2	2	5.17E+04	4.59E+04	3.00E+04	2.46E+04	1.88E+04	2.05E+04	6.5	6.5	6.5	6.5	6.5	6.5
Q5FVC7	Acap2	Arf-GAP with coiled-coil, ANK repeat and PH domain-containing protein 2	91.57	1	1	1	1	1	2	1	1	1	1	1	2	3.54E+03	7.27E+03	2.88E+04	2.83E+03	1.80E+03	3.83E+04	1.4	1.4	1.9	1.4	1.4	3.2
Q5XI22	Acat2	Acetyl-CoA acetyltransferase, cytosolic	41.11	5	6	4	6	5	4	5	6	4	6	5	4	3.93E+05	4.80E+05	2.23E+05	2.85E+05	1.32E+05	7.75E+04	29.5	37	23.4	37	33.2	23.4
P16638	Aclv	ATP-citrate synthase	120.54	20	21	12	20	19	13	20	21	12	20	19	13	3.38E+05	4.28E+05	1.23E+05	2.81E+05	2.68E+05	5.65E+04	27.9	28.4	17.5	27.8	26.5	18.3
Q63270	Aco1	Cytoplasmic aconitate hydratase	98.19	5	3	4	3	5	5	5	3	4	3	5	5	4.57E+04	2.71E+04	1.87E+04	1.51E+04	1.75E+04	2.13E+04	7.3	4.4	7	4.4	7.3	8.2
Q9ER34	Aco2	Aconitate hydratase, mitochondrial	85.43	2	1	2	1	1	2	2	1	2	1	1	2	6.72E+03	3.66E+03	4.63E+03	1.28E+03	2.82E+03	5.78E+03	3.6	1.7	3.6	1.9	1.7	3.6
Q64559	Acot7	Cytosolic acyl coenzyme A thioester hydrolase	40.97	2	2	2	2	2	2	2	2	2	2	2	2	6.09E+04	5.29E+04	5.76E+04	2.11E+04	4.00E+04	9.85E+03	5.9	5.9	5.9	5.9	5.9	5.9
P41498	Acp1	Low molecular weight phosphotyrosine protein phosphatase	18.22	4	4	2	4	4	2	4	4	2	4	4	2	2.08E+05	2.04E+05	1.41E+04	1.43E+05	5.73E+04	3.10E+04	27	27	18.9	27	27	15.7
Q6AY33	Acrbp	Acrosin-binding protein	35.92	2	1	1	2	0	0	2	1	1	2	0	0	1.24E+04	1.51E+04	2.14E+05	1.38E+04	0.00E+00	0.00E+00	8.2	3.2	3.2	8.2	0	0
Q9WUY6	Acrv1	Acrosomal vesicle protein 1	28.59	2	2	1	1	1	0	2	2	1	1	1	0	3.51E+04	6.18E+04	9.85E+03	3.85E+03	1.60E+04	0.00E+00	9.7	9.7	2.6	7.1	2.6	0
Q924N5	Acsbg1	Long-chain-fatty-acid--CoA ligase ACSBG1	80.52	38	39	33	37	37	32	38	39	33	37	37	32	4.11E+06	8.88E+06	1.96E+06	5.32E+06	3.62E+06	1.27E+06	55.6	58.5	54	55.6	55.6	50.2
P18163	Acsl1	Long-chain-fatty-acid--CoA ligase 1	78.18	4	3	2	3	2	3	4	3	2	3	2	3	2.74E+04	8.88E+03	8.18E+03	2.67E+03	8.54E+02	2.87E+03	7	5.3	3.7	4.4	3.7	5.3
P60711	Actb	Actin, cytoplasmic 1	41.74	29	33	29	31	30	23	1	1	1	1	1	1	4.48E+07	5.34E+07	3.95E+07	3.07E+07	2.23E+07	2.33E+07	90.4	92.5	91.5	91.7	91.7	85.6
P63259	Actg1	Actin, cytoplasmic 2	41.79	29	33	29	31	30	23	1	1	1	1	1	1	2.47E+05	2.92E+05	1.95E+05	1.13E+05	1.40E+05	8.90E+04	90.4	92.5	91.5	91.7	91.7	85.6
P63269	Actg2	Actin, gamma-enteric smooth muscle	42.01	23	28	26	27	22	21	1	2	2	2	1	1	8.37E+06	1.41E+07	9.83E+06	6.61E+06	5.60E+06	6.73E+06	71.9	81.4	80.6	79.6	77.7	74.3
Q4KM87	Actl6a	Actin-like 6A	47.42	1	2	1	0	1	1	1	2	1	0	1	1	6.01E+03	2.00E+04	1.65E+04	0.00E+00	1.61E+03	1.63E+03	3.3	7.5	4.2	0	4.2	4.2
Q4QR76	Actl7b	Actin-like protein 7B	45.49	6	5	5	3	3	2	6	5	5	3	3	2	8.43E+04	1.09E+05	7.31E+04	2.07E+04	1.71E+04	2.70E+03	27.8	22.3	27.6	14.9	15.1	10.6
Q6GMN8	Actn1	Alpha-actinin-1	102.61	27	25	25	24	21	23	16	14	15	14	11	13	1.82E+05	1.67E+05	1.38E+05	7.78E+04	5.16E+04	8.09E+04	42.2	37.3	38.9	34.7	32.1	35.2
Q9QXQ0	Actn4	Alpha-actinin-4	102.97	28	31	26	23	27	24	17	20	16	13	17	14	1.05E+06	9.11E+05	6.63E+05	4.00E+05	4.11E+05	4.12E+05	45.2	47	42	38	43.5	38.2
P85515;B2RYJ7	Actr1a	Alpha-centractin	42.61	5	7	3	4	3	3	5	7	3	4	3	3	1.23E+05	1.69E+05	3.40E+04	8.32E+04	5.39E+04	4.00E+04	20.5	22.6	12.5	15.7	13.3	13
Q5M7U6	Actr2	Actin-related protein 2	44.73	5	6	2	6	4	2	5	6	2	6	4	2	2.71E+05	9.63E+04	2.72E+04	1.12E+05	6.19E+04	2.57E+04	21.6	27.4	6.1	27.4	12.7	6.1
A0A0G2K1C0	Actr3	Actin-related protein 3	47.58	6	8	4	6	6	2	6	8	4	6	6	2	1.73E+05	1.67E+05	4.13E+04	5.90E+04	1.32E+05	5.99E+03	23.9	28.9	14.3	23.9	23.9	5.3
Q5M876	Acy3	N-acyl-aromatic-L-amino acid amidohydrolase (carboxylate-forming)	35.42	7	7	6	7	4	4	7	7	6	7	4	4	3.49E+05	3.01E+05	1.51E+05	3.15E+05	2.13E+05	8.17E+04	26	26	25.7	26	15.4	23.2
Q920P6	Ada	Adenosine deaminase	39.90	1	1	0	1	1	0	1	1	0	1	1	0	1.02E+04	3.67E+04	0.00E+00	3.64E+03	4.97E+03	0.00E+00	5.4	5.4	0	5.4	5.4	0
D4A4X6	Adamts12	ADAMTS-like 2	105.57	1	1	1	1	1	1	1	1	1	1	1	1	1.42E+04	9.15E+03	8.81E+03	9.38E+03	5.44E+03	6.60E+03	2	2	2	2	2	2
Q63028	Add1	Alpha-adducin	80.34	14	15	13	14	15	10	14	15	13	14	15	10	1.61E+05	4.28E+05	7.22E+04	1.89E+05	1.48E+05	4.82E+04	33.6	36.1	30.1	32.8	36.1	20.3
D3ZCH7	Add3	Adducin 3 (Gamma), isoform CRA_a	74.96	5	6	2	6	6	1	5	6	2	6	6	1	2.47E+04	1.71E+05	1.42E+04	3.77E+04	4.84E+04	7.40E+03	12.8	14.5	5.2	14.9	15.5	2.7
A0A0G2JSI4	Adgre5	Adhesion G protein-coupled receptor E5	99.39	4	4	3	4	3	3	4	4	3	4	3	3	6.14E+04	3.71E+04	3.46E+04	6.01E+04	3.57E+04	3.02E+04	7.1	7.1	3.7	7.1	3.7	3.7
P06757	Adh1	Alcohol dehydrogenase 1	39.65	16	18	11	16	17	11	16	18	11	16	17	11	4.55E+06	1.37E+07	3.00E+06	5.78E+06	3.19E+06	1.79E+06	58	64.4	46.8	58	58	46.8
Q7TQ90	Adh4	Alcohol dehydrogenase 4 class-2	93.85	3	3	3	3	3	3	3	3	3	3	3	3	4.19E+04	8.71E+04	2.46E+04	3.52E+04	2.78E+04	1.24E+04	6.8	6.8	6.8	6.8	6.8	6.8
Q562C9	Adi1	1,2-dihydroxy-3-keto-5-methylthiopentene dioxygenase	21.46	6	6	4	5	3	5	6	6	4	5	3	5	2.05E+05	5.88E+05	7.13E+05	2.83E+05	5.21E+05	5.32E+05	44.7	44.7	28.5	33	26.3	33
A0A0G2K845	Adipoq	Adiponectin, C1Q and collagen domain-containing	23.47	2	2	2	2	2	2	2	2	2	2	2	2	4.24E+05	9.11E+05	8.02E+05	1.79E+05	1.40E+06	8.02E+05	12.4	12.4	12.4	12.4	12.4	12.4
Q64640	Adk	Adenosine kinase	40.13	7	6	5	6	4	6	7	6	5	6	4	6	2.33E+05	2.38E+05	9.69E+04	1.42E+05	9.16E+04	4.31E+04	24.1	21.9	17.2	21.9	14.1	20.5
Q02589	Adprh	[Protein ADP-ribosylarginine] hydrolase	39.96	5	6	3	4	5	4	5	6	3	4	5	4	1.95E+05	2.98E+05	9.41E+04	4.31E+04	5.15E+04	2.69E+04	21	23.8	11.9	16.3	21	18
D3ZW08	Adsl	Adenylosuccinate lyase	54.85	5	5	3	6	4	4	5	5	3	6	4	4	7.29E+04	1.08E+05	2.23E+04	6.33E+04	4.61E+04	2.50E+04	15.9	15.9	9.7	21.1	12	13.8
D4AEP0	Adss	Adenylosuccinate synthetase isozyme 2	50.09	2	2	2	2	2	2	2	2	2	2	2	2	2.33E+04	4.26E+04	3.77E+04	1.28E+04	1.08E+04	9.64E+03	4.8	4.8	4.8	4.8	4.8	4.8
A0A0H2UHL3	Aebp1	Adipocyte enhancer-binding protein 1	127.99	9	10	7	6	9	7	9	10	7	6	9	7	9.21E+04	7.32E+04	4.84E+04	1.94E+04	5.50E+04	4.66E+04	10.6	11.7	7.5	7.4	10.7	8.1
P36953	Afam	Afamin	69.34	42	48	41	40	44	41	42	48	41	40	44	41	1.92E+07	1.52E+07	1.68E+07	1.58E+07	1.95E+07	1.55E+07	70.7	72.2	63.8	70.2	72.2	63.8
F1M9N7	Agfg1	Arf-GAP domain and FG repeat-containing protein 1	58.05	3	3	3	2	2	2	3	3	3	2	2	2	1.83E+04	4.90E+04	1.51E+04	1.14E+04	1.51E+04	1.20E+04	7.9	7.9	7.9	6.1	6.1	5.9
A0A0G2K7G2	Agfg2	ArfGAP with FG repeats 2	50.10	2	2	1	2	2	1	2	2	1	2	2	1	1.08E+04	4.94E+04	8.74E+03	8.93E+03	1.06E+04	3.56E+03	7.6	7.6	3.9	7.6	7.6	3.9
D4A2F1	Agrn	Agrin	206.59	2	2	2	1	2	2	2	2	2	1	2	2	3.32E+03	7.96E+03	5.39E+03	3.70E+01	2.54E+03	1.02E+04	1.5	1.5	1.5	0.6	1.5	1.5
P01015	Agt	Angiotensinogen	51.98	11	12	9	11	11	9	11	12	9	11	11	9	2.18E+06	2.21E+06	2.94E+06	2.47E+06	3.58E+06	2.85E+06	28.1	28.7	24.7	28.1	28.1	24.7
P10760	Ahcy	Adenosylhomocysteinase	47.54	12	11	12	12	10	11	12	11	12	12	10	11	1.20E+06	1.23E+06	6.21E+05	7.51E+05	5.64E+05	3.42E+05	37.3	35.2	37.3	37.3	28.5	35.2
A0A140TAI8	Ahcyl1	S-adenosylhomocysteine hydrolase-like protein 1	52.90	4	6	5	5	5	5	4	6	5	5	5	5	5.36E+04	1.62E+05	7.81E+04	6.91E+04	4.41E+04	3.03E+04	12	15.8	11.6	13.7	13.3	11.6
A0A0G2JUA5	Ahnak	AHNAK nucleoprotein	581.12	39	45	36	37	37	34	39	45	36	37	37	34	1.81E+05	2.44E+05	8.73E+04	1.74E+05	1.05E+05	6.00E+04	24.6	26.4	19.7	22.8	24.6	25.5
B0BN63	Ahsa1	Activator of Hsp90 ATPase activity 1	38.10	2	4	3	2	2	1	2	4	3	2	2	1	2.83E+04	1.18E+05	1.84E+04	1.33E+04	1.54E+04	3.13E+03	7.7	19.8	13.3	9.2	9.2	3.6
P24090	Ahsg	Alpha-2-HS-glycoprotein	37.98	23	24	23	23	24	22	21	22	21	21	22	20	1.16E+08	1.22E+08	1.36E+08	1.22E+08	1.12E+08	1.37E+08	66.8	66.8	71.3	66.8	71.3	66.5
Q4G079	Aimp1	Aminoacyl tRNA synthetase complex-interacting multifunctional protein 1	34.57	2	2	0	1	2	0	2	2	0	1	2	0	1.94E+04	9.56E+04	0.00E+00	4.61E+03	1.38E+04	0.00E+00	10.2	10.2	0	6.3	10.2	0
Q5FWY5	Aip	AH receptor-interacting protein	37.60	2	2	1	1	1	0	2	2	1	1	1	0	2.68E+04	4.47E+04	4.32E+03	6.33E+03	1.31E+05	0.00E+00	9.4	9.4	4.2	4.2	5.2	0
P39069	Ak1	Adenylate kinase isoenzyme 1	21.58	7	9	5	6	7	4	7	9	5	6	7	4	8.46E+05	9.68E+05	2.76E+05	2.58E+05	4.06E+05	2.37E+05	46.9	53.1	40.2	40.2	46.9	28.4
Q5QD51	Akap12	A-kinase anchor protein 12	181.11	11	12	7	11	11	4	11	12	7	11	11	4	5.47E+04	9.52E+04	3.35E+04	3.26E+04	2.67E+04	9.23E+03	11.1	11.8	6.3	10.8	11.1	4.6
O35774	Akap4	A-kinase anchor protein 4	93.49	6	5	7	6	3	4	6	5	7	6	3	4	1.71E+04	2.39E+04	4.44E+04	2.08E+04	4.32E+03	8.90E+03	11.1	9.4	13.3	11.1	6.7	8.4
F1LPB4	Akap9	A-kinase-anchoring protein 9	433.94	2	3	2	3	2	2	2	3	2	3	2	2	2.15E+04	4.07E+03	1.19E+04	1.39E+04	1.27E+04	4.42E+03	1	1.4	1	1.4	1	1
P51635	Akr1a1	Alcohol dehydrogenase [NADP(+)]	36.51	5	5	5	4	6	3	5	5	5	4	6	3	1.19E+05	2.13E+05	1.27E+05	8.07E+04	1.43E+05	9.78E+04	17.2	17.2	17.8	13.8	21.8	11.1
P07943	Akr1b1	Aldose reductase	35.80	10	12	11	10	11	12	9	11	10	9	10	11	1.12E+06	1.35E+06	2.06E+06	6.49E+05	1.06E+06	9.99E+05	41.5	52.2	45.3	41.5	45.3	48.1
Q5RJP0	Akr1b7	Aldose reductase-related protein 1	36.12	3	4	4	3	4	4	1	1	1	1	1	1	3.32E+05	5.18E+05	2.33E+05	3.39E+05	2.10E+05	1.05E+05	13.3	16.1	16.1	13.3	16.1	16.1
G3V786	Akr1b8	Aldo-keto reductase family 1, member B8	36.16	12	15	12	12	12	11	9	11	8	9	8	7	1.05E+06	2.22E+06	8.15E+05	1.33E+06	6.89E+05	3.15E+05	57	68.7	50.9	54.4	50.9	48.1
P23457	Akr1c9	3-alpha-hydroxysteroid dehydrogenase	37.03	5	6	5	5	5	4	5	6	5	5	5	4	2.23E+05	5.08E+05	3.48E+05	2.23E+05	1.21E+05	1.74E+05	23.3	26.1	23.3	23.3	23.3	18.6
Q8CG45	Akr7a2	Aflatoxin B1 aldehyde reductase member 2	40.68	7	7	6	7	7	5	7	7	6	7	7	5	6.95E+05	8.77E+05	5.35E+05	5.04E+05	2.84E+05	2.77E+05	31.1	31.1	22.9	31.1	31.1	19.9
P38918	Akr7a3	Aflatoxin B1 aldehyde reductase member 3	36.75	2	3	1	2	2	0	2	3	1	2	2	0	5.35E+04	4.58E+04	1.39E+04	4.49E+04	3.25E+04	0.00E+00	8	12.8	3.4	8	8	0
Q3HSE5	Akt2	Non-specific serine/threonine protein kinase	55.63	2	2	1	1	2	1	2	2	1	1	2	1	2.33E+04	1.17E+04	5.60E+03	5.54E+03	1.07E+04	1.83E+03	5.4	5.4	3.3	2.1	5.4	3.3
P06214	Alad	Delta-aminolevulinic acid dehydratase	36.03	13	11	11	12	14	8	13	11	11	12	14	8	4.63E+05	6.89E+05	2.26E+05	5.65E+05	4.35E+05	9.87E+04	67.6	57.6	60	58.8	69.1	49.1
P02770	Alb	Serum albumin	68.73	88	91	88	88	91	85	86	89	85	86	89	82	2.90E+08	3.12E+08	2.86E+08	3.22E+08	3.26E+08	2.84E+08	82.9	82.9	80.6	82.9	82.9	80.9
Q3T1L0	Aldh16a1	Aldehyde dehydrogenase family 16 member A1	85.41	7	6	4	6	7	2	7	6	4	6	7	2	1.57E+05	1.30E+05	2.08E+04	9.56E+04	1.01E+05	8.10E+03	11	9.7	6.6	9.7	11	3.7
P51647	Aldh1a1	Retinal dehydrogenase 1	54.46	27	32	29	28	28	26	21	25	23	23	21	20	5.00E+06	1.24E+07	5.23E+06	5.11E+06	4.71E+06	2.44E+06	58.9	63.5	62.9	60.1	59.3	61.7
Q63639	Aldh1a2	Retinal dehydrogenase 2	56.64	8	8	5	4	5	4	7	7	5	4	4	4	2.36E+05	1.48E+05	7.86E+04	5.35E+04	6.22E+04	4.56E+04	27.6	27.6	15.1	11.8	15.4	13.1
A0A0G2JUS6	Aldh1a3	Aldehyde dehydrogenase family 1 member A3	56.09	4	4	2	3	3	3	3	3	2	3	2	3	2.87E+04	2.18E+04	1.73E+04	1.30E+04	1.22E+04	1.32E+04	9	9	4.7	6.8	6.8	6.8
P13601	Aldh1a7	Aldehyde dehydrogenase, cytosolic 1	54.56	9	10	9	7	10	7	3	3	3	2	3	1	8.47E+04	1.28E+05	2.57E+04	5.87E+04	4.16E+04	7.05E+03	19	21	20.4	20	21	16.4
G3V7I5	Aldh1b1	Aldehyde dehydrogenase X, mitochondrial	57.66	0	1	0	0	0	0	0	1	0	0	0	0	0.00E+00	1.44E+04	0.00E+00	0.00E+00	0.00E+00	0.00E+00	0	2.3	0	0	0	0

Uniprot accession number	Gene symbol	Protein name	Mol. weight [kDa]	No. Peptides Control wk1	No. Peptides Control wk8	No. Peptides Control wk14	No. Peptides Heat wk1	No. Peptides Heat wk8	No. Peptides Heat wk14	No. Unique peptides Control wk1	No. Unique peptides Control wk8	No. Unique peptides Control wk14	No. Unique peptides Heat wk1	No. Unique peptides Heat wk8	No. Unique peptides Heat wk14	iBAQ Control wk1	iBAQ Control wk8	iBAQ Control wk14	iBAQ Heat wk1	iBAQ Heat wk8	iBAQ Heat wk14	Sequence coverage Control wk1 [%]	Sequence coverage Control wk8 [%]	Sequence coverage Control wk14 [%]	Sequence coverage Heat wk1 [%]	Sequence coverage Heat wk8 [%]	Sequence coverage Heat wk14 [%]
P28037	Aldh1l1	Cytosolic 10-formyltetrahydrofolate dehydrogenase	98.87	17	18	12	16	16	8	17	18	12	16	16	8	1.21E+05	1.47E+05	2.56E+04	1.08E+05	7.67E+04	1.18E+04	29.3	30.9	20.7	27.2	27.9	12.9
F1LN88	Aldh2	Aldehyde dehydrogenase, mitochondrial	56.52	13	14	9	10	12	11	13	14	9	10	12	11	6.12E+05	5.30E+05	3.27E+05	2.10E+05	2.88E+05	1.83E+05	36.8	38.7	22.7	31.8	34.5	32.2
G3V7J0	Aldh6a1	Aldehyde dehydrogenase family 6, subfamily A1, isoform CRA_b	57.75	5	4	3	3	3	3	5	4	3	3	3	3	1.35E+05	8.22E+04	4.91E+04	2.50E+04	2.61E+04	2.23E+04	15.9	14	12.1	12.1	11.2	12.1
Q64057	Aldh7a1	Alpha-aminoadipic semialdehyde dehydrogenase	58.75	9	11	8	10	10	7	9	11	8	10	10	7	4.59E+05	5.84E+05	1.83E+05	3.25E+05	2.47E+05	8.72E+04	23.7	29.7	22.4	27.6	27.6	20.2
A0A0G2JSI1	Aldh9a1	4-trimethylaminobutyraldehyde dehydrogenase	54.05	17	21	16	16	15	15	17	21	16	16	15	15	1.02E+06	1.69E+06	9.22E+05	8.20E+05	4.96E+05	5.06E+05	57.7	60.8	51.7	53.3	46.7	47.1
P05065	Aldoa	Fructose-bisphosphate aldolase A	39.35	14	14	11	14	14	11	11	11	9	11	11	8	9.49E+05	1.35E+06	5.65E+05	6.78E+05	9.51E+05	4.51E+05	55.5	55.5	42.3	55.5	55.5	36.5
Q66HT1	Aldob	Fructose-bisphosphate aldolase B	39.53	0	0	3	1	1	4	0	0	3	1	1	4	0.00E+00	0.00E+00	2.35E+04	6.26E+03	1.67E+04	7.78E+04	0	0	11.3	3.6	3.6	14.8
A0A0G2K3Q6	Aldoc	Fructose-bisphosphate aldolase C	40.48	8	8	6	7	8	6	5	5	4	4	5	3	7.84E+04	1.93E+05	1.20E+05	8.58E+04	1.02E+05	1.34E+05	28.7	28.7	24.7	24.9	28.7	23.9
D3ZXH7	Alyref	Aly/REF export factor	19.92	1	1	0	1	1	0	1	1	0	1	1	0	7.12E+04	1.46E+04	0.00E+00	1.70E+04	8.55E+03	0.00E+00	14.3	14.3	0	14.3	14.3	0
Q64240	Ambp	Protein AMBP;Alpha-1-microglobulin;Inter-alpha-trypsin inhibitor light chain;Trypstatin	38.85	19	23	21	20	22	21	19	23	21	20	22	21	4.63E+07	4.31E+07	4.41E+07	4.86E+07	4.36E+07	4.13E+07	53.6	56.2	53.6	53.6	56.2	53.6
E9PSQ1	Amy1a	Alpha-amylase	58.93	11	10	8	9	10	8	11	10	8	9	10	8	4.98E+05	2.19E+05	4.19E+05	2.85E+05	3.09E+05	4.51E+05	36.3	33.2	24.2	27.3	30.3	24.2
P22282	Andpro	Cystatin-related protein 1	21.06	7	7	3	7	6	5	1	1	1	1	1	1	1.69E+06	2.92E+06	2.11E+04	1.04E+06	6.93E+05	4.23E+05	42.6	42.6	28.4	42.6	38.6	38.1
A0A0G2JSU6	Andpro	Cystatin	21.07	7	7	2	7	6	4	1	1	0	1	1	0	1.60E+05	1.58E+05	0.00E+00	9.89E+04	3.04E+04	0.00E+00	42.6	42.6	17	42.6	38.6	26.7
Q5GAM5	Ang2	Angiogenin ribonuclease 2	18.53	2	2	2	2	2	1	2	2	2	2	2	1	1.25E+06	7.67E+05	4.74E+05	7.92E+05	6.02E+05	5.79E+05	13.2	13.2	13.2	13.2	13.2	7.2
F7FHP0	Angptl3	Angiopoietin-like 3	52.62	0	1	0	0	1	1	0	1	0	0	1	1	0.00E+00	5.44E+03	0.00E+00	0.00E+00	2.13E+03	4.88E+03	0	4.8	0	0	4.8	2.4
Q5U313	Ankrd13a	Ankyrin repeat domain 13a	67.32	1	1	2	1	1	1	1	1	2	1	1	1	7.85E+03	1.42E+04	1.58E+04	6.50E+03	3.17E+03	2.65E+03	2.2	2.2	4.2	2.2	2.2	2
A0A0G2K7X0	Anp32a	Acidic leucine-rich nuclear phosphoprotein 32 family member A	26.32	3	5	4	4	3	2	3	5	4	4	3	2	1.15E+05	1.19E+06	2.90E+05	4.25E+05	1.31E+05	3.36E+04	15.7	21.4	19.2	19.2	15.7	10.9
Q9EST6	Anp32b	Acidic leucine-rich nuclear phosphoprotein 32 family member	31.06	2	4	3	2	2	1	2	4	3	2	2	1	1.53E+04	2.99E+05	8.71E+04	3.20E+04	8.52E+03	4.33E+03	9.6	17.3	16.5	10.3	9.6	5.1
Q5XIE0	Anp32e	Acidic leucine-rich nuclear phosphoprotein 32 family member	29.42	3	3	2	3	3	2	3	3	2	3	3	2	1.37E+05	4.79E+05	1.56E+05	1.28E+05	1.45E+05	4.00E+04	18.6	17.1	9.7	17.1	17.1	9.7
F1LT78	Antxr2	Anthrax toxin receptor	53.27	1	1	1	1	1	1	1	1	1	1	1	1	2.45E+04	1.81E+04	1.68E+04	2.15E+04	1.56E+04	1.62E+04	2.7	2.7	2.7	2.7	2.7	2.7
P07150	Anxa1	Annexin A1	38.83	4	4	4	5	3	4	4	4	4	5	3	4	8.77E+04	7.71E+04	5.94E+04	6.41E+04	2.76E+04	3.95E+04	16.8	16.8	16.8	22.3	12.1	16.8
Q07936	Anxa2	Annexin A2	38.68	9	9	9	10	12	10	9	9	9	10	12	10	3.56E+05	3.91E+05	1.29E+05	4.92E+05	6.55E+05	1.60E+05	36	36.9	33.9	41.6	48.7	34.8
P14669	Anxa3	Annexin A3	36.36	2	1	4	3	1	3	2	1	4	3	1	3	7.24E+03	2.11E+04	5.11E+04	2.31E+04	4.68E+03	2.87E+04	5.9	3.4	15.1	9.3	3.4	11.7
Q66HH8	Anxa5	Annexin A5	35.77	1	2	2	2	2	1	1	2	2	2	2	1	4.87E+03	2.11E+04	9.16E+03	2.11E+04	2.56E+04	2.79E+03	2.8	6.6	6.6	6.6	6.3	2.8
Q6IMZ3;P48037	Anxa6	Annexin A6	75.76	4	3	1	3	3	2	4	3	1	3	3	2	2.48E+04	1.70E+04	1.10E+03	1.53E+04	4.73E+04	3.70E+03	10.4	5.2	2.4	5.2	5.2	3.7
F1LRQ1	Aox1	Aldehyde oxidase 1	146.90	24	30	23	26	26	19	24	30	23	26	26	19	1.82E+05	6.95E+05	3.01E+05	2.79E+05	1.94E+05	1.71E+05	28.1	34.6	26.6	31.4	31.4	24.4
A0A096P6M6	Aox2	Aldehyde oxidase 2	147.93	2	2	0	2	1	0	2	2	0	2	1	0	3.21E+03	9.10E+03	0.00E+00	5.07E+03	1.74E+03	0.00E+00	1.5	1.5	0	1.5	0.6	0
A0A0G2K1Z5	Aox3	Aldehyde oxidase 3	146.66	24	27	14	25	22	10	24	27	14	25	22	10	2.72E+05	4.73E+05	1.01E+05	2.50E+05	1.34E+05	3.22E+04	27.7	29	15.5	28.4	25.7	11.6
A0A0G2K2V2	Ap1b1	AP-1 complex subunit beta-1	103.82	9	11	6	9	9	4	5	6	3	4	4	2	6.27E+04	8.32E+04	1.84E+04	5.65E+04	4.34E+04	1.06E+04	14.4	18.2	7.7	11.8	11.8	4.5
Q32Q06	Ap1m1	AP-1 complex subunit mu-1	48.56	1	1	1	0	1	1	1	1	1	0	1	1	4.80E+03	3.01E+04	1.78E+04	0.00E+00	1.53E+04	1.96E+04	2.6	2.6	2.6	0	2.6	2.6
Q66HM2	Ap2a2	AP-2 complex subunit alpha-2	104.17	4	4	5	4	5	3	4	4	5	4	5	3	5.82E+04	3.30E+04	2.29E+04	3.68E+04	2.72E+04	3.13E+04	4.9	4.9	5.9	4.4	5.6	3.7
P62944	Ap2b1	AP-2 complex subunit beta	104.55	7	9	6	8	8	4	3	4	3	3	3	2	1.04E+05	8.88E+04	3.09E+04	1.17E+05	4.20E+04	1.93E+04	9.1	10.5	7.7	10.4	10.4	4.5
A0A140TAH5	Ap2m1	AP-2 complex subunit mu	49.53	3	3	1	3	3	1	3	3	1	3	3	1	3.29E+04	4.44E+04	3.00E+03	2.82E+04	3.42E+04	3.83E+03	7.8	7.8	2.1	7.8	7.8	2.1
A0A0H2UHH2	Apcs	Serum amyloid P-component	31.62	14	16	14	16	16	15	14	16	14	16	16	15	1.18E+07	7.86E+06	9.09E+06	9.78E+06	1.07E+07	8.41E+06	63.3	63.3	60.7	63.3	63.3	60.7
P13676	Apeh	Acylamino-acid-releasing enzyme	81.38	8	8	6	8	8	6	8	8	6	8	8	6	1.40E+05	1.51E+05	6.18E+04	1.11E+05	6.37E+04	4.37E+04	22.1	19.8	15.6	19.8	20.1	15.6
P43138	Apex1	DNA-(apurinic or apyrimidinic site) lyase	35.54	1	0	1	1	2	0	1	0	1	1	2	0	1.18E+04	0.00E+00	2.70E+03	7.58E+03	2.09E+04	0.00E+00	5.7	0	4.1	5.7	9.8	0
D3ZUI1	Apip	Methylthioribulose-1-phosphate dehydratase	27.05	2	2	1	2	2	1	2	2	1	2	2	1	3.33E+04	5.43E+04	1.17E+04	2.23E+04	2.05E+04	2.53E+03	11.6	11.6	5.8	11.6	11.6	5.8
P04639	Apoa1	Apolipoprotein A-I;Proapolipoprotein A-I	30.06	31	32	30	32	31	33	31	32	30	32	31	33	2.87E+08	2.73E+08	2.54E+08	3.35E+08	2.58E+08	2.38E+08	72.6	72.6	69.1	72.6	72.6	71
B0BNM1	Apoa1bp	NAD(P)H-hydrate epimerase	30.89	6	6	2	5	5	2	6	6	2	5	5	2	3.87E+05	4.28E+05	6.40E+04	1.90E+05	1.68E+05	2.12E+04	30.5	30.5	12.4	30.5	30.5	12.4
P04638	Apoa2	Apolipoprotein A-II;Proapolipoprotein A-II	11.44	6	6	6	6	6	6	6	6	6	6	6	6	9.95E+06	6.87E+06	7.92E+06	9.07E+06	4.19E+06	5.40E+06	50	50	50	50	50	50
P02651	Apoa4	Apolipoprotein A-IV	44.46	45	47	40	46	47	41	45	47	40	46	47	41	1.55E+08	1.43E+08	1.63E+08	1.70E+08	1.62E+08	1.40E+08	81.6	81.6	81.6	81.6	81.6	81.6
F1M6Z1	Apob	Apolipoprotein B-100;Apolipoprotein B-48	509.69	86	90	92	93	92	90	86	90	92	93	92	90	3.65E+05	3.42E+05	5.13E+05	4.41E+05	3.16E+05	3.82E+05	26	26.9	28	28.1	28.5	27.7
P19939	Apoc1	Apolipoprotein C-I	9.86	3	3	3	3	3	3	3	3	3	3	3	3	1.19E+07	9.40E+06	9.72E+06	1.34E+07	8.14E+06	7.85E+06	22.7	22.7	22.7	22.7	22.7	22.7
G3V8D4	Apoc2	Apolipoprotein C-II	10.70	5	5	5	6	5	4	5	5	5	6	5	4	2.66E+07	1.53E+07	1.32E+07	3.15E+07	1.58E+07	1.72E+07	49.5	49.5	47.4	49.5	47.4	47.4
A0A0G2K8Q1	Apoc3	Apolipoprotein C-III	11.03	3	4	4	3	4	3	3	4	4	3	4	3	5.52E+07	5.62E+07	4.69E+07	6.30E+07	4.00E+07	4.15E+07	43	51	51	43	51	43
P55797	Apoc4	Apolipoprotein C-IV	14.53	4	4	3	4	3	4	4	4	3	4	3	4	3.50E+06	2.99E+06	3.91E+06	3.19E+06	1.90E+06	3.90E+06	35.5	35.5	28.2	35.5	28.2	35.5
M0R4S2	Apod	Apolipoprotein D	21.61	5	5	4	5	5	5	5	5	4	5	5	5	4.86E+05	3.71E+05	3.12E+05	5.40E+05	3.14E+05	4.00E+05	29.1	29.1	22.2	29.1	29.1	29.1
A0A0G2K151	Apoe	Apolipoprotein E	41.20	29	29	27	27	29	27	29	29	27	27	29	27	9.42E+07	8.68E+07	8.67E+07	9.90E+07	1.01E+08	8.20E+07	58.2	59.1	58.2	55.7	59.1	56
Q5M889	Apof	Apolipoprotein F	33.84	3	3	3	2	3	3	3	3	3	2	3	3	2.34E+05	8.32E+04	2.45E+05	4.58E+04	1.63E+05	7.33E+04	15.3	15.3	15.3	10.7	15.3	15.3
Q5I0M1	Apoh	Beta-2-glycoprotein 1	38.46	23	24	21	23	24	23	23	24	21	23	24	23	4.73E+07	3.73E+07	5.25E+07	3.51E+07	4.48E+07	4.94E+07	55.7	58.8	57.4	58.3	58.8	58
P14630	Apom	Apolipoprotein M	21.51	6	6	5	6	5	6	6	6	5	6	5	6	8.06E+06	7.28E+06	8.03E+06	8.65E+06	7.15E+06	6.47E+06	35.8	35.8	32.6	35.8	31.6	35.8
Q5M890	Apon	Apolipoprotein N	28.23	6	6	7	6	6	7	6	6	7	6	6	7	2.28E+06	1.90E+06	2.35E+06	2.38E+06	1.88E+06	2.35E+06	30.6	30.6	38.4	30.6	30.6	38.4
Q6P6Q5	App	Amyloid-beta A4 protein	82.80	3	3	3	3	3	3	3	3	3	3	3	3	8.57E+04	8.60E+04	3.65E+04	6.52E+04	6.01E+04	3.19E+04	7.1	7.1	7.1	7.1	7.1	7.1
B4F779	Appl2	Adaptor protein, phosphotyrosine interaction, PH domain and leucine zipper containing 2	74.12	14	15	8	13	13	8	14	15	8	13	13	8	1.17E+05	2.58E+05	6.41E+04	1.08E+05	6.08E+04	3.42E+04	33.2	35.2	17.4	31.7	31.9	17.5
P36972	Aprt	Adenine phosphoribosyltransferase	19.55	7	8	5	6	6	5	7	8	5	6	6	5	4.19E+05	5.01E+05	1.61E+05	3.27E+05	2.27E+05	1.10E+05	57.8	58.3	43.3	50.6	50.6	43.3
Q66H80	Arcn1	Coatomer subunit delta	57.20	6	6	3	5	5	3	6	6	3	5	5	3	8.66E+04	1.00E+05	4.64E+04	5.29E+04	5.12E+04	4.23E+04	12.1	12.1	6.1	10.4	10.4	6.1
P84079	Arf1	ADP-ribosylation factor 1	20.70	12	11	10	11	12	9	2	2	2	2	2	1	1.98E+06	3.23E+06	1.44E+06	1.54E+06	1.13E+06	8.01E+05	73.5	70.7	65.7	73.5	73.5	65.7
A0A0G2JV81	Arf3	ADP-ribosylation factor 3	20.57	11	10	9	10	10	8	1	1	1	1	0	0	3.14E+04	2.94E+04	2.52E+04	1.77E+04	0.00E+00	0.00E+00	73.5	70.7	65.7	73.5	57.5	49.7
P61751	Arf4	ADP-ribosylation factor 4	20.40	7	7	7	7	7	6	3	3	3	3	3	3	4.99E+05	5.94E+05	2.98E+05	2.87E+05	1.67E+05	1.44E+05	66.1	66.1	66.1	66.1	66.1	58.3
P84083	Arf5	ADP-ribosylation factor 5	20.53	8	8	8	8	8	7	3	3	3	3	3	3	2.61E+05	3.56E+05	1.17E+05	1.98E+05	1.16E+05	4.66E+04	70.6	70.6	70.6	70.6	70.6	62.8
P62332	Arf6	ADP-ribosylation factor 6	20.08	3	4	0	2	4	2	3	4	0	2	4	2	4.58E+05	6.49E+05	0.00E+00	3.56E+05	4.70E+05	8.95E+03	33.7	42.3	0	27.4	42.3	24
A0A0G2K4J0	Arfgap3	ADP-ribosylation factor GTPase-activating protein 3	57.67	1	1	1	1	1	1	1	1	1	1	1	1	9.39E+03	1.62E+04	2.86E+03	5.63E+03	2.71E+03	1.60E+03	3.6	3.6	3.6	3.6	3.6	3.6
D4A6C5	Arhgap1	Rho GTPase-activating protein 1	50.62	11	11	7	9	9	10	11	11	7	9	9	10	2.03E+05	4.37E+05	7.39E+04	1.57E+05	9.03E+04	7.75E+04	33.5	33.5	20.5	26.4	24.1	31.2
Q5XI73	Arhgdia	Rho GDP-dissociation inhibitor 1	23.41	5	6	5	7	5	7	5	6	5	7	5	7	7.30E+05	7.54E+05	8.43E+05	5.38E+05	3.98E+05	5.84E+05	42.6	50	48.5	54.9	47.5	54.9
Q5M860	Arhgdib	Rho GDP dissociation inhibitor beta	22.88	2	1	1	1	1	1	2	1	1	1	1	1	1.35E+05	1.69E+04	5.61E+03	1.33E+04	7.00E+03	5.36E+03	21	10.5	10.5	10.5	10.5	10.5
D3ZXL1	Arih1	RBR-type E3 ubiquitin transferase	64.02	3	5	2	4	3	2	3	5	2	4	3	2	4.02E+05	2.85E+05	1.50E+04	3.08E+05	3.57E+05	6.62E+03	7.7	13.2	5.2	10.8	7.7	5.2
P61212	Arl1	ADP-ribosylation factor-like protein 1	20.41	3	2	2	2	2	2	3	2	2	2	2	2	1.06E+05	1.10E+05	6.60E+04	4.18E+04	2.30E+04	2.71E+04	26	18.2	18.2	18.2	18.2	18.2
F8WG91	Arl3	ADP-ribosylation factor-like protein 3	20.87	4	3	5	3	3	4	4	3	5	3	3	4	2.42E+05	3.75E+05	4.39E+05	1.95E+05	1.18E+05	1.26E+05	35.5	26.3	40.9	26.3	26.3	30.6
D3ZPP2	Arl8a;Arl8b	ADP-ribosylation factor-like protein 8B	21.39	1	1	1	1	1	2	1	1	1	1	1	2	4.54E+04	3.49E+04	3.61E+04	2.92E+04	7.77E+03	8.94E+03	5.4	5.4	5.4	5.4	5.4	10.2
Q6AYT5	Armt1	Protein-glutamate O-methyltransferase	50.18	6	8	5	5	4	2	6	8	5	5	4	2	1.38E+05	2.05E+05	6.77E+04	9.48E+04	3.91E+04	1.97E+04	16.6	23	14.8	14.4	12.1	6.4
O88656	Arpc1b	Actin-related protein 2/3 complex subunit 1B	41.06	6	6	6	5	5	6	6	6	6	5	5	6	2.80E+05	2.12E+05	2.03E+05	1.20E+05	1.17E+05	1.33E+05	24.7	24.7	24.7	20.2	20.2	24.7
A0A0G2K905	Arpc2	Actin-related protein 2/3 complex subunit 2	32.50	2	1	0	2	2	0	2	1	0	2	2	0	1.31E+05	5.74E+04	0.00E+00	4.65E+04	4.57E+04	0.00E+00	10.2	3.2	0	10.2	10.2	0
B2GV73	Arpc3	Actin-related protein 2/3 complex subunit 3	20.54	1	2	1	1	2	1	1	2	1	1	2	1	1.42E+05	2.00E+05	8.19E+04	6.37E+04	1.81E+05	6.00E+04	6.2	13.5	6.2	6.2	13.5	6.2
B2RZ72	Arpc4	Actin-related protein 2/3 complex subunit 4	19.67	2	1	1	2	1	1	2	1	1	2	1	1	2.18E+05	1.30E+05	4.83E+04	1.12E+05	1.16E+05	3.59E+04	19.6	6.5	6.5	19.6	6.5	6.5
Q4KLF8	Arpc5	Actin-related protein 2/3 complex subunit 5	16.32	1	2	1	1	1	1	1	2	1	1	1	1	1.08E+05	4.38E+04	2.32E+04	1.50E+04	1.99E+04	1.22E+04	12.6	21.2	8.6	12.6	12.6	8.6
Q6AYJ9	Art3	NAD(P)(+)--arginine ADP-ribosyltransferase	41.71	2	2	2	1	1	0	2	2	2	1	1	0	4.01E+04	5.01E+04	5.20E+04	2.38E+04	2.10E+04	0.00E+00	9.6	9.6	9.6	4.8	4.8	0
A0A0G2K2W6	Ash1l	Histone-lysine N-methyltransferase	326.47	0	0	1	1	1	1	0	0	1	1	1	1	0.00E+00	0.00E+00	8.57E+03	1.04E+04	2.10E+03	1.59E+04	0	0	0.6	0.6	0.4	0.6
Q4QRB8	Asl	Argininosuccinate lyase	51.39	4	5	2	4	3	2	4	5	2	4	3	2	1.13E+05	2.04E+05	5.90E+04	9.37E+04	7.37E+04	1.62E+04	11.7	14.1	4.3	11.7	6.9	5
D4AA35	Asmtl	Acetylserotonin O-methyltransferase-like	24.25	2	2	2	2	1	2	2	2	2	2	1	2	5.79E+04	6.25E+04	4.17E+04	4.70E+04	6.78E+03	3.44E+04	12.4	12.4	12.4	12.4	8	12.4
G3V9T7	Asna1	ATPase Asna1	38.82	6	6	3	4	4	2	6	6	3	4	4	2	2.09E+05	2.94E+05	1.68E+05	1.57E+05	1.06E+05	5.63E+04	25.3	25.3	12.9	16.7	16.7	10.1
P49088	Asns	Asparagine synthetase [glutamine-hydrolyzing]	64.25	15	16	8	15	15	6	15	16	8	15	15	6	1.00E+06	9.63E+05	1.91E+05	6.29E+05	4.42E+05	6.24E+04	36.2	36.2	23	36.2	33.2	16
Q8VI04	Asrgl1	Isoaspartyl peptidase/L-asparaginase	34.41	6	7	7	6	6	2	6	7	7	6	6	2	3.14E+05	3.60E+05	1.36E+05	2.99E+05	1.92E+05	6.57E+03	21.6	25.8	25.8	21.6	21.6	7.5
P09034	Ass1	Argininosuccinate synthase	46.50	23	27	22	24	23	16	23	27	22	24	23	16	4.46E+06	1.07E+07	2.22E+06	4.53E+06	3.21E+06	9.05E+05	56.6	59.5	55.8	58	56.6	47.6
D4A2N1	Ate1	Arginyl-tRNA--protein transferase 1	58.22	1	1	0	0	0	0	1	1	0	0	0	0	5.54E+03	2.33E+04	0.00E+00	0.00E+00	0.00E+00	0.00E+00	3.5	3.5	0	0	0	0
Q6AZ50	Atg3	Ubiquitin-like-conjugating enzyme ATG3	35.82	2	3	0	2	1	1	2	3	0	2	1	1	1.92E+04	1.50E+05	0.00E+00	2.52E+04	5.47E+03	9.28E+03	6.4	10.5	0	6.1	3.2	3.2
Q641Y5	Atg7	Ubiquitin-like modifier-activating enzyme ATG7	77.44	2	3	3	1	2	1	2	3	3	1	2	1	5.87E+03	1.37E+04	9.47E+03	1.24E+03	4.12E+03	2.50E+03	4.6	7	7	1.6	4.6	2.4
O35567	Atic	Bifunctional purine biosynthesis protein PURH	64.21	11	11	6	10	9	5	11	11	6	10	9	5	1.40E+05	1.58E+05	5.27E+04	6.99E+04	4.96E+04	2.97E+04	29.6	29.6	16.6	27	24.3	14.4
Q9WUC4	Atox1	Copper transport protein ATOX1	7.29	3	3	3	3	3	3	3	3	3	3	3	3	8.53E+05	9.77E+05	6.72E+05	4.08E+05	2.82E+05	3.68E+05	47.1	47.1	47.1	47.1	47.1	47.1
G3V6D3	Atp5b	ATP synthase subunit beta;ATP synthase subunit beta, mitochondrial	56.34	8	4	4	5	6	4	8	4	4	5	6	4	2.92E+05	3.55E+04	5.49E+04	3.22E+04	1.27E+05	4.41E+04	27.2	11.2	12.3	16.3	17.6	14.4
A0A0G2K099	Atp5fa1	ATP synthase subunit alpha, mitochondrial	54.30	6	4	5	3	6	4	6	4	5	3	6	4	8.39E+04	3.85E+04	2.73E+04	1.78E+04	5.67E+04	1.80E+04	18.7	11.4	14.4	9.8	18.3	11.8
D4A133	Atp6v1a	ATPase H+-transporting V1 subunit A	68.26	7	7	4	6	6	3	7	7	4	6	6	3	1.07E+05	1.30E+05	2.10E+04	7.26E+04	5.81E+04	8.38E+03	18.5	15.6	8.3	15.9	13.5	8.1

Uniprot accession number	Gene symbol	Protein name	Mol. weight [kDa]	No. Peptides Control wk1	No. Peptides Control wk8	No. Peptides Control wk14	No. Peptides Heat wk1	No. Peptides Heat wk8	No. Peptides Heat wk14	No. Unique peptides Control wk1	No. Unique peptides Control wk8	No. Unique peptides Control wk14	No. Unique peptides Heat wk1	No. Unique peptides Heat wk8	No. Unique peptides Heat wk14	iBAQ Control wk1	iBAQ Control wk8	iBAQ Control wk14	iBAQ Heat wk1	iBAQ Heat wk8	iBAQ Heat wk14	Sequence coverage Control wk1 [%]	Sequence coverage Control wk8 [%]	Sequence coverage Control wk14 [%]	Sequence coverage Heat wk1 [%]	Sequence coverage Heat wk8 [%]	Sequence coverage Heat wk14 [%]
B2GUV5	Atp6v1g1	V-type proton ATPase subunit G 1	13.71	2	2	1	2	1	2	2	2	1	2	1	2	1.06E+05	1.67E+05	4.83E+04	7.79E+04	7.23E+04	5.06E+04	13.6	13.6	12.7	22	12.7	22
Q99J86	Atrn	Attractin	158.67	4	4	4	4	5	4	4	4	4	4	5	4	2.47E+04	2.71E+04	2.46E+04	1.95E+04	3.88E+04	2.62E+04	3.4	3.4	3.4	3.4	4.3	3.4
Q9ER24	Atxn10	Ataxin-10	53.73	5	5	3	4	4	4	5	5	3	4	4	4	4.83E+04	6.75E+04	2.79E+04	2.89E+04	1.80E+04	1.61E+04	13.3	13.3	8.2	10.5	10.9	10.9
Q3B8R6	Azgp1	Zinc-alpha-2-glycoprotein	34.03	10	10	10	10	10	10	10	10	10	10	10	10	1.93E+06	1.54E+06	2.26E+06	1.76E+06	2.36E+06	1.98E+06	42.2	42.2	42.2	42.2	42.2	42.2
P07151	B2m	Beta-2-microglobulin	13.72	4	3	4	3	3	4	4	3	4	3	3	4	1.74E+06	9.35E+05	3.16E+06	8.66E+05	1.51E+06	3.30E+06	43.7	36.1	43.7	36.1	36.1	43.7
Q6MG49	Bag6	Large proline-rich protein BAG6	120.01	8	10	6	9	9	3	8	10	6	9	9	3	2.16E+05	2.46E+05	1.10E+05	1.41E+05	1.38E+05	7.00E+04	12	14.9	10.4	10.7	10.7	4.1
Q9R1T1	Banf1	Barrier-to-autointegration factor	10.04	1	2	2	2	3	1	1	2	2	2	3	1	2.12E+04	2.78E+05	6.51E+04	3.09E+04	9.81E+04	5.73E+04	13.5	42.7	42.7	21.3	50.6	29.2
Q05175	Basp1	Brain acid soluble protein 1	21.79	1	1	2	3	1	2	1	1	2	3	1	2	1.80E+04	5.74E+04	1.38E+04	7.83E+04	4.77E+03	1.90E+04	12.7	12.7	19.1	29.5	12.7	19.1
D3ZT71	Bcl2l13	BCL2-like protein 13	46.73	2	3	1	2	2	1	2	3	1	2	2	1	2.40E+04	4.98E+04	1.95E+03	1.31E+04	9.63E+03	6.07E+02	7.8	11.1	3.7	7.8	7.8	4.1
A0A0A0MXX5	Bdh2	3-hydroxybutyrate dehydrogenase type 2	27.68	1	1	2	2	2	1	1	1	2	2	2	1	1.67E+04	7.65E+03	1.38E+04	2.21E+04	9.62E+03	1.08E+04	4.7	4.7	9.8	9.8	9.8	5.1
Q5HZA7	Bin1	Myc box-dependent-interacting protein 1	45.83	1	1	1	1	1	0	1	1	1	1	1	0	1.33E+04	2.40E+04	8.12E+02	1.15E+04	7.58E+03	0.00E+00	4.6	4.6	4.6	4.6	4.6	0
A1A5L1	Blmh	Bleomycin hydrolase	52.45	4	2	2	4	6	2	4	2	2	4	6	2	7.31E+04	2.22E+04	1.10E+04	2.53E+04	1.05E+05	2.91E+04	13	5.7	8.6	13.4	16	7.9
P46844	Blvra	Biliverdin reductase A	33.57	7	8	8	6	8	5	7	8	8	6	8	5	4.61E+05	3.08E+05	9.60E+04	1.36E+05	1.39E+05	3.66E+04	30.5	35.3	35.9	26.1	35.3	24.4
B5DF65	Blvrb	Biliverdin reductase B	22.09	4	4	4	3	3	3	4	4	4	3	3	3	1.20E+05	1.69E+05	8.66E+04	9.38E+04	3.86E+04	4.79E+04	39.8	39.8	39.8	27.7	27.7	37.9
Q6P6G4	Bpgm	Phosphoglycerate mutase	30.08	2	2	0	1	2	0	2	2	0	1	2	0	5.78E+04	8.56E+04	0.00E+00	3.09E+04	1.89E+04	0.00E+00	10.5	10.5	0	3.1	10.5	0
Q9Z1N4	Bpnt1	3(2),5-bisphosphate nucleotidase 1	33.17	4	4	2	3	3	2	4	4	2	3	3	2	3.79E+04	9.37E+04	1.66E+04	3.24E+04	2.12E+04	9.45E+03	22.1	22.1	9.4	16.6	16.6	9.4
Q4V8K5	Brox	BRO1 domain-containing protein BROX	46.19	2	2	1	1	1	1	2	2	1	1	1	1	2.51E+04	3.38E+04	1.01E+04	6.56E+03	7.99E+03	3.63E+03	5.1	5.1	2.7	2.7	2.7	2.7
A0A140TAI2	Btd	Biotinidase	59.82	11	12	9	11	11	10	11	12	9	11	11	10	7.77E+05	4.85E+05	6.21E+05	4.82E+05	9.15E+05	5.80E+05	26	29.3	22.8	26	27.9	24.7
Q6P7P5	Bzw1	Basic leucine zipper and W2 domain-containing protein 1	48.04	2	2	1	2	1	0	2	2	1	2	1	0	3.04E+04	1.16E+04	3.50E+03	7.89E+03	3.89E+03	0.00E+00	7.9	7.9	5.7	7.9	5.7	0
P31720	C1qa	Complement C1q subcomponent subunit A	25.92	3	3	3	5	6	5	3	3	3	5	6	5	4.09E+05	2.31E+05	4.07E+05	6.51E+05	9.85E+05	5.86E+05	16.7	16.7	16.7	28.2	32.7	24.5
G3V7N9	C1qb	Complement C1q subcomponent subunit B	26.65	4	4	5	5	5	5	4	4	5	5	5	5	1.06E+06	9.20E+05	1.39E+06	1.38E+06	3.09E+06	1.40E+06	19	19	24.5	24.5	24.5	24.5
A0A0H2UHK1	C1qc	Complement C1q subcomponent subunit C	26.09	6	7	7	7	6	6	6	7	7	7	6	6	1.34E+06	1.07E+06	2.55E+06	1.63E+06	4.34E+06	1.92E+06	31.5	33.1	42.3	33.1	31.5	35.5
B5DEH7	C1r	Complement C1r subcomponent	80.42	31	35	32	32	34	31	31	35	32	32	34	31	4.13E+06	2.81E+06	2.88E+06	4.00E+06	5.17E+06	2.50E+06	62	63.2	62.8	62.7	63.5	60.8
F1LP96	C1rl	Complement C1r subcomponent-like protein	53.96	3	3	2	4	3	3	3	3	2	4	3	3	2.68E+04	2.44E+04	4.05E+04	3.09E+04	1.35E+04	6.07E+04	12.3	12.3	6.8	13.9	12.3	8.4
G3V7L3	C1s	Complement C1s subcomponent	77.71	21	22	20	21	21	21	21	22	20	21	21	21	3.54E+06	2.67E+06	2.59E+06	3.67E+06	4.69E+06	2.39E+06	44.5	42.8	42.8	44.5	44.5	43.9
Q6MG73	C2	Complement C2	83.70	24	25	24	23	26	28	12	12	12	12	13	13	4.07E+05	2.88E+05	4.85E+05	3.02E+05	6.30E+05	5.54E+05	46.7	46.7	46.8	44.6	50.5	50.7
M0RBF1	C3	Complement C3	186.32	193	203	188	200	192	187	180	190	175	187	179	174	1.72E+08	1.46E+08	1.65E+08	1.85E+08	1.69E+08	1.57E+08	89.1	90.4	89.2	90	89.7	88.9
P08649	C4	Complement C4	192.16	113	120	107	110	115	108	6	7	5	5	5	5	4.06E+06	3.33E+06	3.46E+06	3.27E+06	3.13E+06	3.00E+06	70.8	71.2	68.3	69.5	70.9	68.8
Q6MG90	C4b	Complement C4B	192.12	111	117	104	107	111	105	26	28	25	25	25	25	5.17E+06	3.91E+06	4.47E+06	4.73E+06	7.02E+06	4.21E+06	68.3	69	66.7	67.6	68.4	67.2
Q5M891	C4bpa	C4b-binding protein alpha chain	67.20	26	27	25	25	25	24	26	27	25	25	25	24	2.78E+06	2.72E+06	3.97E+06	3.56E+06	6.04E+06	4.01E+06	49.6	52.2	49.1	51.1	51.7	49.1
A0A5C5	C4bpb	C4b-binding protein beta chain	28.63	6	6	7	7	6	7	6	6	7	7	6	7	8.73E+05	8.28E+05	9.92E+05	9.28E+05	1.10E+06	8.81E+05	32.6	33.7	35.7	35.7	32.6	35.7
A0A096P6L9	C5	Complement C5	189.08	98	104	99	101	103	101	92	97	92	94	96	94	1.07E+07	7.71E+06	9.75E+06	1.21E+07	1.30E+07	9.04E+06	70.7	72.9	68.1	72.2	72.4	70.2
Q811M5	C6	Complement component C6	105.11	46	53	40	47	48	45	3	3	2	2	2	3	4.82E+06	4.37E+06	5.11E+06	4.08E+06	5.22E+06	5.01E+06	57.5	59.4	53.9	56.6	56.6	55.5
F1M7F7	C6	Complement component C6	104.32	44	52	40	47	48	44	1	2	2	2	2	2	3.78E+03	8.75E+04	8.14E+04	4.99E+04	7.37E+04	1.29E+05	55.7	58.1	53.4	56.2	56.2	54.1
A0A0G2K7X7	C7	Complement C7	93.66	32	34	29	32	32	26	32	34	29	32	32	26	3.02E+06	1.95E+06	2.20E+06	2.62E+06	2.22E+06	2.14E+06	49.9	50.2	42.9	48.3	49.9	40.2
D3ZWD6	C8a	Complement C8 alpha chain	66.27	35	42	34	38	39	36	35	42	34	38	39	36	1.33E+07	1.25E+07	1.19E+07	1.28E+07	1.25E+07	1.17E+07	75.6	79.2	69	76.3	77.5	69.3
P55314	C8b	Complement component C8 beta chain	66.67	40	46	38	41	40	38	40	46	38	41	40	38	1.78E+07	1.32E+07	1.38E+07	1.63E+07	1.65E+07	1.39E+07	62	63.3	60.3	63.5	59.6	60.3
D3ZPI8	C8g	Complement C8 gamma chain	18.41	13	15	11	13	14	11	13	15	11	13	14	11	1.34E+07	1.03E+07	9.67E+06	1.13E+07	1.40E+07	9.29E+06	78.7	82.3	74.4	79.9	79.9	74.4
F7F389	C9	Complement component C9	65.29	40	43	38	43	41	40	40	43	38	43	41	40	3.93E+07	2.86E+07	3.83E+07	3.50E+07	3.14E+07	3.65E+07	61.7	61.4	60.2	62.1	62.1	64.5
P27139	Ca2	Carbonic anhydrase 2	29.11	4	5	3	4	4	4	4	5	3	4	4	4	8.84E+04	3.16E+05	3.27E+04	2.39E+05	8.79E+04	1.40E+05	25.4	35	20	25.4	25.4	29.6
P14141	Ca3	Carbonic anhydrase 3	29.43	9	11	8	8	7	11	9	11	8	8	7	11	5.66E+05	7.10E+05	3.44E+05	4.20E+05	1.89E+05	3.83E+05	51.2	59.6	45.4	50	40.8	62.7
A0A0G2JZH0	Cab39	Calcium-binding protein 39	39.87	1	1	1	1	1	0	1	1	1	1	1	0	4.12E+04	4.08E+04	5.34E+03	1.72E+04	2.10E+04	0.00E+00	3.2	3.2	3.2	3.2	3.2	0
Q68FX6	Cabs1	Calcium-binding and spermatid-specific protein 1	42.26	11	12	11	10	9	10	11	12	11	10	9	10	5.19E+05	1.20E+06	5.91E+05	7.30E+05	1.38E+05	9.72E+04	53.6	54.6	53.6	50.8	46.9	50.8
M0R8P3	Cabyr	Calcium-binding tyrosine phosphorylation-regulated	43.04	1	2	1	1	1	0	1	2	1	1	1	0	7.75E+04	1.47E+05	3.57E+04	3.13E+04	6.92E+03	0.00E+00	2.5	10.2	2.5	2.5	2.5	0
Q6AYK6	Cacybp	Calcyclin-binding protein	26.54	4	5	3	2	3	2	4	5	3	2	3	2	4.20E+04	1.05E+05	8.20E+04	3.36E+04	4.17E+04	3.49E+04	24	32.8	17.5	11.4	20.1	13.5
A0A0G2JUT1	Cadm1	Cell adhesion molecule 1	42.83	2	2	1	2	2	0	2	2	1	2	2	0	1.04E+05	1.53E+04	4.20E+03	5.48E+04	3.42E+04	0.00E+00	11.7	11.7	5.5	11.7	11.7	0
P47728	Calb2	Calretinin	31.40	9	7	4	10	6	3	9	7	4	10	6	3	6.22E+05	4.57E+05	1.34E+05	6.97E+05	7.44E+04	3.16E+04	43.5	31.4	18.8	41.7	26.6	13.7
G3V9E3	Cald1	Non-muscle caldesmon	60.61	7	8	6	4	6	5	7	8	6	4	6	5	7.05E+04	1.99E+05	4.98E+04	1.82E+04	2.69E+04	2.39E+04	13.2	16.4	12.1	9.4	15.1	10
P0DP31	Calm3	Calmodulin-3	16.84	8	8	5	8	8	4	5	5	5	5	5	4	8.44E+05	9.38E+05	8.36E+05	1.17E+06	4.90E+05	2.90E+05	38.3	38.3	28.2	38.3	38.3	28.2
Q5U206	Calml3	Calmodulin-like protein 3	16.80	5	4	0	5	4	0	2	1	0	2	1	0	6.66E+04	3.28E+04	0.00E+00	7.61E+04	2.52E+05	0.00E+00	32.2	23.5	0	32.2	23.5	0
P18418	Calr	Calreticulin	48.00	12	13	10	11	10	8	12	13	10	11	10	8	1.42E+06	1.00E+06	5.35E+05	4.48E+05	3.36E+05	3.32E+05	47.6	49.5	43.8	46.4	43.8	40.4
G3V6S3	Calu	Calumenin	37.06	6	5	2	5	4	1	6	5	2	5	4	1	3.29E+05	3.05E+05	3.13E+04	3.31E+05	2.40E+05	1.62E+04	34.3	30.8	7.6	25.4	21.9	5.1
P15791	Camk2d	Calcium/calmodulin-dependent protein kinase type II subunit delta	60.08	3	3	1	1	4	0	3	3	1	1	4	0	2.29E+04	2.53E+04	3.11E+03	2.08E+03	3.80E+04	0.00E+00	6.6	6.6	2.3	1.9	10.1	0
P97536	Cand1	Cullin-associated NEDD8-dissociated protein 1	136.36	25	24	23	23	23	16	25	24	23	23	23	16	2.13E+05	2.93E+05	1.95E+05	1.80E+05	1.26E+05	6.54E+04	27.8	27.9	27	27.3	26.7	17.2
P35565	Canx	Calnexin	67.25	1	1	2	1	1	1	1	1	2	1	1	1	8.47E+04	2.54E+05	2.09E+05	3.35E+03	6.90E+03	1.50E+05	2.5	2.5	5.2	1.9	1.9	2.5
Q08163	Cap1	Adenylyl cyclase-associated protein 1	51.59	16	18	18	15	16	17	16	18	18	15	16	17	1.13E+06	1.42E+06	5.97E+05	6.74E+05	6.57E+05	2.80E+05	59.1	61	62.9	56.5	55.5	62.9
Q6AYC4	Capg	Macrophage-capping protein	38.80	8	8	8	8	7	7	8	8	8	8	7	7	7.29E+05	7.99E+05	5.32E+05	2.47E+05	3.19E+05	2.56E+05	38.1	38.1	38.1	38.1	32.7	37.5
F1LS29	Capn1	Calpain-1 catalytic subunit	82.10	8	8	4	8	7	4	8	8	4	8	7	4	4.35E+04	6.83E+04	2.88E+04	6.04E+04	3.22E+04	3.61E+04	14	14	8.1	14	12.6	8.3
Q07009	Capn2	Calpain-2 catalytic subunit	79.92	13	13	9	13	13	8	13	13	9	13	13	8	1.73E+05	2.20E+05	8.01E+04	9.45E+04	7.21E+04	5.13E+04	25	25.4	16.7	25	25	15.7
M0RD20	Capns1	Calpain small subunit 1	25.45	4	4	5	5	5	5	4	4	5	5	5	5	2.33E+05	1.66E+05	1.10E+05	1.83E+05	1.20E+05	9.74E+04	30	30	36.2	36.2	36.2	36.2
A0A0G2K8H0	Caprin1	Caprin-1	79.63	2	4	3	2	2	2	2	4	3	2	2	2	3.71E+04	7.92E+04	2.19E+04	3.41E+04	4.25E+04	1.63E+04	4.2	7.4	5.7	4.2	4.2	3.1
B2GUZ5	Capza1	F-actin-capping protein subunit alpha-1	32.91	5	5	4	5	4	5	4	4	3	4	3	4	5.54E+05	6.17E+05	3.07E+05	3.91E+05	2.96E+05	1.75E+05	30.8	29.4	21.7	30.8	25.5	25.9
Q3T1K5	Capza2	F-actin-capping protein subunit alpha-2	32.97	4	5	5	6	5	5	3	4	4	5	4	4	2.32E+05	3.14E+05	1.59E+05	1.84E+05	1.37E+05	8.71E+04	25.5	30.8	30.4	35	30.8	30.8
Q5XI32	Capzb	F-actin-capping protein subunit beta	30.63	8	9	7	8	7	4	8	9	7	8	7	4	7.47E+05	1.06E+06	4.37E+05	4.38E+05	2.51E+05	2.00E+05	34.9	37.1	32.4	34.9	29.8	22.4
Q9WU49	Carhsp1	Calcium-regulated heat stable protein 1	15.91	3	3	3	2	2	2	3	3	3	2	2	2	2.59E+05	3.19E+05	1.48E+05	1.56E+05	8.68E+04	7.63E+04	51.7	51.7	51.7	35.4	27.2	27.2
P43527	Casp1	Caspase-1;Caspase-1 subunit p20;Caspase-1 subunit p10	45.58	4	4	0	4	2	0	4	4	0	4	2	0	5.70E+04	9.80E+04	0.00E+00	4.68E+04	1.04E+04	0.00E+00	10.7	10.7	0	10.7	5.7	0
A0A0G2JSY2	Cast	Calpastatin	73.16	2	3	1	1	1	1	2	3	1	1	1	1	1.10E+04	4.04E+04	8.52E+03	4.49E+03	7.03E+03	8.48E+02	7.3	9.3	5.3	1.9	1.9	5.3
P04762	Cat	Catalase	59.76	15	15	16	14	11	16	15	15	16	14	11	16	1.07E+06	1.86E+06	1.94E+06	6.72E+05	1.49E+06	1.79E+06	43.5	41.4	43.1	36.1	31.5	43.1
M0R3X6	Cbr1	Carbonyl reductase [NADPH] 1	30.61	14	16	14	14	13	11	13	15	13	13	12	10	1.94E+06	5.79E+06	2.82E+06	2.07E+06	1.42E+06	1.11E+06	69.3	73.3	69.3	69.3	65.3	50.2
B2GV72	Cbr3	Carbonyl reductase 3	30.84	8	9	6	8	7	6	7	8	5	7	6	5	2.13E+05	5.03E+05	1.65E+05	2.27E+05	1.64E+05	1.07E+05	41.5	42.2	32.9	41.5	31.4	27.1
Q99MB4	Cbwd1	COBW domain-containing protein 1	43.93	3	4	3	3	2	2	3	4	3	3	2	2	1.31E+04	4.71E+04	1.34E+04	1.65E+04	2.31E+03	3.68E+03	16.8	20.8	17	16.8	6.1	6.3
Q5RJK5	Cbx3	Chromobox 3	20.81	2	2	2	3	1	3	2	2	2	3	1	3	1.97E+05	1.00E+05	3.49E+04	2.46E+05	9.23E+04	2.75E+04	15.3	15.3	14.2	23	6.6	14.2
G3V827	Ccbl1	Kynurenine--oxoglutarate transaminase 1, mitochondrial	51.58	4	4	1	2	4	2	4	4	1	2	4	2	2.60E+04	4.10E+04	1.33E+04	6.07E+03	2.50E+04	1.50E+04	12.3	14.2	2.8	9	12.3	6.1
A0A0G2KAL0	Ccdc17	Coiled-coil domain-containing 17	63.19	2	2	1	2	1	0	2	2	1	2	1	0	9.09E+04	1.30E+06	1.93E+02	1.15E+05	6.94E+05	0.00E+00	5.3	5.3	2.5	5.3	2.5	0
Q5FVN3	Ccl9	Ccl9-like protein	13.10	2	2	1	2	2	1	2	2	1	2	2	1	3.20E+05	2.00E+05	1.02E+05	1.72E+05	2.38E+05	4.69E+04	16.2	16.2	9.4	16.2	16.2	9.4
E9PSS2	Ccs	Superoxide dismutase [Cu-Zn]	23.98	2	2	2	3	1	1	2	2	2	3	1	1	2.10E+04	6.34E+04	1.18E+04	3.90E+04	1.31E+04	1.33E+03	19.3	19.3	19.3	25	3.9	3.9
Q5XIM9	Cct2	T-complex protein 1 subunit beta	57.46	9	11	7	9	7	5	9	11	7	9	7	5	1.82E+05	1.71E+05	6.80E+04	7.99E+04	8.20E+04	1.43E+04	27.9	33.5	22.6	27.5	22.2	15.9
Q6P502	Cct3	T-complex protein 1 subunit gamma	60.65	10	11	6	8	9	5	10	11	6	8	9	5	1.62E+05	2.31E+05	6.61E+04	1.05E+05	1.14E+05	2.50E+04	26.2	27.9	14.7	21.3	22.9	12.5
Q7TPB1	Cct4	T-complex protein 1 subunit delta	58.10	9	10	12	8	9	8	9	10	12	8	9	8	1.37E+05	1.36E+05	1.20E+05	8.29E+04	7.04E+04	1.71E+04	29.5	32.7	36.5	23.6	32.5	23.7
Q68FQ0	Cct5	T-complex protein 1 subunit epsilon	59.54	13	14	9	14	12	4	13	14	9	14	12	4	1.21E+05	2.13E+05	8.16E+04	8.31E+04	1.04E+05	1.46E+04	38.1	38.3	24.4	38.3	36.2	10.7
Q3MHS9	Cct6a	T-complex protein 1 subunit 6A (Zeta 1)	58.02	9	8	5	7	7	4	9	8	5	7	7	4	1.70E+05	2.28E+05	8.52E+04	1.06E+05	1.06E+05	1.75E+04	27.7	23	17.1	19.8	18.3	14.9
D4AC23	Cct7	T-complex protein 1 subunit eta	59.66	7	8	7	7	5	5	7	8	7	7	5	5	1.30E+05	1.27E+05	6.47E+04	9.30E+04	8.19E+04	2.61E+04	17.3	19.5	17.3	17.3	10.8	10.8
D4ACB8	Cct8	T-complex protein 1 subunit theta	59.59	9	11	10	10	10	9	9	11	10	10	10	9	1.09E+05	2.18E+05	1.09E+05	1.06E+05	8.00E+04	2.81E+04	21.2	29	24.3	25.2	26.1	22.4
A0A0G2JVY2	Cd163	CD163 molecule	119.61	9	9	10	8	10	9	9	9	10	8	10	9	1.46E+05	1.09E+05	9.17E+04	1.35E+05	1.20E+05	7.91E+04	11.6	11.6	12.1	10.2	12.6	11.9
B1PLB1	Cd34	CD34 antigen	41.24	1	1	1	2	1	1	1	1	1	2	1	1	4.69E+04	5.52E+04	1.86E+04	3.90E+04	2.34E+04	4.37E+04	3.1	3.1	3.1	5.4	3.1	3.1
O70509	Cd44	CD44 antigen	39.73	1	1	0	1	1	0	1	1	0	1	1	0	1.64E+05	3.80E+04	0.00E+00	1.02E+05	1.25E+05	0.00E+00	3.3	3.3	0	3.3	3.3	0
P27274	Cd59	CD59 glycoprotein	13.79	3	3	3	3	3	3	3	3	3	3	3	3	1.08E+05	1.47E+05	9.84E+04	1.02E+05	9.81E+04	7.95E+04	23	23	23	23	23	23
Q4KM75	Cd5l	CD5 antigen-like	37.86	5	7	8	7	8	9	5	7	8	7	8	9	1.72E+05	1.27E+06	8.04E+05	7.15E+05	6.82E+05	8.66E+05	16.8	26.9	27.5	22.5	27.5	27.5
D4AC20	Cda	Cytidine deaminase	16.11	1	1	0	1	1	1	1	1	0	1	1	1	1.02E+06	4.36E+05	0.00E+00	8.69E+05	3.43E+05	1.11E+04	8.2	8.2	0	8.2	8.2	8.2
A0A0G2K3C1	Cdc37	Hsp90 co-chaperone Cdc37	43.00	5	5	3	4	4	1	5	5	3	4	4	1	1.46E+05	1.70E+05	3.86E+04	8.11E+04	8.75E+04	4.68E+03	17.3	17.3	12.4	15.4	15.4	3
Q8CFN2	Cdc42	Cell division control protein 42 homolog	21.26	5	6	4	5	4	3	4	5	3	4	3	2	8.26E+05	1.30E+06	4.22E+05	6.76E+05	4.00E+05	2.99E+05	36.6	37.2	30.9	36.6	30.9	22
Q9R0T4	Cdh1	Cadherin-1	98.71	3	3	1	3	2	1	3	3	1	3	2	1	5.59E+04	3.63E+04	1.70E+04	2.40E+04	1.16E+04	1.63E+04	6.5	6.5	2	6.5	5	2
P55281	Cdh17	Cadherin-17	91.86	2	2	3	2	2	3	2	2	3	2	2	3	2.77E+04	2.65E+04	3.44E+04	1.94E+04	1.51E+04	1.54E+04	3.5	3.5	6.8	3.5	3.5	6.8
F1M7E5	Cdh5	Cadherin-5	87.13	6	6	5	6	5	5	6	6	5	6	5	5	1.48E+05	1.30E+05	1.19E+05	8.75E+04	5.68E+04	1.51E+05	8.9	8.9	7.2	8.9	7.6	7.2

Uniprot accession number	Gene symbol	Protein name	Mol. weight [kDa]	No. Peptides Control wk1	No. Peptides Control wk8	No. Peptides Control wk14	No. Peptides Heat wk1	No. Peptides Heat wk8	No. Peptides Heat wk14	No. Unique peptides Control wk1	No. Unique peptides Control wk8	No. Unique peptides Control wk14	No. Unique peptides Heat wk1	No. Unique peptides Heat wk8	No. Unique peptides Heat wk14	iBAQ Control wk1	iBAQ Control wk8	iBAQ Control wk14	iBAQ Heat wk1	iBAQ Heat wk8	iBAQ Heat wk14	Sequence coverage Control wk1 [%]	Sequence coverage Control wk8 [%]	Sequence coverage Control wk14 [%]	Sequence coverage Heat wk1 [%]	Sequence coverage Heat wk8 [%]	Sequence coverage Heat wk14 [%]
A0A0G2K0B0	Cdv3	Protein CDV3 homolog	29.65	1	1	1	1	1	0	1	1	1	1	1	0	2.50E+04	3.06E+04	6.74E+03	8.50E+03	1.47E+04	0.00E+00	10.7	10.7	10.7	10.7	10.7	0
Q4QQT3	Celf1	CUGBP Elav-like family member 1	52.21	1	2	1	1	2	0	1	2	1	1	2	0	2.50E+04	8.02E+04	4.86E+03	1.37E+04	5.53E+04	0.00E+00	3.7	6.6	3.7	3.7	6.6	0
Z4YNP1	Celf2	CUGBP Elav-like family member 2	55.06	2	2	1	2	2	1	2	2	1	2	2	1	3.13E+04	5.54E+04	8.52E+03	1.98E+04	1.64E+04	1.27E+04	6.6	6.6	3.5	6.6	6.6	3.5
D4AA05	Ces1a	Carboxylic ester hydrolase	62.36	2	2	2	2	1	1	2	2	2	2	1	1	1.32E+05	3.99E+04	7.47E+04	1.58E+05	7.09E+04	9.54E+04	5.9	5.9	5.9	5.9	3.2	3.2
P10959	Ces1c	Carboxylesterase 1C	60.17	25	28	25	27	27	24	8	8	8	8	8	8	1.33E+07	9.56E+06	1.04E+07	1.06E+07	1.15E+07	1.13E+07	61	63.9	61	63.2	63.2	61
D3ZGK7	Ces1c	Carboxylic ester hydrolase	64.23	19	22	19	21	21	18	2	2	2	2	2	2	5.84E+05	7.60E+04	5.14E+05	6.13E+05	4.67E+05	5.07E+05	40.2	43	40.2	42.3	42.3	40.2
P16303	Ces1d	Carboxylesterase 1D	62.15	18	21	18	12	15	17	3	3	4	2	3	3	1.33E+06	1.23E+06	7.84E+05	5.27E+05	5.63E+05	6.87E+05	38.2	47.6	44.1	29	34.5	43.2
G3V7J5	Ces2e	Carboxylic ester hydrolase	63.58	7	6	4	7	6	5	4	3	2	4	3	3	2.04E+05	1.80E+05	1.06E+05	2.09E+05	2.73E+05	6.42E+04	22.6	18.7	14.3	22.6	18.7	16.9
Q4V8E4	Cfap36	Cilia- and flagella-associated protein 36	39.59	9	11	9	9	9	8	9	11	9	9	9	8	3.10E+05	7.29E+05	5.95E+05	2.29E+05	1.61E+05	1.04E+05	42.9	50.4	42.9	42.9	42.9	37.3
G3V615	Cfb	Complement factor B	85.35	37	41	36	38	39	39	5	5	5	5	5	5	6.19E+06	3.42E+06	2.57E+06	4.50E+06	5.16E+06	2.46E+06	52.6	54.5	48.9	52.6	53.9	52.6
A0A0U1RRP[illegible]	Cfb	Complement factor B	123.97	44	49	43	44	47	49	0	0	0	0	0	0	3.86E+06	2.67E+06	3.69E+06	2.80E+06	3.57E+06	3.60E+06	47	48.3	44.5	45.7	48.8	48.7
G3V7H3	Cfd	Complement factor D	28.54	6	6	5	6	5	5	6	6	5	6	5	5	1.68E+06	1.12E+06	1.81E+06	9.38E+05	1.15E+06	1.60E+06	39.5	39.5	29.7	39.5	29.7	29.7
G3V9R2	Cfh	Complement factor H	140.23	84	99	89	88	87	86	80	94	84	83	82	82	3.66E+07	3.19E+07	3.93E+07	3.85E+07	3.67E+07	3.74E+07	75.5	78.4	76.3	75.5	76.8	74.9
Q5I0M3	Cfhr1	Complement component factor H-like 1	30.62	10	10	10	10	10	10	7	7	7	7	7	7	1.02E+07	7.16E+06	1.05E+07	8.56E+06	7.16E+06	9.48E+06	56.9	56.9	56.9	56.9	56.9	56.9
F1LWS4	Cfhr2	Uncharacterized protein	65.87	10	13	13	10	12	14	9	12	12	9	11	13	2.08E+05	3.43E+05	4.89E+05	3.25E+05	5.44E+05	5.20E+05	27.2	34.1	34.1	27.5	34	35.9
A0A0G2K135	Cfi	Complement factor I	69.77	33	35	32	34	32	32	33	35	32	34	32	32	1.04E+07	5.66E+06	5.91E+06	5.99E+06	5.88E+06	6.66E+06	55.1	53.4	53.8	55.3	52.2	51
P45592	Cfl1	Cofilin-1	18.53	10	11	10	11	11	10	10	11	10	11	11	10	2.40E+06	4.54E+06	2.45E+06	2.72E+06	2.19E+06	1.38E+06	61.4	62	61.4	61.4	62	61.4
B0BNN4	Cfp	Complement factor properdin	50.57	5	5	4	5	5	4	5	5	4	5	5	4	4.41E+05	3.93E+05	3.64E+05	3.64E+05	4.24E+05	3.08E+05	15.5	15.5	13.8	15.5	15.5	13.8
A0A0A0MXV3	Cgref1	Cell growth regulator with EF hand domain protein 1, isoform CRA_b	35.32	2	2	1	3	2	2	2	2	1	3	2	2	9.70E+04	6.84E+04	8.69E+03	1.17E+05	5.28E+04	5.06E+04	12	11.7	3.4	15	12	6.4
Q5PPG5	Chga	Chromogranin-A	51.90	3	4	4	3	5	4	3	4	4	3	5	4	2.31E+05	2.30E+05	2.22E+05	2.41E+05	2.73E+05	2.28E+05	15.1	17.6	17.6	15.1	21.7	17.6
F1M8B7	Chmp2b	Charged multivesicular body protein 2B	23.93	1	1	0	1	0	0	1	1	0	1	0	0	1.41E+04	5.31E+04	0.00E+00	1.11E+04	0.00E+00	0.00E+00	4.7	4.7	0	4.7	0	0
Q8CGS4	Chmp3	Charged multivesicular body protein 3	25.06	1	2	0	1	1	0	1	2	0	1	1	0	3.79E+04	1.58E+05	0.00E+00	3.38E+04	1.81E+04	0.00E+00	4	8.1	0	4	4	0
M0RCH6	Chmp4b	Charged multivesicular body protein 4b	24.81	3	3	2	3	3	2	3	3	2	3	3	2	6.94E+04	1.30E+05	6.57E+04	7.59E+04	3.95E+04	3.05E+04	23.4	23.4	11.3	23.4	23.4	11.3
Q4QQV8	Chmp5	Charged multivesicular body protein 5	24.58	1	1	0	0	0	0	1	1	0	0	0	0	1.47E+05	7.17E+04	0.00E+00	0.00E+00	0.00E+00	0.00E+00	9.6	9.6	0	0	0	0
Q5M7T1	Ciao1	Probable cytosolic iron-sulfur protein assembly protein CIAO1	37.62	2	3	2	2	2	2	2	3	2	2	2	2	1.92E+04	5.55E+04	2.51E+04	1.99E+04	9.50E+03	8.86E+03	9.1	12.7	9.1	9.1	9.1	9.1
Q5RJS3	Ciao2a	Cytosolic iron-sulfur assembly component 2A	18.38	1	1	1	1	0	1	1	1	1	1	0	1	1.29E+04	4.47E+04	1.31E+04	3.51E+04	0.00E+00	7.52E+03	6.9	6.9	6.9	6.9	0	6.9
Q5XID1	Ciapin1	Anamorsin	33.04	2	3	2	2	1	1	2	3	2	2	1	1	4.64E+04	1.04E+05	4.47E+04	1.27E+04	7.82E+03	6.32E+03	12.3	19.7	12.3	12.3	4.2	4.2
P60825	Cirbp	Cold-inducible RNA-binding protein	18.61	1	2	2	2	1	1	1	2	2	2	1	1	5.47E+04	1.15E+05	4.32E+04	4.57E+04	3.02E+04	8.56E+03	6.4	18.6	18.6	18.6	6.4	6.4
P07335	Ckb	Creatine kinase B-type	42.73	19	21	17	19	19	16	18	20	16	18	18	15	5.52E+06	4.80E+06	3.23E+06	1.53E+06	1.22E+06	2.67E+06	62.7	65.6	58.5	62.7	62.7	58.5
A0A0G2JSP8	Ckm	Creatine kinase M-type	43.02	6	5	3	6	5	7	5	4	2	5	4	6	8.17E+04	6.73E+04	2.33E+04	8.35E+04	1.85E+04	1.06E+05	19.9	17.3	9.4	19.9	15	22.3
Q5BJT9	Ckmt1	Creatine kinase U-type, mitochondrial	46.96	2	1	0	2	3	0	2	1	0	2	3	0	8.26E+03	3.06E+03	0.00E+00	4.78E+03	5.31E+04	0.00E+00	7.7	3.8	0	7.7	10	0
O88201	Clec11a	C-type lectin domain family 11 member A	36.39	6	7	8	8	5	7	6	7	8	8	5	7	5.36E+05	3.12E+05	2.37E+05	3.31E+05	2.03E+05	2.09E+05	27.4	30.8	31.1	31.1	20.7	24.4
D3ZUU6	Clec3b	C-type lectin domain family 3, member B	22.31	13	14	12	12	12	12	13	14	12	12	12	12	1.06E+07	9.08E+06	7.54E+06	9.76E+06	8.61E+06	6.27E+06	72.3	72.8	69.3	69.3	69.3	69.3
Q6MG61	Clic1	Chloride intracellular channel protein 1	26.98	13	13	10	11	13	12	13	13	10	11	13	12	1.03E+06	1.43E+06	4.55E+05	8.74E+05	6.27E+05	3.05E+05	76.3	76.8	64.7	69.7	76.8	76.3
Q5M883	Clic2	Chloride intracellular channel protein 2	28.16	6	6	4	5	5	4	5	5	3	4	4	3	2.04E+05	1.58E+05	4.21E+04	5.86E+04	8.56E+04	3.19E+04	36.3	36.3	20.8	30.2	30.2	20.8
D3ZY91	Clic3	Chloride intracellular channel protein	26.78	2	2	3	2	2	2	2	2	3	2	2	2	1.96E+05	1.04E+05	1.12E+05	6.24E+04	4.02E+04	6.92E+04	15.2	15.2	19.4	15.2	15.2	15.2
G3V8C4	Clic4	Chloride intracellular channel protein 4	28.67	10	11	9	11	9	8	8	9	7	9	7	6	3.41E+05	5.00E+05	2.93E+05	2.50E+05	1.37E+05	1.68E+05	42.7	44.3	41.1	44.3	42.7	36.8
F1M9X4	Clic6	Chloride intracellular channel protein 6	64.28	6	8	5	8	5	5	4	6	3	6	3	3	1.06E+05	1.98E+05	6.23E+04	1.47E+05	6.84E+04	3.28E+04	16.8	20.9	13.2	22.4	12.7	13.2
Q6Q0N0	Clstn1	Calsyntenin-1	106.26	6	6	4	6	6	5	6	6	4	6	6	5	1.29E+05	8.37E+04	2.95E+04	8.90E+04	6.30E+04	4.26E+04	9.2	9.2	6.4	9.2	9.2	7.4
A0A0G2JYW3	Clta	Clathrin light chain A	25.58	1	2	1	2	2	1	1	2	1	2	2	1	2.75E+04	3.06E+05	1.54E+04	1.26E+05	1.63E+04	2.13E+04	7.2	13.6	7.2	10.6	13.6	7.2
F1M779	Cltc	Clathrin heavy chain	191.56	23	22	19	22	21	16	23	22	19	22	21	16	2.63E+06	3.65E+05	1.87E+05	6.78E+05	1.23E+06	2.55E+05	19.8	18.7	16.6	18.4	16.6	13
G3V836	Clu	Clusterin	51.42	18	19	19	19	20	19	18	19	19	19	20	19	3.75E+07	3.51E+07	3.44E+07	4.47E+07	4.34E+07	3.19E+07	51.5	52.8	54.1	44.5	55.5	54.1
A0A0U1RRV5	Cluh	Clustered mitochondria protein homolog	151.16	2	2	2	2	1	2	2	2	2	2	1	2	1.11E+04	1.93E+04	6.86E+03	7.28E+03	2.43E+04	1.34E+04	2.4	2.4	2.4	2.4	1.5	2.4
Q7TP52	Cmbl	Carboxymethylenebutenolidase homolog	27.90	2	3	2	1	2	1	2	3	2	1	2	1	2.94E+04	1.00E+05	5.41E+04	2.31E+04	4.26E+04	4.94E+03	9.8	15.5	12.2	6.5	12.2	5.7
Q4KM73	Cmpk1	UMP-CMP kinase	22.17	8	9	3	9	8	3	8	9	3	9	8	3	2.48E+05	5.15E+05	1.27E+05	3.07E+05	1.29E+05	6.89E+04	41.8	45.9	16.8	45.9	41.8	16.8
P62634	Cnbp	Cellular nucleic acid-binding protein	19.46	3	3	2	3	3	2	3	3	2	3	3	2	4.96E+05	7.89E+05	3.59E+05	3.55E+05	2.89E+05	1.56E+05	23.2	23.2	15.3	23.2	23.2	15.3
Q6Q0N1	Cndp2	Cytosolic non-specific dipeptidase	52.69	21	21	21	18	17	17	21	21	21	18	17	17	1.37E+06	1.19E+06	8.15E+05	6.40E+05	5.17E+05	3.86E+05	59.4	54.7	57.3	56.8	52	49.9
Q08290	Cnn1	Calponin-1	33.34	6	7	6	6	4	5	6	7	6	6	4	5	2.37E+05	6.11E+05	1.56E+05	2.49E+05	3.09E+05	5.43E+04	29.3	29.6	26.6	29.3	25.6	24.9
D3ZRX9	Cnn2	Calponin	24.07	3	4	5	2	3	3	3	3	4	2	3	3	3.28E+06	2.38E+06	1.56E+05	3.72E+06	6.32E+06	3.18E+04	18.7	23.7	31.1	11	18.7	21
P37397	Cnn3	Calponin-3	36.43	2	3	3	2	1	2	2	2	2	2	1	2	2.33E+04	6.63E+04	3.41E+04	1.94E+04	4.07E+03	1.43E+04	9.7	13	10.6	9.7	3.9	7.3
A0JN30	Cnpy2	Canopy 2 homolog	20.71	1	2	1	0	1	2	1	2	1	0	1	2	1.02E+05	5.51E+04	1.27E+04	0.00E+00	2.15E+04	3.23E+04	6.6	15.4	8.8	0	6.6	15.4
A0A0G2KAJ7	Col12a1	Collagen alpha-1(XII) chain	342.52	3	2	0	3	2	1	3	2	0	3	2	1	4.73E+03	1.04E+03	0.00E+00	4.75E+03	9.98E+02	3.56E+02	1	0.7	0	1	0.7	0.3
D3ZZT9	Col14a1	Collagen type 14 alpha 1 chain	192.56	29	26	20	25	25	23	29	26	20	25	25	23	4.72E+05	2.18E+05	1.35E+05	1.85E+05	1.88E+05	1.87E+05	23.3	21	16.6	20.1	20.9	19.6
F1LR02	Col18a1	Collagen type 18 alpha 1 chain	134.64	4	3	3	4	4	3	4	3	3	4	4	3	5.82E+04	2.20E+04	2.44E+04	3.85E+04	5.83E+04	2.83E+04	3.6	2.9	2.8	3.6	3.6	2.8
P02454	Col1a1	Collagen type 1 alpha-1 chain	137.95	19	13	14	17	15	14	19	13	14	17	15	14	1.14E+06	1.98E+05	3.25E+05	3.02E+05	1.79E+05	2.19E+05	19.5	14.4	16.2	16.4	15.8	13.7
F1LS40	Col1a2	Collagen type 1 alpha-2 chain	129.63	12	9	11	10	11	9	12	9	11	10	11	9	4.32E+05	7.90E+04	1.04E+05	1.23E+05	6.36E+04	6.48E+04	13.5	10.3	12.2	11	12.8	10.7
P13941	Col3a1	Collagen type 3 alpha-1 chain	138.93	9	9	6	8	7	6	6	6	4	6	6	4	1.45E+05	4.31E+04	3.47E+04	7.23E+04	4.51E+04	3.93E+04	7.2	7.2	5	6.2	5.3	5
D3ZUL3	Col6a1	Collagen type 6 alpha-1 chain	108.80	3	2	3	2	2	2	3	2	3	2	2	2	8.49E+04	2.85E+04	1.14E+04	5.60E+04	3.27E+04	2.08E+04	3.3	2.4	3.3	2.4	2.4	2.4
P22734	Comt	Catechol O-methyltransferase	29.60	7	6	7	6	5	6	7	6	7	6	5	6	2.84E+05	2.33E+05	2.72E+05	1.04E+05	7.76E+04	1.31E+05	50	40.2	49.2	40.2	33.3	39.4
G3V6T1	Copa	Coatomer subunit alpha	138.36	12	11	8	10	11	6	12	11	8	10	11	6	7.22E+04	8.72E+04	1.59E+04	5.63E+04	5.37E+04	7.02E+03	16.3	15.5	12.2	13.7	15.5	9.1
P23514	Copb1	Coatomer subunit beta	107.01	9	9	4	8	7	2	9	9	4	8	7	2	6.96E+04	6.52E+04	1.78E+04	3.77E+04	3.38E+04	4.14E+03	13.3	14.1	7.1	13.3	11.9	4.1
O35142	Copb2	Coatomer subunit beta	102.55	6	9	5	9	7	4	6	9	5	9	7	4	4.59E+04	9.01E+04	2.24E+04	4.26E+04	4.80E+04	6.52E+03	10.9	16.2	9.3	15.6	12.9	8.2
G3V8Q1	Cope	Coatomer subunit epsilon	34.65	3	3	1	3	3	2	3	3	1	3	3	2	2.74E+05	2.35E+05	4.50E+04	2.68E+05	1.58E+05	3.50E+04	14	14	3.9	14	14	9.4
A0A0G2K1F3	Copg1	Coatomer subunit gamma-1	101.00	5	5	2	6	5	1	5	5	2	6	5	1	4.14E+04	5.52E+04	8.91E+03	3.97E+04	3.14E+04	2.54E+03	9.2	9.2	3.6	10.9	8.6	2.5
P61203	Cops2	COP9 signalosome complex subunit 2	51.60	3	3	3	3	3	3	3	3	3	3	3	3	1.04E+05	1.55E+05	8.50E+04	6.83E+04	9.86E+04	4.66E+04	11.1	11.1	11.1	11.1	11.1	11.1
Q68FW9	Cops3	COP9 signalosome complex subunit 3	47.86	3	5	4	4	3	3	3	5	4	4	3	3	4.43E+04	8.24E+04	5.48E+04	4.87E+04	4.30E+04	2.20E+04	13.5	18.2	16.3	16.3	13.5	12.8
Q68FS2	Cops4	COP9 signalosome complex subunit 4	46.29	9	9	7	8	8	4	9	9	7	8	8	4	1.34E+05	2.14E+05	8.41E+04	1.44E+05	9.34E+04	3.36E+04	34.5	30.8	25.4	30	30	13.1
F7EUU4	Cops5	COP9 signalosome subunit 5	43.65	4	5	3	4	2	2	4	5	3	4	2	2	5.39E+04	7.92E+04	1.33E+04	4.89E+04	1.32E+04	5.69E+03	12.3	18.3	9	12.3	8.7	5.4
D3ZI16	Cops6	COP9 signalosome complex subunit 6	37.70	2	3	3	2	2	2	2	3	3	2	2	2	6.62E+04	1.60E+05	1.43E+05	4.05E+04	3.38E+04	4.16E+04	10.2	14.5	14.5	10.2	10.2	10.2
Q6P4Z9	Cops8	COP9 signalosome complex subunit 8	23.24	2	3	1	2	2	2	2	3	1	2	2	2	1.04E+05	1.80E+05	4.22E+04	7.71E+04	1.71E+05	3.77E+04	13.9	18.7	6.7	13.9	11.5	13.9
D4A8T3	Copz1	Coatomer protein complex, subunit zeta 1	20.20	3	4	2	3	2	1	3	4	2	3	2	1	1.02E+05	3.70E+05	4.10E+04	1.51E+05	9.38E+04	1.11E+04	26.6	35	18.6	26.6	18.6	13
Q91ZN1	Coro1a	Coronin-1A	51.07	5	5	5	5	5	2	5	5	5	5	5	2	9.55E+04	7.13E+04	3.29E+04	4.90E+04	3.93E+04	2.60E+04	22.1	22.1	22.1	22.1	22.1	7.8
G3V940	Coro1b	Coronin-1B	53.94	4	4	2	2	3	2	4	4	2	2	3	2	9.19E+04	1.18E+05	2.14E+04	4.65E+04	3.11E+04	1.03E+04	19.4	21.9	9.7	10.7	17.8	11.2
G3V624	Coro1c	Coronin-1C	53.18	4	4	2	4	3	2	4	4	2	4	3	2	7.69E+04	5.82E+04	2.71E+03	2.43E+04	1.87E+04	5.78E+03	11.4	11.4	5.1	11.2	9.7	3.6
A0A0A0MXU2	Coro7	Coronin-7	86.14	2	2	3	1	2	3	2	2	3	1	2	3	1.18E+04	1.23E+04	1.65E+04	8.26E+03	4.91E+03	8.22E+03	3.4	3.4	4.7	2	3.4	4.7
B0BNA5	Cotl1	Coactosin-like protein	15.93	1	0	0	0	0	0	1	0	0	0	0	0	1.09E+05	0.00E+00	0.00E+00	0.00E+00	0.00E+00	0.00E+00	11.3	0	0	0	0	0
G3V7K3	Cp	Ceruloplasmin	120.66	90	95	84	90	91	88	16	16	15	15	13	15	1.18E+08	1.02E+08	1.14E+08	1.30E+08	1.15E+08	1.13E+08	83.3	84.2	83.1	82.9	77.7	78.6
P13635	Cp	Ceruloplasmin	120.84	75	80	70	76	79	73	1	1	1	1	1	0	9.23E+03	1.17E+04	1.06E+03	1.19E+04	4.44E+03	0.00E+00	67.6	68.6	68.1	67.9	67.9	67.9
Q9EQV9	Cpb2	Carboxypeptidase B2	48.83	12	12	12	12	12	11	12	12	12	12	12	11	1.39E+06	9.14E+05	1.03E+06	8.63E+05	8.26E+05	9.47E+05	46.2	46.2	46.2	46.2	46.2	44.3
Q9EQV8	Cpn1	Carboxypeptidase N catalytic chain	51.98	17	21	15	19	17	15	17	21	15	19	17	15	5.21E+06	4.56E+06	4.89E+06	5.03E+06	4.21E+06	4.38E+06	61.7	68.7	57.5	67.4	57.3	54.5
F1LQT4	Cpn2	Carboxypeptidase N subunit 2	62.64	22	23	24	24	25	24	22	23	24	24	25	24	9.78E+06	7.27E+06	9.94E+06	9.29E+06	9.88E+06	8.66E+06	51.7	55.2	56.6	56.1	57.5	54
Q6IRK9	Cpq	Carboxypeptidase Q	52.04	8	8	8	9	8	9	8	8	8	9	8	9	6.77E+05	5.47E+05	4.58E+05	6.41E+05	6.99E+05	5.23E+05	22.7	22.7	22.7	22.7	22.7	27.5
Q4G063	Creld2	Cysteine-rich with EGF-like domain protein 2	38.25	3	4	3	4	3	0	3	4	3	4	3	0	4.35E+04	5.26E+04	3.87E+04	5.40E+04	1.19E+04	0.00E+00	11.5	14.3	9.7	14.3	11.2	0
P63255	Crip1	Cysteine-rich protein 1	8.55	2	2	2	2	2	1	2	2	2	2	2	1	1.43E+07	7.75E+06	8.26E+06	4.94E+06	4.61E+06	7.12E+06	36.4	36.4	36.4	36.4	36.4	19.5
P36201	Crip2	Cysteine-rich protein 2	22.70	5	5	5	4	5	5	5	5	5	4	5	5	5.92E+05	8.59E+05	2.90E+05	1.41E+05	2.14E+05	1.78E+05	43.3	43.3	43.3	38.5	43.3	43.3
P12020	Crisp1	Cysteine-rich secretory protein 1	27.85	3	4	4	2	3	2	3	4	4	2	3	2	1.25E+05	4.91E+05	5.39E+05	3.47E+04	1.29E+05	1.02E+05	12.6	19.1	19.1	8.5	12.6	8.5
P48199	Crp	C-reactive protein	25.47	12	12	12	12	12	12	12	12	12	12	12	12	1.83E+08	1.52E+08	1.72E+08	1.78E+08	1.70E+08	1.49E+08	62.2	62.2	62.2	62.2	62.2	62.2
P22283	Crp2	Cystatin-related protein 2	21.01	5	5	1	2	4	1	5	5	1	2	4	1	1.13E+05	3.90E+05	3.27E+03	2.55E+04	6.57E+04	7.16E+03	30.7	30.7	6.2	9.7	22.2	6.2
A0A0G2K568	Crym	Ketimine reductase mu-crystallin	33.43	2	2	2	2	1	2	2	2	2	2	1	2	3.73E+04	3.97E+04	5.62E+04	4.21E+04	1.12E+04	1.42E+04	6.1	6.1	6.1	6.1	3.2	6.1
Q6AYT0	Cryz	Quinone oxidoreductase	34.98	3	2	0	2	2	0	3	2	0	2	2	0	4.06E+04	7.03E+04	0.00E+00	3.73E+04	2.69E+04	0.00E+00	18.2	10	0	10	10	0
A0A0G2K5P7	Csad	Cysteine sulfinic acid decarboxylase	52.82	2	2	2	1	2	3	2	2	2	1	2	3	2.87E+04	2.93E+04	3.82E+04	1.54E+04	1.22E+04	3.65E+04	6.6	6.6	5.9	3.6	6.6	8.9
M0R7K9	Csap1	Common salivary protein 1	12.95	4	3	3	3	2	4	4	3	3	3	2	4	1.49E+06	1.39E+05	9.39E+04	6.44E+05	1.14E+05	2.30E+05	44.7	34.2	36	34.2	25.4	44.7
P18395	Csde1	Cold shock domain-containing protein E1	88.89	4	4	2	3	4	1	4	4	2	3	4	1	1.04E+04	2.18E+04	7.41E+03	6.38E+03	6.75E+03	2.62E+03	6.3	6.3	3.4	4.8	6.3	2.4
D3ZPR0	Cse1l	Chromosome segregation 1-like	110.21	8	8	6	8	7	4	8	8	6	8	7	4	2.98E+04	3.77E+04	1.23E+05	3.00E+04	3.61E+04	5.98E+04	11.7	11.7	9.2	11.7	10.4	6.2
A0A0G2KA61	Csnk2b	Casein kinase II subunit beta	17.42	3	2	3	3	3	1	3	2	3	3	3	1	1.41E+05	1.94E+05	1.27E+05	9.58E+04	2.22E+05	1.38E+04	27.2	16.6	27.2	27.2	27.2	7.3
F1LS79	Cspg4	Chondroitin sulfate proteoglycan 4	252.01	2	2	3	2	2	2	2	2	3	2	2	2	1.56E+04	9.10E+03	1.21E+04	5.87E+03	9.21E+03	1.09E+04	1.2	1.2	1.9	1.2	1.2	1.3

Uniprot accession number	Gene symbol	Protein name	Mol. weight [kDa]	No. Peptides Control wk1	No. Peptides Control wk8	No. Peptides Control wk14	No. Peptides Heat wk1	No. Peptides Heat wk8	No. Peptides Heat wk14	No. Unique peptides Control wk1	No. Unique peptides Control wk8	No. Unique peptides Control wk14	No. Unique peptides Heat wk1	No. Unique peptides Heat wk8	No. Unique peptides Heat wk14	iBAQ Control wk1	iBAQ Control wk8	iBAQ Control wk14	iBAQ Heat wk1	iBAQ Heat wk8	iBAQ Heat wk14	Sequence coverage Control wk1 [%]	Sequence coverage Control wk8 [%]	Sequence coverage Control wk14 [%]	Sequence coverage Heat wk1 [%]	Sequence coverage Heat wk8 [%]	Sequence coverage Heat wk14 [%]
P47875	Csrp1	Cysteine and glycine-rich protein 1	20.61	7	8	7	8	7	6	7	8	7	8	7	6	1.60E+06	2.96E+06	1.58E+06	4.37E+05	5.63E+05	9.97E+05	47.2	47.2	46.6	47.2	46.6	46.6
Q5U202	Csrp2	Cysteine and glycine-rich protein 2	20.07	1	1	2	2	1	2	1	1	2	2	1	2	8.51E+03	1.39E+04	7.87E+03	1.10E+04	6.26E+03	1.61E+04	8.2	8.2	13.6	13.6	8.2	13.6
G3V9M0	Cst	Cystatin	16.14	3	2	0	3	2	3	3	2	0	3	2	3	2.60E+05	1.80E+05	0.00E+00	2.49E+05	6.22E+04	2.12E+04	27.1	20.1	0	27.1	20.1	27.1
G3V6M1	Cst12	Cystatin-12	15.16	3	3	1	3	3	1	3	3	1	3	3	1	1.80E+05	1.85E+05	4.25E+04	2.03E+05	5.02E+05	2.18E+04	30.5	30.5	7	30.5	30.5	7
P14841	Cst3	Cystatin-C	15.44	4	4	4	4	4	4	4	4	4	4	4	4	6.22E+05	4.00E+05	1.32E+06	6.19E+05	8.19E+05	9.15E+05	42.1	42.1	42.1	42.1	42.1	42.1
Q8VHC1	Cst6	Cystatin-B	16.79	2	2	2	1	2	2	2	2	2	1	2	2	1.23E+05	9.06E+04	1.50E+05	6.03E+04	1.21E+05	1.35E+05	21.5	21.5	21.5	14.1	21.5	21.5
D3ZMS9	Cst9l	Cystatin-9-like	16.00	1	1	1	1	1	1	1	1	1	1	1	1	2.24E+05	1.43E+05	7.53E+04	1.37E+05	3.27E+05	4.03E+04	13.1	13.1	13.1	13.1	13.1	13.1
P01041	Cstb	Cystatin-B	11.20	2	3	2	2	3	2	2	3	2	2	3	2	3.57E+05	5.01E+05	3.61E+05	1.53E+05	1.20E+05	1.85E+05	43.9	55.1	43.9	43.9	55.1	43.9
A0A0G2JYF7	Ctnna1	Catenin alpha 1	89.32	0	1	1	1	1	0	0	1	1	1	1	0	0.00E+00	5.80E+03	1.55E+03	3.48E+03	5.96E+03	0.00E+00	0	1.5	1.5	1.5	1.5	0
Q4KM58	Ctnnbip1	Catenin, beta-interacting protein 1	9.20	1	0	1	0	1	1	1	0	1	0	1	1	2.97E+04	0.00E+00	2.66E+04	0.00E+00	9.04E+04	3.18E+04	18.5	0	18.5	0	18.5	18.5
Q6AYS3	Ctsa	Carboxypeptidase	51.22	11	11	11	11	10	12	11	11	11	11	10	12	1.11E+06	9.56E+05	7.59E+05	9.89E+05	7.91E+05	6.02E+05	26.3	26.3	26.3	26.3	26.3	26.3
Q6IN22	Ctsb	Cathepsin B	37.54	9	8	8	6	9	8	9	8	8	6	9	8	5.62E+05	5.04E+05	4.15E+05	4.98E+05	5.31E+05	3.11E+05	31.3	28	28	20.4	31.3	28
P80067	Ctsc	Dipeptidyl peptidase 1	52.24	3	4	3	3	5	4	3	4	3	3	5	4	6.62E+04	4.93E+04	2.47E+04	4.86E+04	4.68E+04	3.27E+04	9.7	14.1	12.1	9.7	16.7	14.7
Q6P6T6	Ctsd	Cathepsin D	44.62	5	5	4	5	5	4	5	5	4	5	5	4	2.69E+05	2.37E+05	1.77E+05	1.75E+05	1.29E+05	1.09E+05	16.5	16.5	16.5	16.5	16.5	16.5
Q499S6	Ctsf	Cathepsin F	51.83	3	3	3	3	3	2	3	3	3	3	3	2	1.44E+05	1.58E+05	4.13E+04	7.55E+04	7.90E+04	2.30E+04	10.4	10.4	10.4	10.4	10.4	6.5
Q9R1T3	Ctsz	Cathepsin Z	34.19	5	4	3	3	5	3	5	4	3	3	5	3	1.37E+05	1.18E+05	7.18E+04	3.65E+04	5.56E+04	4.27E+04	18.6	15.4	12.1	11.4	18.6	12.1
A0A0G2JZ13	Cttn	Src substrate cortactin	52.68	5	4	3	3	4	3	5	4	3	3	4	3	4.97E+04	1.21E+05	1.38E+04	3.00E+04	2.91E+04	1.24E+04	15.9	13.8	11	11.7	13.8	11
B1WBY1	Cul1	Cullin-1	89.69	4	4	2	4	2	4	4	4	2	4	2	4	1.85E+04	2.16E+04	9.87E+03	2.11E+04	2.19E+03	4.85E+03	6.1	6.1	3.5	6.1	3.6	6.1
A0A0G2JSP3	Cul3	Cullin-3	86.47	4	4	4	4	4	2	4	4	4	4	4	2	2.02E+04	2.56E+04	1.46E+04	1.82E+04	1.66E+04	6.50E+03	7	7	7	7	7	4.3
D4A8H8	Cyfip1	Cytoplasmic FMR1-interacting protein	145.26	3	3	2	3	3	2	3	3	2	3	3	2	7.23E+03	1.04E+04	4.63E+03	7.05E+03	7.55E+03	1.27E+03	3	3	1.8	3	3	1.8
Q921A4	Cygb	Cytoglobin	21.50	2	2	2	1	1	2	2	2	2	1	1	2	1.69E+04	2.11E+04	3.39E+04	6.50E+03	1.68E+04	2.90E+04	12.6	12.6	12.6	8.9	8.9	12.6
A0A0G2JSR8	Cyp17a1	Cytochrome P450, family 17, subfamily a, polypeptide 1	57.26	4	4	3	2	3	0	4	4	3	2	3	0	1.96E+04	4.09E+04	9.19E+03	2.04E+04	2.44E+04	0.00E+00	10.7	10.7	8.3	4.1	6.9	0
F1LMP9	Dab2	Disabled homolog 2	82.22	5	5	3	5	5	4	5	5	3	5	5	4	8.75E+04	1.19E+05	5.38E+04	5.54E+04	4.19E+04	3.50E+04	11.2	11.2	6.5	11.2	11.2	9.3
F1M8K0	Dag1	Dystroglycan 1	96.71	2	3	2	2	2	2	2	3	2	2	2	2	3.42E+04	5.65E+04	4.97E+04	4.75E+04	2.71E+04	3.60E+04	4.3	5.8	4.3	4.3	4.3	4.3
P15178	Dars	Aspartate--tRNA ligase, cytoplasmic	57.13	4	3	3	4	5	3	4	3	3	4	5	3	3.45E+04	3.45E+04	2.45E+04	2.99E+04	2.64E+04	1.15E+04	8.8	7	7	9.2	11	7
Q4KLZ3	Dazap1	DAZ associated protein 1	43.09	2	2	1	2	2	1	2	2	1	2	2	1	1.41E+05	2.77E+05	1.32E+05	1.26E+05	8.41E+04	2.96E+04	7.7	7.7	3.7	7.7	7.7	3.7
P11030	Dbi	Acyl-CoA-binding protein	10.03	3	3	2	3	3	2	3	3	2	3	3	2	1.77E+06	3.29E+06	1.63E+06	1.98E+06	2.30E+06	9.16E+05	47.1	47.1	39.1	47.1	47.1	39.1
P56702	Dbil5	Diazepam-binding inhibitor-like 5	9.86	3	3	3	3	3	2	3	3	3	3	3	2	3.29E+05	6.53E+05	5.92E+05	5.16E+05	2.25E+05	3.58E+04	44.8	44.8	44.8	44.8	44.8	29.9
Q9JHL4	Dbnl	Drebrin-like protein	48.61	7	8	5	7	9	2	7	8	5	7	9	2	9.07E+04	1.88E+05	5.54E+04	1.05E+05	7.69E+04	1.03E+04	22.9	27.5	15.4	23.4	30.5	5
Q01129	Dcn	Decorin	39.81	7	7	6	6	7	7	7	7	6	6	7	7	1.41E+06	3.74E+05	4.36E+05	3.37E+05	2.34E+05	6.24E+05	19.8	19.8	17.5	19.8	19.8	19.8
A0A0G2K428	Dctn1	Dynactin subunit 1	139.84	3	5	1	1	1	1	3	5	1	1	1	1	5.39E+03	2.69E+04	8.52E+02	2.49E+03	2.19E+03	3.79E+03	3.6	7.1	1.4	0.8	0.8	1.4
A0A0G2JUC7	Dctn2	Dynactin subunit 2	46.22	3	4	2	2	2	3	3	4	2	2	2	3	3.90E+04	9.12E+04	3.92E+04	1.96E+04	2.32E+04	2.29E+04	13.6	18.8	10.2	10.2	10.2	13.6
D3ZRV0	Dcun1d1	DCN1-like protein	24.06	2	2	2	1	1	2	2	2	2	1	1	2	3.42E+04	3.75E+04	2.56E+04	2.82E+04	3.72E+03	9.52E+03	14	14	14	5.8	5.8	14
Q6MG60	Ddah2	N(G),N(G)-dimethylarginine dimethylaminohydrolase 2	29.69	2	2	2	2	1	2	2	2	2	2	1	2	1.39E+04	3.09E+04	2.15E+04	9.05E+03	2.14E+03	1.44E+04	10.5	10.5	10.5	10.5	5.6	10.5
G3V8T4	Ddb1	DNA damage-binding protein 1	126.94	5	8	5	4	5	4	5	8	5	4	5	4	4.65E+04	6.85E+04	2.56E+04	2.89E+04	2.34E+04	1.09E+04	6.1	10.5	7.4	4.9	6.1	5.2
D3ZJ91	Ddhd2	DDHD domain-containing 2	79.57	1	2	1	2	2	0	1	2	1	2	2	0	5.86E+03	2.72E+04	2.92E+03	9.49E+03	4.76E+03	0.00E+00	2.7	6.3	3.6	6.3	6.3	0
D3ZAS9	Ddrgk1	DDRGK domain-containing 1	38.61	1	1	1	1	1	1	1	1	1	1	1	1	1.88E+04	1.22E+04	9.09E+03	1.07E+04	3.81E+03	7.33E+02	5	5	5	5	5	5
Q641Y8	Ddx1	ATP-dependent RNA helicase DDX1	82.50	4	6	5	3	4	3	4	6	5	3	4	3	2.54E+04	6.47E+04	1.17E+04	2.10E+04	2.92E+04	7.32E+03	7.6	12.3	9.9	6.5	7.6	7.6
E9PT29	Ddx17	DEAD-box helicase 17	72.46	9	9	4	8	7	4	3	3	1	3	3	1	8.73E+03	1.90E+04	4.57E+02	2.08E+03	9.95E+03	2.89E+02	16.8	16.8	7.2	15.1	13.4	7.2
Q68FX3	Ddx19a	DEAD-box polypeptide 19a	53.90	2	3	0	2	2	1	2	3	0	2	2	1	7.22E+03	2.88E+04	0.00E+00	6.73E+03	5.23E+03	1.20E+03	5.2	7.5	0	5.2	5.2	5.2
Q5U216	Ddx39a	ATP-dependent RNA helicase DDX39A	49.11	8	8	7	7	7	5	3	3	2	3	3	1	4.80E+04	9.34E+04	7.97E+04	4.16E+04	2.92E+04	1.74E+04	27.6	27.6	24.4	24.8	24.8	19
Q63413	Ddx39b	Spliceosome RNA helicase Ddx39b	49.04	10	10	10	9	9	8	5	5	5	5	5	4	1.02E+06	1.11E+06	3.74E+05	6.30E+05	4.75E+05	1.42E+05	35.7	35.7	33.4	32.9	32.9	27.3
D3ZN21	Ddx3y	DEAD-box helicase 3, Y-linked	72.99	6	8	3	6	8	4	3	5	1	3	5	1	1.95E+04	4.05E+04	2.08E+03	1.25E+04	2.62E+04	2.28E+03	10	12.3	5.3	10	12.3	6.7
F1LQD1	Ddx4	Probable ATP-dependent RNA helicase DDX4	77.41	11	13	9	11	10	7	9	11	8	9	8	5	8.43E+04	2.26E+05	8.57E+04	5.90E+04	4.92E+04	1.80E+04	21.2	28.5	19.6	23.3	20.1	13.4
Q6AYI1	Ddx5	DEAD box polypeptide 5	69.24	8	10	4	9	7	4	2	4	1	4	3	1	9.03E+04	1.76E+05	5.02E+04	6.33E+04	6.89E+04	1.46E+04	16.3	20.7	8.1	18.5	15	8.1
D4ADT5	Ddx58	DEAD box polypeptide 58	68.36	2	3	2	2	1	2	2	3	2	2	1	2	1.53E+04	3.10E+04	6.43E+03	3.08E+03	3.00E+03	4.99E+03	3.8	7.2	5.4	5.2	1.8	5.4
D3ZD73	Ddx6	DEAD box polypeptide 6	54.24	2	2	2	0	0	1	2	2	2	0	0	1	4.34E+03	3.57E+04	1.72E+04	0.00E+00	0.00E+00	3.13E+03	7.2	7.2	7.2	0	0	4.1
G3V734	Decr1	2,4-dienoyl-CoA reductase, mitochondrial	36.13	2	2	0	2	1	1	2	2	0	2	1	1	5.20E+04	2.67E+04	0.00E+00	1.27E+04	3.20E+03	5.76E+03	9.6	9.6	0	9.6	3	6.6
Q32ZG8	Defb24	Beta-defensin	9.62	2	3	1	3	3	1	2	3	1	3	3	1	3.52E+05	7.28E+05	1.68E+05	5.07E+05	7.85E+05	1.32E+05	31.3	45.8	12	45.8	45.8	12
D4A518	Dennd4a	DENN domain-containing 4A	209.78	2	3	3	2	3	3	2	3	3	2	3	3	6.14E+04	9.58E+04	1.86E+05	3.89E+04	1.78E+05	1.83E+05	2	2.8	2.8	1.9	2.8	2.8
Q6P725	Des	Desmin	53.42	3	3	3	2	3	3	1	1	1	0	1	1	8.73E+03	1.82E+04	1.68E+04	0.00E+00	3.09E+03	1.04E+04	6.8	6.8	6.8	3.8	6.8	6.8
D4A9W3	Dglucy	D-glutamate cyclase	66.06	2	3	2	0	0	2	2	3	2	0	0	2	5.75E+03	1.86E+04	3.22E+03	0.00E+00	0.00E+00	4.86E+03	5.7	7.1	5.7	0	0	5.7
Q6AY53	Dhps	Deoxyhypusine synthase	40.71	2	2	2	2	2	2	2	2	2	2	2	2	6.40E+04	1.18E+05	1.22E+05	5.46E+04	8.82E+04	1.08E+05	6.8	6.8	6.8	6.8	6.8	6.8
G3V978	Dhrs11	Dehydrogenase/reductase 11	28.37	2	3	1	3	2	1	2	3	1	3	2	1	2.92E+04	4.86E+04	4.76E+03	3.82E+04	2.76E+04	9.89E+03	10.8	15.8	6.2	15.8	10.8	6.2
Q5RK17	Diablo	Diablo homolog	26.91	1	1	1	1	0	1	1	1	1	1	0	1	4.71E+04	5.80E+04	4.08E+04	4.72E+04	0.00E+00	7.16E+03	4.2	4.2	4.2	4.2	0	4.2
F1M775	Diaph1	Protein diaphanous homolog 1	140.30	1	0	1	1	0	1	1	0	1	1	0	1	8.89E+03	0.00E+00	1.21E+03	5.66E+02	0.00E+00	7.73E+02	1.7	0	1.7	1.7	0	1.7
Q5U2P0	Dis3l	DIS3-like exonuclease 1	120.76	1	2	1	0	1	2	1	2	1	0	1	2	2.76E+04	4.80E+04	9.03E+04	0.00E+00	1.29E+03	4.41E+04	2.3	3.7	1.4	0	1.4	3.7
D3ZIL9	Dis3l2	DIS3-like exonuclease 2	98.40	2	2	1	2	1	1	2	2	1	2	1	1	6.70E+03	9.99E+03	6.53E+03	7.92E+03	1.71E+03	2.56E+03	2.5	2.5	1.1	2.5	1.4	1.1
B1H219	Dkk3	Dickkopf WNT-signaling pathway inhibitor 3	38.74	6	6	7	7	7	7	6	6	7	7	7	7	6.68E+05	5.72E+05	1.99E+05	7.67E+05	4.73E+05	2.48E+05	24.1	24.1	28.2	28.2	28.2	28.2
G3V927	Dlgap4	Disks large-associated protein 4	108.02	1	2	1	1	2	1	1	2	1	1	2	1	5.89E+03	3.48E+04	1.20E+05	6.43E+03	1.29E+05	1.61E+05	1.2	3	1.8	1.2	3	1.8
A0A0G2K5B1	Dnaaf1	Dynein assembly factor 1, axonemal	70.87	3	4	4	3	4	3	3	4	4	3	4	3	2.75E+04	5.43E+04	4.95E+04	2.27E+04	1.70E+04	5.46E+03	5.8	7.5	7.5	5.6	7.5	5.6
D4A599	Dnah17	Dynein, axonemal, heavy chain 17	508.99	4	4	4	2	2	4	4	4	4	2	2	4	3.05E+04	4.03E+04	4.09E+04	2.74E+04	2.56E+04	3.05E+04	1	1	1	0.5	0.5	1
P63036	Dnaja1	DnaJ homolog subfamily A member 1	44.87	3	5	3	3	3	2	3	5	3	3	3	2	6.01E+04	1.28E+05	3.66E+04	3.32E+04	3.54E+04	1.51E+04	11.6	21.4	11.1	11.6	11.6	6
Q5M9H7	Dnaja2	DnaJ homolog subfamily A member 2	45.75	5	5	4	4	4	4	5	5	4	4	4	4	6.25E+04	1.94E+05	3.58E+04	6.08E+04	4.10E+04	9.18E+03	23.1	23.1	19.4	19.4	20.6	15.8
Q4QR73	Dnaja4	DnaJ homolog subfamily A member 4	61.88	3	5	2	6	3	0	3	5	2	6	3	0	1.69E+04	5.30E+04	4.39E+03	6.27E+04	5.04E+03	0.00E+00	6.3	11.7	4.3	13.7	6.3	0
D3ZAC5	Dnajb3	DnaJ homolog subfamily B member 3	26.58	1	1	0	0	0	0	1	1	0	0	0	0	1.17E+04	4.61E+04	0.00E+00	0.00E+00	0.00E+00	0.00E+00	5.4	5.4	0	0	0	0
G3V8B8	Dnajc7	DnaJ homolog subfamily C member 7	50.10	1	3	1	1	0	0	1	3	1	1	0	0	4.39E+03	4.21E+04	5.24E+03	2.66E+04	0.00E+00	0.00E+00	3	11.9	3	3	0	0
O35303	Dnm1l	Dynamin-1-like protein	83.91	6	8	3	6	6	2	6	8	3	6	6	2	2.15E+04	5.15E+04	1.46E+04	3.11E+04	1.81E+04	8.12E+03	10.2	15	5.4	11.7	10.9	3.8
Q08877	Dnm3	Dynamin-3	97.91	1	2	2	1	1	2	1	2	2	1	1	2	1.26E+04	1.71E+04	7.93E+03	6.58E+03	1.94E+03	1.43E+03	1.2	2.4	2.4	1.2	1.2	2.4
Q4V8H5	Dnpep	Aspartyl aminopeptidase	52.56	12	12	11	13	12	11	12	12	11	13	12	11	7.07E+05	5.34E+05	3.66E+05	5.32E+05	5.54E+05	1.09E+05	42.9	37.3	37.1	45.5	42.9	37.1
O55096	Dpp3	Dipeptidyl peptidase 3	83.04	10	11	5	10	9	7	10	11	5	10	9	7	1.41E+05	1.77E+05	8.66E+04	8.91E+04	6.50E+04	9.76E+04	22.2	24.5	10.4	24	17.9	13.6
F1M7X5	Dpp4	Dipeptidyl peptidase 4	88.05	2	1	1	1	1	2	2	1	1	1	1	2	1.50E+04	3.36E+03	4.21E+03	9.90E+03	5.30E+03	4.66E+03	2.6	1.3	1.4	1.3	1.3	2.7
Q9EPB1	Dpp7	Dipeptidyl peptidase 2	55.11	8	7	4	7	6	5	8	7	4	7	6	5	5.72E+05	3.03E+05	9.48E+04	2.30E+05	1.48E+05	1.14E+05	31	25.6	12.6	25.6	19.8	14.8
B2RZ77	Dpt	Dermatopontin	24.20	7	7	7	7	7	7	7	7	7	7	7	7	1.21E+06	6.51E+05	6.80E+05	9.47E+05	8.95E+05	6.35E+05	50.5	50.5	50.5	50.5	50.5	50.5
A0A0G2K355	Dpyd	Dihydropyrimidine dehydrogenase [NADP(+)]	102.56	10	11	5	10	10	4	10	11	5	10	10	4	3.95E+04	1.44E+05	1.22E+04	7.99E+04	4.95E+04	8.45E+03	15.5	18	7.7	15.5	15.5	5.9
P47942	Dpysl2	Dihydropyrimidinase-related protein 2	62.28	19	22	17	17	18	15	18	20	16	16	17	14	6.79E+05	1.27E+06	4.76E+05	5.26E+05	3.93E+05	2.66E+05	46.3	54.2	45.1	43.9	46.9	41.3
Q62952	Dpysl3	Dihydropyrimidinase-related protein 3	61.97	2	4	1	2	1	2	1	2	0	1	0	1	9.77E+03	1.50E+04	0.00E+00	5.71E+03	0.00E+00	1.91E+03	5.1	8.9	2.8	5.1	2.8	5.4
F1LYX9	Dsg2	Desmoglein 2	122.29	5	5	6	5	5	6	5	5	6	5	5	6	6.50E+04	3.87E+04	4.33E+04	6.00E+04	4.78E+04	5.03E+04	6.9	6.9	7.8	6.9	6.9	7.8
F1LMV6	Dsp	Desmoplakin	332.39	9	4	7	10	20	5	9	4	7	10	20	5	1.04E+04	9.83E+03	8.54E+03	1.54E+04	7.33E+04	6.45E+03	4.4	1.7	3.4	5.1	9.5	2.1
Q62598	Dspp	Dentin sialophosphoprotein	70.18	2	2	1	2	2	1	2	2	1	2	2	1	3.91E+04	8.49E+04	4.79E+04	5.93E+04	3.05E+04	4.22E+04	4.4	4.4	2.5	4.4	4.4	2.5
D3ZC56	Dst	Dystonin	847.20	3	3	5	3	5	5	3	3	5	3	5	5	5.22E+03	5.51E+03	5.41E+03	5.01E+03	1.72E+04	1.18E+04	0.5	0.7	0.9	0.6	1	0.9
Q7M0E3	Dstn	Destrin	18.53	6	7	6	7	7	6	6	7	6	7	7	6	5.18E+05	1.56E+06	8.79E+05	6.27E+05	7.08E+05	5.31E+05	37.6	39.4	37.6	39.4	39.4	33.9
G3V9L3	Dusp3	Dual-specificity phosphatase 3	21.10	4	5	2	4	4	2	4	5	2	4	4	2	1.41E+05	4.14E+05	7.78E+04	1.20E+05	9.03E+04	7.77E+04	28.1	33.3	18.2	28.1	30.2	18.2
F1LRT9	Dync1h1	Cytoplasmic dynein 1 heavy chain 1	531.80	27	26	20	27	28	13	27	26	20	27	28	13	2.98E+04	3.30E+04	1.69E+04	2.59E+04	3.04E+04	3.62E+03	8.6	8.6	6.4	8.2	8.5	4.1
G3V7G0	Dync1li1	Cytoplasmic dynein 1 light intermediate chain 1	56.67	3	3	2	3	3	2	2	2	2	2	2	2	1.28E+04	1.62E+04	5.28E+03	9.98E+03	1.31E+04	2.81E+03	9.4	9.4	6.9	9.4	9.4	6.9
A0A096MIY2	Dync1li2	Cytoplasmic dynein 1 light intermediate chain 2	51.55	3	3	1	3	3	1	2	2	1	2	2	1	1.53E+04	3.87E+04	3.83E+03	1.83E+04	1.73E+04	2.22E+03	8.7	8.7	3.4	8.7	8.7	3.4
P63170	Dynll1	Dynein light chain 1, cytoplasmic	10.37	2	3	3	3	3	3	1	1	1	1	1	1	3.75E+05	8.64E+05	4.93E+05	3.73E+05	6.91E+05	1.47E+05	37.1	67.4	67.4	67.4	67.4	67.4
Q78P75	Dynll2	Dynein light chain 2, cytoplasmic	10.35	2	3	3	3	3	3	1	1	1	1	1	1	1.14E+05	2.91E+05	9.60E+04	1.25E+05	1.02E+05	2.79E+04	37.1	67.4	67.4	67.4	67.4	67.4
Q6AYG5	Echdc1	Ethylmalonyl-CoA decarboxylase	32.63	4	3	1	3	2	1	4	3	1	3	2	1	7.34E+04	1.47E+05	2.38E+04	8.15E+04	3.92E+04	1.77E+04	15.4	12.4	4.3	11	8.7	4.3
Q62894	Ecm1	Extracellular matrix protein 1	63.25	31	31	29	31	31	29	31	31	29	31	31	29	5.48E+06	5.09E+06	4.70E+06	5.94E+06	5.36E+06	4.63E+06	67.4	66.2	64.1	67.4	67.4	65.3
F1M446	Ecpas	Ecm29 proteasome adaptor and scaffold	203.92	2	2	1	2	1	0	2	2	1	2	1	0	3.06E+03	2.72E+03	1.27E+02	1.22E+03	7.25E+02	0.00E+00	1.7	1.7	0.8	1.7	0.8	0
P62630	Eef1a1	Elongation factor 1-alpha 1	50.11	20	22	19	20	19	13	20	22	19	20	19	13	7.06E+06	8.16E+06	3.52E+06	4.05E+06	3.20E+06	1.42E+06	56.1	57.6	47.2	56.1	47.2	41.3
B5DEN5	Eef1b2	Elongation factor 1-beta 2	24.68	6	6	5	7	7	4	5	5	5	6	6	3	5.65E+05	9.53E+05	4.09E+05	4.23E+05	2.73E+05	8.49E+04	44.9	44.9	39.6	48	48	36.9
Q68FR9	Eef1d	Elongation factor 1-delta	31.33	8	10	7	8	6	7	7	9	7	7	5	6	4.26E+05	6.94E+05	3.78E+05	3.31E+05	2.36E+05	1.37E+05	42.7	44.1	38.4	42.7	29.9	34.2
Q68FR6	Eef1g	Elongation factor 1-gamma	50.06	8	8	8	10	9	6	8	8	8	10	9	6	3.03E+05	4.62E+05	2.22E+05	2.36E+05	2.00E+05	7.28E+04	31.1	31.4	26.5	31.4	31.1	17.4
P05197	Eef2	Elongation factor 2	95.28	36	31	25	31	31	25	36	31	25	31	31	25	1.39E+06	1.40E+06	5.03E+05	7.12E+05	7.28E+05	2.60E+05	53.6	44.4	38.5	47.6	44.4	40.6
Q6AXN2	Efemp1	EGF-containing fibulin extracellular matrix protein 1	54.65	16	16	14	15	16	14	16	16	14	15	16	14	3.93E+06	2.63E+06	1.95E+06	2.49E+06	3.03E+06	1.65E+06	47.9	47.9	48.1	47.9	49.9	48.1
A0A0G2K2R5	Efemp2	EGF-containing fibulin extracellular matrix protein 2	49.39	6	5	3	6	5	2	6	5	3	6	5	2	2.51E+05	1.12E+05	8.80E+04	1.60E+05	1.55E+05	4.51E+04	17.2	13.3	7.7	17.2	13.3	5.9
Q4FZY0	Efhd2	EF-hand domain-containing protein D2	26.76	4	4	4	4	4	4	4	4	4	4	4	4	1.87E+05	1.96E+05	1.25E+05	8.28E+04	7.25E+04	5.92E+04	15.1	15.1	15.1	15.1	15.1	15.1
D3ZXJ5	Efl1	Elongation factor-like GTPase 1	125.69	1	1	0	1	1	0	1	1	0	1	1	0	3.82E+03	7.00E+03	0.00E+00	2.79E+03	1.44E+03	0.00E+00	1.3	1.3	0	1.3	1.3	0

Uniprot accession number	Gene symbol	Protein name	Mol. weight [kDa]	No. Peptides Control wk1	No. Peptides Control wk8	No. Peptides Control wk14	No. Peptides Heat wk1	No. Peptides Heat wk8	No. Peptides Heat wk14	No. Unique peptides Control wk1	No. Unique peptides Control wk8	No. Unique peptides Control wk14	No. Unique peptides Heat wk1	No. Unique peptides Heat wk8	No. Unique peptides Heat wk14	iBAQ Control wk1	iBAQ Control wk8	iBAQ Control wk14	iBAQ Heat wk1	iBAQ Heat wk8	iBAQ Heat wk14	Sequence coverage Control wk1 [%]	Sequence coverage Control wk8 [%]	Sequence coverage Control wk14 [%]	Sequence coverage Heat wk1 [%]	Sequence coverage Heat wk8 [%]	Sequence coverage Heat wk14 [%]
Q641Z6	Ehd1	EH domain-containing protein 1	60.60	13	15	14	13	15	13	13	15	14	13	15	13	3.37E+05	3.60E+05	2.88E+05	1.86E+05	1.83E+05	2.06E+05	35	39.1	37.3	35.8	40.1	37.1
Q4V8H8	Ehd2	EH domain-containing protein 2	61.24	11	12	10	9	10	10	11	12	10	9	10	10	5.60E+05	5.39E+05	3.89E+05	2.39E+05	2.66E+05	1.62E+05	32.2	35	30.9	27.8	27.8	28.7
Q8R3Z7	Ehd4	EH domain-containing protein 4	61.47	2	4	1	2	3	1	2	4	1	2	3	1	1.59E+04	5.58E+04	2.94E+03	3.94E+03	1.16E+04	1.26E+03	5	9.8	2.4	4.6	7.4	2.4
A0A096MIS3	Eif2b4	Translation initiation factor eIF-2B subunit delta	57.52	1	1	1	1	1	1	1	1	1	1	1	1	9.84E+03	3.18E+04	2.35E+03	1.07E+04	1.01E+04	9.80E+02	4.6	4.6	4.6	4.6	4.6	4.6
P68101	Eif2s1	Eukaryotic translation initiation factor 2 subunit 1	36.11	6	6	4	2	6	3	6	6	4	2	6	3	9.73E+04	6.46E+04	1.22E+05	3.76E+04	4.90E+04	3.20E+04	23.8	24.1	17.5	6.3	24.8	12.1
Q6P685	Eif2s2	Eukaryotic translation initiation factor 2 subunit 2	38.24	1	2	2	1	1	2	1	2	2	1	1	2	3.56E+04	4.08E+04	4.47E+04	1.52E+04	6.94E+03	2.91E+04	3.6	6.9	6.9	3.6	3.6	6.9
P81795	Eif2s3	Eukaryotic translation initiation factor 2 subunit 3	51.08	3	3	1	3	3	1	3	3	1	3	3	1	2.09E+04	5.77E+04	4.83E+03	1.44E+04	1.90E+04	3.56E+03	10.2	10.2	3.8	10.2	10.2	3.8
Q4G061	Eif3b	Eukaryotic translation initiation factor 3 subunit B	90.91	2	4	3	2	4	3	2	4	3	2	4	3	1.29E+05	1.05E+05	9.54E+04	6.66E+04	7.01E+04	1.04E+05	3.4	8.5	6.3	3.4	8.5	6.3
Q6AYK8	Eif3d	Eukaryotic translation initiation factor 3 subunit D	63.99	2	3	1	2	3	0	2	3	1	2	3	0	8.83E+03	4.15E+04	8.63E+02	5.17E+03	2.08E+04	0.00E+00	5.8	5.8	3.5	5.8	5.8	0
Q5RK09	Eif3g	Eukaryotic translation initiation factor 3 subunit G	35.65	3	3	3	1	3	2	3	3	3	1	3	2	3.33E+04	1.12E+05	7.13E+04	2.01E+04	2.38E+04	2.60E+04	12.8	12.8	12.8	5	12.8	10
A0JPM9	Eif3j	Eukaryotic translation initiation factor 3 subunit J	29.19	1	1	1	2	1	1	1	1	1	2	1	1	7.70E+03	1.42E+04	2.17E+04	1.49E+04	3.49E+03	8.62E+03	4.6	4.6	4.6	13.1	4.6	4.6
Q6P3V8	Eif4a1	Eukaryotic translation initiation factor 4A-1	46.15	13	14	10	13	12	9	9	9	5	9	8	6	9.47E+05	9.29E+05	6.93E+05	5.95E+05	5.55E+05	2.84E+05	48.3	50	29.3	48.3	42.4	31.3
Q5RKI1	Eif4a2	Eukaryotic translation initiation factor 4A-2	46.40	7	8	7	6	6	4	3	3	2	2	2	1	8.27E+04	1.06E+05	5.47E+04	7.79E+04	4.46E+04	5.39E+03	24.3	26	20.1	18.4	18.4	12.8
Q3B8Q2	Eif4a3	Eukaryotic translation initiation factor 4A-3	46.84	2	4	3	2	2	1	1	2	1	1	1	1	2.86E+04	3.14E+04	1.52E+04	2.09E+04	2.24E+04	5.46E+03	6.1	11.2	7.8	6.1	6.1	3.9
A0A1W2Q627	Eif4e	Eukaryotic translation initiation factor 4E	25.15	2	2	3	3	2	2	2	2	3	3	2	2	9.90E+04	1.34E+05	9.40E+04	7.20E+04	5.50E+04	2.98E+04	11.9	11.9	11.9	11.9	11.9	11.9
D4AD15	Eif4g1	Eukaryotic translation initiation factor 4 gamma-1	175.09	4	2	1	4	2	2	4	2	1	4	2	2	1.12E+04	8.13E+03	3.36E+03	8.20E+03	6.86E+03	1.49E+03	3.2	1.6	0.6	3.3	1.6	1.6
Q5XI72	Eif4h	Eukaryotic translation initiation factor 4H	27.32	4	5	2	4	3	0	4	5	2	4	3	0	4.89E+04	1.68E+05	2.24E+04	6.90E+04	3.24E+04	0.00E+00	33.5	35.9	16.9	33.5	26.2	0
Q3T1J1	Eif5a	Eukaryotic translation initiation factor 5A-1	16.83	11	12	11	10	9	8	11	12	11	10	9	8	2.61E+06	3.07E+06	1.23E+06	1.33E+06	1.21E+06	7.61E+05	78.6	78.6	78.6	77.9	77.9	77.9
A0A0G2K110	Eif6	Eukaryotic translation initiation factor 6	26.73	3	5	3	2	4	2	3	5	3	2	4	2	1.37E+05	2.67E+05	9.39E+04	5.16E+04	1.03E+05	5.28E+04	15.4	35.4	19.9	11.4	32.9	9.8
B5DF91	Elavl1	ELAV-like protein	36.17	3	3	1	3	2	1	3	3	1	3	2	1	1.28E+05	1.89E+05	4.48E+04	9.74E+04	4.73E+04	2.26E+04	10.7	10.7	3.4	10.7	7.4	3.4
Q6P6T4	Eml2	Echinoderm microtubule-associated protein-like 2	70.71	2	2	3	2	2	2	2	2	3	2	2	2	1.26E+04	1.77E+04	3.17E+04	1.20E+04	8.85E+03	2.15E+04	5.1	5.1	6.3	5.1	5.1	5.1
M0R5J4	Eno1	Alpha-enolase	47.07	9	8	7	8	6	5	9	8	7	8	6	5	3.44E+05	2.35E+05	1.28E+05	1.34E+05	2.10E+05	4.51E+04	30.2	25.6	22.8	26	18.7	14.5
D3ZDT1	Epb41l2	Erythrocyte membrane protein band 4.1-like 2	102.59	4	4	2	5	3	1	4	4	2	5	3	1	1.28E+04	2.97E+04	2.08E+03	1.39E+04	6.06E+03	8.85E+03	6.6	6.8	4	8.1	5.3	1.3
A3E0T0	Epb41l3	Erythrocyte membrane protein band 4.1-like 3	96.95	2	2	0	2	2	0	2	2	0	2	2	0	7.10E+03	1.96E+04	0.00E+00	4.67E+03	4.99E+03	0.00E+00	3.4	3.4	0	3.4	3.4	0
Q5RKK3	Ephx2	Bifunctional epoxide hydrolase 2	62.33	6	5	5	7	5	5	6	5	5	7	5	5	2.58E+04	4.40E+04	1.35E+04	4.00E+04	1.37E+04	1.37E+04	15.5	13.7	13.7	17.5	12.6	13.7
D4A2Z2	Eppin	Epididymal peptidase inhibitor	15.68	3	3	3	3	3	3	3	3	3	3	3	3	3.44E+05	5.12E+05	3.42E+05	2.55E+05	2.99E+05	1.88E+05	23.9	23.9	23.9	23.9	23.9	23.9
A0A0G2JZI2	Eprs	Glutamyl-prolyl-tRNA synthetase	169.86	18	21	18	18	19	10	18	21	18	18	19	10	6.72E+04	1.22E+05	3.65E+04	6.58E+04	5.43E+04	1.19E+04	19	21.6	18.5	19.2	19.4	12.1
B2RYQ5	Erh	Enhancer of rudimentary homolog	12.26	2	2	1	2	2	1	2	2	1	2	2	1	1.96E+05	2.73E+05	7.55E+04	1.44E+05	1.70E+05	4.32E+04	21.2	21.2	10.6	21.2	21.2	10.6
P52555	Erp29	Endoplasmic reticulum resident protein 29	28.57	3	3	1	2	2	2	3	3	1	2	2	2	6.71E+04	3.93E+04	1.13E+04	1.89E+04	9.30E+03	1.23E+04	15	15	3.5	9.2	9.2	9.2
Q5VLR5	Erp44	Endoplasmic reticulum protein 44	46.88	2	2	3	1	2	2	2	2	3	1	2	2	1.71E+05	1.80E+05	3.04E+05	1.33E+05	2.72E+05	2.76E+05	10.1	10.1	13.5	5.7	10.1	9.1
B0BNE5	Esd	S-formylglutathione hydrolase	31.36	11	11	10	10	6	10	11	11	10	10	6	10	1.20E+06	1.72E+06	5.68E+05	7.16E+05	3.18E+05	3.73E+05	69.1	69.1	68.8	68.8	42.6	69.1
Q5U2Q7	Etf1	Eukaryotic peptide chain release factor subunit 1	49.03	6	5	4	5	4	4	6	5	4	5	4	4	9.20E+04	1.25E+05	4.92E+04	6.22E+04	3.98E+04	3.31E+04	19.7	13.5	11.2	17.4	11	11.2
P13803	Etfa	Electron transfer flavoprotein subunit alpha, mitochondrial	34.95	1	1	1	0	0	1	1	1	1	0	0	1	4.43E+03	1.76E+04	1.24E+04	0.00E+00	0.00E+00	5.25E+03	3.9	3.9	3.9	0	0	3.9
Q68FU3	Etfb	Electron transfer flavoprotein subunit beta	27.69	1	1	1	1	0	1	1	1	1	1	0	1	2.37E+04	2.63E+04	1.75E+04	2.97E+03	0.00E+00	1.15E+04	8.2	8.2	8.2	8.2	0	8.2
A0A0G2K850	Ewsr1	RNA-binding protein EWS	67.94	2	2	1	2	2	1	2	2	1	2	2	1	4.42E+04	7.63E+04	1.04E+04	2.31E+04	3.56E+04	2.05E+03	4.3	4.3	2.9	4.3	4.3	2.9
G3V901	Ext1	Exostosin glycosyltransferase 1	86.31	2	2	2	2	2	1	2	2	2	2	2	1	1.72E+04	7.00E+03	9.99E+03	1.10E+04	2.26E+04	4.44E+03	4.2	4.2	4.2	4.2	4.2	2.8
A0A0G2K890	Ezr	Ezrin	69.29	12	10	9	10	9	8	9	7	7	8	6	6	3.85E+05	1.18E+05	2.52E+05	1.27E+05	9.66E+04	1.59E+05	28.2	24.3	21.5	24.6	21.7	18.8
A0A0H2UHR6	F10	Coagulation factor X	55.48	20	20	19	20	18	20	20	20	19	20	18	20	1.50E+06	2.01E+06	2.39E+06	2.14E+06	2.40E+06	2.32E+06	41.3	41.3	44.5	43.1	36.8	47
A0A0G2K4I9	F11	Coagulation factor XI	69.60	20	19	18	20	19	20	20	19	18	20	19	20	1.54E+06	9.30E+05	1.36E+06	1.44E+06	1.12E+06	1.45E+06	47.3	47.4	42.3	47.1	45.8	44.9
A0A0H2UI19	F12	Coagulation factor XII	66.72	24	29	24	25	25	22	24	29	24	25	25	22	9.75E+06	7.96E+06	1.01E+07	8.03E+06	1.15E+07	8.66E+06	66.7	68	64.8	67	66.7	60.4
G3V811	F13a1	Coagulation factor XIII A chain	83.05	15	14	15	15	15	14	4	4	4	4	4	4	5.59E+05	3.23E+05	4.16E+05	5.17E+05	4.36E+05	3.27E+05	31.8	31.8	29.1	31.8	31.8	28.7
O08619	F13a1	Coagulation factor XIII A chain	82.66	12	11	12	12	12	11	1	1	1	1	1	1	1.52E+04	8.47E+03	1.00E+04	2.47E+04	1.46E+04	1.14E+04	24.7	24.7	22	24.7	24.7	21.6
F6Q1N1	F13b	Coagulation factor XIII B chain	74.88	32	34	31	32	31	27	32	34	31	32	31	27	2.93E+06	2.26E+06	2.45E+06	3.12E+06	2.92E+06	2.67E+06	57.5	57.8	53.7	57.4	55.4	52.7
G3V843	F2	Prothrombin	70.39	48	51	48	48	49	47	41	44	41	41	42	40	7.14E+07	6.23E+07	7.66E+07	7.69E+07	6.65E+07	7.53E+07	56.2	56.2	54.5	55.4	55.4	54.5
A0A0G2K3W2	F5	Coagulation factor V	190.99	4	3	6	5	5	4	4	3	6	5	5	4	1.51E+04	1.32E+04	9.84E+04	1.74E+04	1.89E+04	8.41E+04	2.9	2	4.6	3.7	3.6	3.3
Q8K3U6	F7	Coagulation factor VII	50.40	10	8	8	9	8	9	10	8	8	9	8	9	1.82E+05	1.40E+05	2.42E+05	1.75E+05	1.65E+05	1.46E+05	30.7	24	25.1	26.5	24.2	28.5
P16296	F9	Coagulation factor IX	51.81	18	19	19	18	19	19	18	19	19	18	19	19	1.19E+07	1.30E+07	1.50E+07	1.44E+07	1.21E+07	1.47E+07	49.8	51.5	49.8	48.9	49.8	48.5
P07483	Fabp3	Fatty acid-binding protein, heart	14.78	5	6	4	5	6	3	5	6	4	5	6	3	3.58E+05	3.91E+05	1.09E+05	5.09E+05	3.88E+05	6.51E+04	40.6	47.4	30.1	40.6	47.4	19.5
Q5XFV4	Fabp4	Fatty acid-binding protein, adipocyte	14.74	3	3	4	2	3	4	3	3	4	2	3	4	7.70E+05	7.74E+05	1.05E+06	2.41E+05	2.44E+05	5.85E+05	22.7	22.7	28.8	15.9	22	28.8
P55053	Fabp5	Fatty acid-binding protein, epidermal	15.06	4	4	1	4	5	3	4	4	1	4	5	3	4.14E+05	3.82E+05	5.69E+04	2.22E+05	3.47E+05	2.11E+04	48.1	48.1	15.6	48.1	54.8	34.8
P55054	Fabp9	Fatty acid-binding protein 9	15.09	7	9	8	7	7	8	7	9	8	7	7	8	3.14E+06	4.07E+06	3.49E+06	2.45E+06	1.06E+06	8.24E+05	53.8	61.4	60.6	53.8	53.8	60.6
Q8R2E7	Fadd	FAS-associated death domain protein	23.12	2	2	0	2	0	1	2	2	0	2	0	1	3.64E+04	2.46E+04	0.00E+00	9.00E+03	0.00E+00	4.28E+03	15.4	15.4	0	15.4	0	9.6
D4A777	Fam114a1	Family with sequence similarity 114, member A1	60.76	3	4	4	4	4	4	3	4	4	4	4	4	5.98E+04	7.38E+04	2.73E+04	2.31E+04	2.27E+04	1.95E+04	9.3	14.6	14.6	14.6	14.6	14.6
Q9ESN0	Fam129a	Protein Niban	103.46	20	23	18	21	18	14	20	23	18	21	18	14	2.94E+05	7.45E+05	1.66E+05	3.35E+05	1.59E+05	9.16E+04	31.8	37.7	28.6	35	29.5	24.2
B4F7E8	Fam129b	Niban-like protein 1	84.73	9	10	8	4	6	6	9	10	8	4	6	6	1.11E+05	1.58E+05	7.16E+04	2.36E+04	4.46E+04	2.90E+04	18.2	21.7	17.4	7.9	12.7	14.2
A0A0G2JSY5	Fam221a	Protein FAM221A	27.49	2	2	2	2	2	1	2	2	2	2	2	1	5.18E+04	1.30E+05	3.54E+04	4.51E+04	1.95E+04	6.52E+03	18.5	18.5	18.5	18.5	18.5	7.6
B2GUZ9	Fam49b	Fam49b protein	36.78	4	3	1	3	2	2	4	3	1	3	2	2	8.98E+04	1.11E+05	1.22E+04	3.36E+04	1.21E+04	2.53E+04	19.8	15.7	8.3	16.4	12.3	12.3
F1LMH7	Fap	Fibroblast activation protein, alpha	87.71	3	1	1	3	2	1	3	1	1	3	2	1	3.41E+04	7.97E+03	1.61E+03	1.70E+04	2.30E+04	1.13E+04	4.7	2	1.4	4.7	3.4	1.4
Q68FT7	Farsb	Phenylalanyl-tRNA synthetase subunit beta	65.65	3	2	2	2	2	2	3	2	2	2	2	2	3.23E+04	4.46E+04	2.28E+04	1.90E+04	1.82E+04	1.50E+04	5.3	3.7	3.7	3.4	3.4	3.7
P12785	Fasn	Fatty acid synthase	272.65	8	10	6	7	8	4	8	10	6	7	8	4	2.88E+04	2.00E+04	9.32E+03	1.14E+04	1.44E+04	3.61E+03	6.3	7.4	4.3	5.6	6.1	3.4
D3ZQ25	Fbln1	Fibulin-1	78.07	20	21	17	19	18	18	4	5	3	4	4	4	3.09E+06	1.74E+06	1.50E+06	3.10E+06	1.99E+06	1.85E+06	35.6	38	31.1	35	32.3	32.9
B1WC21	Fbln1	Fibulin-1	75.38	17	17	15	16	15	15	1	1	1	1	1	1	2.12E+05	1.11E+05	1.63E+05	1.84E+05	1.76E+05	1.37E+05	32.7	34.2	28	32.1	29.3	29.9
Q9WVH8	Fbln5	Fibulin-5	50.16	7	7	5	7	7	6	7	7	5	7	7	6	6.22E+05	4.12E+05	2.80E+05	4.13E+05	2.57E+05	2.93E+05	19.6	19.6	14.3	19.6	19.6	17.9
G3V9M6	Fbn1	Fibrillin 1	311.95	6	9	4	9	8	5	6	9	4	9	8	5	1.40E+04	1.12E+04	5.35E+03	1.24E+04	7.59E+03	5.03E+03	2.8	4.6	1.9	4.6	4.2	2.3
P19112	Fbp1	Fructose-1,6-bisphosphatase 1	39.61	6	7	6	6	5	4	6	7	6	6	5	4	1.15E+05	1.89E+05	1.20E+05	7.50E+04	3.64E+04	2.32E+04	24.8	28.7	25.3	24.8	18.7	15.4
Q9Z1N1	Fbp2	Fructose-1,6-bisphosphatase isozyme 2	36.89	1	2	1	2	1	1	1	2	1	2	1	1	3.21E+04	5.04E+04	5.03E+03	3.87E+04	2.08E+04	4.27E+03	3.5	8.6	3.5	8.6	3.5	3.5
Q923V4	Fbxo6	F-box only protein 6	32.79	1	1	1	1	1	0	1	1	1	1	1	0	1.81E+04	3.34E+04	0.00E+00	1.64E+04	7.57E+03	0.00E+00	3.5	3.5	3.5	3.5	3.5	0
D3Z9G1	Fbxw17	F-box and WD-40 domain protein 17	54.33	2	4	4	3	3	3	2	4	4	3	3	3	2.74E+05	2.38E+05	3.52E+04	1.56E+05	1.49E+05	1.25E+04	6.1	14.1	14.1	8.8	9.2	9.2
D3ZJF8	Fcgbp	Fc fragment of IgG-binding protein	275.16	8	11	8	8	9	5	7	10	7	7	8	4	2.05E+04	2.84E+04	8.74E+03	1.49E+04	1.93E+04	2.69E+03	5.4	7	5.1	5.2	5.8	3
F7EZQ4	Fcgbpl1	Fc fragment of IgG-binding protein-like 1	275.74	36	29	33	27	31	16	35	28	32	26	30	15	3.41E+05	1.34E+05	1.86E+05	7.00E+04	1.42E+05	1.56E+04	22.8	19.5	21.2	17.7	21	10.2
Q5M8B4	Fcna	Ficolin-1	36.60	8	8	7	9	8	7	8	8	7	9	8	7	5.54E+05	3.88E+05	5.13E+05	6.14E+05	7.20E+05	5.35E+05	36.4	33.1	30.7	38.8	33.1	30.7
F1LND7	Fdps	Farnesyl pyrophosphate synthase	40.80	4	3	5	4	3	3	4	3	5	4	3	3	1.04E+05	8.44E+04	2.58E+04	1.19E+05	4.56E+04	3.33E+04	13	10.5	16.1	11.9	10.5	10.2
Q5XI19	Fermt2	Fermitin family homolog 2	77.88	6	9	7	5	4	6	6	9	7	5	4	6	7.06E+04	1.38E+05	7.07E+04	3.64E+04	1.81E+04	3.64E+04	14	19.6	14.3	12.5	10	13.8
Q6IRS6	Fetub	Fetuin-B	43.17	16	16	15	17	15	16	16	16	15	17	15	16	8.22E+06	8.37E+06	8.65E+06	9.80E+06	1.17E+07	9.02E+06	59.5	52.7	51.4	58.3	52.7	57.5
Q7TQ70	Fga	Fibrinogen alpha chain	86.66	39	35	34	36	38	31	39	35	34	36	38	31	1.27E+07	6.92E+06	8.97E+06	5.57E+06	5.81E+06	7.46E+06	49.2	47.8	48	47.8	48.6	42.8
P14480	Fgb	Fibrinogen beta chain	54.24	37	38	39	35	36	36	37	38	39	35	36	36	1.81E+07	7.81E+06	1.24E+07	7.87E+06	6.87E+06	1.21E+07	74.5	73.5	73.5	73.5	73.5	71
F1LM54	Fgfr1	Fibroblast growth factor receptor	81.09	2	2	2	2	2	1	2	2	2	2	2	1	2.03E+04	1.97E+04	1.86E+04	2.87E+04	3.02E+04	8.43E+03	3.4	3.4	3.4	3.4	3.4	1.7
P02680	Fgg	Fibrinogen gamma chain	50.63	26	23	24	21	23	23	26	23	24	21	23	23	1.91E+07	7.19E+06	1.44E+07	8.10E+06	6.88E+06	1.34E+07	60.9	51.5	57.8	51.7	52.1	53
Q5M8C6	Fgl1	Fibrinogen-like protein 1	36.48	2	2	1	2	2	1	2	2	1	2	2	1	3.95E+04	2.41E+04	3.73E+04	1.68E+04	2.45E+04	4.05E+04	9.6	9.6	5.1	9.6	9.6	5.1
G3V7P2	Fgl2	Fibrinogen-like protein 2	48.66	2	2	1	1	2	1	2	2	1	1	2	1	6.94E+04	5.21E+04	5.80E+04	3.44E+04	1.04E+05	4.38E+04	6.8	6.8	4.4	2.3	6.8	4.4
Q6P792	Fhl1	Four and a half LIM domains protein 1	33.58	8	9	6	7	6	6	8	9	6	7	6	6	5.61E+05	8.83E+05	3.46E+05	3.76E+05	2.23E+05	2.72E+05	34.1	39.2	22.3	33.8	28.7	22.3
O35115	Fhl2	Four and a half LIM domains protein 2	32.09	5	5	4	5	4	3	5	5	4	5	4	3	1.54E+05	2.12E+05	7.67E+04	5.72E+04	4.36E+04	4.44E+04	21.1	21.1	17.9	21.1	17.9	13.6
Q4FZR8	Fhl4	Four and a half LIM domains protein 4	32.12	4	3	3	3	0	0	4	3	3	3	0	0	6.39E+04	1.15E+05	7.36E+04	5.23E+04	0.00E+00	0.00E+00	20.7	17.9	15	17.9	0	0
P84817	Fis1	Mitochondrial fission 1 protein	16.99	2	3	3	3	2	3	2	3	3	3	2	3	1.23E+05	2.33E+05	2.41E+05	1.06E+05	6.49E+04	1.13E+05	15.8	23.7	23.7	23.7	15.8	23.7
Q5U2V1	Fkbp10	Peptidylprolyl isomerase	64.79	7	7	3	5	6	2	7	7	3	5	6	2	9.12E+04	4.20E+04	1.10E+04	1.31E+04	1.37E+04	5.70E+03	13.4	13.4	6.7	9.5	11	5
Q62658	Fkbp1a	Peptidyl-prolyl cis-trans isomerase FKBP1A	11.92	3	3	2	3	2	1	3	3	2	3	2	1	5.97E+05	6.08E+05	1.80E+05	2.86E+05	2.31E+05	1.52E+05	40.7	40.7	28.7	40.7	28.7	15.7
G3V6L9	Fkbp3	Peptidyl-prolyl cis-trans isomerase	25.18	2	4	3	3	3	0	2	4	3	3	3	0	4.57E+04	1.89E+05	1.38E+05	5.11E+04	4.17E+04	0.00E+00	10.7	26.8	21.9	21.9	21.9	0
Q9QVC8	Fkbp4	Peptidyl-prolyl cis-trans isomerase FKBP4	51.45	6	6	7	6	5	4	6	6	7	6	5	4	8.78E+04	1.42E+05	6.68E+04	5.97E+04	4.92E+04	1.84E+04	16.4	16.4	18.1	16.4	14.2	12
Q5U2T9	Fkbp5	Peptidyl-prolyl cis-trans isomerase FKBP5	50.96	6	8	5	6	4	4	6	8	5	6	4	4	6.65E+04	1.33E+05	2.67E+04	5.71E+04	3.70E+04	1.28E+04	14.7	27	12.1	14.7	12.3	12.9
Q66H94	Fkbp9	Peptidyl-prolyl cis-trans isomerase FKBP9	63.13	2	1	0	1	0	0	2	1	0	1	0	0	5.29E+04	1.32E+04	0.00E+00	6.44E+03	0.00E+00	0.00E+00	3.7	2.1	0	2.1	0	0
C0JPT7	Flna	Filamin A	280.49	31	36	26	31	25	20	31	36	26	31	25	20	9.49E+04	2.46E+05	8.20E+04	7.16E+04	5.07E+04	3.19E+04	19.2	21.1	15.3	18.7	15.3	12.4
Q91ZT1	Flt4	Vascular endothelial growth factor receptor 3	153.32	9	9	9	8	9	9	9	9	9	8	9	9	2.59E+05	1.94E+05	1.73E+05	2.42E+05	2.31E+05	2.19E+05	9.1	9.1	9.5	8.1	9.1	9.5
G3V6E7	Fmod	Fibromodulin	43.13	11	11	9	9	9	8	11	11	9	9	9	8	1.21E+07	3.14E+06	2.92E+06	3.75E+06	2.27E+06	1.98E+06	37.8	37.8	29.3	33.8	29.3	26.3
F1LST1	Fn1	Fibronectin	262.75	117	140	113	119	123	111	1	2	1	2	2	1	1.44E+07	1.06E+07	1.40E+07	1.65E+07	1.54E+07	1.18E+07	68.7	71.2	67.7	69.2	69.3	67.2
A0A096P6L8	Fn1	Fibronectin	272.44	117	139	113	118	122	111	1	1	1	1	1	1	3.20E+03	2.62E+03	1.25E+03	2.96E+03	2.40E+03	1.67E+03	65.8	68.2	64.9	66.2	66.4	64.4
B2RYN1	Fn3krp	Fructosamine-3-kinase-related protein	34.17	2	2	1	1	1	1	2	2	1	1	1	1	2.03E+04	6.88E+04	1.60E+04	2.00E+04	1.59E+04	1.20E+04	7.4	7.4	4.9	2.6	2.6	4.9
A0A0G2KAM4	Fscn1	Fascin	53.88	2	3	2	3	3	1	2	3	2	3	3	1	5.78E+04	4.29E+04	4.63E+03	4.77E+04	4.14E+04	3.09E+03	4.7	7.1	4.7	7.1	7.1	2.6
A0A0G2K296	Fsip2	Fibrous sheath-interacting protein 2	570.68	1	1	1	1	1	1	1	1	1	1	1	1	1.92E+03	6.01E+03	3.39E+03	8.14E+02	6.59E+03	2.98E+03	0.5	0.5	0.5	0.5	0.5	0.5

Uniprot accession number	Gene symbol	Protein name	Mol. weight [kDa]	No. Peptides Control wk1	No. Peptides Control wk8	No. Peptides Control wk14	No. Peptides Heat wk1	No. Peptides Heat wk8	No. Peptides Heat wk14	No. Unique peptides Control wk1	No. Unique peptides Control wk8	No. Unique peptides Control wk14	No. Unique peptides Heat wk1	No. Unique peptides Heat wk8	No. Unique peptides Heat wk14	iBAQ Control wk1	iBAQ Control wk8	iBAQ Control wk14	iBAQ Heat wk1	iBAQ Heat wk8	iBAQ Heat wk14	Sequence coverage Control wk1 [%]	Sequence coverage Control wk8 [%]	Sequence coverage Control wk14 [%]	Sequence coverage Heat wk1 [%]	Sequence coverage Heat wk8 [%]	Sequence coverage Heat wk14 [%]
F8WG88;Q62632	Fstl1	Follistatin-related protein 1	60.67	7	7	7	8	8	7	7	7	7	8	8	7	4.60E+05	2.65E+05	2.59E+05	3.20E+05	2.48E+05	2.44E+05	17.6	17.6	17.6	21.3	21.3	17.6
Q99PW7	Fstl3	Follistatin-related protein 3	27.11	2	2	3	2	4	4	2	2	3	2	4	4	4.18E+04	3.71E+04	7.81E+04	5.00E+04	8.26E+04	7.00E+04	16.8	16.8	20.3	16.8	23.4	23.4
Q66HI5	Fth1	Ferritin	21.10	8	9	5	6	9	5	8	9	5	6	9	5	1.30E+06	1.17E+06	3.10E+05	6.67E+05	9.69E+05	2.27E+05	59.9	72.5	45.1	40.1	72.5	45.1
P02793	Ftl1	Ferritin light chain 1	20.75	6	8	4	5	5	4	6	8	4	5	5	4	2.01E+06	2.35E+06	1.27E+05	4.79E+05	1.61E+06	8.67E+04	53	57.4	35.5	44.3	44.3	35.5
A0A140TAJ3	Fubp1	Far upstream element-binding protein 1	67.53	6	8	6	6	6	5	5	7	6	5	5	5	4.76E+04	7.95E+04	4.07E+04	4.50E+04	3.98E+04	1.45E+04	9.8	11.2	9.2	9.8	10	10.4
A0A0G2JSJ8	Fuca1	Tissue alpha-L-fucosidase	53.47	6	6	3	5	7	3	6	6	3	5	7	3	2.83E+05	2.63E+05	2.12E+05	1.73E+05	1.42E+05	8.01E+04	21.6	21.6	11.9	16.7	24	10.2
Q5PQK2	Fus	FUS RNA-binding protein	52.67	3	2	0	2	2	1	3	2	0	2	2	1	4.68E+04	9.40E+04	0.00E+00	1.37E+04	7.64E+04	1.56E+03	14.5	7.3	0	7.3	7.3	4.6
D3ZYS7	G3bp1	G3BP stress granule assembly factor 1	51.79	1	1	2	1	1	1	1	1	2	1	1	1	2.53E+04	3.37E+04	3.26E+04	9.38E+03	9.37E+03	1.16E+04	3.2	3.2	6	3.2	3.2	3.2
P05370	G6pdx	Glucose-6-phosphate 1-dehydrogenase	59.38	15	17	12	18	16	11	15	17	12	18	16	11	4.81E+05	7.74E+05	1.89E+05	4.38E+05	2.41E+05	1.03E+05	33.8	38.1	28	40	35	24.3
M0R544	Gaa	Lysosomal alpha-glucosidase	106.20	3	2	3	3	3	2	3	2	3	3	3	2	1.54E+04	1.30E+04	1.89E+04	1.72E+04	1.49E+04	7.43E+03	4.3	2.9	4.3	4.3	4.3	2.4
Q0VGK0	Gabarapl1	Gamma-aminobutyric acid receptor-associated protein-like 1	14.04	1	1	1	1	1	1	1	1	1	1	1	1	5.27E+04	7.99E+04	3.48E+04	2.81E+04	2.92E+04	1.75E+04	14.5	14.5	14.5	14.5	14.5	14.5
Q5RKH2	Galk1	Galactokinase 1	42.38	7	8	6	6	6	4	7	8	6	6	6	4	2.08E+05	3.19E+05	1.46E+05	2.06E+05	1.08E+05	4.65E+04	23	23.2	19.9	23	23	16.3
A0A0G2JTQ5	Galk2	N-acetylgalactosamine kinase	49.07	1	3	1	1	1	0	1	3	1	1	1	0	2.75E+04	4.67E+04	4.76E+03	2.07E+04	1.68E+04	0.00E+00	3.4	7.4	3.4	3.4	3.4	0
G3V960	Gamt	Guanidinoacetate N-methyltransferase	26.38	7	7	5	6	5	4	7	7	5	6	5	4	4.73E+05	6.24E+05	2.52E+05	2.28E+05	1.56E+05	1.13E+05	60.6	60.6	46.6	53.8	47.5	38.1
D3ZAN3	Ganab	Alpha glucosidase 2 alpha neutral subunit	90.57	5	4	4	3	4	3	5	4	4	3	4	3	1.17E+05	6.83E+04	3.67E+04	7.10E+04	7.19E+04	3.87E+04	10.4	7.7	7.7	6.1	7.7	6.1
P04797	Gapdh	Glyceraldehyde-3-phosphate dehydrogenase	35.83	18	22	18	17	18	19	15	17	14	14	15	15	1.50E+07	3.52E+07	1.08E+07	1.36E+07	9.85E+06	6.93E+06	66.4	68.8	67.9	65.5	66.4	68.8
B1WBQ8	Gapdhs	Glyceraldehyde-3-phosphate dehydrogenase	46.72	5	7	5	5	5	5	3	3	2	3	3	2	1.34E+05	1.83E+05	6.70E+04	1.30E+05	5.24E+04	1.73E+04	13.2	15	12.5	13.2	13.2	12.5
G3V7G8	Gars	Glycine--tRNA ligase	81.79	8	8	6	5	6	3	8	8	6	5	6	3	8.10E+04	9.25E+04	3.90E+04	4.58E+04	2.94E+04	7.26E+03	16.6	18.8	14	12.9	13.3	5.4
G3V918	Gart	Trifunctional purine biosynthetic protein adenosine-3	107.58	9	11	5	9	8	4	9	11	5	9	8	4	1.78E+05	2.05E+05	1.72E+05	1.69E+05	1.43E+05	1.73E+05	15.9	18.4	7.5	14.8	13	5.9
M0RBH9	Gas1	Growth arrest-specific 1	40.22	3	3	3	4	3	2	3	3	3	4	3	2	5.70E+04	4.98E+04	4.45E+04	3.41E+04	2.15E+04	2.44E+04	18.3	18.3	18.3	22.7	18.3	12.8
A0A0G2JTB2	Gbe1	Glucan (1,4-alpha-), branching enzyme 1	75.71	2	2	2	2	1	1	2	2	2	2	1	1	1.84E+04	1.86E+04	9.01E+03	1.61E+04	1.42E+04	6.60E+03	6.3	6.3	6.3	6.3	2.3	2.3
Q5PQW8	Gbp2	Interferon-induced guanylate-binding protein 2	67.36	10	10	9	8	10	6	10	10	9	8	10	6	2.32E+05	4.10E+05	1.78E+05	1.32E+05	1.66E+05	1.24E+05	17.3	17.3	15.4	14	17.3	10.8
D3ZV82	Gbp7	Guanylate binding protein 7	71.35	5	4	5	2	2	5	5	4	5	2	2	5	3.23E+04	5.06E+04	3.03E+05	1.34E+04	8.07E+03	2.90E+04	14.5	11.2	13.3	4.3	4.3	12.1
Q68FY4	Gc	Vitamin D-binding protein	53.52	54	57	52	52	53	50	54	57	52	52	53	50	8.43E+07	9.03E+07	5.19E+07	5.88E+07	4.39E+07	4.08E+07	82.8	87	86.6	82.8	86.3	86.3
P19468	Gclc	Glutamate--cysteine ligase catalytic subunit	72.62	7	8	3	6	5	3	7	8	3	6	5	3	1.70E+05	3.29E+05	4.89E+04	1.27E+05	6.95E+04	2.06E+04	17.1	20.4	9.7	13.7	12.1	8.9
P48508	Gclm	Glutamate--cysteine ligase regulatory subunit	30.55	4	4	3	4	2	1	4	4	3	4	2	1	1.43E+05	1.79E+05	7.19E+04	8.53E+04	3.72E+04	2.04E+04	20.8	20.8	15	20.8	10.2	4.7
F1LRI5	Gcn1l1	GCN1 eIF2 alpha kinase activator-like 1	293.07	3	3	3	3	3	2	3	3	3	3	3	2	5.61E+04	5.48E+04	9.78E+02	5.82E+04	3.30E+04	3.43E+02	1.6	1.5	1.6	1.5	1.5	1.2
Q9JKB7	Gda	Guanine deaminase	50.90	21	20	21	22	19	19	21	20	21	22	19	19	1.79E+06	1.75E+06	1.18E+06	1.26E+06	8.19E+05	7.91E+05	55.3	53.5	53.3	55.3	49.8	51.5
P50398	Gdi1	Rab GDP dissociation inhibitor alpha	50.54	20	21	20	19	20	19	14	15	14	13	14	13	8.53E+05	1.12E+06	6.02E+05	5.46E+05	4.72E+05	3.58E+05	54.4	58.8	53.2	56.6	56.6	51.2
P50399	Gdi2	Rab GDP dissociation inhibitor beta	50.54	18	20	17	17	15	15	12	14	11	11	9	9	3.87E+05	3.92E+05	4.27E+05	1.83E+05	1.65E+05	2.61E+05	59.3	59.6	56.9	51.5	51.5	47.9
A0A0G2KB56	Gfpt1	Glutamine--fructose-6-phosphate aminotransferase [isomerizing] 1	78.92	1	1	0	1	1	0	1	1	0	1	1	0	6.22E+02	4.07E+03	0.00E+00	1.86E+03	9.92E+02	0.00E+00	2	2	0	2	2	0
A0A0G2K423	Ghr	Growth hormone receptor	27.07	7	7	8	7	8	9	7	7	8	7	8	9	3.44E+05	4.26E+05	6.93E+05	3.75E+05	4.74E+05	7.41E+05	44.6	44.6	45.5	44.6	45.5	50.2
A0A0G2K527	Git1	ARF GTPase-activating protein GIT1	83.37	2	3	2	2	2	2	2	3	2	2	2	2	1.89E+04	3.04E+04	1.07E+04	1.63E+04	9.56E+03	1.49E+04	2.9	4.8	2.9	2.9	2.9	2.9
F1LQ73	Glb1l3	Beta-galactosidase	73.93	5	5	2	5	6	3	5	5	2	5	6	3	8.37E+04	9.93E+04	5.12E+04	1.21E+05	1.17E+05	2.61E+04	12	12	5.7	12	13.2	7.3
F1M5V2	Glipr2	GLI pathogenesis-related 2	18.99	6	6	6	4	4	5	6	6	6	4	4	5	2.60E+05	3.28E+05	2.08E+05	1.35E+05	8.28E+04	1.12E+05	45.3	45.3	45.3	37.6	24.7	37.6
Q6P7Q4	Glo1	Lactoylglutathione lyase	20.82	1	1	1	1	1	1	1	1	1	1	1	1	3.41E+04	2.04E+04	5.93E+04	1.87E+04	2.14E+04	5.00E+04	5.4	5.4	5.4	5.4	5.4	5.4
Q9JLZ1	Glrx3	Glutaredoxin-3	37.85	7	6	6	8	6	5	7	6	6	8	6	5	2.42E+05	3.46E+05	1.94E+05	2.04E+05	8.21E+04	4.04E+04	32	27.9	28.5	35.6	27.9	24
P10860	Glud1	Glutamate dehydrogenase 1, mitochondrial	61.42	3	2	2	1	2	3	3	2	2	1	2	3	3.40E+04	6.68E+03	8.91E+03	5.47E+04	3.18E+03	8.58E+03	8.2	6.5	5.2	3.6	4.7	7
P09606	Glul	Glutamine synthetase	42.27	19	23	15	19	17	14	19	23	15	19	17	14	9.99E+06	1.54E+07	3.65E+06	8.79E+06	6.72E+06	1.62E+06	70.2	74.3	67.6	71.3	68.9	65.1
G3V9L4	Glycam1	Glycosylation-dependent cell adhesion molecule 1	15.38	1	1	1	1	1	1	1	1	1	1	1	1	3.59E+05	2.76E+05	2.16E+05	3.90E+05	2.01E+05	2.01E+05	6.8	6.8	6.8	6.8	6.8	6.8
Q0VGK3	Glyctk	Glycerate kinase	55.19	0	1	0	1	0	0	0	1	0	1	0	0	0.00E+00	4.12E+03	0.00E+00	2.21E+03	0.00E+00	0.00E+00	0	2.1	0	2.1	0	0
Q6IN37	Gm2a	GM2 ganglioside activator	21.49	6	5	6	4	5	5	6	5	6	4	5	5	1.51E+06	9.29E+05	1.09E+06	8.37E+05	1.07E+06	7.34E+05	36.7	32.7	36.7	31.7	32.7	36.7
Q3MHS7	Gmds	GDP-mannose 4, 6-dehydratase	42.09	1	2	2	1	1	1	1	2	2	1	1	1	5.35E+03	1.62E+04	1.29E+04	1.25E+04	4.12E+03	6.92E+03	3.2	7	7	3.2	3.2	3.2
Q63228	Gmfb	Glia maturation factor beta	16.74	4	5	4	5	5	4	4	5	4	5	5	4	4.26E+05	7.06E+05	2.74E+05	2.29E+05	1.53E+05	9.64E+04	35.9	35.9	32.4	35.9	35.9	32.4
A0A0G2K824	Gmppa	Mannose-1-phosphate guanyltransferase alpha	46.65	2	2	0	2	1	0	2	2	0	2	1	0	4.29E+04	1.71E+04	0.00E+00	5.09E+03	2.80E+03	0.00E+00	7.8	7.8	0	7.8	3.5	0
F1LRV6	Gmpr	GMP reductase	37.46	2	2	1	2	1	0	2	2	1	2	1	0	3.60E+04	4.50E+04	1.05E+03	1.71E+04	2.36E+03	0.00E+00	7.8	7.8	2.9	7.8	2.9	0
Q4V7C6	Gmps	GMP synthase [glutamine-hydrolyzing]	76.76	7	8	5	6	6	6	7	8	5	6	6	6	8.15E+04	1.49E+05	6.38E+04	4.86E+04	3.48E+04	2.19E+04	16.7	19.9	12.6	13.6	15.2	15.2
P04897	Gnai2	Guanine nucleotide-binding protein G(i) subunit alpha-2	40.50	4	4	3	4	4	2	4	4	3	4	4	2	6.47E+04	9.17E+04	3.45E+04	4.22E+04	2.29E+04	2.44E+04	14.4	14.4	9.6	14.4	14.4	5.6
P54311	Gnb1	Guanine nucleotide-binding protein G(I)/G(S)/G(T) subunit beta-1	37.38	1	3	1	2	2	2	1	3	1	2	2	2	4.39E+04	1.02E+05	3.52E+04	4.96E+04	4.38E+04	3.59E+04	3.8	11.5	3.8	7.9	7.9	7.9
P54313	Gnb2	Guanine nucleotide-binding protein G(I)/G(S)/G(T) subunit beta-2	37.33	4	4	2	2	2	3	4	4	2	2	2	3	1.68E+05	1.25E+05	3.97E+04	7.86E+04	4.72E+04	4.85E+04	17.1	17.1	9.1	7.9	7.9	13.2
M0RCH5	Gnpda1	Glucosamine-6-phosphate isomerase	27.99	2	2	2	2	2	2	2	2	2	2	2	2	6.22E+04	5.67E+04	4.61E+04	6.65E+04	8.83E+04	2.56E+04	16.4	16.4	9.6	16.4	9.6	9.6
B0BNH1	Gnptg	N-acetylglucosamine-1-phosphotransferase subunit gamma	34.13	4	4	3	4	4	3	4	4	3	4	4	3	2.56E+05	1.90E+05	2.01E+05	2.65E+05	2.31E+05	2.16E+05	17.6	17.6	14.1	17.6	17.6	14.1
F6T071	Gorasp2	Golgi reassembly-stacking protein 2	39.93	3	4	1	3	3	2	3	4	1	3	3	2	5.64E+04	8.13E+04	2.85E+04	5.14E+04	1.06E+04	9.21E+03	11.4	16.8	4.1	11.4	11.4	7.3
P00507	Got2	Aspartate aminotransferase, mitochondrial	47.31	0	1	1	0	0	0	0	1	1	0	0	0	0.00E+00	4.50E+03	9.40E+03	0.00E+00	0.00E+00	0.00E+00	0	3.5	3.5	0	0	0
D3ZQU7	Gp1ba	Glycoprotein Ib platelet subunit alpha	78.27	3	3	3	3	3	3	3	3	3	3	3	3	5.62E+04	6.04E+04	1.14E+05	9.67E+04	4.84E+04	9.33E+04	5.2	5.2	5.2	5.2	5.2	5.2
O35077	Gpd1	Glycerol-3-phosphate dehydrogenase [NAD(+)], cytoplasmic	37.45	13	13	12	12	12	7	12	12	11	11	11	6	8.72E+05	8.66E+05	5.59E+05	5.45E+05	4.25E+05	2.30E+05	35.2	39	32.4	35.2	32.7	21.8
D3ZAP9	Gpd1l	Glycerol-3-phosphate dehydrogenase [NAD(+)]	38.07	5	5	5	5	4	5	4	4	4	4	3	4	1.75E+05	2.34E+05	1.18E+05	8.76E+04	6.90E+04	7.00E+04	16	16	20.8	16	13.4	20.8
G3V8B1	Gpld1	Phosphatidylinositol-glycan-specific phospholipase D	93.67	34	33	30	34	33	30	34	33	30	34	33	30	6.33E+06	5.04E+06	4.72E+06	6.26E+06	5.37E+06	4.37E+06	51.2	51.2	44.6	51.2	51.2	47.2
A0A0G2JZZ0	Gpr116	Probable G-protein coupled receptor 116	153.16	3	4	6	3	4	6	3	4	6	3	4	6	5.35E+04	4.18E+04	5.05E+04	3.27E+04	3.68E+04	5.68E+04	3	4	5.9	3	3.8	5.9
A0A0G2JT06	Gps1	COP9 signalosome complex subunit 1	58.88	6	8	4	7	8	2	6	8	4	7	8	2	1.24E+05	1.86E+05	9.99E+04	1.10E+05	7.44E+04	1.85E+04	16.5	20.2	11	16.9	18.8	5.7
M0RAM5	Gpx1	Glutathione peroxidase 1	22.16	7	8	6	8	6	5	7	8	6	8	6	5	3.49E+05	1.11E+06	2.17E+05	5.27E+05	6.23E+04	1.60E+05	52.5	60.5	41	51.5	45.5	34
A0A0G2K531	Gpx3	Glutathione peroxidase 3	25.27	6	7	6	6	7	6	6	7	6	6	7	6	6.88E+06	6.48E+06	8.85E+06	1.03E+07	1.43E+07	7.67E+06	32.4	32.4	32.4	32.4	32.4	32.4
A0A0G2K398	Gpx4	Phospholipid hydroperoxide glutathione peroxidase	22.07	1	4	4	3	1	4	1	4	4	3	1	4	0.00E+00	1.52E+05	1.51E+05	6.92E+04	8.98E+03	9.73E+04	4.6	23	23	17.3	5.6	23
G3V8V1	Grn	Granulins	65.16	10	10	7	10	10	7	10	10	7	10	10	7	1.02E+06	8.03E+05	8.06E+05	8.04E+05	6.39E+05	6.15E+05	29.4	29.4	21.9	29.4	29.4	21.9
A0A096MJ11	Gsdmd	Gasdermin D	53.21	3	5	5	4	2	5	3	5	5	4	2	5	1.20E+05	2.14E+05	5.47E+04	7.51E+04	3.38E+04	5.75E+04	8.6	14.1	13.7	12.3	5.9	14.5
A0A0G2K7W7	Gsk3a	Glycogen synthase kinase-3 alpha	50.80	2	2	1	2	1	1	2	2	1	2	1	1	1.47E+04	2.20E+04	1.40E+03	6.59E+03	4.50E+03	3.00E+03	9.6	9.6	2.9	9.6	2.9	2.9
A0A0G2JSH4	Gsk3b	Glycogen synthase kinase-3 beta	46.71	2	2	1	2	2	1	2	2	1	2	2	1	1.81E+04	2.41E+04	7.54E+03	1.02E+04	5.33E+03	4.06E+03	7.9	7.9	5.7	7.9	7.9	5.7
Q68FP1	Gsn	Gelsolin	86.07	43	51	37	44	42	40	43	51	37	44	42	40	3.36E+07	3.19E+07	2.34E+07	3.52E+07	2.98E+07	2.35E+07	70.6	77.2	68.7	72.7	71.8	71.8
Q6AYD5	Gspt1	Eukaryotic peptide chain release factor GTP-binding subunit ERF3B-like	68.75	5	4	5	5	3	5	5	4	5	5	3	5	4.61E+05	2.76E+05	1.03E+05	3.76E+05	2.24E+05	7.95E+04	12.4	9.7	11.2	12.4	5.8	11.2
P46413	Gss	Glutathione synthetase	52.34	7	8	5	7	4	3	7	8	5	7	4	3	1.17E+05	2.04E+05	3.74E+04	9.63E+04	3.01E+04	1.47E+04	23	23	18.6	23	14.6	8.6
P00502	Gsta1	Glutathione S-transferase alpha-1	25.61	10	11	8	10	8	10	7	8	5	7	5	7	7.84E+05	1.45E+06	4.56E+05	8.82E+05	2.47E+05	2.63E+05	52.7	61.7	34.7	52.7	35.6	52.7
P04904	Gsta3	Glutathione S-transferase alpha-3	25.32	15	21	17	18	16	16	11	17	13	14	12	12	2.48E+07	5.27E+07	2.11E+07	2.65E+07	1.94E+07	1.33E+07	71.9	81	74.2	78.3	76.9	72.9
P14942	Gsta4	Glutathione S-transferase alpha-4	25.51	5	5	4	5	4	5	4	4	3	4	3	4	1.89E+05	2.25E+05	6.26E+04	1.49E+05	8.53E+04	6.60E+04	25.2	25.2	21.2	25.2	21.2	24.3
Q6AXY0	Gsta6	Glutathione S-transferase A6	25.81	6	7	6	5	6	6	4	5	4	3	4	4	4.06E+05	7.90E+05	2.85E+05	3.07E+05	3.73E+05	1.31E+05	26.6	29.7	26.6	22.5	26.6	26.6
P04905	Gstm1	Glutathione S-transferase Mu 1	25.91	17	21	20	18	18	17	12	16	14	13	12	11	3.82E+06	1.15E+07	2.64E+06	3.74E+06	2.39E+06	1.19E+06	65.6	71.1	71.6	66.5	64.2	65.6
P08010	Gstm2	Glutathione S-transferase Mu 2	25.70	23	24	21	23	23	22	9	10	7	9	9	8	1.05E+07	2.05E+07	9.54E+06	8.41E+06	6.96E+06	5.72E+06	74.8	78.4	74.3	74.8	78.4	74.3
P08009	Gstm3	Glutathione S-transferase Yb-3	25.68	15	15	16	14	16	16	3	3	3	3	3	3	5.99E+04	1.18E+05	8.04E+04	7.60E+04	6.39E+04	2.87E+04	60.1	60.1	63.8	52.8	63.8	63.8
Q9Z1B2	Gstm5	Glutathione S-transferase Mu 5	26.63	13	15	14	12	12	12	12	14	13	11	11	11	3.24E+06	5.86E+06	2.83E+06	3.05E+06	2.13E+06	8.46E+05	68.9	70.2	66.7	61.8	55.6	61.8
B0BN47	Gstm6	Glutathione S-transferase Mu 6	25.63	11	11	11	11	12	10	7	7	6	7	7	6	5.67E+05	6.00E+05	7.17E+05	3.98E+05	5.62E+05	1.86E+05	50.5	50.5	49.5	50.5	55.5	45.4
A0A0G2K4U2	Gstm7	Glutathione S-transferase, mu 7	25.66	17	17	17	16	17	17	0	0	0	0	0	0	2.66E+05	3.15E+05	2.60E+05	1.68E+05	1.78E+05	1.16E+05	60.1	60.1	63.8	52.8	63.8	63.8
Q6AXR6	Gsto1	Glutathione S-transferase omega-1	27.68	1	2	2	1	2	2	1	2	2	1	2	2	3.30E+04	8.04E+04	5.67E+04	2.24E+04	1.28E+04	3.48E+04	8.3	14.1	14.1	8.3	14.1	14.1
P04906	Gstp1	Glutathione S-transferase P	23.44	12	13	12	10	12	11	12	13	12	10	12	11	2.14E+06	3.67E+06	3.54E+06	9.24E+05	1.71E+06	2.18E+06	63.3	63.3	64.3	55.7	62.4	64.8
Q01579	Gstt1	Glutathione S-transferase theta-1	27.47	6	8	4	5	5	3	6	8	4	5	5	3	2.13E+05	3.19E+05	1.26E+05	8.44E+04	3.57E+04	5.41E+04	30	35.8	24.6	25	25	18.3
P30713	Gstt2	Glutathione S-transferase theta-2	27.44	8	8	7	8	8	7	6	6	6	6	6	6	4.02E+05	1.08E+06	5.05E+05	4.99E+05	5.10E+05	2.89E+05	35.2	35.2	34.8	35.2	35.2	34.8
D3Z8I7	Gstt3	Glutathione S-transferase, theta 3	23.38	9	9	7	9	8	7	7	7	6	7	6	6	2.43E+06	6.61E+06	2.79E+06	2.67E+06	2.13E+06	1.39E+06	34.8	34.8	33.3	34.8	33.8	33.3
A0A0G2K6H2	Gstz1	Maleylacetoacetate isomerase	23.86	4	7	4	6	4	3	4	7	4	6	4	3	2.30E+05	4.75E+05	4.41E+04	1.48E+05	7.47E+04	3.47E+04	30.2	57.2	37.2	51.2	32.1	26
F1LQQ8	Gusb	Beta-glucuronidase	74.79	10	6	2	9	5	3	10	6	2	9	5	3	2.40E+05	1.72E+04	8.71E+03	3.89E+04	2.51E+04	1.26E+04	27.9	17.1	5.1	23.9	11	10.2
D3ZK97	H3f3c	Histone H3	15.36	0	0	1	0	1	0	0	0	1	0	1	0	0.00E+00	0.00E+00	6.96E+04	0.00E+00	7.36E+04	0.00E+00	0	0	23.5	0	23.5	0
D4A7D7	H6pd	Hexose-6-phosphate dehydrogenase	89.84	3	2	3	3	2	2	3	2	3	3	2	2	3.65E+04	1.70E+04	4.53E+03	2.52E+04	2.10E+04	5.24E+03	5.1	3.1	3.9	5.1	3.1	2.4
Q6L711	Habp2	Hyaluronan-binding protein 2	62.09	18	20	17	20	18	16	18	20	17	20	18	16	3.28E+06	3.15E+06	2.75E+06	3.11E+06	3.15E+06	2.32E+06	50.7	51.8	50.4	51.8	50.7	49.3
A0A0G2K713	Hao2	Hydroxyacid oxidase 2	43.80	6	6	3	5	5	2	6	6	3	5	5	2	6.11E+04	1.09E+05	1.67E+04	7.09E+04	4.07E+04	9.60E+03	23.5	23.5	13.9	20.2	19.9	10.9
Q4QQV4	Hars	Dead end homolog 1	57.36	7	6	6	8	6	3	7	6	6	8	6	3	1.42E+05	9.19E+04	6.57E+04	7.15E+04	3.70E+04	3.15E+04	17.1	15	15.2	19.5	15	8.5
Q62669	Hba-a1	Globin a1	16.02	9	9	8	9	8	8	2	2	2	2	2	2	2.33E+06	2.89E+06	1.22E+06	3.16E+06	7.92E+05	3.28E+06	74.8	74.8	73.5	74.8	59.2	73.5
A0A0G2JSV6	Hba-a2	Globin c2	15.28	10	10	9	10	8	10	8	8	7	8	6	8	1.15E+08	1.34E+08	4.27E+07	1.29E+08	3.62E+07	6.92E+07	78.2	78.2	58.5	78.2	78.2	78.2

Uniprot accession number	Gene symbol	Protein name	Mol. weight [kDa]	No. Peptides Control wk1	No. Peptides Control wk8	No. Peptides Control wk14	No. Peptides Heat wk1	No. Peptides Heat wk8	No. Peptides Heat wk14	No. Unique peptides Control wk1	No. Unique peptides Control wk8	No. Unique peptides Control wk14	No. Unique peptides Heat wk1	No. Unique peptides Heat wk8	No. Unique peptides Heat wk14	iBAQ Control wk1	iBAQ Control wk8	iBAQ Control wk14	iBAQ Heat wk1	iBAQ Heat wk8	iBAQ Heat wk14	Sequence coverage Control wk1 [%]	Sequence coverage Control wk8 [%]	Sequence coverage Control wk14 [%]	Sequence coverage Heat wk1 [%]	Sequence coverage Heat wk8 [%]	Sequence coverage Heat wk14 [%]
Q63910	Hba-a3	Alpha globin	15.52	6	6	6	6	6	6	4	4	4	4	4	4	5.53E+05	8.68E+05	2.90E+05	5.39E+05	9.20E+04	7.32E+05	54.9	54.9	54.9	54.9	54.9	54.9
P02091	Hbb	Hemoglobin subunit beta-1	15.98	17	19	16	18	17	18	0	0	0	0	0	0	6.91E+07	8.47E+07	2.94E+07	8.34E+07	2.01E+07	5.21E+07	87.1	87.1	87.1	87.1	87.1	87.1
A0A0G2JSW3	Hbb	Globin a4	15.97	15	17	14	16	15	15	1	1	1	1	1	1	6.00E+04	4.67E+04	2.68E+04	1.06E+05	5.60E+04	5.32E+04	87.1	87.1	85.7	87.1	87.1	85.7
A0A0G2JTW9	Hbb-b1	Beta-globin	15.99	11	11	10	11	10	11	0	0	0	0	0	0	3.57E+06	4.26E+06	1.67E+06	4.76E+06	6.25E+05	4.20E+06	74.8	74.8	74.8	74.8	59.2	74.8
A0A0G2K2P6	Hbs1l	HBS1-like protein	74.80	1	2	2	1	1	1	1	2	2	1	1	1	4.97E+03	2.01E+04	4.46E+03	1.36E+03	1.54E+03	1.47E+03	2.7	5.6	5.6	2.7	2.7	2.7
A0A0G2QC41	Hdac6	Histone deacetylase	125.49	1	1	2	2	1	0	1	1	2	2	1	0	4.47E+03	5.59E+03	1.76E+03	7.50E+03	1.41E+03	0.00E+00	1	1	2.2	2.2	1	0
D3ZKT8	Hddc2	HD domain containing 2	22.99	2	3	2	2	3	2	2	3	2	2	3	2	7.58E+04	1.60E+05	7.55E+04	4.67E+04	4.62E+04	5.41E+04	18.1	23.6	12.1	18.1	23.6	12.1
D4A500	Hddc3	HD domain containing 3	20.25	1	1	1	1	1	1	1	1	1	1	1	1	1.96E+04	3.24E+04	6.68E+04	4.19E+04	4.13E+04	1.84E+04	7.8	7.8	7.8	7.8	7.8	7.8
F1LPC7	Hdgf	Hepatoma-derived growth factor	26.44	5	5	4	5	3	4	5	5	4	5	3	4	2.72E+05	2.83E+05	9.21E+04	2.22E+05	5.68E+04	6.22E+04	33.3	33.3	29.1	33.3	21.9	26.2
Q3KRF2	Hdlbp	Vigilin	141.69	7	7	6	6	6	5	7	7	6	6	6	5	2.85E+04	4.05E+04	2.52E+04	1.65E+04	1.61E+04	1.29E+04	8.4	8.4	7.3	7	7	6.5
D3ZHC4	Hebp2	Heme binding protein 2	22.95	3	3	2	3	2	0	3	3	2	3	2	0	2.85E+04	9.86E+04	1.17E+04	2.62E+04	2.22E+04	0.00E+00	19.7	19.7	12.3	19.7	13.8	0
F1M9J4	Heg1	Heart development protein with EGF-like domains 1	139.84	1	2	0	2	2	2	1	2	0	2	2	2	4.81E+03	5.78E+03	0.00E+00	6.53E+03	9.02E+03	1.02E+04	1.9	2.9	0	2.9	2.9	2.9
Q5PQN1	Herc4	Probable E3 ubiquitin-protein ligase HERC4	118.54	2	2	1	2	2	1	2	2	1	2	2	1	1.11E+04	1.04E+04	4.93E+03	7.12E+03	4.81E+03	1.65E+03	2.1	2.1	1.1	2.1	2.1	1.1
Q641X3	Hexa	Beta-hexosaminidase subunit alpha	60.54	2	3	1	2	2	2	2	3	1	2	2	2	4.81E+04	3.20E+04	3.24E+03	2.64E+04	1.65E+04	2.05E+04	8.9	11	5.7	8.9	8.9	8.9
F1LR87	Hexb	Beta-hexosaminidase subunit beta	61.50	2	1	2	2	0	1	2	1	2	2	0	1	4.83E+04	2.83E+04	3.50E+04	1.64E+04	0.00E+00	7.58E+03	4.8	1.9	4.8	4.8	0	3
Q5EBA7	Hgfac	HGF activator	70.74	18	20	17	19	19	21	18	20	17	19	19	21	2.01E+06	1.99E+06	2.85E+06	2.28E+06	2.84E+06	2.87E+06	44	48.7	37.8	44.6	44.6	51.1
A0A0G2K3R7	Hikeshi	Protein Hikeshi	20.58	1	1	1	1	1	0	1	1	1	1	1	0	5.67E+04	3.96E+04	1.49E+04	3.98E+04	1.93E+04	0.00E+00	6.8	6.8	6.8	6.8	6.8	0
P62959	Hint1	Histidine triad nucleotide-binding protein 1	13.78	6	7	7	6	4	6	6	7	7	6	4	6	2.31E+06	3.96E+06	2.44E+06	1.13E+06	8.02E+05	1.27E+06	71.4	72.2	72.2	66.7	46.8	71.4
A0A0G2K7W8	Hint3	Histidine triad nucleotide-binding protein 3	14.32	1	2	1	2	2	1	1	2	1	2	2	1	1.98E+04	2.93E+04	2.03E+04	4.00E+04	1.94E+04	9.93E+03	7.7	18.5	7.7	18.5	18.5	7.7
P62804	Hist1h4b	Histone H4	11.37	2	2	4	1	5	1	2	2	4	1	5	1	3.18E+04	4.86E+04	6.71E+05	7.25E+03	8.07E+05	6.56E+03	19.4	21.4	40.8	11.7	41.7	11.7
D4ACV3	Hist2h2ac	Histone H2A	13.65	1	2	1	1	2	1	1	2	1	1	2	1	3.05E+04	3.80E+04	1.24E+05	5.54E+03	5.13E+05	5.15E+03	15.1	22.2	15.1	15.1	22.2	15.1
D3Z708	Hist2h3c2	Histone H3	15.39	1	0	1	0	0	0	1	0	1	0	0	0	1.35E+05	0.00E+00	1.95E+04	0.00E+00	0.00E+00	0.00E+00	23.5	0	23.5	0	0	0
P05708;M0RAQ6	Hk1	Hexokinase-1	102.41	5	7	6	5	4	3	5	7	6	5	4	3	4.97E+04	7.48E+04	1.60E+04	2.50E+04	4.16E+04	3.25E+03	6.9	9.4	8.1	6.9	5.6	4.4
A0A0G2K1N3	Hmbs	Porphobilinogen deaminase	37.79	1	1	1	1	1	1	1	1	1	1	1	1	2.06E+04	3.04E+04	1.79E+04	3.08E+03	1.16E+04	5.27E+03	5.8	5.8	5.8	5.8	5.8	5.8
A0A096MJ40	Hmcn1	Hemicentin 1	551.99	4	1	1	3	2	1	4	1	1	3	2	1	7.89E+04	4.78E+02	7.56E+01	3.38E+04	3.05E+04	9.67E+03	1.2	0.2	0.2	1	0.8	0.4
D3ZCR3	Hmgb1	High mobility group protein B1 pseudogene	24.68	5	6	7	5	5	6	4	5	6	4	4	5	1.47E+06	5.92E+06	1.93E+06	2.14E+06	8.66E+05	7.96E+05	28.6	28.6	35.7	28.6	28.6	29.1
P17425	Hmgcs1	Hydroxymethylglutaryl-CoA synthase, cytoplasmic	57.43	8	8	7	7	6	6	7	7	7	6	5	6	9.64E+04	1.26E+05	4.35E+04	8.74E+04	4.77E+04	1.71E+04	22.9	22.9	20.8	17.3	15.6	18.8
Q68G44	Hmgcs2	Hydroxymethylglutaryl-CoA synthase, mitochondrial	56.89	13	13	5	12	11	5	12	12	5	11	10	5	4.31E+05	8.08E+05	1.71E+05	3.83E+05	2.03E+05	9.85E+04	38.6	38.6	15.9	35	31.7	15.9
M0R5F8	Hmgn5	High mobility group nucleosome-binding domain-containing protein 5	45.46	2	2	0	4	3	1	2	2	0	4	3	1	5.77E+04	6.89E+04	0.00E+00	6.98E+04	1.79E+04	3.20E+04	11.2	11.2	0	18.2	14.9	3.7
Q6P6G9	Hnrnpa1	Heterogeneous nuclear ribonucleoprotein A1	33.62	2	1	3	1	2	1	2	1	3	1	2	1	6.85E+04	3.18E+04	3.75E+04	2.66E+04	3.24E+04	7.88E+03	8.3	3.2	13.4	3.2	8.3	3.2
F1LNF1	Hnrnpa2b1	Heterogeneous nuclear ribonucleoproteins A2/B1	37.30	13	12	11	11	12	10	13	12	11	11	12	10	1.42E+06	2.05E+06	7.95E+05	7.48E+05	7.82E+05	2.80E+05	46.9	38.6	40.6	38.9	44	36.4
Q6URK4	Hnrnpa3	Heterogeneous nuclear ribonucleoprotein A3	39.65	12	13	10	12	13	9	12	13	10	12	13	9	1.11E+06	2.16E+06	6.93E+05	9.84E+05	8.93E+05	3.69E+05	34.3	36.1	35.6	34.3	36.1	28
Q9QX80	Hnrnpab	Heterogeneous nuclear ribonucleoprotein A/B	30.85	6	6	6	6	6	5	5	5	5	5	5	4	5.73E+05	5.86E+05	3.67E+05	3.27E+05	2.11E+05	1.61E+05	27.4	27.4	27.4	27.4	27.4	22.8
A0A0G2K7B3	Hnrnpc	Heterogeneous nuclear ribonucleoprotein C	33.06	2	4	3	3	4	1	2	4	3	3	4	1	1.79E+04	1.13E+05	3.75E+04	4.48E+04	4.15E+04	3.92E+03	8.3	16	12.3	12.3	16	4
Q9JI54	Hnrnpd	Heterogeneous nuclear ribonucleoprotein D0	38.22	8	9	7	8	7	5	7	8	6	7	6	4	5.54E+05	1.16E+06	5.11E+05	4.38E+05	3.09E+05	2.67E+05	22.9	23.2	18.4	22.9	21	18.1
A0A0G2KAZ7	Hnrnpdl	Heterogeneous nuclear ribonucleoprotein D-like	46.31	3	5	3	4	4	2	1	3	1	2	2	0	1.73E+04	6.73E+04	6.69E+03	1.88E+04	2.36E+04	0.00E+00	8.1	11.7	8.1	10	10	4.3
Q794E4	Hnrnpf	Heterogeneous nuclear ribonucleoprotein F	45.73	7	8	7	8	8	3	6	7	6	7	7	3	7.57E+05	9.19E+05	3.00E+05	6.17E+05	4.47E+05	9.12E+04	28.9	33.7	30.1	32	32	12
A0A0G2JTG7	Hnrnph1	Heterogeneous nuclear ribonucleoprotein H	49.20	6	7	5	5	6	4	5	6	4	4	5	4	1.76E+05	3.60E+05	2.25E+05	1.57E+05	2.89E+05	1.08E+05	19.4	19.8	16.9	16.9	19.4	13.1
Q5D059	Hnrnpk	Heterogeneous nuclear ribonucleoprotein K	51.03	11	13	9	15	13	10	11	13	9	15	13	10	7.80E+05	7.99E+05	3.83E+05	5.22E+05	4.40E+05	1.23E+05	40.5	42.9	31.7	44.6	42.9	36
F1LQ48	Hnrnpl	Heterogeneous nuclear ribonucleoprotein L	67.90	10	12	8	9	9	8	10	12	8	9	9	8	4.31E+05	7.07E+05	2.95E+05	2.79E+05	3.24E+05	1.01E+05	31.3	34.7	23.3	26.5	21.3	24.4
D4A3E1	Hnrnpll	Heterogeneous nuclear ribonucleoprotein L-like	64.36	1	2	1	2	1	0	1	2	1	2	1	0	2.82E+03	2.43E+04	7.71E+03	1.01E+04	2.28E+03	0.00E+00	3.4	6.3	2.9	6.3	3.4	0
F1LV13	Hnrnpm	Heterogeneous nuclear ribonucleoprotein M	73.72	6	7	4	4	6	3	6	7	4	4	6	3	3.69E+04	1.08E+05	3.12E+04	1.94E+04	5.86E+04	1.08E+04	13.3	15.5	10.1	9.6	13.2	6.8
Q6IMY8	Hnrnpu	Heterogeneous nuclear ribonucleoprotein U	87.73	8	10	10	8	9	8	8	10	10	8	9	8	1.61E+05	3.10E+05	1.50E+05	1.05E+05	1.51E+05	5.35E+04	16.3	22.2	22.8	15.7	17.5	15.9
D4ABT8	Hnrnpul2	Heterogeneous nuclear ribonucleoprotein U-like 2	84.86	3	4	1	5	3	1	3	4	1	5	3	1	1.09E+04	2.75E+04	1.00E+03	8.69E+03	8.26E+03	5.97E+02	6.7	8.5	1.9	9.8	6.6	3.1
A0A0H2UHM3	Hp	Haptoglobin	38.43	21	22	18	21	21	18	21	22	18	21	21	18	1.48E+07	1.17E+07	1.12E+07	1.79E+07	9.98E+06	1.63E+07	48	48	44.5	48	48	43.4
P27605	Hprt1	Hypoxanthine-guanine phosphoribosyltransferase	24.48	10	10	7	10	10	8	10	10	7	10	10	8	1.64E+06	2.24E+06	1.03E+06	1.23E+06	9.27E+05	4.97E+05	64.7	64.7	49.5	64.7	64.7	54.6
P20059	Hpx	Hemopexin	51.35	31	34	31	31	32	31	31	34	31	31	32	31	3.61E+07	2.41E+07	3.94E+07	2.76E+07	3.95E+07	3.77E+07	63.5	64.3	62.4	62.4	63.5	62.4
A0A0G2K9Y5	Hrg	Histidine-rich glycoprotein	57.93	29	31	28	29	30	27	29	31	28	29	30	27	6.41E+07	6.72E+07	7.38E+07	7.45E+07	8.02E+07	7.45E+07	54	55.5	55.7	54	55.5	52.2
P52759	Hrsp12	Ribonuclease UK114	14.30	2	2	0	2	2	1	2	2	0	2	2	1	1.58E+05	3.37E+05	0.00E+00	1.65E+05	8.59E+04	1.48E+04	14.6	14.6	0	14.6	14.6	7.3
Q8K3X8	Hspb1	Heat shock factor-binding protein 1	8.58	1	1	0	1	1	0	1	1	0	1	1	0	9.53E+04	1.71E+05	0.00E+00	5.60E+04	4.05E+04	0.00E+00	32.9	32.9	0	32.9	32.9	0
B0BMW2	Hsd17b10	3-hydroxyacyl-CoA dehydrogenase type-2	27.25	2	1	1	0	1	0	2	1	1	0	1	0	3.69E+04	1.09E+04	1.88E+04	0.00E+00	3.48E+03	0.00E+00	19.5	10	9.6	0	10	0
P82995	Hsp90aa1	Heat shock protein HSP 90-alpha	84.81	36	40	33	37	36	32	24	28	22	25	25	21	3.28E+06	5.16E+06	3.64E+06	3.66E+06	1.92E+06	1.33E+06	58.1	65.5	57.3	58.4	63.7	50.3
P34058	Hsp90ab1	Heat shock protein HSP 90-beta	83.28	36	36	30	36	34	31	22	22	17	22	21	18	2.28E+06	3.33E+06	1.84E+06	1.83E+06	1.39E+06	8.63E+05	64.6	59.8	50.1	61.5	61.2	52.6
A0A0A0MY09	Hsp90b1	Endoplasmin	92.90	23	21	19	21	21	20	21	19	17	19	19	18	7.94E+05	7.35E+05	4.40E+05	3.47E+05	2.80E+05	2.58E+05	35.4	33.2	30	31.8	32.5	28.9
P0DMW1	Hspa1b	Heat shock 70 kDa protein 1B	70.18	11	10	8	12	11	7	4	3	2	5	4	2	5.61E+04	5.36E+04	1.29E+04	1.63E+05	1.15E+05	1.48E+04	22.8	21.2	17.8	23.1	23.1	16.1
P55063	Hspa1l	Heat shock 70 kDa protein 1-like	70.55	12	14	12	13	11	9	5	7	6	6	4	4	1.16E+05	2.44E+05	1.89E+05	2.17E+05	1.28E+05	2.94E+04	26.5	28.9	25.4	26.7	24.6	20.1
P14659	Hspa2	Heat shock-related 70 kDa protein 2	69.64	25	30	23	27	23	20	15	20	15	17	13	11	1.19E+06	2.30E+06	1.67E+06	9.60E+05	6.23E+05	3.14E+05	52.6	54.5	49.4	49.1	45.7	42.3
F1LRV4	Hspa4	Heat shock 70 kDa protein 4	94.03	26	26	24	24	23	17	24	24	22	23	21	16	3.81E+05	5.05E+05	2.31E+05	2.97E+05	1.51E+05	1.15E+05	41.7	39.3	40.2	43.3	39.5	31
F7F2F3	Hspa4l	Heat shock 70 kDa protein 4L	114.31	26	32	29	26	18	17	24	30	27	25	16	16	4.22E+05	7.65E+05	5.46E+05	4.17E+05	1.34E+05	7.95E+04	32.8	38.1	35.7	34.4	24	23.5
P06761	Hspa5	78 kDa glucose-regulated protein	72.35	27	27	24	27	23	21	25	25	22	25	21	19	2.02E+06	1.97E+06	1.29E+06	1.14E+06	1.04E+06	9.51E+05	51.1	48.8	43.1	52.1	39.1	34.1
P63018	Hspa8	Heat shock cognate 71 kDa protein	70.87	29	32	24	28	29	26	18	21	15	17	18	16	3.90E+06	4.43E+06	2.40E+06	2.96E+06	2.28E+06	1.25E+06	62.4	65.6	54.6	59.3	60.8	56.3
F1M953	Hspa9	Stress-70 protein, mitochondrial	73.74	3	3	5	3	4	3	3	3	5	3	4	3	2.11E+04	1.11E+04	1.60E+04	5.17E+03	1.94E+04	1.47E+04	4	5.4	9.6	4	6	5.9
G3V913	Hspb1	Heat shock protein beta-1	22.81	6	7	6	7	5	6	6	7	6	7	5	6	6.93E+05	8.28E+05	4.26E+05	6.04E+05	3.35E+05	2.68E+05	60.2	68.4	63.6	68.4	55.3	63.6
Q6IMX7	Hspbp1	Hsp70-binding protein 1	39.19	0	1	0	0	0	0	0	1	0	0	0	0	0.00E+00	1.47E+04	0.00E+00	0.00E+00	0.00E+00	0.00E+00	0	4.5	0	0	0	0
P63039	Hspd1	60 kDa heat shock protein, mitochondrial	60.96	7	8	8	6	4	5	7	8	8	6	4	5	2.02E+05	3.95E+04	4.98E+04	3.99E+04	2.56E+04	2.99E+04	24.6	29	23.4	20.6	13.6	15.7
Q66HA8	Hsph1	Heat shock protein 105 kDa	96.42	6	5	5	4	4	3	5	4	4	3	3	3	3.42E+05	1.28E+05	9.41E+04	2.27E+05	1.09E+05	1.61E+04	11.1	9	9	7.1	7.1	6.1
Q9QZK5	Htra1	Serine protease HTRA1	51.33	3	3	3	3	2	1	3	3	3	3	2	1	5.97E+04	4.47E+04	3.54E+04	2.31E+04	2.62E+04	2.77E+04	8.1	8.1	8.1	8.1	6.2	1.9
F1M963	Hyal1	Hyaluronidase	50.70	6	6	6	6	6	7	6	6	6	6	6	7	6.99E+05	6.53E+05	7.23E+05	6.65E+05	6.86E+05	8.11E+05	25.8	25.8	25.8	25.8	18.3	27.2
F1LZ14	Hyi	Hydroxypyruvate isomerase	30.59	2	2	2	2	2	2	2	2	2	2	2	2	1.31E+05	1.35E+05	1.21E+05	8.69E+04	7.30E+04	4.31E+04	7.9	7.9	7.9	7.9	7.9	7.9
Q6P136	Hyou1	Hypoxia up-regulated protein 1	111.22	5	5	3	3	3	2	5	5	3	3	3	2	4.51E+04	3.06E+04	3.08E+04	1.81E+04	1.28E+04	7.80E+03	11.5	10.2	6.3	6	6.5	4.4
F1M8A5	Hypk	Huntingtin-interacting protein K	14.66	1	1	1	1	1	1	1	1	1	1	1	1	8.12E+04	2.35E+05	7.49E+04	8.81E+04	1.01E+05	5.75E+04	14	14	14	14	14	14
Q711G3	Iah1	Isoamyl acetate-hydrolyzing esterase 1 homolog	28.00	4	4	4	4	3	3	4	4	4	4	3	3	8.92E+04	2.29E+05	1.39E+05	6.17E+04	6.47E+04	4.76E+04	32.9	32.9	32.9	32.9	23.7	23.7
A0A0G2JVL8	Iars	Isoleucyl-tRNA synthetase	143.58	3	3	0	3	3	0	3	3	0	3	3	0	1.12E+04	5.35E+03	0.00E+00	1.06E+04	1.05E+04	0.00E+00	2.5	2.5	0	2.5	2.5	0
F1LVL2	Icoslg	Inducible T-cell co-stimulator ligand	34.85	5	5	5	5	5	5	5	5	5	5	5	5	1.20E+06	1.16E+06	1.49E+06	1.14E+06	1.44E+06	1.16E+06	20.2	20.2	20.2	20.2	20.2	20.2
A0A0G2K7Q7	Ide	Insulin-degrading enzyme	113.16	3	5	3	4	5	2	3	5	3	4	5	2	1.90E+04	2.22E+04	3.85E+03	1.15E+04	3.98E+04	1.77E+04	3.5	7.5	4.1	5.9	7.5	2.6
P41562	Idh1	Isocitrate dehydrogenase [NADP] cytoplasmic	46.73	11	13	7	11	11	6	10	12	6	10	10	5	5.97E+05	5.50E+05	1.31E+05	4.76E+05	5.20E+05	5.99E+04	28.3	30.4	20.3	28.3	28.3	17.4
P56574	Idh2	Isocitrate dehydrogenase [NADP], mitochondrial	50.97	4	3	2	3	3	1	3	2	1	2	2	0	4.77E+04	3.42E+04	3.40E+03	9.68E+03	1.67E+04	0.00E+00	10.4	8.4	4.9	8.4	8.4	2
F1MAC0	Ifit47	Interferon gamma-inducible protein 47	47.43	2	3	1	3	2	1	2	3	1	3	2	1	2.08E+04	4.55E+04	7.14E+03	9.69E+03	1.08E+04	4.85E+03	7.1	10	2.9	10	7.1	2.9
M0R8H7	Ifnar2	Interferon alpha and beta receptor subunit 2	57.92	0	0	1	0	0	1	0	0	1	0	0	1	0.00E+00	0.00E+00	7.10E+03	0.00E+00	0.00E+00	6.09E+03	0	0	4.5	0	0	4.5
F1LY69	Ift140	Intraflagellar transport 140	165.88	0	1	0	0	0	0	0	1	0	0	0	0	0.00E+00	1.58E+03	0.00E+00	0.00E+00	0.00E+00	0.00E+00	0	0.7	0	0	0	0
A0A0G2JX40	Igf1	Insulin-like growth factor I	16.08	4	4	4	4	4	4	4	4	4	4	4	4	7.20E+06	4.03E+06	5.51E+06	5.45E+06	5.03E+06	5.99E+06	29.4	29.4	29.4	29.4	29.4	29.4
F1LRE2	Igfals	Insulin-like growth factor-binding protein complex acid labile subunit	66.90	21	21	21	20	21	22	21	21	21	20	21	22	1.51E+07	1.30E+07	1.77E+07	1.64E+07	1.88E+07	1.55E+07	49.9	49.9	48.3	49.9	49.9	53.6
P12843	Igfbp2	Insulin-like growth factor-binding protein 2	32.85	7	7	7	7	7	7	7	7	7	7	7	7	8.92E+05	6.33E+05	9.52E+05	9.08E+05	1.30E+06	9.24E+05	35.9	35.9	35.9	35.9	35.9	35.9
P15473	Igfbp3	Insulin-like growth factor-binding protein 3	31.68	11	14	14	14	11	14	11	14	14	14	11	14	3.42E+06	3.14E+06	2.76E+06	3.83E+06	2.64E+06	2.06E+06	43.2	43.2	43.2	43.2	43.2	43.2
P21744	Igfbp4	Insulin-like growth factor-binding protein 4	27.75	3	3	4	3	3	4	3	3	4	3	3	4	1.03E+05	7.95E+04	3.14E+05	1.22E+05	1.81E+05	1.26E+05	16.9	16.9	22.8	16.9	16.9	22.8
A0A0G2JVW1	Igfbp5	Insulin-like growth factor-binding protein 5	30.31	6	6	4	5	5	4	6	6	4	5	5	4	1.10E+06	8.45E+05	3.23E+05	1.22E+06	5.94E+05	3.92E+05	31.4	31.4	15.9	24.7	22.5	15.9

Uniprot accession number	Gene symbol	Protein name	Mol. weight [kDa]	No. Peptides Control wk1	No. Peptides Control wk8	No. Peptides Control wk14	No. Peptides Heat wk1	No. Peptides Heat wk8	No. Peptides Heat wk14	No. Unique peptides Control wk1	No. Unique peptides Control wk8	No. Unique peptides Control wk14	No. Unique peptides Heat wk1	No. Unique peptides Heat wk8	No. Unique peptides Heat wk14	iBAQ Control wk1	iBAQ Control wk8	iBAQ Control wk14	iBAQ Heat wk1	iBAQ Heat wk8	iBAQ Heat wk14	Sequence coverage Control wk1 [%]	Sequence coverage Control wk8 [%]	Sequence coverage Control wk14 [%]	Sequence coverage Heat wk1 [%]	Sequence coverage Heat wk8 [%]	Sequence coverage Heat wk14 [%]
P35572	Igfbp6	Insulin-like growth factor-binding protein 6	24.19	6	6	5	6	5	5	6	6	5	6	5	5	7.89E+05	5.54E+05	4.67E+05	7.38E+05	5.09E+05	3.91E+05	38.5	38.5	35	38.5	35	35
F1M9B2	Igfbp7	Insulin-like growth factor-binding protein 7	28.95	4	5	5	4	4	5	4	5	5	4	4	5	3.75E+05	2.31E+05	3.02E+05	2.28E+05	2.04E+05	2.88E+05	20.6	25.3	25.3	20.6	20.6	25.3
P20760	Igg-2a	Ig gamma-2A chain C region	35.19	22	23	21	22	22	20	19	20	18	19	19	17	1.04E+08	1.19E+08	1.49E+08	1.13E+08	1.23E+08	1.47E+08	83.2	86.3	82	83.2	83.2	78.9
P20761	Igh-1a	Ig gamma-2B chain C region	36.50	12	15	12	13	14	12	12	15	12	13	14	12	5.90E+07	8.98E+07	8.19E+07	5.68E+07	8.38E+07	8.86E+07	72.4	76	72.4	73.3	74.8	72.4
Q925N6	Igsf1	Immunoglobulin superfamily member 1	147.29	5	5	4	5	6	4	5	5	4	5	6	4	2.87E+04	2.87E+04	3.47E+04	5.77E+04	7.15E+04	2.12E+04	5.5	5.5	4.5	5.5	6.4	4.5
F7F5P4	Il18bp	Interleukin 18 binding protein	21.32	1	1	1	1	1	1	1	1	1	1	1	1	1.26E+05	1.17E+05	9.63E+04	9.02E+04	9.34E+04	9.07E+04	6.7	6.7	6.7	6.7	6.7	6.7
F1M9B9	Il1rap	Interleukin-1 receptor accessory protein	65.57	2	3	4	2	2	4	2	3	4	2	2	4	7.70E+04	8.11E+04	4.97E+04	9.09E+04	1.20E+05	6.07E+04	4.2	6.1	7.4	4.2	4.2	7.4
G3V8T6	Il6r	Interleukin-6 receptor subunit alpha	49.28	1	1	1	1	1	1	1	1	1	1	1	1	2.57E+04	1.84E+04	2.31E+04	2.86E+04	2.38E+04	2.26E+04	2.6	2.6	2.6	2.6	2.6	2.6
Q99J82	Ilk	Integrin-linked protein kinase	51.37	5	7	4	4	6	2	5	7	4	4	6	2	9.43E+04	2.05E+05	6.74E+04	5.78E+04	5.77E+04	2.12E+04	14.8	21.2	10.6	11.7	18.1	5.3
F1M978	Impa1	Inositol monophosphatase 1	30.50	1	1	2	1	1	1	1	1	2	1	1	1	3.04E+04	2.27E+04	1.94E+04	1.10E+04	2.35E+04	4.52E+03	4	4	8.7	4	4	4
Q5GFD9	Impact	Protein IMPACT	36.00	2	2	1	2	0	0	2	2	1	2	0	0	1.86E+04	4.22E+04	2.41E+04	1.01E+04	0.00E+00	0.00E+00	11.7	11.7	7.6	7.6	0	0
D3ZLZ7	Impdh1	Inosine-5-monophosphate dehydrogenase 1	55.29	2	1	0	2	1	0	2	1	0	2	1	0	2.13E+04	1.37E+04	0.00E+00	8.07E+03	6.46E+03	0.00E+00	3.9	2.3	0	3.9	2.3	0
E9PU28	Impdh2	Inosine-5-monophosphate dehydrogenase 2	55.81	2	2	3	3	2	3	2	2	3	3	2	3	1.74E+04	3.47E+04	2.73E+04	2.42E+04	2.22E+04	1.27E+04	6.8	6.8	9.5	9.5	6.8	9.5
P17490	Inha	Inhibin alpha chain	39.50	3	3	2	3	3	3	3	3	2	3	3	3	1.50E+05	1.34E+05	8.27E+04	1.65E+05	1.26E+05	3.87E+04	12.8	12.8	8.7	12.8	12.8	12.8
A0A0G2K0C6	Inhbb	Inhibin beta B chain	44.77	1	1	1	1	1	1	1	1	1	1	1	1	3.40E+04	1.80E+04	4.02E+04	2.03E+04	2.53E+04	3.19E+04	3.7	3.7	3.7	3.7	3.7	3.7
Q5RJK6	Inpp1	Inositol polyphosphate-1-phosphatase	43.36	3	3	1	2	1	2	3	3	1	2	1	2	6.87E+04	8.90E+04	1.97E+04	2.10E+04	1.39E+04	1.84E+04	9.3	9.3	3	5.8	3	5.8
Q9WUK0	Insl3	Insulin-like 3	14.11	4	4	3	4	4	3	4	4	3	4	4	3	4.59E+06	3.70E+06	3.08E+06	6.60E+06	5.77E+06	2.43E+06	42.2	42.2	42.2	42.2	42.2	42.2
D4A2D7	Ipo4	Importin 4	118.93	7	7	5	7	8	5	7	7	5	7	8	5	5.79E+04	5.53E+04	1.81E+05	3.83E+04	3.39E+04	1.66E+05	9.3	8	6.7	9	9.3	6.7
D4A781	Ipo5	Importin 5	123.70	22	25	22	22	23	18	22	25	22	22	23	18	3.47E+05	4.12E+05	2.79E+05	2.93E+05	1.61E+05	6.88E+04	31.3	37.1	31.2	30.6	32	24.9
G3V7Q7	Iqgap1	IQ motif containing GTPase activating protein 1	188.83	19	23	16	16	20	16	18	22	15	15	19	15	1.48E+05	2.07E+05	1.25E+05	1.03E+05	1.15E+05	1.31E+05	17.5	21.7	15.6	15	18.5	14.8
F1LW74	Iqgap2	IQ motif containing GTPase activating protein 2	162.97	21	28	16	23	25	17	20	27	15	22	24	16	9.28E+04	2.22E+05	4.04E+04	9.08E+04	8.60E+04	2.25E+04	20.2	27.7	15.2	20.8	23.8	16.1
Q5XIB0	Irf3	Interferon regulatory factor 3	47.28	1	2	1	1	1	1	1	2	1	1	1	1	6.93E+03	2.64E+04	2.97E+03	2.86E+03	1.37E+03	1.47E+03	2.6	7.4	4.8	2.6	4.8	4.8
Q6AYF9	Irgc	Interferon-inducible GTPase 5	50.56	1	2	2	2	1	1	1	2	2	2	1	1	1.11E+03	2.84E+03	2.64E+04	8.58E+03	3.49E+03	6.59E+03	3	6.3	6.3	6.3	3	3
Q6AYK3	Isyna1	Inositol-3-phosphate synthase 1	60.88	17	18	19	18	16	13	17	18	19	18	16	13	1.27E+06	1.74E+06	6.68E+05	1.07E+06	8.24E+05	2.65E+05	40.8	40.9	42.4	42.4	40.8	29.8
A0A0G2JSK5	Itgb1	Integrin beta-1	88.34	3	2	2	4	3	1	3	2	2	4	3	1	8.07E+04	4.83E+04	7.29E+04	1.18E+05	1.01E+05	6.33E+04	5.5	3.9	4.1	8.1	5.5	2.5
Q5PQQ8	Itgbl1	Integrin beta-like protein 1	53.90	4	6	2	6	5	0	4	6	2	6	5	0	1.67E+05	8.77E+04	1.86E+04	1.14E+05	6.26E+04	0.00E+00	12.1	16.8	6.7	16.8	14.4	0
B2RYM3	Itih1	Inter-alpha trypsin inhibitor, heavy chain 1	100.59	47	51	48	49	47	47	47	51	48	49	47	47	2.95E+07	2.50E+07	3.44E+07	3.02E+07	2.76E+07	3.08E+07	58.8	60.7	60.3	60.4	59.8	60.2
D3ZFH5	Itih2	Inter-alpha trypsin inhibitor, heavy chain 2	92.37	32	32	30	32	32	28	26	27	25	26	26	23	2.84E+07	2.77E+07	3.09E+07	2.93E+07	2.92E+07	2.85E+07	56.5	56.5	55.9	56.5	56.5	52.3
D3ZBS2	Itih3	Inter-alpha-trypsin inhibitor heavy chain H3	99.07	44	51	42	46	47	44	40	47	38	42	43	40	5.44E+07	5.07E+07	4.52E+07	6.04E+07	4.70E+07	4.13E+07	58.3	60.9	58.7	60	59	59.3
Q5EBC0	Itih4	Inter alpha-trypsin inhibitor, heavy chain 4	103.75	65	70	63	66	66	64	1	1	1	1	1	1	6.35E+07	5.29E+07	6.91E+07	6.23E+07	5.71E+07	6.46E+07	75.1	75.9	75.9	75.9	75.1	75.9
D3ZFC6	Itih4	Inter-alpha-trypsin inhibitor heavy chain family, member 4	103.75	64	70	62	65	65	63	0	1	0	0	0	0	0.00E+00	5.75E+05	0.00E+00	0.00E+00	0.00E+00	0.00E+00	73.5	76.6	74.2	74.2	73.5	74.2
Q5XIE8	Itm2b	Integral membrane protein 2B	30.31	2	2	2	2	2	2	2	2	2	2	2	2	5.35E+04	4.06E+04	3.30E+04	5.20E+04	5.14E+04	3.65E+04	10.9	10.9	10.9	10.9	10.9	10.9
D3ZW55	Itpa	Inosine triphosphate pyrophosphatase	21.93	4	4	2	4	3	2	4	4	2	4	3	2	3.11E+05	2.07E+05	6.46E+04	1.34E+05	1.16E+05	4.63E+04	29.8	29.8	11.6	29.8	22.7	11.6
P12007	Ivd	Isovaleryl-CoA dehydrogenase, mitochondrial	46.44	1	1	0	0	0	0	1	1	0	0	0	0	0.00E+00	0.00E+00	0.00E+00	0.00E+00	0.00E+00	0.00E+00	2.1	2.1	0	0	0	0
G3V6G1	Jchain	Immunoglobulin joining chain	17.78	4	6	4	5	5	5	4	6	4	5	5	5	1.66E+06	5.19E+06	1.82E+06	1.88E+06	2.57E+06	1.58E+06	31.4	59.7	31.4	35.2	35.2	35.2
Q6P0K8	Jup	Junction plakoglobin	81.80	10	8	1	8	17	3	10	8	1	8	17	3	4.56E+04	1.30E+04	7.87E+02	2.23E+04	3.59E+05	2.98E+03	19.5	16.4	2	15.2	33	7.2
Q5XIM7	Kars	Lysine--tRNA ligase	71.62	3	3	3	3	1	2	3	3	3	3	1	2	2.72E+04	4.13E+04	2.19E+04	1.36E+04	3.05E+03	2.40E+03	8	8	8	8	1.9	3.4
D4A5J1	Kbtbd11	Kelch repeat and BTB domain-containing 11	67.85	10	11	5	8	8	5	10	11	5	8	8	5	1.08E+05	2.70E+05	4.73E+04	7.03E+04	1.02E+05	3.71E+04	28.3	30.3	12.5	25.1	24.2	12.5
M0R961	Khsrp	Far upstream element-binding protein 2	74.21	14	16	12	15	15	9	13	15	12	14	14	9	2.29E+05	4.25E+05	1.02E+05	2.07E+05	1.57E+05	4.00E+04	23.7	29.3	23.3	27.7	27.7	14.1
D3ZI07	Kif3b	Kinesin-like protein	85.26	2	2	2	2	1	1	2	2	2	2	1	1	4.93E+03	1.65E+04	3.37E+03	6.84E+03	2.22E+03	1.18E+03	3.6	3.6	3.6	3.6	1.7	1.9
Q2PQA9	Kif5b	Kinesin-1 heavy chain	109.53	6	10	6	9	9	6	6	10	6	9	9	6	5.54E+05	4.33E+05	1.56E+05	7.69E+05	4.47E+05	1.49E+05	8.7	13.8	8.9	12.6	13	8.6
A0A0G2JX00	Klk1c9	Kallikrein 1-related peptidase C9	32.21	4	4	2	2	2	0	4	4	2	2	2	0	1.48E+05	2.27E+05	9.24E+03	6.47E+04	6.40E+04	0.00E+00	22	22	9.3	12.4	12.4	0
Q5FVS2	Klkb1	Kallikrein B, plasma 1	71.28	29	31	29	30	29	29	29	31	29	30	29	29	9.56E+06	7.79E+06	9.64E+06	9.13E+06	8.41E+06	8.95E+06	58.2	59.7	58.2	62.4	58.2	58.2
A0A0G2JWF0	Kmt2e	Lysine methyltransferase 2E	176.90	2	2	1	2	2	2	2	2	1	2	2	2	1.71E+04	1.03E+06	5.41E+04	2.05E+06	6.19E+05	9.43E+05	0.9	0.9	0.7	0.9	0.9	0.9
P08934	Kng1	Kininogen-1	70.93	29	30	26	30	29	26	27	28	24	28	27	24	4.30E+07	4.41E+07	4.96E+07	4.63E+07	4.73E+07	4.63E+07	48.2	48.4	44	48.4	48.4	44
A0A0G2KA54	Kng1	Kininogen-1	70.44	26	26	24	26	27	24	2	2	1	2	2	1	2.01E+04	5.39E+04	3.23E+04	4.82E+04	3.45E+04	3.01E+04	41.7	41.7	40.5	41.7	41.7	40.5
P08932	Kng2	T-kininogen 2	47.70	27	27	26	27	28	26	0	0	0	0	0	0	1.75E+07	1.65E+07	2.85E+07	1.52E+07	1.69E+07	2.38E+07	63	63	62.3	63	63	62.3
Q6AXN6	Knstrn	Small kinetochore-associated protein	34.89	2	2	2	2	1	1	2	2	2	2	1	1	1.78E+04	7.87E+04	3.19E+04	3.39E+04	4.62E+03	2.04E+03	10.9	10.9	10.9	10.9	7.1	7.1
F2Z3Q8;P52296	Kpnb1	Importin subunit beta-1	97.18	9	7	7	7	8	6	9	7	7	7	8	6	2.66E+05	1.39E+05	8.12E+04	3.28E+05	2.99E+05	2.84E+04	15.4	12.7	12.7	12.7	13.7	11.6
G3V9A5	Kprp	Keratinocyte proline-rich protein	76.41	1	1	1	1	1	1	1	1	1	1	1	1	1.17E+04	8.63E+03	1.11E+04	1.34E+03	5.34E+03	5.79E+03	1.4	1.4	1.4	1.4	1.4	1.4
A0A0G2K2V6	Krt10	Keratin, type I cytoskeletal 10	56.81	12	11	11	11	11	9	1	1	1	1	1	0	1.25E+03	5.22E+03	0.00E+00	0.00E+00	0.00E+00	0.00E+00	22.4	22.4	18.2	18.2	18.2	14.5
Q63279	Krt19	Keratin, type I cytoskeletal 19	44.64	13	12	12	9	14	11	3	3	4	2	3	4	2.22E+05	7.09E+04	1.77E+05	2.02E+04	5.10E+04	1.06E+05	36.2	36.2	39	23.6	39.2	36.2
A0A0G2K7N1	Krt72	Keratin, type II cytoskeletal 72	60.44	1	1	1	2	3	1	1	1	1	1	1	1	1.04E+05	4.18E+05	6.49E+04	2.20E+05	7.20E+05	5.91E+04	3.1	3.1	3.1	4.7	6	3.1
Q10758	Krt8	Keratin, type II cytoskeletal 8	54.02	5	3	4	4	5	5	2	1	1	1	1	2	8.82E+04	4.14E+04	7.03E+04	2.37E+04	2.37E+04	5.66E+04	12.6	8.3	9.9	10.1	11.6	12.4
D3ZPW6	Lage3	L antigen family, member 3	15.67	2	2	2	2	1	2	2	2	2	2	1	2	1.77E+05	3.19E+05	1.19E+05	1.24E+05	8.56E+04	1.49E+05	28.4	28.4	28.4	28.4	14.2	28.4
F1M614	Lama2	Laminin subunit alpha 2	343.86	26	22	24	26	28	23	26	22	24	26	28	23	1.01E+05	5.47E+04	5.96E+04	8.80E+04	8.01E+04	4.53E+04	13.5	11.7	12.5	13.8	14.6	11.9
F1LTF8	Lama4	Laminin subunit alpha 4	196.95	4	3	4	4	3	3	4	3	4	4	3	3	1.15E+04	6.21E+03	6.39E+03	7.94E+03	7.75E+03	4.54E+03	2.8	2.1	2.8	2.8	2.1	1.9
F1MAN8	Lama5	Laminin subunit alpha 5	403.77	3	3	2	3	3	2	3	3	2	3	3	2	3.29E+03	4.51E+03	1.71E+03	5.82E+03	2.25E+03	2.57E+03	1.2	1.2	0.9	1.2	1.2	0.9
D3ZQN7	Lamb1	Laminin subunit beta-1	197.39	17	15	9	16	15	10	17	15	9	16	15	10	1.83E+05	1.03E+05	5.06E+04	1.22E+05	1.01E+05	4.70E+04	17.2	15.5	8.8	16.1	15.5	9.9
M0R6K0	Lamb2	Laminin subunit beta-2	196.53	6	8	5	7	8	5	6	8	5	7	8	5	3.56E+04	3.33E+04	4.50E+03	3.22E+04	3.14E+04	6.05E+03	5.9	7.6	4.6	6.6	7.6	4.7
F1MAA7	Lamc1	Laminin subunit gamma 1	177.38	16	16	13	17	15	9	16	16	13	17	15	9	1.50E+05	1.90E+05	1.32E+05	1.83E+05	1.61E+05	7.69E+04	13.5	13.5	10.1	14.1	12.6	8.2
A0A0G2K023	Lamc3	Laminin subunit gamma 3	172.53	13	12	10	12	14	9	13	12	10	12	14	9	5.10E+04	4.20E+04	2.29E+04	3.69E+04	5.38E+04	2.45E+04	14.2	12.2	10.9	12.8	14.8	7.8
Q9QX69	Lancl1	LanC-like protein 1	45.24	6	7	5	7	6	3	6	7	5	7	6	3	1.39E+05	3.10E+05	2.27E+05	1.25E+05	1.01E+05	7.12E+04	21.8	25.1	16	25.1	22.6	10.3
Q68FS4	Lap3	Cytosol aminopeptidase	56.15	10	10	7	6	8	8	10	10	7	6	8	8	2.07E+05	1.42E+05	1.76E+05	7.87E+04	9.94E+04	1.28E+05	32.2	28.1	23.5	17.3	24.9	24.3
Q5PPJ6	Lars	Leucyl-tRNA synthetase	134.28	2	4	2	1	3	2	2	4	2	1	3	2	9.37E+03	2.04E+04	6.52E+04	8.50E+03	1.28E+04	3.14E+04	3.3	5.6	2.8	1.2	3.5	2.8
Q99MZ8	Lasp1	LIM and SH3 domain protein 1	29.97	2	3	2	2	2	2	2	3	2	2	2	2	1.47E+05	2.34E+05	7.74E+04	8.81E+04	3.19E+04	5.83E+04	10.3	16	10.3	10.3	10.3	10.3
Q3MID7	Lbp	Lipopolysaccharide-binding protein	53.50	3	3	2	3	3	2	3	3	2	3	3	2	1.37E+05	1.29E+05	1.22E+05	1.25E+05	1.08E+05	1.22E+05	9.1	9.1	6.9	9.1	9.1	6.9
O35849	Lcat	Phosphatidylcholine-sterol acyltransferase	49.88	12	13	11	13	12	12	12	13	11	13	12	12	3.35E+06	2.80E+06	2.61E+06	3.14E+06	2.61E+06	2.17E+06	43.4	43.4	32.7	43.4	43.4	40.9
Q5XI38	Lcp1	Lymphocyte cytosolic protein 1	70.12	18	18	14	17	16	14	17	17	13	16	15	13	7.15E+05	4.91E+05	2.21E+05	4.20E+05	3.08E+05	2.72E+05	39.1	39.1	30.9	34.1	29.7	30.1
P04642	Ldha	L-lactate dehydrogenase A chain	36.45	8	8	8	10	8	5	7	7	7	9	7	4	2.88E+05	2.62E+05	1.49E+05	2.47E+05	2.29E+05	9.61E+04	31	31	38.6	44.6	31	24.4
P42123	Ldhb	L-lactate dehydrogenase B chain	36.61	11	12	9	11	11	8	10	11	8	10	10	7	9.43E+05	1.70E+06	7.00E+05	8.09E+05	7.99E+05	3.14E+05	40.7	45.5	33.5	40.7	40.7	32.6
Q6AYX2	Ldhc	L-lactate dehydrogenase	35.71	4	3	4	4	3	3	4	3	4	4	3	3	1.04E+05	1.48E+05	1.37E+05	8.45E+04	4.07E+04	1.83E+04	22.3	18.1	22.3	22.3	18.1	18.4
D4A526	Lect2	Leukocyte cell-derived chemotaxin 2	16.60	1	1	0	1	1	0	1	1	0	1	1	0	2.36E+04	3.04E+03	0.00E+00	4.80E+04	1.77E+04	0.00E+00	9.3	9.3	0	9.3	9.3	0
P11762	Lgals1	Galectin-1	14.86	11	10	11	11	9	11	11	10	11	11	9	11	1.79E+07	1.02E+07	7.42E+06	4.99E+06	2.84E+06	3.86E+06	86.7	86.7	86.7	86.7	80.7	86.7
A0A0G2JXB1	Lgals3	Galectin-3	26.34	4	5	5	5	5	5	4	5	5	5	5	5	5.34E+05	6.29E+05	1.09E+05	3.20E+05	1.87E+05	1.00E+05	15.1	19.4	19.4	19.4	19.4	19.4
O70513	Lgals3bp	Galectin-3-binding protein	63.74	11	10	10	9	12	11	11	10	10	9	12	11	6.03E+05	3.29E+05	4.47E+05	4.66E+05	1.34E+06	3.68E+05	24.6	21.4	21.8	20.9	26.3	24.6
Q5PPG2	Lgmn	Legumain	49.48	2	2	1	2	2	1	2	2	1	2	2	1	8.84E+04	6.75E+04	3.26E+04	3.96E+04	3.60E+04	3.91E+04	11.5	11.5	6	11.5	11.5	6
Q5I0D5	Lhpp	Phospholysine phosphohistidine inorganic pyrophosphate phosphatase	29.19	1	1	1	1	1	0	1	1	1	1	1	0	2.75E+04	4.67E+04	4.07E+03	2.58E+04	5.92E+03	0.00E+00	7.8	7.8	7.8	7.8	7.8	0
F1LR10	Lima1	LIM domain and actin-binding protein 1	83.80	2	2	1	2	2	2	2	2	1	2	2	2	1.07E+04	2.04E+04	4.89E+03	1.37E+03	5.62E+03	2.79E+03	4.9	4.9	3.3	4.9	4.9	4.9
Q4KM31	Limd2	LIM domain-containing protein 2	14.24	1	1	1	1	1	1	1	1	1	1	1	1	1.72E+04	1.75E+04	7.49E+03	7.56E+03	6.26E+03	2.02E+03	13.3	13.3	13.3	13.3	13.3	13.3
C0KUC5	Lims1	LIM and senescent cell antigen-like-containing domain protein	41.61	3	5	3	4	4	3	3	5	3	4	4	3	1.01E+05	1.86E+05	4.14E+04	5.96E+04	5.29E+04	3.69E+04	10.2	18	10.2	18	18	14.4
D4A0Q1	Lin28b	Lin-28 homolog B	26.93	1	1	1	1	1	1	1	1	1	1	1	1	1.56E+06	1.18E+06	1.72E+06	1.44E+06	1.57E+06	2.23E+06	4	4	4	4	4	4
G3V8R5	Lipe	Hormone-sensitive lipase	116.84	5	5	2	5	4	1	5	5	2	5	4	1	2.71E+04	2.75E+04	1.37E+03	1.12E+04	1.73E+04	1.92E+02	8.4	8.4	3.6	8.4	7	2.1
Q8VBX1	Lipg	Endothelial lipase	55.92	1	1	1	1	1	1	1	1	1	1	1	1	8.83E+03	1.90E+03	1.15E+04	1.64E+04	1.27E+04	8.40E+03	5.1	5.1	5.1	5.1	5.1	5.1
Q6AYF2	Lmcd1	LIM and cysteine-rich domains 1	41.09	2	2	4	1	0	4	2	2	4	1	0	4	6.49E+03	1.56E+04	3.13E+04	3.56E+02	0.00E+00	2.91E+04	11.8	7.9	18.4	6.6	0	18.4
G3V8L3	Lmna	Lamin A, isoform CRA_b	74.31	12	11	11	11	17	10	2	2	2	2	2	2	2.09E+05	1.82E+05	1.28E+05	9.44E+04	2.86E+05	6.30E+04	23.2	21.4	23.3	21.5	31.9	20.5
P48679	Lmna	Prelamin-A/C	74.32	10	9	9	9	17	8	0	0	0	0	2	0	0.00E+00	0.00E+00	0.00E+00	0.00E+00	2.40E+04	0.00E+00	19.4	17.6	19.5	17.7	30.2	16.7
G3V7U4	Lmnb1	Lamin-B1	66.69	1	2	2	1	2	2	1	2	2	1	1	2	1.70E+04	1.67E+04	2.59E+04	4.42E+03	6.24E+03	1.78E+04	2.4	4.4	4.4	2.4	3.7	4.4
F1LWD1	LOC100359978	Ucharacterized protein	14.16	4	3	3	3	3	3	3	2	2	2	2	2	1.50E+05	9.64E+04	1.04E+05	1.39E+05	2.87E+05	2.26E+05	39.7	28.6	28.6	28.6	28.6	28.6
D3ZIF6	LOC100360095	Urinary protein 1-like	10.65	3	3	3	3	3	3	3	3	3	3	3	3	2.83E+06	2.07E+06	2.80E+06	2.73E+06	2.06E+06	2.48E+06	58	58	58	58	58	58
F1M3H2	LOC100360367	Uncharacterized protein	11.19	1	1	2	1	1	2	0	0	1	0	0	1	0.00E+00	0.00E+00	8.32E+03	0.00E+00	0.00E+00	7.21E+04	9.1	9.1	20.2	9.1	9.1	20.2

Uniprot accession number	Gene symbol	Protein name	Mol. weight [kDa]	No. Peptides Control wk1	No. Peptides Control wk8	No. Peptides Control wk14	No. Peptides Heat wk1	No. Peptides Heat wk8	No. Peptides Heat wk14	No. Unique peptides Control wk1	No. Unique peptides Control wk8	No. Unique peptides Control wk14	No. Unique peptides Heat wk1	No. Unique peptides Heat wk8	No. Unique peptides Heat wk14	iBAQ Control wk1	iBAQ Control wk8	iBAQ Control wk14	iBAQ Heat wk1	iBAQ Heat wk8	iBAQ Heat wk14	Sequence coverage Control wk1 [%]	Sequence coverage Control wk8 [%]	Sequence coverage Control wk14 [%]	Sequence coverage Heat wk1 [%]	Sequence coverage Heat wk8 [%]	Sequence coverage Heat wk14 [%]
M0RDI9	LOC100360610	Uncharacterized protein	10.58	1	1	2	1	1	2	0	0	1	0	0	1	0.00E+00	0.00E+00	2.18E+05	0.00E+00	0.00E+00	1.95E+05	24.5	24.5	43.9	24.5	24.5	43.9
F1LTY5	LOC100361052	Uncharacterized protein	15.31	3	3	3	3	3	3	3	3	3	3	3	3	3.06E+06	4.10E+06	6.03E+06	2.43E+06	4.22E+06	5.97E+06	23.9	23.9	23.9	23.9	23.9	23.9
F1M0B7	LOC100361705	Uncharacterized protein	12.63	2	2	1	2	2	1	1	1	0	1	1	0	1.30E+05	3.16E+05	0.00E+00	1.08E+05	3.13E+05	0.00E+00	43.1	43.1	26.7	43.1	43.1	26.7
A0A0G2JYC4	LOC100361907	Complement factor H-related protein B	44.58	12	13	12	12	12	14	11	12	11	11	11	13	1.11E+06	1.02E+06	1.57E+06	1.61E+06	1.03E+06	1.33E+06	41.4	43.4	42.4	41.4	36.2	43.4
D3ZBB2	LOC100361952	Uncharacterized protein	13.15	4	3	4	4	4	3	3	2	3	3	3	2	2.72E+05	1.28E+05	4.78E+05	1.35E+06	2.98E+05	5.31E+05	30	30	30	30	30	30
D3ZWC1	LOC100362150	Uncharacterized protein	12.30	3	3	2	3	2	3	3	3	2	3	2	3	7.11E+05	5.62E+05	2.05E+05	2.01E+05	2.45E+05	2.85E+05	30.4	30.4	30.4	30.4	29.5	30.4
F1M5X4	LOC100362687	Uncharacterized protein	13.73	0	1	0	0	0	0	0	1	0	0	0	0	0.00E+00	1.53E+04	0.00E+00	0.00E+00	0.00E+00	0.00E+00	0	12.1	0	0	0	0
D4A5Y5	LOC100363779	Uncharacterized protein	13.02	1	1	2	1	1	2	1	1	1	1	1	1	4.47E+05	3.67E+05	9.10E+05	2.86E+05	2.74E+05	5.83E+05	12.7	12.7	30.5	12.7	12.7	30.5
G3V6H0	LOC100363782	RCG48149, isoform CRA_b	22.18	6	7	6	7	6	4	3	3	2	3	3	1	8.90E+05	1.19E+06	4.94E+05	6.46E+05	4.43E+05	2.29E+05	34.8	38.8	30.8	38.8	34.8	25.9
D3ZMY4	LOC100364733	Uncharacterized protein	12.78	2	2	2	2	2	2	1	1	1	1	1	1	9.14E+04	3.57E+04	3.26E+04	6.92E+04	1.65E+04	4.29E+04	26.5	26.5	26.5	26.5	26.5	26.5
O70177	LOC100365112	Carboxylic ester hydrolase	62.24	5	5	5	5	5	5	2	2	3	2	2	3	3.02E+04	1.05E+04	1.80E+05	5.12E+04	1.96E+04	8.84E+04	12.1	12.1	12.8	12.1	12.1	12.8
M0R3M3	LOC100910109	Uncharacterized protein	29.44	2	1	2	0	3	1	2	1	2	0	3	1	7.36E+03	3.48E+03	2.89E+04	0.00E+00	7.83E+04	1.20E+03	6.1	5.7	6.1	0	9.5	5.7
D3ZVI9	LOC100911365	Parkinson disease 7 domain containing 1	23.26	2	2	0	2	2	0	2	2	0	2	2	0	7.34E+04	9.13E+04	0.00E+00	4.42E+04	4.71E+04	0.00E+00	20	20	0	20	20	0
A0A0G2JWJ4	LOC100911515	Triosephosphate isomerase	29.06	13	12	10	13	12	9	2	1	1	2	2	0	2.38E+04	2.06E+04	1.91E+04	1.83E+04	4.19E+03	0.00E+00	65.8	62	50.2	65.8	60.8	46.4
M0R7P3	LOC100912026	Urinary protein 3-like	10.99	3	3	3	3	3	2	3	3	3	3	3	2	1.76E+06	8.06E+05	1.10E+06	1.39E+06	8.34E+05	8.70E+05	47	47	47	47	47	29
Q99MI5	LOC100912604	Spermidine synthase	34.00	4	4	4	3	3	3	4	4	4	3	3	3	1.36E+05	1.01E+05	8.91E+04	4.01E+04	3.13E+04	5.90E+04	19.9	24.5	21.2	16.6	16.6	13.2
D3ZFY8	LOC100912618	Ubiquitin-conjugating enzyme E2 V1	16.36	4	5	2	4	4	2	4	5	2	4	4	2	1.33E+05	1.46E+05	1.23E+05	7.04E+04	6.49E+04	3.81E+04	32	40.1	17.7	32	32	17.7
A0A0G2JW12	LOC100368996	Complement C4-like	192.25	112	120	108	111	115	110	0	0	0	0	0	0	3.97E+07	2.87E+07	3.13E+07	3.50E+07	3.85E+07	3.09E+07	70.3	70.9	68.6	69.5	70.8	69.1
Q1RP74	LOC100369005	RCG53953, isoform CRA_a	27.25	2	2	3	3	2	3	2	2	3	3	2	3	4.98E+04	5.86E+04	2.42E+04	3.79E+04	1.15E+04	1.58E+04	14.8	14.8	18.9	18.9	10.7	18.9
A0A0G2K926	LOC297568	Murinoglobulin-1	163.72	129	133	132	132	130	131	6	6	6	6	7	6	2.16E+08	1.86E+08	2.03E+08	2.15E+08	2.08E+08	2.11E+08	74.3	74.9	74.9	76.1	76	76
A0A096MIX6	LOC298111	Alpha2u globulin	19.82	3	3	3	3	3	3	2	2	2	2	2	2	5.01E+05	4.37E+05	7.92E+05	4.08E+05	2.61E+05	8.71E+05	17.3	17.3	17.3	17.3	17.3	17.3
A0A0G2JYK0	LOC299282	Serine protease inhibitor A3N	67.98	38	39	41	39	41	40	0	0	0	0	0	0	6.70E+06	5.83E+06	4.03E+06	6.06E+06	7.02E+06	4.39E+06	57	57.6	58.5	57.6	60.6	58.5
[illegible]	LOC299282	Serine protease inhibitor A3N	46.31	33	34	35	35	37	34	0	0	0	0	0	0	6.10E+06	4.61E+06	6.28E+06	4.77E+06	5.73E+06	8.65E+06	70.2	71.2	78.6	78.1	82.5	78.6
F7FAY5	LOC360919	Similar to alpha-fetoprotein	70.32	13	15	15	13	15	16	13	15	15	13	15	16	6.08E+05	5.81E+05	8.60E+05	6.73E+05	7.44E+05	7.65E+05	36.6	39	38	35.4	36.9	39.3
A0A0G2K9F1	LOC362863	First gene upstream of Nt5dc3	46.02	1	1	0	1	1	1	1	1	0	1	1	1	2.78E+03	7.36E+04	0.00E+00	2.16E+03	9.61E+02	1.63E+03	7.1	7.1	0	7.1	7.1	7.1
D4A4D5	LOC498555	Similar to 60S acidic ribosomal protein P2	11.71	2	2	2	2	2	2	2	2	2	2	2	2	2.56E+05	5.63E+05	3.12E+05	1.90E+05	4.62E+05	1.42E+05	45.2	45.2	45.2	45.2	45.2	45.2
F1M3H8	LOC681410	Hypothetical protein	30.08	3	3	2	3	3	2	3	3	2	3	3	2	1.54E+05	1.79E+05	6.16E+04	9.27E+04	6.68E+04	1.85E+04	16.9	16.9	10.3	16.9	16.9	10.3
F1M1R0	LOC690813	Uncharacterized protein	14.89	3	3	3	3	3	3	1	1	1	1	1	1	2.35E+05	4.89E+05	7.42E+05	3.80E+05	4.76E+04	1.33E+06	17.6	17.6	17.6	17.6	17.6	17.6
D4A400	Lpo	Lactoperoxidase	78.25	2	2	1	2	2	1	2	2	1	2	2	1	2.22E+04	3.16E+04	1.24E+04	2.00E+04	2.23E+04	2.13E+04	6.3	6.3	2.9	6.3	6.3	2.9
Q5XI07	Lpp	Lipoma-preferred partner homolog	68.26	4	5	2	3	3	3	4	5	2	3	3	3	5.97E+04	7.05E+04	1.30E+04	3.45E+04	1.79E+04	5.50E+03	11.1	14.7	6	7.4	7.6	9.5
Q5I0E1	Lrg1	Leucine-rich alpha-2-glycoprotein 1	36.32	0	2	3	2	2	2	0	2	3	2	2	2	0.00E+00	1.39E+04	6.54E+04	1.44E+04	1.37E+04	8.29E+03	0	8.4	18.4	8.4	8.4	10.2
G3V928	Lrp1	LDL receptor-related protein 1	504.88	17	15	7	14	15	6	17	15	7	14	15	6	2.81E+04	2.26E+04	1.21E+04	1.36E+04	1.65E+04	6.51E+03	5.4	4.8	2.2	4.7	4.8	1.9
G3V7B2	Lrrc46	Leucine-rich repeat-containing protein 46	36.02	6	6	6	6	4	3	6	6	6	6	4	3	1.54E+05	2.96E+05	1.93E+05	1.10E+05	5.97E+04	7.06E+03	21.7	21.4	21.7	22.3	13.3	11.8
Q5RJR8	Lrrc59	Leucine-rich repeat-containing protein 59	34.87	3	3	0	3	3	0	3	3	0	3	3	0	9.68E+04	9.11E+04	0.00E+00	5.24E+04	2.68E+04	0.00E+00	12.4	12.4	0	12.4	12.4	0
F1LTX4	Lrrn4	Leucine-rich repeat neuronal 4	80.90	5	5	4	5	5	5	5	5	4	5	5	5	2.39E+05	1.22E+05	9.35E+04	1.35E+05	5.74E+04	7.00E+04	12.9	12.9	10.3	12.9	12.9	12.9
D4A7U6	Lsm3	U6 snRNA-associated Sm-like protein LSm3	11.85	3	3	3	2	2	2	3	3	3	2	2	2	6.97E+05	7.38E+05	3.24E+05	4.55E+05	2.08E+05	1.26E+05	67.6	67.6	67.6	32.4	47.1	47.1
D4A2C6	Lsm4	U6 snRNA-associated Sm-like protein LSm4	15.20	3	2	1	3	2	0	3	2	1	3	2	0	5.71E+04	1.88E+04	8.10E+03	3.25E+04	5.96E+03	0.00E+00	31.2	23.9	15.2	31.2	23.9	0
Q4QQV6	Lsp1	Lymphocyte specific 1	36.56	2	2	1	2	2	2	2	2	1	2	2	2	3.78E+04	5.93E+04	2.54E+04	2.97E+04	2.93E+04	1.62E+04	8.2	8.2	3.9	8.2	8.2	8.2
Q499P2	Lta4h	Leukotriene A(4) hydrolase;Leukotriene A-4 hydrolase	69.09	12	11	12	13	11	11	12	11	12	13	11	11	4.85E+05	3.48E+05	2.59E+05	2.89E+05	1.77E+05	1.29E+05	26.2	23.4	25.2	28.2	24.5	23.6
D3ZAA3	Ltbp1	Latent-transforming growth factor beta-binding protein 1	186.60	5	5	4	5	6	5	5	5	4	5	6	5	4.72E+04	2.64E+04	1.46E+04	3.57E+04	3.19E+04	1.20E+04	4.1	4.1	3.1	4.1	4.7	3.6
A0A0G2K588	Ltbp4	Latent-transforming growth factor beta-binding protein 4	154.01	10	9	10	12	11	7	10	9	10	12	11	7	1.31E+05	6.70E+04	5.41E+04	1.03E+05	5.37E+04	3.50E+04	9.7	8.1	8.8	10.8	9.7	6.3
P51886	Lum	Lumican	38.28	14	15	12	15	13	12	14	15	12	15	13	12	6.98E+06	5.15E+06	5.35E+06	6.77E+06	5.76E+06	4.64E+06	40.2	41.4	38.5	43.2	39.3	38.5
Q64361	Lxn	Latexin	25.58	1	1	0	1	1	1	1	1	0	1	1	1	2.88E+04	1.93E+04	0.00E+00	1.45E+04	1.17E+04	1.49E+04	8.1	8.1	0	8.1	8.1	8.1
D3ZQK8	Ly75	Lymphocyte antigen 75	199.11	1	1	0	1	1	0	1	1	0	1	1	0	4.67E+03	3.54E+03	0.00E+00	0.00E+00	1.12E+03	0.00E+00	0.8	0.8	0	0.4	0.8	0
P70470	Lypla1	Acyl-protein thioesterase 1	24.71	5	5	4	4	4	4	5	5	4	4	3	4	2.51E+05	5.04E+05	3.68E+05	2.39E+05	1.45E+05	1.47E+05	35.7	35.7	29.6	29.6	18.3	29.6
Q9QYL8	Lypla2	Acyl-protein thioesterase 2	24.81	3	3	1	3	2	0	3	3	1	3	2	0	1.45E+05	2.45E+05	2.84E+04	6.28E+04	6.94E+04	0.00E+00	26.8	26.8	11.3	26.8	19	0
D3ZD19	Lyve1	Extracellular link domain-containing 1	37.27	3	3	3	3	3	3	3	3	3	3	3	3	3.61E+05	2.29E+05	2.20E+05	2.63E+05	2.07E+05	1.80E+05	10.2	10.2	10.2	10.2	10.2	10.2
F1M8E9	Lyz2	Lysozyme	16.72	3	3	4	2	4	4	3	3	4	2	4	4	2.48E+06	1.13E+06	1.53E+06	1.26E+06	2.21E+06	1.28E+06	33.1	33.8	53.4	17.6	52.7	53.4
Q562C6	Lztfl1	Leucine zipper transcription factor-like protein 1	34.64	4	7	5	6	7	2	4	7	5	6	7	2	1.01E+05	2.77E+05	9.63E+04	1.18E+05	6.49E+04	1.85E+04	18.4	32.8	21.7	27.8	32.8	9.4
A0A0G2JWA8	Macf1	Microtubule-actin cross-linking factor 1	830.73	2	2	2	2	2	2	2	2	2	2	2	2	2.50E+04	1.43E+04	1.23E+04	1.08E+04	1.33E+04	1.81E+04	0.5	0.5	0.5	0.5	0.5	0.5
D4A4J3	Man2a2	Alpha-mannosidase	131.96	4	4	2	4	4	3	4	4	2	4	4	3	2.49E+04	2.07E+04	8.32E+03	2.43E+04	2.87E+04	1.25E+04	4.5	4.5	3	4.5	4.5	3.8
Q6P762	Man2b1	Alpha-mannosidase	114.33	4	4	2	4	4	2	4	4	2	4	4	2	3.31E+04	2.31E+04	1.01E+04	2.78E+04	2.76E+04	1.18E+04	6.9	6.9	2.7	6.9	6.9	2.7
Q5M9I2	Man2c1	Alpha-mannosidase;Alpha-mannosidase 2C1	115.84	6	8	3	7	8	3	6	8	3	7	8	3	3.08E+04	4.31E+04	1.08E+04	3.48E+04	4.39E+04	7.80E+03	9.5	12.3	5.6	9.9	12.5	4.8
P01048	Map1	T-kininogen 1	47.78	24	25	21	24	24	20	7	8	6	7	7	5	1.79E+06	1.57E+06	2.86E+06	1.81E+06	2.08E+06	2.57E+06	45.6	46.7	42.6	45.6	45.6	41.9
F1LRL9	Map1b	Microtubule-associated protein 1B	269.64	14	18	10	16	15	8	14	18	10	16	15	8	2.54E+04	7.53E+04	1.46E+04	3.65E+04	1.58E+04	6.32E+03	8.6	11.5	6.7	8.8	9.1	5.8
P36506	Map2k2	Dual specificity mitogen-activated protein kinase kinase 2	44.28	1	1	1	1	1	1	1	1	1	1	1	1	1.82E+04	2.28E+04	1.15E+04	8.16E+03	7.68E+03	5.94E+03	3.5	3.5	3.5	3.5	3.5	3.5
F1LP57	Map2k4	Dual specificity mitogen-activated protein kinase kinase 4	42.40	4	4	2	4	3	0	4	4	2	4	3	0	1.35E+04	2.42E+04	9.20E+03	1.38E+04	5.81E+03	0.00E+00	14	14	7.3	14	11.3	0
Q5M7W5	Map4	Microtubule-associated protein 4	110.30	8	10	7	9	9	7	8	10	7	9	9	7	4.26E+05	2.73E+05	1.23E+05	1.54E+05	1.70E+05	1.53E+05	11.3	12.6	9.7	11.3	12.6	9.7
P63086	Mapk1	Mitogen-activated protein kinase 1	41.28	5	7	0	6	5	1	4	5	0	4	3	1	6.45E+04	9.92E+04	0.00E+00	4.24E+04	2.24E+04	3.38E+03	30.7	36.6	0	33.2	28.2	6.7
G3V617	Mapk14	Mitogen-activated protein kinase 14	41.27	5	5	4	3	3	3	5	5	4	3	3	3	1.34E+05	3.56E+05	4.68E+04	3.04E+05	6.51E+05	7.72E+03	18.9	18.9	15.8	9.2	9.2	13.6
P21708	Mapk3	Mitogen-activated protein kinase 3	43.08	8	9	5	8	7	6	7	7	5	6	5	6	2.13E+05	2.96E+05	1.15E+05	1.24E+05	1.35E+05	6.69E+04	40.8	43.2	27.1	40.8	28.9	26.6
Q66HR2	Mapre1	Microtubule-associated protein RP/EB family member 1	30.00	5	5	5	5	5	4	5	5	5	5	5	4	1.98E+05	3.60E+05	1.20E+05	1.48E+05	1.04E+05	3.46E+04	22.8	22.8	22	22.8	22.8	14.6
P30009	Marcks	Myristoylated alanine-rich C-kinase substrate	29.79	3	4	3	4	4	3	3	4	3	4	4	3	9.38E+04	6.53E+04	5.80E+04	2.25E+05	7.19E+04	4.44E+04	27.2	28.5	26.2	36.6	36.6	26.2
A0A0G2K613	Marcksl1	MARCKS-related protein	19.72	0	0	0	2	0	0	0	0	0	2	0	0	0.00E+00	0.00E+00	0.00E+00	2.83E+05	0.00E+00	0.00E+00	0	0	0	24.1	0	0
A0A0H2UHA1	Masp1	Mannan-binding lectin serine protease 1	80.11	22	24	19	23	23	21	22	24	19	23	23	21	9.17E+05	8.14E+05	8.70E+05	1.21E+06	1.02E+06	7.24E+05	43	45.5	39.5	44.7	44.7	42.8
A2VCV7	Masp2	Mannan-binding lectin serine protease 2	75.57	17	19	16	17	18	13	17	19	16	17	18	13	6.54E+05	5.62E+05	6.75E+05	7.19E+05	7.05E+05	5.92E+05	41.3	43.9	34.6	36.9	42.6	31.1
Q6P688	Mat2a	S-adenosylmethionine synthase	39.72	4	4	4	4	4	4	4	4	4	4	4	4	2.11E+05	2.91E+05	8.28E+04	1.95E+05	9.69E+04	4.16E+04	16.3	16.3	16.3	16.3	16.3	16.3
A0A0G2JT30	Mat2b	Methionine adenosyltransferase 2 subunit beta	36.24	5	5	3	4	4	2	5	5	3	4	4	2	8.45E+04	9.77E+04	2.82E+04	4.13E+04	3.26E+04	1.91E+04	18.3	18.3	10.5	15.2	15.2	8.4
A0A0G2JSR7	Matr3	Matrin-3	94.50	2	2	2	2	2	1	2	2	2	2	2	1	6.20E+03	1.41E+04	1.43E+03	3.91E+03	4.30E+03	7.52E+02	3.2	3.2	3.2	3.2	3.2	1.7
Q66HG9	Mavs	Mitochondrial antiviral-signaling protein	53.80	4	5	3	4	3	2	4	5	3	4	3	2	4.31E+04	5.99E+04	9.77E+04	1.77E+04	1.62E+04	1.27E+05	13.6	16.2	10.3	13.6	10.8	7.5
P19999	Mbl1	Mannose-binding protein A	25.31	7	9	6	6	7	5	7	9	6	6	7	5	1.40E+06	2.42E+06	1.30E+06	1.50E+06	2.01E+06	1.39E+06	41.2	47.1	41.2	38.2	41.2	37.4
P08661	Mbl2	Mannose-binding protein C	26.01	4	6	2	4	3	2	4	6	2	4	3	2	3.65E+04	1.86E+05	5.44E+04	8.29E+04	1.02E+05	5.53E+04	22.1	26.6	16.4	16	21.3	16.4
D3ZP96	Mcm2	DNA helicase	102.14	1	1	0	0	0	0	1	1	0	0	0	0	2.05E+04	4.07E+03	0.00E+00	0.00E+00	0.00E+00	0.00E+00	2.2	2.2	0	0	0	0
D3ZFP4	Mcm3	DNA helicase	91.66	1	0	0	0	0	0	1	0	0	0	0	0	4.13E+03	0.00E+00	0.00E+00	0.00E+00	0.00E+00	0.00E+00	4.2	0	0	0	0	0
G3V681	Mcm4	DNA helicase	96.57	1	0	0	0	0	0	1	0	0	0	0	0	1.10E+04	0.00E+00	0.00E+00	0.00E+00	0.00E+00	0.00E+00	2	0	0	0	0	0
P09650	Mcpt1	Mast cell protease 1	28.62	1	2	3	2	1	3	1	2	3	2	1	3	6.46E+04	8.03E+04	1.40E+05	6.52E+03	4.91E+04	1.85E+05	6.9	10.8	18.5	14.6	6.9	18.5
O88989	Mdh1	Malate dehydrogenase, cytoplasmic	36.48	2	3	2	2	3	3	2	3	2	2	3	3	3.59E+04	4.42E+04	1.65E+04	1.53E+04	1.25E+05	2.30E+04	8.7	11.7	11.1	8.7	14.7	14.7
P04636	Mdh2	Malate dehydrogenase, mitochondrial	35.68	0	0	0	1	2	0	0	0	0	1	2	0	0.00E+00	0.00E+00	0.00E+00	2.75E+03	2.82E+04	0.00E+00	0	0	0	4.1	8	0
F1LQQ1	Me1	Malic enzyme	54.96	3	4	3	4	4	2	3	4	3	4	4	2	2.25E+04	6.72E+04	1.02E+04	3.41E+04	2.97E+04	3.59E+03	10.1	14.1	10.1	14.1	14.1	6.4
A0A0G2JV28	Mea1	Male-enhanced antigen 1	22.40	1	2	2	2	0	0	1	2	2	2	0	0	4.72E+04	1.61E+05	2.72E+04	7.56E+04	0.00E+00	0.00E+00	8.2	14.4	14.4	14.4	0	0
D3ZSY2	Mei1	Meiosis defective 1	140.75	1	2	1	0	1	0	1	2	1	0	1	0	8.38E+02	7.84E+05	2.97E+03	0.00E+00	1.09E+04	0.00E+00	0.9	2.6	0.9	0	0.9	0

Uniprot accession number	Gene symbol	Protein name	Mol. weight [kDa]	No. Peptides Control wk1	No. Peptides Control wk8	No. Peptides Control wk14	No. Peptides Heat wk1	No. Peptides Heat wk8	No. Peptides Heat wk14	No. Unique peptides Control wk1	No. Unique peptides Control wk8	No. Unique peptides Control wk14	No. Unique peptides Heat wk1	No. Unique peptides Heat wk8	No. Unique peptides Heat wk14	iBAQ Control wk1	iBAQ Control wk8	iBAQ Control wk14	iBAQ Heat wk1	iBAQ Heat wk8	iBAQ Heat wk14	Sequence coverage Control wk1 [%]	Sequence coverage Control wk8 [%]	Sequence coverage Control wk14 [%]	Sequence coverage Heat wk1 [%]	Sequence coverage Heat wk8 [%]	Sequence coverage Heat wk14 [%]
A0A0G2JY19	Met	Hepatocyte growth factor receptor	157.14	2	3	2	3	2	1	2	3	2	3	2	1	1.06E+04	1.23E+04	1.42E+04	1.08E+04	1.01E+04	9.02E+03	2.5	3.8	2.1	3.8	2.5	1.3
G3V6A9	Mfap4	Microfibril-associated protein 4	28.81	2	2	2	2	2	2	2	2	2	2	2	2	2.73E+06	8.50E+05	8.71E+05	1.05E+06	1.23E+06	8.33E+05	17.2	17.2	17.2	17.2	17.2	17.2
A0A0G2K506	Mfge8	Lactadherin	51.14	4	5	5	5	5	4	4	5	5	5	5	4	1.28E+05	9.12E+04	8.73E+04	1.39E+05	1.08E+05	8.81E+04	10.9	12.8	13.5	13.5	12.8	10.7
Q8R431	Mgll	Monoglyceride lipase	33.50	4	6	3	5	5	4	4	6	3	5	5	4	8.26E+04	2.57E+05	5.58E+04	6.17E+04	5.36E+04	3.36E+04	21.8	31.4	19.5	24.8	24.8	24.1
Q5RK05	Mgp	Matrix Gla protein	12.05	2	2	2	2	2	2	2	2	2	2	2	2	6.40E+05	7.15E+05	8.22E+05	6.60E+05	1.18E+06	7.82E+05	23.3	23.3	23.3	23.3	23.3	23.3
D3ZSU7	Mien1	Migration and invasion enhancer 1	12.33	0	0	0	1	0	0	0	0	0	1	0	0	0.00E+00	0.00E+00	0.00E+00	5.92E+04	0.00E+00	0.00E+00	0	0	0	9.6	0	0
G3V7H2	Minpp1	Multiple inositol polyphosphate phosphatase 1	54.60	16	16	16	16	15	16	16	16	16	16	15	16	3.84E+06	3.09E+06	2.90E+06	3.50E+06	3.33E+06	2.68E+06	44.7	44.7	44.7	44.7	41.6	44.7
D3ZKP6	Mlkl	Mixed lineage kinase domain-like pseudokinase	53.31	2	2	2	2	2	2	2	2	2	2	2	2	5.00E+04	4.77E+04	1.95E+04	3.12E+04	4.69E+04	2.77E+04	6	6	6	6	6	6
C0M4B0	Mmp19	Matrix metallopeptidase 19	58.29	6	6	4	5	5	3	6	6	4	5	5	3	1.12E+05	6.22E+04	6.51E+04	9.65E+04	7.80E+04	4.18E+04	17.2	17.2	10.1	15.1	15.1	7.9
E9PSM5	Mmp2	72 kDa type IV collagenase	74.24	6	4	7	6	4	7	6	4	7	6	4	7	8.06E+04	4.20E+04	7.27E+04	8.88E+04	5.45E+04	7.53E+04	12.5	8.4	14.3	12.5	8.4	14.3
Q68FX1	Mpi	Mannose-6-phosphate isomerase	46.42	3	4	2	2	4	2	3	4	2	2	4	2	1.36E+05	1.79E+05	6.90E+04	7.03E+04	7.45E+04	2.23E+04	10.6	14.2	6.9	6.9	14.2	6.9
D3ZGE2	Mpo	Myeloperoxidase	51.88	3	4	1	3	3	1	3	4	1	3	3	1	4.24E+04	4.98E+04	9.44E+03	2.94E+04	4.64E+04	1.43E+04	7.2	9.4	2.8	7.2	7.2	2.8
P97532	Mpst	3-mercaptopyruvate sulfurtransferase	32.94	3	3	3	2	2	2	3	3	3	2	2	2	6.20E+04	1.11E+05	6.70E+04	3.75E+04	3.19E+04	1.61E+04	19.5	19.5	19.5	13.5	13.5	15.2
F1LMA7	Mrc2	C-type mannose receptor 2	170.63	12	12	9	11	11	7	12	12	9	11	11	7	1.69E+05	9.35E+04	3.14E+04	5.09E+04	4.48E+04	1.51E+04	14.6	14.6	11.6	13.1	13.1	8.8
Q5HZE4	Mri1	Methylthioribose-1-phosphate isomerase	39.59	2	3	3	3	4	3	2	3	3	3	4	3	1.22E+05	2.81E+05	8.93E+04	1.38E+05	9.62E+04	6.15E+04	12.7	19.5	17.9	19.5	24.7	17.9
Q9ERA7	Msln	Mesothelin	68.88	4	3	3	4	3	3	4	3	3	4	3	3	8.73E+04	2.62E+04	5.95E+04	3.50E+04	2.42E+04	5.46E+04	11.2	9.9	9	11.2	9.9	9
A0A1W2Q6E9	Msn	Moesin	67.65	14	12	11	13	11	11	10	9	8	9	8	9	4.84E+05	3.45E+05	1.23E+05	1.82E+05	1.56E+05	9.62E+04	29.3	21.2	21.7	26.6	24	19.8
F7FMS0	Mst1	Macrophage-stimulating 1	83.14	25	25	28	26	27	28	25	25	28	26	27	28	1.50E+06	1.37E+06	1.38E+06	1.40E+06	1.23E+06	1.35E+06	46.5	46.5	49.5	47	47.9	49.5
A0A0G2K583	Mtap	S-methyl-5-thioadenosine phosphorylase	31.09	5	4	2	5	4	2	5	4	2	5	4	2	1.13E+05	1.02E+05	1.48E+04	6.47E+04	6.19E+04	6.75E+03	25.8	19.8	9.5	25.8	19.8	9.5
G3V6S5	Mthfd1	C-1-tetrahydrofolate synthase	100.96	13	11	5	12	9	2	13	11	5	12	9	2	1.12E+05	1.46E+05	2.33E+04	9.40E+04	5.22E+04	9.79E+03	21.1	14.8	10.1	16.6	12.4	3.7
P62775	Mtpn	Myotrophin	12.86	2	2	3	2	2	3	2	2	3	2	2	3	3.51E+05	5.70E+05	4.33E+05	2.81E+05	2.23E+05	1.92E+05	32.2	32.2	38.1	32.2	32.2	38.1
G3V8A4	Mtr	Methionine synthase	139.19	2	2	1	0	1	0	2	2	1	0	1	0	3.47E+03	4.43E+03	2.93E+03	0.00E+00	2.87E+03	0.00E+00	2.2	2.2	0.9	0	1.3	0
D3ZAU0	Muc5b	Mucin 5B, oligomeric mucus/gel-forming	449.07	2	1	5	2	2	2	2	1	5	2	2	2	2.71E+02	1.64E+02	4.37E+03	3.52E+02	1.82E+02	3.88E+02	0.7	0.4	2.3	1.1	0.7	1
D4A6E3	Mug1	Murinoglobulin-1	165.32	119	124	118	120	119	118	3	2	2	3	2	2	3.58E+06	1.65E+06	8.95E+05	4.08E+06	3.49E+06	2.04E+06	73.6	74.2	72	73.6	73.6	73.2
Q03626	Mug1	Murinoglobulin-1	165.32	119	128	118	119	120	119	0	3	0	0	0	1	5.91E+07	5.97E+07	6.85E+07	5.27E+07	6.36E+07	6.90E+07	73.6	74.2	72	73.6	73.6	73.2
A0A0G2JUP5	Mug1	Murinoglobulin-1	161.36	100	106	101	102	102	101	0	0	0	0	0	1	0.00E+00	0.00E+00	0.00E+00	0.00E+00	0.00E+00	1.85E+03	65	65.6	63.7	65.2	65.2	66.6
Q6IE52	Mug2	Murinoglobulin-2	161.59	89	95	89	91	90	87	2	2	3	3	3	2	2.51E+06	2.47E+06	3.23E+06	3.93E+06	2.65E+06	4.08E+06	59.5	60.1	59.2	60.3	59.7	60.2
M0R5V7	Mug2	Murinoglobulin-2	151.96	89	95	89	89	88	87	3	3	3	3	3	3	1.78E+05	1.33E+05	1.84E+05	1.59E+05	1.77E+05	1.41E+05	64.8	65	66.7	65.1	64.5	66.4
D4A7F2	Mycbp	Myc-binding protein	11.97	0	2	1	0	1	0	0	2	1	0	1	0	0.00E+00	1.59E+05	2.72E+04	0.00E+00	6.19E+04	0.00E+00	0	30.1	19.4	0	19.4	0
Q641W2	Myg1	UPF0160 protein MYG1, mitochondrial	42.89	6	6	4	5	5	3	6	6	4	5	5	3	1.41E+05	2.03E+05	1.06E+05	7.82E+04	5.78E+04	3.89E+04	21	21	15.7	16.3	16.3	12.6
E9PTU4	Myh11	Myosin-11	227.29	5	11	8	6	7	5	4	10	7	5	6	4	2.22E+04	3.82E+04	1.05E+04	2.42E+04	3.55E+04	5.74E+03	3.9	9.5	6.8	4.7	5.4	4.3
A0A0G2K484	Myh4	Myosin-4	222.69	4	2	1	4	2	2	4	2	1	4	2	2	3.22E+04	6.76E+03	4.05E+03	4.58E+04	6.19E+03	5.94E+03	2.6	1.4	0.5	2.6	1.4	1.5
G3V6P7	Myh9	Myosin, heavy polypeptide 9, non-muscle	226.41	19	19	10	16	19	10	18	18	9	15	18	9	6.62E+04	8.11E+04	2.01E+04	4.07E+04	6.50E+04	1.85E+04	17.1	16	9.5	14	14.8	9
P02600	Myl1	Myosin light chain 1/3, skeletal muscle isoform	20.68	3	3	2	3	2	1	2	2	2	2	1	1	4.96E+04	4.01E+04	7.82E+03	6.16E+04	9.09E+04	1.02E+03	19.6	19.6	13.2	19.6	12.7	6.3
A0A0G2JSW0	Myl12b	Myosin regulatory light chain 12B	19.78	2	3	1	5	6	2	2	3	1	5	6	2	2.99E+05	3.27E+05	1.62E+07	1.43E+05	5.71E+05	4.11E+04	22.1	28.5	10.5	34.9	34.9	22.1
A0A0G2JWE1	Myl6	Myosin light polypeptide 6	12.53	5	6	4	6	6	4	3	4	2	4	4	2	2.63E+06	3.62E+06	1.54E+06	2.30E+06	2.08E+06	9.58E+05	55	59.5	43.2	65.8	65.8	43.2
D3ZDI6	Mylip	E3 ubiquitin-protein ligase MYLIP	49.89	2	2	2	1	2	2	2	2	2	1	2	2	1.45E+05	6.43E+05	1.03E+06	2.74E+04	5.34E+05	7.71E+05	6.1	6.1	6.1	2.9	6.1	6.1
A0A0G2K0Q7	Mylk	Myosin light chain kinase	214.00	10	13	12	11	11	9	10	13	12	11	11	9	2.12E+05	1.17E+06	4.43E+05	2.94E+05	8.52E+05	3.23E+05	8	10.5	9.6	9.2	9.5	7.8
Q63355	Myo1c	Unconventional myosin-Ic	119.81	2	2	1	2	2	2	2	2	1	2	2	2	6.81E+03	5.53E+03	2.65E+03	5.21E+03	2.50E+03	1.37E+03	2.8	2.8	1.1	2.8	2.8	2.8
D4A5I9	Myo6	Myosin VI	148.13	0	1	1	1	1	0	0	1	1	1	1	0	0.00E+00	2.61E+02	1.88E+02	1.53E+03	5.00E+02	0.00E+00	0	1.3	1.3	1.3	1.3	0
Q8CJE3	Myo7a	Myosin VIIA	251.11	1	1	1	1	1	1	1	1	1	1	1	1	3.66E+03	1.73E+03	1.21E+04	8.12E+02	3.05E+03	1.44E+03	0.4	0.4	0.4	0.4	0.4	0.4
A0A0G2K7R1	N/A	Uncharacterized protein (Belongs to the histone H2B family)	13.13	2	0	1	2	3	1	2	0	1	2	3	1	2.64E+04	0.00E+00	8.62E+04	3.45E+04	1.23E+06	7.35E+03	20.3	0	12.7	20.3	21.2	12.7
F1LTJ5	N/A	Uncharacterized protein	263.11	19	19	13	19	18	14	19	19	13	19	18	14	1.32E+05	9.54E+04	4.58E+04	1.28E+05	1.03E+05	5.87E+04	12	11.6	9	11.7	11.1	9.4
D4A3D1	N/A	Uncharacterized protein	11.15	2	3	3	3	3	2	2	3	3	3	3	2	4.28E+06	3.00E+06	1.90E+06	2.68E+06	3.65E+06	2.45E+06	24.2	40.4	40.4	40.4	40.4	24.2
F1LXY6	N/A	Uncharacterized protein	11.25	7	7	6	7	7	6	7	7	6	7	7	6	1.06E+07	4.36E+06	8.84E+06	5.60E+06	4.19E+06	1.05E+07	88	88	83	88	88	83
D4ACR1	N/A	Uncharacterized protein	13.71	5	4	5	5	5	4	4	3	4	4	4	3	2.52E+06	1.52E+06	5.27E+05	1.84E+06	2.33E+06	9.49E+05	65.3	47.1	65.3	65.3	65.3	49.6
F1LZH0	N/A	Uncharacterized protein	13.61	1	1	1	1	1	1	1	1	1	1	1	1	5.30E+06	7.98E+06	9.66E+06	1.01E+07	7.89E+06	1.31E+07	12.2	12.2	12.2	12.2	12.2	12.2
G3V9J1	N/A	Uncharacterized protein	97.34	49	54	52	50	52	55	16	19	18	17	18	20	5.07E+06	4.89E+06	5.75E+06	5.35E+06	5.75E+06	5.27E+06	56.1	59.9	57.1	57	57.6	60.9
D3ZE63	N/A	Uncharacterized protein	12.61	1	2	1	1	2	1	1	2	1	1	2	1	1.83E+05	2.68E+05	1.12E+05	1.49E+05	1.13E+05	6.59E+04	7.8	17.4	7.8	7.8	17.4	7.8
D4A5L9	N/A	Uncharacterized protein	11.64	2	2	4	1	1	1	2	2	4	1	1	1	3.65E+04	7.88E+04	2.02E+05	9.73E+03	3.02E+04	4.90E+04	31.4	31.4	39	17.1	17.1	17.1
G3V8Z5	N/A	Uncharacterized protein	14.28	4	5	4	4	4	4	2	3	2	2	2	2	8.75E+06	1.10E+07	8.17E+06	1.06E+07	1.22E+07	9.82E+06	24	24	24	24	24	24
M0R936	N/A	Uncharacterized protein	15.44	3	3	3	3	3	4	3	3	3	3	3	4	4.37E+05	1.59E+06	1.33E+06	5.17E+05	1.91E+06	1.62E+06	27.9	27.9	27.1	27.9	27.9	27.9
F1M937	N/A	Uncharacterized protein	12.93	3	3	3	3	2	2	3	3	3	3	2	2	1.75E+05	4.29E+05	1.61E+05	1.41E+05	6.92E+04	5.90E+04	21.4	21.4	21.4	21.4	21.4	21.4
M0R9A3	N/A	Uncharacterized protein	12.00	3	3	1	2	2	2	3	3	1	2	2	2	6.05E+05	3.84E+05	2.86E+04	3.28E+05	7.28E+04	4.07E+05	31.8	31.8	12.1	22.4	22.4	21.5
P02761	N/A	Major urinary protein	20.74	6	6	7	6	5	7	5	5	6	5	4	6	3.17E+06	1.65E+06	3.08E+06	4.42E+06	2.35E+06	3.37E+06	29.8	29.8	34.3	29.8	29.8	34.3
M0RA79	N/A	Uncharacterized protein	10.96	7	7	6	6	6	6	7	7	6	6	6	6	6.01E+06	3.62E+06	4.05E+06	5.30E+06	3.82E+06	5.19E+06	80.8	80.8	80.8	80.8	80.8	80.8
D3ZFH6	N/A	Uncharacterized protein	29.59	2	0	1	1	0	0	2	0	1	1	0	0	1.41E+05	0.00E+00	5.95E+03	1.01E+04	0.00E+00	0.00E+00	14.7	0	7.4	7.4	0	0
M0R4G1	N/A	Uncharacterized protein	12.94	1	1	2	1	1	2	1	1	1	1	1	1	2.92E+06	4.54E+06	1.52E+06	3.90E+06	6.33E+06	2.00E+06	12.8	12.8	30.8	12.8	12.8	30.8
F1M0U4	N/A	Uncharacterized protein	13.44	1	1	1	1	1	1	1	1	1	1	1	1	4.40E+05	6.29E+05	5.10E+05	7.79E+05	9.01E+05	1.02E+06	9.2	9.2	9.2	9.2	9.2	9.2
D4A6W6	N/A	Uncharacterized protein	28.16	1	0	0	0	1	0	1	0	0	0	1	0	2.04E+03	0.00E+00	0.00E+00	0.00E+00	7.04E+03	0.00E+00	4.3	0	0	0	4.3	0
D3Z8P5	N/A	Uncharacterized protein	35.27	4	4	3	4	4	4	4	4	3	4	4	4	1.06E+05	2.81E+05	6.67E+04	1.06E+05	8.86E+04	5.62E+04	19.4	19.4	15.7	19.4	19.4	19.4
F1LTN6	N/A	Uncharacterized protein	24.92	16	18	17	18	17	17	10	12	11	12	11	12	1.32E+08	1.43E+08	1.84E+08	1.66E+08	1.44E+08	1.59E+08	57.5	57.5	57.5	57.5	57.5	57.5
M0R816	N/A	Uncharacterized protein	10.64	2	3	2	3	2	2	1	2	1	2	1	1	5.27E+07	7.61E+07	7.74E+07	6.42E+07	5.97E+07	4.78E+07	33	33	33	33	33	33
P20767	N/A	Ig lambda-2 chain C region	11.32	8	9	9	9	9	9	8	9	9	9	9	9	2.73E+07	3.71E+07	6.95E+07	3.69E+07	4.49E+07	6.06E+07	89.4	97.1	89.4	97.1	97.1	89.4
A0A0G2K477	N/A	Uncharacterized protein	51.14	18	19	18	18	19	18	0	0	0	0	0	0	3.05E+07	2.53E+07	3.29E+07	2.94E+07	2.66E+07	3.48E+07	59	59.9	59	59	59.9	59
D3ZPL2	N/A	Uncharacterized protein	11.33	3	3	3	2	3	3	3	3	3	2	3	3	1.80E+07	2.10E+07	2.89E+07	1.72E+07	2.25E+07	2.91E+07	37.1	37.1	37.1	31.4	37.1	37.1
A0A0G2JVP4	N/A	Uncharacterized protein	51.71	19	24	18	21	20	17	19	24	18	21	20	17	6.88E+06	1.66E+07	6.68E+06	1.23E+07	1.23E+07	7.63E+06	55.5	56.8	54.5	55.7	55.7	52.3
M0R9U2	N/A	Uncharacterized protein	10.85	7	8	7	7	7	7	7	8	7	7	7	7	5.87E+06	2.36E+07	7.94E+06	5.81E+06	9.20E+06	7.32E+06	83.7	83.7	83.7	83.7	83.7	83.7
D4A4L6	N/A	Uncharacterized protein	12.97	7	6	6	7	5	7	0	0	0	0	0	0	8.76E+06	9.19E+06	8.54E+06	8.49E+06	9.07E+06	1.47E+07	74.4	74.4	68.4	74.4	68.4	74.4
P20762	N/A	Ig gamma-2C chain C region	36.57	18	20	18	19	18	19	15	17	15	16	15	16	1.65E+07	9.97E+06	1.85E+07	1.33E+07	8.97E+06	1.24E+07	86.6	86.6	86.6	86.6	80.2	86.6
A0A0G2K7P6	N/A	Uncharacterized protein	10.23	4	4	4	4	4	4	2	2	2	2	2	2	6.54E+06	8.36E+06	9.79E+06	7.29E+06	8.68E+06	8.29E+06	38.3	38.3	38.3	38.3	38.3	38.3
A0A0G2JZV7	N/A	Uncharacterized protein	12.16	5	5	5	5	5	5	3	3	3	3	3	3	8.58E+06	8.64E+06	8.26E+06	1.05E+07	8.43E+06	7.11E+06	72.1	72.1	72.1	72.1	72.1	72.1
A0A0G2JXF0	N/A	Uncharacterized protein	11.80	3	5	3	3	5	4	2	4	2	2	4	3	7.29E+06	6.07E+06	7.10E+06	6.00E+06	8.31E+06	1.01E+07	24.1	61.1	24.1	24.1	61.1	38.9
M0RBK4	N/A	Uncharacterized protein	11.51	3	3	3	3	3	3	3	3	3	3	3	3	6.83E+06	6.51E+06	9.70E+06	7.96E+06	8.03E+06	7.66E+06	42.5	42.5	42.5	42.5	42.5	42.5
P01836	N/A	Ig kappa chain C region, A allele	11.73	13	14	12	14	14	12	8	9	7	9	9	8	5.47E+06	8.38E+06	2.31E+06	3.45E+06	7.84E+06	9.97E+06	95.3	95.3	95.3	95.3	95.3	95.3
M0R7M5	N/A	Uncharacterized protein	14.65	6	6	3	5	6	5	4	4	1	3	4	3	6.89E+06	5.41E+06	9.78E+06	6.42E+06	7.64E+06	7.20E+06	53	40.9	23.5	50.8	53	53
A0A0G2K4K2	N/A	Uncharacterized protein	10.41	3	3	3	3	3	3	1	1	1	1	1	1	4.49E+06	4.14E+06	6.62E+06	5.42E+06	7.11E+06	8.36E+06	41.7	41.7	41.7	41.7	41.7	41.7
A0A0G2JUY4	N/A	Uncharacterized protein	12.42	6	6	6	6	6	5	2	2	2	2	2	1	3.28E+06	4.70E+06	2.67E+06	1.57E+06	6.41E+06	4.24E+06	54.5	54.5	54.5	54.5	54.5	51.8
D3ZEP5	N/A	Uncharacterized protein	10.58	5	6	5	5	6	4	3	4	3	3	4	2	9.19E+05	4.35E+06	2.97E+06	2.16E+06	5.61E+06	1.98E+06	62.9	62.9	62.9	62.9	62.9	56.7
A0A0G2K0N6	N/A	Uncharacterized protein	10.75	3	3	3	2	3	3	3	3	3	2	3	3	1.04E+06	2.87E+06	4.85E+06	2.75E+06	5.44E+06	6.34E+06	45.4	45.4	45.4	28.9	45.4	45.4
D3ZQR5	N/A	Uncharacterized protein	12.77	3	3	3	3	3	3	2	2	2	2	2	2	4.85E+06	4.56E+06	5.11E+06	3.29E+06	5.07E+06	7.02E+06	37.1	37.1	37.1	37.1	37.1	37.1
M0RAZ1	N/A	Uncharacterized protein	11.11	5	5	5	4	5	4	4	4	4	3	4	3	3.53E+06	3.12E+06	3.86E+06	3.43E+06	4.93E+06	5.71E+06	54.9	54.9	31.4	31.4	54.9	31.4
A0A0G2JXB7	N/A	Uncharacterized protein	12.89	3	3	1	3	4	1	2	2	1	2	3	1	3.90E+04	4.07E+06	2.39E+06	2.78E+06	4.87E+06	3.52E+06	30.2	30.2	13.8	30.2	31.9	13.8
M0RBD5	N/A	Uncharacterized protein	11.02	4	4	4	4	4	4	3	3	3	3	3	3	3.53E+06	3.54E+06	3.99E+06	6.00E+06	4.51E+06	5.53E+06	47	47	47	47	47	47
A0A0G2JW41	N/A	Uncharacterized protein	13.03	3	2	3	2	3	3	2	1	2	1	2	2	4.35E+06	3.25E+06	6.49E+06	2.62E+06	4.16E+06	6.75E+06	36.4	26.3	36.4	26.3	36.4	36.4
D3ZC54	N/A	Uncharacterized protein	13.13	5	5	3	4	4	4	5	5	3	4	4	4	2.89E+06	2.77E+06	1.95E+06	3.07E+06	3.58E+06	2.91E+06	50.4	50.4	33.3	50.4	50.4	50.4
M0RAB8	N/A	Uncharacterized protein	11.10	4	4	3	4	4	3	4	4	3	4	4	3	3.44E+06	2.19E+06	1.64E+06	2.98E+06	3.42E+06	1.71E+06	61	61	52	61	76	52
A0A0G2K61[illegible]	N/A	Uncharacterized protein	10.34	4	4	4	4	4	4	3	3	3	3	3	3	1.06E+06	1.31E+06	2.75E+06	1.03E+06	3.33E+06	2.79E+06	47.9	47.9	47.9	47.9	47.9	47.9
F1LWD0	N/A	Uncharacterized protein	11.92	4	4	4	4	4	4	4	4	4	4	4	4	1.87E+06	1.37E+06	1.08E+06	1.92E+06	3.16E+06	1.99E+06	50	50	50	50	50	50
P01681	N/A	Ig kappa chain V region S211	11.43	2	2	2	2	2	2	2	2	2	2	2	2	2.76E+06	3.96E+06	2.71E+06	2.56E+06	3.11E+06	2.57E+06	36.7	36.7	36.7	36.7	36.7	36.7
A0A0G2K4I8	N/A	Uncharacterized protein	12.68	2	2	1	2	2	1	2	2	1	2	2	1	1.17E+06	2.26E+06	2.21E+06	1.69E+06	3.03E+06	2.36E+06	19.6	19.6	9.8	19.6	19.6	9.8
P81828	N/A	Urinary protein 2	11.07	1	1	1	1	1	1	1	1	1	1	1	1	7.56E+06	2.83E+06	2.04E+06	5.39E+06	2.98E+06	2.49E+06	13.9	13.9	13.9	13.9	13.9	13.9
A0A0G2JX36	N/A	Uncharacterized protein	13.23	4	4	3	4	3	4	4	4	3	4	3	4	1.73E+06	5.64E+06	3.62E+06	2.40E+06	2.81E+06	6.78E+06	28.6	28.6	24.4	28.6	24.4	28.6
E9PSU8	N/A	Uncharacterized protein	15.16	3	3	3	3	3	3	3	3	3	3	3	3	2.83E+06	2.32E+06	2.49E+06	4.42E+06	2.79E+06	2.22E+06	31.4	31.4	31.4	31.4	31.4	31.4

Uniprot accession number	Gene symbol	Protein name	Mol. weight [kDa]	No. Peptides Control wk1	No. Peptides Control wk8	No. Peptides Control wk14	No. Peptides Heat wk1	No. Peptides Heat wk8	No. Peptides Heat wk14	No. Unique peptides Control wk1	No. Unique peptides Control wk8	No. Unique peptides Control wk14	No. Unique peptides Heat wk1	No. Unique peptides Heat wk8	No. Unique peptides Heat wk14	iBAQ Control wk1	iBAQ Control wk8	iBAQ Control wk14	iBAQ Heat wk1	iBAQ Heat wk8	iBAQ Heat wk14	Sequence coverage Control wk1 [%]	Sequence coverage Control wk8 [%]	Sequence coverage Control wk14 [%]	Sequence coverage Heat wk1 [%]	Sequence coverage Heat wk8 [%]	Sequence coverage Heat wk14 [%]
A0A0G2K8C3	N/A	Uncharacterized protein	12.74	1	1	1	1	1	1	1	1	1	1	1	1	3.27E+06	3.14E+06	1.79E+06	4.68E+06	2.73E+06	2.79E+06	13.8	13.8	13.8	13.8	13.8	13.8
A0A0G2K290	N/A	Uncharacterized protein	13.91	6	6	6	6	6	6	2	2	2	2	2	2	1.85E+06	2.66E+06	2.30E+06	5.22E+06	2.53E+06	4.25E+06	48.4	48.4	48.4	48.4	48.4	48.4
M0R4Z4	N/A	Uncharacterized protein	13.29	3	3	3	3	3	3	1	1	1	1	1	1	2.15E+06	9.12E+05	3.10E+06	1.86E+06	2.52E+06	3.32E+06	18.6	18.6	18.6	18.6	18.6	18.6
M0R8G6	N/A	Uncharacterized protein	11.00	2	3	4	2	3	4	2	3	4	2	3	4	7.34E+05	1.25E+06	1.54E+06	6.78E+05	2.40E+06	2.29E+06	35.6	36.6	36.6	35.6	36.6	36.6
F1LZ11	N/A	Uncharacterized protein	14.07	3	4	3	3	3	3	3	4	3	3	3	3	2.31E+06	2.42E+06	1.82E+06	1.81E+06	2.39E+06	3.37E+06	33.1	34.7	33.1	33.1	33.1	33.1
A0A0G2JZN1	N/A	Uncharacterized protein	10.31	2	3	2	2	2	2	2	3	2	2	2	2	1.77E+06	1.05E+06	9.14E+05	1.08E+06	2.19E+06	1.26E+06	33.3	42.7	33.3	33.3	33.3	33.3
D3ZHM9	N/A	Uncharacterized protein	11.84	5	5	5	5	5	5	3	3	3	3	3	3	1.48E+06	1.62E+06	2.33E+06	1.11E+06	2.16E+06	1.51E+06	34.3	34.3	34.3	34.3	34.3	34.3
M0RDF0	N/A	Uncharacterized protein	12.11	3	3	1	3	3	2	2	2	1	2	2	2	1.35E+06	2.19E+06	1.85E+06	2.29E+06	1.95E+06	1.58E+06	34.3	34.3	14.8	34.3	34.3	27.8
D3ZFF8	N/A	Uncharacterized protein	12.99	3	5	2	3	5	3	3	5	2	3	5	3	8.03E+05	1.66E+06	1.14E+06	1.06E+06	1.83E+06	1.43E+06	39.3	45.3	28.2	39.3	45.3	39.3
M0RC23	N/A	Uncharacterized protein	11.19	4	5	3	3	4	3	1	2	1	1	2	1	2.68E+06	1.62E+06	1.55E+06	1.20E+06	1.76E+06	1.71E+06	34.3	57.8	30.4	30.4	53.9	30.4
D3ZQM9	N/A	Uncharacterized protein	12.94	3	3	3	2	3	3	2	2	2	1	2	2	3.50E+05	1.15E+06	1.94E+05	7.10E+05	1.68E+06	3.92E+05	29.3	29.3	29.3	29.3	29.3	29.3
D3ZE00	N/A	Uncharacterized protein	10.85	4	4	4	4	4	4	1	1	1	1	1	1	5.61E+05	7.37E+05	1.63E+06	7.58E+05	1.66E+06	1.98E+06	50	50	50	50	50	50
F1M663	N/A	Uncharacterized protein	12.73	3	3	3	3	3	3	2	2	2	2	2	2	7.14E+05	1.43E+06	1.67E+06	5.92E+05	1.56E+06	1.39E+06	28.7	28.7	28.7	28.7	28.7	28.7
A0A0G2JWX0	N/A	Uncharacterized protein	15.51	4	4	3	4	4	4	4	4	3	4	4	4	7.36E+05	1.11E+06	1.52E+06	1.24E+06	1.56E+06	1.36E+06	39	39	24.8	39	39	39
F1LZY6	N/A	Uncharacterized protein	10.48	2	2	2	2	2	2	1	1	1	1	1	1	8.46E+05	8.35E+05	1.34E+06	7.82E+05	1.36E+06	9.68E+05	33	33	33	33	33	33
A0A0G2JV42	N/A	Uncharacterized protein	12.58	1	1	1	1	1	1	1	1	1	1	1	1	1.82E+06	9.74E+05	1.21E+06	6.90E+05	1.20E+06	1.49E+06	16.5	16.5	16.5	16.5	16.5	16.5
D3ZAB3	N/A	Uncharacterized protein	13.26	1	2	2	2	2	2	1	2	2	2	2	2	6.86E+05	1.21E+06	1.46E+06	5.47E+05	1.19E+06	2.22E+06	13.4	17.6	17.6	17.6	17.6	17.6
A0A0G2K245	N/A	Uncharacterized protein	12.61	1	1	1	1	1	1	1	1	1	1	1	1	6.47E+05	1.27E+06	7.87E+05	9.29E+05	1.09E+06	9.38E+05	14	14	14	14	14	14
P11517	N/A	Hemoglobin subunit beta-2	15.98	14	15	13	14	14	13	3	4	3	3	3	2	4.75E+06	5.10E+06	1.17E+06	4.29E+06	1.06E+06	2.84E+06	78.2	78.2	78.2	78.2	78.2	75.5
D4ADL1	N/A	Uncharacterized protein	12.91	3	3	3	4	3	3	2	2	2	3	2	2	4.73E+05	4.13E+05	1.83E+05	7.00E+05	9.03E+05	3.28E+05	45.8	45.8	45.8	45.8	45.8	45.8
M0R4X3	N/A	Uncharacterized protein	10.71	3	3	3	3	3	3	2	2	2	2	2	2	5.89E+04	2.99E+05	2.27E+06	5.22E+04	8.75E+05	2.07E+06	28.1	28.1	28.1	28.1	28.1	28.1
M0RAV0	N/A	Uncharacterized protein	10.13	4	4	4	4	4	3	3	3	3	3	3	2	8.58E+05	1.26E+06	1.30E+06	8.24E+05	8.16E+05	8.77E+05	60.2	60.2	60.2	60.2	60.2	50.5
F1LPR6	N/A	Uncharacterized protein	51.40	10	11	9	9	10	9	9	10	9	8	9	9	1.82E+06	1.13E+06	2.73E+06	1.47E+06	7.43E+05	2.21E+06	43.6	44	42.1	41.1	37.4	42.1
M0RE02	N/A	Uncharacterized protein	12.80	3	3	3	3	3	3	2	2	2	2	2	2	2.00E+06	8.57E+05	3.23E+06	1.83E+06	7.40E+05	2.44E+06	54.7	54.7	54.7	54.7	54.7	54.7
F1LWW1	N/A	Uncharacterized protein	12.37	1	1	1	1	2	1	1	1	1	1	2	1	1.82E+05	5.38E+05	1.14E+06	9.49E+05	7.38E+05	8.14E+05	13.3	13.3	13.3	13.3	27.4	13.3
F1M7B3	N/A	Uncharacterized protein	11.20	5	5	5	5	5	5	3	3	3	3	3	3	7.91E+05	6.18E+05	4.67E+05	6.52E+05	6.99E+05	5.09E+05	51	51	51	51	51	51
M0RDW9	N/A	Uncharacterized protein	11.86	2	2	2	2	2	2	2	2	2	2	2	2	1.14E+06	1.11E+06	8.73E+05	8.97E+05	6.50E+05	9.73E+05	34.6	34.6	34.6	34.6	34.6	34.6
M0RDF2	N/A	Uncharacterized protein	11.18	4	4	4	4	4	4	3	3	3	3	3	3	9.93E+05	3.44E+05	1.71E+06	9.74E+05	6.27E+05	2.00E+06	46.5	46.5	46.5	46.5	46.5	46.5
F1LYU4	N/A	Uncharacterized protein	13.38	3	3	2	3	3	2	2	2	1	2	2	1	7.96E+05	2.53E+05	2.22E+04	4.13E+05	5.65E+05	1.80E+04	49.2	49.2	33.9	49.2	49.2	33.9
A0A0G2K9Y0	N/A	Uncharacterized protein	51.59	17	18	17	17	18	17	0	0	0	0	0	0	6.13E+05	5.94E+05	7.79E+05	6.45E+05	5.63E+05	8.73E+05	55.9	56.7	55.9	55.9	56.7	55.9
A0A0G2K2D9	N/A	Uncharacterized protein	11.67	1	1	1	1	1	1	1	1	1	1	1	1	7.45E+04	4.51E+05	2.94E+03	4.04E+05	5.55E+05	1.45E+04	15.2	15.2	15.2	15.2	15.2	15.2
P83121	N/A	Urinary protein 3	11.10	2	2	2	2	2	1	2	2	2	2	2	1	1.00E+06	3.40E+05	4.51E+05	8.29E+05	5.10E+05	3.38E+05	32.7	32.7	32.7	32.7	32.7	13.9
M0R693	N/A	Uncharacterized protein	12.71	2	2	2	2	2	1	2	2	2	2	2	1	1.18E+05	2.90E+05	9.25E+04	1.25E+05	5.09E+05	8.90E+02	41.9	41.9	41.9	41.9	41.9	20.5
M0R789	N/A	Uncharacterized protein	10.49	1	1	1	1	1	1	1	1	1	1	1	1	3.06E+05	4.87E+05	9.68E+05	2.49E+05	4.60E+05	1.93E+06	19.6	19.6	19.6	19.6	19.6	19.6
F1M3X3	N/A	Uncharacterized protein	13.01	3	3	3	3	3	3	1	1	1	1	1	1	1.75E+05	1.50E+05	5.20E+05	1.15E+05	4.21E+05	8.49E+05	32.5	32.5	32.5	32.5	32.5	32.5
F1LYF1	N/A	Uncharacterized protein	15.28	3	5	4	5	4	3	2	3	2	3	3	3	1.76E+05	2.88E+05	6.11E+05	4.89E+05	4.13E+05	6.64E+04	27.1	27.9	27.9	27.9	27.9	27.9
A0A0G2JUY3	N/A	Uncharacterized protein	12.74	2	3	2	3	3	2	2	3	2	3	3	2	2.62E+05	6.46E+05	5.02E+04	5.23E+05	3.82E+05	2.17E+05	18.3	31.3	31.3	31.3	31.3	31.3
A0A0G2K4W9	N/A	Uncharacterized protein	12.89	2	3	3	3	2	3	2	3	3	3	2	3	1.17E+05	5.61E+05	4.55E+05	2.97E+05	3.57E+05	6.78E+05	20.8	34.2	34.2	34.2	20.8	34.2
A0A0G2JZS9	N/A	Uncharacterized protein	10.81	1	1	1	1	1	1	1	1	1	1	1	1	5.98E+04	5.71E+05	5.42E+05	1.03E+05	3.55E+05	2.40E+05	15.5	15.5	15.5	15.5	15.5	15.5
D4A3L8	N/A	Uncharacterized protein	14.69	2	3	2	3	3	3	2	3	2	3	3	3	2.88E+05	1.60E+05	1.59E+05	7.73E+05	3.31E+05	2.28E+05	17.4	28.8	17.4	28.8	28.8	28.8
A0A0G2K3K8	N/A	Uncharacterized protein	12.40	2	2	1	2	2	1	2	2	1	2	2	1	2.40E+05	2.33E+06	3.41E+04	2.67E+05	3.11E+05	2.91E+04	20.7	20.7	20.7	20.7	20.7	20.7
A0A0G2K0M4	N/A	Uncharacterized protein	10.18	1	1	2	2	2	2	1	1	2	2	2	2	2.90E+05	1.22E+05	4.70E+05	2.41E+05	2.92E+05	5.68E+05	18.3	18.3	25.8	25.8	25.8	25.8
M0R4C5	N/A	Uncharacterized protein	14.57	1	2	1	1	1	1	1	2	1	1	1	1	3.06E+05	2.11E+06	5.34E+05	2.02E+05	2.63E+05	7.54E+05	6.7	11.9	6.7	6.7	6.7	6.7
D3ZZ08	N/A	Uncharacterized protein	13.19	2	2	2	2	2	2	2	2	2	2	2	2	3.83E+05	2.96E+05	3.73E+05	6.90E+05	2.55E+05	4.46E+05	24.2	24.2	24.2	24.2	24.2	24.2
F1MAE7	N/A	Uncharacterized protein	12.26	2	3	1	3	3	2	2	3	1	3	3	2	3.32E+05	4.40E+06	1.37E+05	9.59E+05	2.36E+05	2.37E+05	20.5	26.5	7.7	26.5	26.5	26.5
F1M2W3	N/A	Uncharacterized protein	14.78	2	1	1	1	2	1	2	1	1	1	2	1	2.13E+05	1.85E+04	2.30E+05	3.39E+04	2.34E+05	4.16E+03	15.6	15.6	11.1	11.1	15.6	11.1
M0R7Q2	N/A	Uncharacterized protein	13.15	3	3	2	3	3	2	3	3	2	3	3	2	2.18E+05	2.41E+05	5.51E+05	6.10E+05	2.11E+05	1.11E+06	30.8	30.8	21.4	30.8	30.8	21.4
A0A0G2JZL1	N/A	Uncharacterized protein	14.95	2	2	2	3	2	2	2	2	2	3	2	2	3.65E+05	2.06E+05	5.74E+05	9.25E+05	1.98E+05	8.08E+05	13.5	13.5	13.5	23.3	13.5	13.5
A0A0G2K5X3	N/A	Uncharacterized protein	13.32	2	2	1	1	2	2	2	2	1	1	2	2	1.42E+05	1.85E+05	8.14E+04	3.24E+04	1.78E+05	9.16E+04	17.5	17.5	10.8	10.8	17.5	17.5
A0A0G2K304	N/A	Uncharacterized protein	12.59	2	3	2	2	3	3	0	1	0	0	1	1	6.96E+04	2.05E+05	1.27E+05	3.41E+05	1.75E+05	1.61E+05	19	19	19	19	19	19
A0A0G2K8K8	N/A	Uncharacterized protein	13.45	4	5	3	4	3	3	4	5	3	4	3	3	5.44E+05	2.84E+06	5.80E+05	4.00E+05	1.44E+05	2.54E+05	57.9	71.1	47.9	57.9	47.9	41.3
A0A0G2K7S9	N/A	Uncharacterized protein	13.00	2	2	2	2	2	2	1	1	1	1	1	1	7.96E+04	6.92E+04	2.36E+05	1.42E+05	1.39E+05	1.93E+05	22.2	22.2	22.2	22.2	22.2	22.2
D3ZMS7	N/A	Uncharacterized protein	12.72	1	0	0	1	1	0	1	0	0	1	1	0	1.28E+05	0.00E+00	0.00E+00	1.88E+05	1.36E+05	0.00E+00	7	0	0	7	7	0
A0A0G2JT70	N/A	Uncharacterized protein	10.36	3	3	3	3	3	3	1	1	1	1	1	1	5.73E+04	7.44E+04	1.27E+05	4.23E+04	1.32E+05	1.87E+05	41.7	41.7	41.7	41.7	41.7	41.7
A0A0G2K9Z5	N/A	Uncharacterized protein	13.03	4	4	3	4	3	3	3	3	2	3	2	2	2.67E+04	1.05E+05	1.52E+05	1.10E+05	9.73E+04	1.34E+05	42.4	42.4	42.4	42.4	35.6	42.4
A0A0G2JY98	N/A	Uncharacterized protein	15.38	2	5	3	3	4	1	0	2	0	0	2	0	2.67E+04	3.97E+04	4.03E+04	3.76E+04	9.25E+04	3.31E+04	18.6	33.6	19.3	19.3	33.6	7.9
P81827	N/A	Urinary protein 1	10.96	1	1	1	1	1	1	1	1	1	1	1	1	5.28E+05	1.72E+05	6.72E+05	1.15E+06	9.01E+04	9.13E+05	10.9	10.9	10.9	10.9	10.9	10.9
A0A0G2K7I1	N/A	Uncharacterized protein	10.15	0	2	2	1	1	1	0	2	2	1	1	1	0.00E+00	3.46E+05	1.02E+05	2.24E+03	7.54E+04	4.55E+04	0	35.4	35.4	18.8	18.8	18.8
F1LN61	N/A	Uncharacterized protein	50.38	16	17	16	17	17	17	1	1	0	1	1	1	8.86E+02	4.12E+04	8.38E+04	5.14E+04	6.06E+04	1.27E+05	54.4	56.4	52.9	56.4	56.4	56.4
M0RBX3	N/A	Uncharacterized protein	13.05	2	2	2	2	2	2	2	2	2	2	2	2	9.94E+04	9.73E+04	8.80E+04	1.81E+05	4.70E+04	7.18E+04	21.4	21.4	21.4	21.4	21.4	21.4
M0R845	N/A	Uncharacterized protein	12.49	1	2	2	1	2	2	1	1	1	0	1	1	9.08E+04	1.13E+05	9.03E+03	0.00E+00	4.63E+04	6.07E+03	9.9	18	18	8.1	18	18
D3ZME3	N/A	Uncharacterized protein	33.43	2	3	3	2	2	3	1	1	1	1	1	1	4.18E+04	2.88E+04	1.20E+04	6.58E+03	4.44E+04	2.02E+04	10.3	12.9	12.9	10.3	10.3	12.9
M0R692	N/A	Uncharacterized protein	10.86	7	6	6	7	5	7	1	1	1	1	1	1	1.58E+05	4.64E+04	1.53E+05	1.04E+05	4.44E+04	7.00E+04	88.8	88.8	81.6	88.8	81.6	88.8
M0RDL2	N/A	Uncharacterized protein	11.27	3	3	3	2	3	3	1	1	1	0	1	1	0.00E+00	1.04E+05	5.08E+04	0.00E+00	3.26E+04	1.29E+05	30.4	30.4	30.4	19.6	30.4	30.4
A0A0G2K828	N/A	Uncharacterized protein	13.22	3	3	2	3	3	2	2	2	1	2	2	1	1.09E+05	3.82E+04	2.47E+04	6.10E+04	2.63E+04	1.81E+05	33.6	33.6	16.8	33.6	33.6	16.8
F1M5L5	N/A	Uncharacterized protein	12.91	2	2	2	2	2	2	1	1	1	1	1	1	1.54E+05	1.31E+05	7.87E+04	7.91E+04	1.54E+04	5.66E+04	25.6	25.6	25.6	25.6	25.6	25.6
P56571	N/A	ES1 protein homolog, mitochondrial	28.17	1	2	2	1	1	2	1	2	2	1	1	2	2.57E+03	5.34E+04	1.73E+04	2.10E+03	4.70E+03	1.27E+04	9.4	13.2	13.2	9.4	9.4	13.2
A0A0G2K458	N/A	Uncharacterized protein	12.65	1	0	1	0	1	1	1	0	1	0	1	1	5.00E+03	0.00E+00	1.17E+05	0.00E+00	4.16E+03	1.97E+05	12.2	0	12.2	0	12.2	12.2
Q498R7	N/A	UPF0587 protein C1orf123 homolog	18.09	1	1	1	1	0	1	1	1	1	1	0	1	9.91E+04	6.35E+04	1.16E+04	4.81E+04	0.00E+00	2.30E+04	10.6	10.6	10.6	10.6	0	10.6
Q66H24	N/A	Uncharacterized protein C9orf40 homolog	18.15	1	1	0	2	0	0	1	1	0	2	0	0	5.84E+03	4.33E+04	0.00E+00	1.86E+04	0.00E+00	0.00E+00	22.9	22.9	0	30.1	0	0
D3ZD89	Naa15	N(alpha)-acetyltransferase 15, NatA auxiliary subunit	101.01	3	3	1	2	2	1	3	3	1	2	2	1	7.27E+03	1.92E+04	4.18E+03	3.98E+03	5.18E+03	7.11E+02	3.1	3.1	1	2	2	1
M0R9L0	Naca	Nascent polypeptide-associated complex subunit alpha	220.19	4	2	3	4	4	2	4	2	3	4	4	2	2.19E+04	4.01E+04	8.94E+03	2.59E+04	2.07E+04	2.27E+03	2.6	1.3	2	2.6	2.6	1.3
F1M7W7	Nae1	NEDD8-activating enzyme E1 regulatory subunit	60.42	3	5	4	2	4	3	3	5	4	2	4	3	8.46E+04	9.18E+04	1.05E+06	4.74E+04	3.78E+04	7.51E+05	6.9	12.9	12.9	4.7	7.5	7.5
A0A0G2K0I3	Nampt	Nicotinamide phosphoribosyltransferase	54.09	8	8	5	6	6	6	8	8	5	6	6	6	1.02E+05	1.70E+05	3.60E+04	7.37E+04	4.28E+04	4.26E+04	30.1	27.4	19.2	20.5	16.9	21.5
B1WC26	Nans	N-acetylneuraminate synthase	40.05	8	8	5	6	6	3	8	8	5	6	6	3	3.85E+05	4.96E+05	1.45E+05	1.45E+05	1.26E+05	1.35E+05	35.9	28.1	20.1	23.1	24.8	12.5
G3V6H9	Nap1l1	Nucleosome assembly protein 1-like 1	45.37	7	9	9	9	9	7	7	8	8	8	8	6	4.24E+05	8.42E+05	3.33E+05	3.05E+05	3.44E+05	1.31E+05	34.8	37.3	37.3	37.3	37.3	32.5
A0A0H2UHZ2	Nap1l4	Nucleosome assembly protein 1-like 4	44.04	5	8	5	7	6	5	5	7	4	6	5	4	1.98E+05	3.33E+05	1.37E+05	1.48E+05	9.74E+04	4.93E+04	23	28.4	18.3	28.4	25.6	18.3
P54921	Napa	Alpha-soluble NSF attachment protein	33.19	0	2	1	2	4	0	0	2	1	2	4	0	0.00E+00	1.98E+04	3.32E+03	3.09E+04	2.78E+04	0.00E+00	0	11.2	7.8	11.2	20.3	0
A0A0G2K350	Napg	NSF attachment protein gamma	34.66	2	2	2	2	1	1	2	2	2	2	1	1	1.77E+04	3.82E+04	1.61E+04	1.41E+04	4.48E+03	2.81E+03	9.9	9.9	9.9	9.9	5.4	4.5
G3V709	Naprt	Nicotinate phosphoribosyltransferase	58.60	2	3	1	3	3	2	2	3	1	3	3	2	1.50E+04	1.46E+04	1.08E+03	6.62E+03	4.96E+03	5.52E+03	5	7.4	2.4	7.4	6.7	4.1
F1LPV0	Nars	Asparaginyl-tRNA synthetase	64.13	10	11	8	10	9	7	10	11	8	10	9	7	3.06E+05	3.52E+05	1.34E+05	1.79E+05	8.70E+04	7.73E+04	26	27.1	21.3	26	23.3	17.9
Q66HD3	Nasp	Nuclear autoantigenic sperm protein	84.20	9	9	12	10	8	7	9	9	12	10	8	7	8.96E+04	1.83E+05	1.67E+05	7.90E+04	3.24E+04	3.39E+04	22.2	22.3	25	22.2	20.1	16.2
P50297	Nat1	Arylamine N-acetyltransferase 1	33.44	2	3	3	3	3	3	2	3	3	3	3	3	6.89E+04	1.77E+05	9.80E+04	1.15E+05	6.45E+04	4.40E+04	9.3	12.4	12.4	12.4	12.4	12.4
F1LUV9	Ncam1	Neural cell adhesion molecule 1	91.64	5	4	6	6	7	4	5	4	6	6	7	4	6.02E+04	7.04E+04	5.07E+04	8.99E+04	6.37E+04	7.20E+04	8.3	6.2	10.1	10.2	11.4	6.7
Q5U328	Ncl	Nucleolin	77.28	0	2	3	1	0	2	0	2	3	1	0	2	0.00E+00	1.37E+04	3.48E+04	4.83E+03	0.00E+00	2.12E+03	0	6.3	7.1	1.7	0	3.9
Q6JE36	Ndrg1	Protein NDRG1	42.95	7	8	6	6	8	4	7	8	6	6	8	4	2.24E+05	5.00E+05	2.08E+05	5.94E+04	8.51E+04	1.13E+05	37.8	38.3	34.3	34	38.3	20.1
A0A0G2JSU4	Ndrg2	Protein NDRG2	39.26	9	10	8	9	9	4	9	10	8	9	9	4	2.54E+05	5.60E+05	1.87E+05	2.72E+05	1.46E+05	9.64E+04	45.9	45.9	31.1	39.8	43.1	18.5
A0A096MK15	Neb	Nebulin	772.09	6	6	4	4	6	6	6	6	4	4	6	6	1.39E+05	1.31E+05	3.84E+04	5.56E+04	2.51E+05	6.08E+04	1.3	1.4	0.9	0.9	1.1	1.3
A0A0G2K0B4	Nedd4	E3 ubiquitin-protein ligase NEDD4	102.43	7	7	5	6	6	5	7	7	5	6	6	5	7.25E+04	6.78E+04	5.44E+04	3.65E+04	3.94E+04	5.17E+04	11.7	11.7	9.6	9.7	10.2	9.6
P97603	Neo1	Neogenin	150.64	9	9	10	9	9	11	9	9	10	9	9	11	9.91E+04	4.93E+04	5.66E+04	7.61E+04	6.86E+04	5.08E+04	10.4	10.4	12.6	10.4	10.4	13.5

Uniprot accession number	Gene symbol	Protein name	Mol. weight [kDa]	No. Peptides Control wk1	No. Peptides Control wk8	No. Peptides Control wk14	No. Peptides Heat wk1	No. Peptides Heat wk8	No. Peptides Heat wk14	No. Unique peptides Control wk1	No. Unique peptides Control wk8	No. Unique peptides Control wk14	No. Unique peptides Heat wk1	No. Unique peptides Heat wk8	No. Unique peptides Heat wk14	iBAQ Control wk1	iBAQ Control wk8	iBAQ Control wk14	iBAQ Heat wk1	iBAQ Heat wk8	iBAQ Heat wk14	Sequence coverage Control wk1 [%]	Sequence coverage Control wk8 [%]	Sequence coverage Control wk14 [%]	Sequence coverage Heat wk1 [%]	Sequence coverage Heat wk8 [%]	Sequence coverage Heat wk14 [%]
F1LM84	Nid1	Nidogen-1	137.04	15	14	14	12	18	14	15	14	14	12	18	14	1.55E+05	1.09E+05	1.35E+05	9.24E+04	1.67E+05	1.39E+05	16.2	15.6	16.8	13.4	21.5	17.6
Q7TQ94	Nit1	Nitrilase homolog 1	36.09	11	12	12	12	13	10	11	12	12	12	13	10	4.55E+05	6.04E+05	4.19E+05	3.51E+05	2.73E+05	1.91E+05	55.4	58.7	59.6	59.6	63	54.4
Q497B0	Nit2	Omega-amidase NIT2	30.70	3	3	2	3	2	1	3	3	2	3	2	1	8.00E+04	7.34E+04	6.28E+04	8.06E+04	4.86E+04	4.70E+04	19.6	19.6	12	19.6	13	5.4
P19804	Nme2	Nucleoside diphosphate kinase B	17.28	5	5	5	6	5	4	5	5	5	6	5	4	8.25E+05	9.61E+05	6.42E+05	6.95E+05	5.82E+05	3.26E+05	47.4	47.4	46.7	56.6	46.7	34.2
G3V816	Nme3	Nucleoside diphosphate kinase	19.12	1	1	1	1	1	1	1	1	1	1	1	1	1.19E+04	6.75E+03	4.81E+04	1.90E+04	3.20E+04	2.65E+04	10.1	10.1	10.1	10.1	10.1	10.1
A0A0G2K5K3	Nmral1	NmrA-like family domain-containing protein 1	33.11	1	1	1	1	1	1	1	1	1	1	1	1	8.44E+04	1.36E+05	4.71E+04	1.51E+04	1.32E+04	3.02E+04	5.4	5.4	5.4	5.4	5.4	5.4
Q8K1Q0	Nmt1	Glycylpeptide N-tetradecanoyltransferase 1	56.86	2	2	2	2	2	2	2	2	2	2	2	2	2.25E+04	2.77E+04	1.21E+04	1.15E+04	1.52E+04	3.91E+03	5.2	5.2	5.2	5.2	5.2	5.2
Q5FVM4	Nono	Non-POU domain-containing octamer-binding protein	54.93	1	1	1	1	1	1	1	1	1	1	1	1	1.44E+04	1.93E+04	9.80E+03	7.55E+03	1.49E+04	6.91E+03	2.9	2.9	2.9	2.9	2.9	2.9
F1LQX7	Notch3	Neurogenic locus notch homolog protein 3	244.21	2	2	2	2	2	2	2	2	2	2	2	2	5.11E+03	4.09E+03	4.34E+03	2.88E+03	5.31E+03	2.65E+03	1.1	1.1	1.1	1.1	1.1	1.1
F1M9V7	Npepps	Aminopeptidase	103.34	17	19	15	16	17	13	17	19	15	16	17	13	2.62E+05	2.83E+05	1.00E+05	1.56E+05	1.25E+05	6.55E+04	26.3	30.2	25.8	25.3	26.3	21.2
Q66H59	Npl	N-acetylneuraminate lyase	35.12	3	4	2	4	3	3	3	4	2	4	3	3	4.96E+04	6.75E+04	7.34E+04	6.38E+04	3.21E+04	2.15E+04	14.7	18.1	6.9	18.1	14.7	10.6
F1LQX9	Nploc4	Nuclear protein localization protein 4 homolog	68.13	2	3	0	2	2	1	2	3	0	2	2	1	2.08E+04	3.46E+04	0.00E+00	7.62E+03	7.23E+03	2.19E+03	5.3	6.9	0	5.3	5.3	3
P13084	Npm1	Nucleophosmin	32.56	4	4	5	3	4	2	4	4	5	3	4	2	3.89E+05	2.85E+05	2.38E+05	8.25E+04	1.60E+05	1.66E+04	29.8	24.7	31.2	20.2	24.7	12
G3V700	Nrd1	Nardilysin	133.00	13	17	14	14	12	6	13	17	14	14	12	6	6.45E+04	2.53E+05	6.75E+04	9.46E+04	4.73E+04	6.02E+03	16	21.5	18.2	16.4	15.8	6.6
F1LQ81	Nsf	Vesicle-fusing ATPase	82.63	11	12	7	10	10	7	11	12	7	10	10	7	8.31E+04	1.37E+05	4.29E+04	8.11E+04	3.42E+04	2.06E+04	16.9	18.5	11.4	16.9	15.7	11.4
A0A0G2K911	Nsfl1c	NSFL1 cofactor p47	37.25	6	8	7	7	7	7	6	8	7	7	7	7	1.21E+05	1.92E+05	1.64E+05	1.08E+05	1.05E+05	5.12E+04	29.4	35.9	32.6	32.6	32.6	32.6
D3ZMY7	Nt5c2	5'-nucleotidase, cytosolic II	67.76	2	2	1	2	2	0	2	2	1	2	2	0	2.95E+04	4.26E+04	5.06E+03	2.07E+04	9.06E+03	0.00E+00	5.1	5.1	2.9	5.1	5.1	0
Q6AYP7	Nt5c3b	7-methylguanosine phosphate-specific 5-nucleotidase	34.54	6	7	5	5	5	5	6	7	5	5	5	5	1.38E+05	2.46E+05	4.88E+04	9.64E+04	8.54E+04	3.16E+04	27.7	31.3	22.7	24.3	24.3	22.7
Q5BJX0	Ntmt1	N-terminal Xaa-Pro-Lys N-methyltransferase 1	25.46	2	2	2	2	2	2	2	2	2	2	2	2	8.51E+05	8.87E+05	7.56E+05	8.15E+05	9.74E+05	6.03E+05	17.9	17.9	17.9	17.9	17.9	17.9
F7ES73	Nub1	Negative regulator of ubiquitin-like proteins 1	70.06	1	1	0	1	1	0	1	1	0	1	1	0	6.58E+03	1.77E+04	0.00E+00	2.19E+03	4.35E+03	0.00E+00	3.4	3.4	0	3.4	3.4	0
Q5I0L4	Nubp1	Cytosolic Fe-S cluster assembly factor NUBP1	34.05	2	2	1	2	2	0	2	2	1	2	2	0	3.47E+04	1.30E+05	3.92E+03	4.36E+04	1.99E+04	0.00E+00	11.2	11.2	5.6	11.2	11.2	0
Q63083	Nucb1	Nucleobindin-1	53.51	7	6	5	7	6	6	7	6	5	7	6	6	1.88E+05	1.34E+05	1.03E+05	1.44E+05	9.38E+04	8.46E+04	22.9	19.4	14.2	22.7	20.7	19.6
G3V8R1	Nucb2	Nucleobindin-2	50.12	6	6	3	6	6	5	6	6	3	6	6	5	5.52E+05	5.45E+05	8.17E+04	4.23E+05	4.18E+05	7.06E+04	21.4	20.5	10.7	22.4	22.4	18.3
A0A0G2K0V8	Nudc	Nuclear migration protein nudC	32.40	8	8	7	9	8	6	8	8	7	9	8	6	3.99E+05	5.25E+05	2.34E+05	2.96E+05	1.87E+05	9.35E+04	37.3	37.3	35.5	41.2	35.8	31.2
Q5M823	Nudcd2	NudC domain-containing protein 2	17.67	2	2	1	2	2	1	2	2	1	2	2	1	1.30E+05	1.77E+05	2.13E+05	1.31E+05	3.01E+04	1.90E+03	18.5	18.5	7	18.5	18.5	11.5
D3ZYH3	Nudt10	Nudix hydrolase 11	18.59	5	6	4	4	4	2	5	6	4	4	4	2	3.78E+05	9.99E+05	1.56E+05	3.36E+05	2.28E+05	7.05E+04	47	47	42.7	42.7	42.7	22
D4A1D4	Nudt14	Nudix (Nucleoside diphosphate linked moiety X)-type motif 14	24.43	2	2	2	2	2	1	2	2	2	2	2	1	2.57E+05	4.40E+05	1.41E+05	1.24E+05	8.62E+04	3.24E+04	14	14	14	14	14	7.7
Q6AY63	Nudt5	ADP-sugar pyrophosphatase	24.12	5	5	2	5	5	2	5	5	2	5	5	2	2.14E+05	3.86E+05	6.43E+04	2.07E+05	6.44E+04	4.31E+04	20.5	20.5	7.3	20.5	20.5	7.3
P61972	Nutf2	Nuclear transport factor 2	14.48	4	4	4	4	4	4	4	4	4	4	4	4	1.34E+06	1.71E+06	1.03E+06	1.05E+06	1.08E+06	6.93E+05	51.2	51.2	51.2	51.2	51.2	51.2
Q6AYE5	Oaf	Out at first protein homolog	31.78	2	2	4	4	3	2	2	2	4	4	3	2	1.33E+05	7.57E+04	1.34E+05	1.51E+05	7.10E+04	7.60E+04	6	6	11.7	10.6	7.1	6.4
P21769	Odf1	Outer dense fiber protein 1	27.35	3	2	2	2	0	1	3	2	2	2	0	1	3.30E+04	6.35E+04	2.93E+04	3.45E+04	0.00E+00	6.77E+03	13.1	9.8	9.8	9.8	0	5.3
G3V7X0	Odf2	Outer dense fiber protein 2	81.35	5	5	5	4	2	2	5	5	5	4	2	2	1.86E+04	2.08E+04	1.82E+04	2.07E+04	2.26E+03	2.40E+03	9.1	9.1	9.1	7.5	3.8	3.8
D3ZVB7	Ogn	Osteoglycin	34.07	6	6	3	6	5	2	6	6	3	6	5	2	5.98E+05	3.64E+05	3.74E+05	5.07E+05	2.83E+05	2.82E+05	25.8	25.8	16.8	25.8	24.2	10.4
A0JPJ7	Ola1	Obg-like ATPase 1	44.54	5	6	6	5	4	5	5	6	6	5	4	5	7.37E+04	1.39E+05	9.38E+04	5.57E+04	3.04E+04	5.17E+04	17.4	24.2	24.2	17.4	14.1	21.5
G3V8H7	Olfml3	Olfactomedin-like protein 3	47.22	3	3	1	3	3	1	3	3	1	3	3	1	7.94E+04	3.04E+04	2.32E+04	5.79E+04	3.46E+04	1.62E+04	12	12	2.9	12	12	2.9
G3V7Y2	Omd	Osteomodulin	49.69	3	3	4	4	4	3	3	3	4	4	4	3	5.60E+05	1.62E+05	1.66E+05	4.03E+05	1.35E+05	1.82E+05	12.1	13.2	15.6	15.6	15.6	12.1
A0A0H2UHF8	Orm1	Alpha-1-acid glycoprotein	26.71	1	0	2	1	1	2	1	0	2	1	1	2	9.34E+03	0.00E+00	3.12E+05	8.50E+04	3.68E+04	2.44E+05	3.8	0	6	3.8	3.8	6
D4A9D8	Osbp	Oxysterol-binding protein	77.81	2	3	2	3	2	2	2	3	2	3	2	2	2.89E+04	4.93E+04	1.16E+04	1.85E+04	9.12E+03	7.93E+03	4.1	6.7	4.1	5.9	4.1	4.1
Q4QQS3	Oscp1	Protein OSCP1	43.31	1	1	1	1	1	0	1	1	1	1	1	0	9.02E+03	1.01E+04	1.29E+04	1.68E+03	1.75E+03	0.00E+00	3.2	3.2	3.2	3.2	3.2	0
Q9WVS2	Osgep	Probable tRNA N6-adenosine threonylcarbamoyltransferase	36.36	6	6	5	4	6	3	6	6	5	4	6	3	5.80E+04	8.41E+04	3.41E+04	2.88E+04	2.40E+04	2.12E+04	25.4	25.4	20.6	16.4	25.4	11.9
Q6P686	Ostf1	Osteoclast-stimulating factor 1	23.67	3	3	1	3	2	0	3	3	1	3	2	0	1.02E+05	1.79E+05	6.80E+03	7.34E+04	4.91E+04	0.00E+00	26.6	26.6	12.1	26.6	17.8	0
B2RYG6	Otub1	Ubiquitin thioesterase OTUB1	31.27	10	10	9	10	9	8	10	10	9	10	9	8	3.83E+05	5.08E+05	4.48E+05	4.60E+05	3.00E+05	1.91E+05	57.2	57.2	53.9	57.2	50.6	50.9
D3ZUC9	Oxsr1	Oxidative-stress responsive 1	58.20	3	3	1	2	2	0	2	2	0	1	1	0	2.49E+04	4.62E+04	4.99E+03	2.28E+04	1.60E+04	0.00E+00	10.4	10.4	3.4	6.3	7.6	0
P04785	P4hb	Protein disulfide-isomerase	56.95	11	11	8	11	10	10	11	11	8	11	10	10	6.50E+05	3.96E+05	2.88E+05	2.33E+05	2.28E+05	2.26E+05	31.6	31.2	24.8	32.4	30.1	28.7
Q6AYD3	Pa2g4	Proliferation-associated protein 2G4	43.66	8	6	7	6	8	5	8	6	7	6	8	5	8.56E+04	1.03E+05	3.99E+04	3.39E+04	7.99E+04	1.64E+04	23.4	18	20.8	15.2	23.9	12.4
Q9EPH8	Pabpc1	Polyadenylate-binding protein 1	70.70	19	20	16	17	18	9	12	13	11	12	12	5	3.26E+05	5.19E+05	2.33E+05	2.63E+05	2.18E+05	4.30E+04	37.9	42.5	33.3	34.9	36.2	20.6
B5DF80	Pabpc6	Polyadenylate-binding protein	71.03	10	12	9	7	9	6	3	5	4	2	3	2	1.38E+04	6.68E+04	2.66E+04	5.47E+03	1.09E+04	1.45E+03	20.7	27.1	22.6	15.1	19	13.7
Q9QY17	Pacsin2	Protein kinase C and casein kinase substrate in neurons 2 protein	55.98	3	3	3	4	2	3	3	3	3	4	2	3	3.32E+04	9.28E+04	7.30E+04	4.10E+04	2.99E+04	4.25E+04	7	7	7	9.2	4.7	7
P63004	Pafah1b1	Platelet-activating factor acetylhydrolase IB subunit alpha	46.67	4	4	4	4	5	3	4	4	4	4	5	3	7.07E+04	6.97E+04	6.17E+04	6.16E+04	6.78E+04	2.13E+04	13.7	13.7	12	13.7	17.8	9.3
O35264	Pafah1b2	Platelet-activating factor acetylhydrolase IB subunit beta	25.58	7	7	7	6	7	6	7	7	7	6	7	6	1.62E+06	2.41E+06	1.56E+06	9.20E+05	8.87E+05	7.33E+05	60.7	60.7	60.7	59.4	60.7	59.4
O35263	Pafah1b3	Platelet-activating factor acetylhydrolase IB subunit gamma	25.86	1	1	2	1	1	1	1	1	2	1	1	1	1.72E+04	1.60E+04	1.62E+04	2.10E+04	1.15E+04	6.75E+03	9.5	9.5	12.9	9.5	9.5	9.5
P04176	Pah	Phenylalanine-4-hydroxylase	51.82	22	26	21	24	23	17	22	26	21	24	23	17	8.02E+05	2.13E+06	3.49E+05	1.18E+06	7.18E+05	1.89E+05	63.4	65.6	62.7	60.7	60.7	47.5
P51583	Paics	Multifunctional protein ADE2	47.10	8	8	4	7	7	2	8	8	4	7	7	2	3.32E+05	6.24E+05	1.82E+05	4.10E+05	2.66E+05	1.58E+05	25.6	22.4	14.6	23.1	23.1	8.5
D3ZZF8	Paip1	Poly(A)-binding protein-interacting protein 1	42.06	3	3	2	2	1	2	3	3	2	2	1	2	5.50E+04	1.30E+05	9.08E+04	7.48E+04	2.91E+04	3.91E+04	11.4	12.3	6.3	6.3	3.3	6.3
Q64303	Pak2	Serine/threonine-protein kinase PAK 2	57.96	4	4	2	4	3	2	4	4	2	4	3	2	1.21E+05	1.74E+05	2.86E+04	5.88E+04	5.18E+04	1.76E+04	9.4	9.4	5	9.4	6.1	5
F1M265	Palld	Palladin	108.34	1	2	0	0	0	0	1	2	0	0	0	0	1.72E+03	7.23E+03	0.00E+00	0.00E+00	0.00E+00	0.00E+00	1.3	2.2	0	0	0	0
D3ZD40	Papln	Papilin, proteoglycan-like sulfated glycoprotein	138.60	7	6	7	7	8	7	7	6	7	7	8	7	4.25E+04	2.84E+04	7.65E+04	3.34E+04	4.24E+04	1.42E+05	7.7	6.4	8.2	7.8	9	8.2
O88767	Park7	Protein deglycase DJ-1	19.97	7	9	6	6	7	5	7	9	6	6	7	5	1.42E+06	2.96E+06	1.53E+06	1.08E+06	9.54E+05	7.03E+05	67.2	67.7	55	55	67.2	48.1
Q5U2U3	Parp3	Poly [ADP-ribose] polymerase	58.87	2	2	0	1	1	0	2	2	0	1	1	0	2.02E+04	3.84E+04	0.00E+00	1.09E+04	1.00E+04	0.00E+00	4	4	0	2.3	2.3	0
G3V818	Parva	Alpha-parvin	42.32	5	5	5	5	5	3	5	5	5	5	5	3	1.35E+05	1.85E+05	7.39E+04	5.84E+04	5.18E+04	2.03E+04	16.4	16.4	16.4	16.4	16.4	11.8
Q6AYU5	Pcbp2	Poly(rC)-binding protein 2	38.58	9	8	8	9	9	9	7	5	5	7	6	6	3.33E+05	6.47E+05	4.49E+05	4.07E+05	2.61E+05	1.76E+05	46	41.1	35.6	46	44.1	44.1
Q6AY48	Pcbp3	Poly(rC)-binding protein 3	33.78	5	6	4	4	5	3	3	3	1	2	2	0	4.32E+04	6.76E+04	2.69E+03	2.14E+04	6.41E+03	0.00E+00	24.1	28.5	17.9	17.6	21.9	14.1
A0A140TAB9;P22062	Pcmt1	Protein-L-isoaspartate(D-aspartate) O-methyltransferase	21.19	3	2	1	3	1	2	3	2	1	3	1	2	1.33E+05	1.13E+05	2.26E+04	1.01E+05	6.53E+04	1.24E+04	35.2	29.6	5.6	35.2	9.7	15.3
P04961	Pcna	Proliferating cell nuclear antigen	28.75	1	2	1	1	2	1	1	2	1	1	2	1	2.35E+04	9.72E+04	2.25E+04	2.59E+04	2.26E+04	1.28E+03	8	13	8	8	13	8
A0A0H2UHW4	Pcnp	PEST proteolytic signal-containing nuclear protein	20.08	1	1	1	2	1	1	1	1	1	2	1	1	4.79E+03	2.06E+04	1.26E+04	2.82E+03	8.69E+02	3.77E+03	9	9	6.9	9	9	6.9
Q5RJN2	Pcolce	Procollagen C-endopeptidase enhancer 1	53.15	13	13	11	13	13	10	13	13	11	13	13	10	2.49E+06	6.48E+05	6.14E+05	1.03E+06	9.05E+05	5.19E+05	43.8	43.8	43.8	43.8	43.8	40.2
G3V6X7	Pcsk1n	ProSAAS	27.47	1	1	1	1	1	1	1	1	1	1	1	1	1.37E+04	2.13E+04	1.92E+04	1.94E+04	1.45E+04	6.92E+03	5.8	5.8	5.8	5.8	5.8	5.8
P41413	Pcsk5	Proprotein convertase subtilisin/kexin type 5	201.31	3	4	4	4	3	3	3	4	4	4	3	3	8.04E+03	1.50E+04	4.63E+03	1.14E+04	3.59E+03	5.65E+03	2.7	3.4	3.3	3.4	2.7	2.4
P59996	Pcsk9	Proprotein convertase subtilisin/kexin type 9	74.71	5	7	7	7	7	5	5	7	7	7	7	5	6.58E+04	5.31E+04	1.04E+05	8.37E+04	6.60E+04	5.92E+04	9	11.9	11.9	11.9	11.9	8.1
O88637	Pcyt2	Ethanolamine-phosphate cytidylyltransferase	45.22	2	1	0	2	1	0	2	1	0	2	1	0	7.88E+03	1.02E+04	0.00E+00	6.24E+03	2.24E+03	0.00E+00	5.2	3	0	5.2	3	0
Q62785	Pdap1	28 kDa heat- and acid-stable phosphoprotein	20.61	2	3	3	3	2	3	2	3	3	3	2	3	5.30E+04	1.47E+05	1.24E+05	7.76E+04	2.95E+04	6.64E+04	16	21.5	21.5	21.5	16	21.5
D3ZSC2	Pdcd2l	Programmed cell death 2-like	39.73	2	2	2	1	1	1	2	2	2	1	1	1	3.30E+04	5.14E+04	5.78E+04	1.22E+04	1.08E+03	2.51E+03	7.5	7.5	7.5	4.7	4.7	4.7
D4ADF5	Pdcd5	Programmed cell death 5	14.20	1	1	1	1	1	1	1	1	1	1	1	1	1.95E+05	3.23E+05	1.93E+05	1.69E+05	1.19E+05	7.77E+04	10.4	10.4	10.4	10.4	10.4	10.4
A0A140TAA4	Pdcd6ip	Programmed cell death 6-interacting protein	95.88	14	17	12	17	13	11	14	17	12	17	13	11	2.00E+05	3.11E+05	1.16E+05	1.94E+05	9.10E+04	3.67E+04	26.4	30.9	22	29	23.5	20.9
Q6TUH0	Pde12	2,5-phosphodiesterase 12	78.89	1	1	0	1	1	0	1	1	0	1	1	0	3.94E+03	1.05E+04	0.00E+00	4.81E+03	3.44E+03	0.00E+00	3.5	3.5	0	3.5	3.5	0
A0A0H2UHM5	Pdia3	Protein disulfide-isomerase A3	57.08	10	11	9	10	10	8	10	11	9	10	10	8	2.13E+05	1.45E+05	9.40E+04	6.55E+04	1.48E+05	6.63E+04	21.2	26.3	23.7	21.6	20.8	17.1
G3V6T7	Pdia4	Protein disulfide-isomerase A4	72.75	5	5	6	2	2	6	5	5	6	2	2	6	1.20E+05	1.37E+05	1.01E+05	9.26E+03	2.68E+04	4.44E+04	10.7	10.7	12.4	5.8	5.3	12.4
A0A0G2JSZ5	Pdia6	Protein disulfide-isomerase A6	48.76	7	8	7	6	7	8	7	8	7	6	7	8	6.82E+05	4.21E+05	2.18E+05	1.58E+05	1.49E+05	1.42E+05	25.8	28.1	24.5	20.2	25.8	27.9
P52944	Pdlim1	PDZ and LIM domain protein 1	35.58	4	3	3	3	2	2	4	3	3	3	2	2	6.11E+04	7.91E+04	4.38E+04	2.35E+05	1.11E+04	1.25E+04	15.3	11.3	11.9	11.6	7.6	8
Q6AYD6	Pdlim2	PDZ and LIM domain protein 2	37.58	5	6	3	6	4	3	5	6	3	6	4	3	1.28E+05	2.60E+05	6.99E+04	8.21E+04	8.61E+04	4.13E+04	18.3	18.3	11.2	18.3	14.3	11.2
A0A0G2JSM3	Pdlim3	PDZ and LIM domain protein 3	34.42	5	5	3	5	5	3	5	5	3	5	5	3	2.27E+05	3.66E+05	3.72E+04	6.53E+04	7.52E+04	2.43E+04	23.4	23.4	13	22.2	22.2	13
Q62920	Pdlim5	PDZ and LIM domain protein 5	63.20	4	5	5	5	5	4	4	5	5	5	5	4	4.05E+04	9.11E+04	3.28E+04	2.86E+04	2.87E+04	9.36E+03	9.3	11.3	11.3	11.3	11.3	8.6
B5DFK8	Pdxdc1	Pyridoxal-dependent decarboxylase domain-containing protein 1	86.80	0	0	0	1	0	0	0	0	0	1	0	0	0.00E+00	0.00E+00	0.00E+00	3.58E+03	0.00E+00	0.00E+00	0	0	0	2.4	0	0
Q5U318	Pea15	Astrocytic phosphoprotein PEA-15	15.04	4	4	4	5	4	4	4	4	4	5	4	4	1.05E+06	1.74E+06	1.23E+06	9.87E+05	5.53E+05	6.82E+05	34.6	34.6	34.6	42.3	34.6	42.3
P31044	Pebp1	Phosphatidylethanolamine-binding protein 1;Hippocampal cholinergic neurostimulating peptide	20.80	11	11	11	11	10	9	11	11	11	11	10	9	3.61E+06	6.97E+06	3.91E+06	2.92E+06	2.11E+06	1.25E+06	83.4	83.4	83.4	83.4	83.4	74.9
Q5I0D7	Pepd	Xaa-Pro dipeptidase	54.75	13	15	10	13	12	11	13	15	10	13	12	11	6.54E+05	5.94E+05	5.33E+05	6.18E+05	5.42E+05	4.39E+05	33.5	37.6	25.8	35.4	33.5	25.8
D3ZC81	Pex10	Peroxisomal biogenesis factor 10	37.11	1	1	1	1	1	1	1	1	1	1	1	1	5.10E+05	6.11E+05	5.32E+05	4.80E+05	4.78E+05	2.84E+05	3.4	3.4	3.4	3.4	3.4	3.4
A0A0G2JY69	Pex19	Peroxisomal biogenesis factor 19	31.86	4	4	3	3	3	1	4	4	3	3	3	1	4.47E+04	8.08E+04	2.55E+04	3.33E+04	1.97E+04	6.27E+03	24.6	24.6	18.8	18.4	18.4	6.1
A0A0G2JTN4	Pfas	Phosphoribosylformylglycinamidine synthase	144.39	10	11	11	11	11	9	10	11	11	11	11	9	9.81E+04	1.47E+05	6.50E+04	5.67E+04	5.51E+04	3.65E+04	12.4	13.7	13.7	13.7	13.7	11.9
B0BN18	Pfdn2	Prefoldin subunit 2	16.58	1	1	2	1	1	1	1	1	2	1	1	1	7.74E+04	9.95E+04	6.36E+04	5.35E+04	3.81E+04	3.50E+04	7.8	7.8	16.9	7.8	7.8	7.8
M0R5N4	Pfdn4	Prefoldin subunit 4	15.78	1	1	1	1	1	1	1	1	1	1	1	1	1.19E+05	3.09E+05	1.73E+05	2.05E+05	1.09E+05	6.22E+04	8.6	8.6	8.6	8.6	8.6	8.6
B5DFN4	Pfdn5	Prefoldin 5	17.33	4	5	3	5	5	3	4	5	3	5	5	3	2.67E+05	4.04E+05	1.12E+05	1.66E+05	8.18E+04	8.08E+04	37.7	42.9	27.9	42.9	42.9	27.9
P30835	Pfkl	ATP-dependent 6-phosphofructokinase, liver type	85.34	5	4	4	5	4	3	3	2	3	3	2	3	2.45E+04	1.12E+05	9.86E+04	6.38E+04	4.70E+04	7.71E+04	9.1	6.8	9.6	9.5	6.8	7.2
Q52KS1	Pfkm	ATP-dependent 6-phosphofructokinase	85.34	5	5	2	5	3	1	4	4	2	4	2	1	3.62E+04	2.29E+04	1.11E+04	2.18E+04	5.42E+03	2.69E+03	7.9	7.9	4.1	7.9	5.3	1.9

Uniprot accession number	Gene symbol	Protein name	Mol. weight [kDa]	No. Peptides Control wk1	No. Peptides Control wk8	No. Peptides Control wk14	No. Peptides Heat wk1	No. Peptides Heat wk8	No. Peptides Heat wk14	No. Unique peptides Control wk1	No. Unique peptides Control wk8	No. Unique peptides Control wk14	No. Unique peptides Heat wk1	No. Unique peptides Heat wk8	No. Unique peptides Heat wk14	iBAQ Control wk1	iBAQ Control wk8	iBAQ Control wk14	iBAQ Heat wk1	iBAQ Heat wk8	iBAQ Heat wk14	Sequence coverage Control wk1 [%]	Sequence coverage Control wk8 [%]	Sequence coverage Control wk14 [%]	Sequence coverage Heat wk1 [%]	Sequence coverage Heat wk8 [%]	Sequence coverage Heat wk14 [%]
P47860	Pfkp	ATP-dependent 6-phosphofructokinase, platelet type	85.72	15	16	10	15	13	6	13	14	9	13	11	6	2.32E+05	3.49E+05	1.27E+05	2.33E+05	1.05E+05	3.54E+04	26.8	27.4	18.4	28.4	22.6	12.4
P62963	Pfn1	Profilin-1	14.96	6	6	3	5	6	3	2	2	2	2	2	1	2.22E+06	5.89E+05	2.55E+05	4.55E+05	4.23E+05	2.67E+05	61.4	61.4	39.3	61.4	61.4	30
P25113	Pgam1	Phosphoglycerate mutase 1	28.83	4	4	3	5	4	4	4	4	3	5	4	4	1.47E+05	1.12E+05	6.37E+04	7.33E+04	8.76E+04	3.64E+04	24.4	22	20.1	32.7	30.7	22
P85968	Pgd	6-phosphogluconate dehydrogenase, decarboxylating	53.24	14	17	12	16	14	9	14	17	12	16	14	9	6.86E+05	9.50E+05	2.98E+05	5.63E+05	3.68E+05	1.77E+05	46	48.7	40.4	48.7	46	36.2
D3ZY02	Pgghg	Protein-glucosylgalactosylhydroxylysine glucosidase	76.95	3	4	1	3	2	0	3	4	1	3	2	0	1.83E+04	3.51E+04	3.54E+03	1.65E+04	7.56E+03	0.00E+00	5.3	6.7	1.9	5.2	3.7	0
P16617	Pgk1	Phosphoglycerate kinase 1	44.54	13	14	12	10	13	10	13	14	12	10	13	10	7.79E+05	8.59E+05	5.38E+05	3.58E+05	4.92E+05	4.71E+05	51.8	51.8	48	36.9	51.8	39.1
G3V8D5	Pgls	6-phosphogluconolactonase	30.82	3	3	2	2	3	1	3	3	2	2	3	1	6.91E+04	1.25E+05	1.96E+04	5.01E+04	4.76E+04	1.43E+04	21	21	18.2	18.2	21	5.5
M0R485	Pglyrp2	Peptidoglycan recognition protein 2	47.10	15	16	15	14	15	14	15	16	15	14	15	14	4.26E+06	3.31E+06	5.90E+06	4.56E+06	3.48E+06	6.14E+06	51	51.7	51	51	51	51
B2RYN0	Pgm3	Phosphoacetylglucosamine mutase	59.68	6	8	3	5	4	3	6	8	3	5	4	3	1.09E+05	1.04E+05	4.09E+04	4.48E+04	1.67E+04	2.96E+04	16.4	20.1	8.5	14.2	9.8	8.5
D3ZDK7	Pgp	Glycerol-3-phosphate phosphatase	34.60	10	10	10	9	9	6	10	10	10	9	9	6	7.17E+05	7.64E+05	9.97E+05	5.86E+05	2.04E+05	1.50E+05	40.2	40.2	42.1	39.3	37.1	22.7
Q7TPJ6;	Phf5a	PHD finger-like domain-containing protein 5A	11.49	1	1	0	0	0	0	1	1	0	0	0	0	1.64E+04	4.22E+04	0.00E+00	0.00E+00	0.00E+00	0.00E+00	15.7	15.7	0	0	0	0
O08651	Phgdh	D-3-phosphoglycerate dehydrogenase	56.49	10	10	11	11	11	11	10	10	11	11	11	11	5.05E+05	6.07E+05	2.84E+05	1.99E+05	1.88E+05	1.09E+05	35.3	35.3	36.2	37.1	37.1	36.2
D3ZP47	Phpt1	Phosphohistidine phosphatase 1	14.01	2	2	3	2	2	2	2	2	3	2	2	2	5.65E+04	6.34E+04	1.18E+05	3.08E+04	3.41E+04	5.51E+04	25	25	34.7	25	25	19.4
D3ZGM7	Pi16	Peptidase inhibitor 16	52.15	7	7	5	7	7	6	7	7	5	7	7	6	1.01E+06	5.44E+05	4.22E+05	9.57E+05	6.16E+05	5.44E+05	31.7	31.7	22.8	31.7	31.7	28.8
A0A0G2K5U5	Pigr	Polymeric immunoglobulin receptor	84.60	7	6	11	7	8	11	7	6	11	7	8	11	7.37E+04	5.49E+04	7.69E+04	6.09E+04	7.65E+04	1.24E+05	12.2	9.9	17.6	12.2	14.6	17.6
B0BNL2	Pin1	Peptidyl-prolyl cis-trans isomerase	18.33	2	4	3	3	2	3	2	4	3	3	2	3	1.75E+05	4.54E+05	2.00E+05	6.27E+04	1.12E+05	9.62E+04	27.9	50.3	37	41.2	27.9	37
M0RCP9	Pin4	Peptidyl-prolyl cis-trans isomerase	13.82	0	1	1	1	1	1	0	1	1	1	1	1	0.00E+00	3.85E+04	1.56E+04	1.72E+04	8.35E+03	1.61E+04	0	9.2	9.2	9.2	9.2	9.2
G3V812	Pip	Prolactin-inducible protein homolog	16.44	0	1	1	0	0	2	0	1	1	0	0	2	0.00E+00	1.26E+04	2.14E+04	0.00E+00	0.00E+00	1.07E+05	0	13	13	0	0	24
Q5M827	Pir	Pirin	32.18	4	6	5	5	4	5	4	6	5	5	4	5	5.61E+04	2.47E+05	7.80E+04	8.87E+04	4.38E+04	5.01E+04	16.8	25.4	25.1	25.1	16.8	25.1
D3ZCD4	Pitpnb	Phosphatidylinositol transfer protein beta isoform	31.62	3	3	3	3	2	3	3	3	3	3	2	3	6.53E+04	8.02E+04	6.79E+04	3.44E+04	3.36E+04	4.21E+04	19.5	19.5	19.5	19.5	11	19.5
D3ZTP9	Piwil1	Piwi-like protein	98.57	5	6	6	4	6	4	5	6	6	4	6	4	1.84E+04	4.05E+04	5.77E+04	8.83E+03	1.59E+04	2.00E+04	8.8	10.6	9.5	6.1	8.9	5.5
P11980	Pkm	Pyruvate kinase PKM	57.82	25	29	25	28	28	23	2	2	2	3	3	2	2.62E+05	2.81E+05	1.70E+05	1.94E+05	1.38E+05	1.08E+05	59.7	62.3	53.3	61.2	61.2	49.7
A0A0G2JVG[illegible]	Pkm	Pyruvate kinase	53.19	25	29	26	27	27	24	2	2	3	2	2	3	3.77E+06	4.15E+06	2.54E+06	2.29E+06	2.00E+06	1.36E+06	67.3	70.1	64.2	67.3	67.3	60.3
D3ZY51	Pkp1	Plakophilin 1	67.22	3	2	1	0	4	3	3	2	1	0	4	3	5.07E+03	1.69E+03	1.47E+03	0.00E+00	2.72E+04	2.57E+03	6.8	5	2.5	0	8.6	6.1
D3ZJ50	Pkp3	Plakophilin 3	89.90	0	0	1	1	2	1	0	0	1	1	2	1	0.00E+00	0.00E+00	1.58E+04	2.87E+02	4.99E+03	2.05E+01	0	0	1.5	1.3	3.3	1.3
P97535	Pla1a	Phospholipase A1 member A	50.20	0	1	0	2	2	0	0	1	0	2	2	0	0.00E+00	1.07E+05	0.00E+00	1.62E+04	2.17E+04	0.00E+00	0	5.3	0	8.1	8.1	0
A0A0G2JTD0	Pla2g16	HRAS-like suppressor 3	17.75	3	3	2	3	3	2	3	3	2	3	3	2	1.58E+05	2.70E+05	6.43E+04	1.62E+05	2.95E+04	4.31E+04	21.9	21.9	14.4	21.9	21.9	14.4
Q5M7T7	Pla2g7	Platelet-activating factor acetylhydrolase	49.49	7	6	6	7	7	4	7	6	6	7	7	4	2.88E+05	2.32E+05	2.91E+05	3.39E+05	6.03E+05	2.06E+05	23.4	20.2	20.2	23.4	23.4	12.7
P54319	Plaa	Phospholipase A-2-activating protein	87.08	4	5	3	4	3	3	4	5	3	4	3	3	1.75E+04	2.25E+04	4.40E+03	1.21E+04	1.08E+04	3.65E+03	8.3	9.4	6.2	7.8	6.7	6.8
G3V9D1	Plcd1	Phosphoinositide phospholipase C	85.91	2	1	2	2	2	2	2	1	2	2	2	2	1.97E+04	1.80E+04	1.02E+04	1.27E+04	2.76E+03	1.20E+04	3	1.6	3	3	3	3.3
A0A0G2K1J5	Plec	Plectin	499.23	5	4	3	3	4	3	5	4	3	3	4	3	2.00E+04	6.28E+03	1.30E+04	7.96E+03	1.11E+03	1.96E+04	1.5	1.1	0.7	0.9	1.1	0.7
Q01177	Plg	Plasminogen	90.54	76	86	75	77	81	70	67	76	66	69	72	63	8.63E+07	7.70E+07	8.19E+07	7.49E+07	6.00E+07	7.53E+07	82.5	83.6	81.5	81.9	84.9	80.3
M0RA08	Plin3	Perilipin	47.34	11	14	7	13	9	6	11	14	7	13	9	6	1.98E+05	6.58E+05	9.11E+04	2.73E+05	1.80E+05	4.12E+04	45.7	55	24.7	53.9	35.2	18.3
F1LPK7	Pls3	Plastin-3	70.75	11	12	10	8	13	8	10	11	9	7	12	7	1.32E+05	1.91E+05	9.09E+04	3.21E+04	1.43E+05	4.06E+04	26.5	28.7	26.2	22.5	30.3	22.1
E9PSP1	Pltp	Phospholipid transfer protein	54.45	8	8	10	8	9	9	8	8	10	8	9	9	5.91E+05	5.68E+05	7.83E+05	7.85E+05	6.96E+05	6.61E+05	26.6	25.4	33.5	26.6	29.4	31.5
B5DEZ8	Plxdc2	Plexin domain containing 2	59.42	2	2	1	2	2	1	2	2	1	2	2	1	4.23E+04	2.26E+04	2.84E+04	5.03E+04	3.01E+04	1.75E+04	5.1	5.1	3.2	5.1	5.1	3.2
B5DF46	Pmm2	Phosphomannomutase	27.71	6	7	5	4	5	4	6	7	5	4	5	4	1.91E+05	3.27E+05	1.16E+05	1.02E+05	6.09E+04	3.29E+04	31.8	35.1	24	20.2	24.8	19.4
P85973	Pnp	Purine nucleoside phosphorylase	32.30	4	3	4	4	4	4	4	3	4	4	4	4	1.32E+05	7.21E+04	5.59E+04	3.90E+04	9.03E+04	4.08E+04	19.4	14.2	17.6	19.4	19.4	17.6
O88794	Pnpo	Pyridoxine-5-phosphate oxidase	30.18	3	3	2	3	3	2	3	3	2	3	3	2	1.82E+05	2.42E+05	1.47E+04	1.52E+05	9.93E+04	2.04E+04	14.2	14.2	11.1	14.2	14.2	11.1
D3ZWE3	Pof1b	POF1B, actin-binding protein	67.66	2	2	1	1	4	0	2	2	1	1	4	0	1.20E+04	1.83E+04	4.95E+03	7.99E+03	1.17E+05	0.00E+00	6.6	6.6	4.6	4.6	8.3	0
D4A5A6	Polr2a	DNA-directed RNA polymerase	217.20	2	2	2	2	1	2	2	2	2	2	1	2	1.80E+04	1.94E+04	6.57E+03	1.61E+04	6.96E+02	1.02E+04	2	2	2	2	1.4	2
D4A531	Polr2i	DNA-directed RNA polymerase subunit	14.52	2	2	1	2	2	1	2	2	1	2	2	1	4.53E+04	1.10E+05	2.14E+04	4.70E+04	3.90E+04	1.17E+04	28	28	9.6	28	28	9.6
P55159	Pon1	Serum paraoxonase/arylesterase 1	39.36	12	13	10	12	10	10	12	13	10	12	10	10	2.38E+07	1.81E+07	1.71E+07	2.77E+07	1.76E+07	1.41E+07	66.2	66.8	62.3	71	60.6	62.3
A0A097BW25	Postn	Periostin	87.15	21	19	19	20	19	19	21	19	19	20	19	19	9.03E+05	4.59E+05	4.91E+05	7.51E+05	4.68E+05	4.24E+05	43.9	41	41.4	40	40	41.4
F7EPH4	Ppa1	Pyrophosphatase (inorganic) 1	32.77	6	9	9	7	7	9	6	9	9	7	7	9	4.00E+05	6.01E+05	4.71E+05	2.43E+05	1.35E+05	2.42E+05	41.5	53.3	42.6	45.3	45.3	42.6
Q99ME0	Ppbp	CXC chemokine RTCK1	12.16	1	1	1	1	1	1	1	1	1	1	1	1	4.71E+04	2.82E+04	4.99E+04	1.98E+04	5.10E+03	2.07E+03	13.5	13.5	18	13.5	13.5	13.5
P10111	Ppia	Peptidyl-prolyl cis-trans isomerase A	17.87	4	4	4	3	4	3	4	4	4	3	4	3	2.53E+05	2.70E+05	5.99E+04	1.84E+05	1.04E+06	4.58E+04	41.5	41.5	38.4	25	41.5	30.5
P24368	Ppib	Peptidyl-prolyl cis-trans isomerase B	23.80	2	0	0	1	3	0	2	0	0	1	3	0	3.60E+04	0.00E+00	0.00E+00	6.30E+03	9.33E+04	0.00E+00	12	0	0	6	17.1	0
Q6AYQ9	Ppic	Peptidyl-prolyl cis-trans isomerase	23.01	3	3	2	2	2	3	3	3	2	2	2	3	3.47E+05	2.75E+05	8.82E+04	2.98E+05	1.45E+05	1.70E+05	27.4	27.4	21.7	11.8	11.8	27.4
Q6DGG0	Ppid	Peptidyl-prolyl cis-trans isomerase D	40.77	3	3	3	3	3	2	3	3	3	3	3	2	5.31E+04	4.20E+04	1.43E+04	2.47E+04	1.20E+04	3.50E+03	8.6	8.6	8.6	8.6	8.6	5.4
Q4KLI4	Ppil1	Peptidyl-prolyl cis-trans isomerase	18.25	0	1	0	1	0	0	0	1	0	1	0	0	0.00E+00	2.36E+04	0.00E+00	7.76E+03	0.00E+00	0.00E+00	0	8.4	0	8.4	0	0
D4A5T8	Ppl	Periplakin	204.14	5	5	5	3	3	5	5	5	5	3	3	5	9.02E+03	1.10E+04	6.76E+03	4.25E+03	3.53E+03	5.20E+03	3.2	3.5	3.5	1.8	2.1	3.2
A0A0H2UHE5	Ppm1a	Protein phosphatase 1A	53.46	5	5	4	5	4	3	3	3	2	3	2	2	6.27E+04	1.02E+05	5.28E+04	2.40E+04	1.74E+04	4.74E+04	12.5	12.5	10.6	12.5	10.6	10.2
Q642F2	Ppm1b	Protein phosphatase 1B	43.53	7	8	8	6	5	5	5	6	6	4	3	4	1.94E+05	3.48E+05	1.51E+05	1.09E+05	5.76E+04	6.82E+04	27	29.3	26.5	21.9	17	21.4
A0A0H2UHT5	Ppm1g	Protein phosphatase 1G	58.72	2	2	0	1	1	0	2	2	0	1	1	0	2.31E+04	1.19E+04	0.00E+00	7.02E+03	1.49E+03	0.00E+00	8.3	10.5	0	3	3	0
Q4FZT2	Ppme1	Protein phosphatase methylesterase 1	42.32	2	2	4	2	2	3	2	2	4	2	2	3	4.90E+04	4.56E+04	1.62E+05	2.90E+04	3.15E+04	1.30E+05	8	8	16.3	7.8	7.8	13.5
P62138	Ppp1ca	Serine/threonine-protein phosphatase PP1-alpha catalytic subunit	37.51	9	10	9	10	9	6	2	2	1	2	2	1	3.82E+05	6.13E+05	3.39E+05	3.17E+05	2.42E+05	1.11E+05	29.1	33.3	30.3	33.3	27.9	24.8
P62142	Ppp1cb	Serine/threonine-protein phosphatase PP1-beta catalytic subunit	37.19	9	10	10	10	9	7	2	2	2	2	2	2	9.62E+04	1.58E+05	5.96E+04	1.04E+05	8.53E+04	2.70E+04	31.5	35.8	35.8	35.8	30.3	30.3
P63088	Ppp1cc	Serine/threonine-protein phosphatase PP1-gamma catalytic subunit	36.98	9	10	9	9	8	6	2	2	1	1	1	1	6.07E+04	7.22E+04	2.87E+04	4.36E+04	3.36E+04	4.98E+03	28.2	32.5	31	31	25.4	25.4
Q99MC0	Ppp1r14a	Protein phosphatase 1 regulatory subunit 14A	16.70	1	1	1	1	2	1	1	1	1	1	2	1	5.69E+04	1.54E+05	3.77E+04	3.57E+04	2.21E+05	1.50E+04	12.2	12.2	12.2	12.2	19.7	12.2
Q8K3F3	Ppp1r14b	Protein phosphatase 1 regulatory subunit 14B	15.96	3	3	2	3	1	2	3	3	2	3	1	2	1.92E+05	2.75E+05	1.02E+05	1.59E+05	2.75E+04	5.10E+04	40.1	40.1	26.5	40.1	17	26.5
Q5HZV9	Ppp1r7	Protein phosphatase 1 regulatory subunit 7	41.30	9	10	10	11	8	7	9	10	10	11	8	7	2.98E+05	4.21E+05	2.89E+05	3.01E+05	1.29E+05	9.65E+04	40.8	46.1	42.5	47.5	30.3	32.2
P63331	Ppp2ca	Serine/threonine-protein phosphatase 2A catalytic subunit alpha isoform	35.61	10	10	8	10	9	6	1	1	0	1	1	0	5.42E+05	8.24E+05	2.45E+05	4.43E+05	3.58E+05	1.05E+05	46.9	40.1	37.9	46.9	38.8	30.7
P62716	Ppp2cb	Serine/threonine-protein phosphatase 2A catalytic subunit beta isoform	35.58	10	10	9	10	9	7	1	1	1	1	1	1	4.84E+04	5.10E+04	4.53E+03	1.66E+04	8.16E+03	6.11E+03	46.9	40.1	42.1	46.9	38.8	35
Q5XI34	Ppp2r1a	Protein phosphatase 2 (Formerly 2A), regulatory subunit A (PR 65), alpha isoform	65.32	15	17	14	14	16	13	15	17	14	14	16	13	3.02E+05	4.27E+05	2.28E+05	2.11E+05	1.99E+05	1.27E+05	32.6	37.7	31.4	33.3	35.5	30.4
P36876	Ppp2r2a	Serine/threonine-protein phosphatase 2A 55 kDa regulatory subunit B alpha isoform	51.68	3	3	2	3	3	2	3	3	2	3	3	2	5.36E+04	6.06E+04	1.18E+04	3.53E+04	3.67E+04	2.45E+03	8.1	8.1	5.6	8.1	8.1	5.6
B2RYQ2	Ppp2r4	Serine/threonine-protein phosphatase 2A activator	36.62	3	4	3	2	3	3	3	4	3	2	3	3	1.33E+05	1.22E+05	6.63E+04	2.51E+04	4.76E+04	2.47E+04	18.3	26.3	18.3	14.2	18.3	18.3
D4A1A5	Ppp2r5c	Serine/threonine-protein phosphatase 2A 56 kDa regulatory subunit	60.87	2	2	1	2	1	1	2	2	1	2	1	1	2.18E+04	2.65E+04	8.75E+03	1.55E+04	1.20E+04	8.72E+03	6.5	6.5	2.5	6.5	2.5	2.5
P63329	Ppp3ca	Serine/threonine-protein phosphatase 2B catalytic subunit alpha isoform	58.64	3	3	3	2	3	2	3	3	3	2	3	2	1.07E+05	1.36E+05	6.17E+04	2.79E+04	2.57E+04	3.20E+04	7.3	7.3	7.3	4	7.3	4
F1LRK9	Ppp4r1	Serine/threonine-protein phosphatase 4 regulatory subunit 1	103.78	3	3	0	4	2	1	3	3	0	4	2	1	9.81E+03	1.04E+04	0.00E+00	1.43E+04	1.67E+03	4.54E+02	5.7	6.9	0	7.5	4.6	1.1
P53042	Ppp5c	Serine/threonine-protein phosphatase 5	56.92	3	5	4	4	2	3	3	5	4	4	2	3	3.16E+04	8.42E+04	4.44E+04	2.79E+04	6.48E+03	6.14E+03	10	12.8	12.6	12.6	5	8.8
D3ZBT9	Ppp6r3	Protein phosphatase 6, regulatory subunit 3	97.51	1	1	1	1	1	0	1	1	1	1	1	0	6.20E+03	1.44E+04	1.40E+03	8.66E+03	6.79E+03	0.00E+00	1.6	1.6	1.6	1.6	1.6	0
P45479	Ppt1	Palmitoyl-protein thioesterase 1	34.46	5	5	3	4	4	4	5	5	3	4	4	4	1.47E+05	2.32E+05	1.75E+05	1.64E+05	1.19E+05	5.35E+04	21.9	21.9	13.1	19	19	16
F1LQ66	Prdm2	PR domain zinc finger protein 2	187.54	1	1	1	1	1	1	1	1	1	1	1	1	4.43E+06	2.93E+06	8.68E+05	4.37E+06	4.58E+06	3.83E+06	0.5	0.5	0.5	0.5	0.5	0.5
A0A0G2K3Z9	Prdx1	Peroxiredoxin-1	22.16	12	13	9	13	12	10	11	12	8	12	11	9	4.63E+06	7.15E+06	2.67E+06	4.11E+06	3.38E+06	1.62E+06	56.3	63.8	51.8	60.3	56.3	51.8
A0A0G2JSH9	Prdx2	Peroxiredoxin-2	21.80	11	14	11	13	11	12	11	14	11	13	11	12	5.74E+06	6.54E+06	2.72E+06	5.23E+06	2.25E+06	2.73E+06	82.3	88.4	82.3	86.4	82.3	82.3
Q9Z0V5	Prdx4	Peroxiredoxin-4	31.01	4	5	6	5	3	6	3	4	5	4	2	5	9.63E+05	1.25E+06	8.25E+05	8.21E+05	4.61E+05	3.91E+05	24.5	28.2	33.3	28.2	15.4	33.3
O35244	Prdx6	Peroxiredoxin-6	24.82	13	12	11	12	12	12	13	12	11	12	12	12	2.07E+06	2.28E+06	1.20E+06	8.70E+05	8.01E+05	8.81E+05	76.3	76.3	71.4	76.3	73.2	76.3
F1LRA5	Prg4	Proteoglycan 4	115.81	1	0	2	1	3	3	1	0	2	1	3	3	6.12E+02	0.00E+00	9.14E+03	1.98E+03	7.40E+03	1.71E+04	1.1	0	2	1.1	3.1	3.1
A1L1M0	Prkaca	cAMP-dependent protein kinase catalytic subunit alpha	40.61	7	7	6	7	5	5	2	2	2	2	2	2	4.24E+04	1.15E+05	9.52E+04	5.69E+04	3.09E+04	1.56E+04	28.8	28.8	23.4	28.8	17.1	17.1
P68182	Prkacb	cAMP-dependent protein kinase catalytic subunit beta	40.71	7	8	7	7	4	6	2	3	3	2	1	3	1.47E+05	2.62E+05	8.97E+04	1.49E+05	6.47E+04	5.02E+04	30.8	33.3	27.9	30.8	12.3	21.7
P09456	Prkar1a	cAMP-dependent protein kinase type I-alpha regulatory subunit	43.09	4	6	4	4	5	5	4	6	4	4	5	5	8.08E+05	8.48E+05	8.65E+05	7.33E+05	7.76E+05	8.44E+05	10.5	16.8	12.3	12.9	13.4	15
A0A0G2K405	Prkar2a	cAMP-dependent protein kinase type II-alpha regulatory subunit	48.15	7	8	3	8	6	1	5	6	2	6	4	0	4.19E+04	1.34E+05	6.52E+03	4.50E+04	2.12E+04	0.00E+00	23.9	27	11.6	27	21.3	3.3
P12369	Prkar2b	cAMP-dependent protein kinase type II-beta regulatory subunit	46.12	8	12	5	10	7	5	6	10	4	8	5	4	2.25E+05	7.12E+05	1.66E+05	3.82E+05	1.38E+05	7.43E+04	28.6	36.3	18.5	35.8	25.2	18.5
B1WC34	Prkcsh	Protein kinase C substrate 80K-H	59.22	4	5	5	3	2	5	4	5	5	3	2	5	1.07E+05	6.93E+04	1.16E+05	3.20E+04	1.91E+04	7.95E+04	10.5	12.4	15	6.5	4.6	15
A0A0G2K9I8	Prmt1	Protein arginine N-methyltransferase 1	40.50	5	5	4	5	5	3	5	5	4	5	5	3	1.36E+05	1.61E+05	9.20E+04	1.52E+05	1.35E+05	3.41E+04	18.7	18.7	15.9	19.5	19.5	11.6
D4A0E8	Prmt5	Protein arginine N-methyltransferase 5	72.69	4	4	2	2	3	0	4	4	2	2	3	0	5.05E+04	6.33E+04	3.01E+04	3.67E+04	2.67E+04	0.00E+00	7.8	8.8	3.8	3.8	5.2	0
P13852	Prnp	Major prion protein	27.80	1	1	1	1	1	1	1	1	1	1	1	1	1.03E+05	1.92E+05	1.47E+05	8.44E+04	1.54E+05	7.86E+04	4.7	4.7	4.7	4.7	4.7	4.7
F7FMY6	Proc	Vitamin K-dependent protein C	54.02	15	18	15	18	15	15	15	18	15	18	15	15	2.39E+06	1.96E+06	2.95E+06	2.52E+06	2.00E+06	2.89E+06	36.7	38.2	37.1	38.4	36.7	36.7

Uniprot accession number	Gene symbol	Protein name	Mol. weight [kDa]	No. Peptides Control wk1	No. Peptides Control wk8	No. Peptides Control wk14	No. Peptides Heat wk1	No. Peptides Heat wk8	No. Peptides Heat wk14	No. Unique peptides Control wk1	No. Unique peptides Control wk8	No. Unique peptides Control wk14	No. Unique peptides Heat wk1	No. Unique peptides Heat wk8	No. Unique peptides Heat wk14	iBAQ Control wk1	iBAQ Control wk8	iBAQ Control wk14	iBAQ Heat wk1	iBAQ Heat wk8	iBAQ Heat wk14	Sequence coverage Control wk1 [%]	Sequence coverage Control wk8 [%]	Sequence coverage Control wk14 [%]	Sequence coverage Heat wk1 [%]	Sequence coverage Heat wk8 [%]	Sequence coverage Heat wk14 [%]
M0R5R0	Pros1	Vitamin K-dependent protein S	74.61	17	19	15	18	19	17	17	19	15	18	19	17	2.57E+06	2.34E+06	2.74E+06	2.98E+06	3.09E+06	2.68E+06	30.1	31.6	26.1	31.3	32.9	31.3
G3V8K8	Proz	Protein Z, vitamin K-dependent plasma glycoprotein	45.38	13	13	11	13	13	11	13	13	11	13	13	11	3.92E+06	2.80E+06	2.89E+06	4.04E+06	3.42E+06	3.03E+06	43.3	43.3	38.2	43.3	43.3	38.2
A0A0G2JSV3	Prps1	Ribose-phosphate pyrophosphokinase 1	34.81	7	6	4	7	6	4	7	6	4	7	6	4	1.88E+05	2.86E+05	7.38E+04	1.74E+05	1.31E+05	3.63E+04	40.9	27.4	18.2	40.9	36.8	28
G3V7B5	Prpsap1	Phosphoribosyl pyrophosphate synthase-associated protein 1	42.50	1	1	1	1	1	0	1	1	1	1	1	0	1.86E+04	2.44E+04	1.26E+03	7.76E+03	1.15E+04	0.00E+00	3.9	3.9	3.9	3.9	3.9	0
P00762	Prss1	Anionic trypsin-1	25.96	2	2	1	2	2	1	2	2	1	2	2	1	4.73E+05	4.59E+05	5.46E+05	5.00E+05	6.70E+05	5.86E+05	15	15	8.1	15	15	8.1
F1LLW4	Prss35	Inactive serine protease 35	45.47	2	2	2	2	2	2	2	2	2	2	2	2	1.90E+05	1.75E+05	1.02E+05	9.25E+04	1.69E+05	1.05E+05	7.1	7.1	7.1	7.1	7.1	7.1
Q6AYG3	Prune	Protein prune homolog	50.00	1	1	1	1	1	1	1	1	1	1	1	1	0.00E+00	1.35E+04	4.14E+03	5.68E+03	2.74E+03	6.40E+02	2.4	2.4	2.4	2.4	2.4	2.4
P10960	Psap	Sulfated glycoprotein 1	61.12	20	21	18	21	21	18	1	1	1	1	1	1	5.73E+06	4.72E+06	2.87E+06	4.54E+06	3.64E+06	1.95E+06	44	47.1	41.9	47.1	47.1	40.1
F7EPE0	Psap	Prosaposin	61.45	20	21	18	21	21	18	1	1	1	1	1	1	4.36E+05	3.98E+05	3.07E+05	3.74E+05	2.34E+05	2.10E+05	43.3	46.3	41.1	46.3	46.3	39.3
P02782	Psbpc1	Prostatic steroid-binding protein C1	12.76	3	3	0	3	3	2	3	3	0	3	3	2	1.58E+06	3.21E+06	0.00E+00	1.62E+06	9.32E+05	1.23E+05	53.2	53.2	0	53.2	53.2	37.8
P02781;A0A0H2UHR8	Psbpc2	Prostatic steroid-binding protein C2	12.83	4	4	0	3	4	2	4	4	0	3	4	2	1.26E+06	3.12E+06	0.00E+00	1.46E+06	7.13E+05	1.13E+05	31.2	34.8	0	30.4	31.2	16.1
P18420	Psma1	Proteasome subunit alpha type-1	29.52	8	10	7	8	9	5	8	10	7	8	9	5	6.60E+05	6.80E+05	1.60E+05	4.42E+05	5.07E+05	7.17E+04	47.9	51	41.8	47.5	47.9	36.1
P17220	Psma2	Proteasome subunit alpha type-2	25.93	9	8	6	8	9	5	9	8	6	8	9	5	1.34E+06	7.93E+05	4.34E+05	8.96E+05	1.12E+06	1.59E+05	50	49.6	34.6	49.6	50	34.2
P18422	Psma3	Proteasome subunit alpha type-3	28.42	4	6	4	5	5	3	4	6	4	5	5	3	6.51E+05	5.35E+05	2.60E+05	5.74E+05	5.10E+05	9.24E+04	17.6	25.5	17.6	23.1	23.1	14.1
P21670	Psma4	Proteasome subunit alpha type-4	29.50	7	6	7	7	8	6	7	6	7	7	8	6	1.00E+06	5.91E+05	3.97E+05	8.47E+05	8.46E+05	1.68E+05	43.3	40.2	42.9	43.3	46.7	39.8
Q6P9V6	Psma5	Proteasome subunit alpha type-5	26.41	6	9	7	7	7	7	6	9	7	7	7	7	1.46E+06	1.41E+06	1.31E+06	1.11E+06	1.20E+06	5.08E+05	39.4	45.6	39.4	42.7	42.7	39.4
P60901	Psma6	Proteasome subunit alpha type-6	27.40	9	9	5	9	9	6	9	9	5	9	9	6	6.61E+05	6.40E+05	2.86E+05	6.65E+05	7.92E+05	2.04E+05	38.2	41.9	24	38.2	38.2	28.9
A0A0G2K0W9	Psma7	Proteasome subunit alpha type-7	27.86	10	9	8	9	10	9	10	9	8	9	10	9	1.95E+06	1.08E+06	8.23E+05	1.32E+06	1.39E+06	4.95E+05	54	50.8	42.3	50.8	54	45.6
Q6PDW4	Psmb1	Proteasome subunit beta type-1	26.41	7	7	8	7	7	7	7	7	8	7	7	7	1.40E+06	1.37E+06	6.55E+05	1.19E+06	1.17E+06	3.22E+05	42.9	42.9	42.9	42.9	42.9	42.9
Q4KM35	Psmb10	Proteasome subunit beta type-10	29.04	3	3	3	3	2	3	3	3	3	3	2	3	4.64E+05	5.08E+05	3.11E+05	3.01E+05	3.62E+05	1.99E+05	12.8	12.8	12.8	12.8	9.2	12.8
P40307	Psmb2	Proteasome subunit beta type-2	22.91	5	5	6	5	6	4	5	5	6	5	6	4	6.42E+05	3.14E+05	9.92E+05	5.33E+05	6.70E+05	2.29E+05	39.8	35.3	40.8	35.3	40.8	30.3
P40112	Psmb3	Proteasome subunit beta type-3	22.97	4	4	3	4	4	3	4	4	3	4	4	3	4.76E+05	2.44E+05	2.54E+05	3.59E+05	5.14E+05	6.35E+04	23.9	23.9	23.9	23.9	23.9	23.9
G3V8U9	Psmb4	Proteasome subunit beta type-4	25.76	6	6	5	6	5	4	6	6	5	6	5	4	1.11E+06	8.86E+05	3.87E+05	9.05E+05	8.69E+05	1.35E+05	38.4	38.4	36.6	38.4	36.6	32.3
G3V7Q6	Psmb5	Proteasome subunit beta type-5	28.56	3	3	2	3	3	2	3	3	2	3	3	2	1.55E+05	6.88E+04	3.29E+04	1.13E+05	8.73E+04	2.24E+04	14.1	14.1	10.3	14.1	14.1	10.3
A0A0G2JSL0	Psmb6	Proteasome subunit beta type-6	25.30	3	3	3	2	3	2	3	3	3	2	3	2	2.85E+05	1.66E+05	1.95E+05	2.13E+05	1.93E+05	7.32E+04	13	13	13	8.8	13	8.8
P28064	Psmb8	Proteasome subunit beta type-8	30.57	5	6	2	6	6	2	5	6	2	6	6	2	3.40E+05	2.70E+05	7.95E+04	2.44E+05	2.03E+05	5.20E+04	22.5	27.2	9.4	27.2	27.2	9.4
Q6MGA6	Psmb9	Proteasome subunit beta type-9	23.34	4	3	3	4	4	2	4	3	3	4	4	2	1.85E+05	1.15E+05	7.36E+04	1.54E+05	1.48E+05	6.13E+04	21	14.2	16.9	21	21	12.3
P62193	Psmc1	26S protease regulatory subunit 4	49.18	5	8	4	6	8	4	5	8	4	6	8	4	1.48E+05	2.13E+05	5.14E+04	9.86E+04	1.17E+05	2.86E+04	22.5	31.8	14.3	22.3	31.8	16.8
G3V7L6	Psmc2	26S protease regulatory subunit 7	48.63	7	10	3	10	10	4	7	10	3	10	10	4	1.28E+05	2.16E+05	5.33E+04	1.32E+05	1.20E+05	3.47E+04	21	32.6	8.8	32.6	32.6	13.2
Q6P6U2	Psmc3	26S protease regulatory subunit 6A	49.55	9	11	7	9	9	6	9	11	7	9	9	6	1.33E+05	3.23E+05	1.03E+05	1.52E+05	1.42E+05	3.60E+04	26.9	31.9	25.3	26.9	29.2	18.3
Q63570	Psmc4	26S protease regulatory subunit 6B	47.41	4	4	4	4	4	4	4	4	4	4	4	4	2.78E+04	6.38E+04	1.18E+05	6.40E+04	5.53E+04	4.79E+04	15.6	15.1	11.2	15.6	15.6	12.2
P62198	Psmc5	26S protease regulatory subunit 8	45.63	5	8	5	4	6	5	5	8	5	4	6	5	6.63E+04	1.71E+05	7.11E+04	8.20E+04	1.31E+05	3.46E+04	16.3	26.4	17	13.3	21.9	18.5
G3V6W6	Psmc6	26S protease regulatory subunit 10B	45.80	6	7	3	7	7	3	6	7	3	7	7	3	2.00E+05	2.47E+05	5.21E+04	1.69E+05	1.74E+05	1.79E+04	23.1	26.1	9.9	26.1	26.1	9.9
A0A0G2JTW5	Psmd1	26S proteasome non-ATPase regulatory subunit 1	105.62	11	9	6	10	9	4	11	9	6	10	9	4	1.17E+05	1.33E+05	2.53E+04	9.50E+04	8.40E+04	5.83E+03	19.5	15.8	13.9	20	17.2	8.5
A0A0G2JWX1	Psmd11	26S proteasome non-ATPase regulatory subunit 11	55.92	5	5	4	5	4	4	5	5	4	5	4	4	1.01E+05	9.22E+04	5.33E+04	6.41E+04	5.50E+04	2.89E+04	14.2	14.2	10.8	14.2	11	10.8
Q5XIC6	Psmd12	26S proteasome non-ATPase regulatory subunit 12	52.94	4	3	2	2	2	0	4	3	2	2	2	0	4.09E+04	3.94E+04	1.33E+04	1.67E+04	1.17E+04	0.00E+00	10.5	5.5	7	3.5	3.5	0
Q4V8E2	Psmd14	26S proteasome non-ATPase regulatory subunit 14	34.58	2	2	0	1	2	1	2	2	0	1	2	1	1.56E+05	1.61E+05	0.00E+00	3.48E+04	9.09E+04	3.50E+04	10.3	10.3	0	5.2	10.3	5.2
Q4FZT9	Psmd2	26S proteasome non-ATPase regulatory subunit 2	100.19	8	12	7	13	10	5	8	12	7	13	10	5	1.05E+05	1.45E+05	5.52E+04	1.09E+05	6.94E+04	1.64E+04	13.1	21	14.2	22	15.1	8.5
Q5U2S7	Psmd3	26S proteasome non-ATPase regulatory subunit 3	60.69	6	7	6	6	6	3	6	7	6	6	6	3	9.16E+04	8.06E+04	1.21E+05	8.46E+04	7.46E+04	1.03E+05	17.4	19.4	16.6	17.4	17.4	7.2
O88321	Psmd4	26S proteasome non-ATPase regulatory subunit 4	41.07	4	4	3	3	4	3	4	4	3	3	4	3	2.08E+05	4.95E+05	1.84E+05	1.37E+05	1.62E+05	7.98E+04	13.4	13.4	10.8	10.8	13.4	10.8
G3V8G2	Psmd5	26S proteasome non-ATPase regulatory subunit 5	55.85	3	3	2	3	2	1	3	3	2	3	2	1	4.59E+04	5.73E+04	2.33E+04	3.60E+04	9.30E+03	5.67E+03	8.3	8.3	5.6	8.3	5.4	2.6
Q6PCT9	Psmd6	26S proteasome non-ATPase regulatory subunit 5	45.60	6	7	7	6	6	4	6	7	7	6	6	4	8.15E+04	1.01E+05	6.20E+04	8.00E+04	8.66E+04	2.73E+04	19	22.4	21.9	18.3	19	11.8
G3V9P0	Psmd9	26S proteasome non-ATPase regulatory subunit 9	24.82	1	1	1	1	1	1	1	1	1	1	1	1	4.72E+04	3.84E+04	1.11E+04	1.99E+04	2.10E+04	4.05E+03	7.2	7.2	7.2	7.2	7.2	7.2
Q6P9V7	Psme1	Proteasome activator complex subunit 1	28.64	10	12	11	10	9	10	10	12	11	10	9	10	1.25E+06	2.03E+06	1.15E+06	9.67E+05	7.56E+05	9.11E+05	45.8	57.8	50.2	50.2	41.4	47.4
Q63798	Psme2	Proteasome activator complex subunit 2	26.86	12	10	3	11	8	6	12	10	3	11	8	6	4.45E+05	5.65E+05	1.38E+05	2.81E+05	1.69E+05	7.60E+04	61.3	63.9	16	54.2	47.1	34.5
Q5FVM2	Psme3	Proteaseome (Prosome, macropain) 28 subunit, 3	29.51	2	3	1	3	3	0	2	3	1	3	3	0	1.32E+04	3.07E+04	6.10E+03	3.26E+04	2.77E+04	0.00E+00	7.9	13.8	3.5	13.8	13.8	0
D3ZB30	Ptbp1	Polypyrimidine tract-binding protein 1	56.94	8	8	7	6	7	7	8	8	7	6	7	7	2.79E+05	3.98E+05	8.87E+04	1.23E+05	1.24E+05	4.74E+04	25.8	25.8	19.6	18.3	23.2	19.6
O54857	Pten	Phosphatase and tensin homolog	47.12	2	2	0	2	2	1	2	2	0	2	2	1	3.37E+04	4.79E+04	0.00E+00	2.07E+04	3.76E+04	1.14E+04	5	5	0	5	5	3
Q63530	Pter	Phosphotriesterase-related protein	39.15	2	3	2	2	2	1	2	3	2	2	2	1	4.65E+04	1.04E+05	7.92E+03	3.33E+04	2.59E+04	3.59E+02	7.4	14.9	11.7	7.4	7.4	4.3
P83868	Ptges3	Prostaglandin E synthase 3	18.72	4	6	5	4	4	4	4	6	5	4	4	4	5.19E+05	2.30E+06	1.00E+06	7.53E+05	6.61E+05	2.82E+05	30.6	33.8	32.5	27.5	27.5	31.2
Q5BK81	Ptgr2	Prostaglandin reductase 2	38.14	8	8	8	6	7	5	8	8	8	6	7	5	3.74E+05	6.25E+05	2.79E+05	2.45E+05	1.75E+05	6.65E+04	41	40.7	41.3	31.6	36.2	33.6
P06302	Ptma	Prothymosin alpha	12.38	1	2	2	1	1	1	1	2	2	1	1	1	7.35E+03	4.23E+04	1.30E+05	2.27E+04	1.78E+03	5.33E+03	11.6	24.1	24.1	11.6	11.6	12.5
P04550	Ptms	Parathymosin	11.56	1	1	1	1	1	1	1	1	1	1	1	1	1.07E+06	1.10E+06	4.84E+05	9.38E+05	3.20E+05	4.26E+05	10.8	10.8	10.8	10.8	10.8	10.8
P41499	Ptpn11	Tyrosine-protein phosphatase non-receptor type 11	68.46	6	8	7	9	8	3	6	8	7	9	8	3	3.76E+04	1.46E+05	6.27E+04	6.01E+04	2.88E+04	1.29E+04	14.7	17.9	14.6	19.4	17.9	8.4
A0A0G2K064	Ptpn6	Tyrosine-protein phosphatase non-receptor type 6	67.62	4	4	3	3	1	3	4	4	3	3	1	3	7.53E+04	9.13E+04	1.30E+04	7.53E+03	3.31E+03	1.73E+03	10.1	10.1	8.6	8.6	4.9	8.6
P04157	Ptprc	Receptor-type tyrosine-protein phosphatase C	143.27	2	0	0	0	0	0	2	0	0	0	0	0	6.33E+03	0.00E+00	0.00E+00	0.00E+00	0.00E+00	0.00E+00	5.5	0	0	0	0	0
A0A0G2K561	Ptprg	Protein-tyrosine-phosphatase	149.92	2	3	2	3	2	2	2	3	2	3	2	2	1.47E+04	1.62E+04	1.85E+04	2.58E+04	1.02E+04	2.36E+04	1.7	2.8	2	2.8	1.7	2
G3V8L9	Ptrf	Polymerase I and transcript release factor	43.91	5	6	6	5	4	4	5	6	6	5	4	4	2.56E+05	3.21E+05	3.47E+05	9.23E+04	3.86E+04	9.54E+04	27	27	27	27	22.7	22.7
F1LPS8	Pura	Transcriptional activator protein Pur-alpha	31.90	3	3	1	2	2	0	3	3	1	2	2	0	1.76E+05	1.90E+05	3.33E+04	9.92E+04	7.82E+04	0.00E+00	20.1	20.1	8	11.1	11.1	0
A0A0G2JUX	Purb	Transcriptional activator protein Pur-beta	33.53	1	1	0	1	0	1	1	1	0	1	0	1	5.97E+02	2.22E+03	0.00E+00	1.05E+04	0.00E+00	1.05E+03	5.4	5.4	0	5.4	0	5.4
A0A0G2JWB6	Pxdn	Peroxidasin	165.21	2	1	1	1	1	1	2	1	1	1	1	1	5.57E+03	2.84E+03	3.00E+03	3.08E+03	2.13E+03	2.29E+03	1.5	0.7	0.7	0.7	0.7	0.7
G3V6Y6	Pygb	Alpha-1,4 glucan phosphorylase	96.77	8	7	7	10	7	5	4	4	4	6	3	2	5.25E+04	4.87E+04	2.00E+04	3.06E+04	1.82E+04	1.33E+04	15.4	14.2	14.2	17.8	13.7	9.8
P09811	Pygl	Glycogen phosphorylase, liver form	97.48	13	12	9	14	12	8	9	9	6	10	8	5	9.74E+04	1.07E+05	4.55E+04	9.01E+04	5.98E+04	3.44E+04	21.4	20.7	16.1	22.6	20.1	13.5
G3V8V3	Pygm	Alpha-1,4 glucan phosphorylase	97.29	9	8	5	9	8	7	4	4	1	4	3	3	6.30E+04	3.33E+04	7.71E+03	3.65E+04	1.64E+04	1.13E+04	15.3	14.4	9.5	15.3	14	12
Q66H61	Qars	Glutamine--tRNA ligase	87.70	3	4	1	3	3	0	3	4	1	3	3	0	6.77E+04	1.10E+05	2.17E+03	7.70E+04	1.08E+05	0.00E+00	5.3	8.5	2.1	5.3	5.3	0
Q6IUU3	Qsox1	Sulfhydryl oxidase 1	82.41	17	15	12	15	16	12	17	15	12	15	16	12	5.03E+05	2.12E+05	2.72E+05	2.57E+05	3.80E+05	2.57E+05	33.2	29.2	26	28.1	31.2	26
E9PU16	Rab1	Ras-related protein Rab-1A	33.54	5	6	5	6	5	4	2	2	1	2	2	1	2.37E+05	2.98E+05	3.81E+04	1.09E+05	1.26E+05	9.29E+03	20	22.7	17	22.7	20	17
O35509	Rab11b	Ras-related protein Rab-11B	24.49	8	8	7	8	8	6	8	8	7	8	8	6	8.13E+05	8.92E+05	4.99E+05	6.61E+05	4.00E+05	2.84E+05	46.8	46.8	38.5	46.8	46.8	34.9
P35286	Rab13	Ras-related protein Rab-13	22.90	3	4	3	4	3	4	2	2	1	2	2	2	7.15E+04	1.66E+05	3.84E+04	7.45E+04	4.50E+04	3.09E+04	17.2	21.2	16.3	21.2	17.2	21.2
B0BMW0	Rab14	Ras-related protein Rab-14	23.90	6	6	5	3	5	4	6	6	5	3	5	4	3.40E+05	4.82E+05	3.09E+05	1.48E+05	1.39E+05	1.95E+05	40	39.5	34.9	27	32.6	34.9
Q5EB77	Rab18	Ras-related protein Rab-18	22.98	7	7	5	7	7	5	7	7	5	7	7	5	3.57E+05	3.90E+05	2.17E+05	3.34E+05	2.67E+05	2.00E+05	42.2	42.2	33	42.2	42.2	33
Q6AXT5	Rab21	Ras-related protein Rab-21	24.16	2	2	1	3	1	2	2	2	1	3	1	2	2.67E+04	3.00E+04	2.99E+04	2.72E+04	3.41E+04	9.94E+03	13.5	13.5	7.6	17.9	7.6	12.1
F1LP82	Rab2a	Ras-related protein Rab-2A	22.80	4	4	3	4	4	2	4	4	3	4	4	2	3.24E+05	3.88E+05	7.78E+04	2.21E+05	1.28E+05	4.94E+04	26.7	26.7	20.4	26.7	26.7	13.6
Q5U316	Rab35	Ras-related protein Rab-35	23.03	1	1	1	1	1	0	1	1	1	1	1	0	1.42E+05	1.57E+05	4.23E+04	7.83E+04	4.70E+04	0.00E+00	7	7	7	7	7	0
A1L1J8	Rab5b	Ras-related protein Rab-5B	23.67	4	3	1	4	3	1	2	1	0	2	1	0	3.32E+04	3.37E+04	0.00E+00	4.53E+04	1.34E+04	0.00E+00	22.8	16.3	4.7	22.8	16.3	4.7
B0BNK1	Rab5c	Ras-related protein Rab-5C	23.43	5	4	3	4	4	2	3	2	2	2	2	1	1.65E+05	1.92E+05	5.70E+04	1.79E+05	9.12E+04	4.03E+04	28.2	21.8	16.7	21.8	21.8	10.2
A0A0H2UHP9	Rab6a	Ras-related protein Rab-6A	23.55	5	5	3	4	3	3	5	5	3	4	3	3	4.83E+05	5.29E+05	3.29E+05	3.57E+05	2.61E+05	2.09E+05	24	24	17.8	24	18.3	17.8
P09527	Rab7a	Ras-related protein Rab-7a	23.50	10	10	8	9	8	8	10	10	8	9	8	8	7.33E+05	8.15E+05	3.79E+05	3.69E+05	3.37E+05	2.36E+05	63.8	63.8	49.8	57	48.8	53.6
P35280	Rab8a	Ras-related protein Rab-8A	23.67	2	3	3	3	2	3	1	1	1	1	1	1	6.43E+04	7.13E+04	2.42E+04	2.53E+04	4.67E+04	1.53E+04	12.1	15.9	15.9	15.9	12.1	15.9
P70550	Rab8b	Ras-related protein Rab-8B	23.60	1	2	3	3	1	3	0	0	1	1	0	1	0.00E+00	0.00E+00	2.64E+04	1.21E+04	0.00E+00	1.31E+04	5.3	9.2	15.9	15.9	5.3	15.9
Q62835	Rabep2	Rab GTPase-binding effector protein 2	61.97	4	4	2	4	3	3	4	4	2	4	3	3	6.58E+04	1.08E+05	1.92E+04	3.42E+04	2.08E+04	1.88E+04	10.8	10.8	5.2	10.8	8.3	7.8
Q6RUV5	Rac1	Ras-related C3 botulinum toxin substrate 1	21.45	5	5	4	5	4	4	4	4	3	4	3	3	8.04E+05	1.00E+06	5.92E+05	5.66E+05	5.06E+05	3.58E+05	23.4	23.4	23.4	23.4	18.8	23.4
P63245	Rack1	Receptor of activated protein C kinase 1	35.08	4	3	4	4	5	3	4	3	4	4	5	3	1.15E+05	9.73E+04	6.61E+04	6.87E+04	1.77E+05	8.39E+04	28.7	19.9	28.7	28.7	23.7	23.3
Q4KMA2	Rad23b	UV excision repair protein RAD23 homolog B	43.50	5	6	3	4	4	2	5	6	3	4	4	2	1.84E+05	2.62E+05	5.14E+04	6.26E+04	5.29E+04	1.02E+04	14	17.1	11.8	11.6	14	9.6
F1LQ62	Ralb	Ras-related protein Ral-B;Ras-related protein Ral-A	23.26	1	2	1	1	1	1	1	2	1	1	1	1	4.39E+04	1.25E+05	4.16E+04	1.82E+04	1.52E+04	1.36E+04	7.8	11.2	7.8	7.8	7.8	7.8
P62828	Ran	GTP-binding nuclear protein Ran	24.42	11	11	8	10	10	6	11	11	8	10	10	6	1.99E+06	2.18E+06	1.45E+06	1.56E+06	9.00E+05	5.33E+05	66.2	66.2	57.4	63	63	50.9
D4A2G9	Ranbp1	RAN-binding protein 1	23.60	5	5	4	5	5	5	5	5	4	5	5	5	9.09E+05	1.18E+06	9.20E+05	7.82E+05	2.54E+05	3.96E+05	43.3	43.3	36.9	43.3	43.3	42.4
F1MAA5	Rangap1	RAN GTPase-activating protein 1	63.14	3	4	2	4	4	0	3	4	2	4	4	0	2.43E+04	1.17E+05	2.45E+04	4.58E+04	1.85E+04	0.00E+00	5.8	7.5	4.1	7.8	7.8	0
P62836	Rap1a	Ras-related protein Rap-1A	20.99	6	6	5	5	6	6	2	2	2	2	2	2	2.25E+05	2.07E+05	8.26E+04	9.70E+04	1.06E+05	9.38E+04	48.9	48.9	43.5	33.2	48.9	48.9
Q62636	Rap1b	Ras-related protein Rap-1b	20.80	7	7	7	5	7	7	3	3	4	2	3	3	1.73E+06	1.63E+06	1.35E+06	8.08E+05	6.36E+05	1.08E+06	63	63	57.6	33.2	63	63
P40329	Rars	Arginine--tRNA ligase, cytoplasmic	75.81	5	5	2	5	5	1	5	5	2	5	5	1	4.10E+04	3.62E+04	1.31E+04	2.18E+04	2.31E+04	1.53E+03	9.1	9.1	3.5	9.1	9.1	1.8
G3V9H0	Rasa1	Ras GTPase-activating protein 1	111.66	1	1	1	1	1	0	1	1	1	1	1	0	2.13E+03	3.10E+03	9.24E+02	1.68E+03	6.03E+02	0.00E+00	1.4	1.4	1.4	1.4	1.4	0
B5DFB2	Rbbp4	RB-binding protein 4, chromatin-remodeling factor	47.66	4	3	3	2	3	2	3	2	3	1	2	2	1.09E+05	1.07E+05	2.33E+04	3.25E+04	4.02E+04	7.48E+03	22.6	13.9	19.5	5.9	13.9	10.8
Q71UF4	Rbbp7	Histone-binding protein RBBP7	47.82	4	4	1	5	5	2	3	3	1	4	4	2	9.62E+04	1.29E+05	9.44E+02	6.73E+04	5.46E+04	1.89E+03	19.5	19.5	2.8	21.9	21.9	5.2
O88350	Rbbp9	Putative hydrolase RBBP9	21.00	2	2	2	2	1	1	2	2	2	2	1	1	7.80E+04	1.05E+05	7.50E+04	3.43E+04	2.90E+04	2.73E+04	22.6	22.6	22.6	22.6	10.8	10.8
G3V6P6	Rbm3	RNA-binding protein 3	16.98	4	4	4	4	4	4	4	4	4	4	4	4	1.41E+06	1.54E+06	7.92E+05	9.53E+05	6.58E+05	4.35E+05	42.3	42.3	42.3	42.3	42.3	42.3

Uniprot accession number	Gene symbol	Protein name	Mol. weight [kDa]	No. Peptides Control wk1	No. Peptides Control wk8	No. Peptides Control wk14	No. Peptides Heat wk1	No. Peptides Heat wk8	No. Peptides Heat wk14	No. Unique peptides Control wk1	No. Unique peptides Control wk8	No. Unique peptides Control wk14	No. Unique peptides Heat wk1	No. Unique peptides Heat wk8	No. Unique peptides Heat wk14	iBAQ Control wk1	iBAQ Control wk8	iBAQ Control wk14	iBAQ Heat wk1	iBAQ Heat wk8	iBAQ Heat wk14	Sequence coverage Control wk1 [%]	Sequence coverage Control wk8 [%]	Sequence coverage Control wk14 [%]	Sequence coverage Heat wk1 [%]	Sequence coverage Heat wk8 [%]	Sequence coverage Heat wk14 [%]
Q27W01	Rbm8a	RNA-binding protein 8A	19.89	3	1	1	2	2	1	3	1	1	2	2	1	8.58E+04	2.92E+04	3.80E+04	7.60E+04	1.69E+04	1.55E+04	31	6.3	6.3	17.2	17.2	6.3
P04916	Rbp4	Retinol-binding protein 4	23.22	13	13	14	13	14	13	13	13	14	13	14	13	1.22E+07	6.54E+06	1.01E+07	9.54E+06	1.26E+07	8.75E+06	61.2	61.7	61.7	61.2	61.2	60.2
Q498D8	Rbx1	Ring-box 1	12.27	3	3	2	3	3	2	3	3	2	3	3	2	3.47E+05	6.79E+05	3.02E+05	3.64E+05	3.02E+05	1.57E+05	30.6	30.6	30.6	30.6	30.6	30.6
F1LVV4	Rcc2	Regulator of chromosome condensation 2	46.65	0	1	0	0	1	1	0	1	0	0	1	1	0.00E+00	1.23E+04	0.00E+00	0.00E+00	8.32E+03	3.89E+03	0	4.9	0	0	4.9	4.9
D3ZJW6	rCG_21066	Uncharacterized protein	13.06	2	2	2	2	2	2	1	1	1	1	1	1	5.56E+05	4.93E+05	1.25E+06	1.95E+06	8.64E+05	1.31E+06	18.8	18.8	18.8	18.8	18.8	18.8
D3ZUB0	Rcn1	Reticulocalbin 1	38.09	6	4	4	5	5	5	6	4	4	5	5	5	2.26E+05	9.80E+04	5.13E+04	6.94E+04	2.39E+04	4.62E+04	35.7	28.3	20.9	25.8	31.7	23.4
I6L9G5	Rcn3	Reticulocalbin-3	37.94	5	3	4	4	3	2	5	3	4	4	3	2	1.76E+05	2.47E+04	6.68E+04	8.45E+04	1.07E+04	2.66E+04	30.5	20.4	22	22	20.4	8.8
E9PT65	Rdx	Radixin	68.49	8	7	4	8	5	1	5	5	2	5	3	0	8.85E+04	1.31E+05	1.25E+04	5.89E+04	1.87E+04	0.00E+00	16.6	15.4	9.1	17.5	9.4	1.2
Q5XI60	Reep6	Receptor expression-enhancing protein 6	23.31	3	3	3	3	3	3	3	3	3	3	3	3	6.35E+05	9.02E+05	2.87E+05	5.87E+05	6.36E+05	1.93E+05	18	18	18	18	18	18
P51607	Renbp	N-acylglucosamine 2-epimerase	49.60	2	2	2	2	3	2	2	2	2	2	3	2	2.94E+04	5.26E+04	2.22E+04	2.35E+04	2.35E+04	1.23E+04	6.7	6.7	6.7	6.7	10	6.7
Q641W6	RGD1309049	RCG43512	16.56	1	1	1	1	1	1	1	1	1	1	1	1	1.62E+04	6.01E+04	7.45E+04	8.55E+03	4.38E+03	1.30E+04	15.6	15.6	15.6	15.6	15.6	15.6
A0A0G2K896	RGD1310507	Similar to RIKEN cDNA 1300017J02	76.72	27	28	26	28	27	26	27	28	26	28	27	26	1.93E+06	1.61E+06	1.76E+06	1.67E+06	1.58E+06	1.67E+06	53	53	53.7	55.6	53.1	50.1
F7FM32	RGD1311345	Queuosine salvage protein	39.06	1	2	1	1	1	1	1	2	1	1	1	1	5.33E+04	8.01E+04	3.75E+04	3.39E+04	3.38E+04	9.50E+03	3.2	10	3.2	3.2	3.2	3.2
F1M171	RGD1311933	Similar to RIKEN cDNA 2310057J18	38.48	3	4	4	5	4	4	3	4	4	5	4	4	1.22E+05	1.73E+05	2.33E+05	1.60E+05	1.61E+05	1.62E+05	14.9	18.5	18.5	18.8	18.5	18.5
D3ZY47	RGD1559896	Similar to RIKEN cDNA 2310022B05	35.67	1	2	2	1	1	1	1	2	2	1	1	1	8.93E+03	1.79E+04	1.41E+04	1.37E+04	8.14E+03	3.87E+03	6.5	9.9	9.9	6.5	6.5	3.4
D3ZN59	RGD1559962	Similar to High mobility group protein B2	24.02	2	2	3	1	3	1	1	1	2	0	2	0	7.69E+03	9.28E+04	2.11E+05	0.00E+00	2.75E+04	0.00E+00	11.5	11.5	11.5	5.7	11.5	5.7
D3ZHA7	RGD1560334	Similar to Myosin light chain 1 slow a	22.81	5	5	3	5	5	2	4	4	2	4	4	1	8.72E+04	2.57E+05	2.27E+04	1.34E+05	9.12E+04	2.38E+03	33.8	33.8	21.3	33.8	33.8	13.5
M0RCN6	RGD1563231	Similar to immunoglobulin kappa-chain VK-1	12.44	1	1	1	1	1	1	1	1	1	1	1	1	3.32E+06	2.17E+06	2.19E+06	3.01E+06	2.54E+06	3.21E+06	13.2	13.2	13.2	13.2	13.2	13.2
A0A0G2K975	RGD1564614	Similar to complement factor H-related protein	85.81	20	24	22	21	22	20	19	22	20	19	20	19	9.60E+05	6.83E+05	6.40E+05	9.25E+05	7.44E+05	6.42E+05	41.8	45.2	44.2	42	44.2	41.2
D3ZYE2	RGD1565617	Uncharacterized protein	13.17	1	2	1	2	2	1	1	1	1	1	1	1	8.51E+05	1.59E+06	1.13E+06	5.93E+05	1.52E+06	1.37E+06	13.3	39.2	13.3	39.2	39.2	13.3
F1M7I8	RGD1565617	Similar to Ig variable region, light chain	13.58	1	2	1	2	2	1	1	1	1	1	1	1	1.02E+04	1.67E+05	9.35E+04	8.05E+03	3.53E+05	5.68E+04	12.9	37.9	12.9	37.9	37.9	12.9
D3ZUQ1	RGD1565682	Lipase	44.44	5	6	5	4	5	5	5	6	5	4	5	5	2.33E+05	2.76E+05	3.55E+05	2.38E+05	2.63E+05	2.90E+05	16.6	20.9	17.6	13.4	17.6	16.6
Q62639	Rheb	GTP-binding protein Rheb	20.48	1	1	1	2	1	0	1	1	1	2	1	0	4.86E+04	1.13E+05	3.49E+04	1.77E+04	1.38E+04	0.00E+00	8.7	8.7	8.7	14.1	8.7	0
P61589	Rhoa	Transforming protein RhoA	21.78	10	10	10	9	10	9	10	10	10	9	10	9	2.08E+06	2.43E+06	1.22E+06	1.40E+06	1.00E+06	9.63E+05	67.4	67.4	67.4	67.4	67.4	54.9
A0A096MK75	Rhog	Ras homolog family member G	19.87	5	6	4	5	5	4	4	5	3	4	4	3	2.61E+05	4.06E+05	1.74E+05	3.15E+05	1.58E+05	1.58E+05	44.4	45.5	33.7	44.4	44.4	33.7
O55004	Rnase4	Ribonuclease 4	16.90	6	6	6	6	6	6	6	6	6	6	6	6	1.39E+06	1.77E+06	1.96E+06	1.30E+06	1.33E+06	1.85E+06	43.5	43.5	43.5	43.5	43.5	43.5
Q6J2U6	Rnf114	E3 ubiquitin-protein ligase RNF114	25.66	4	4	0	4	4	0	4	4	0	4	4	0	5.19E+04	9.49E+04	0.00E+00	6.03E+04	3.19E+04	0.00E+00	20.1	20.1	0	20.1	20.1	0
Q3ZAU6	Rnf14	RBR-type E3 ubiquitin transferase	54.11	1	1	0	1	1	0	1	1	0	1	1	0	4.74E+04	3.71E+04	0.00E+00	2.94E+04	3.49E+03	0.00E+00	4	4	0	4	4	0
D3Z8P1	Rnf7	Ring finger protein 7	12.71	1	2	1	2	2	1	1	2	1	2	2	1	1.72E+04	9.42E+04	2.38E+04	3.64E+04	2.50E+04	3.11E+03	10.6	18.6	10.6	18.6	18.6	10.6
E2RUH2	Rnh1	Ribonuclease inhibitor	49.92	22	22	18	22	21	16	22	22	18	22	21	16	6.29E+06	4.86E+06	8.41E+05	5.31E+06	2.41E+06	4.42E+05	71.7	70.8	64	69.7	68.4	57.5
G3V6V1	Rnpep	Aminopeptidase B	72.69	7	7	6	7	6	4	7	7	6	7	6	4	1.09E+05	1.57E+05	9.15E+04	7.82E+04	2.51E+04	3.52E+04	15.5	15.5	14.6	15.4	13.4	9.8
A0A0G2K0B7	Ropn1l	Rhophilin-associated tail protein 1-like	22.94	2	2	2	2	1	2	2	2	2	2	1	2	6.11E+04	1.88E+05	7.93E+04	7.24E+04	1.73E+04	2.56E+04	12.6	13.1	12.6	13.1	7.8	12.6
D4A7L6	Rpia	Ribose 5-phosphate isomerase A	32.47	2	2	2	2	2	2	2	2	2	2	2	2	9.25E+04	1.17E+05	4.82E+04	5.86E+04	5.66E+04	4.05E+04	10.6	10.6	10.6	10.6	10.6	10.6
D4A1P2	Rpl10l	60S ribosomal protein L10	24.56	1	1	1	0	1	1	1	1	1	0	1	1	2.25E+03	2.39E+04	6.37E+04	0.00E+00	4.37E+04	3.45E+04	12.6	13.6	12.6	0	13.6	12.6
Q4V8I6	Rpl11	60S ribosomal protein L11	19.02	0	2	0	0	2	0	0	2	0	0	2	0	0.00E+00	3.00E+04	0.00E+00	0.00E+00	7.11E+04	0.00E+00	0	13.8	0	0	13.8	0
P23358	Rpl12	60S ribosomal protein L12	17.85	3	3	2	3	3	1	3	3	2	3	3	1	7.78E+04	1.99E+05	5.01E+04	4.59E+04	1.67E+05	4.91E+03	30.3	30.3	18.8	30.3	30.3	9.7
P61314	Rpl15	60S ribosomal protein L15	24.15	2	0	1	1	3	1	2	0	1	1	3	1	1.95E+04	0.00E+00	5.71E+03	2.32E+03	5.62E+04	2.53E+03	12.7	0	3.4	6.9	16.2	3.4
Q6PDV8	Rpl22	60S ribosomal protein L22	14.76	2	2	2	2	2	2	2	2	2	2	2	2	1.49E+05	2.07E+05	4.55E+04	8.30E+04	2.45E+05	2.65E+04	30.5	30.5	30.5	30.5	30.5	30.5
P62832	Rpl23	60S ribosomal protein L23	14.87	0	0	0	1	1	0	0	0	0	1	1	0	0.00E+00	0.00E+00	0.00E+00	2.15E+04	4.81E+04	0.00E+00	0	0	0	14.3	14.3	0
P21531	Rpl3	60S ribosomal protein L3	46.14	0	0	1	0	1	1	0	0	1	0	1	1	0.00E+00	0.00E+00	1.07E+04	0.00E+00	5.27E+03	3.25E+03	0	0	6	0	3	3
P62890	Rpl30	60S ribosomal protein L30	12.78	1	1	2	3	4	2	1	1	2	3	4	2	3.21E+04	6.15E+04	4.66E+04	7.93E+04	2.54E+05	1.11E+04	13.9	16.5	30.4	40.9	51.3	27
Q6P3V9	Rpl4	60S ribosomal protein L4	47.30	1	3	1	0	2	0	1	3	1	0	2	0	5.53E+03	2.81E+04	1.30E+04	0.00E+00	3.05E+04	0.00E+00	5.2	8.6	5.2	0	7.8	0
D3ZHP8	Rpl5l1;Rpl5	60S ribosomal protein L5	34.43	1	2	1	1	3	1	1	2	1	1	3	1	2.26E+04	2.82E+04	9.97E+03	1.86E+04	8.16E+04	2.31E+03	6.1	8.4	6.1	4	12.8	4.7
B0K031	Rpl7	60S ribosomal protein L7	30.31	0	1	0	0	1	1	0	1	0	0	1	1	0.00E+00	1.51E+04	0.00E+00	0.00E+00	8.27E+04	7.52E+03	0	7.3	0	0	7.3	7.3
P19945	Rplp0	60S acidic ribosomal protein P0	34.22	3	2	1	3	3	1	3	2	1	3	3	1	4.37E+04	7.79E+04	1.23E+04	4.13E+04	1.10E+05	1.26E+04	11.4	8.2	3.8	11.4	11.4	4.4
P19944	Rplp1	60S acidic ribosomal protein P1	11.50	2	3	3	2	3	3	2	3	3	2	3	3	1.25E+06	7.03E+05	3.36E+05	2.38E+05	6.68E+05	1.06E+05	60.5	74.6	74.6	60.5	74.6	74.6
Q6PDW1	Rps12	40S ribosomal protein S12	14.52	5	4	3	4	4	2	5	4	3	4	4	2	5.83E+05	4.66E+05	5.69E+05	1.96E+05	4.10E+05	4.84E+05	54.5	37.9	31.8	43.2	37.9	30.3
P62845	Rps15	40S ribosomal protein S15	17.04	1	1	1	0	1	1	1	1	1	0	1	1	3.37E+05	3.84E+04	1.09E+04	0.00E+00	3.26E+04	8.77E+03	18.6	18.6	18.6	0	18.6	18.6
D4A6G6	Rps19	40S ribosomal protein S19	16.12	1	1	0	1	1	0	1	1	0	1	1	0	2.86E+04	3.50E+04	0.00E+00	2.75E+03	1.28E+04	0.00E+00	9	9	0	9	9	0
A0A0U1RVI9	Rps2	40S ribosomal protein S2	28.59	3	2	0	2	3	0	3	2	0	2	3	0	1.49E+05	2.42E+04	0.00E+00	1.36E+04	6.11E+04	0.00E+00	17.6	10.5	0	13.5	15.4	0
A0A0G2JXC3	Rps21	40S ribosomal protein S21	8.87	1	2	1	0	1	0	1	2	1	0	1	0	1.49E+04	9.86E+04	1.74E+04	0.00E+00	9.46E+04	0.00E+00	19.8	19.8	18.5	0	18.5	0
P62982	Rps27a	Ubiquitin-40S ribosomal protein S27a	17.95	3	3	2	3	4	2	3	3	2	3	4	2	5.71E+05	1.20E+06	7.79E+05	6.33E+05	8.74E+05	4.89E+05	25.6	25.6	16	25.6	34	16
P62909	Rps3	40S ribosomal protein S3	26.67	3	3	2	3	3	4	3	3	2	3	3	4	4.35E+04	3.26E+04	4.20E+04	1.78E+04	8.86E+04	2.84E+04	15.2	15.2	10.3	15.2	15.2	20.6
X1WI37	Rps4x	40S ribosomal protein S4, X isoform	29.47	0	0	1	1	2	1	0	0	1	1	2	1	0.00E+00	0.00E+00	1.22E+04	1.10E+03	3.08E+04	5.87E+03	0	0	6.5	6.5	13.7	6.5
A0A0G2K200	Rps5	40S ribosomal protein S5	19.33	1	2	1	1	0	0	1	2	1	1	0	0	7.12E+04	9.64E+04	3.15E+04	5.06E+03	0.00E+00	0.00E+00	11.7	21.6	11.7	9.9	0	0
D3Z8E0	Rps6ka3	Ribosomal protein S6 kinase	83.72	4	5	5	5	4	5	4	5	5	5	4	5	1.44E+04	4.08E+04	1.39E+04	1.99E+04	1.20E+04	9.54E+03	7	8.6	8.6	8.6	7	8.6
P62083	Rps7	40S ribosomal protein S7	22.13	3	4	2	2	3	1	3	4	2	2	3	1	5.96E+04	8.06E+04	2.39E+04	1.34E+04	7.57E+04	3.57E+03	27.3	36.6	24.7	11.9	21.1	15.5
P38983	Rpsa	40S ribosomal protein SA	32.82	4	6	3	5	6	4	4	6	3	5	6	4	2.00E+05	2.67E+05	2.37E+04	1.14E+05	2.87E+05	2.65E+04	27.1	36.9	18.6	34.2	38	23.1
F1M853	Rrbp1	Ribosome-binding protein 1	157.50	6	9	4	6	6	3	6	9	4	6	6	3	1.43E+04	2.20E+04	4.58E+03	1.68E+04	1.07E+04	4.05E+03	5.5	8.6	3.4	5.5	5.5	2.5
D4A8F2	Rsu1	Ras suppressor protein 1	31.34	1	1	1	1	1	1	1	1	1	1	1	1	3.70E+04	7.26E+04	1.28E+04	1.82E+04	1.79E+04	7.80E+03	8.7	8.7	8.7	8.7	8.7	8.7
E9PSS8	RT1-A1	RT1 class Ia, locus A1	41.24	4	4	3	4	3	3	1	1	1	1	1	1	1.09E+05	1.09E+05	3.15E+04	7.56E+04	5.17E+04	2.65E+04	11.7	11.7	9	11.7	9	9
Q6MGB8	RT1-A2	RT1 class Ia, locus A2	41.39	3	3	2	4	4	1	1	1	1	1	1	0	2.09E+04	1.29E+04	1.21E+04	1.75E+04	2.09E+04	0.00E+00	10.1	10.1	7.4	13.7	13.7	3.6
P15978	RT1-Aw2	Class I histocompatibility antigen, Non-RT1.A alpha-1 chain	36.57	5	5	4	6	6	4	3	3	3	3	3	3	1.90E+05	2.11E+05	1.27E+05	2.59E+05	2.08E+05	1.38E+05	20.1	20.1	16.9	24.1	24.1	16.9
Q6AYT3	Rtcb	tRNA-splicing ligase RtcB homolog	55.25	4	6	5	6	7	3	4	6	5	6	7	3	8.10E+04	1.83E+05	7.08E+04	1.10E+05	6.81E+04	1.16E+04	9.7	15	13.9	14.1	17.2	8.1
A0A0H2UHX1	Rtn3	Reticulon-3	28.23	1	1	1	1	1	1	1	1	1	1	1	1	1.08E+03	3.34E+04	2.75E+03	3.19E+03	6.54E+03	1.10E+03	15.3	15.3	15.3	15.3	15.3	15.3
F7EMB2	Rtraf	RNA transcription, translation and transport factor	28.17	1	0	1	1	1	0	1	0	1	1	1	0	1.32E+04	0.00E+00	1.03E+04	1.57E+04	1.91E+04	0.00E+00	8.2	0	8.2	8.2	8.2	0
P60123	Ruvbl1	RuvB-like 1	50.21	7	8	7	7	7	2	7	8	7	7	7	2	7.89E+04	1.03E+05	9.19E+04	5.54E+04	6.15E+04	9.39E+03	21.3	26.5	21.9	20.6	20.4	6.1
G3V8T5	Ruvbl2	RuvB-like 2	51.11	5	7	5	4	5	4	5	7	5	4	5	4	8.14E+04	1.30E+05	8.06E+04	4.20E+04	6.56E+04	1.80E+04	12.3	14.9	12.7	10.4	12.3	10.2
P35467	S100a1	Protein S100-A1	10.56	3	3	3	3	3	3	3	3	3	3	3	3	3.80E+06	2.62E+06	2.57E+06	1.06E+06	1.32E+06	1.26E+06	42.6	42.6	42.6	42.6	42.6	42.6
Q6B345	S100a11	Protein S100-A11	11.07	2	1	1	0	2	1	2	1	1	0	2	1	2.16E+05	5.35E+04	1.28E+05	0.00E+00	2.03E+05	2.27E+04	27.6	16.3	16.3	0	27.6	16.3
P05942	S100a4	Protein S100-A4	11.78	1	1	1	1	1	1	1	1	1	1	1	1	3.29E+05	2.95E+05	1.66E+05	1.61E+05	1.07E+05	1.00E+05	16.8	16.8	16.8	16.8	16.8	16.8
P05964	S100a6	Protein S100-A6	10.04	3	3	3	1	2	2	3	3	3	1	2	2	2.02E+05	2.00E+05	9.34E+04	1.86E+04	2.70E+05	1.52E+05	56.2	56.2	56.2	9	28.1	47.2
P04631	S100b	Protein S100-B	10.74	3	4	3	3	3	3	3	4	3	3	3	3	5.63E+06	1.04E+07	3.61E+06	5.32E+06	3.28E+06	3.52E+06	40.2	44.6	40.2	40.2	40.2	40.2
Q5M878	Saa4	Serum amyloid A protein	14.97	11	13	10	11	10	11	11	13	10	11	10	11	6.03E+07	4.78E+07	4.55E+07	6.56E+07	3.92E+07	3.27E+07	67.7	72.3	67.7	67.7	67.7	67.7
Q6AXQ0	Sae1	SUMO-activating enzyme subunit 1	38.51	5	6	4	6	5	2	5	6	4	6	5	2	1.09E+05	1.27E+05	6.06E+04	5.88E+04	2.68E+04	9.95E+03	24.1	29.8	20.1	29.8	23.5	9.7
Q6AY18	Sar1a	GTP-binding protein SAR1a	22.40	4	4	4	2	0	4	4	4	3	2	0	3	2.38E+05	3.73E+05	1.86E+05	9.18E+04	0.00E+00	1.25E+05	47	47	42.4	25.3	0	40.9
Q5HZY2	Sar1b	GTP-binding protein SAR1b	22.41	2	2	2	2	2	2	2	2	1	2	2	1	6.33E+04	1.61E+05	1.13E+04	2.16E+05	3.22E+04	3.09E+03	16.2	16.2	15.7	16.2	16.2	15.7
Q498U4	Sarnp	SAP domain-containing ribonucleoprotein	23.61	2	2	2	2	1	2	2	2	2	2	1	2	8.30E+04	1.28E+05	3.35E+04	4.13E+04	1.79E+04	1.59E+04	9	9	9	9	4.8	9
A0A0G2JZG7	Sars	Serine--tRNA ligase, cytoplasmic	61.36	6	8	6	6	5	2	6	8	6	6	5	2	8.29E+04	1.44E+05	6.59E+04	8.30E+04	3.82E+04	1.04E+04	18.5	23.1	20	18.5	16	7.8
A0A0G2JTU6	Sbp	Prostatic spermine-binding protein	26.10	1	3	1	1	1	0	1	3	1	1	1	0	6.72E+03	2.61E+05	1.58E+03	3.28E+03	4.33E+03	0.00E+00	7.2	17	7.2	7.2	7.2	0
F7FEM5	Sbsn	Suprabasin	69.44	4	4	4	4	4	3	4	4	4	4	4	3	1.18E+05	1.47E+05	5.18E+04	1.27E+05	1.16E+05	4.28E+04	18.5	18.5	18.5	18.5	18.5	7.9
G3V921	Scel	Sciellin	72.85	1	2	1	2	1	2	1	2	1	2	1	2	3.59E+04	3.34E+04	3.92E+04	1.76E+04	4.19E+04	9.20E+04	1.7	4.6	1.7	4.6	1.7	4.6
P02780	Scgb2a2	Secretoglobin family 2A member 2	10.73	4	4	2	4	4	3	4	4	2	4	4	3	1.59E+06	2.76E+06	5.28E+03	1.04E+06	6.60E+05	1.46E+05	46.3	46.3	20	46.3	46.3	43.2
F1LQ55	Scp2	Non-specific lipid-transfer protein	58.79	1	1	2	1	1	2	1	1	2	1	1	2	3.66E+04	3.25E+04	1.36E+04	1.74E+04	1.08E+04	5.94E+03	1.8	1.8	3.8	1.8	1.8	3.8
Q920A6	Scpep1	Retinoid-inducible serine carboxypeptidase	51.17	7	7	7	7	7	7	7	7	7	7	7	7	4.96E+05	4.83E+05	2.69E+05	1.67E+05	2.19E+05	1.23E+05	21.7	21.7	21.7	21.7	21.7	21.7
Q6AY84	Scrn1	Secernin-1	46.40	3	2	1	3	3	3	3	2	1	3	3	3	1.61E+05	1.40E+05	1.16E+03	5.94E+04	4.93E+04	2.63E+04	10.1	7	3.1	10.1	10.1	10.1
Q6AYR8	Scrn2	Secernin-2	46.50	7	9	6	9	7	5	7	9	6	9	7	5	1.30E+05	2.66E+05	8.98E+04	8.77E+04	5.82E+04	1.57E+04	28.1	40.9	25.3	40.9	37.4	18.4
Q5XFW8	Sec13	Protein SEC13 homolog	35.55	3	3	1	3	1	1	3	3	1	3	1	1	6.78E+04	1.08E+05	1.87E+04	2.93E+04	1.30E+04	7.67E+03	15.5	15.5	3.4	15.5	3.4	3.4
A0A0G2JZM[illegible]	Sec23a	Protein transport protein SEC23	84.71	6	5	2	4	2	2	6	5	2	4	2	2	6.22E+04	2.46E+04	1.35E+04	3.24E+04	1.23E+04	9.94E+03	10.1	8.8	4.4	7.2	3.6	4.4
A0A0G2JZF0	Sec24c	SEC24 homolog C, COPII coat complex component	114.70	2	3	2	1	2	1	2	3	2	1	2	1	7.02E+03	1.07E+04	1.85E+03	1.18E+03	1.10E+04	9.44E+02	2.5	4.1	2.5	1.2	2.5	1.2
A0A0G2K0X9	Sec31a	Protein transport protein Sec31A	131.97	10	10	7	10	10	5	10	10	7	10	10	5	9.18E+04	1.21E+05	3.34E+04	5.43E+04	4.21E+04	7.88E+03	15	14.1	9.8	15	14.7	5.9
F1LRJ9	Selenbp1	Selenium-binding protein 1	55.11	18	20	19	20	17	17	18	20	19	20	17	17	7.14E+05	1.36E+06	1.24E+06	6.35E+05	4.15E+05	1.56E+06	52.2	55.6	52.8	57.3	49.2	46.4
P25236	Selenop	Selenoprotein P	43.08	9	10	11	10	9	11	9	10	11	10	9	11	2.22E+06	2.02E+06	1.52E+06	2.22E+06	2.25E+06	1.44E+06	21.6	23.1	23.1	21.6	21.6	23.1
F7EY63	Sell	L-selectin	49.10	2	2	2	2	2	2	2	2	2	2	2	2	4.39E+04	6.65E+04	7.59E+04	2.73E+04	3.09E+04	8.48E+04	7	7	7	7	7	7
Q6P6X2	Semg1	Semenogelin-1	45.55	6	2	0	3	6	0	6	2	0	3	6	0	1.21E+05	5.83E+03	0.00E+00	1.53E+04	1.35E+05	0.00E+00	15	5.6	0	9.2	15	0
D3ZFY0	Sephs1	Selenophosphate synthetase 1	42.89	4	5	2	4	3	1	4	5	2	4	3	1	8.82E+04	1.54E+05	8.33E+03	5.37E+04	4.85E+04	2.37E+03	14.8	20.2	9.2	14.8	11.7	5.4
B3GNI6	Sept11	Septin-11	49.34	9	10	6	7	7	5	9	10	6	7	7	5	2.28E+05	3.53E+05	1.31E+05	1.62E+05	9.58E+04	1.08E+05	20.7	23.1	17.9	20.3	20.5	15.4
Q91Y81	Sept2	Septin-2	41.59	7	8	6	7	7	6	7	8	6	7	7	6	2.09E+05	3.60E+05	1.39E+05	1.76E+05	1.97E+05	9.29E+04	33	33.8	30.5	29.4	33	30.5

Uniprot accession number	Gene symbol	Protein name	Mol. weight [kDa]	No. Peptides Control wk1	No. Peptides Control wk8	No. Peptides Control wk14	No. Peptides Heat wk1	No. Peptides Heat wk8	No. Peptides Heat wk14	No. Unique peptides Control wk1	No. Unique peptides Control wk8	No. Unique peptides Control wk14	No. Unique peptides Heat wk1	No. Unique peptides Heat wk8	No. Unique peptides Heat wk14	iBAQ Control wk1	iBAQ Control wk8	iBAQ Control wk14	iBAQ Heat wk1	iBAQ Heat wk8	iBAQ Heat wk14	Sequence coverage Control wk1 [%]	Sequence coverage Control wk8 [%]	Sequence coverage Control wk14 [%]	Sequence coverage Heat wk1 [%]	Sequence coverage Heat wk8 [%]	Sequence coverage Heat wk14 [%]
Q9WVC0	Sept7	Septin-7	50.58	8	8	8	8	9	6	8	8	8	8	9	6	1.32E+05	1.85E+05	1.86E+05	1.70E+05	9.38E+04	9.71E+04	22	22	26.8	22	22	20.6
Q9QZR6	Sept9	Septin-9	63.79	8	10	6	11	11	5	8	10	6	11	11	5	1.07E+05	1.82E+05	3.41E+04	1.15E+05	8.76E+04	1.20E+04	21.1	22.7	11.9	24.3	24.3	13.3
A0A0G2JY31	Serpina1	Alpha-1-antiproteinase	46.12	19	27	20	21	24	20	19	27	20	21	24	20	2.85E+07	3.52E+07	3.60E+07	2.66E+07	3.12E+07	2.68E+07	50.4	59.1	51.8	56.2	57.7	51.8
Q62975	Serpina10	Protein Z-dependent protease inhibitor	50.24	16	18	19	16	16	18	16	18	19	16	16	18	4.16E+06	3.58E+06	4.97E+06	4.28E+06	4.27E+06	4.88E+06	48.4	43.3	51.6	43.1	42.7	49.8
Q7TPA5	Serpina11	Serpin A11	47.02	5	5	6	4	6	6	5	5	6	4	6	6	1.65E+05	9.07E+04	2.18E+05	1.11E+05	1.60E+05	2.28E+05	12.1	12.1	14.9	9.7	14.9	14.9
A0A0G2JSK1	Serpina3c	Serine protease inhibitor A3C	46.48	30	31	30	31	33	28	1	1	2	2	2	1	1.89E+06	2.28E+06	9.62E+05	2.69E+06	1.16E+06	1.90E+06	67.3	67.3	64.9	67.3	71.2	64.9
P05545	Serpina3k	Serine protease inhibitor A3K	46.56	34	36	33	35	36	32	6	7	6	7	6	6	5.86E+07	5.20E+07	6.55E+07	5.90E+07	6.98E+07	6.58E+07	76	76.4	73.6	76.4	79.8	73.6
P05544	Serpina3l	Serine protease inhibitor A3L	46.28	39	40	42	40	42	40	3	3	3	3	3	2	1.11E+08	9.31E+07	1.14E+08	1.02E+08	1.12E+08	1.11E+08	79.7	80.6	81.8	80.6	85	81.4
F1LR92	Serpina3m	Serine protease inhibitor A3M	46.84	23	24	22	23	23	22	20	21	20	20	20	19	1.05E+07	7.13E+06	1.09E+07	7.59E+06	1.15E+07	1.01E+07	59.9	58.2	56.8	57.8	58.9	57.5
A0A0H2UHI5	Serpina3n	Serine protease inhibitor A3N	45.48	30	30	30	31	32	30	14	14	14	14	14	14	6.73E+06	4.99E+06	7.46E+06	5.66E+06	8.12E+06	7.19E+06	66.7	66.7	73.8	73.8	77.7	73.8
Q5M8C3	Serpina4	Serine protease inhibitor A4	48.05	18	18	17	18	18	18	18	18	17	18	18	18	2.13E+07	1.65E+07	2.60E+07	1.83E+07	2.14E+07	2.58E+07	54.4	54.4	52.5	54.4	54.4	54.4
F7EMJ6	Serpina5	Serine protease inhibitor A5	49.45	6	5	3	5	4	2	6	5	3	5	4	2	1.84E+05	1.22E+05	5.26E+04	8.50E+04	8.73E+04	1.99E+04	21.9	20.1	14.5	20.1	16.3	6.3
P31211	Serpina6	Corticosteroid-binding globulin	44.67	16	18	16	16	17	17	16	18	16	16	17	17	7.90E+06	6.00E+06	7.35E+06	6.16E+06	1.35E+07	5.47E+06	46.7	50	48.7	46.7	48.7	48.7
D3ZKA0	Serpinb13	Serine protease inhibitor B13	44.25	0	1	1	1	3	1	0	1	1	1	3	1	0.00E+00	4.48E+03	1.73E+03	9.39E+02	1.42E+05	2.49E+03	0	3.3	3.3	3.3	8.2	3.3
G3V6C1	Serpinb5	Serine protease inhibitor B5	42.07	0	0	3	0	4	0	0	0	3	0	4	0	0.00E+00	0.00E+00	9.92E+03	0.00E+00	1.40E+05	0.00E+00	0	0	9.1	0	13.6	0
Q6P9U0	Serpinb6	Serine protease inhibitor B6	43.02	7	7	6	7	7	6	7	7	6	7	7	6	4.22E+05	4.59E+05	4.25E+05	2.72E+05	3.25E+05	2.22E+05	25.6	25.6	19	25.6	25.6	19
Q6AYF8	Serpinb9	Serine protease inhibitor B9	42.30	7	9	5	10	7	1	7	9	5	10	7	1	2.19E+05	2.82E+05	7.70E+04	1.37E+05	1.04E+05	2.22E+04	27	33.7	16.3	36.1	26.5	4.5
Q5M7T5	Serpinc1	Serine protease inhibitor C1	52.23	29	29	33	30	29	29	23	23	26	23	23	23	1.21E+07	9.58E+06	1.17E+07	9.05E+06	1.22E+07	1.11E+07	66.9	66.9	67.7	67.3	60.9	61.5
A0A0G2K8K3	Serpind1	Heparin cofactor 2	58.02	19	20	20	22	21	20	19	20	20	22	21	20	7.17E+06	4.98E+06	9.14E+06	7.71E+06	6.44E+06	8.78E+06	46	46.6	46.8	49.5	47.4	46.8
Q80ZA3	Serpinf1	Alpha-2 antiplasmin	46.47	20	22	20	20	20	21	20	22	20	20	20	21	1.45E+07	9.52E+06	1.59E+07	1.30E+07	1.10E+07	1.58E+07	54.5	56.7	58.1	58.6	47.8	51.4
F7FHF3	Serpinf2	Serpin family F member 2	62.29	15	16	17	15	18	15	15	16	17	15	18	15	4.47E+06	3.57E+06	4.64E+06	4.09E+06	6.27E+06	4.43E+06	37.4	42.4	40.8	36.5	50.4	37.5
Q6P734	Serping1	Plasma protease C1 inhibitor	55.61	29	30	29	29	28	27	29	30	29	29	28	27	3.19E+07	2.18E+07	2.33E+07	2.61E+07	2.42E+07	2.30E+07	63.1	63.3	62.1	62.3	62.3	60.1
Q5RJR9	Serpinh1	Serine protease inhibitor H1	46.56	2	1	2	1	1	2	2	1	2	1	1	2	5.85E+04	3.05E+03	6.09E+03	2.00E+03	7.82E+02	9.38E+03	8.6	5.5	8.6	5.5	3.1	8.6
A0A0G2JSU3	Set	Protein SET	33.38	4	6	4	7	5	4	4	6	4	7	5	4	3.52E+05	6.61E+05	4.42E+05	2.92E+05	1.87E+05	5.32E+04	26	30.8	29.4	35.3	26	29.4
D4ADE5	Setd7	Histone-lysine N-methyltransferase SETD7	40.51	2	3	3	2	2	2	2	3	3	2	2	2	4.47E+04	8.52E+04	2.19E+04	2.74E+04	1.67E+04	1.71E+04	7.7	10.1	10.1	7.7	7.7	7.4
D3ZQM0	Sf3a1	Splicing factor 3a, subunit 1	88.59	3	3	2	3	3	2	3	3	2	3	3	2	1.16E+05	2.47E+05	3.58E+04	1.07E+05	2.56E+05	3.33E+04	5.9	5.9	4.3	5.9	5.9	4.3
G3V9A3	Sfn	RCG31390	27.75	4	6	6	6	10	6	2	4	4	4	8	4	9.78E+04	1.32E+05	8.39E+04	9.60E+04	1.80E+06	1.67E+04	18.1	28.2	23.4	29	44.8	23.4
A0A0G2K8K0	Sfpq	Splicing factor proline and glutamine rich	75.09	3	3	1	2	2	1	3	3	1	2	2	1	3.30E+04	2.73E+04	1.40E+04	2.00E+04	2.67E+04	4.35E+03	6	6	2.2	3.6	4.6	2.2
A0A0H2UHK0	Sfr1	Swi5-dependent recombination DNA repair protein 1 homolog	29.02	3	3	2	3	1	1	3	3	2	3	1	1	6.89E+04	1.16E+05	3.38E+04	4.16E+04	1.15E+04	9.44E+03	14.5	14.5	10.2	14.5	5.5	4.7
O70593	Sgta	Small glutamine-rich tetratricopeptide repeat-containing protein alpha	34.16	3	4	2	4	3	2	3	4	2	4	3	2	1.38E+05	1.97E+05	5.56E+04	1.64E+05	4.43E+04	2.72E+04	12.1	15.9	7.3	15.9	11.8	7.3
B5DFD8	Sh3bgrl	SH3 domain-binding glutamic acid-rich-like protein	12.80	2	2	1	2	2	1	2	2	1	2	2	1	4.74E+04	8.56E+04	5.62E+04	6.39E+04	8.55E+04	2.61E+04	24.6	24.6	15.8	24.6	24.6	15.8
B2RZ27	Sh3bgrl3	SH3 domain binding glutamic acid-rich protein-like 3	10.48	1	1	0	1	2	0	1	1	0	1	2	0	1.77E+05	1.28E+04	0.00E+00	1.39E+04	1.15E+05	0.00E+00	35.5	35.5	0	20.4	55.9	0
O35964	Sh3gl1	Endophilin-A2	41.49	4	4	2	4	3	3	4	4	2	4	3	3	7.22E+04	4.73E+04	1.98E+04	2.37E+04	1.64E+04	5.68E+03	21.2	21.2	7.9	21.2	16.6	12.2
Q9JKT0	Sh3gl3	Endophilin-A3	35.31	2	4	2	3	3	1	2	4	2	3	3	1	2.29E+04	1.35E+05	4.33E+04	1.37E+04	1.34E+04	3.06E+03	7.1	16.3	9.6	12.5	12.5	5.4
Q71F54	Sh3rf1	E3 ubiquitin-protein ligase SH3RF1	93.88	0	0	0	0	1	0	0	0	0	0	1	0	0.00E+00	0.00E+00	0.00E+00	0.00E+00	1.19E+04	0.00E+00	0	0	0	0	1.3	0
A0A0H2UHJ[illegible]	Shbg	Sex hormone-binding globulin	48.81	11	10	10	10	11	10	11	10	10	10	11	10	8.52E+05	6.86E+05	8.50E+05	1.12E+06	1.07E+06	6.62E+05	40.9	38	38.7	38	40.9	38.7
B1H291	Shcbp1l	SHC-binding and spindle-associated 1-like	70.50	4	5	6	4	1	3	4	5	6	4	1	3	2.83E+04	7.69E+04	1.03E+05	2.78E+04	1.30E+04	3.90E+04	9.1	11.9	11	9.1	2	7.8
Q6TXG7	Shmt1	Serine hydroxymethyltransferase	75.37	9	9	7	8	8	7	9	9	7	8	8	7	2.08E+05	3.75E+05	6.63E+04	1.88E+05	8.98E+04	3.31E+04	22.2	22.2	17.5	20.3	20.9	17.5
A0A0G2JWM2	Sirt2	NAD-dependent protein deacetylase sirtuin-2	43.16	6	6	5	3	5	3	6	6	5	3	5	3	9.83E+04	1.80E+05	5.82E+04	4.73E+04	2.71E+04	2.08E+04	17.5	17.5	15.5	12.1	17.3	9.3
A0A0G2K4X8	Skp1	S-phase kinase-associated protein 1	18.93	7	7	5	7	7	6	7	7	5	7	7	6	5.17E+05	8.93E+05	2.23E+05	4.56E+05	3.04E+05	1.47E+05	65.5	65.5	50.3	67.9	65.5	58.2
Q09073	Slc25a5	ADP/ATP translocase 2;ADP/ATP translocase 2, N-terminally processed	32.90	0	0	1	1	2	0	0	0	1	1	2	0	0.00E+00	0.00E+00	7.21E+03	1.10E+04	4.02E+04	0.00E+00	0	0	4.7	3	7	0
Q9JJ19	Slc9a3r1	Na(+)/H(+) exchange regulatory cofactor NHE-RF1	38.83	7	6	5	7	6	5	7	6	5	7	6	5	1.18E+05	1.09E+05	1.54E+05	8.16E+04	3.64E+04	9.01E+04	21.3	21.3	21.3	21.3	21.3	21.3
A0A096MK98	Slfn5	Schlafen family member 5	101.05	2	3	2	2	3	2	2	3	2	2	3	2	8.27E+03	1.03E+04	2.66E+04	6.34E+03	7.26E+03	2.27E+04	2.8	3.3	2.8	2.8	3.9	2.7
Q64298	Smcp	Sperm mitochondrial-associated cysteine-rich protein	15.15	6	6	5	7	7	2	6	6	5	7	7	2	1.26E+06	2.25E+06	6.10E+05	2.06E+06	7.15E+05	9.30E+03	44.8	44.8	29.7	62.1	62.1	13.1
Q6IE50	Smoc1	SPARC-related modular calcium binding protein 1	49.78	2	1	1	2	2	1	2	1	1	2	2	1	3.16E+04	1.05E+04	6.55E+03	1.78E+04	1.32E+04	6.79E+03	4.2	2	2.2	4.2	4.2	2.2
Q5XIA6	Smpd1	Sphingomyelin phosphodiesterase	69.76	8	6	7	6	7	7	8	6	7	6	7	7	1.24E+05	8.96E+04	1.03E+05	1.02E+05	8.59E+04	9.86E+04	17.5	12.9	17.4	15	17.4	17.4
D3ZII8	Smyd5	SET and MYND domain containing 5	47.07	1	0	0	1	1	1	1	0	0	1	1	1	3.18E+04	0.00E+00	0.00E+00	2.95E+03	1.55E+03	3.70E+03	3.4	0	0	2.6	2.6	3.4
A0A0G2K0I[illegible]	Sncg	Gamma-synuclein	13.05	2	3	2	2	2	2	2	3	2	2	2	2	5.13E+05	5.04E+05	4.34E+05	1.09E+05	1.25E+05	2.67E+05	26.8	28.5	26.8	26.8	26.8	26.8
D4A8Y5	Snd1	Staphylococcal nuclease domain-containing protein 1	99.05	3	2	0	2	2	0	3	2	0	2	2	0	1.60E+04	1.24E+04	0.00E+00	5.62E+03	6.86E+03	0.00E+00	7.5	4	0	4	4	0
D3ZNR4	Sned1	Sushi, nidogen and EGF-like domain-containing protein 1	150.75	1	2	2	2	2	2	1	2	2	2	2	2	3.77E+03	5.69E+03	1.16E+04	7.57E+03	5.51E+03	1.14E+04	1	2	2	2	2	2
Q5RK19	Snf8	Vacuolar-sorting protein SNF8	28.88	2	2	1	2	1	1	2	2	1	2	1	1	4.53E+04	5.32E+04	3.33E+04	2.91E+04	9.33E+03	9.81E+03	10.1	10.1	4.7	10.1	4.7	4.7
Q5U214	Snrpa	Small nuclear ribonucleoprotein polypeptide A	31.18	1	1	1	1	1	1	1	1	1	1	1	1	6.96E+04	8.82E+04	4.34E+04	5.31E+04	5.29E+04	2.23E+04	6.8	6.8	6.8	6.8	6.8	6.8
D3ZCL3	Snrpc	U1 small nuclear ribonucleoprotein C	17.36	1	3	1	1	2	2	1	3	1	1	2	2	1.47E+04	4.92E+05	1.53E+04	2.98E+04	5.60E+04	1.21E+04	7.5	19.5	7.5	11.3	18.9	19.5
M0R8K2	Snrpd2l	Small nuclear ribonucleoprotein Sm D2	13.52	1	1	1	1	1	1	1	1	1	1	1	1	9.79E+04	2.86E+05	1.33E+05	8.62E+04	1.18E+05	4.81E+04	8.5	8.5	8.5	8.5	8.5	8.5
M0R907	Snrpd3	Small nuclear ribonucleoprotein Sm D3	13.92	4	4	4	4	3	3	4	4	4	4	3	3	2.50E+05	2.61E+05	1.67E+05	1.46E+05	1.21E+05	2.91E+04	37.3	37.3	37.3	37.3	29.4	31.7
Q99N27	Snx1	Sorting nexin-1	59.04	9	9	8	8	6	7	8	8	7	7	5	6	1.97E+05	2.60E+05	9.07E+04	1.03E+05	8.79E+04	6.75E+04	20.7	20.7	18	18.4	14.4	15.7
B2RYP4	Snx2	Sorting nexin-2	58.53	10	11	7	9	9	6	9	10	6	8	8	5	2.69E+05	3.42E+05	1.09E+05	1.33E+05	1.27E+05	5.51E+04	23.3	25.2	18.9	23.3	21.2	14.8
G3V8U4	Snx27	Sorting nexin-27	59.53	1	2	1	2	2	0	1	2	1	2	2	0	6.37E+03	1.83E+04	1.17E+03	6.13E+03	7.80E+03	0.00E+00	2.7	4.4	1.7	4.4	4.4	0
B1H267	Snx5	Sorting nexin-5	46.79	7	6	6	6	4	6	7	6	6	6	4	6	1.73E+05	2.48E+05	1.29E+05	1.12E+05	6.91E+04	4.29E+04	27.5	24.8	23.5	23.5	11.9	23.5
B5DEY8	Snx6	Sorting nexin-6	46.64	2	3	1	1	2	0	2	3	1	1	2	0	2.88E+04	4.20E+04	1.10E+04	1.95E+03	1.20E+04	0.00E+00	7.1	11.6	4.4	4.4	7.1	0
Q08420	Sod3	Extracellular superoxide dismutase [Cu-Zn]	26.62	7	7	7	7	7	7	7	7	7	7	7	7	6.20E+06	4.68E+06	5.34E+06	6.14E+06	7.61E+06	5.75E+06	32.8	32.8	32.8	32.8	32.8	32.8
E9PSJ4	Spag9	Sperm-associated antigen 9	146.00	0	1	0	1	1	1	0	1	0	1	1	1	0.00E+00	1.18E+03	0.00E+00	1.05E+03	2.23E+02	7.23E+03	0	0.6	0	0.8	0.8	0.8
P16975	Sparc	SPARC	34.30	8	8	7	8	8	6	8	8	7	8	8	6	3.41E+06	1.18E+06	7.73E+05	1.26E+06	8.27E+05	6.63E+05	48.5	48.5	42.2	48.5	48.5	37.9
G3V7X5	Sparcl1	SPARC-like protein 1	70.55	15	16	12	18	17	13	15	16	12	18	17	13	8.05E+05	6.78E+05	4.92E+05	1.01E+06	6.23E+05	3.69E+05	36.8	38.8	27.6	42.3	42.3	32.8
A0A0H2UHA4	Spata18	Mitochondria-eating protein	67.79	3	3	3	3	2	0	3	3	3	3	2	0	2.40E+04	3.59E+04	4.08E+04	2.53E+04	8.05E+03	0.00E+00	7.3	7.3	7.3	7.3	5.1	0
F1LSR7	Spata20	Spermatogenesis-associated protein 20	88.31	15	17	17	18	16	11	15	17	17	18	16	11	2.56E+05	4.62E+05	2.87E+05	2.51E+05	9.21E+04	3.75E+04	28.1	31.4	33.1	35.1	28.5	24.1
P09656	Spink3	Serine protease inhibitor Kazal-type 3	8.57	2	1	2	2	2	1	2	1	2	2	2	1	2.85E+05	2.77E+04	5.35E+04	1.14E+05	2.27E+05	1.19E+04	32.9	17.7	32.9	32.9	32.9	15.2
A0A0G2K946	Spock2	SPARC/osteonectin, cwcv and kazal-like domains proteoglycan 2	47.01	6	7	8	6	6	8	6	7	8	6	6	8	1.83E+05	1.77E+05	1.79E+05	1.34E+05	1.02E+05	1.14E+05	23.1	24.7	28.2	23.1	23.1	28.2
Q3B7D6	Spon1	Spondin-1	90.76	6	6	5	3	4	5	6	6	5	3	4	5	1.42E+05	7.95E+04	5.82E+04	5.86E+04	7.95E+04	7.38E+04	15.6	15.6	12	6.2	8.6	12
P08721	Spp1	Osteopontin	34.96	0	1	0	1	1	0	0	1	0	1	1	0	0.00E+00	2.31E+03	0.00E+00	2.15E+04	3.32E+03	0.00E+00	0	4.1	0	4.1	4.1	0
A0A0G2K9X1	Spp2	Secreted phosphoprotein 24	14.86	2	2	2	1	1	2	2	2	2	1	1	2	2.29E+04	2.95E+04	9.50E+04	3.72E+04	2.75E+04	6.69E+04	17.8	17.8	17.8	8.9	8.9	17.8
P18297	Spr	Sepiapterin reductase	28.13	7	7	8	8	5	7	7	7	8	8	5	7	4.66E+05	5.11E+05	1.87E+05	2.92E+05	1.23E+05	1.63E+05	40.5	40.5	46.6	46.6	31.3	40.8
D3ZAR3	Sprr2d	Small proline-rich protein 2D	8.86	1	1	1	1	1	1	1	1	1	1	1	1	5.05E+04	2.47E+04	2.33E+04	9.04E+03	1.11E+05	1.18E+04	16	16	16	16	16	16
Q6IRK8	Sptan1	Spectrin alpha chain, non-erythrocytic 1	282.38	62	71	49	63	64	40	62	71	49	63	64	40	3.05E+05	5.27E+05	1.51E+05	2.83E+05	2.40E+05	6.79E+04	36.2	38.7	27	36.6	36.1	23
A0A0G2JZY6	Sptbn1	Spectrin beta chain, non-erythrocytic 1	267.90	41	49	29	46	43	23	41	49	29	46	43	23	2.46E+05	4.15E+05	6.30E+04	1.84E+05	2.84E+05	3.33E+04	28.7	33.3	20.4	30.7	30	15.8
Q9WUD9	Src	Proto-oncogene tyrosine-protein kinase Src	59.97	2	1	1	1	0	1	2	1	1	1	0	1	1.30E+04	1.24E+04	4.28E+03	2.90E+03	0.00E+00	2.41E+03	5	3.2	1.9	3.2	0	1.9
A0A0G2K2M9	Srrm2	Serine/arginine repetitive matrix 2	295.11	2	2	2	2	2	0	2	2	2	2	2	0	4.36E+04	3.76E+04	1.46E+04	1.07E+04	7.51E+03	0.00E+00	1.1	1.1	1.1	1.1	1.1	0
Q66HM7	Ssb	Lupus La protein homolog	47.79	5	6	2	4	4	1	5	6	2	4	4	1	1.38E+05	1.54E+05	1.69E+04	1.48E+05	7.78E+04	7.96E+03	15.2	17.6	6.3	10.8	10.8	3.9
P50503	St13	Hsc70-interacting protein	41.28	3	5	5	3	4	5	3	5	5	3	4	5	3.42E+05	5.89E+05	3.58E+05	2.82E+05	1.43E+05	2.05E+05	9.5	16.3	15.2	9.5	12.2	15.2
F1M9D6	Stat1	Signal transducer and activator of transcription	87.25	12	14	6	12	10	7	12	14	6	12	10	7	1.41E+05	2.31E+05	7.90E+04	1.07E+05	7.57E+04	7.26E+04	22.6	25.8	11.3	22	18.3	10.8
P52631	Stat3	Signal transducer and activator of transcription 3	88.04	7	8	3	7	5	2	7	8	3	7	5	2	6.43E+04	1.23E+05	1.87E+04	4.71E+04	2.79E+04	9.54E+03	15.5	17.1	7.7	15.5	11.9	5.3
A0A0G2JXI4	Stat5a	Signal transducer and activator of transcription	86.97	2	3	2	2	2	2	2	3	2	2	2	2	3.66E+04	4.04E+04	3.99E+04	3.42E+04	3.27E+04	4.19E+04	2.8	4.4	2.8	2.8	2.8	2.8
O35814	Stip1	Stress-induced-phosphoprotein 1	62.57	15	18	13	18	18	16	15	18	13	18	18	16	4.90E+05	7.79E+05	3.04E+05	3.84E+05	2.75E+05	1.28E+05	31.7	34.4	29.1	39.8	36.5	36.8
G3V9Q4	Stk38	Non-specific serine/threonine protein kinase	54.16	1	1	1	1	1	1	1	1	1	1	1	1	1.21E+04	1.62E+04	8.57E+03	5.90E+03	5.97E+03	3.83E+03	3.4	3.4	3.4	3.4	3.4	3.4
A0A0G2K007	Stk39	STE20/SPS1-related proline-alanine-rich protein kinase	56.03	1	1	2	2	1	1	0	0	1	1	0	1	0.00E+00	0.00E+00	4.98E+03	2.66E+03	0.00E+00	2.26E+03	3.6	3.6	6.5	6.5	3.6	3
Q5XIG8	Strap	Serine-threonine kinase receptor-associated protein	38.46	5	6	4	5	4	2	5	6	4	5	4	2	9.89E+04	1.37E+05	1.11E+05	8.48E+04	5.98E+04	1.01E+04	20.6	22.3	16.3	17.1	16.3	8.6
B4F7C9	Stt3a	Dolichyl-diphosphooligosaccharide--protein glycosyltransferase subunit STT3A	80.60	1	0	0	1	0	0	1	0	0	1	0	0	1.30E+04	0.00E+00	0.00E+00	2.58E+03	0.00E+00	0.00E+00	2.7	0	0	2.7	0	0
B0BN85	Sugt1	Suppressor of G2 allele of SKP1 homolog	38.09	6	7	4	5	2	2	6	7	4	5	2	2	1.61E+05	1.98E+05	1.74E+04	5.66E+04	1.21E+04	3.10E+03	30.1	33.6	19.3	25.9	8.6	11.3
P17988	Sult1a1	Sulfotransferase 1A1	33.91	13	13	8	13	12	6	13	13	8	13	12	6	5.53E+05	1.40E+06	1.89E+05	5.86E+05	3.11E+05	1.09E+05	70.4	70.4	49.1	70.4	60.1	34

Uniprot accession number	Gene symbol	Protein name	Mol. weight [kDa]	No. Peptides Control wk1	No. Peptides Control wk8	No. Peptides Control wk14	No. Peptides Heat wk1	No. Peptides Heat wk8	No. Peptides Heat wk14	No. Unique peptides Control wk1	No. Unique peptides Control wk8	No. Unique peptides Control wk14	No. Unique peptides Heat wk1	No. Unique peptides Heat wk8	No. Unique peptides Heat wk14	iBAQ Control wk1	iBAQ Control wk8	iBAQ Control wk14	iBAQ Heat wk1	iBAQ Heat wk8	iBAQ Heat wk14	Sequence coverage Control wk1 [%]	Sequence coverage Control wk8 [%]	Sequence coverage Control wk14 [%]	Sequence coverage Heat wk1 [%]	Sequence coverage Heat wk8 [%]	Sequence coverage Heat wk14 [%]
A0A0G2K291	Sult1d1	Sulfotransferase 1 family member D1	36.21	5	6	6	5	5	5	5	6	6	5	5	5	2.76E+05	2.79E+05	1.97E+05	1.23E+05	1.52E+05	1.97E+05	25.1	27.4	27.4	25.1	25.1	25.1
Q99ND5	Sult1e1	Sulfotransferase	35.36	1	1	0	1	1	0	1	1	0	1	1	0	2.11E+04	1.54E+04	0.00E+00	1.42E+03	2.77E+03	0.00E+00	5.1	5.1	0	5.1	5.1	0
F1M2K3	Sumo2	Small ubiquitin-related modifier 2	10.77	1	1	1	0	1	1	1	1	1	0	1	1	3.37E+05	2.06E+05	2.03E+05	0.00E+00	2.46E+05	3.90E+04	12.8	12.8	12.8	0	12.8	12.8
A0A1W2Q689	Supt5h	Transcription elongation factor SPT5	56.70	1	1	1	1	1	0	1	1	1	1	1	0	1.24E+03	6.64E+03	4.10E+03	1.10E+03	1.98E+03	0.00E+00	2.9	2.9	2.9	2.9	2.9	0
A0A0G2JSZ2	Svs4	Seminal vesicle secretory protein 4	11.93	4	4	2	3	3	2	4	4	2	3	3	2	1.06E+06	3.68E+05	1.58E+04	2.57E+05	5.44E+05	6.48E+03	45.9	45.9	45	39.6	39.6	45.9
A0A0G2JTC7	Svs5	Seminal vesicle secretory protein 5	13.62	3	2	0	3	3	1	3	2	0	3	3	1	9.23E+04	3.83E+04	0.00E+00	6.76E+04	1.20E+05	1.20E+03	32.5	23.6	0	32.5	34.1	13
D3ZRE7	Swap70	Switch-associated protein 70	68.77	3	4	2	3	3	1	3	4	2	3	3	1	2.22E+04	4.10E+04	8.71E+03	1.81E+04	1.24E+04	3.39E+03	6.2	8.4	5	6.2	6.2	2.7
M0R735	Syncrip	Heterogeneous nuclear ribonucleoprotein Q	62.67	2	3	3	2	2	4	2	3	3	2	2	4	4.88E+04	7.50E+04	4.37E+04	2.89E+04	1.68E+04	3.52E+04	5	7.1	7.8	5	5	10.1
A0A096MK54	Synm	Synemin	140.76	2	1	1	1	2	0	2	1	1	1	2	0	6.12E+04	1.18E+05	1.36E+03	8.85E+02	3.23E+04	0.00E+00	2	1.2	1.2	1.2	1.5	0
A0A096MJZ7	Synrg	Synergin gamma	71.80	1	1	0	1	1	0	1	1	0	1	1	0	4.67E+03	8.61E+03	0.00E+00	2.06E+03	1.95E+03	0.00E+00	3.3	3.3	0	3.3	3.3	0
P31232	Tagln	Transgelin	22.60	16	17	16	11	16	14	16	17	16	11	16	14	1.75E+06	3.53E+06	3.59E+06	4.25E+05	1.45E+06	2.75E+06	76.6	80.1	76.6	59.2	76.6	70.6
Q5XFX0	Tagln2	Transgelin-2	22.39	13	14	12	13	14	12	13	14	12	13	14	12	1.41E+06	1.98E+06	8.79E+05	6.02E+05	9.64E+05	5.43E+05	81.4	86.9	76.9	80.9	86.9	76.9
Q9EQS0	Taldo1	Transaldolase	37.46	3	2	1	2	3	1	3	2	1	2	3	1	2.66E+04	1.01E+04	1.29E+03	3.43E+03	3.23E+04	1.30E+03	22	6.8	3.3	6.8	10.7	3.3
I6L9G6	Tardbp	TAR DNA-binding protein 43	32.15	4	5	1	3	4	0	4	5	1	3	4	0	1.63E+05	4.02E+05	1.80E+04	1.23E+05	1.27E+05	0.00E+00	24.2	32.6	4.6	19.6	28.1	0
A0A0G2K9V6	Tars	Threonine--tRNA ligase, cytoplasmic	83.39	4	4	3	3	3	2	4	4	3	3	3	2	2.57E+04	1.95E+04	3.03E+04	5.37E+03	1.40E+04	1.32E+04	6.6	6.6	5.3	5.4	4.3	4
Q6PEC1	Tbca	Tubulin-specific chaperone A	12.74	1	1	1	1	1	0	1	1	1	1	1	0	1.81E+05	3.80E+05	7.76E+04	1.95E+05	1.50E+05	0.00E+00	7.4	7.4	7.4	7.4	7.4	0
Q5PQJ7	Tbcel	Tubulin-specific chaperone cofactor E-like protein	48.05	3	5	3	4	3	2	3	5	3	4	3	2	1.53E+04	4.85E+04	1.15E+04	1.69E+04	1.16E+04	3.02E+03	10.4	15.1	10.4	13	10.4	8.3
Q4KLL0	Tcea1	Transcription elongation factor A protein 1	33.89	2	2	1	3	2	1	2	2	1	3	2	1	2.76E+04	3.73E+04	1.53E+04	2.98E+04	1.75E+04	6.93E+03	13.6	7.6	4.3	16.9	7.6	4.3
P83941	Tceb1	Transcription elongation factor B polypeptide 1	12.47	4	4	3	4	3	3	4	4	3	4	3	3	4.14E+05	6.69E+05	4.15E+05	4.10E+05	2.22E+05	1.82E+05	48.2	48.2	37.5	48.2	30.4	37.5
P28480	Tcp1	T-complex protein 1 subunit alpha	60.36	4	4	5	4	5	3	4	4	5	4	5	3	8.96E+04	9.27E+04	6.37E+04	4.84E+04	4.56E+04	5.44E+04	11.2	11.2	12.9	11	12.8	7.7
Q5XI00	Tcp11	T-complex protein 11 homolog	62.61	6	7	5	6	4	2	6	7	5	6	4	2	9.15E+04	1.70E+05	6.85E+04	9.02E+04	3.77E+04	2.04E+04	22.6	24.4	17.1	20.8	17.5	6.9
Q2LAP6	Tes	Testin	47.63	2	2	2	2	1	1	2	2	2	2	1	1	2.08E+04	3.65E+04	5.29E+03	1.59E+04	1.05E+04	3.28E+03	7.9	7.9	7.9	7.9	4.5	4.5
P12346	Tf	Serotransferrin	76.39	53	56	46	53	52	46	52	55	45	52	51	45	2.68E+07	2.04E+07	2.72E+07	2.24E+07	2.47E+07	2.29E+07	77.1	77.8	73.8	76.5	74.6	73.4
Q4R1A4	Tfg	TRK-fused gene protein	31.03	1	1	1	1	1	0	1	1	1	1	1	0	4.08E+04	5.75E+04	6.83E+03	9.40E+03	1.61E+04	0.00E+00	6	6	6	6	6	0
Q5PQU8	Tfpi	Tissue factor pathway inhibitor	28.60	3	3	3	3	3	3	3	3	3	3	3	3	2.66E+05	2.34E+05	3.12E+05	2.41E+05	3.52E+05	2.29E+05	19.1	19.1	19.1	19.1	19.1	19.1
G3V679	Tfrc	Transferrin receptor protein 1	85.88	2	2	0	2	1	0	2	2	0	2	1	0	2.08E+04	3.62E+03	0.00E+00	9.14E+03	9.54E+02	0.00E+00	2.8	3	0	3	1.3	0
Q99PD6	Tgfb1i1	Transforming growth factor beta-1-induced transcript 1 protein	50.12	1	1	0	1	1	0	1	1	0	1	1	0	2.80E+03	1.05E+04	0.00E+00	8.20E+02	7.44E+02	0.00E+00	2	2	0	2	2	0
D4A8G5	Tgfbi	Transforming growth factor, beta-induced	74.75	13	13	13	12	13	13	13	13	13	12	13	13	2.86E+05	2.42E+05	2.55E+05	3.12E+05	2.59E+05	2.57E+05	29.1	29.1	29.3	28.5	29.1	29.3
P26342	Tgfbr3	Transforming growth factor beta receptor type 3	94.10	2	2	3	1	2	3	2	2	3	1	2	3	5.18E+04	4.52E+04	8.68E+04	2.08E+04	3.65E+04	8.04E+04	4.2	4.2	5.6	1.8	4.2	5.6
D4A5U3	Tgm3	Protein-glutamine gamma-glutamyltransferase E	77.23	2	1	1	0	3	2	2	1	1	0	3	2	1.40E+04	2.95E+03	1.93E+03	0.00E+00	6.71E+04	3.29E+03	3.3	1.9	1.4	0	5.9	4.5
Z4YP11	Tgm4	Protein-glutamine gamma-glutamyltransferase 4	75.55	9	3	6	9	3	2	9	3	6	9	3	2	1.35E+05	1.58E+04	4.68E+04	9.06E+04	4.84E+03	1.62E+03	19.9	7	14.2	19.9	9.3	3.3
M0R979	Thbs1	Thrombospondin 1	127.04	5	7	7	4	5	6	5	7	7	4	5	6	2.97E+04	2.86E+04	2.54E+04	2.57E+04	1.06E+04	1.43E+04	6.6	8.2	8.1	5.2	6.6	7.3
F1LMS5	Thbs4	Thrombospondin-4	105.83	18	18	16	18	18	15	16	16	14	16	16	14	8.89E+05	5.59E+05	3.29E+05	1.10E+06	5.41E+05	3.71E+05	28.8	28.8	25.5	28.8	28.8	24.2
Q5M7T9	Thnsl2	Threonine synthase-like 2	54.14	11	14	6	11	9	4	11	14	6	11	9	4	1.02E+05	2.30E+05	9.01E+04	1.16E+05	6.04E+04	4.64E+04	32.2	36.7	20.4	32.2	25.2	11.8
P24155	Thop1	Thimet oligopeptidase	78.39	4	4	4	3	3	3	4	4	4	3	3	3	2.17E+04	5.25E+04	3.23E+04	2.13E+04	1.02E+04	9.94E+03	6.7	6.7	6.7	5.5	5.2	5.5
P30120	Timp1	Metalloproteinase inhibitor 1	23.79	4	4	3	4	4	2	4	4	3	4	4	2	6.49E+04	4.97E+04	3.62E+04	1.16E+05	2.02E+05	2.09E+04	30.4	30.4	23.5	30.4	30.4	14.7
P30121	Timp2	Metalloproteinase inhibitor 2	24.36	3	4	3	4	4	1	3	4	3	4	4	1	1.49E+05	1.67E+05	4.29E+04	1.79E+05	1.77E+05	4.35E+04	20.5	20.5	26.8	20.5	20.5	6.4
A2VCX1	Tiprl	TIP41-like protein	31.22	2	2	1	1	2	0	2	2	1	1	2	0	1.37E+04	3.31E+04	2.27E+03	2.88E+04	1.27E+04	0.00E+00	7.7	7.7	3.7	4.1	7.7	0
Q4KLZ6	Tkfc	Triokinase/FMN cyclase	59.44	10	12	9	10	9	9	10	12	9	10	9	9	2.14E+05	2.85E+05	2.33E+05	1.47E+05	6.87E+04	5.57E+04	26.3	29.8	24.6	27.2	22.7	21.5
G3V826	Tkt	Transketolase	71.16	5	6	6	4	5	5	5	6	6	4	5	5	1.09E+05	9.03E+04	4.50E+04	3.38E+04	2.04E+04	2.40E+04	17.6	18.9	18.9	15	14.2	14.8
D3ZHE7	Tktl2	Transketolase-like 2	68.36	3	4	4	4	3	2	3	4	4	4	3	2	1.07E+04	5.48E+04	1.45E+04	2.32E+04	1.24E+04	9.32E+03	7.7	10.2	10.2	10.2	7.7	5.6
G3V852	Tln1	Talin-1	269.67	51	55	42	46	40	36	51	55	42	46	40	36	2.80E+05	3.94E+05	1.42E+05	1.70E+05	1.25E+05	7.13E+04	31.4	34.1	27	26.8	23.9	22.8
Q6AXW2	Tmod3	Tropomodulin-3	39.47	2	3	1	3	3	1	2	3	1	3	3	1	5.47E+04	1.86E+05	1.44E+04	6.68E+04	6.58E+04	4.89E+03	6	11.6	3.1	11.6	11.6	3.1
Q62733	Tmpo	Lamina-associated polypeptide 2, isoform beta	50.28	2	2	2	2	2	2	2	2	2	2	2	2	2.92E+04	3.30E+04	1.89E+04	2.11E+04	1.82E+04	1.19E+04	6.4	6.4	6.4	6.4	6.4	6.4
F1LQP9	Tnpo1	Transportin 1	101.27	3	2	1	3	3	1	3	2	1	3	3	1	9.00E+03	5.29E+03	8.82E+02	1.13E+04	1.07E+04	4.22E+02	5.3	3.9	2.2	6.1	6.1	1.7
F1LN42	Tns1	Tensin 1	203.91	1	2	3	3	1	2	1	2	3	3	1	2	3.64E+03	8.86E+03	6.17E+03	1.63E+03	4.54E+02	2.11E+03	1	1.7	2.5	2.5	0.7	1.4
Q3KRD5	Tomm34	Mitochondrial import receptor subunit TOM34	34.46	3	3	2	3	2	1	3	3	2	3	2	1	4.09E+04	8.13E+04	1.88E+04	2.86E+04	5.92E+03	3.42E+03	12	12	9.1	12	7.1	4.2
F1MAB9	Tpd52	Tumor protein D52	24.27	1	1	1	1	1	1	1	1	1	1	1	1	4.33E+04	3.95E+04	5.03E+04	7.78E+03	2.47E+03	1.46E+04	5.4	5.4	5.4	5.4	5.4	5.4
Q6PCT3	Tpd52l2	Tumor protein D54	23.99	4	4	2	4	4	1	4	4	2	4	4	1	1.19E+05	1.97E+05	2.08E+04	9.63E+04	4.31E+04	6.89E+03	23.6	23.6	13.2	23.6	23.6	6.4
P48500	Tpi1	Triosephosphate isomerase	26.85	14	14	12	14	13	11	3	3	3	3	3	2	8.56E+05	1.93E+06	1.10E+06	7.86E+05	1.01E+06	4.35E+05	77.9	77.9	66.3	77.9	72.7	65.9
Q63607	Tpm1	Alpha-tropomyosin 3	32.85	8	11	13	7	9	11	0	0	1	0	0	0	1.61E+05	3.39E+05	2.52E+05	6.20E+04	7.77E+04	1.50E+05	22.9	33.1	33.8	22.5	28.2	24.3
Q923Z2	Tpm1	Tropomyosin 1, alpha	32.79	8	10	12	8	9	11	2	1	3	2	2	3	9.44E+03	3.24E+03	4.84E+04	3.82E+04	7.35E+03	8.44E+04	26.1	33.1	36.6	25.7	31.3	31
A0A0G2JSQ4	Tpm1	Tropomyosin 1, alpha	28.56	8	11	10	7	8	10	2	2	1	1	1	2	1.81E+04	3.34E+04	4.14E+04	7.32E+04	0.00E+00	2.33E+04	31	42.7	34.3	25	31.5	32.7
Q63610	Tpm3	Tropomyosin alpha-3 chain	29.01	17	19	17	16	16	16	13	14	13	12	12	12	2.58E+06	4.31E+06	2.42E+06	1.98E+06	1.46E+06	1.31E+06	40.7	47.2	40.7	37.9	37.9	37.9
P09495	Tpm4	Tropomyosin alpha-4 chain	28.51	15	18	15	15	14	14	9	11	9	9	9	9	8.71E+05	7.84E+05	7.12E+05	3.17E+05	2.52E+05	5.44E+05	33.1	44	33.1	36.7	33.1	33.1
Q642E6	Tpp1	Tripeptidyl-peptidase 1	61.31	1	1	0	1	1	0	1	1	0	1	1	0	7.53E+04	7.05E+04	0.00E+00	2.18E+04	3.42E+04	0.00E+00	3.7	3.7	0	3.7	3.7	0
Q64560	Tpp2	Tripeptidyl-peptidase 2	138.29	13	16	7	13	14	4	13	16	7	13	14	4	8.14E+04	1.32E+05	3.54E+04	4.67E+04	5.18E+04	1.10E+04	15.1	18.4	9.3	15.1	16.7	4.6
G3V8E5	Tpsab1	Tryptase	34.24	1	1	0	0	1	0	1	1	0	0	1	0	0.00E+00	4.61E+04	0.00E+00	0.00E+00	7.35E+04	0.00E+00	3.2	3.2	0	0	3.2	0
P63029	Tpt1	Translationally-controlled tumor protein	19.46	5	5	4	4	4	4	5	5	4	4	4	4	4.00E+06	3.44E+06	1.53E+06	2.32E+06	1.23E+06	9.86E+05	58.7	58.7	31.4	51.7	50	31.4
O08629	Trim28	Transcription intermediary factor 1-beta	88.96	14	14	8	14	11	5	14	14	8	14	11	5	1.60E+05	3.15E+05	9.06E+04	9.66E+04	7.25E+04	2.36E+04	36	36	25.6	36	29.3	16
D4ABW9	Trim29	Tripartite motif protein 29	65.77	2	1	1	1	3	1	2	1	1	1	3	1	9.22E+03	1.37E+03	1.98E+04	1.42E+03	4.58E+04	6.09E+03	4.1	1.5	2.6	1.5	5.5	2.6
A0A140UHW6	Trmt1	tRNA (guanine(26)-N(2))-dimethyltransferase	69.37	1	1	0	0	1	0	1	1	0	0	1	0	5.10E+03	6.58E+03	0.00E+00	0.00E+00	1.36E+03	0.00E+00	3.1	3.1	0	0	3.1	0
D3Z8M8	Tsc22d1	TSC22 domain family protein 1	106.79	1	1	0	1	1	0	1	1	0	1	1	0	8.29E+03	3.82E+04	0.00E+00	3.03E+04	1.09E+04	0.00E+00	1.1	1.1	0	1.1	1.1	0
D3ZFW1	Tsen15	tRNA-splicing endonuclease subunit Sen15	14.01	1	1	1	1	1	1	1	1	1	1	1	1	2.09E+04	2.54E+04	4.50E+04	1.40E+04	1.31E+04	1.98E+04	14.1	14.1	14.1	14.1	14.1	14.1
G3V8X6	Tsku	Tsukushin	38.08	1	1	1	2	1	1	1	1	1	2	1	1	6.84E+04	5.21E+04	7.96E+03	4.23E+05	5.99E+04	6.66E+04	4.8	4.8	4.8	8.8	4.8	4.8
Q71SY3	Tsn	Translin	26.17	5	6	6	5	5	5	5	6	6	5	5	5	3.21E+05	4.46E+05	3.52E+05	2.65E+05	1.87E+05	1.55E+05	34.2	37.7	37.7	34.2	34.2	34.2
Q9JHB5	Tsnax	Translin-associated protein X	33.01	1	4	2	3	2	0	1	4	2	3	2	0	5.65E+04	1.47E+05	3.10E+04	1.44E+05	2.88E+04	0.00E+00	6.2	19.7	10	13.1	10	0
G3V762	Tsta3	Tissue specific transplantation antigen P35B	35.80	7	9	5	8	5	2	7	9	5	8	5	2	3.05E+05	5.50E+05	6.79E+04	3.09E+05	9.01E+04	1.92E+04	26.5	31.8	18.1	30.2	20.9	9.7
D4ACL2	Ttc38	Tetratricopeptide repeat domain 38	57.06	2	3	3	3	2	3	2	3	3	3	2	3	1.41E+04	1.64E+04	1.05E+04	1.03E+04	5.07E+03	7.52E+03	4.7	7.6	7.6	7.6	5.5	7.6
P19814	Ttgn1	Trans-Golgi network integral membrane protein TGN38	38.30	1	1	0	1	1	0	1	1	0	1	1	0	2.42E+04	1.07E+04	0.00E+00	1.10E+04	2.02E+04	0.00E+00	3.4	3.4	0	3.4	3.4	0
D4A1Q9	Ttll12	Tubulin tyrosine ligase-like 12	73.90	8	8	8	7	6	4	8	8	8	7	6	4	1.21E+05	1.60E+05	6.94E+04	9.23E+04	7.70E+04	2.63E+04	17.5	17.5	18	15.6	13.8	10.3
P02767	Ttr	Transthyretin	15.72	11	13	11	11	12	11	11	13	11	11	12	11	5.58E+07	6.07E+07	6.82E+07	9.08E+07	3.98E+07	6.11E+07	70.1	74.1	71.4	70.1	74.1	71.4
P68370	Tuba1a	Tubulin alpha-1A chain	50.14	27	29	26	26	24	24	0	0	0	0	0	0	5.82E+06	1.02E+07	5.56E+06	5.11E+06	3.79E+06	2.18E+06	70.1	70.1	66.5	70.1	69.6	66.3
Q6P9V9	Tuba1b	Tubulin alpha-1B chain	50.15	27	29	27	25	23	25	0	0	0	0	0	0	5.85E+05	1.12E+06	2.13E+05	5.30E+05	4.17E+05	1.15E+05	70.1	70.1	69.6	69.8	69.4	66.5
Q6AYZ1	Tuba1c	Tubulin alpha-1C chain	49.94	27	29	27	26	24	23	2	2	2	2	2	1	1.25E+05	1.37E+05	4.29E+04	7.75E+04	6.41E+04	2.12E+04	70.4	70.4	69.9	70.4	69.9	61.2
Q68FR8	Tuba3a	Tubulin alpha-3 chain	49.96	23	26	23	22	20	20	2	3	2	2	2	2	4.18E+05	7.60E+05	2.75E+05	3.72E+05	2.07E+05	5.07E+04	67.1	68.2	65.1	67.1	60.9	62
Q5XIF6	Tuba4a	Tubulin alpha-4A chain	49.92	21	22	20	18	21	19	2	2	1	1	4	1	1.13E+04	8.71E+03	2.18E+03	6.53E+03	7.23E+05	3.44E+03	53.6	53.6	51.3	50	59.8	48.2
P85108	Tubb2a	Tubulin beta-2A chain	49.91	21	24	20	23	23	21	4	4	4	5	5	5	2.80E+05	3.72E+05	2.09E+05	1.21E+05	1.61E+05	9.51E+04	63.6	65.4	61.1	67.9	68.1	64.5
Q4QRB4	Tubb3	Tubulin beta-3 chain	50.42	24	26	23	24	22	21	10	12	9	10	9	7	1.20E+06	2.31E+06	7.81E+05	1.21E+06	8.27E+05	3.33E+05	66.4	68.2	60.4	66.2	64.2	60.2
B4F7C2	Tubb4a	Tubulin beta-4A chain	49.59	20	23	21	20	21	20	0	0	0	0	0	0	0.00E+00	0.00E+00	0.00E+00	0.00E+00	0.00E+00	0.00E+00	58.1	59	58.3	58.1	58.3	58.3
G3V7C6	Tubb4b	Tubulin beta-4B chain	61.19	26	32	27	27	27	26	1	2	2	1	1	2	1.27E+07	1.99E+07	1.18E+07	1.03E+07	7.95E+06	4.08E+06	60	65.1	60.9	60.8	60.9	60.9
P69897	Tubb5	Tubulin beta-5 chain	49.67	23	27	24	23	24	24	5	5	5	4	4	5	1.55E+06	2.45E+06	1.30E+06	1.60E+06	7.17E+05	6.21E+05	67.1	70.7	67.3	68	68.2	67.3
Q4QQV0	Tubb6	Tubulin beta-6 chain	50.06	13	14	13	12	12	11	2	3	3	1	2	1	3.52E+04	1.23E+05	3.54E+04	1.68E+03	1.33E+04	7.87E+03	35.1	40.7	38	32.7	33.1	28.2
Q5RJR2	Twf1	Twinfilin-1	40.09	5	6	3	4	4	0	5	6	3	4	4	0	1.42E+05	2.02E+05	2.05E+04	9.86E+04	6.45E+04	0.00E+00	17.7	24.6	16	14	14	0
P11232	Txn	Thioredoxin	11.67	4	5	4	5	4	5	4	5	4	5	4	5	5.08E+06	8.87E+06	3.42E+06	5.29E+06	3.62E+06	1.58E+06	30.5	35.2	30.5	35.2	30.5	35.2
B0K010	Txndc17	Thioredoxin domain-containing 17	14.09	1	3	2	3	2	1	1	3	2	3	2	1	8.14E+04	3.70E+05	1.51E+05	1.27E+05	9.52E+04	7.79E+04	11.4	24.4	21.1	24.4	21.1	11.4
F1LV53	Txndc2	Thioredoxin domain-containing protein 2	57.49	2	2	1	2	0	2	2	2	1	2	0	2	2.23E+04	2.07E+04	2.95E+03	2.00E+04	0.00E+00	2.96E+03	4.5	4.5	2.7	4.5	0	4.5
D3ZZC1	Txndc5	Thioredoxin domain-containing protein 5	46.35	7	7	3	7	7	2	7	7	3	7	7	2	2.92E+05	1.75E+05	4.65E+04	7.49E+04	6.79E+04	2.03E+04	22.1	22.1	9.1	22.1	22.1	7.4
Q5M7W1	Txnip	Thioredoxin-interacting protein	44.02	2	3	2	2	2	2	2	3	2	2	2	2	1.62E+04	4.19E+04	2.03E+04	1.62E+04	1.79E+04	1.55E+04	5.8	9.1	5.8	5.8	5.8	5.8
A0A0G2K737	Txnl1	Thioredoxin-like protein 1	32.70	11	11	9	10	10	8	11	11	9	10	10	8	9.96E+05	1.39E+06	4.03E+05	7.73E+05	4.93E+05	2.79E+05	51.7	51.7	48.6	48.6	48.6	40.8
A0A0G2JUN[illegible]	Txnrd1	Thioredoxin reductase 1, cytoplasmic	54.50	2	3	3	2	0	3	2	3	3	2	0	3	2.55E+04	1.95E+04	3.36E+04	5.59E+03	0.00E+00	1.99E+04	6.4	8.7	8.7	5.6	0	8.7
A0A0G2K764	Txnrd3	Thioredoxin reductase 3	67.67	7	7	4	5	6	2	7	7	4	5	6	2	6.50E+04	7.65E+04	3.37E+04	3.16E+04	1.79E+04	7.71E+03	15.5	15.5	7.5	10.4	12.2	5.1
D3ZD03	Tyk2	Tyrosine-protein kinase	133.29	1	1	1	1	1	1	1	1	1	1	1	1	4.61E+05	2.44E+05	4.77E+05	2.31E+05	3.13E+05	5.35E+05	1	1	1	1	1	1
F2Z3T9	U2af2	U2 snRNP auxiliary factor large subunit	53.12	1	2	2	2	2	1	1	2	2	2	2	1	5.77E+03	5.08E+04	1.53E+04	9.16E+03	1.92E+04	4.99E+03	4.5	6.2	6.2	6.2	6.2	4.5
B5DEH4	Uap1l1	UDP-N-acetylglucosamine pyrophosphorylase 1-like 1	56.44	1	2	1	2	2	1	1	2	1	2	2	1	2.99E+03	1.42E+04	8.57E+03	6.22E+03	4.94E+03	7.44E+03	3.6	8.1	3.6	8.1	8.1	3.6
Q5U300	Uba1	Ubiquitin-like modifier-activating enzyme 1	117.79	29	33	31	32	26	28	19	22	22	21	17	19	6.78E+05	9.71E+05	4.83E+05	4.93E+05	2.85E+05	2.56E+05	39.2	44.1	41.5	40	36.2	39.1
A0A0G2K8A5	Uba1y	Ubiquitin-activating enzyme, Chr Y	117.83	14	15	14	15	13	13	4	4	5	4	4	4	2.18E+04	4.71E+04	7.34E+04	1.92E+04	7.82E+03	2.13E+04	16.4	16.8	18.2	17.4	16.4	15.7

Uniprot accession number	Gene symbol	Protein name	Mol. weight [kDa]	No. Peptides Control wk1	No. Peptides Control wk8	No. Peptides Control wk14	No. Peptides Heat wk1	No. Peptides Heat wk8	No. Peptides Heat wk14	No. Unique peptides Control wk1	No. Unique peptides Control wk8	No. Unique peptides Control wk14	No. Unique peptides Heat wk1	No. Unique peptides Heat wk8	No. Unique peptides Heat wk14	iBAQ Control wk1	iBAQ Control wk8	iBAQ Control wk14	iBAQ Heat wk1	iBAQ Heat wk8	iBAQ Heat wk14	Sequence coverage Control wk1 [%]	Sequence coverage Control wk8 [%]	Sequence coverage Control wk14 [%]	Sequence coverage Heat wk1 [%]	Sequence coverage Heat wk8 [%]	Sequence coverage Heat wk14 [%]
F1LS72	Uba2	Ubiquitin-like modifier-activating enzyme 2	66.34	3	3	2	3	3	1	3	3	2	3	3	1	3.47E+04	4.12E+04	1.34E+04	1.39E+04	9.16E+03	1.23E+03	11.4	11.4	7.4	11.4	11.4	2
Q99MI7	Uba3	NEDD8-activating enzyme E1 catalytic subunit	51.72	2	3	2	2	2	1	2	3	2	2	2	1	4.08E+04	3.35E+04	1.62E+04	2.86E+04	9.26E+03	3.66E+03	6.7	11.9	6.5	6.7	6.7	5.2
Q5M7A4	Uba5	Ubiquitin-like modifier-activating enzyme 5	44.90	0	0	1	2	1	1	0	0	1	2	1	1	0.00E+00	0.00E+00	2.35E+04	1.48E+04	1.89E+03	5.00E+03	0	0	3	6.2	3	3
D4A8H3	Uba6	Ubiquitin-like modifier-activating enzyme 6	117.93	18	25	12	19	21	9	18	25	12	19	21	9	1.32E+05	3.64E+05	2.87E+04	1.43E+05	1.37E+05	3.20E+04	25.5	34.1	17	27	29.4	10.5
A0A0G2JYC6	Ubap2l	Ubiquitin-associated protein 2-like	112.51	1	1	1	1	1	1	1	1	1	1	1	1	3.00E+03	9.10E+03	3.66E+03	1.69E+03	2.73E+03	1.14E+03	2.3	2.3	2.3	2.3	2.3	2.3
F1M5C9	Ube2d2	Ubiquitin-conjugating enzyme E2 D2	13.60	2	2	1	2	2	1	2	2	1	2	2	1	1.66E+06	1.97E+06	7.33E+05	1.18E+06	1.09E+06	3.35E+05	24.6	24.6	9.3	24.6	24.6	9.3
A0A0G2JYC6	Ube2h	Ubiquitin-conjugating enzyme E2H	17.17	0	1	1	1	1	0	0	1	1	1	1	0	0.00E+00	8.79E+04	1.23E+04	1.05E+04	1.68E+04	0.00E+00	0	9.9	9.9	9.9	9.9	0
D3ZNQ6	Ube2n	Ubiquitin-conjugating enzyme E2M	20.90	1	1	2	1	1	1	1	1	2	1	1	1	3.66E+04	7.91E+04	1.13E+05	1.95E+04	8.70E+03	1.10E+04	8.7	8.7	13.1	8.7	8.7	8.7
Q9EQX9	Ube2n	Ubiquitin-conjugating enzyme E2 N	17.12	3	3	2	3	2	3	3	3	2	3	2	3	2.09E+05	2.42E+05	1.27E+05	1.68E+05	1.50E+05	7.62E+04	21.7	21.7	16.4	21.7	16.4	23.7
Q3B7D1	Ube2z	Ubiquitin-conjugating enzyme E2 Z	38.35	1	2	0	1	1	0	1	2	0	1	1	0	2.06E+04	1.04E+05	0.00E+00	9.46E+03	1.21E+04	0.00E+00	2.8	5.6	0	2.8	2.8	0
A0A140TAI1	Ubqln1	Ubiquilin-1	62.01	4	6	4	5	4	4	2	4	2	3	2	2	3.37E+05	4.79E+05	2.58E+05	3.22E+05	2.34E+05	3.19E+04	9.5	19.6	10.8	15.3	9.5	10.8
D4A4A63	Ubqln2	Ubiquilin-2	67.26	5	5	5	5	5	4	3	3	3	3	3	2	6.00E+04	1.30E+05	5.62E+04	5.96E+04	6.77E+04	1.65E+04	12.1	12.1	12.1	12.1	12.1	9.7
A0A0G2JU89	Ubr4	E3 ubiquitin-protein ligase UBR4	573.87	2	2	1	1	2	1	2	2	1	1	2	1	2.02E+04	2.13E+04	3.66E+03	2.17E+04	1.60E+04	4.66E+03	0.9	0.9	0.3	0.3	0.9	0.3
Q499N6	Ubxn1	UBX domain-containing protein 1	33.58	3	3	3	3	3	1	3	3	3	3	3	1	4.49E+04	1.15E+05	5.10E+04	1.84E+04	3.09E+04	1.75E+04	18.2	18.2	18.2	18.2	18.2	4
Q00981	Uchl1	Ubiquitin carboxyl-terminal hydrolase isozyme L1	24.84	4	4	4	4	4	4	4	4	4	4	4	4	6.72E+05	5.11E+05	3.71E+05	4.26E+05	2.90E+05	1.90E+05	38.6	38.6	38.6	38.6	38.6	38.6
D4A8J6	Uchl3	Ubiquitin carboxyl-terminal hydrolase isozyme L3	26.11	8	8	6	8	7	4	8	8	6	8	7	4	6.65E+05	1.06E+06	4.51E+05	5.68E+05	3.23E+05	1.80E+05	47.4	47.4	38.3	43	43.5	28.3
Q9ES53	Ufd1l	Ubiquitin fusion degradation protein 1 homolog	34.49	1	2	2	0	1	1	1	2	2	0	1	1	2.10E+04	5.43E+04	2.44E+04	0.00E+00	7.09E+03	6.28E+03	3.9	7.2	7.2	0	3.3	3.9
A0A0G2K266	Ufl1	E3 UFM1-protein ligase 1	83.63	2	3	0	3	3	0	2	3	0	3	3	0	1.16E+04	3.12E+04	0.00E+00	2.18E+04	8.93E+03	0.00E+00	3.5	5.7	0	5.7	5.7	0
G3V6C4	Ugdh	UDP-glucose 6-dehydrogenase	54.89	3	3	3	2	3	3	3	3	3	2	3	3	3.00E+04	5.02E+04	1.46E+04	2.03E+04	2.21E+04	1.10E+04	8.5	8.5	8.5	6.7	8.5	8.5
A0A0G2K542	Ugp2	UTP--glucose-1-phosphate uridylyltransferase	56.89	8	7	7	7	7	8	8	7	7	7	7	8	2.81E+05	2.25E+05	2.57E+05	1.90E+05	1.86E+05	1.54E+05	21.1	17.6	19.3	17.6	17.6	21.1
Q4QQS7	Umps	Uridine monophosphate synthetase	52.38	4	4	2	3	4	3	4	4	2	3	4	3	9.51E+04	1.31E+05	6.11E+04	5.20E+04	5.23E+04	4.16E+04	12.7	12.7	7.9	10.8	12.7	10.8
F1LY19	Upf1	Regulator of nonsense transcripts 1	122.64	2	4	3	1	2	3	2	4	3	1	2	3	5.93E+03	1.97E+04	1.32E+04	3.17E+03	4.60E+03	6.51E+03	3.9	6.3	5.3	1.6	3.9	5.3
D4A7S4	Urb1	URB1 ribosome biogenesis homolog	255.80	1	1	1	1	1	1	1	1	1	1	1	1	6.92E+04	4.13E+04	4.45E+02	8.22E+04	6.23E+04	4.93E+03	0.8	0.8	0.6	0.8	0.8	0.6
B0BN55	Urod	Uroporphyrinogen decarboxylase	40.58	7	6	6	6	4	5	7	6	6	6	4	5	3.90E+05	1.37E+05	1.03E+05	1.78E+05	1.23E+05	4.93E+04	37.1	30	34.3	31.1	17.7	25.6
P41542	Uso1	General vesicular transport factor p115	107.16	7	9	7	7	8	6	7	9	7	7	8	6	4.04E+04	9.32E+04	3.14E+04	3.20E+04	2.15E+04	1.23E+04	10.3	12.7	9.7	9.8	11.5	8.6
A0A0G2JYY4	Usp14	Ubiquitin carboxyl-terminal hydrolase	52.29	6	4	3	5	4	3	6	4	3	5	4	3	8.37E+04	8.01E+04	5.28E+04	7.39E+04	4.54E+04	2.04E+04	22.1	15.3	9.6	16.4	15.3	9.6
D3ZVQ0	Usp5	Ubiquitin carboxyl-terminal hydrolase	95.78	24	25	23	24	22	21	24	25	23	24	22	21	5.74E+05	7.78E+05	3.65E+05	3.96E+05	2.80E+05	1.57E+05	43.6	46.7	43	46.4	43.6	40.1
A2RRU3	Uip15	U3 small nucleolar RNA-associated protein 15 homolog	59.52	1	1	1	1	1	0	1	1	1	1	1	0	2.48E+04	4.00E+04	0.00E+00	0.00E+00	4.01E+04	0.00E+00	1.5	1.5	1.5	1.5	1.5	0
G3V7L1	Utrn	Utrophin	391.31	2	2	2	2	2	2	2	2	2	2	2	2	2.91E+03	3.32E+03	4.04E+03	3.41E+03	2.84E+03	3.51E+03	1	1	1	1	1	1
Q04462	Vars	Valine--tRNA ligase	140.37	10	10	7	8	11	6	10	10	7	8	11	6	8.44E+04	1.64E+05	4.55E+04	6.96E+04	6.56E+04	2.10E+04	11.7	11.5	8.1	9.8	13	7
D3ZAE6	Vasn	Vasorin	72.32	1	1	1	1	1	0	1	1	1	1	1	0	2.71E+04	6.18E+03	1.28E+04	9.36E+03	1.36E+04	0.00E+00	1.5	1.5	1.5	1.5	1.5	0
Q3MIE4	Vat1	Synaptic vesicle membrane protein VAT-1 homolog	43.12	13	13	13	13	12	13	13	13	13	13	12	13	1.01E+06	1.54E+06	1.04E+06	7.05E+05	4.78E+05	5.35E+05	55.2	55.2	55.2	55.2	50.5	55.2
P29534	Vcam1	Vascular cell adhesion protein 1	81.25	11	12	12	10	10	13	11	12	12	10	10	13	2.65E+05	1.94E+05	3.65E+05	2.52E+05	1.74E+05	2.60E+05	18.3	20.3	21.2	18.3	17.9	22.1
R9PXU6	Vcl	Vinculin	116.57	27	28	31	28	26	26	27	28	31	28	26	26	4.61E+05	4.49E+05	4.12E+05	2.97E+05	2.03E+05	2.37E+05	35.2	37.8	41.7	36.1	32.9	35
P46462	Vcp	Transitional endoplasmic reticulum ATPase	89.35	35	41	27	34	35	19	35	41	27	34	35	19	9.54E+05	9.78E+05	5.69E+05	7.28E+05	8.76E+05	2.38E+05	59.1	63.6	49.1	57.6	55.2	41.4
Q9Z2L0	Vdac1	Voltage-dependent anion-selective channel protein 1	30.76	1	0	0	0	3	1	1	0	0	0	3	1	1.30E+04	0.00E+00	0.00E+00	0.00E+00	8.81E+04	2.81E+03	4.9	0	0	0	15.9	4.9
G3V8C3	Vim	Vimentin	53.70	33	37	26	31	29	22	31	35	24	29	27	20	1.48E+06	3.31E+06	1.43E+06	1.13E+06	1.03E+06	6.71E+05	67.8	68.7	61.8	65.9	64.6	55.8
Q4KLZ0	Vnn1	Vanin 1	57.01	1	1	0	0	1	0	1	1	0	0	1	0	5.14E+03	5.93E+03	0.00E+00	0.00E+00	1.13E+03	0.00E+00	2.5	2.5	0	0	2.5	0
D4A183	Vnn3	Vanin 3	56.42	2	1	2	3	3	2	2	1	2	3	3	2	5.22E+03	3.58E+03	2.85E+04	6.14E+03	2.56E+04	2.56E+04	5.6	2.8	5.8	8.6	9	5.8
D4A899	Vps13a	Vacuolar protein sorting-associated protein 13A	266.49	2	2	2	0	1	1	2	2	2	0	1	1	4.62E+03	6.46E+03	3.62E+03	0.00E+00	1.19E+03	7.59E+02	1.5	1.5	1.5	0	0.7	0.7
Q6AY86	Vps26a	Vacuolar protein sorting-associated protein 26A	38.11	1	4	1	0	1	1	1	4	1	0	1	1	1.12E+04	4.14E+04	3.79E+03	0.00E+00	1.15E+04	4.73E+03	4	15.9	6.4	0	4	6.4
A0A0G2JTS3	Vps29	Vacuolar protein sorting-associated protein 29	23.60	1	1	1	1	1	1	1	1	1	1	1	1	2.69E+05	1.29E+05	1.31E+05	1.06E+05	1.01E+05	8.59E+04	6.2	6.2	6.2	6.2	6.2	6.2
G3V8A5	Vps35	Vacuolar protein sorting-associated protein 35	91.73	10	10	9	10	9	7	10	10	9	10	9	7	1.77E+05	1.99E+05	1.14E+05	1.19E+05	9.20E+04	4.52E+04	16.2	16.2	15.1	16.2	14.7	11.7
Q4KLL7	Vps4b	Vacuolar protein sorting-associated protein 4B	49.45	3	4	2	3	3	3	3	4	2	3	3	3	5.97E+04	9.29E+04	2.38E+04	2.66E+04	3.53E+04	1.26E+04	13.1	16	7.2	13.1	12.4	12.4
A0A096MKH2	Vta1	Vacuolar protein sorting-associated protein VTA1 homolog	33.98	2	2	2	2	2	2	2	2	2	2	2	2	1.54E+04	2.88E+04	2.60E+04	3.36E+04	1.80E+04	1.95E+04	6.1	6.1	6.1	6.1	6.1	6.1
Q3KR94	Vtn	Vitronectin	54.72	24	24	20	24	22	20	24	24	20	24	22	20	4.69E+07	4.98E+07	5.09E+07	5.69E+07	5.51E+07	4.60E+07	51.3	51.3	43.1	51.3	48.3	43.1
A0A0H2UH90	Vwa5a	von Willebrand factor A domain-containing protein 5A	88.08	12	14	9	13	11	10	12	14	9	13	11	10	2.83E+05	4.22E+05	8.96E+04	2.81E+05	1.16E+05	4.01E+04	22.1	25	17.7	23.1	18	16.8
F1M957	Vwf	von Willebrand factor	308.98	7	7	5	3	6	4	7	7	5	3	6	4	2.30E+04	2.24E+04	2.27E+04	6.15E+03	8.82E+03	7.13E+03	4.8	4.8	3.9	2.4	4.1	3.1
F8WFH8	Wars	Tryptophan--tRNA ligase, cytoplasmic	53.43	7	7	5	6	6	4	7	7	5	6	6	4	1.57E+05	2.50E+05	1.10E+05	1.04E+05	6.94E+04	4.20E+04	22.5	22.5	17.3	18.5	19.8	13.5
G3V721	Wbp2	WW domain-binding protein 2	28.16	2	2	1	2	2	1	2	2	1	2	2	1	4.36E+04	1.31E+05	5.68E+04	3.59E+04	2.51E+04	3.48E+04	7.6	7.6	3.8	7.6	7.6	3.8
Q5RKI0	Wdr1	WD repeat-containing protein 1	66.18	4	3	4	3	3	3	4	3	4	3	3	3	3.85E+04	2.88E+04	1.98E+04	2.08E+04	2.93E+04	1.56E+04	11.2	5.8	11.2	5.8	5.8	9.7
D3ZX63	Wdr54	WD repeat-containing protein 54	35.59	4	4	4	4	4	2	4	4	4	4	4	2	1.11E+05	1.53E+05	8.17E+04	6.04E+04	3.36E+04	1.27E+04	20.7	20.7	20.7	20.7	20.7	13.8
Q7TPT7	Wdr77	Methylosome protein 50	37.73	2	3	3	3	3	3	2	3	3	3	3	3	7.18E+04	6.19E+04	2.23E+04	7.44E+04	5.51E+04	5.25E+04	8.9	12.9	12.9	12.9	12.9	12.9
D3ZKN4	Whamm	WASP homolog-associated protein with actin, membranes and microtubules	89.63	1	1	1	1	1	1	1	1	1	1	1	1	9.20E+04	1.93E+05	2.82E+05	1.90E+05	1.16E+05	2.92E+05	3	3	3	3	3	3
F1LQS6	Xdh	Xanthine dehydrogenase/oxidase	146.26	20	21	18	19	19	18	20	21	18	19	19	18	3.27E+05	2.95E+05	2.23E+05	1.57E+05	2.28E+05	1.66E+05	24	27.1	22.7	24	24	22
A0A0G2JV31	Xpnpep1	Xaa-Pro aminopeptidase 1	74.67	23	25	20	23	21	19	23	25	20	23	21	19	1.23E+06	1.71E+06	7.75E+05	8.69E+05	4.71E+05	2.89E+05	49.1	50.9	44.1	50.8	41.3	41.7
Q80U96	Xpo1	Exportin-1	123.04	4	4	5	3	2	2	4	4	5	3	2	2	2.70E+04	5.51E+04	2.28E+04	1.51E+04	6.89E+03	2.45E+03	5	5	6	3.7	2.8	2.6
Q3ZAV2	Ybx1	Nuclease-sensitive element-binding protein 1	36.20	2	3	2	2	2	2	2	2	2	2	2	2	7.12E+04	1.82E+05	2.97E+04	2.77E+04	4.69E+04	1.68E+04	15	17.5	15	15	15	15
D4A3P0	Ybx2	Y box-binding protein 2	38.09	7	10	5	5	6	5	7	9	5	5	6	5	6.71E+05	1.54E+06	4.52E+05	4.17E+05	2.11E+05	6.10E+04	41.5	46.5	28.4	28.4	36.8	28.4
Q62764	Ybx3	Y-box-binding protein 3	38.85	2	5	3	3	4	3	2	4	3	3	4	3	6.91E+03	1.47E+05	7.56E+04	2.88E+04	2.69E+04	2.86E+04	12.5	28.5	26	20.5	26.3	16.6
P35213	Ywhab	14-3-3 protein beta/alpha;14-3-3 protein beta/alpha, N-terminally processed	28.05	12	13	11	12	12	11	7	8	7	7	7	7	1.69E+06	2.90E+06	1.21E+06	1.45E+06	9.69E+05	5.42E+05	55.3	59.3	47.2	55.3	55.3	47.2
P62260	Ywhae	14-3-3 protein epsilon	29.17	18	18	17	19	18	13	16	16	15	17	16	11	2.57E+06	3.98E+06	2.15E+06	2.73E+06	1.15E+06	1.13E+06	70.6	70.6	69	70.6	70.6	56.1
P61983	Ywhag	14-3-3 protein gamma;14-3-3 protein gamma, N-terminally processed	28.30	8	8	8	8	8	8	4	4	4	4	4	4	2.66E+05	3.52E+05	2.47E+05	3.04E+05	1.95E+05	2.15E+05	31.2	31.2	34.8	31.2	31.2	34.8
P68511	Ywhah	14-3-3 protein eta	28.21	9	12	8	11	9	8	7	10	6	9	7	6	5.33E+05	1.56E+06	4.01E+05	5.17E+05	3.56E+05	1.03E+05	42.3	50.4	32.5	43.9	36.6	32.5
P68255	Ywhaq	14-3-3 protein theta	27.78	15	15	14	15	13	14	13	13	12	13	11	12	2.09E+06	2.99E+06	1.46E+06	1.87E+06	1.02E+06	7.45E+05	49.8	49.8	44.9	49.8	44.9	49.8
P63102	Ywhaz	14-3-3 protein zeta/delta	27.77	16	18	16	19	17	15	13	15	14	16	14	13	7.87E+06	1.13E+07	6.21E+06	6.36E+06	6.19E+06	3.23E+06	64.9	70.6	56.7	70.6	70.6	52.2
M0R5Y9	Zbtb8os	Zinc finger and BTB domain-containing 8 opposite strand	19.59	1	1	1	1	1	1	1	1	1	1	1	1	6.03E+03	7.01E+03	5.32E+03	6.59E+04	2.00E+04	2.28E+04	10.2	10.2	10.2	10.2	10.2	10.2
D4A7U1	Zyx	Zyxin	60.30	5	7	5	4	4	4	5	7	5	4	4	4	1.02E+05	1.71E+05	5.23E+04	5.80E+04	4.42E+04	2.21E+04	19.9	25.4	19.9	11.5	11.5	16.5

Column explanations

Uniprot accession number: First, or leading, protein ID annotation in UniProtKB/Swiss-Prot Rattus norvegicus database (Nov 2018).

Gene symbol: Leading gene symbol in UniProtKB/Swiss-Prot Rattus norvegicus database (Nov 2018).

Protein name: Protein name from the UniProtKB/Swiss-Prot Rattus norvegicus database (Nov 2018).

iBAQ: The sum of all the peptides intensities divided by the number of observable peptides of a protein.

N/A: Data not available/ applicable.

7. Bibliography

(Includes references cited in Chapters 1 and 5, and Appendix 1)

Absalan, F., Movahedin, M., Mowla, S.J., 2010. Germ cell apoptosis induced by experimental cryptorchidism is mediated by molecular pathways in mouse testis. Andrologia 42, 5–12.

Adam, M., Schwarzer, J.U., Köhn, F.M, Strauss, L., Poutanen, M., Mayerhofer, A., 2011. Mast cell tryptase stimulates production of decorin by human testicular peritubular cells: possible role of decorin in male infertility by interfering with growth factor signaling. Hum. Reprod. 26, 2613–2625.

Adam, M., Urbanski, H.F., Garyfallou, V.T., Welsch, U., Köhn, F.M., Ullrich Schwarzer, J., Strauss, L., Poutanen, M., Mayerhofer, A., 2012. High levels of the extracellular matrix proteoglycan decorin are associated with inhibition of testicular function. Int. J. Androl. 35, 550–561.

Aebersold, R., Mann, M., 2016. Mass-spectrometric exploration of proteome structure and function. Nature 537, 347–355.

Agarwal, A., Ayaz, A., Samanta, L., Sharma, R., Assidi, M., Abuzenadah, A.M., Sabanegh, E., 2015. Comparative proteomic network signatures in seminal plasma of infertile men as a function of reactive oxygen species. Clin. Proteom. 12, 23.

Agarwal, A., Durairajanayagam, D., Halabi, J., Peng, J., Vazquez-Levin, M., 2014. Proteomics, oxidative stress and male infertility. Reprod. Biomed. Online 29, 32–58.

Agarwal, A., Prabakaran, S., Allamaneni, S., 2006. What an andrologist/urologist should know about free radicals and why. Urology 67, 2–8.

Agoulnik A.I., Huang Z., Ferguson L., 2012. Spermatogenesis in Cryptorchidism, in: Chan W.Y., Blomberg L. (Eds.) Germline Development: Methods and Protocols. Springer, New York, pp. 127–147.

Ahotupa, M., Huhtaniemi, I., 1992. Impaired detoxification of reactive oxygen and consequent oxidative stress in experimentally cryptorchid rat testis. Biol. Reprod. 46, 1114–1118.

Aitken, R.J., Baker, M.A., 2006. Oxidative stress, sperm survival and fertility control. Mol. Cell. Endocrinol. 250, 66–69.

Alekseev, O.M., Richardson, R.T., O'Rand, M.G., 2009. Linker histones stimulate HSPA2 ATPase activity through NASP binding and inhibit CDC2/Cyclin B1 complex formation during meiosis in the mouse. Biol. Reprod. 81, 739–748.

Anand-Ivell, R., Heng, K., Hafen, B., Setchell, B.P., Ivell, R., 2009. Dynamics of INSL3 peptide expression in the rodent testis. Biol. Reprod. 81, 480–487.

Anton, F., Morales, C., Aguilar, R., Bellido, C., Aguilar, E., Gaytan, F., 1998. A comparative study of mast cells and eosinophil leukocytes in the mammalian testis. J. Vet. Med. Ser. A 45, 209–218.

Aoki, A., Fawcett, D.W., 1978. Is there a local feedback from the seminiferous tubules affecting activity of the Leydig cells? Biol. Reprod. 19, 144–158.

Aoki, V.W., Carrell, D.T., 2003. Human protamines and the developing spermatid: their structure, function, expression and relationship with male infertility. Asian J. Androl. 5, 315–324.

Aoki, V.W., Moskovtsev, S.I., Willis, J., Liu, L., Mullen, J.B.M., Carrell, D.T., 2005. DNA Integrity Is Compromised in Protamine-Deficient Human Sperm. J. Androl. 26, 741–748.

Archambeault, D.R., Yao, H.H.-C., 2010. Activin A, a product of fetal Leydig cells, is a unique paracrine regulator of Sertoli cell proliferation and fetal testis cord expansion. Proc. Natl. Acad. Sci. 107, 10526–10531.

Arrotéia, K.F., Garcia, P.V., Barbieri, M.F., Justino, M.L., and Pereira, L., 2012. The epididymis: embryology, structure, function and its role in fertilization and infertility. in: Pereira, L., (Ed.) Embryology—updates and highlights on classic topics. Intech, Rijeka, pp. 41–66

Ascoli, M., Fanelli, F., Segaloff, D.L., 2002. The lutropin/choriogonadotropin receptor, a 2002 perspective. Endocr. Rev. 23, 141-174.

Au, C.L., Robertson, D.M., de Kretser, D.M., 1983. In Vitro Bioassay of Inhibin in Testes of Normal and Cryptorchid Rats. Endocrinology. 112, 239–244.

Au, C.L., Robertson, D.M., de Kretser, D.M., 1987. Changes in Testicular Inhibin after a Single Episode of Heating of Rat Testes. Endocrinology 120, 973–977.

Aubry, F., Satie, A.P., Rioux-Leclercq, N., Meyts, R.D., Spagnoli, G.C., Chomez, P., De Backer, O., Jégou, B., Samson, M., 2001. MAGE-A4, a germ cell specific marker, is expressed differentially in testicular tumors. Cancer 92, 2778–2785.

Banerjee, S., Chambliss, K.L., Mineo, C., Shaul, P.W., 2014. Recent insights into non-nuclear actions of estrogen receptor alpha. Steroids 81, 64–69.

Banks, S., King, S.A., Irvine, D.S., Saunders, P.T., 2005. Impact of a mild scrotal heat stress on DNA integrity in murine spermatozoa. Reproduction 129, 505–514.

Barakat, B., Itman, C., Mendis, S.H., Loveland, KL.., 2012. Activins and inhibins in mammalian testis development: New models, new insights. Mol. Cell. Endocrinol. 359, 66–77.

Bartkova, J., Falck, J., Rajpert-De Meyts, E., Skakkebaek, N.E., Lukas, J., Bartek, J., 2001. Chk2 tumour suppressor protein in human spermatogenesis and testicular germ-cell tumours. Oncogene 20, 5897–5902.

Bartlett, J.E., Lee, S.M.Y., Mishina, Y., Behringer, R.R., Yang, N., Wolf, J., Temelcos, C., Hutson, J.M., 2002. Gubernacular development in Müllerian inhibiting substance receptor-deficient mice. BJU Int. 89, 113–118.

Bartlett, J.M.S., Sharpe, R.M., 1987. Effect of local heating of the rat testis on the levels in interstitial fluid of a putative paracrine regulator of the Leydig cells and its relationship to changes in Sertoli cell secretory function. J. Reprod. Fertil. 80, 279–287.

Batruch, I., Smith, C.R., Mullen, B.J., Grober, E., Lo, K.C., Diamandis, E.P., Jarvi, K.A., 2012. Analysis of seminal plasma from patients with non-obstructive azoospermia and identification of candidate biomarkers of male infertility. J. Proteome Res. 11, 1503–1511.

Beckmann, R.P., Mizzen, L., Welch, W.J., 1990. Interaction of Hsp 70 with newly synthesized proteins: implications for protein folding and assembly. Science 248, 850–854.

Behre, H.M., Yeung, C. H., Holstein, A. F., Weinbauer, G. F., Gassner, P., Nieschlag, E., 2001. Diagnosis of Male Infertility and Hypogonadism, in: van Ahlen, H. (Ed.), Andrology: male reproductive health and dysfunction. Springer, Berlin, Heidelberg, pp.89–124.

Beitins, I.Z., Lipson, L.G. and McArthur, J.W., 1977. Immunoreactive luteinizing hormone, follicle stimulating hormone and their subunits in tissue culture media from normal and adenomatous, human pituitary fragments. J. Clin. Endocrin. Metab. 45, 1271–1280.

Bergh, A.R.J., 1982. Local differences in Leydig cell morphology in the adult rat testis: evidence for a local control of Leydig cells by adjacent seminiferous tubules. Int. J. Androl. 5, 325–330.

Birk, D.E., Brückner, P., 2011. Collagens, suprastructures, and collagen fibril assembly, in: Mecham R. (Eds.), The extracellular matrix: an overview. Springer, Berlin, Heidelberg, pp. 77–115.

Bisht, S., Faiq, M., Tolahunase, M., Dada, R., 2017. Oxidative stress and male infertility. Nat. Rev. Urol. 14, 470.

Blackstock, W.P., Weir, M.P., 1999. Proteomics: quantitative and physical mapping of cellular proteins. Trends Biotechnol. 17, 121–127.

Blanco-Rodriguez, J., Martinez-Garcia, C., 1998. Apoptosis precedes detachment of germ cells from the seminiferous epithelium after hormone suppression by short-term oestradiol treatment of rats. Int. J. Androl. 21, 109–115.

Blanco-Rodriguez, J., Martinez-Garcia, C., 1998. Apoptosis pattern elicited by several apoptogenic agents on the seminiferous epithelium of the adult rat testis. J. Androl. 19, 487–497.

Bliss, S.P., Navratil, A.M., Xie, J., Roberson, M.S., 2010. GnRH signaling, the gonadotrope and endocrine control of fertility. Front. Neuroendocrinol. 31, 322–340.

Boonyaratanakornkit, V., Scott, M.P., Ribon, V., Sherman, L., Anderson, S.M., Maller, J.L., Miller, W.T., Edwards, D.P., 2001. Progesterone receptor contains a proline-rich motif that directly interacts with SH3 domains and activates c-Src family tyrosine kinases. Mol. Cell 8, 269–280.

Bowler, K., 1972. The effect of repeated applications of heat on spermatogenesis in the rat: a histological study. J. Reprod. Fertil. 28, 325–333.

Brady, R.O., 1951. Biosynthesis of radioactive testosterone in vitro. J. Biol. Chem. 193, 145–148.

Bromfield, E.G., Aitken, R.J., Nixon, B., 2015. Novel characterization of the HSPA2-stabilizing protein BAG6 in human spermatozoa. Mol. Hum. Reprod. 21, 755–769.

Bromfield, E.G., Aitken, R.J., McLaughlin, E.A., Nixon, B., 2017. Proteolytic degradation of heat shock protein A2 occurs in response to oxidative stress in male germ cells of the mouse. Mol. Hum. Reprod. 23, 91–105.

Brown, C.W., Houston-Hawkins, D.E., Woodruff, T.K., Matzuk, M.M., 2000. Insertion of Inhbb into the Inhba locus rescues the Inhba-null phenotype and reveals new activin functions. Nat. Genet. 25, 453–457.

Buzzard, J.J., Farnworth, P.G., de Kretser, D.M., O'Connor, A.E., Wreford, N.G., Morrison, J.R., 2003. Proliferative phase Sertoli cells display a developmentally regulated response to activin in vitro. Endocrinology 144, 474–483.

Byskov, A.G., 1986. Differentiation of mammalian embryonic gonad. Physiol. Rev. 66, 71–117.

Cai, H., Ren, Y., Li, X.X., Yang, J.L., Zhang, C.P., Chen, M., Fan, C.H., Hu, X.Q., Hu, Z.Y., Gao, F., 2011. Scrotal heat stress causes a transient alteration in tight junctions and induction of TGF-β expression. Int. J. Androl. 34, 352–362.

Calvel, P., Kervarrec, C., Lavigne, R., Vallet-Erdtmann, V., Guerrois, M., Rolland, A.D., Chalmel, F., Jégou, B., Pineau, C., 2009. CLPH, a novel casein kinase 2-phosphorylated disordered protein, is specifically associated with postmeiotic germ cells in rat spermatogenesis. J. Proteome Res. 8, 2953–2965.

Candas, V., Becmeur, F., Bothorel, B., Hoeft, A., 1993. Qualitative assessment of thermal and evaporative adjustments of human scrotal skin in response to heat stress. Int. J. Androl. 16, 137–142.

Canick, J.A., Makris, A., Gunsalus, G.L., Ryan, K.J., 1979. Testicular Aromatization in Immature Rats: Localization and Stimulation after Gonadotropin Administration in Vivo. Endocrinology. 104, 285–288.

Carlsen, E., Andersson, A.M., Petersen, J.H., Skakkebæk, N.E., 2003. History of febrile illness and variation in semen quality. Hum. Reprod. 18, 2089–2092.

Carreau, S., Hess, R.A., 2010. Oestrogens and spermatogenesis. Philos. Trans. R. Soc. Lond. B. Biol. Sci. 365, 1517–1535.

Carrell, D.T., Emery, B.R., Hammoud, S., 2007. Altered protamine expression and diminished spermatogenesis: what is the link? Hum. Reprod. Update 13, 313-327.

Carrell, D.T., Liu, L., 2001. Altered protamine 2 expression is uncommon in donors of known fertility, but common among men with poor fertilizing capacity, and may reflect other abnormalities of spermiogenesis. J. Androl. 22, 604-610.

Castoria, G., Barone, M.V., Di Domenico, M., Bilancio, A., Ametrano, D., Migliaccio, A., Auricchio, F., 1999. Non-transcriptional action of oestradiol and progestin triggers DNA synthesis. EMBO J. 18, 2500–2510.

Castrillon, D.H., Quade, B.J., Wang, T., Quigley, C., Crum, C.P., 2000. The human VASA gene is specifically expressed in the germ cell lineage. Proc. Natl. Acad. Sci. 97, 9585–9590.

Cedenho, A.P., Lima, S.B., Cenedeze, M.A., Spaine, D.M., Ortiz, V., Oehninger, S., 2006. Oligozoospermia and heat-shock protein expression in ejaculated spermatozoa. Hum. Reprod. 21, 1791–1794.

Chang, C., Lee, S.O., Wang, R.-S., Yeh, S., Chang, T.-M., 2013. Androgen receptor (AR) physiological roles in male and female reproductive systems: lessons learned from AR-knockout mice lacking AR in selective cells. Biol. Reprod. 89, 21.

Chappel, S., Miller, C. and Hyland, L., 1984. Regulation of the pulsatile releases of luteinizing and follicle-stimulating hormones in ovariectomized hamsters. Biol. Reprod. 30, 628–636.

Chen, J.L., Walton, K.L., Winbanks, C.E., Murphy, K.T., Thomson, R.E., Makanji, Y., Qian, H., Lynch, G.S., Harrison, C.A., Gregorevic, P., 2014. Elevated expression of activins promotes muscle wasting and cachexia. FASEB J. 28, 1711–1723.

Chen, S.-H., Li, D., Xu, C., 2012. Downregulation of Col1a1 induces differentiation in mouse spermatogonia. Asian J. Androl. 14, 842.

Chen, Y., Wu, H., Winnall, W.R., Loveland, K.L., Makanji, Y., Phillips, D.J., Smith, J.A., Hedger, M.P., 2011. Tumour necrosis factor-α stimulates human neutrophils to release preformed activin A. Immunol. Cell Biol. 89, 889–896.

Chen, Z., Yuhanna, I.S., Galcheva-Gargova, Z., Karas, R.H., Mendelsohn, M.E., Shaul, P.W., 1999. Estrogen receptor α mediates the nongenomic activation of endothelial nitric oxide synthase by estrogen. J. Clin. Invest. 103, 401.

Cheng, C.Y., Mruk, D.D., 2012. The blood-testis barrier and its implications for male contraception. Pharmacol. Rev. 64, 16–64.

Chirico, W.J., Waters, M.G., Blobel, G., 1988. 70K heat shock related proteins stimulate protein translocation into microsomes. Nature 332, 805.

Chowdhury, A., Steinberger, E., 1970. Early changes in the germinal epithelium of rat testes following exposure to heat. J. Reprod. Fertil. 22, 205–212.

Christensen, A.K., Mason, N.R., 1965. Comparative ability of seminiferous tubules and interstitial tissue of rat testes to synthesize androgens from progesterone-4-^{14}C in vitro. Endocrinology 76, 646–656.

Chu, D.S., Liu, H., Nix, P., Wu, T.F., Ralston, E.J., Yates III, J.R., Meyer, B.J., 2006. Sperm chromatin proteomics identifies evolutionarily conserved fertility factors. Nature 443, 101.

Cipriano, S.C., Chen, L., Kumar, T.R., Matzuk, M.M., 2000. Follistatin Is a Modulator of Gonadal Tumor Progression and the Activin-Induced Wasting Syndrome in Inhibin-Deficient Mice. Endocrinology 141, 2319–2327.

Clayton, R.N., Shakespear, R.A., Duncan, J.A., Munson, P.J. and Rodbard, D., 1979. Radioiodinated nondegradable gonadotropin-releasing hormone analogs: new probes for the investigation of pituitary gonadotropin-releasing hormone receptors. Endocrinology 105, 1369–1381.

Clermont, Y., 1963. The cycle of the seminiferous epithelium in man. Am. J. Anat. 112, 35–51.

Clermont, Y., 1966a. Renewal of spermatogonia in man. Am. J. Anat. 118, 509–524.

Clermont, Y., 1966b. Spermatogenesis in man. A study of the spermatogonial population. Fertil. Steril. 17, 705–721.

Clermont, Y., 1972. Kinetics of spermatogenesis in mammals: seminiferous epithelium cycle and spermatogonial renewal. Physiol. Rev. 52, 198–236.

Clermont, Y., Perey, B., 1957. Quantitative study of the cell population of the seminiferous tubules in immature rats. Am. J. Anat. 100, 241–267.

Coleman, K., Smith, C., 2001. Intracellular signaling pathways: nongenomic actions of estrogens and ligand-independent activation of estrogen receptors. Front. Biosci. 6, D1379–1391.

Com, E., Evrard, B., Roepstorff, P., Aubry, F., Pineau, C., 2003. New insights into the rat spermatogonial proteome: identification of 156 additional proteins. Mol. Cell. Proteom. 2, 248–261.

Cooke, H.J., Saunders, P.T., 2002. Mouse models of male infertility. Nat. Rev. Genet. 3, 790–801.

Cornwall, G.A., 2009. New insights into epididymal biology and function. Hum. Reprod. Update 15, 213–227.

Cornwall, G.A., von Horsten, H.H., 2007. Sperm Maturation in the epididymis, in: Carrell D.T. (Ed.) The genetics of male infertility. Humana Press, Totowa, New Jersey, pp. 211–231.

Crofton, P.M., Evans, A.E., Groome, N.P., Taylor, M.R., Holland, C.V., Kelnar, C.J., 2002. Inhibin B in boys from birth to adulthood: relationship with age, pubertal stage, FSH and testosterone. Clin. Endocrinol. 56, 215–221.

Cui, Z., Agarwal, A., da Silva, B., Sharma, R., Sabanegh, E., 2018. Evaluation of seminal plasma proteomics and relevance of FSH in identification of nonobstructive azoospermia: A preliminary study. Andrologia 50, e12999.

Culty, M., 2009. Gonocytes, the forgotten cells of the germ cell lineage. Birth Defects Res. C Embryo Today 87, 1–26.

Dadoune, J. P., 1995. The nuclear status of human sperm cells. Micron 26, 323–345.

Dahl, E., Herrick, J., 1959. A vascular mechanism for maintaining testicular temperature by counter-current exchange. Surg. Gynecol. Obstet. 108, 697–705.

de Kretser, D.M, Hedger, M.P, Loveland, K.L, Phillips, D.J, 2002. Inhibins, activins and follistatin in reproduction. Hum. Reprod. Update 8, 529–541.

de Kretser, D.M., Kerr, J.B., 1988. The cytology of the testis, in: Knobil E., Neil J.D. (Eds.), The physiology of reproduction. Raven Press Ltd., New York, vol. 1, pp.837–932.

de Kretser, D.M., O'Hehir, R.E., Hardy, C.L., Hedger, M.P., 2012. The roles of activin A and its binding protein, follistatin, in inflammation and tissue repair. Mol. Cell. Endocrinol. 359, 101–106.

de Kretser, D.M., Sharpe, R.M., Swanston, I.A., 1979. Alterations in Steroidogenesis and Human Chorionic Gonadotropin Binding in the Cryptorchid Rat Testis. Endocrinology 105, 135–138.

de Kretser, D.M., Temple-Smith, P.D., Kerr, J.B., 1982. Anatomical and Functional Aspects of the Male Reproductive Organs, in: Bandhauer, J., Frick, K. (Eds.), Disturbances in Male Fertility. Springer, Berlin, Heidelberge, pp. 1–131.

de Mateo, S., Castillo, J., Estanyol, J.M., Ballescà, J.L., Oliva, R., 2011. Proteomic characterization of the human sperm nucleus. Proteomics 11, 2714–2726.

De Plaen, E., De Backer, O., Arnaud, D., Bonjean, B., Chomez, P., Martelange, V., Avner, P., Baldacci, P., Babinet, C., Hwang, S.-Y., 1999. A New Family of Mouse Genes Homologous to the HumanMAGEGenes. Genomics 55, 176–184.

de Rooij, D.G., Grootegoed, J.A., 1998. Spermatogonial stem cells. Curr. Opin. Cell Biol. 10, 694–701.

de Rooij, D.G., Russell, L.D., 2000. All you wanted to know about spermatogonia but were afraid to ask. J. Androl. 21, 776–798.

DeFalco, T., Potter, S.J., Williams, A.V., Waller, B., Kan, M.J., Capel, B., 2015. Macrophages contribute to the spermatogonial niche in the adult testis. Cell Rep. 12, 1107–1119.

Desai, N., Ludgin, J., Sharma, R., Anirudh, R.K., Agarwal, A., 2013. Female and Male Gametogenesis, in: Falcone, T., Hurd, W.W. (Eds.), Clinical Reproductive Medicine and Surgery: A Practical Guide. Springer, Cham, pp. 43–62.

Desmots, F., Russell, H.R., Michel, D., McKinnon, P.J., 2008. Scythe regulates apoptosis-inducing factor stability during endoplasmic reticulum stress-induced apoptosis. J. Biol. Chem. 283, 3264–3271.

Di Cunto, F., Imarisio, S., Camera, P., Boitani, C., Altruda, F., Silengo, L., 2002. Essential role of citron kinase in cytokinesis of spermatogenic precursors. J. Cell Sci. 115, 4819–4826.

Dierschke, D.J., Bhattacharya, A.N., Atkinson, L.E. and Knobil, E., 1970. Circhoral oscillations of plasma LH levels in the ovariectomized rhesus monkey. Endocrinology 87, 850–853.

Dihazi, H., Dihazi, G.H., Nolte, J., Meyer, S., Jahn, O., Müller, G.A., Engel, W., 2009. Multipotent adult germline stem cells and embryonic stem cells: comparative proteomic approach. J. Proteome Res. 8, 5497–5510.

Dix, D.J., Allen, J.W., Collins, B.W., Mori, C., Nakamura, N., Poorman-Allen, P., Goulding, E.H., Eddy, E., 1996. Targeted gene disruption of Hsp70-2 results in failed meiosis, germ cell apoptosis, and male infertility. Proc. Natl. Acad. Sci. 93, 3264–3268.

Dix, D.J., Allen, J.W., Collins, B.W., Poorman-Allen, P., Mori, C., Blizard, D.R., Brown, P.R., Goulding, E.H., Strong, B.D., Eddy, E., 1997. HSP70-2 is required for desynapsis of synaptonemal complexes during meiotic prophase in juvenile and adult mouse spermatocytes. Development 124, 4595–4603.

Domanico, S.Z., DeNagel, D.C., Dahlseid, J.N., Green, J.M., Pierce, S.K., 1993. Cloning of the gene encoding peptide-binding protein 74 shows that it is a new member of the heat shock protein 70 family. Mol. Cell. Biol. 13, 3598–3610.

Dorrington, J.H., Armstrong, D.T., 1975. Follicle-stimulating hormone stimulates estradiol-17beta synthesis in cultured Sertoli cells. Proc. Natl. Acad. Sci. 72, 2677–2681.

Drabovich, A.P., Dimitromanolakis, A., Saraon, P., Soosaipillai, A., Batruch, I., Mullen, B., Jarvi, K., Diamandis, E.P., 2013. Differential diagnosis of azoospermia with proteomic biomarkers ECM1 and TEX101 quantified in seminal plasma. Sci. Transl. Med. 5, 212ra160.

Dufau, M.L., Veldhuis, J.D., Fraioli, F., Johnson, M.L., Beitins, I.Z., 1983. Mode of Secretion of Bioactive Luteinizing Hormone in Man. J. Clin. Endocrinol. Metab. 57, 993–1000.

Durairajanayagam, D., Agarwal, A., Ong, C., 2014a. Causes, effects and molecular mechanisms of testicular heat stress. Reprod. Biomed. Online 30, 14–27.

Durairajanayagam, D., Sharma, R.K., du Plessis, S.S., Agarwal, A., 2014b. Testicular heat stress and sperm quality, in: du Plessis, S.S., Agarwal, A., Sabanegh Jr., E.S. (Eds.), Male Infertility: A Complete Guide to Lifestyle and Environmental Factors. Springer, New York, pp. 105–125.

Dym, M., Kokkinaki, M., He, Z., 2009. Spermatogonial stem cells: mouse and human comparisons. Birth Defects Res. C Embryo Today 87, 27–34.

Ehmcke, J., Schlatt, S., 2006. A revised model for spermatogonial expansion in man: lessons from non-human primates. Reproduction 132, 673-680.

Eik-Nes, K.B., Hall, P.F., 1966. Secretion of steroid hormones in vivo. Vitam. Horm. 23, 153–208.

Elkin, N.D., Piner, J.A., Sharpe, R.M., 2010. Toxicant-induced leakage of germ cell–specific proteins from seminiferous tubules in the rat: Relationship to blood-testis barrier integrity and prospects for biomonitoring. Toxicol. Sci. 117, 439–448.

Eppink, B., Krawczyk, P.M., Stap, J., Kanaar, R., 2012. Hyperthermia-induced DNA repair deficiency suggests novel therapeutic anti-cancer strategies. Int. J. Hyperth. 28, 509–517.

Evans, R.M., Mangelsdorf, D.J., 2014. Nuclear receptors, RXR, and the big bang. Cell 157, 255–266.

Fang, J., Wang, H., Xi, W., Cheng, G., Wang, S., Su, S., Zhang, S., Deng, Y., Song, Z., Xu, A., 2015. Downregulation of tNASP inhibits proliferation through regulating cell cycle-related proteins and inactive ERK/MAPK signal pathway in renal cell carcinoma cells. Tumor Biol. 36, 5209–5214.

Favor J. 1999. Mechanisms of mutation induction in germ cells of the mouse as assessed by the specific locus test. Mutat. Res. 428, 227–236.

Ferdous, Z., Peterson, S., Tseng, H., Anderson, D., Iozzo, R., Grande-Allen, K., 2010. A role for decorin in controlling proliferation, adhesion, and migration of murine embryonic fibroblasts. J. Biomed. Mater. Res. Part A 93, 419–428.

Ford, S.L., Reinhart, A.J., Lukyanenko, Y., Hutson, J.C., Stocco, D.M., 1999. Pregnenolone synthesis in immature rat Sertoli cells. Mol. Cell. Endocrinol. 157, 87–94.

Fowler, D., 1969. The relationship between air temperature, scrotal surface area and testis temperature in rams. Anim. Prod. Sci. 9, 258–261.

Franke, F.E., Pauls, K., Rey, R., Marks, A., Bergmann, M., Steger, K., 2004. Differentiation markers of Sertoli cells and germ cells in fetal and early postnatal human testis. Anat. Embryol. 209, 169–177.

Fraune, J., Schramm, S., Alsheimer, M., Benavente, R., 2012. The mammalian synaptonemal complex: protein components, assembly and role in meiotic recombination. Exp. Cell Res. 318, 1340–1346.

Fridd, C., Murphy, J., Linke, C., Bonfiglio, T., 1975. Response of rat testis to localized induced hyperthermia. Urology 5, 76–82.

Frye, C., 2009. Steroids, reproductive endocrine function, and affect. A review. Minerva Ginecol. 61, 541–562.

Fujisawa, M., Matsumoto, O., Kamidono, S., Hirose, F., Kojima, K., Yoshida, S., 1988. Changes of enzymes involved in DNA synthesis in the testes of cryptorchid rats. J. Reprod. Fertil. 84, 123–130.

Fukuda, T., Hedinger, C., Groscurth, P., 1975. Ultrastructure of developing germ cells in the fetal human testis. Cell Tissue Res. 161, 55–70.

Furland, N.E., Luquez, J.M., Oresti, G.M., Aveldaño, M.I., 2011. Mild testicular hyperthermia transiently increases lipid droplet accumulation and modifies sphingolipid and glycerophospholipid acyl chains in the rat testis. Lipids 46, 443–454.

Garriott, M., Chrisman, C., 1980. Hyperthermia induced dissociation of the X-Y bivalent in mice. Environ. Mutagen. 2, 465–471.

Gasinska, A., Hill, S., 1989. The effect of hyperthermia on the mouse testis. Neoplasma 37, 357-366.

Gaskell, T.L., Esnal, A., Robinson, L.L., Anderson, R.A., Saunders, P.T., 2004. Immunohistochemical profiling of germ cells within the human fetal testis: identification of three subpopulations. Biol. Reprod. 71, 2012–2021.

Gay, V.L. and Sheth, N.A., 1972. Evidence for a periodic release of LH in castrated male and female rats. Endocrinology 90, 158–162.

Giebel, L.B., Dworniczak, B.P., Bautz, E., 1988. Developmental regulation of a constitutively expressed mouse mRNA encoding a 72-kDa heat shock-like protein. Dev. Biol. 125, 200–207.

Ginsburg, M., Snow, M., Mclaren, A., 1990. Primordial germ cells in the mouse embryo during gastrulation. Development 110, 521–528.

Goldoni, S., Humphries, A., Nyström, A., Sattar, S., Owens, R.T., McQuillan, D.J., Ireton, K., Iozzo, R.V., 2009. Decorin is a novel antagonistic ligand of the Met receptor. J. Cell Biol. 185, 743–754.

Gomez Perdiguero, E., K. Klapproth, C. Schulz, K. Busch, E. Azzoni, L. Crozet, H. Garner, C.Trouillet, M.F. de Bruijn, F. Geissmann, and H.R. Rodewald. 2015.Tissue-resident macrophages originate from yolk-sac- derived erythro-myeloid progenitors. Nature 518, 547–551.

Goulis, D.C., Mintziori, G., Koliakos, N., Hatzichristou, D., Papadimas, I., Hatzimouratidis, K., Goulis, D.G., 2011. Inhibin B and anti-Müllerian hormone in spermatic vein of subfertile men with varicocele. Reprod. Sci. 18, 551–555.

Govin, J., Caron, C., Escoffier, E., Ferro, M., Kuhn, L., Rousseaux, S., Eddy, E.M., Garin, J., Khochbin, S., 2006. Post-meiotic shifts in HSPA2/HSP70.2 chaperone activity during mouse spermatogenesis. J. Biol. Chem. 281, 37888–37892

Govin, J., Gaucher, J., Ferro, M., Debernardi, A., Garin, J., Khochbin, S., Rousseaux, S., 2011. Proteomic strategy for the identification of critical actors in reorganization of the post-meiotic male genome. Mol. Hum. Reprod. 18, 1–13.

Greenbaum, M.P., Yan, W., Wu, M.-H., Lin, Y.-N., Agno, J.E., Sharma, M., Braun, R.E., Rajkovic, A., Matzuk, M.M., 2006. TEX14 is essential for intercellular bridges and fertility in male mice. Proc. Natl. Acad. Sci. 103, 4982–4987.

Gregory, S.J., Kaiser, U.B., 2004. Regulation of gonadotropins by inhibin and activin. Semin. Reprod. Med. 22, 253–267

Guillaume, E., Dupaix, A., Moertz, E., Courtens, J.-L., Jégou, B., Pineau, C., 2000. Proteome analysis of spermatogonia: identification of a first set of 53 proteins. Proteomics 1, 1–20.

Guo, Q., Kumar, T.R., Woodruff, T., Hadsell, L.A., DeMayo, F.J., Matzuk, M.M., 1998. Overexpression of mouse follistatin causes reproductive defects in transgenic mice. Mol. Endocrinol. 12, 96–106.

Guo, X., Zhang, P., Huo, R., Zhou, Z., Sha, J., 2008. Analysis of the human testis proteome by mass spectrometry and bioinformatics. Proteom. Clin. Appl. 2, 1651–1657.

Guo, X., Zhao, C., Wang, F., Zhu, Y., Cui, Y., Zhou, Z., Huo, R., Sha, J., 2010. Investigation of human testis protein heterogeneity using 2-dimensional electrophoresis. J. Androl. 31, 419–429.

Hales, D.B., 2002. Testicular macrophage modulation of Leydig cell steroidogenesis. J. Reprod. Immunol. 57, 3–18.

Hall, J., Guyton, A., 2011. Guyton and Hall Textbook of Medical Physiology, twelfth ed. WB Saunders, Philadelphia, pp. 973–986.

Handel, M.A., Schimenti, J.C., 2010. Genetics of mammalian meiosis: regulation, dynamics and impact on fertility. Nat. Rev. Genet. 11, 124–136.

Hagemeyer, N., Kierdorf, K., Frenzel, K., Xue, J., Ringelhan, M., Abdullah, Z., Godin, I., Wieghofer, P., Jordão, M.J.C., Ulas, T. and Yorgancioglu, G., 2016. Transcriptome-based profiling of yolk sac-derived macrophages reveals a role for Irf8 in macrophage maturation. EMBO J. 35, 1730–1744.

Harrison, R.G., Weiner, J.S., 1949. Vascular patterns of the mammalian testis and their functional significance. J. Exp. Biol. 26, 304–316.

Hashimoto, O., Nakamura, T., Shoji, H., Shimasaki, S., Hayashi, Y., Sugino, H., 1997. A Novel Role of Follistatin, an Activin-binding Protein, in the Inhibition of Activin Action in Rat Pituitary Cells Endocytotic Degradation Of Activin And Its Acceleration By Follistatin Associated With Cell-Surface Heparan Sulfate. J. Biol. Chem. 272, 13835–13842.

He, Z., Feng, L., Zhang, X., Geng, Y., Parodi, D.A., Suarez-Quian, C., Dym, M., 2005. Expression of Col1a1, Col1a2 and procollagen I in germ cells of immature and adult mouse testis. Reproduction 130, 333–341.

Hedger, M.P., de Kretser, D.M., 2013. The activins and their binding protein, follistatin—diagnostic and therapeutic targets in inflammatory disease and fibrosis. Cytokine Growth Factor Rev. 24, 285–295.

Hedger, M.P., McFarlane, J.R., de Kretser, D.M., Risbridger, G.P., 1994. Multiple factors with steroidogenesis-regulating activity in testicular interbular fluid from normal and experimentally cryptorchid adult rats. Steroids 59, 676–685.

Hedger, M.P., Muir, J.A., 2000. Differential Actions of Gonadotropin-Releasing Hormone and Human Chorionic Gonadotropin on Interstitial Fluid Volume and Immunoglobulin G Concentrations in Adult Rat Testis. J. Androl. 21, 747–752.

Hedger, M.P., Winnall, W.R., 2012. Regulation of activin and inhibin in the adult testis and the evidence for functional roles in spermatogenesis and immunoregulation. Mol. Cell. Endocrinol. 359, 30–42.

Hedger, M.P., Winnall, W.R., Phillips, D.J., de Kretser, D.M., 2011. The regulation and functions of activin and follistatin in inflammation and immunity. Vitam. Horm. 85, 255–297.

Henriksen, K., Hakovirta, H., Parvinen, M., 1995. In-situ quantification of stage-specific apoptosis in the rat seminiferous epithelium: effects of short-term experimental cryptorchidism. Int. J. Androl. 18, 256–262.

Hess, R.A., de Franca, L.R., 2009. Spermatogenesis and cycle of the seminiferous epithelium, in: Cheng C.Y. (Ed.), Molecular mechanisms in spermatogenesis. Springer, New York, vol. 636, pp. 1–15.

Hikim, A.P., Lue, Y., Yamamoto, C.M., Vera, Y., Rodriguez, S., Yen, P.H., Soeng, K., Wang, C., Swerdloff, R.S., 2003. Key apoptotic pathways for heat-induced programmed germ cell death in the testis. Endocrinology 144, 3167–3175.

Hikim, A.P., Rajavashisth, T.B., Hikim, I.S., Lue, Y., Bonavera, J.J., Leung, A., Wang, C., Swerdloff, R.S., 1997. Significance of apoptosis in the temporal and stage-specific loss of germ cells in the adult rat after gonadotropin deprivation. Biol. Reprod. 57, 1193–1201.

Hikim, A.P., Wang, C., Leung, A., Swerdloff, R.S., 1995. Involvement of apoptosis in the induction of germ cell degeneration in adult rats after gonadotropin-releasing hormone antagonist treatment. Endocrinology 136, 2770–2775.

Hilscher, B., Bülthoff-Ohnolz, B., Krämer, U., Birke, A., Pelzer, H., Gauss, G., 1974. Kinetics of gametogenesis. Cell Tissue Res. 154, 443–470.

Hilscher, W., 1991. REVIEW The genetic control and germ cell kinetics of the female and male germ line in mammals including man. Hum. Reprod. 6, 1416–1425.

Hjollund, N.H.I., Storgaard, L., Ernst, E., Bonde, J.P., Olsen, J., 2002. Impact of diurnal scrotal temperature on semen quality. Reprod. Toxicol. 16, 215–221.

Holdsworth-Carson, S., Craythorn, R., Winnall, W., Dhaliwal, K., Genovese, R., Nowell, C., Rogers, P., de Kretser, D., Hedger, M., Girling, J., 2014. Follistatin is essential for normal postnatal development and function of mouse oviduct and uterus. Reprod. Fertil. Dev. 27, 985–999.

Hou, Y., Wang, X., Lei, Z., Ping, J., Liu, J., Ma, Z., Zhang, Z., Jia, C., Jin, M., Li, X., 2015. Heat Stress Induced Metabolic Changes and Altered Male Reproductive Function. J. Proteome Res. 14, 1495–1503.

Houston, B.J., Nixon, B., Martin, J.H., De Iuliis, G.N., Trigg, N.A., Bromfield, E.G., McEwan, K.E., Aitken, R.J., 2018. Heat exposure induces oxidative stress and DNA damage in the male germ line. Biol. Reprod. 98, 593–606.

Huang, S.Y., Lin, J.H., Chen, Y.H., Chuang, C.k., Lin, E.C., Huang, M.C., Sunny Sun, H.F., Lee, W.C., 2005. A reference map and identification of porcine testis proteins using 2-DE and MS. Proteomics 5, 4205–4212.

Huang, S.Y., Lin, J.H., Teng, S.H., Sun, H.S., Chen, Y.-H., Chen, H.H., Liao, J.Y., Chung, M.-T., Chen, M.-Y., Chuang, C.-k., 2011. Differential expression of porcine testis proteins during postnatal development. Anim. Reprod. Sci. 123, 221–233.

Huang, X.Y., Guo, X.-j., Shen, J., Wang, Y.-f., Chen, L., Xie, J., Wang, N.-l., Wang, F.-q., Zhao, C., Huo, R., 2008. Construction of a proteome profile and functional analysis of the proteins involved in the initiation of mouse spermatogenesis. J. Proteome Res. 7, 3435–3446.

Huckins, C., 1978. The morphology and kinetics of spermatogonial degeneration in normal adult rats: an analysis using a simplified classification of the germinal epithelium. The Anat. Rec. 190, 905–926.

Huhtaniemi, I., 2003. Gonadotrophin actions on the testis-genotypes and phenotypes of gonadotrophin and gonadotrophin receptor mutations. Endocr. Dev. 5, 81–103.

Hunt, C.R., Gasser, D.L., Chaplin, D.D., Pierce, J.C., Kozak, C.A., 1993. Chromosomal localization of five murine HSP70 gene family members: Hsp70. 1, Hsp70-2, Hsp70-3, Hsc70t, and Grp78. Genomics 16, 193–198.

Huszar, G., Stone, K., Dix, D., Vigue, L., 2000. Putative creatine kinase M-isoform in human sperm is identifiedas the 70-kilodalton heat shock protein HspA2. Biol. Reprod. 63, 925–932.

Hutson, J.M., Baker, M., Terada, M., Zhou, B., Paxton, G., 1994. Hormonal control of testicular descent and the cause of cryptorchidism. Reprod. Fertil. Dev. 6, 151–156.

Iacob, D., Cai, J., Tsonis, M., Babwah, A., Chakraborty, C., Bhattacharjee, R., Lala, P., 2008. Decorin-mediated inhibition of proliferation and migration of the human trophoblast via different tyrosine kinase receptors. Endocrinology 149, 6187–6197.

Ikeda, M., Kodama, H., Fukuda, J., Shimizu, Y., Murata, M., Kumagai, J., Tanaka, T., 1999. Role of radical oxygen species in rat testicular germ cell apoptosis induced by heat stress. Biol. Reprod. 61, 393–399.

Imamoğlu, M., Bülbül, S.S., kaklikkaya, N., Sarihan, H., 2012. Oxidative, inflammatory and immunologic status in children with undescended testes. Pediatr. Int. 54, 816–819.

Intasqui, P., Agarwal, A., Sharma, R., Samanta, L., Bertolla, R., 2018. Towards the identification of reliable sperm biomarkers for male infertility: A sperm proteomic approach. Andrologia. 50, e12919.

Intasqui, P., Antoniassi, M.P., Camargo, M., Nichi, M., Carvalho, V.M., Cardozo, K.H.M., Zylbersztejn, D.S., Bertolla, R.P., 2015. Differences in the seminal plasma proteome are associated with oxidative stress levels in men with normal semen parameters. Fertil. Steril. 104, 292–301.

Ishii, T., Matsuki, S., Iuchi, Y., Okada, F., Toyosaki, S., Tomita, Y., Ikeda, Y., Fujii, J., 2005. Accelerated impairment of spermatogenic cells in SOD1-knockout mice under heat stress. Free Radic. Res. 39, 697–705.

Ishikawa, T., 2012. Surgical recovery of sperm in non-obstructive azoospermia. Asian J. Androl. 14, 109.

Ivell, R., 2007. Lifestyle impact and the biology of the human scrotum. Reprod. Biol. Endocrinol. 5, 1477–1482.

Izu, H., Inouye, S., Fujimoto, M., Shiraishi, K., Naito, K., Nakai, A., 2004. Heat shock transcription factor 1 is involved in quality-control mechanisms in male germ cells. Biol. Reprod. 70, 18–24.

Jégou, B., 1992. 3 The sertoli cell. Baillière`s Clin. Endocrinol. Metab. 6, 273–311.

Jegou, B., Laws, A.O., de Kretser, D.M., 1984. Changes in testicular function induced by short-term exposure of the rat testis to heat: further evidence for interaction of germ cells, Sertoli cells and Leydig cells. Int. J. Androl. 7, 244–257.

Jegou, B., Risbridger, G.P., de Kretser, D.M., 1983. Effects of experimental cryptorchidism on testicular function in adult rats. J. Androl. 4, 88–94.

Jensen, T.K., Andersson, A.-M., Hjollund, N.H.I., Scheike, T., Kolstad, H., Giwercman, A., Henriksen, T.B., Ernst, E., Bonde, J.P., Olsen, J., 1997. Inhibin B as a Serum Marker of Spermatogenesis: Correlation to Differences in Sperm Concentration and Follicle-Stimulating Hormone Levels. A Study of 349 Danish Men 1. Clin. Endocrinol. Metab. 82, 4059–4063.

Jodar, M., Oliva, R., 2014. Protamine alterations in human spermatozoa, in: Baldi E., Muratori M. (Eds.), Genetic Damage in Human Spermatozoa, Advances in Experimental Medicine and Biology book series. Springer, New York , vol 791, pp. 83–102.

Johnston, D.S., Jelinsky, S.A., Bang, H.J., DiCandeloro, P., Wilson, E., Kopf, G.S., Turner, T.T., 2005. The mouse epididymal transcriptome: transcriptional profiling of segmental gene expression in the epididymis. Biol. Reprod. 73, 404–413.

Johnston, D.S., Turner, T.T., Finger, J.N., Owtscharuk, T.L., Kopf, G.S., Jelinsky, S.A., 2007. Identification of epididymis-specific transcripts in the mouse and rat by transcriptional profiling. Asian J. Androl. 9, 522–527.

Jones, K.L., de Kretser, D.M., Patella, S., Phillips, D.J., 2004. Activin A and follistatin in systemic inflammation. Mol. Cell. Endocrinol. 225, 119–125.

Jones, K.L., Mansell, A., Patella, S., Scott, B.J., Hedger, M.P., de Kretser, D.M., Phillips, D.J., 2007. Activin A is a critical component of the inflammatory response, and its binding protein, follistatin, reduces mortality in endotoxemia. Proc. Natl. Acad. Sci. 104, 16239–16244.

Jost A, Vigier B, Prepin J, Perchellet JP., 1973. Studies on sex differentiation in mammals. Recent Prog. Horm. Res. 29, 1–41.

Kampinga, H.H., Hageman, J., Vos, M.J., Kubota, H., Tanguay, R.M., Bruford, E.A., Cheetham, M.E., Chen, B. and Hightower, L.E., 2009. Guidelines for the nomenclature of the human heat shock proteins. Cell Stress and Chaperones, 14, 105–111.

Kandeel, F., Swerdloff, R., 1988. Role of temperature in regulation of spermatogenesis and the use of heating as a method for contraception. Int. J. Gynecol. Obstet. 27, 477–478.

Kanter, M., Aktas, C., 2009. Effects of scrotal hyperthermia on Leydig cells in long-term: a histological, immunohistochemical and ultrastructural study in rats. J. Mol. Histol. 40, 123–130.

Kanter, M., Aktas, C., Erboga, M., 2013. Heat stress decreases testicular germ cell proliferation and increases apoptosis in short term: an immunohistochemical and ultrastructural study. Toxicol. Ind. Health 29, 99–113.

Kerr, J.B., 1991. Ultrastructure of the seminiferous epithelium and intertubular tissue of the human testis. J. Electron Microsc. Tech. 19, 215–240.

Kerr, J.B., Loveland, K.L., O'Bryan, M.K., de Kretser, D.M., 2006. Cytology of the testis and intrinsic control mechanisms, in: Neil J.D. (Ed.), Knobil and Neill's Physiology of Reproduction. Elsevier, New York, pp. 827–947.

Kessler-Icekson, G., Schlesinger, H., Freimann, S., Kessler, E., 2006. Expression of procollagen C-proteinase enhancer-1 in the remodeling rat heart is stimulated by aldosterone. Int. J. Biochem. Cell Biol. 38, 358–365.

Kessler, E., Takahara, K., Biniaminov, L., Brusel, M., Greenspan, D.S., 1996. Bone morphogenetic protein-1: the type I procollagen C-proteinase. Science 271, 360–362.

Kierszenbaum, A.L., 2001. Transition nuclear proteins during spermiogenesis: unrepaired DNA breaks not allowed. Mol. Reprod. Dev. 58, 357–358.

Kierszenbaum, A.L., Tres, L.L., 1975. Structural and transcriptional features of the mouse spermatid genome. J. Cell Biol. 65, 258–270.

Kim, B., Park, K., Rhee, K., 2013. Heat stress response of male germ cells. Cell. Mol. Life Sci. 70, 2623–2636.

King, S.R., LaVoie, H.A., 2009. Regulation of the Early Steps in Gonadal Steroidogenesis, In: Chedrese P. (Ed.), Reproductive Endocrinology: A molecular approach. Springer, Boston, pp. 175–193.

Knoblaugh, S.E., True, L., Tretiakova, M., Hukkanen, R.R., 2018. Male reproductive system, in: Treuting P.M., Dintzis S.M., Montine K.S. (Eds.), Comparative Anatomy and Histology: A Mouse, Rat and Human Atlas. Elsevier; Philadelphia, pp. 335–363.

Kovac, J.R., Pastuszak, A.W., Lamb, D.J., 2013. The use of genomics, proteomics, and metabolomics in identifying biomarkers of male infertility. Fertil. Steril. 99, 998–1007.

Kumar, V., Abbas, A.K., Aster, J.C., 2017. Robbins Basic Pathology, tenth ed. Elsevier, Philadelphia.

Lagarrigue, M., Becker, M., Lavigne, R., Deininger, S.-O., Walch, A., Aubry, F., Suckau, D., Pineau, C., 2011. Revisiting rat spermatogenesis with MALDI imaging at 20-µm resolution. Mol. Cell. Proteom. 10, M110. 005991.

Lamb, D., 2009. A look towards the future: advances in andrology expected to revolutionize the diagnosis and treatment of the infertile male, in: in: Lipshultz L., Howards S., Niederberger C. (Eds.), Infertility in the male. Cambridge University Press, Cambridge, pp. 642–653.

Landreh, L., 2014. Identification and characterization of stem Leydig cells in the testis, Department of Women's and Children's Health. Doctoral dissertation, Karolinska Institute, Solna, Sweden.

Lawson, K.A., and Pederson, R. A., 1992. Clonal analysis of cell fate during gastrulation and early neurulation in the mouse, CIBA Foundation Symposium 165, discussion 21–26

Le Gac, F., de Kretser, D.M., 1982. Inhibin production by Sertoli cell cultures. Mol. Cell. Endocrinol. 28, 487–498.

Lee, C.H., Cho, Y.H., 1999. Aspects of mammalian spermatogenesis: electrophoretical analysis of protamines in mammalian species. Mol. Cells 9, 556–559.

Lee, J., Richburg, J.H., Shipp, E.B., Meistrich, M.L., Boekelheide, K., 1999. The Fas System, a Regulator of Testicular Germ Cell Apoptosis, Is Differentially Up-Regulated in Sertoli Cell Versus Germ Cell Injury of the Testis. Endocrinology 140, 852–858.

Légaré, C., Thabet, M., Sullivan, R., 2004. Expression of heat shock protein 70 in normal and cryptorchid human excurrent duct. Mol. Hum. Reprod. 10, 197–202.

Lewis, J.D., Abbott, D.W., Ausió, J., 2003a. A haploid affair: core histone transitions during spermatogenesis. Biochem. Cell Biol. 81, 131–140.

Lewis, J.D., Song, Y., de Jong, M.E., Bagha, S.M., Ausió, J., 2003b. A walk though vertebrate and invertebrate protamines. Chromosoma 111, 473–482.

Li, J., Liu, F., Liu, X., Liu, J., Zhu, P., Wan, F., Jin, S., Wang, W., Li, N., Liu, J., 2011. Mapping of the human testicular proteome and its relationship with that of the epididymis and spermatozoa. Mol. Cell. Proteom. 10, M110.004630.

Lin, S.Y., 2003. Genetically engineered mouse models for the study of follistatin biology. Doctoral dissertation, Institute of Reproduction and Development, Monash University, Melbourne, Australia.

Lin, S.Y., Craythorn, R.G., O'Connor, A.E., Matzuk, M.M., Girling, J.E., Morrison, J.R., de Kretser, D.M., 2008. Female infertility and disrupted angiogenesis are actions of specific follistatin isoforms. Mol. Endocrinol. 22, 415–429.

Liu, M., Ru, Y., Gu, Y., Tang, J., Zhang, T., Wu, J., Yu, F., Yuan, Y., Xu, C., Wang, J., 2018. Disruption of Ssp411 causes impaired sperm head formation and male sterility in mice. Biochim. Biophys. Acta 1862, 660–668.

Liu, Y., 2010. Temperature control of spermatogenesis and prospect of male contraception. Front. Biosci. 2, 730–755.

Loveland, K.L., and Hedger, M.P., 2015. Activins and inhibins in Sertoli cell biology: implications for testis development and function, in: Griswold, M.D. (Ed.), Sertoli Cell Biology. Academic Press, Oxford, pp. 201–232.

Lue, Y.H., Lasley, B.L., Laughlin, L.S., Swerdloff, R.S., Hikim, A.P.S., Leung, A., Overstreet, J.W., Wang, C., 2002. Mild testicular hyperthermia induces profound transitional spermatogenic suppression through increased germ cell apoptosis in adult cynomolgus monkeys (Macaca fascicularis). J. Androl. 23, 799–805.

Lue, Y.H., Sinha Hikim, A.P., Swerdloff, R.S., Im, P., Taing, K.S., Bui, T., Leung, A., Wang, C., 1999. Single Exposure to Heat Induces Stage-Specific Germ Cell Apoptosis in Rats: Role of Intratesticular Testosterone on Stage Specificity. Endocrinology 140, 1709–1717.

Lue, Y., Sinha Hikim, A.P., Wang, C., Im, M., Leung, A., Swerdloff, R.S., 2000. Testicular Heat Exposure Enhances the Suppression of Spermatogenesis by Testosterone in Rats: The “Two-Hit” Approach to Male Contraceptive Development 1. Endocrinology 141, 1414–1424.

Lysiak, J.J., Nguyen, Q.A.T., Turner, T.T., 2000. Fluctuations in rat testicular interstitial oxygen tensions are linked to testicular vasomotion: persistence after repair of torsion. Biol. Reprod. 63, 1383–1389.

Macri, L., Silverstein, D., Clark, R.A., 2007. Growth factor binding to the pericellular matrix and its importance in tissue engineering. Adv. Drug Deliv. Rev. 59, 1366–1381.

Maddocks, S., Hargreave, T., Reddie, K., Fraser, H., Kerr, J., Sharpe, R., 1993. Intratesticular hormone levels and the route of secretion of hormones from the testis of the rat, guinea pig, monkey and human. Int. J. Androl. 16, 272–278.

Maddocks, S., Sharpe, R., 1989. Interstitial fluid volume in the rat testis: androgen-dependent regulation by the seminiferous tubules? J. Endocrinology 120, 215–NP.

Maeshima, A., Mishima, K., Yamashita, S., Nakasatomi, M., Miya, M., Sakurai, N., Sakairi, T., Ikeuchi, H., Hiromura, K., Hasegawa, Y., 2014. Follistatin, an Activin Antagonist, Ameliorates Renal Interstitial Fibrosis in a Rat Model of Unilateral Ureteral Obstruction. BioMed Res. Int. 2014, 376191.

Maloney, S.K., Bonomelli, J.M., DeSouza, J., 2003. Scrotal heating stimulates panting and reduces body temperature similarly in febrile and non-febrile rams (Ovis aries). Comp. Biochem. Physiol. Part A: Mol. Integr. Physiol. 135, 565–573.

Manku, G., Culty, M., 2015. Mammalian gonocyte and spermatogonia differentiation: recent advances and remaining challenges. Reproduction 149, R139–R157.

Marconi, M., Keudel, A., Diemer, T., Bergmann, M., Steger, K., Schuppe, H.C., Weidner, W., 2012. Combined trifocal and microsurgical testicular sperm extraction is the best technique for testicular sperm retrieval in “low-chance” nonobstructive azoospermia. Eur. Urol. 62, 713–719.

Marian, J., Conn, P.M., 1983. Subcellular localization of the receptor for gonadotropin-releasing hormone in pituitary and ovarian tissue. Endocrinology 112, 104–112.

Martínez-Heredia, J., Estanyol, J.M., Ballescà, J.L., Oliva, R., 2006. Proteomic identification of human sperm proteins. Proteomics 6, 4356–4369.

Mass, E., Ballesteros, I., Farlik, M., Halbritter, F., Günther, P., Crozet, L., Jacome-Galarza, C.E., Händler, K., Klughammer, J., Kobayashi, Y. and Gomez-Perdiguero, E., 2016. Specification of tissue-resident macrophages during organogenesis. Science 353, aaf4238.

Matsumoto, A., 1989. Hormonal control of spermatogenesis, in: Burger, H., de Kretser, D.M. (Eds.), The Testis. Raven Press, New York, pp. 181–196

Matzuk, M.M., Finegold, M.J., Su, J., Hsueh, A., Bradley, A., 1992. Alpha-inhibin is a tumour-suppressor gene with gonadal specificity in mice. Nature 360, 313–319.

McCarrey, J.R., 1993. Development of the germ cell, in: Desjardins C., Ewing, L.L. (Eds.), Cell Molecular Biology of the Testis. Oxford University Press, New York, pp. 58–89.

McGuinness, M., Orth, J.M., 1992a. Gonocytes of male rats resume migratory activity postnatally. Eur. J. Cell Biol. 59, 196–210.

McGuinness, M.P., Orth, J.M., 1992b. Reinitiation of gonocyte mitosis and movement of gonocytes to the basement membrane in testes of newborn rats in vivo and in vitro. Anat. Rec. 233, 527–537.

McLachlan, R.I., Rajpert-De Meyts, E., Hoei-Hansen, C.E., de Kretser, D.M., Skakkebaek, N.E., 2006. Histological evaluation of the human testis—approaches to optimizing the clinical value of the assessment: mini review. Hum. Reprod. 22, 2–16.

McLean, D.J., Friel, P.J., Johnston, D.S., Griswold, M.D., 2003. Characterization of spermatogonial stem cell maturation and differentiation in neonatal mice. Biol. Reprod. 69, 2085–2091.

McPherson, S., Longo, F., 1993. Chromatin structure-function alterations during mammalian spermatogenesis: DNA nicking and repair in elongating spermatids. Eur. J. Histochem. 37, 109–128.

Meehan, T., Schlatt, S., O'Bryan, M.K., de Kretser, D.M., Loveland, K.L., 2000. Regulation of germ cell and Sertoli cell development by activin, follistatin, and FSH. Dev. Biol. 220, 225–237.

Meinhardt, A., O'Bryan, M.K., McFarlane, J.R., Loveland, K.L., Mallidis, C., Foulds, L.M., Phillips, D.J., de Kretser, D.M., 1998. Localization of follistatin in the rat testis. J. Reprod. Fertil. 112, 233–241.

Mendelsohn, M.E., 2002. Genomic and nongenomic effects of estrogen in the vasculature. Am. J Cardiol. 90, F3-F4.

Mendis-Handagama, S.C., Kerr, J.B., de Kretser, D.M., 1990. Experimental cryptorchidism in the adult mouse: II. A hormonal study. J. Androl. 11, 548–554.

Mendis, S.H., Meachem, S.J., Sarraj, M.A., Loveland, K.L., 2011. Activin A balances Sertoli and germ cell proliferation in the fetal mouse testis. Biol. Reprod. 84, 379–391.

Mescher, A.L., 2013. Junqueira's basic histology: text & atlas, thirteenth ed. McGraw-Hill Medical, New York.

Mieusset, R., Bujan, L., 1995. Testicular heating and its possible contributions to male infertility: a review. Int. J. Androl. 18, 169–184.

Mithraprabhu, S., Mendis, S., Meachem, S.J., Tubino, L., Matzuk, M.M., Brown, C.W., Loveland, K.L., 2010. Activin bioactivity affects germ cell differentiation in the postnatal mouse testis in vivo. Biol. Reprod. 82, 980–990.

Morgentaler, A., Stahl, B.C., Yin, Y., 1999. Testis and temperature: an historical, clinical, and research perspective. J. Androl. 20, 189–195.

Mossadegh-Keller, N., Gentek, R., Gimenez, G., Bigot, S., Mailfert, S., Sieweke, M.H., 2017. Developmental origin and maintenance of distinct testicular macrophage populations. J. Exp. Med. 214, 2829–2841.

Munkelwitz, R., Gilbert, B.R., 1998. Are boxer shorts really better? A critical analysis of the role of underwear type in male subfertility. J. Urol. 160, 1329–1333.

Nagano, R., Tabata, S., Nakanishi, Y., Ohsako, S., Kurohmaru, M., Hayashi, Y., 2000. Reproliferation and relocation of mouse male germ cells (gonocytes) during prespermatogenesis. Anat. Rec. 258, 210–220.

Nakamura, T., Sugino, K., Titani, K., Sugino, H., 1992. Follistatin, an activin-binding protein, associates with heparan sulfate chains of proteoglycans on follicular granulosa cells. J. Biol. Chem. 266, 19432–19437.

Nielsen, C.T., Skakkebæk, N.E., Richardson, D.W., Darling, J.A., Hunter, W.M., Jørgensen, M., Nielsen, A., Ingerslev, O., Keiding, N., Müller, J., 1986. Onset of the Release of Spermatozia (Supermarche) in Boys in Relation to Age, Testicular Growth, Pubic Hair, and Height. J. Clin. Endocrinol. Metab. 62, 532–535.

Nili, N., Cheema, A.N., Giordano, F.J., Barolet, A.W., Babaei, S., Hickey, R., Eskandarian, M.R., Smeets, M., Butany, J., Pasterkamp, G., 2003. Decorin inhibition of PDGF-stimulated vascular smooth muscle cell function: potential mechanism for inhibition of intimal hyperplasia after balloon angioplasty. Am. J. Pathol. 163, 869–878.

Nyman, M.A., Geiger, J., Goldzieher, J.W., 1959. Biosynthesis of estrogen by the perfused stallion testis. J. Biol. Chem 234, 16–18.

O'Donnell, L., Meachem, S.J., Stanton, P.G., McLachlan, R.I., 2006. Endocrine regulation of spermatogenesis. in: Neil J.D. (Ed.), Knobil and Neill's Physiology of Reproduction. Elsevier, New York, pp. 1017–1069.

Ogata, I., Auster, A.S., Matsui, A., Greenwel, P., Geerts, A., D'Amico, T., Fujiwara, K., Kessler, E., Rojkind, M., 1997. Up-regulation of type I procollagen C-proteinase enhancer protein messenger RNA in rats with CCl4-induced liver fibrosis. Hepatology 26, 611–617.

Ohta, Y., Nishikawa, A., Fukazawa, Y., Urushitani, H., Matsuzawa, A., Nishina, Y., Iguchi, T., 1996. Apoptosis in adult mouse testis induced by experimental cryptorchidism. Cell Tissues Organs 157, 195–204.

Oka, S., Shiraishi, K., Fujimoto, M., Katiyar, A., Takii, R., Nakai, A., Matsuyama, H., 2017. Role of heat shock factor 1 in conserving cholesterol transportation in Leydig cell steroidogenesis via steroidogenic acute regulatory protein. Endocrinology 158, 2648–2658.

Okuma, Y., O'Connor, A.E., Hayashi, T., Loveland, K.L., de Kretser, D.M., Hedger, M.P., 2006. Regulated production of activin A and inhibin B throughout the cycle of the seminiferous epithelium in the rat. J. Endocrinol. 190, 331–340.

Oliva, R., 2006. Protamines and male infertility. Hum. Reprod. Update 12, 417–435.

Orth, J.M., 1993. Cell biology of testicular development in the fetusand neonate, in: Desjardins C., Ewing, L.L. (Eds.), Cell Molecular Biology of the Testis. Oxford University Press, New York, pp. 3–42.

Orth, J.M., Gunsalus, G.L., Lamperti, A.A., 1988. Evidence From Sertoli Cell-Depleted Rats Indicates That Spermatid Number in Adults Depends on Numbers of Sertoli Cells Produced During Perinatal Development. Endocrinology 122, 787–794.

Orwig, K.E., Ryu, B.-Y., Avarbock, M.R., Brinster, R.L., 2002. Male germ-line stem cell potential is predicted by morphology of cells in neonatal rat testes. Proc. Natl. Acad. Sci. 99, 11706–11711.

Ozaki, T., Hanaoka, E., Naka, M., Nakagawara, A., Sakiyama, S., 1999. Cloning and characterization of rat BAT3 cDNA. DNA Cell Biol. 18, 503–512.

Paniagua, R., Nistal, M., 1984. Morphological and histometric study of human spermatogonia from birth to the onset of puberty. J. Anat. 139, 535–552.

Parvinen, M., 1982. Regulation of the Seminiferous Epithelium. Endocr. Rev. 3, 404–417.

Patel, K., 1998. Follistatin. Int. J. Biochem. Cell Biol. 30, 1087–1093.

Patil, S.S., Patil, A.B., Patil, M.M., Nikam, P.B., Mahadik, Y.M., Londhe, S.R., Kamble, N.A., 2014. Testicular hyperthermia in Rattus norvegicus: focus on gamatocytic alterations. Int. J. Curr. Microbiol. App. Sci 3, 93–103.

Paul, C., Murray, A.A., Spears, N., Saunders, P.T., 2008. A single, mild, transient scrotal heat stress causes DNA damage, subfertility and impairs formation of blastocysts in mice. Reproduction 136, 73–84.

Payne, A.H., 2007. Steroidogenic Enzymes in Leydig Cells, in: Payne, A.H., Hardy, M.P. (Eds.), The Leydig cell in health and disease. Humana Press, Totowa, pp. 157–171.

Paz, M., Morín, M., del Mazo, J., 2006. Proteome profile changes during mouse testis development. Comp. Biochem Physiol. Part D Genom. and Proteom. 1, 404–415.

Pei, Y., Wu, Y., Qin, Y., 2012. Effects of chronic heat stress on the expressions of heat shock proteins 60, 70, 90, A2, and HSC70 in the rabbit testis. Cell Stress Chaperones 17, 81–87.

Peltola, V., Huhtaniemi, I., Ahotupa, M., 1995. Abdominal position of the rat testis is associated with high level of lipid peroxidation. Biol. Reprod. 53, 1146–1150.

Perey, B., Clermont, Y., Leblond, C., 1961. The wave of the seminiferous epithelium in the rat. Am. J. Anat. 108, 47–77.

Pérez-Crespo, M., Pintado, B., Gutiérrez-Adán, A., 2008. Scrotal heat stress effects on sperm viability, sperm DNA integrity, and the offspring sex ratio in mice. Mol. Reprod. Dev. 75, 40–47.

Peters, H., 1970. Migration of gonocytes into the mammalian gonad and their differentiation. Philosophical Transactions of the Royal Society of London. Ser. B, Biol. Sci. 91–101.

Phillips, D.J., de Kretser, D.M., 1998. Follistatin: a multifunctional regulatory protein. Front. Neuroendocrinol. 19, 287–322.

Radons, J., 2016. The human HSP70 family of chaperones: where do we stand? Cell Stress Chaperones 21, 379–404.

Ramasamy, R., Reifsnyder, J.E., Husseini, J., Eid, P.-A., Bryson, C., Schlegel, P.N., 2013. Localization of sperm during microdissection testicular sperm extraction in men with nonobstructive azoospermia. J. Urol. 189, 643–646.

Ramaswamy, S., Marshall, G.R., Pohl, C.R., Friedman, R.L., Plant, T.M., 2003. Inhibitory and stimulatory regulation of testicular inhibin B secretion by luteinizing hormone and follicle-stimulating hormone, respectively, in the rhesus monkey (Macaca mulatta). Endocrinology 144, 1175–1185.

Ramaswamy, S., Weinbauer, G.F., 2014. Endocrine control of spermatogenesis: Role of FSH and LH/testosterone. Spermatogenesis 4, e996025.

Ravel C., Jaillard S., 2011. The Sertoli cell. Morphologie 95, 151–158.

Rebourcet, D., O'Shaughnessy, P.J., Pitetti, J.L., Monteiro, A., O'Hara, L., Milne, L., Tsai, Y.T., Cruickshanks, L., Riethmacher, D., Guillou, F., Mitchell, R.T., 2014a. Sertoli cells control peritubular myoid cell fate and support adult Leydig cell development in the prepubertal testis. Development 141, 2139–2149.

Rebourcet, D., O'Shaughnessy, P.J., Monteiro, A., Milne, L., Cruickshanks, L., Jeffrey, N., Guillou, F., Freeman, T.C., Mitchell, R.T., Smith, L.B., 2014b. Sertoli cells maintain Leydig cell number and peritubular myoid cell activity in the adult mouse testis. PLoS One 9, e105687.

Redgrove, K.A., Anderson, A.L., McLaughlin, E.A., O'Bryan, M.K., Aitken, R.J., Nixon, B., 2013. Investigation of the mechanisms by which the molecular chaperone HSPA2 regulates the expression of sperm surface receptors involved in human sperm–oocyte recognition. Mol. Hum. Reprod. 19, 120–135.

Redgrove, K.A., Nixon, B., Baker, M.A., Hetherington, L., Baker, G., Liu, D.-Y., Aitken, R.J., 2012. The molecular chaperone HSPA2 plays a key role in regulating the expression of sperm surface receptors that mediate sperm-egg recognition. PLoS One 7, e50851.

Rey, R., 2003. Regulation of spermatogenesis, in: Söder, O. (Ed.), The Developing Testis: Physiology and Pathophysiology. Karger, Basel, pp. 38–55.

Ricard-Blum, S., 2011. The collagen family. Cold Spring Harb. Perspect. Biol. 3, a004978.

Rich, K.A., de Kretser, D.M., 1977. Effect of Differing Degrees of Destruction of the Rat Seminiferous Epithelium on Levels of Serum Follicle Stimulating Hormone and Androgen Binding Protein 1. Endocrinology 101, 959–968.

Rich, K.A., Kerr, J.B., de Kretser, D.M., 1979. Evidence for Leydig cell dysfunction in rats with seminiferous tubule damage. Mol. Cell. Endocrinol. 13, 123–135.

Richter, K., Haslbeck, M., Buchner, J., 2010. The heat shock response: life on the verge of death. Mol. Cell 40, 253–266.

Risbridger, G.P., Kerr, J.B., de Kretser, D.M., 1981a. Evaluation of Leydig cell function and gonadotropin binding in unilateral and bilateral cryptorchidism: evidence for local control of Leydig cell function by the seminiferous tubule. Biol. Reprod. 24, 534–540.

Risbridger, G.P., Kerr, J.B., Peake, R.A., de Kretser, D.M., 1981b. An Assessment of Leydig Cell Function after Bilateral or Unilateral Efferent Duct Ligation: Further Evidence for Local Control of Leydig Cell Function. Endocrinology 109, 1234–1241.

Ritzen, E.M., Van Damme, M., Fröysa, B., Reuter, C., De La Torre, B., Diczfalusv, E., 1981. Identification of estradiol produced by Sertoli cell enriched cultures during incubation with testosterone. J. Steroid Biochem. 14, 533–535.

Rival, C., Lustig, L., Iosub, R., Guazzone, V.A., Schneider, E., Meinhardt, A., Fijak, M., 2006. Identification of a dendritic cell population in normal testis and in chronically inflamed testis of rats with autoimmune orchitis. Cell Tissue Res. 324, 311–318.

Rockett, J.C., Mapp, F.L., Garges, J.B., Luft, J.C., Mori, C., Dix, D.J., 2001. Effects of hyperthermia on spermatogenesis, apoptosis, gene expression, and fertility in adult male mice. Biol. Reprod. 65, 229–239.

Rolland, A.D., Evrard, B., Guitton, N., Lavigne, R., Calvel, P., Couvet, M., Jégou, B., Pineau, C., 2007. Two-dimensional fluorescence difference gel electrophoresis analysis of spermatogenesis in the rat. J. Proteome Res. 6, 683–697.

Rombauts, L., Healy, D., 1995. Inhibins and activins in reproduction. Curr. Obstet. Gynaecol. 5, 155–162.

Roosen-Runge, E.C., Leik, J., 1968. Gonocyte degeneration in the postnatal male rat. Am. J. Anat. 122, 275–299.

Rosario, M., Perkins, S., O'Brien, D., Allen, R., Eddy, E., 1992. Identification of the gene for the developmentally expressed 70 kDa heat-shock protein (P70) of mouse spermatogenic cells. Dev. Biol. 150, 1–11.

Rousseau, G.G., 2013. Fifty years ago: The quest for steroid hormone receptors. Mol. Cell. Endocrinol. 375, 10–13.

Ruggiu, M., Saunders, P.T., Cooke, H.J., 2000. Dynamic subcellular distribution of the DAZL protein is confined to primate male germ cells. J. Androl. 21, 470–477.

Russell L.D., Ettlin R.A., Hikim A.P., Clegg E.D., 1990. Histological and Histopathological Evaluation of the Testis, first ed. Cache River Press, Clearwater.

Sadler, T.W., 2011. Langman's Medical Embryology, twelfth ed. Lippincott Williams & Wilkins, Baltimore.

Sailer, B.L., Sarkar, L.J., Bjordahl, J.A., Jost, L.K., Evenson, D.P., 1997. Effects of heat stress on mouse testicular cells and sperm chromatin structure. J. Androl. 18, 294–301.

Salerni, S., Di Francescomarino, S., Cadeddu, C., Acquistapace, F., Maffei, S., Gallina, S., 2015. The different role of sex hormones on female cardiovascular physiology and function: not only estrogens. Eur. J. Clin. Invest. 45, 634–645

Sapsford, C., 1962. Changes in the cells of the Sex Cords and Seminiferous Tubules during the development of the Testis of the rat and mouse. Aust. J. Zool. 10, 178–192.

Sarge, K., Cullen, K., 1997. Regulation of hsp expression during rodent spermatogenesis. Cell. Mol. Life Sci. 53, 191–197.

Sasaki, T., Gan, E.C., Wakeham, A., Kornbluth, S., Mak, T.W., Okada, H., 2007. HLA-B-associated transcript 3 (Bat3)/Scythe is essential for p300-mediated acetylation of p53. Genes Dev. 21, 848–861.

Sasaki, T., Marcon, E., McQuire, T., Arai, Y., Moens, P.B., Okada, H., 2008. Bat3 deficiency accelerates the degradation of Hsp70-2/HspA2 during spermatogenesis. J. Cell Biol. 182, 449–458.

Sassone-Corsi, P., 2002. Unique chromatin remodeling and transcriptional regulation in spermatogenesis. Science 296, 2176–2178.

Schaefer, L., Iozzo, R.V., 2008. Biological functions of the small leucine-rich proteoglycans: from genetics to signal transduction. J. Biol. Chem. 283, 21305–21309.

Schlatt, S., Ehmcke, J., 2014. Regulation of spermatogenesis: an evolutionary biologist's perspective, Sem. Cell Dev. Biol. 29, 2–16.

Schrewe, H., Gendron-Maguire, M., Harbison, M.L., Gridley, T., 1994. Mice homozygous for a null mutation of activin β B are viable and fertile. Mech. Dev. 47, 43–51.

Schwall, R.H., Robbins, K., Jardieu, P., Chang, L., La, C., Terrel, T.G., 1993. Activin induces cell death in hepatocytes in vivo and in vitro. Hepatology 18, 347–356.

Scieglinska, D. and Krawczyk, Z., 2015. Expression, function, and regulation of the testis-enriched heat shock HSPA2 gene in rodents and humans. Cell Stress and Chaperones, 20, 221-235.

Seachrist, D.D., Johnson, E., Magee, C., Clay, C.M., Graham, J.K., Veeramachaneni, D.R., Keri, R.A., 2012. Overexpression of follistatin in the mouse epididymis disrupts fluid resorption and sperm transit in testicular excurrent ducts. Biol. Reprod. 87, 41.

Seminara, S.B., Hayes, F.J., Crowley Jr, W.F., 1998. Gonadotropin-releasing hormone deficiency in the human (idiopathic hypogonadotropic hypogonadism and Kallmann's syndrome): pathophysiological and genetic considerations. Endocr. Rev. 19, 521–539.

Sengupta, P., 2015. A scientific review of age determination for a laboratory rat: how old is it in comparison with human age? Biomed. Int. 2, 81–89.

Setchell, B.P., Ploen, L., Ritzen, E.M., 2001. Reduction of long-term effects of local heating of the testis by treatment of rats with a GnRH agonist and an anti-androgen. Reproduction 122, 255–263.

Setchell, B.P., Ploen, L., Ritzen, E.M., 2002. Effect of local heating of rat testes after suppression of spermatogenesis by pretreatment with a GnRH agonist and an anti-androgen. Reproduction 124, 133–140.

Setchell, B.P., 1978. The mammalian testis, first ed. Paul Elek, London.

Setchell, B.P., 1998. The parkes lecture heat and the testis. J. Reprod. Fertil. 114, 179–194.

Setchell, B.P., 2006. The effects of heat on the testes of mammals. Anim. Reprod. 3, 81–91.

Sharma, D.C., Joshi, S.G. and Dorfman, R.I., 1967. Biosynthesis of testosterone by monkey testes in vitro. Endocrinology 80, 499–504.

Sharma, R., Agarwal, A., 2011. Spermatogenesis: an overview, in: Zini A., Agarwal A. (Eds.), Sperm Chromatin: Biological and Clinical Applications in Male. Springer, New York, pp. 19–44.

Sharpe, R.M., 1992. Monitoring of spermatogenesis in man-measurement of Sertoli cell-or germ cell-secreted proteins in semen or blood. Int. J. Androl. 15, 201–210.

Sharpe, R.M., Bartlett, J.M.S., 1987. Changes in the secretion of ABP into testicular interstitial fluid with age and in situations of impaired spermatogenesis. Int. J. Androl. 10, 701–710.

Sharpe, R.M., Bartlett, J.M.S., Allenby, G., 1991. Evidence for the control of testicular interstitial fluid volume in the rat by specific germ cell types. J. Endocrinol. 128, 359–NP.

Sharpe, R.M., Cooper, I., 1983. Testicular interstitial fluid as a monitor for changes in the intratesticular environment in the rat. J. Reprod. Fertil. 69, 125–135.

Shenker, N.S., Huynh, J., Farmer, P.J., Hutson, J.M., 2006. A new role for androgen in testicular descent: permitting gubernacular cell proliferation in response to the neuropeptide, calcitonin gene–related peptide. J. Pediatr. Surg. 41, 407–412.

Shi, J.F., Li, Y.K., Ren, K., Xie, Y.J., Yin, W.D. and Mo, Z.C., 2018. Characterization of cholesterol metabolism in Sertoli cells and spermatogenesis. Mol. Med. Rep. 17, 705–713.

Shikone, T., Billig, H., Hsueh, A., 1994. Experimentally induced cryptorchidism increases apoptosis in rat testis. Biol. Reprod. 51, 865–872.

Shiraishi, K., 2012. Heat and oxidative stress in the germ line, in: Agarwal A., Aitken R.J., Alvarez J.G. (Eds.), Studies on Men's Health and Fertility. Humana Press, New Jersey, pp. 149–178.

Shiraishi, K., Takihara, H., Matsuyama, H., 2010. Elevated scrotal temperature, but not varicocele grade, reflects testicular oxidative stress-mediated apoptosis. World J. Urol. 28, 359–364.

Socher, S.A., Yin, Y., Dewolf, W.C., Morgentaler, A., 1997. Temperature-mediated germ cell loss in the testis is associated with altered expression of the cell-cycle regulator p53. J. Urol. 157, 1986–1989.

Sottile, M.L., Nadin, S.B., 2018. Heat shock proteins and DNA repair mechanisms: an updated overview. Cell Stress Chaperones 23, 303–315.

Sreedhar, A.S., Csermely, P., 2004. Heat shock proteins in the regulation of apoptosis: new strategies in tumor therapy: a comprehensive review. Pharmacol. Ther. 101, 227–257.

Stahl, P. J., Schlegel, P. N., Goldstein, M., 2014. Sperm retrieval and quality evaluation. Methods Mol. Biol. 1154, 361–384.

Stanton, P.G., Foo, C.F., Rainczuk, A., Stephens, A.N., Condina, M., O'Donnell, L., Weidner, W., Ishikawa, T., Cruickshanks, L., Smith, L.B., 2016. Mapping the testicular interstitial fluid proteome from normal rats. Proteomics 16, 2391–2402.

Steger, K., 1999. Transcriptional and translational regulation of gene expression in haploid spermatids. Anat. Embryol. 199, 471–487.

Steiglitz, B.M., Keene, D.R., Greenspan, D.S., 2002. PCOLCE2 encodes a functional procollagen C-proteinase enhancer (PCPE2) that is a collagen-binding protein differing in distribution of expression and post-translational modification from the previously described PCPE1. J. Biol. Chem. 277, 49820–49830.

Stein, K.K., Go, J.C., Lane, W.S., Primakoff, P., Myles, D.G., 2006. Proteomic analysis of sperm regions that mediate sperm-egg interactions. Proteomics 6, 3533–3543.

Steinberg, E., Dixon, W.J., 1959. Some observations on the effect of heat on the testicular germinal epithelium. Fertil. Steril. 10, 578–595.

Steinberger, E. and Ficher, M., 1968. Conversion of progesterone to testosterone by testicular tissue at different stages of maturation. Steroids 11, 351–368.

Stocco, D.M., McPhaul, M.J., 2006. Physiology of Testicular Steroidogenesis. in: Neil J.D. (Ed.), Knobil and Neill's Physiology of Reproduction. Elsevier, New York, pp. 1017–1069.

Tan, K.A., De Gendt, K., Atanassova, N., Walker, M., Sharpe, R.M., Saunders, P.T., Denolet, E., Verhoeven, G., 2005. The role of androgens in Sertoli cell proliferation and functional maturation: studies in mice with total or Sertoli cell-selective ablation of the androgen receptor. Endocrinology 146, 2674–2683.

Tanimoto, Y., Tanimoto, K., Sugiyama, F., Horiguchi, H., Murakami, K., Yagami, K.-i., Fukamizu, A., 1999. Male sterility in transgenic mice expressing activin βA subunit gene in testis. Biochem. Biophys. Res. Commun. 259, 699–705.

Thomas, P., 2012. Rapid steroid hormone actions initiated at the cell surface and the receptors that mediate them with an emphasis on recent progress in fish models. Gen. Comp. Endocrinol. 175, 367–383.

Toulis, K.A., Iliadou, P.K., Venetis, C.A., Tsametis, C., Tarlatzis, B.C., Papadimas, I., Goulis, D.G., 2010. Inhibin B and anti-Müllerian hormone as markers of persistent spermatogenesis in men with non-obstructive azoospermia: a meta-analysis of diagnostic accuracy studies. Hum. Reprod. Update 16, 713–724.

Tramontano, F., Malanga, M., Farina, B., Jones, R., Quesada, P., 2000. Heat stress reduces poly (ADPR) polymerase expression in rat testis. Mol. Hum. Reprod. 6, 575–581.

Troppmann, B., Kleinau, G., Krause, G., Gromoll, J., 2013. Structural and functional plasticity of the luteinizing hormone/choriogonadotrophin receptor. Hum. Reprod. Update 19, 583–602.

Tsai, M.-Y., Yeh, S.-D., Wang, R.-S., Yeh, S., Zhang, C., Lin, H.-Y., Tzeng, C.-R., Chang, C., 2006. Differential effects of spermatogenesis and fertility in mice lacking androgen receptor in individual testis cells. Proc. Natl. Acad. Sci. 103, 18975–18980.

Tsuchida, K., Nakatani, M., Yamakawa, N., Hashimoto, O., Hasegawa, Y., Sugino, H., 2004. Activin isoforms signal through type I receptor serine/threonine kinase ALK7. Mol. Cell. Endocrinol. 220, 59–65.

Tsukahara, T., Kimura, S., Ichimiya, S., Torigoe, T., Kawaguchi, S., Wada, T., Yamashita, T., Sato, N., 2009. Scythe/BAT3 regulates apoptotic cell death induced by papillomavirus binding factor in human osteosarcoma. Cancer Sci. 100, 47–53.

Tunc, L., Kırac, M., Gurocak, S., Yucel, A., Kupeli, B., Alkıbay, T., Bozkirli, I., 2006. Can serum Inhibin B and FSH levels, testicular histology and volume predict the outcome of testicular sperm extraction in patients with non-obstructive azoospermia? Int. Urol. Nephrol. 38, 629–635.

Turner, K.J., Mckinnell, C., Mclaren, T.T., Qureshi, S.J., Saunders, P.T., Foster, P.M., Sharpe, R.M., 1996. Detection of germ cell-derived proteins in testicular interstitial fluid: potential for monitoring spermatogenesis in vivo. J. Androl. 17, 127–136.

Turner, T., Bomgardner, D., Jacobs, J., Nguyen, Q., 2003. Association of segmentation of the epididymal interstitium with segmented tubule function in rats and mice. Reproduction 125, 871–878.

van Furth, R. and Cohn, Z.A., 1968. The origin and kinetics of mononuclear phagocytes. J. Exp. Med. 128, 415–435.

Van Zelst, S.J., Zupp, J.L., Hayman, D.L., Setchell, B.P., 1995. XY chromosome dissociation in mice and rats exposed to increased testicular or environmental temperatures. Reprod. Fertil. Dev. 7, 1117–1121.

Vassalli, A., Matzuk, M.M., Gardner, H.A., Lee, K.F., Jaenisch, R., 1994. Activin/inhibin beta B subunit gene disruption leads to defects in eyelid development and female reproduction. Genes Dev. 8, 414–427.

Vera, Y., Diaz-Romero, M., Rodriguez, S., Lue, Y., Wang, C., Swerdloff, R.S., Hikim, A.P.S., 2004. Mitochondria-dependent pathway is involved in heat-induced male germ cell death: lessons from mutant mice. Biol. Reprod. 70, 1534–1540.

Vera, Y., Rodriguez, S., Castanares, M., Lue, Y., Atienza, V., Wang, C., Swerdloff, R.S., Hikim, A.P.S., 2005. Functional role of caspases in heat-induced testicular germ cell apoptosis. Biol. Reprod. 72, 516–522.

Vergouwen, R., Jacobs, S., Huiskamp, R., Davids, J., de Rooij, D., 1991. Proliferative activity of gonocytes, Sertoli cells and interstitial cells during testicular development in mice. J. Reprod. Fertil. 93, 233–243.

Virji, N., Naz, R., 1995. The role of lactate dehydrogenase-C4 in testicular function and infertility. Int. J. Androl. 18, 1–7.

von Strandmann, E.P., Simhadri, V.R., von Tresckow, B., Sasse, S., Reiners, K.S., Hansen, H.P., Rothe, A., Böll, B., Simhadri, V.L., Borchmann, P., 2007. Human leukocyte antigen-B-associated transcript 3 is released from tumor cells and engages the NKp30 receptor on natural killer cells. Immun. 27, 965–974.

Waheeb, R., Hofmann, M.C., 2011. Human spermatogonial stem cells: a possible origin for spermatocytic seminoma. Int. J. Androl. 34, e296–e305.

Waites G , Voglmayr J., 1963. The functional activity and control of the apocrine sweat glands of the scrotum of the ram. Aust. J. Agric. Res. 14, 839–851.

Walker, W.H., 2011. Testosterone signaling and the regulation of spermatogenesis. Spermatogenesis 1, 116–120.

Wang, C., Cui, Y.G., Wang, X.-H., Jia, Y., Sinha Hikim, A., Lue, Y.-H., Tong, J.-S., Qian, L.-X., Sha, J.-H., Zhou, Z.-M., 2007. Transient scrotal hyperthermia and levonorgestrel enhance testosterone-induced spermatogenesis suppression in men through increased germ cell apoptosis. J. Clin. Endocrinol. Metab. 92, 3292–3304.

Wang, R.S., Yeh, S., Tzeng, C.-R., Chang, C., 2009. Androgen receptor roles in spermatogenesis and fertility: lessons from testicular cell-specific androgen receptor knockout mice. Endocr. Rev. 30, 119–132.

Wang, R., Liew, C.C., 1994. The human BAT3 ortholog in rodents is predominantly and developmentally expressedin testis. Mol. Cell. Biochem. 136, 49–57.

Ward, W.S., Partin, A.W., Coffey, D.S., 1989. DNA loop domains in mammalian spermatozoa. Chromosoma 98, 153–159.

Wartenberg, H., 1976. Comparative Cytomorphologic Aspects of the Male Germ Cells, Especially of the “Gonia”. Andrologia 8, 117–130.

Wartenberg, H., 1989. Differentiation and development of the testes, in: Burger, H., de Kretser, D.M. (Eds.), The Testis. Raven Press, New York, pp. 67–118.

Weinbauer, G.F., Luetjens, C.M., Simon, M., Nieschlag, E., 2010. Physiology of Testicular Function, in: van Ahlen, H. (Ed.), Andrology: Male Reproductive Health and Dysfunction. Springer, Berlin, pp. 11–54.

Welsh, M., Saunders, P.T., Atanassova, N., Sharpe, R.M., Smith, L.B., 2009. Androgen action via testicular peritubular myoid cells is essential for male fertility. FASEB J. 23, 4218–4230.

Werdelin, L., Nilsonne, Å., 1999. The evolution of the scrotum and testicular descent in mammals: a phylogenetic view. J. Theor. Biol. 196, 61–72.

Widlak, W., Vydra, N., Malusecka, E., Dudaladava, V., Winiarski, B., Ścieglińska, D., Widlak, P., 2007a. Heat shock transcription factor 1 down-regulates spermatocyte-specific 70 kDa heat shock protein expression prior to the induction of apoptosis in mouse testes. Genes Cells 12, 487–499.

Widlak, W., Winiarski, B., Krawczyk, A., Vydra, N., Malusecka, E., Krawczyk, Z., 2007b. Inducible 70 kDa heat shock protein does not protect spermatogenic cells from damage induced by cryptorchidism. Int. J. Androl. 30, 80–87.

Wijayarathna, R., de Kretser, D., 2016. Activins in reproductive biology and beyond. Hum. Reprod. Update 22, 342–357.

Wilhelm, D., Huang, E., Svingen, T., Stanfield, S., Dinnis, D., Koopman, P., 2006. Comparative proteomic analysis to study molecular events during gonad development in mice. Genes. 44, 168–176.

Wilson, M.D., 2014. A study of male reproductive form and function in a rat model. Asian Pac. J. Reprod. 3, 258–262.

Winnall, W.R., Okuma, Y., Saito, K., Muir, J.A., Hedger, M.P., 2009. Regulation of interleukin 1α, activin and inhibin by lipopolysaccharide in Sertoli cells from prepubertal rats. Mol. Cell. Endocrinol. 307, 169–175.

Winnall, W.R., Wu, H., Sarraj, M.A., Rogers, P.A., de Kretser, D.M., Girling, J.E., Hedger, M.P., 2013. Expression patterns of activin, inhibin and follistatin variants in the adult male mouse reproductive tract suggest important roles in the epididymis and vas deferens. Reprod. Fertil. Dev. 25, 570–580.

Wosnitzer, M., Goldstein, M., Hardy, M.P., 2014. Review of azoospermia. Spermatogenesis 4, e28218.

Yaeram, J., Setchell, B.P., Maddocks, S., 2006. Effect of heat stress on the fertility of male mice in vivo and in vitro. Reprod. Fertil. Dev. 18, 647–653.

Yamakawa, K., Yoshida, K., Nishikawa, H., Kato, T., Iwamoto, T., 2007. Comparative analysis of interindividual variations in the seminal plasma proteome of fertile men with identification of potential markers for azoospermia in infertile patients. J. Androl. 28, 858–865.

Yang, F., Wang, P., 2009. The Mammalian synaptonemal complex: a scaffold and beyond. Genome Dyn. 5, 69–80.

Yeh, S., Tsai, M.Y., Xu, Q., Mu, X.M., Lardy, H., Huang, K.E., Lin, H., Yeh, S.D., Altuwaijri, S., Zhou, X., 2002. Generation and characterization of androgen receptor knockout (ARKO) mice: an in vivo model for the study of androgen functions in selective tissues. Proc. Natl. Acad. Sci. 99, 13498–13503.

Yin, Y., DeWolf, W.C., Morgentaler, A., 1997a. p53 is associated with the nuclear envelope in mouse testis. Biochem. Biophys. Res. Commun. 235, 689–694.

Yin, Y., DeWolf, W.C., Morgentaler, A., 1998. Experimental cryptorchidism induces testicular germ cell apoptosis by p53-dependent and-independent pathways in mice. Biol. Reprod. 58, 492–496.

Yin, Y., Hawkins, K.L., Dewolf, W.C., Morgentaler, A., 1997b. Heat stress causes testicular germ cell apoptosis in adult mice. J. Androl. 18, 159–165.

Yona, S., Kim, K.W., Wolf, Y., Mildner, A., Varol, D., Breker, M., Strauss-Ayali, D., Viukov, S., Guilliams, M., Misharin, A. and Hume, D.A., 2013. Fate mapping reveals origins and dynamics of monocytes and tissue macrophages under homeostasis. Immunity, 38, 79-91.

Yuan, L., Liu, J.-G., Zhao, J., Brundell, E., Daneholt, B., Höög, C., 2000. The murine Scp3 gene is required for synaptonemal complex assembly, chromosome synapsis, and male fertility. Mol. Cell 5, 73–83.

Zhang, X.S., Yuan, J.X., Liu, T., Lue, Y.H., Jin, X., Tao, S.X., Hu, Z.Y., Hikim, A.P.S., Swerdloff, R.S., Wang, C., 2006. Expression of Orphan Receptors TR2, TR3, TR4, and p53 in Heat-Treated Testis of Cynomolgus Monkeys (Macaca fascicularis). J. Androl. 27, 405–413.

Zhao, C., Huo, R., Wang, F.-Q., Lin, M., Zhou, Z.-M., Sha, J.-H., 2007. Identification of several proteins involved in regulation of sperm motility by proteomic analysis. Fertil. Steril. 87, 436–438.

Zhu, H., Cui, Y., Xie, J., Chen, L., Chen, X., Guo, X., Zhu, Y., Wang, X., Tong, J., Zhou, Z., 2010. Proteomic analysis of testis biopsies in men treated with transient scrotal hyperthermia reveals the potential targets for contraceptive development. Proteomics 10, 3480–3493.

Zhu, Y.F., Cui, Y.G., Guo, X.J., Wang, L., Bi, Y., Hu, Y.-Q., Zhao, X., Liu, Q., Huo, R., Lin, M., 2006. Proteomic analysis of effect of hyperthermia on spermatogenesis in adult male mice. J. Proteome Res. 5, 2217–2225.

Zitzmann, M., Nieschlag, E., 2000. Hormone substitution in male hypogonadism. Mol. Cell. Endocrinol. 161, 73–88.

Zoppi, S., Young, M., McPhaul, M., 2002. Regulation of gene expression by the nuclear receptor family, in: Mason J.I. (Ed.), The Genetics of Steroid Biosynthesis. Harwood Academic Publisher, Reading, pp. 376–403.